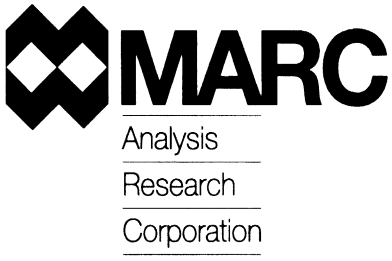

VOLUME E
Demonstration Problems

K6 Additions

Copyright © 1995 MARC Analysis Research Corporation
Printed in U. S. A.
This notice shall be marked on any reproduction of this data, in whole or in part.

MARC Analysis Research Corporation
260 Sheridan Avenue, Suite 309
Palo Alto, CA 94306 USA

Phone: (415) 329-6800
FAX: (415) 323-5892
email: techpubs@marc.com

Document Title: **Volume E, Demonstration Problems, K6 Additions**
Part Number: RF-3019-06
Revision Date: July, 1995

PROPRIETARY NOTICE

MARC Analysis Research Corporation reserves the right to make changes in specifications and other information contained in this document without prior notice.

Although due care has been taken to present accurate information, MARC Analysis Research Corporation DISCLAIMS ALL WARRANTIES WITH RESPECT TO THE CONTENTS OF THIS DOCUMENT (INCLUDING, WITHOUT LIMITATION, WARRANTIES OR MERCHANTABILITY AND FITNESS FOR A PARTICULAR PURPOSE) EITHER EXPRESSED OR IMPLIED. MARC Analysis Research Corporation SHALL NOT BE LIABLE FOR DAMAGES RESULTING FROM ANY ERROR CONTAINED HEREIN, INCLUDING, BUT NOT LIMITED TO, FOR ANY SPECIAL, INCIDENTAL OR CONSEQUENTIAL DAMAGES ARISING OUT OF, OR IN CONNECTION WITH, THE USE OF THIS DOCUMENT.

This software product and its documentation set are copyrighted and all rights are reserved by MARC Analysis Research Corporation. Usage of this product is only allowed under the terms set forth in the MARC Analysis Research Corporation License Agreement. Any reproduction or distribution of this document, in whole or in part, without the prior written consent of MARC Analysis Research Corporation is prohibited.

RESTRICTED RIGHTS NOTICE

This computer software is commercial computer software submitted with "restricted rights." Use, duplication, or disclosure by the government is subject to restrictions as set forth in subparagraph (c)(i)(ii) or the Rights in technical Data and Computer Software clause at DFARS 252.227-7013, NASA FAR Supp. Clause 1852.227-86, or FAR 52.227-19. Unpublished rights reserved under the Copyright Laws of the United States.

TRADEMARKS

All products mentioned are the trademarks, service marks, or registered trademarks of their respective holders.

Preface

This manual contains the updates to *Volume E, Demonstration Problems* for the K6 release. The *Volume E, Demonstration Problems* demonstrates most of the MARC program capabilities. The MARC program is a powerful, modern, general-purpose nonlinear finite element program for structural, thermal, and electromagnetic analyses.

In a typical finite element analysis, you will need to define the:

mesh (which is an *approximate* model of the actual structure);
material properties (Young's modulus, Poisson's ration, etc.);
applied loads (static, dynamic temperature, inertial, etc.);
boundary conditions (geometric and kinematic constraints); and
type of analysis (linear static, nonlinear, buckling, thermal, etc.).

The steps leading up to the actual finite element analysis are generally termed preprocessing; currently, many users accomplish these steps by using an interactive color graphics pre- and post-processing program such as the Mentat II graphics program. After an analysis, the results evaluation phase (post-processing) is where you check the adequacy of the design (and of the approximate finite analysis model) in terms of critical stresses, deflection, temperatures, and so forth.

This update manual is divided into two sections: the *K6 Additions* and the *K6 Changes*. This section, *K6 Additions*, highlights the additions to the MARC K6 release. It is organized similar to the complete *Volume E, Demonstration Problems*.

Volume E, Demonstration Problems is divided into four parts with each part containing two chapters. The manual has eight chapters grouped by the type of demonstration problems.

Part 1

Chapter 1, Introduction provides a general introduction to the problems demonstrated in all parts of *Volume E, Demonstration Problems*. Following the text is a set of cross reference tables showing keywords for the following:

parameter options
model definition options
mesh display options
history definition options
mesh rezoning options
element types
user subroutines

Each keyword is cross-referenced to the problem in which its use is demonstrated

Chapter 2, Linear Analysis	demonstrates most of the element types available to the user. Many linear analysis features are illustrated. The use of adaptive meshing for linear analysis is demonstrated here.
Part II	
Chapter 3, Plasticity and Creep	demonstrates the nonlinear material analysis capabilities. Both plasticity and creep phenomena are covered.
Chapter 4, Large Displacement	demonstrates the program's ability to analyze both large displacement and small strain effects.
Part III	
Chapter 5, Heat Transfer	demonstrates both steady-state and transient heat transfer capabilities.
Chapter 6, Dynamics	demonstrates many types of dynamic problems. These include analyses performed using both the modal and direct integration methods. The influences of fluid coupling and initial stresses on the calculated eigenvalues are shown. Harmonic and spectrum response analysis is also demonstrated here.
Part IV	
Chapter 7, Contact and Advanced Topics	demonstrates some of the special program capabilities of the MARC program. This includes the ability to solve rubber (incompressible), foam, viscoelastic, contact, and composite problems as well as others.

Chapter 8, Advanced Topics	demonstrates the capabilities most recently added to the MARC program. They include the ability to use substructures, in both linear and nonlinear analysis, to perform cracking analysis, analysis of contact problems, the ability to perform coupled thermal-mechanical analysis, electrostatic, magnetostatic and acoustic analysis. The use of adaptive meshing to solve nonlinear analysis is demonstrated here.

Volume E, Demonstration Problems summarizes the physics of each problem and describes the options required to define the problem. Figures are given of the mesh geometry and typical output results. The actual input and user subroutines are not included in the manual. They may be found on the distribution media associated with the MARC installation.

Each problem in *Volume E, Demonstration Problems* has a **Summary of Options Used.** Options and user subroutines are called out in the text by the use of a different type font – such as CONTINUE option, CHANGE STATE option, user subroutine UFCONN and user subroutine UFXORD.

Contents K6 Additions

Chapter 2 Linear Analysis

Chapter 3 Plasticity And Creep

Chapter 4 Large Displacement

Chapter 5 Heat Transfer

Chapter 6 Dynamics

Chapter 7 Contact

Chapter 8 Advanced Topics

Figures K6 Additions

Chapter 2 Linear Analysis

Chapter 3 Plasticity And Creep

Chapter 4 Large Displacement

Chapter 5 Heat Transfer

Chapter 6 Dynamics

Chapter 7 Contact

Chapter 8 Advanced Topics

Tables K6 Additions

Chapter 1 Introduction

Chapter 2 Linear Analysis

Chapter 4 Large Displacement

Chapter 5 Heat Transfer

Chapter 6 Dynamics

Table E 1.0-1 Parameter Option Cross Reference

adaptive					
e2x10c.dat	e2x9d.dat	e3x21d.dat	e7x20c.dat	e8x12c.dat	e8x40.dat
e8x41.dat	e8x42.dat	e8x43.dat	e8x44.dat		
alias					
e2x12d.dat	e2x70.dat	e3x30a.dat	e6x20a.dat	e6x20b.dat	e8x43.dat
all points					
e2x40a.dat	e2x40b.dat	e2x41.dat	e2x68.dat	e3x6.dat	e4x11.dat
e5x17a.dat	e5x17b.dat	e5x18a.dat	e5x18b.dat	e7x23.dat	e8x41.dat
buckle					
e4x12a.dat	e4x12b.dat	e4x12c.dat			
comment					
e5x17b.dat					

Table E 1.0-1 Parameter Option Cross Reference (Continued)

couple					
e7x1b.dat	e7x1c.dat				
dist loads					
e2x40a.dat	e2x40b.dat	e2x41.dat	e2x68.dat	e3x6.dat	e4x11.dat
e5x17a.dat	e5x17b.dat	e5x18a.dat	e5x18b.dat	e6x21.dat	e7x20b.dat
e7x20c.dat	e8x42.dat	e8x43.dat			
dynamic					
e6x18.dat	e6x19.dat	e6x20b.dat	e6x21.dat		
elastic					
e2x10c.dat	e2x9d.dat	e8x40.dat	e8x41.dat		

Table E 1.0-1 Parameter Option Cross Reference (Continued)

elements					
e2x10c.dat	e2x12d.dat	e2x12e.dat	e2x34.dat	e2x40a.dat	e2x40b.dat
e2x41.dat	e2x46d.dat	e2x68.dat	e2x69.dat	e2x70.dat	e2x9d.dat
e3x21d.dat	e3x30a.dat	e3x30b.dat	e3x31.dat	e3x6.dat	e4x11.dat
e4x12a.dat	e4x12b.dat	e4x12c.dat	e4x2a.dat	e4x2b.dat	e4x7b.dat
e5x17a.dat	e5x17b.dat	e5x18a.dat	e5x18b.dat	e6x18.dat	e6x19.dat
e6x20a.dat	e6x20b.dat	e6x21.dat	e7x19b.dat	e7x1b.dat	e7x1c.dat
e7x20b.dat	e7x20c.dat	e7x23.dat	e7x24a.dat	e7x24b.dat	e7x25.dat
e7x26.dat	e7x6b.dat	e8x12c.dat	e8x14f.dat	e8x18b.dat	e8x38a.dat
e8x38b.dat	e8x38c.dat	e8x39.dat	e8x40.dat	e8x41.dat	e8x42.dat
e8x43.dat	e8x44.dat				

Table E 1.0-1 Parameter Option Cross Reference (Continued)

elsto	
e4x2a.dat	e4x2b.dat

Table E 1.0-1 Parameter Option Cross Reference (Continued)

finite					
e3x21d.dat	e3x31.dat	e8x12c.dat	e8x14f.dat	e8x18b.dat	e8x38a.dat
e8x38b.dat	e8x38c.dat	e8x44.dat			
follow for					
e6x21.dat	e7x20b.dat	e7x20c.dat	e8x42.dat	e8x43.dat	
heat					
e5x18a.dat	e5x18b.dat				
istress					
e3x30a.dat					

Table E 1.0-1 Parameter Option Cross Reference (Continued)

large disp					
e3x21d.dat	e3x31.dat	e4x11.dat	e4x12a.dat	e4x12b.dat	e4x12c.dat
e4x2a.dat	e4x2b.dat	e4x7b.dat	e6x21.dat	e7x19b.dat	e7x20b.dat
e7x20c.dat	e7x23.dat	e7x25.dat	e7x26.dat	e8x12c.dat	e8x14f.dat
e8x18b.dat	e8x38a.dat	e8x38b.dat	e8x38c.dat	e8x39.dat	e8x42.dat
e8x43.dat	e8x44.dat				
lump					
e5x18a.dat	e5x18b.dat	e6x19.dat			

Table E 1.0-1 Parameter Option Cross Reference (Continued)

print					
e2x70.dat	e3x30a.dat	e3x30b.dat	e3x31.dat	e4x7b.dat	e5x17a.dat
e5x17b.dat	e6x19.dat	e7x20b.dat	e7x20c.dat	e7x23.dat	e7x26.dat
e8x12c.dat	e8x14f.dat	e8x18b.dat	e8x38a.dat	e8x38b.dat	e8x38c.dat
e8x39.dat	e8x40.dat	e8x43.dat	e8x44.dat		
processor					
e2x12e.dat	e2x46d.dat				
r-p flow					
e3x30a.dat	e3x30b.dat	e7x1b.dat	e7x1c.dat		

Table E 1.0-1 Parameter Option Cross Reference (Continued)

response					
e6x18.dat					
setname					
e2x40a.dat	e2x40b.dat	e2x41.dat	e2x46d.dat	e2x68.dat	e2x70.dat
e3x31.dat	e3x6.dat	e4x11.dat	e5x17a.dat	e5x17b.dat	e5x18a.dat
e5x18b.dat	e6x21.dat	e7x20c.dat	e7x23.dat	e8x42.dat	
shell sect					
e2x40a.dat	e2x40b.dat	e2x41.dat	e2x68.dat	e2x69.dat	e2x70.dat
e3x6.dat	e4x11.dat	e4x7b.dat	e5x18a.dat	e5x18b.dat	e7x24a.dat
e7x24b.dat	e7x25.dat	e7x26.dat	e7x6b.dat	e8x18b.dat	e8x38a.dat
e8x38b.dat	e8x38c.dat				
sizing					
e2x10c.dat	e2x12d.dat	e2x12e.dat	e2x34.dat	e2x40a.dat	e2x40b.dat
e2x41.dat	e2x46d.dat	e2x68.dat	e2x69.dat	e2x70.dat	e2x9d.dat
e3x21d.dat	e3x30a.dat	e3x30b.dat	e3x31.dat	e3x6.dat	e4x11.dat
e4x12a.dat	e4x12b.dat	e4x12c.dat	e4x2a.dat	e4x2b.dat	e4x7b.dat
e5x17a.dat	e5x17b.dat	e5x18a.dat	e5x18b.dat	e6x18.dat	e6x19.dat
e6x20a.dat	e6x20b.dat	e6x21.dat	e7x19b.dat	e7x1b.dat	e7x1c.dat
e7x20b.dat	e7x20c.dat	e7x23.dat	e7x24a.dat	e7x24b.dat	e7x25.dat
e7x26.dat	e7x6b.dat	e8x12c.dat	e8x14f.dat	e8x18b.dat	e8x38a.dat
e8x38b.dat	e8x38c.dat	e8x39.dat	e8x40.dat	e8x41.dat	e8x42.dat
e8x43.dat	e8x44.dat				

Table E 1.0-1 Parameter Option Cross Reference (Continued)

Table E 1.0-1 Parameter Option Cross Reference (Continued)

Table E 1.0-1 Parameter Option Cross Reference (Continued)

thermal					
e2x46d.dat					
title					
e2x10c.dat	e2x12d.dat	e2x12e.dat	e2x34.dat	e2x40a.dat	e2x40b.dat
e2x41.dat	e2x46d.dat	e2x68.dat	e2x69.dat	e2x70.dat	e2x9d.dat
e3x21d.dat	e3x30a.dat	e3x30b.dat	e3x31.dat	e3x6.dat	e4x11.dat
e4x12a.dat	e4x12b.dat	e4x12c.dat	e4x2a.dat	e4x2b.dat	e4x7b.dat
e5x17a.dat	e5x17b.dat	e5x18a.dat	e5x18b.dat	e6x18.dat	e6x19.dat
e6x20a.dat	e6x20b.dat	e6x21.dat	e7x19b.dat	e7x1b.dat	e7x1c.dat
e7x20b.dat	e7x20c.dat	e7x23.dat	e7x24a.dat	e7x24b.dat	e7x25.dat
e7x26.dat	e7x6b.dat	e8x12c.dat	e8x14f.dat	e8x18b.dat	e8x38a.dat
e8x38b.dat	e8x38c.dat	e8x39.dat	e8x40.dat	e8x41.dat	e8x42.dat
e8x43.dat	e8x44.dat				

Table E 1.0-1 Parameter Option Cross Reference (Continued)

Table E 1.0-1 Parameter Option Cross Reference (Continued)

update					
e3x21d.dat	e3x31.dat	e4x7b.dat	e7x25.dat	e8x12c.dat	e8x14f.dat
e8x18b.dat	e8x38a.dat	e8x38b.dat	e8x38c.dat	e8x44.dat	

Table E 1.0-2 Model Definition Option Cross Reference

adaptive					
e2x10c.dat	e2x9d.dat	e7x20c.dat	e8x12c.dat	e8x40.dat	e8x41.dat
e8x42.dat	e8x43.dat	e8x44.dat			
anisotropic					
e7x6b.dat					
attach node					
e2x9d.dat	e7x20c.dat	e8x40.dat	e8x42.dat		
buckle increment					
e4x12c.dat					
change state					
e2x41.dat					
composite					
e7x24a.dat	e7x24b.dat	e7x25.dat	e7x6b.dat		
conn fill					
e2x34.dat					
conn gener					
e2x34.dat	e6x18.dat				

Table E 1.0-2 Model Definition Option Cross Reference (Continued)

connectivity
All MARC input files must have a CONNECTIVITY option.

Table E 1.0-2 Model Definition Option Cross Reference (Continued)

Table E 1.0-2 Model Definition Option Cross Reference (Continued)

contact					
e3x30a.dat	e3x30b.dat	e3x31.dat	e4x7b.dat	e6x19.dat	e7x20b.dat
e7x20c.dat	e7x23.dat	e8x12c.dat	e8x14f.dat	e8x18b.dat	e8x38a.dat
e8x38b.dat	e8x38c.dat	e8x39.dat	e8x42.dat	e8x43.dat	e8x44.dat
contact table					
e3x31.dat	e6x19.dat	e8x38a.dat	e8x38b.dat	e8x38c.dat	e8x44.dat
control					
e2x70.dat	e2x9d.dat	e3x21d.dat	e3x30a.dat	e3x30b.dat	e3x31.dat
e4x12a.dat	e4x12b.dat	e4x12c.dat	e4x2a.dat	e4x2b.dat	e4x7b.dat
e5x17a.dat	e5x17b.dat	e6x21.dat	e7x1b.dat	e7x1c.dat	e7x20b.dat
e7x20c.dat	e7x23.dat	e7x25.dat	e7x26.dat	e8x12c.dat	e8x14f.dat
e8x18b.dat	e8x38a.dat	e8x38b.dat	e8x38c.dat	e8x39.dat	e8x41.dat
e8x42.dat	e8x44.dat				

Table E 1.0-2 Model Definition Option Cross Reference (Continued)

coordinate					
e2x10c.dat	e2x12d.dat	e2x12e.dat	e2x34.dat	e2x40a.dat	e2x40b.dat
e2x41.dat	e2x46d.dat	e2x68.dat	e2x69.dat	e2x70.dat	e2x9d.dat
e3x21d.dat	e3x30a.dat	e3x30b.dat	e3x31.dat	e3x6.dat	e4x11.dat
e4x12a.dat	e4x12b.dat	e4x12c.dat	e4x2b.dat	e4x7b.dat	e5x17a.dat
e5x17b.dat	e5x18a.dat	e5x18b.dat	e6x18.dat	e6x19.dat	e6x20a.dat
e6x20b.dat	e6x21.dat	e7x19b.dat	e7x1b.dat	e7x1c.dat	e7x20b.dat
e7x20c.dat	e7x23.dat	e7x24a.dat	e7x24b.dat	e7x25.dat	e7x26.dat
e7x6b.dat	e8x12c.dat	e8x14f.dat	e8x18b.dat	e8x38a.dat	e8x38b.dat
e8x38c.dat	e8x39.dat	e8x40.dat	e8x41.dat	e8x42.dat	e8x43.dat
e8x44.dat					

Table E 1.0-2 Model Definition Option Cross Reference (Continued)

Table E 1.0-2 Model Definition Option Cross Reference (Continued)

Table E 1.0-2 Model Definition Option Cross Reference (Continued)

define					
e2x40a.dat	e2x40b.dat	e2x41.dat	e2x46d.dat	e2x68.dat	e2x70.dat
e3x31.dat	e3x6.dat	e4x11.dat	e4x12a.dat	e4x12b.dat	e4x12c.dat
e5x17a.dat	e5x17b.dat	e5x18a.dat	e5x18b.dat	e6x19.dat	e6x21.dat
e7x19b.dat	e7x20b.dat	e7x20c.dat	e7x23.dat	e7x6b.dat	e8x42.dat
dist fluxe					
e5x18a.dat	e5x18b.dat				
dist loads					
e2x12d.dat	e2x12e.dat	e2x40a.dat	e2x40b.dat	e2x69.dat	e2x9d.dat
e3x31.dat	e4x2a.dat	e4x2b.dat	e6x20a.dat	e6x20b.dat	e6x21.dat
e7x20b.dat	e7x6b.dat	e8x38a.dat	e8x38b.dat	e8x38c.dat	e8x42.dat
e8x43.dat					

Table E 1.0-2 Model Definition Option Cross Reference (Continued)

error estimate					
e2x34.dat	e8x41.dat				
fail data					
e7x25.dat					
fixed disp					
e2x10c.dat	e2x12d.dat	e2x12e.dat	e2x34.dat	e2x40a.dat	e2x40b.dat
e2x41.dat	e2x46d.dat	e2x68.dat	e2x69.dat	e2x70.dat	e2x9d.dat
e3x21d.dat	e3x30a.dat	e3x30b.dat	e3x31.dat	e3x6.dat	e4x11.dat
e4x12a.dat	e4x12b.dat	e4x12c.dat	e4x2a.dat	e4x2b.dat	e4x7b.dat
e6x18.dat	e6x19.dat	e6x20a.dat	e6x20b.dat	e7x19b.dat	e7x1b.dat
e7x1c.dat	e7x23.dat	e7x24a.dat	e7x24b.dat	e7x25.dat	e7x26.dat
e7x6b.dat	e8x12c.dat	e8x14f.dat	e8x18b.dat	e8x38a.dat	e8x38b.dat
e8x38c.dat	e8x39.dat	e8x40.dat	e8x41.dat	e8x42.dat	e8x43.dat
e8x44.dat					

Table E 1.0-2 Model Definition Option Cross Reference (Continued)

Table E 1.0-2 Model Definition Option Cross Reference (Continued)

fixed temperature					
e5x17a.dat	e5x17b.dat	e5x18a.dat	e5x18b.dat	e7x1b.dat	e7x1c.dat
fluid drag					
e6x20a.dat	e6x20b.dat				
foam					
e7x19b.dat	e7x23.dat				

Table E 1.0-2 Model Definition Option Cross Reference (Continued)

gap data					
e2x70.dat	e7x26.dat				
geometry					
e2x10c.dat	e2x34.dat	e2x40a.dat	e2x40b.dat	e2x41.dat	e2x46d.dat
e2x68.dat	e2x9d.dat	e3x21d.dat	e3x30a.dat	e3x30b.dat	e3x6.dat
e4x11.dat	e4x12a.dat	e4x12b.dat	e4x12c.dat	e4x2a.dat	e4x2b.dat
e4x7b.dat	e5x18a.dat	e5x18b.dat	e6x18.dat	e6x20a.dat	e6x20b.dat
e6x21.dat	e7x19b.dat	e8x12c.dat	e8x14f.dat	e8x18b.dat	e8x38a.dat
e8x38b.dat	e8x38c.dat	e8x39.dat	e8x41.dat	e8x44.dat	

Table E 1.0-2 Model Definition Option Cross Reference (Continued)

initial state
e2x41.dat

Table E 1.0-2 Model Definition Option Cross Reference (Continued)

initial temperature					
e2x46d.dat	e5x17a.dat	e5x17b.dat	e5x18a.dat	e5x18b.dat	e7x1b.dat
e7x1c.dat					
initial velocity					
e6x19.dat					
isotropic					
e2x10c.dat	e2x12d.dat	e2x12e.dat	e2x34.dat	e2x40a.dat	e2x40b.dat
e2x41.dat	e2x46d.dat	e2x68.dat	e2x69.dat	e2x70.dat	e2x9d.dat
e3x21d.dat	e3x30a.dat	e3x30b.dat	e3x31.dat	e3x6.dat	e4x11.dat
e4x12a.dat	e4x12b.dat	e4x12c.dat	e4x2a.dat	e4x2b.dat	e4x7b.dat
e5x17a.dat	e5x17b.dat	e6x18.dat	e6x19.dat	e6x20a.dat	e6x20b.dat
e7x1b.dat	e7x1c.dat	e7x26.dat	e8x12c.dat	e8x14f.dat	e8x18b.dat
e8x38a.dat	e8x38b.dat	e8x38c.dat	e8x39.dat	e8x40.dat	e8x41.dat
e8x42.dat	e8x44.dat				

Table E 1.0-2 Model Definition Option Cross Reference (Continued)

Table E 1.0-2 Model Definition Option Cross Reference (Continued)

mooney					
e8x43.dat					
no print					
e2x40a.dat	e2x40b.dat	e2x41.dat	e2x68.dat	e3x31.dat	e3x6.dat
e4x11.dat	e5x17a.dat	e5x17b.dat	e5x18a.dat	e5x18b.dat	e7x1b.dat
e7x1c.dat	e7x20b.dat	e7x20c.dat	e7x23.dat	e8x12c.dat	e8x14f.dat
e8x18b.dat	e8x38a.dat	e8x38b.dat	e8x38c.dat	e8x40.dat	e8x42.dat
e8x43.dat	e8x44.dat				

Table E 1.0-2 Model Definition Option Cross Reference (Continued)

node fill					
e2x34.dat	e6x18.dat				
ogden					
e7x20b.dat	e7x20c.dat				
optimize					
e2x10c.dat	e2x34.dat	e2x40a.dat	e2x40b.dat	e2x41.dat	e2x46d.dat
e2x68.dat	e2x70.dat	e3x6.dat	e4x11.dat	e4x12a.dat	e4x12b.dat
e4x12c.dat	e5x18a.dat	e5x18b.dat	e6x21.dat	e7x20b.dat	e7x23.dat
e7x26.dat					

Table E 1.0-2 Model Definition Option Cross Reference (Continued)

orientation					
e2x41.dat	e5x18a.dat	e5x18b.dat	e7x24a.dat	e7x24b.dat	e7x25.dat
e7x6b.dat					
orthotropic					
e2x70.dat	e5x18a.dat	e5x18b.dat	e7x24a.dat	e7x24b.dat	e7x25.dat
point load					
e2x10c.dat	e2x68.dat	e2x70.dat	e4x11.dat	e4x12a.dat	e4x12b.dat
e4x12c.dat	e6x20a.dat	e6x20b.dat	e8x39.dat	e8x40.dat	
point temperature					
e2x46d.dat					

Table E 1.0-2 Model Definition Option Cross Reference (Continued)

post					
e2x10c.dat	e2x12d.dat	e2x12e.dat	e2x34.dat	e2x40a.dat	e2x40b.dat
e2x41.dat	e2x46d.dat	e2x68.dat	e2x69.dat	e2x70.dat	e2x9d.dat
e3x21d.dat	e3x30a.dat	e3x30b.dat	e3x31.dat	e3x6.dat	e4x11.dat
e4x12a.dat	e4x12b.dat	e4x12c.dat	e4x2a.dat	e4x2b.dat	e4x7b.dat
e5x17a.dat	e5x17b.dat	e5x18a.dat	e5x18b.dat	e6x18.dat	e6x19.dat
e6x20a.dat	e6x20b.dat	e6x21.dat	e7x19b.dat	e7x1b.dat	e7x1c.dat
e7x20b.dat	e7x20c.dat	e7x23.dat	e7x25.dat	e7x26.dat	e7x6b.dat
e8x12c.dat	e8x14f.dat	e8x18b.dat	e8x38a.dat	e8x38b.dat	e8x38c.dat
e8x39.dat	e8x40.dat	e8x41.dat	e8x42.dat	e8x43.dat	e8x44.dat

Table E 1.0-2 Model Definition Option Cross Reference (Continued)

Table E 1.0-2 Model Definition Option Cross Reference (Continued)

print choice					
e3x21d.dat	e3x30a.dat	e3x30b.dat	e4x2a.dat	e4x2b.dat	e4x7b.dat
e7x19b.dat					
print element					
e2x46d.dat	e2x69.dat	e2x70.dat	e6x19.dat	e7x24a.dat	e7x24b.dat
e7x6b.dat	e8x39.dat				
print node					
e2x46d.dat	e2x70.dat	e6x19.dat	e8x39.dat		

Table E 1.0-2 Model Definition Option Cross Reference (Continued)

restart	
e8x42.dat	e8x44.dat

restart last
e3x31.dat

Table E 1.0-2 Model Definition Option Cross Reference (Continued)

solver					
e2x12e.dat	e2x40a.dat	e2x40b.dat	e2x41.dat	e2x46d.dat	e2x68.dat
e3x6.dat	e4x11.dat	e4x12a.dat	e4x12b.dat	e4x12c.dat	e5x18a.dat
e5x18b.dat	e6x21.dat	e7x23.dat	e8x38b.dat	e8x38c.dat	e8x40.dat
e8x42.dat					
surface					
e2x9d.dat	e7x20c.dat	e8x40.dat	e8x42.dat		

Table E 1.0-2 Model Definition Option Cross Reference (Continued)

tying
e2x70.dat e7x19b.dat e7x25.dat
udump
e3x21d.dat
ufconn
e2x34.dat

Table E 1.0-2 Model Definition Option Cross Reference (Continued)

velocity	
e5x17a.dat	e5x17b.dat

Table E 1.0-2 Model Definition Option Cross Reference (Continued)

work hard					
e3x21d.dat	e3x30a.dat	e3x30b.dat	e8x18b.dat	e8x38a.dat	e8x38b.dat
e8x38c.dat	e8x44.dat				

Table E 1.0-3 Load Incrementation Option Cross Reference

auto increment					
e3x6.dat	e4x7b.dat	e8x39.dat			
auto load					
e2x70.dat	e3x21d.dat	e3x30a.dat	e3x30b.dat	e3x31.dat	e4x11.dat
e4x12a.dat	e4x12b.dat	e4x12c.dat	e4x2a.dat	e4x2b.dat	e6x21.dat
e7x19b.dat	e7x1b.dat	e7x1c.dat	e7x20b.dat	e7x20c.dat	e7x23.dat
e7x25.dat	e8x12c.dat	e8x14f.dat	e8x18b.dat	e8x38a.dat	e8x38b.dat
e8x38c.dat	e8x42.dat	e8x43.dat	e8x44.dat		

Table E 1.0-3 Load Incrementation Option Cross Reference (Continued)

buckle					
e4x12a.dat	e4x12b.dat				
change state					
e2x70.dat					
contact table					
e8x44.dat					
continue					
e2x70.dat	e3x21d.dat	e3x30a.dat	e3x30b.dat	e3x31.dat	e3x6.dat
e4x11.dat	e4x12a.dat	e4x12b.dat	e4x12c.dat	e4x2a.dat	e4x2b.dat
e4x7b.dat	e5x17a.dat	e5x17b.dat	e5x18a.dat	e5x18b.dat	e6x18.dat
e6x19.dat	e6x20b.dat	e6x21.dat	e7x19b.dat	e7x1b.dat	e7x1c.dat
e7x20b.dat	e7x20c.dat	e7x23.dat	e7x25.dat	e7x26.dat	e8x12c.dat
e8x14f.dat	e8x18b.dat	e8x38a.dat	e8x38b.dat	e8x38c.dat	e8x39.dat
e8x42.dat	e8x43.dat	e8x44.dat			
control					
e3x6.dat	e4x11.dat	e5x18a.dat	e5x18b.dat	e6x21.dat	e8x43.dat
e8x44.dat					

Table E 1.0-3 Load Incrementation Option Cross Reference (Continued)

disp change					
e3x31.dat	e6x21.dat	e7x19b.dat	e8x43.dat		
dist fluxes					
e5x18a.dat	e5x18b.dat				
dist loads					
e3x31.dat	e3x6.dat	e4x2a.dat	e4x2b.dat	e6x21.dat	e7x20b.dat
e7x26.dat	e8x42.dat	e8x43.dat			
dynamic change					
e6x19.dat	e6x20b.dat				

Table E 1.0-3 Load Incrementation Option Cross Reference (Continued)

modal shape					
e6x18.dat	e6x21.dat				
motion change					
e3x30a.dat	e3x30b.dat	e7x20b.dat	e7x20c.dat	e8x18b.dat	e8x42.dat
e8x44.dat					
no print					
e3x31.dat	e7x25.dat				
point load					
e2x70.dat	e4x11.dat	e4x12a.dat	e4x12b.dat	e4x12c.dat	e4x7b.dat
e6x20b.dat	e7x25.dat	e8x39.dat			
post increment					
e3x31.dat	e7x25.dat				
print elem					
e7x25.dat					

Table E 1.0-3 Load Incrementation Option Cross Reference (Continued)

proportional increment		
e2x70.dat	e3x21d.dat	e7x25.dat
recover		
e6x18.dat	e6x21.dat	
release		
e8x44.dat		
spectrum		
e6x18.dat		
steady state		
e5x18a.dat		

Table E 1.0-3 Load Incrementation Option Cross Reference (Continued)

temp change					
e5x18a.dat	e5x18b.dat				
time step					
e3x30a.dat	e3x30b.dat	e3x31.dat	e4x11.dat	e6x21.dat	e7x1b.dat
e7x1c.dat	e7x20b.dat	e7x20c.dat	e7x23.dat	e8x12c.dat	e8x14f.dat
e8x18b.dat	e8x38a.dat	e8x38b.dat	e8x38c.dat	e8x42.dat	e8x43.dat
e8x44.dat					
transient					
e5x17a.dat	e5x17b.dat	e5x18b.dat			

Table E 1.0-7 User Subroutine Cross Reference

anelas				
u2x45.f	u2x50.f	u2x53.f	u3x8.f	u8x8.f
ankond				
u5x7a.f				
anplas				
u3x6.f				
crede				
u2x46a.f	u2x46b.f	u2x46c.f	u2x51a.f	u3x13f
crplaw				
u3x12.f	u3x22c.f	u3x24.f		
film				
u3x22a.f	u5x5.f	u5x6.f	u5x8.f	u5x13.f	u5x14.f
flow				
u5x14.f				
flux				
u5x8.f				
forcdt				
u3x26.f	u5x2.f	u7x17.f	u8x26.f	
forcem				
u2x35.f	u2x43.f	u2x46.f		

Table E 1.0-7 User Subroutine Cross Reference (Continued)

gapu					
u2x70					
hooklw					
u8x8.f					
impd					
u3x3.f	u3x3b.f	u3x19.f	u3x19b.f	u3x19c.f	u3x21a.f
u3x21c.f	u2x21d.f	u4x7.f	u8x15b.f		
motion					
u8x16.f	u8x19.f				
orient					
u2x50.f	u2x50b.f	u2.53.f			
plotv					
u2x26.f	u2x26b.f	u2x26c.f	u2x26d.f		
rebar					
u2x14.f	u2x37.f	u2x38.f	u2x39.f	u8x6.f	
sstran					
u8x1.f					
ubeam					
u8x10.f					
ubear					
u7x16.f					

Table E 1.0-7 User Subroutine Cross Reference (Continued)

ufconn					
u2x20.f	u2x27.f	u2x34.f	u2x46a.f	u2x46b.f	u7x15.f
uforms					
u2x4.f	u2x43.f				
ufour					
u7x8c.f	u7x9b.f				
ufxord					
u2x16.f	u2x17.f	u2x18.f	u2x19.f	u2x20.f	u2x55.f
u2x56.f	u3x5.f	u3x16.f	u3x17.f	u3x23.f	u3x27.f
u4x1.f	u4x5.f	u4x7.f	u6x3.f	u7x3.f	u7x15.f
ugroov					
u7x15.f					
uinstr					
u2x38.f	u3x30a.f				
ushell					
u2x40b.f					
ussd					
u6x18.f					
uthick					
u7x15.f	u7x16.f				
utrans					
u2x62.f					

Table E 1.0-7 User Subroutine Cross Reference (Continued)

uveloc
u7.15.f

vswell
u3x13.f

wkslp					
u3x5.f	u3x8.f	u3x30a.f	u3x30b.f	u8x2.f	u8x18.f

Volume E
Demonstration Problems

Chapter 2
Linear Analysis

Chapter 2 Linear Analysis

The MARC program allows the user to perform an elastic analysis using any element in the program. Problems in this chapter deal only with linear, elastic stress analysis and are designed to guide the user through various input options. The problems demonstrate the use of different elements such as plane stress, plane strain, generalized plane strain, axisymmetric, truss, beam, membrane, plate, shell and three-dimensional solids. They also illustrate the selection of isotropic or anisotropic elastic behavior. The options demonstrated are outlined below. For further details, see *Volume C, User Input*.

Mesh generation

- MESH2D
- MESH3D
- Incremental
- FXORD
- User subroutine UFXORD
- User subroutine UFCONN

Kinematic constraints

- Fixed Displacement
- Tying
- Servolinks
- Springs
- Elastic foundations
- Transformations

Loads

- Point loads
- Distributed loads
- Centrifugal loads
- Thermal loads
- Initial stress

Controls

- J-Integral
- Sorting
- Print choices
- Restart
- Case combination

Table E 2.0-1 shows MARC elements and options used in these demonstration problems. It should be pointed out that any example shown here can be considered as the first step in the solution of a nonlinear problem. Extensions to more complex solutions are accomplished by addition of further options using the keyword selection for those options as illustrated in the examples in later chapters.

Table E 2.0-1 Linear Analysis Demonstration Problems

Problem Number (E)	Element Type(s)	Parameter Options	Model Definition	Load Incrementation	User Subroutines	Problem Description
2.1	1	—	—	—	—	Hemisphere under internal pressure.
2.2	2 126 129	—	TRANSFORMATION	—	—	Thick sphere under internal pressure.
2.3	1 2	TRANSFORM	TRANSFORMATION TYING	—	—	Axisymmetric solid/axisymmetric shell intersection.
2.4	10 15	—	TRANSFORMATION TYING	—	UFORMS	Axisymmetric solid/axisymmetric shell intersection.
2.5	5	—	—	—	—	Doubly cantilevered beam.
2.6	13	BEAM SECT	—	-	—	Doubly cantilevered beam, open section.
2.7	14	BEAM SECT	—	—	—	Doubly cantilevered beam, closed section.
2.8	16	—	—	—	—	Curved beam, point load.
2.9	26 124	—	OPTIMIZE	—	—	Plate with circular hole.
2.10	3 114	—	—	—	—	Plane stress disk, diametrically opposing point loads.
2.11	8	SHELL SECT	FXORD	—	—	Square plate by shell elements.
2.12	7 117	PROCESSOR	SOLVER	—	—	3-dimensional plate by 8-node brick elements.
2.13	21	—	—	—	—	3-dimensional plate by 20-node brick elements.

Table E 2.0-1 Linear Analysis Demonstration Problems (Continued)

Problem Number (E)	Element Type(s)	Parameter Options	Model Definition	Load Incrementation	User Subroutines	Problem Description
2.14	21 23	PROCESSOR	—	—	REBAR	3-dimensional cantilever beam, reinforced with rebar, brick elements.
2.15	8	SHELL SECT	TYING FXORD	—	—	Cylinder-sphere intersection, tying type 18.
2.16	8	—	OPTIMIZE	—	UFXORD	Shell roof, element type 8.
2.17	4	—	—	—	UFXORD	Shell roof, element type 4.
2.18	22	—	—	—	UFXORD	Shell roof, element type 22.
2.19	24	—	—	—	UFXORD	Shell roof, element type 24.
2.20	17	—	—	—	—	Pipe band, in-plane, half section.
2.21	52	—	—	—	—	Doubly cantilevered beam, elastic.
2.22	27	J-INT	J-INT	—	—	Double edge notched specimen linear elastic fracture mechanics.
2.23	6	—	TRANSFORMATION	—	—	Thick cylinder under internal pressure.
2.24	9	—	—	—	—	20-bar, 3-dimensional truss.
2.25	11 115	—	CONN GENER NODE FILL	—	—	Strip, bonded edges, υ = .3.
2.26	11 118 125 128	—	—	—	PLOTV	Strip, bonded edges, υ = .4999, constant dilatation.
2.27	19	ELSTO	—	—	UFCONN	Generalized plane strain disk, diametrically opposing point loads.

Table E 2.0-1 Linear Analysis Demonstration Problems (Continued)

Problem Number (E)	Element Type(s)	Parameter Options	Model Definition	Load Incrementation	User Subroutines	Problem Description
2.28	20	—	TYING	—	—	Twist and tension circular bar with varying thickness.
2.29	25	—	FOUNDATION	—	—	Beam in linear elastic foundation with point load.
2.30	28	ELSTO ALIAS	J-INTEGRAL	—	—	Cylindrical notched bar in tension.
2.31	29	SCALE	OPTIMIZE	—	UFCONN	Square plate with round hole, internal pressure, generalized plane strain.
2.32	32	SCALE ALIAS	OPTIMIZE	—	—	Square plate with round hole, internal pressure, generalized plane strain, υ = .5. Mesh as in E 2.31.
2.33	33	CENT LOAD	CONN GENER NODE FILL ROTATION A STIFF SCALE	—	—	Flat spinning disk, υ = .4999.
2.34	34	—	CONN FILL NODE FILL CONN GENER QUALIFY OPTIMIZE	—	—	Bar compressed sideways generalized plane strain.
2.35	35	ELASTIC RESTART	CASE COMBIN	—	FORCEM	Square block, 1/8 model 8 elements, υ = .4999 load case 1: compression; load case 2: bending, combined.
2.36	45	—	FOUNDATION	—	—	Timoshenko beam on elastic foundation.

Table E 2.0-1 Linear Analysis Demonstration Problems (Continued)

Problem Number (E)	Element Type(s)	Parameter Options	Model Definition	Load Incrementation	User Subroutines	Problem Description
2.37	27 46	—	—	—	REBAR	Reinforced cantilever beam.
2.38	29 47	SCALE ISTRESS	OPTIMIZE UFCONN	PROPORTIONAL	REBAR UFCONN UINSTR	Reinforced square plate with round hole, generalized plane strain. Prestressed reinforcement.
2.39	28 48	—	—	—	REBAR	Circular cylinder with reinforcement.
2.40	49	SHELL SECT	—	—	—	Flat square plate, varying thickness, simply supported pressure load.
2.41	50	SHELL SECT	CONN GENER TYING NODE FILL	—	—	Tubular beam with square cross-section cantilevered self weight.
2.42	22	SHELL SECT	FOUNDATION	—	—	Square plate on elastic foundation point load, free edges 1/4 model.
2.43	53 64	—	TYING CONN GENER NODE FILL	—	FORCEM UFORMS	I-beam modeled with plane stress and line elements cantilever, moment load.
2.44	54	—	TYING	—	—	Local load on half-space. Mesh refinement tying.
2.45	55	ANISOTROPIC J-INT	OPTIMIZE J-INTEGRAL	—	ANELAS	Axisymmetric notched bar, anisotropic in longitudinal direction.
2.46	29 56	THERMAL	THERMAL LOADS UFCONN	—	CREDE UFCONN	Square plate with hole, thermal gradient towards outer edge.
2.47	57	TRANSFORM TIE	TRANSFORMATION TYING MESH 3D	—	—	Section of cylinder with uniform internal pressure. TYING to enforce axisymmetric solution.

Table E 2.0-1 Linear Analysis Demonstration Problems (Continued)

Problem Number (E)	Element Type(s)	Parameter Options	Model Definition	Load Incrementation	User Subroutines	Problem Description
2.48	58	—	NODE CIRCLE CONN GENER ROTATION A	—	—	Plane straining with diametrically opposing load (1/2 model).
2.49	59	THERMAL	NODE CIRCLE CONN GENER	—	CREDE	Hollow sphere, spinning gradient across wall thickness.
2.50	60	ANISOTROPIC	NODE CIRCLE	—	ANELAS ORIENT	Generalized plane strain ring with diametrically opposing point loads, circular anisotropy.
2.51	61	THERMAL ELASTIC RESTART	CASE COMBIN	—	CREDE	Square block 1/8 model 8 elements υ = .4999 load case 1: thermal gradient; load case 2: compression, combined.
2.52	66	—	TYING OPTIMIZE	—	—	Twist and tension of a circular bar with varying cross-section, υ = .4999
2.53	67	—	TYING	—	ANELAS ORIENT	Cylinder with helical anisotropy under internal pressure.
2.54	9 68	—	SPRINGS	—	—	Truss cube with shear panels, supported by springs.
2.55	72	SHELL SECT	UFXORD	—	UFXORD	Shell roof, element type 72.
2.56	72	SHELL SECT	UFXORD	—	UFXORD	Cylinder-sphere intersection, element type 72, no tying.
2.57	76 78	BEAM SECT	POINT LOAD	—	—	Cantilever beam, under point load.
2.58	77 79	BEAM SECT	POINT LOAD	—	—	Double cantilever beam under point load.

Table E 2.0-1 Linear Analysis Demonstration Problems (Continued)

Problem Number (E)	Element Type(s)	Parameter Options	Model Definition	Load Incrementation	User Subroutines	Problem Description
2.59	98	BEAM SECT	POINT LOAD	—	—	Cantilever beam under point load.
2.60	11 91 27 93	—	MESH2D MANY TYPES	DIST LOADS	—	Uniform load in a cavity using semi-infinite elements.
2.61	10 92 28 94	—	MESH2D	POINT LOAD POST	—	Point load on a semi-infinite body.
2.62	18	—	UTRANFORM DIST LOADS POST	—	UTRANS	Truncated spherical shell.
2.63	27	—	LORENZI DIST LOADS	CONTINUE POINT LOADS	—	Double edge notch specimen, DeLorenzi method used.
2.64	7	ELASTIC	FIXED DISP DIST LOADS	POINT LOADS	—	Bending on a plate, assumed strain elements used.
2.65	7 75	LARGE DISP	FIXED DISP	AUTO LOAD POINT LOAD	—	Rigid tying test.
2.66	31	BEAM SECT	CONN GENER POINT LOAD NODE FILL	—	—	Bending of a beam.
	31	—	ISOTROPIC	POINT LOAD DIST LOAD	—	Bending of an elbow.
2.67	127 130 21	—	POINT LOAD	—	—	Cantilever beam.
2.68	49	—	POINT LOAD	—	—	Spherical shell under Point Loads.
2.69	95	SHELL SECT	DIST LOAD	—	—	Pipe subjected to bending.
2.70	95 97	—	---	—	—	Flange joint between pressurized pipes.

E 2.68 Linear Analysis of a Hemispherical Cap Loaded by Point Loads

A hemispherical cap with an 18° hole is loaded by two inward and two outward forces (see Figure E 2.68-1).

Elements (Ref. B49.1)

Library element type 49, a 6-node triangular thin shell element, is used.

Model

The dimensions of the cap and the finite element mesh are shown in Figure E 2.68-1. Based on symmetry considerations, only one quarter of the cap is modeled. The mesh is composed of 128 elements and 289 nodes.

Material Properties

The material is elastic with a Young' modulus of 6.835×10^7 N/mm^2 and a Poisson's ratio of 0.3.

Geometry

A uniform thickness of 0.04 mm is assumed. In the thickness direction, three layers are chosen using the SHELL SECT parameter option. Notice that for this problem, which is dominated by nearly inextensional bending, the initial curvature of the elements is important. This means that the default setting for the fifth geometry field must be used.

Loading

The loading consists of 2 inward and 2 outward point loads with a magnitude of 20 N.

Boundary Conditions

Symmetry conditions are imposed on the edges $x = 0$ ($u_x = 0, \varphi = 0$) and $y = 0$ ($u_y = 0, \varphi = 0$). Notice that the rotation constraints only apply for the midside nodes. To suppress the remaining rigid body motion for node 278, the z-displacement is fixed.

Results

The reference solution for the displacements of the points of application of the load is 0.93 (see e.g., J. C. Simo, D. D. Fox, and M. S. Rifai, "On a stress resultant geometrically exact shell model, Part II: The linear theory: computational aspects", *Comp. Meth. Appl. Mech. Eng.*, 79, 21-20, 1990). The results found by MARC (0.93027 for the inward displacement and 0.02708 for the outward displacement) are in close agreement with the reference solution. Finally Figure E 2.68-2 shows the equivalent von Mises stress for layer 1.

Summary of Options Used

Listed below are the options used in example e2x68.dat:

Parameter Options

ELEMENTS
END
SHELL SECT
SIZING
TITLE

Model Definition Options

CONNECTIVITY
COORDINATE
END OPTION
FIXED DISP
GEOMETRY
ISOTROPIC
NO PRINT
OPTIMIZE
POINT LOAD
POST
SOLVER

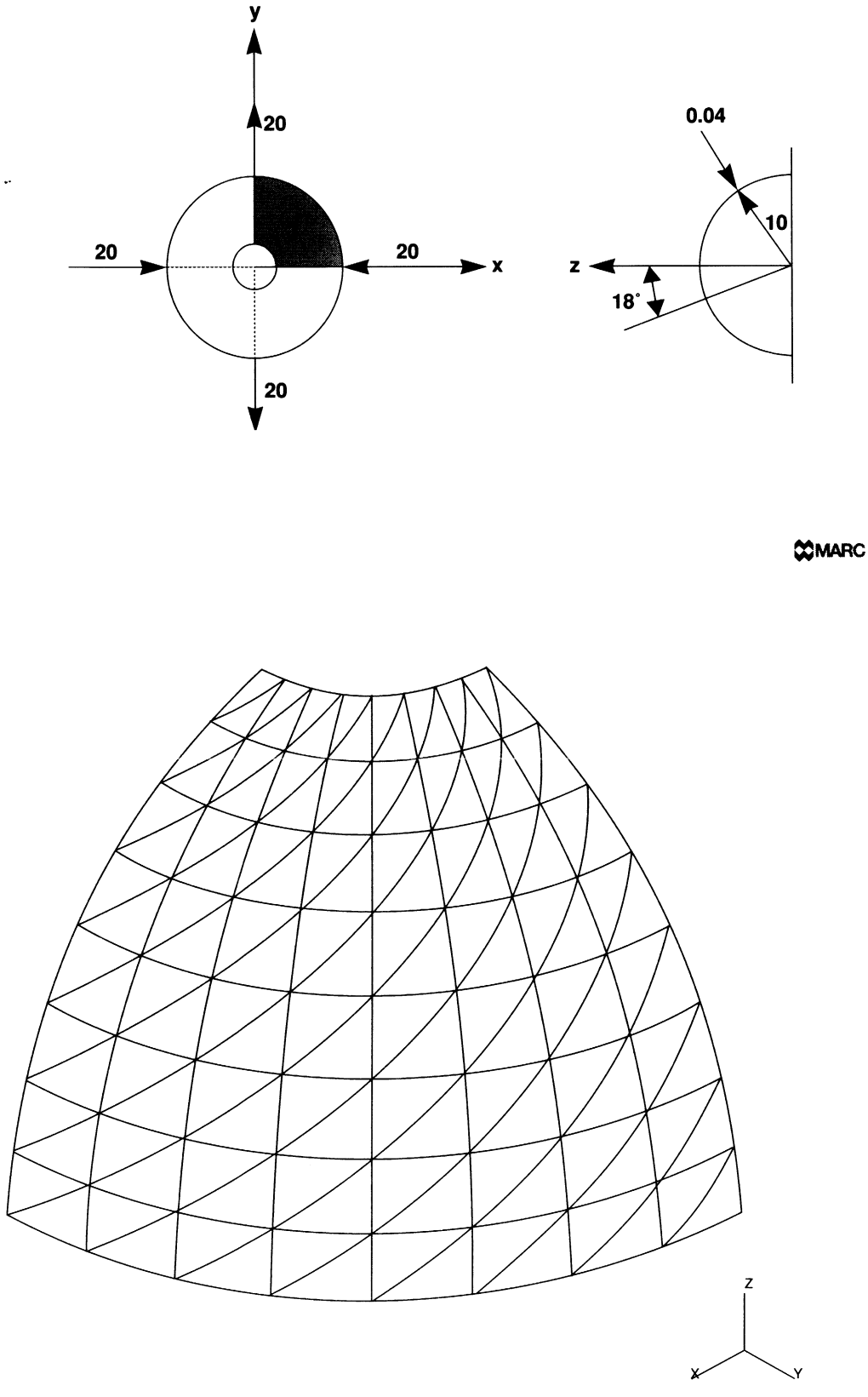

Figure E 2.68-1 Hemispherical Cap, Geometry, Loading, and Finite Element Mesh

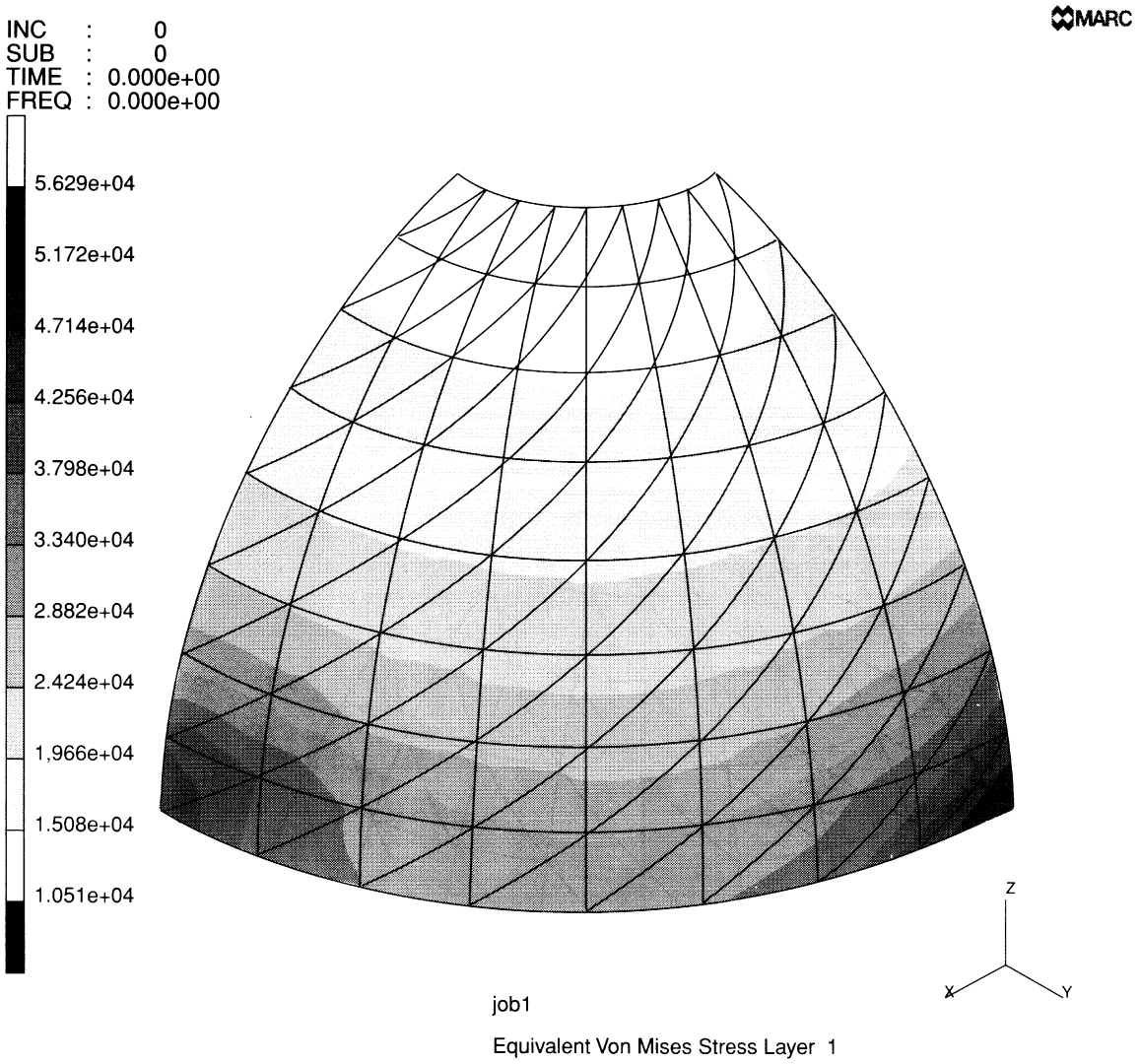

Figure E 2.68-2 Stress Contours Layer 2 (Equivalent von Mises Stress)

E 2.69 Pipe Bend with Axisymmetric Element 95

This problem demonstrates the use of the axisymmetric element with bending (element 95) to model the flexure of a straight pipe. Units [N, mm].

The quadrilateral element 95 represents the cross-section of a ring in the r,z symmetry plane at $\theta = 0°$. A pure axisymmetric deformation induces displacements u,v in the z,r plane which remain constant for θ ranging from 0° to 360° degrees. A flexural deformation in the z,r plane induces different displacements u,v at the opposite sections; $\theta = 0°$ and $\theta = 180°$ along the ring. A twist in the ring induces a circumferential displacement w, equal at every θ, and assigned to the position $\theta = 90$.

Elements (Ref. B95.1)

Thus, five degrees of freedom are associated to each node:

u,v displacements, at 0° and 180°, respectively
w circumferential displacement at 90° angle

Element 95 is integrated numerically in the circumferential direction. The number of integration points (odd number) is given on the SHELL SECT parameter option. The points are equidistant on the half circumference. See Figure E 2.69-1.

Models

The FEM model represents the longitudinal section of the pipe in the z,r plane (x,y plane for Mentat) is shown in Figure E 2.69-2. The FEM mesh consists of 80 type 95 elements for a total of 123 nodes as shown in Figure E 2.69-3.

Material Properties

The Young's modulus of the material is 2.0E5 N/mm^2; the Poisson's ratio is .3.

Loading

A distributed load, $P = 100\ N/mm^2$, is assigned at increment 1, at elements 79 and 80. The load acts as a pressure in the longitudinal direction and is distributed with a sinusoidal variation along θ between 0° and 180° and producing a bending moment around z; $M = \left(2 \cdot \left(P \cdot \frac{\pi}{2} \cdot t \cdot R\right) \cdot R\right) = 2 \cdot 1.57E5 \cdot 100 = 3.1416E7$ applied at the free edge of the beam. See Figure E 2.69-4.

Results

The analytic solution is compared with the MARC, element 95, solution in Table E 2.69-1.

Table E 2.69-1 Analytical Solution

	Analytic	MARC
$Y_{max} = \frac{Ml^2}{2EJ}$	0.624 mm	0.636 mm (Node 122)
$\sigma_{xx} = \frac{Mz}{J}$ $J = \frac{\pi}{4}(R_e^4 - R_i^4) = 3.149E7\ mm^4$	99.73 N/mm^2	100.5 N/mm^2 (Element 80, Node 122)

At increment 0, the y displacement difference is of the order of 1.9% while the stress σ_{xx} value difference is of the order of 0.7%.

Figure E 2.69-5 shows the distribution of the y deflection along the axis of the pipe and the deformed shape under flexural load.

NOTE: Only the deformed shape at 0° can be visualized with the Mentat graphics program even if all the elements variables can be visualized. The displacements and all the nodal quantities referring to 180° can be seen on the output file.

Summary of Options Used

Listed below are the options used in example e2x69.dat:

Parameter Options

ELEMENT
END
SHELL SECT
SIZING
TITLE

Model Definition Options

CONNECTIVITY
COORDINATE
DIST LOADS
END OPTION
FIXED DISP
ISOTROPIC
POST
PRINT ELEM

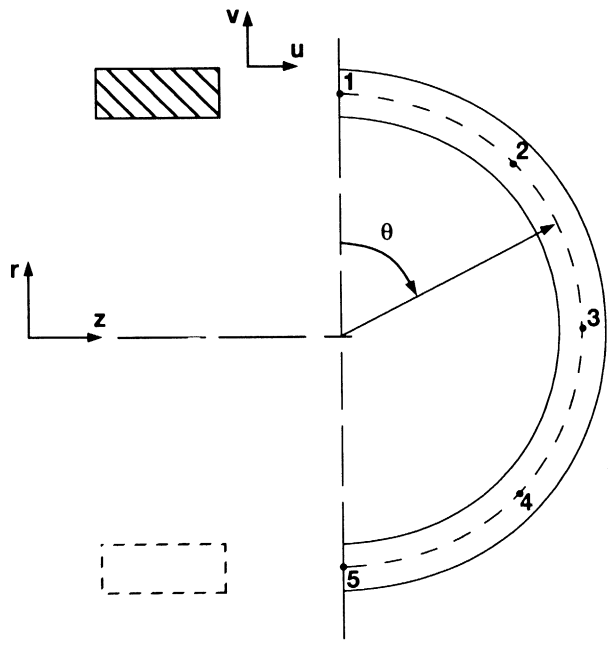

Figure E 2.69-1 Element 95 Layer Points

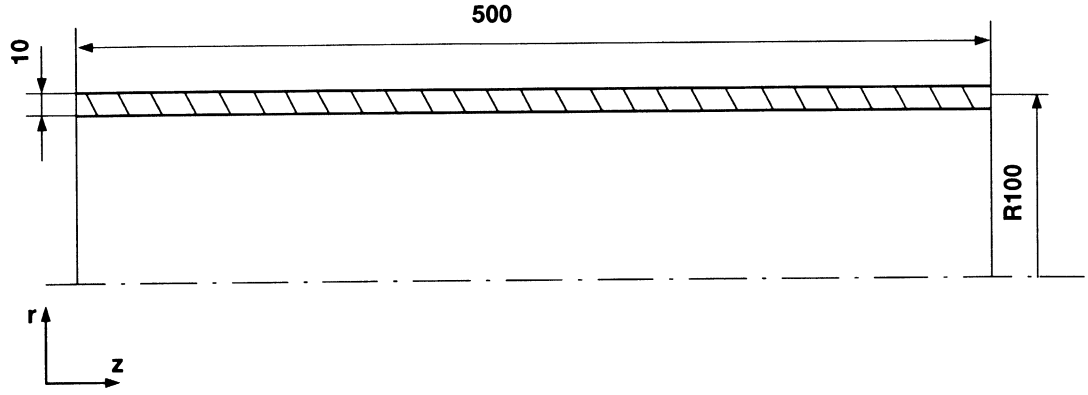

Figure E 2.69-2 Longitudinal Section of the Pipe

MARC

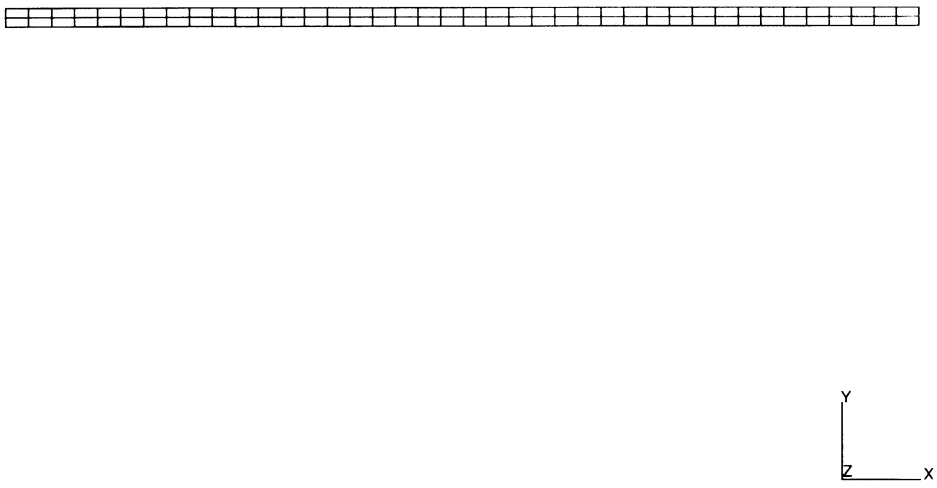

Figure E 2.69-3 FEM Model of the Longitudinal Section of the Pipe

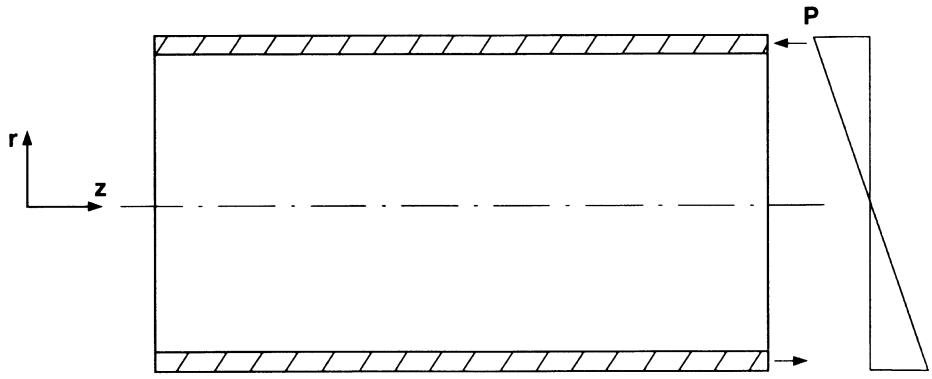

Figure E 2.69-4 Distribution of the Longitudinal Pressure

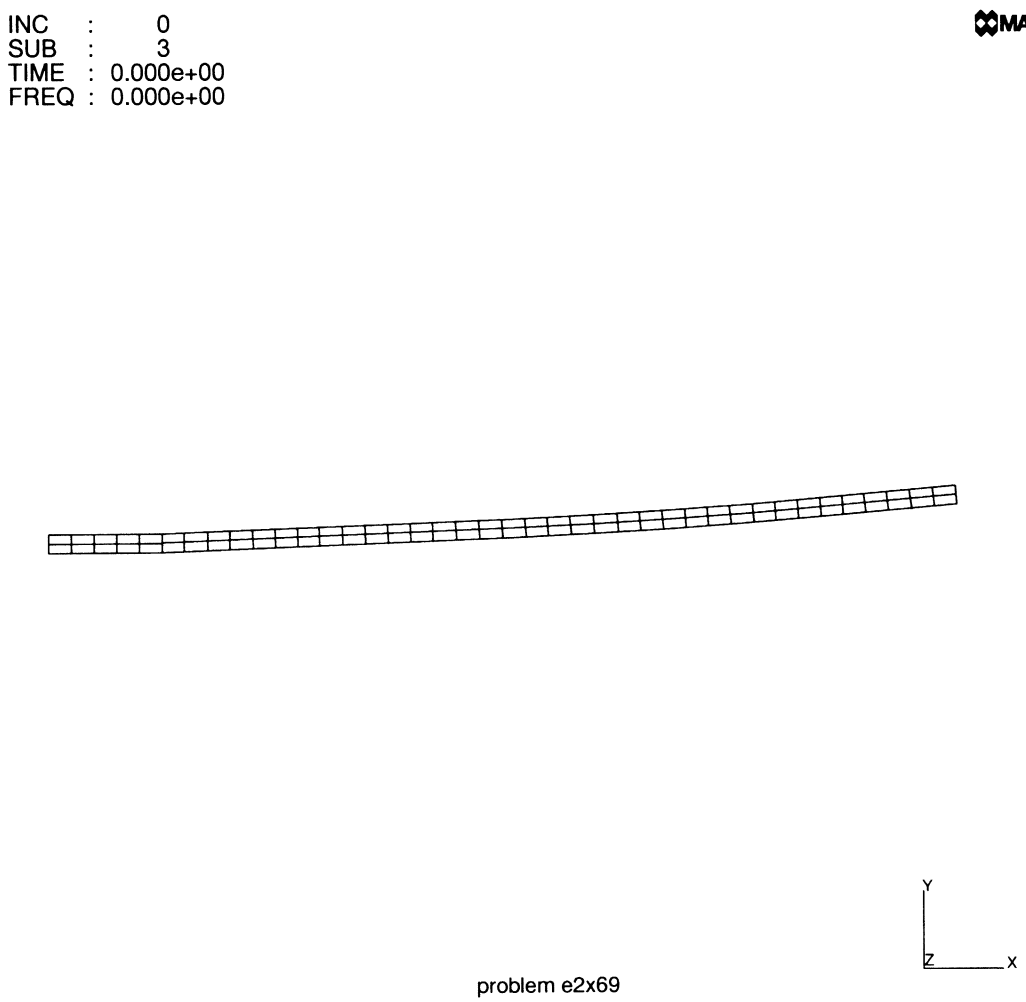

Figure E 2.69-5 Deflection of the Longitudinal Section of the Pipe

E 2.70 Flange Joint Between Pressurized Pipes

This problem demonstrates the capability of the axisymmetric elements 95 together with the axisymmetric gap element 97 to model a flange joint between pressurized pipes including the gasket. These elements may be used even if the loads are nonaxisymmetric as in the case of bending moment and shear applied to the cross-section of one of the pipes.

The model represents an actual joint (see Figure E 2.70-1). A square section cavity is filled with a thoroidal gasket. Under the gasket, a tooth of the right-hand flange penetrates into the left-hand flange. Units [N, m].

Object of the analysis is to compute:

Stresses on the flanges and pipes
Axial loads on each bolt
Value of the applied moment that opens the flanges (loss of pressure)

The quadrilateral element 95 represents the cross-section of a ring in the z,r symmetry plane at $\theta = 0°$. A pure axisymmetric deformation induces displacements u,v in the z,r plane. These remain constant for θ ranging from 0° to 360°. A flexural deformation in the z,r plane induces different displacements u,v at the opposite sections, $\theta = 0°$ and $\theta = 180°$, along the ring. A twist in the ring induces a circumferential displacement w, equal at every θ, and assigned to the position $\theta = 90°$.

The gap element 97 works in the flexural mode. Extra degrees of freedom have been added to account for independent contact and friction between the facing sides of element 95 (q = 0° - 180°).

Elements (Ref. B95.1, B97.1)

Element 95 had five degrees of freedom associated to each node:

u,v displacements at 0° and 180°, respectively.
w circumferential displace at 90° angle

Element 95 is integrated numerically in the circumferential direction. The number of integration points (odd number) is given in the SHELL SECT parameter option. The points are equidistant on the half circumference (see Figure E 2.70-1). Here seven integration points along the half circumference are chosen via the SHELL SECT parameter option.

Element 97 is a 4-node gap and friction link with double contact and friction (0° - 180°). It is designed to be used with element type 95.

Model

The FEM model represents the longitudinal section of the pipe joint in the z,r plane. The mesh consists of 613 elements type 95 and 18 elements type 97 for a total of 751 nodes. The mesh is shown in Figure E 2.70-1.

The 12 bolts are "smeared" into a ring of equivalent stiffness that is represented by the central strip in the shadowed area in Figure E 2.70-1. The remainder of the shaded area represents the "fill" in the section of the bolt.

Material Properties

The two pipes are made with the same material:

E (Young modulus) = 2.05 E11 N/m^2
ν (Poisson ratio) = 0.3

The 12 bolts are modeled with an equivalent axisymmetric ring having material properties:

E (Young modulus) = 2.702 E13 N/m^2
ν (Poisson ratio) = 0.3

The gasket material between bolts is modeled with a coarse mesh of elements type 95 having reduced properties:

E (Young modulus) = 9.04 E10 N/m^2
ν (Poisson ratio) = 0.3

For the bolts and the gasket, the moduli in the hoop direction are strongly reduced.

Loading

Bolts are pre-loaded with an axial force. This is modeled with a local reduction of temperature on the elements modeling the bolts. The bending moment applied to the pipe is assigned with a couple of point loads at the edge of the left pipe as shown in Figure E 2.70-2.

Tying

The bolts are connected with the external faces of flange with a tying that links all the degrees of freedom of the joined nodes as shown in Figure E 2.70-3.

Gap

The contact between the flanges is modeled with 18 gap elements placed as shown in Figure E 2.70-3. Friction is not taken into account. All closure distances are nil; therefore, all gaps are closed until a force greater than 100. N acts on the gap (tensile force). A gap with assigned stiffness represents the gasket.

Boundary Condition

The edge of the right pipe is clamped. Therefore, all degrees of freedom are prescribed to be zero on this edge (see Figure E 2.70-2).

Results

The results produced by the MARC program for the flange joint are shown in the following figures:

Figure E 2.70-3	The von Mises stress at 0° at increment 1 (pre-load)
Figure E 2.70-5	The von Mises stress at 0° at increment 19 (bending moment)

NOTE: Only the deformed shape at 0° can be visualized with the Mentat graphics program even if all the element variables can be visualized. The displacements and all the nodal quantities referring to 180 degrees can be read from the MARC output file.

In Table E 2.70-1, the balance of the bending moment M_z about the symmetry axis is checked by comparing the sum of all moments due to increments of compressive force in the gaps plus the increment of force in the bolts with the moment of the applied load.

Table E 2.70-1 Balance of Moments

Gap	Node 1	Node 2	INC = 1 Force [N]	INC = 19 Force [N]	Δ [N]	Distance [m]	M_z [N · m]
359	359	735	3653.	3651.	-2.	0.0235	-0.0470
360	358	734	2671.	2674.	3.	0.023875	0.0716
361	357	737	2313.	2319.	6.	0.02425	0.1455
362	356	738	2158.	2167.	9.	0.024625	0.2216
363	355	740	2029.	2041.	12.	0.025	0.3000
364	354	739	1871.	1886.	15.	0.025375	0.3806
365	353	751	836.	845.	9.	0.02575	0.2318
366	368	749	1243.	1228.	-15.	0.016	-0.24
367	367	750	1768.	1743.	-25.	0.016375	-0.4094
368	366	741	1788.	1761.	-27.	0.01675	-0.4523
369	365	742	2059.	2028.	-31.	0.017125	-0.5309
370	364	748	2821.	2782.	-39.	0.0175	-0.6825
371	230	747	-74.	0.	74.	0.00825	0.6105
372	228	746	45.	-99.	-144.	0.009375	-1.3500
373	223	744	375.	275.	-100.	0.0105	-1.0500
374	222	736	840.	751.	-89.	0.011625	-1.0346
375	219	745	1047.	997.	-50.	0.01275	-0.6375
376	349	743	760.	713.	-47.	0.014766	-0.6940
Σ			2.82E4		-441.		-5.1665
Bolt Stress [N/m^2]			4.3778E8	4.495E8	1.17E7 (x-1.288E-4/2)		
Bolt Force [N]					-753.	0.0205	-15.45
							-20.62
Applied Moment [N. m]				900 x 2 = 1800.		0.013875	24.98
							Δ% = 17%

Summary of Options Used

Listed below are the options used in example e2x70.dat:

Parameter Options

ALIAS
ELEMENT
END
PRINT
SETNAME
SHELL SECT
SIZING
TITLE

Model Definition Options

CONNECTIVITY
CONTROL
COORDINATE
DEFINE
END OPTION
FIXED DISP
GAP DATA
ISOTROPIC
OPTIMIZE
ORTHOTROPIC
POINT LOAD
POST
PRINT ELEM
PRINT NODE
TYING

Load Incrementation Options

AUTO LOAD
CHANGE STATE
CONTINUE
POINT LOAD
PROPORTIONAL INC

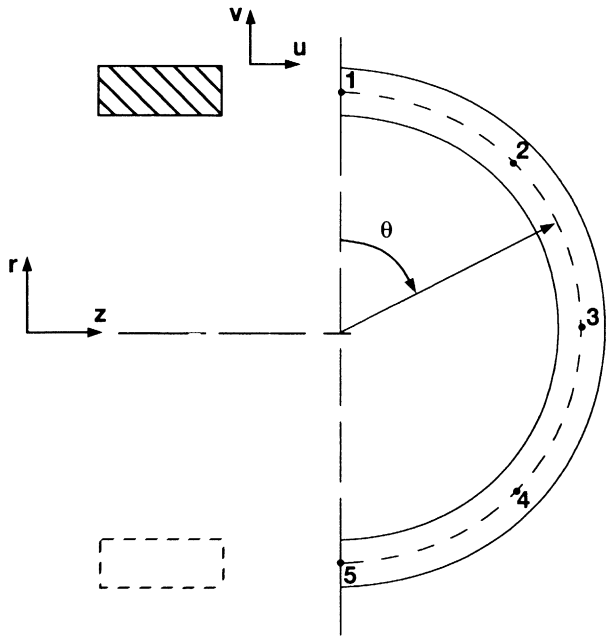

Figure E 2.70-1 Element 95 Layer Points

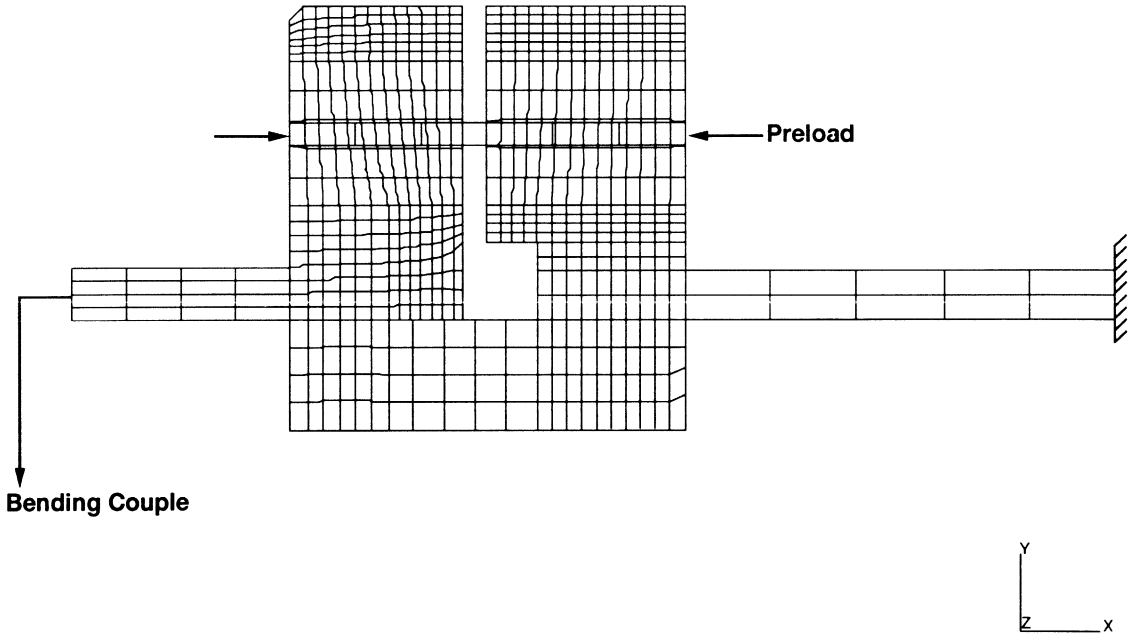

Figure E 2.70-2 Loads on the Flange Joint

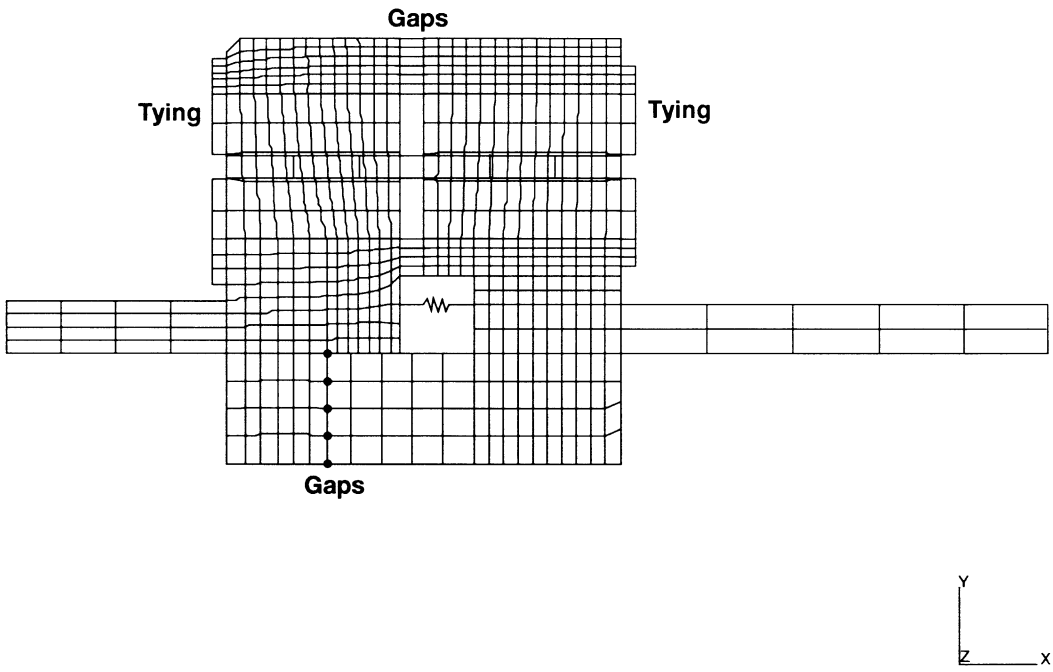

Figure E 2.70-3 Tying in the Flange Joint

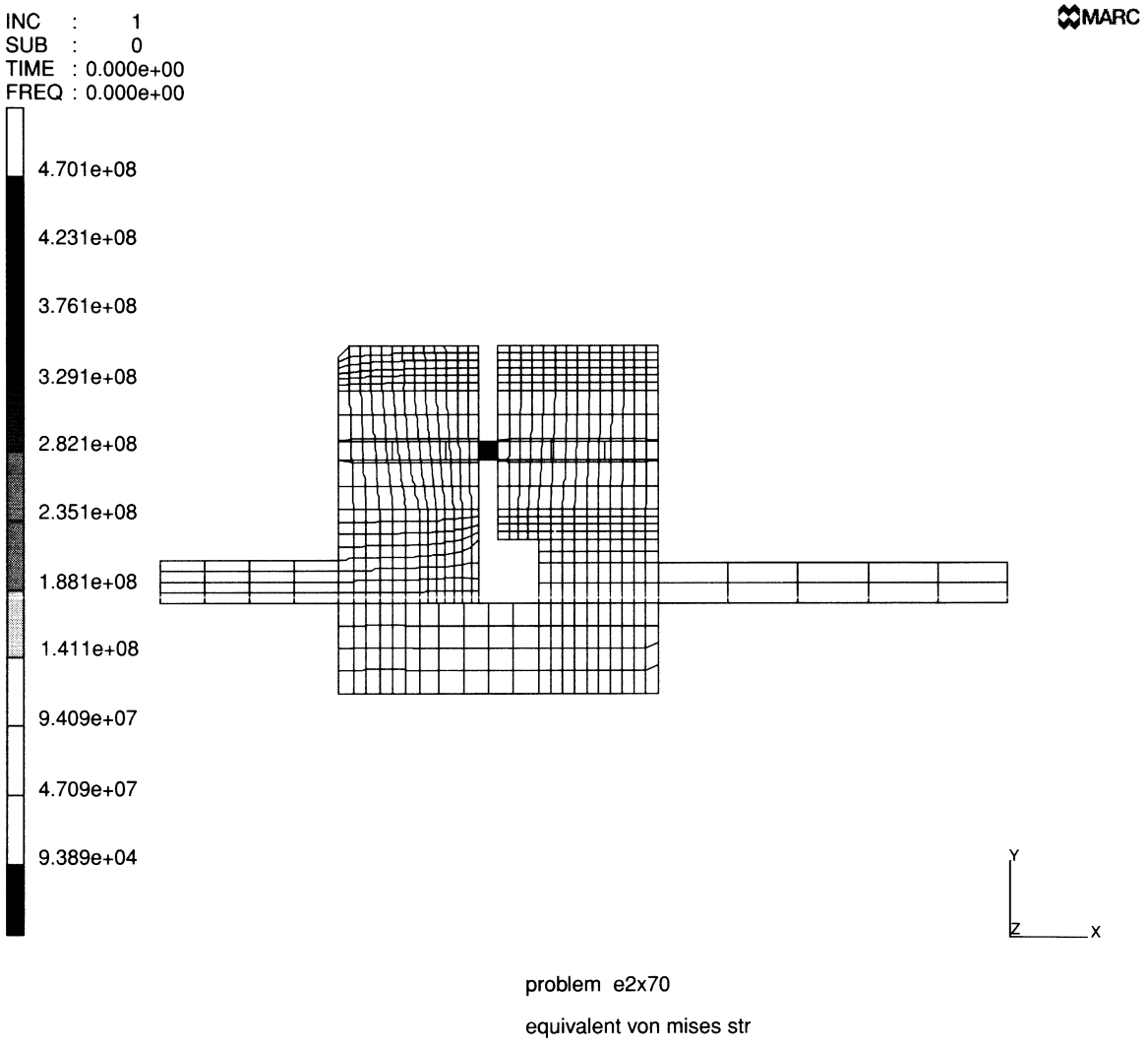

Figure E 2.70-4 von Mises Stress Induced by Preload

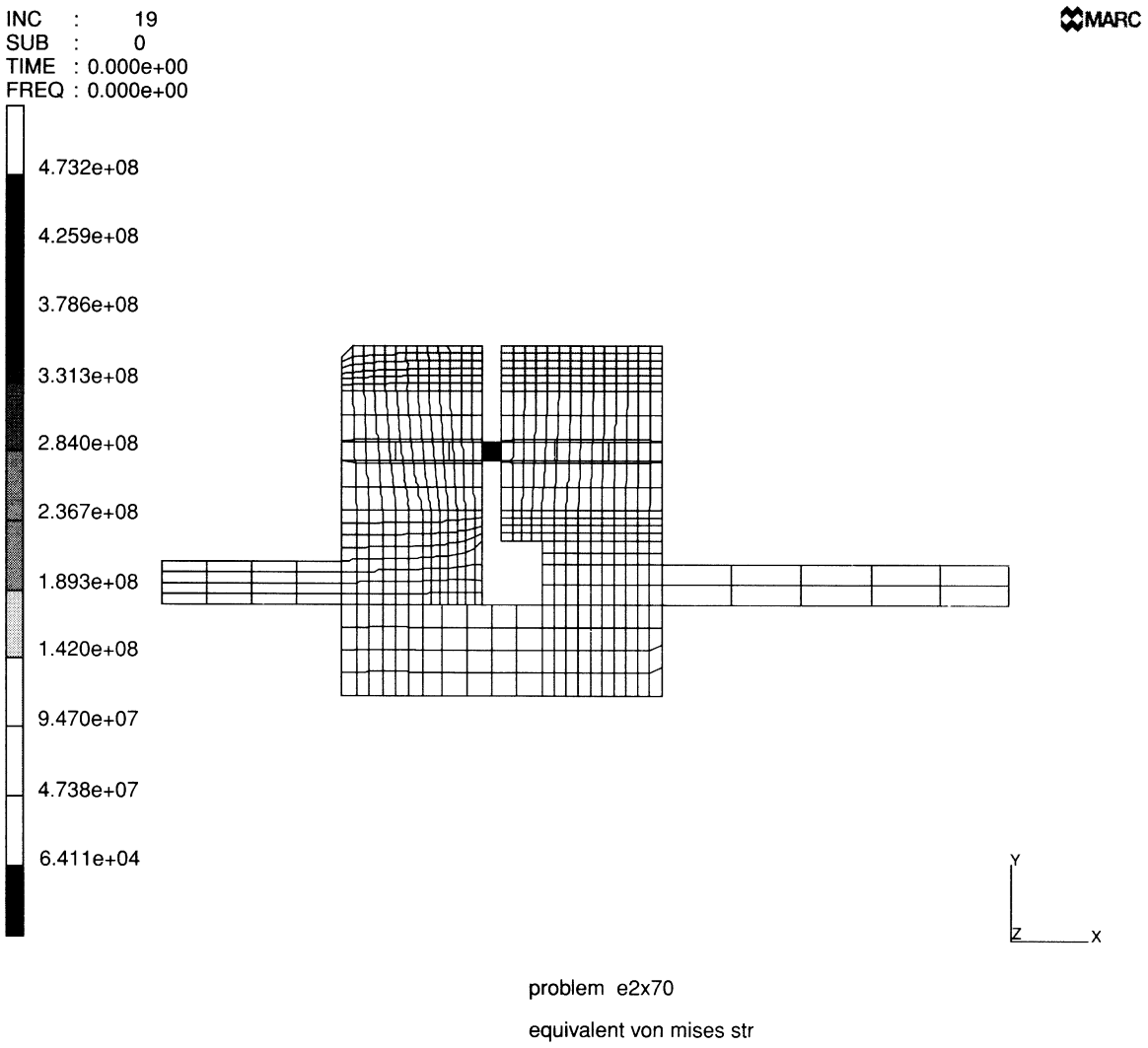

Figure E 2.70-5 von Mises Stress Induced by Moment

E 2.71 Spinning Cantilever Beam

This problem demonstrates the use of MARC element type 98 for the solution of spinning cantilever beam. The beam rotates at a constant angular velocity. The beam also has an initial velocity which induces Coriolis effect. The options ROTATION A and DIST LOADS are used for the input of Centrifugal load. INITIAL VEL option is used to input the initial velocity.

Elements (Ref. B98.1)

The element (Element 98) is a 2-node straight elastic beam in space and includes the transverse shear effects in its formulation.

Model

As shown in Figure E 2.71-1, the finite element mesh consists of five elements and six nodes. The span on the beam is five inches and the cross section of the beam is assumed to be a closed, thin, square section.

Geometry

The GEOMETRY block is used for entering the beam section properties. The section properties (area = 0.0369 inches^2, $I_x = I_y = 6.4693 \times 10^{-3}$ inches^4) are entered through the GEOMETRY block.

Material Properties

The material of the beam is assumed to have a Young's modulus of 3.0e+08 psi, Poisson's ratio of 0.3, and a mass density of 0.281 lb-seconds/inch^4.

Loading

The beam is subjected to Centrifugal loading (IBODY = 100) resulting from the rotation of the beam. With an angular velocity of 20 • radian/seconds ($\omega^2 = 400$) and the axis of rotation is the y axis. The beam has an initial velocity of 100 inches/second in the x-direction which induces Coriolis effect (IBODY = 103).

Boundary Condition

At node 1, all the degrees of freedom are constrained ($U_x = U_y = U_z = \theta_x = \theta_y = \theta_z = 0$).

Results

The deformation of the beam is given is Table E 2.71-1.

Table E 2.71-1 Beam Deflection (Inches)

Node	δ_x(x10^{-4}) (Due to Centrifugal Loading)	δ_y(x10^{-4}) (Due to Coriolis Effect)
1	0.	
2	1.305	1.61
3	2.385	5.022
4	3.203	9.422
5	3.722	14.241
6	3.903	19.135

Summary of Options Used

Listed below are the options used in example e2x71a.dat:

Parameter Options

ELEMENT
END
SIZING
TITLE

Model Definition Options

CONNECTIVITY
COORDINATE
DIST LOADS
END OPTION
FIXED DISP
GEOMETRY
ISOTROPIC
POST
ROTATION A

Listed below are the options used in example e2x71b.dat:

Parameter Options

ELEMENT
END
SIZING
TITLE

Model Definition Options

CONNECTIVITY
COORDINATE
DIST LOADS
END OPTION
FIXED DISP
GEOMETRY
ISOTROPIC
POST
ROTATION A
INITIAL VEL

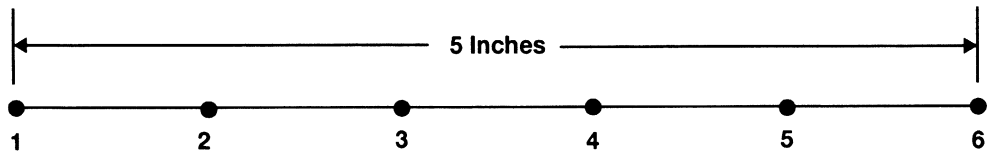

Figure E 2.71-1 Finite Element Model

Volume E
Demonstration Problems

Chapter 3
Plasticity and Creep

Chapter 3 Plasticity And Creep

The MARC program contains an extensive material library. A discussion on the use of these capabilities is found in *Volume A, User Information*. In this chapter, material nonlinearity often exhibited in metals will be demonstrated. Material nonlinearity associated with rubber or polymer materials may be found in Chapter 7. The capabilities demonstrated here may be summarized as:

Variable load paths

- Proportional loads
- Nonproportional loads

Choice of yield functions

- von Mises
- Drucker-Prager, Mohr-Coulomb
- Gurson
- Shima

Strain magnitude

- Infinitesimal plasticity
- Finite strain plasticity

Strain hardening

- Limit Analysis
- Isotropic hardening
- Kinematic hardening

Rate effects

- Deviatoric creep
- Volumetric swelling
- ORNL

Compiled in this chapter are a number of solved problems. Table E 3.0-1 summarizes the element type and options used in these demonstration problems.

Table E 3.0-1 Nonlinear Material Demonstration Problems

Problem Number (E)	Element Type	Parameter Options	Model Definition	Load Incrementation	User Subroutines	Problem Description
3.1	4	TIE SCALE SHELL TRAN SHELL SECT	WORK HARD CONTROL FXORD SHELL TRAN TYING, 2, 6, & 100	AUTO LOAD PROPORTIONAL	—	Combines tension and torsion of a thin-walled cylinder
3.2	67	SCALE	TYING, 1 & 3 WORK HARD CONTROL	AUTO LOAD PROPORTIONAL	—	Combines tension and torsion of a thick-walled cylinder.
3.3	11 115	SCALE	MESH2D CONTROL	AUTO LOAD PROPORTIONAL	IMPD	Limit load analysis of bar.
3.4	16	SCALE SHELL SECT	WORK HARD CONTROL	AUTO LOAD PROPORTIONAL	UFORMS	Bending of prismatic beam.
3.5	15	THERMAL SHELL SECT	UFXORD TRANSFORMATION THERMAL LOAD WORK HARD TEMPERATURE EFFECT CONTROL INITIAL STATE	AUTO THERM CHANGE STATE	WKSLP UFXORD	Hemispherical shell under thermal expansion.
3.6	50	SCALE SHELL SECT	DEFINE CONTROL	AUTO LOAD PROPORTIONAL	ANPLAS	Bending of square plate, simple supported, pressure load.
3.7	10	SCALE	CONTROL RESTART	AUTO LOAD PROPORTIONAL	—	Elastic-plastic analysis of a thick cylinder
3.8	27	SCALE J-INT	J INTEGRAL WORK HARD CONTROL	PROPORTIONAL	WKSLP	Double edge notch specimen under axial tension.

Table E 3.0-1 Nonlinear Material Demonstration Problems (Continued)

Problem Number (E)	Element Type	Parameter Options	Model Definition	Load Incrementation	User Subroutines	Problem Description
3.9	11	SCALE	OPTIMIZE, 2 CONTROL	AUTO LOAD PROPORTIONAL	—	Mises Mohr-Coulomb example.
3.10	26	SCALE	WORK HARD CONTROL OPTIMIZE, 2	AUTO LOAD PROPORTIONAL	—	Plate with hole.
3.11	28	SCALE THERMAL	TYING, 1 WORK HARD CONTROL RESTART	AUTO THERM CHANGE STATE PROPORTIONAL	—	Axisymmetric bar in combined tension and thermal expansion.
3.12	10	CREEP SCALE	CREEP CONTROL	AUTO CREEP	CRPLAW	Creep ring.
3.13	25	THERMAL STATE VARS CREEP	THERMAL LOADS SPRINGS CREEP CONTROL	AUTO CREEP	VSWELL CREDE	Beam under axial thermal gradient.
3.14	16	CREEP SHELL SECT	CONTROL CREEP	DISP CHANGE AUTO CREEP	—	Creep bending of prismatic beam.
3.15	26	POST CREEP ACCUM BUC	OPTIMIZE, 2 CONTROL CREEP	AUTO CREEP CREEP INCREMEN T EXTRAPOLATE	—	Creep of a square plate with central hole.
3.16	15	LARGE DISP SHELL SECT BUCKLE	UFXORD TRANSFORMATION WORK HARD CONTROL	AUTO LOAD PROPORTIONAL BUCKLE	UFXORD	Plastic buckling of externally pressurized hemispherical dome.
3.17	72	SHELL SECT LARGE DISP	UFXORD	AUTO LOAD PROPORTIONAL	UFXORD	Shell roof with nonlinearities.

Table E 3.0-1 Nonlinear Material Demonstration Problems (Continued)

Problem Number (E)	Element Type	Parameter Options	Model Definition	Load Incrementation	User Subroutines	Problem Description
3.18	15 12	LARGE DISP UPDATE FINITE SHELL SECT MATERIAL	WORK HARD TYING, 102 CONTROL GAP DATA	AUTO LOAD DISP CHANGE	—	Olson cup test.
3.19	10 116	LARGE DISP UPDATE FINITE	WORK HARD CONTROL UDUMP	AUTO LOAD PROPORTIONAL	IMPD	Compression of an axisymmetric member, height reduction 20%.
3.20	16	LARGE DISP FOLLOW FOR SHELL TRAN UPDATE FINITE	CONN GENER WORK HARD CONTROL NODE FILL SHELL TRAN	AUTO LOAD PROPORTIONAL	—	Bending of beam into semicircle.
3.21	10 116	UPDATE LARGE DISP FINITE	WORK HARD UDUMP	AUTO LOAD PROPORTIONAL	IMPD	Necking of a cylindrical bar.
3.22	42 28	ALIAS HEAT CREEP THERMAL	INITIAL TEMP CONTROL FILMS TYING, 1 CREEP INITIAL STATE	TRANSIENT AUTO THERM CHANGE STATE AUTO CREEP	FILM CRPLAW	Combined thermal, elastic-plastic, and creep analysis.
3.23	75	SHELL SECT LARGE DISP PROCESSOR	POST CONTROL	AUTO INCREMENT	UFXORD	Analysis of a shell roof with material and geometric nonlinearity. Demonstrate adaptive load control.
3.24	41 26	HEAT CREEP	INITIAL TEMP FIXED TEMP FILMS INITIAL STATE CREEP	TRANSIENT AUTO THERM CREEP CHANGE STATE	CRPLAW	Uncoupled thermal creep stress analysis of a pressure vessel.

Table E 3.0-1 Nonlinear Material Demonstration Problems (Continued)

Problem Number (E)	Element Type	Parameter Options	Model Definition	Load Incrementation	User Subroutines	Problem Description
3.25	11	LARGE DISP UPDATE FOLLOW FOR	POWDER RELATIVE DENSITY DENSITY EFFECTS	TIME STEP AUTO LOAD	—	Hot isostatic pressing of a can demonstrates powder model.
3.26	28	LARGE DISP UPDATE FOLLOW FOR COUPLE	DEFINE POWDER WORK HARD RELATIVE DENSITY TEMP EFFECTS DENSITY EFFECTS FIXED TEMP FORCDT	TRANSIENT	FORCDT	Hot isostatic pressing coupled analysis.
3.27	54	UPDATE FINITE LARGE DISP	DEFINE UFXORD WORK HARD DAMAGE	DISP CHANGE AUTO LOAD	UFXORD	Shear band development, Gurson damage model.
3.28	55	UPDATE FINITE LARGE DISP	DEFINE WORK HARD DAMAGE	DISP CHANGE AUTO LOAD	—	Notched Specimen, Gurson damage model.
3.29	10	CREEP	CREEP	AUTO CREEP	—	Creep ring – implicit procedure.
3.30	18 75	R-P FLOW ISTRESS	CONTACT WORK HARD	AUTO LOAD MOTION CHANGE	WKSLP UINSTR	Deep drawing by a spherical punch.
3.31	11	LARGE DISP UPDATE	CONTACT CONTACT TABLE	AUTO LOAD DISP CHANGE DIST LOADS	—	Formation of geological strata.

E 3.30 3-D Forming of a Circular Blank Using Rigid-Plastic Formulation

This problem demonstrates the program's ability to perform stretchforming by a spherical punch using the CONTACT option and the rigid-plastic formulation. The problem will first be analyzed using membrane elements and then be analyzed with shell elements.

Parameters

The R-P FLOW option is included in the parameter section to indicate that this is a rigid-plastic flow problem. The PRINT,8 option requests the output of incremental displacements in the local system. Element type 18, the 4-node membrane element, is used in the first analysis. Element type 75, the four-node thick shell element, is used in the second analysis. Eleven layers are used through the thickness of the shell. The ISTRESS parameter is used to indicate that an initial stress is going to be imposed which stabilizes the membrane element solution. In the membrane analysis, the ALIAS option is used to change the element type.

Geometry

A shell thickness of 1 cm is specified through the GEOMETRY option in the first field (EGEOM1).

Boundary Conditions

The first boundary condition is used to model the binding in the stretch forming process. The second and third boundary conditions are used to represent the symmetry conditions.

POST

The following variables are written to a formatted post tape:

7 } Equivalent plastic strain
20 } Element thickness
17 } Equivalent von Mises stress

Furthermore, the above three variables are also requested for all shell elements at layer number 4, which is the midsurface.

Control

A full Newton-Raphson iterative procedure is requested. Displacement control is used, with a relative error of 5%. Fifty load steps are prescribed, with a maximum of 30 recycles (iterations) per load step.

Material Properties

The material for all elements is treated as an rigid-plastic material an initial yield stress of 80.6 lbf/cm^2. The yield stress is given in the form of a power law and is defined through the WKSLP user subroutine.

Contact

This option declares that there are three bodies in contact with Coulomb friction between them. A coefficient of friction of 0.3 is associated with each rigid die. The first body represents the work piece. The second body is the lower die, defined as three surfaces of revolution. The first and third surfaces of revolution use a straight line as the generator, the second uses a circle as the generator. The third body (the punch) is defined as two surface of revolution. These surfaces are extended from -0.5 to 101.21 degrees.The rigid surfaces are shown in Figure E 3.30-1. The relative slip velocity is specified as 0.01 cm/sec. The contact tolerance distance is 0.05 cm. When using the rigid-plastic option, nodal based friction should be used. This is because the solution of the stresses may not be accurate.

Load Control

This problem is displacement controlled with a velocity of 1 cm/sec. applied in the negative Z direction with the AUTO LOAD option. The load increment will be applied 40 times. The MOTION CHANGE option is illustrated to control the velocity of the rigid surfaces.

Results

Figure E 3.30-2 shows the deformed body at the end of 40 increments with the deformation at the same scale as the coordinates. Due to the high level of friction, significant transverse deformation is shown along the contact surfaces.

Figure E 3.30-3 shows the equivalent plastic strain contours on the deformed structure at increment 40, with the largest strain level at 60% using membrane elements.

Figure E 3.30-4 shows the equivalent von Mises stress contours on the deformed structure at increment 40 with peak values at 527 lbf/cm^2 using membrane elements.

Figure E 3.30-5 shows the equivalent plastic strain contours on the deformed structure at increment 40, with the largest strain level at 52% using shell elements.

Figure E 3.30-6 shows the equivalent von Mises stress contours on the deformed structure at increment 40 with peak values at 512 lbf/cm^2 using shell elements.

You can observe very good correlation between the two element formulations. And, comparing problem e3x30 with e8x18, there is also very good agreement. As long as springback is not required, the rigid-plastic formulation is viable for performing sheet forming simulations. It is computationally significantly less expensive than the elastic-plastic formulation.

Summary of Options Used

Listed below are the options used in example e3x30a.dat:

Parameter Options

ALIAS
ELEMENT
END
ISTRESS
PRINT
R-P FLOW
SIZING
TITLE

Model Definition Options

CONNECTIVITY
CONTACT
CONTROL
COORDINATE
END OPTION
FIXED DISP
GEOMETRY
ISOTROPIC
OPTIMIZE
POST
PRINT CHOICE
WORK HARD

Load Incrementation Options

AUTO LOAD
CONTINUE
MOTION CHANGE
TIME STEP

Listed below are the user subroutines used in example u3x30a.f:

WKSLP
UINSTR

Listed below are the options used in example e3x30b.dat:

Parameter Options

ELEMENTS
END
PRINT
R-P FLOW
SIZING
TITLE

Model Definition Options

CONNECTIVITY
CONTACT
CONTROL
COORDINATE
END OPTION
FIXED DISP
GEOMETRY
ISOTROPIC
OPTIMIZE
POST
PRINT CHOICE
WORK HARD

Load Incrementation Options

AUTO LOAD
CONTINUE
MOTION CHANGE
TIME STEP

Listed below is the user subroutine used in example u3x30b.f:

WKSLP

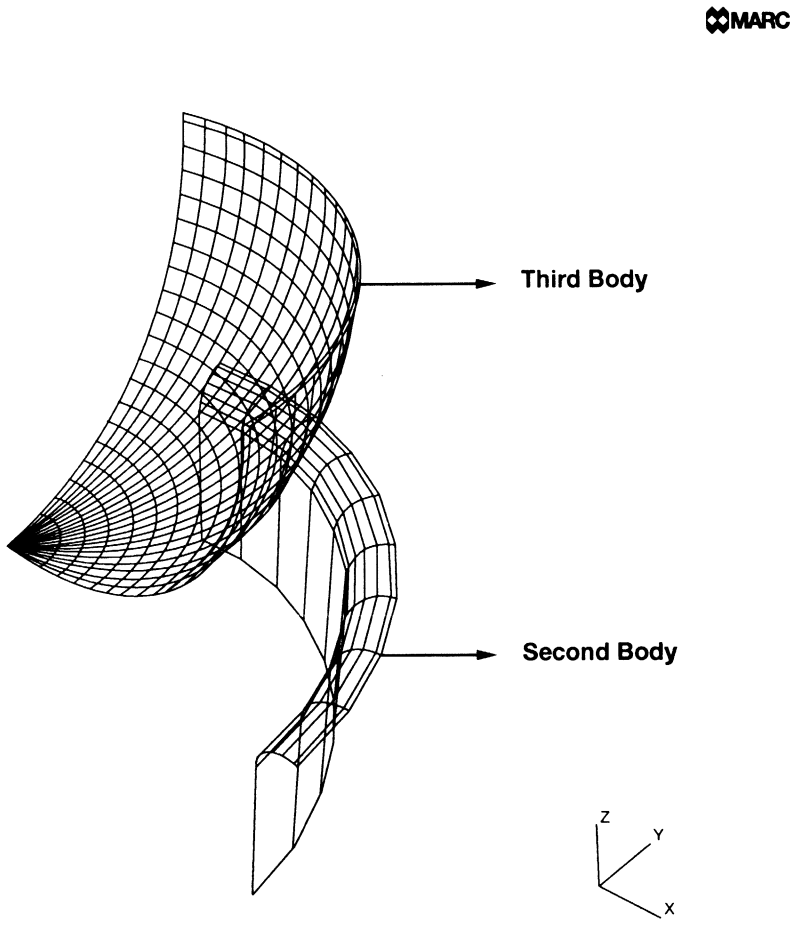

Figure E 3.30-1 Circular Blank Holder and Punch

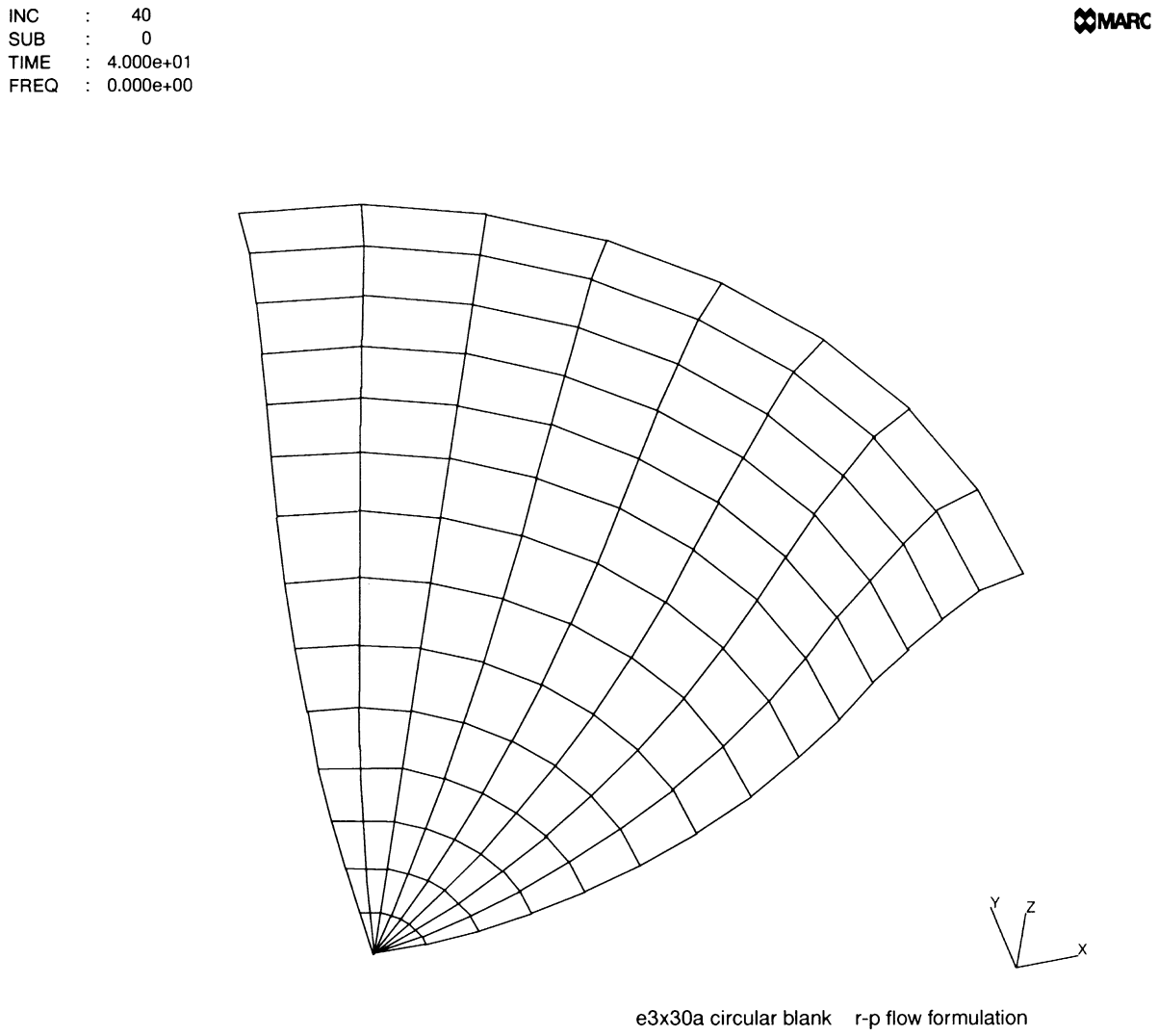

Figure E 3.30-2 Deformed Sheet at Increment 40

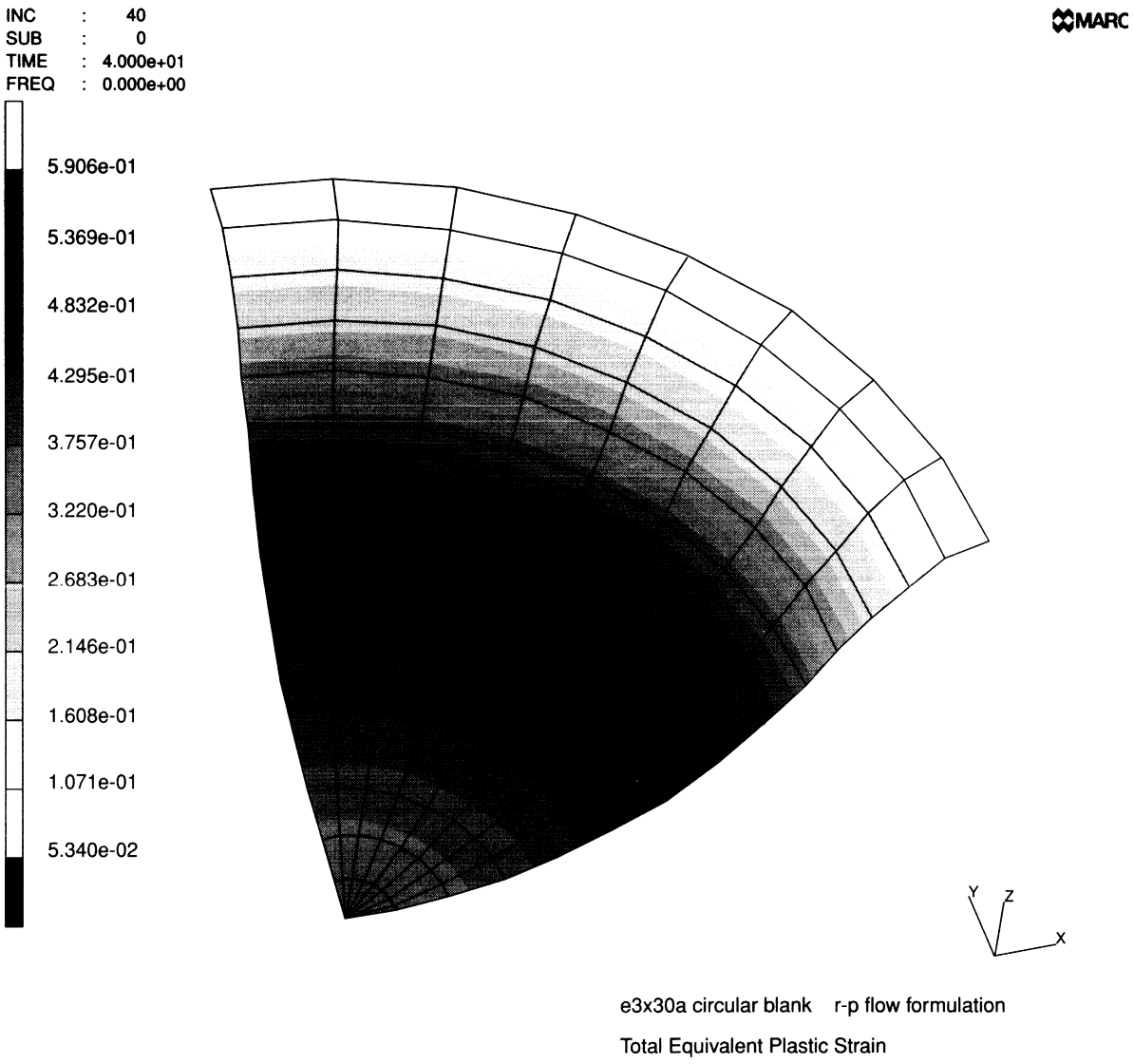

Figure E 3.30-3 Equivalent Plastic Strains in Membrane

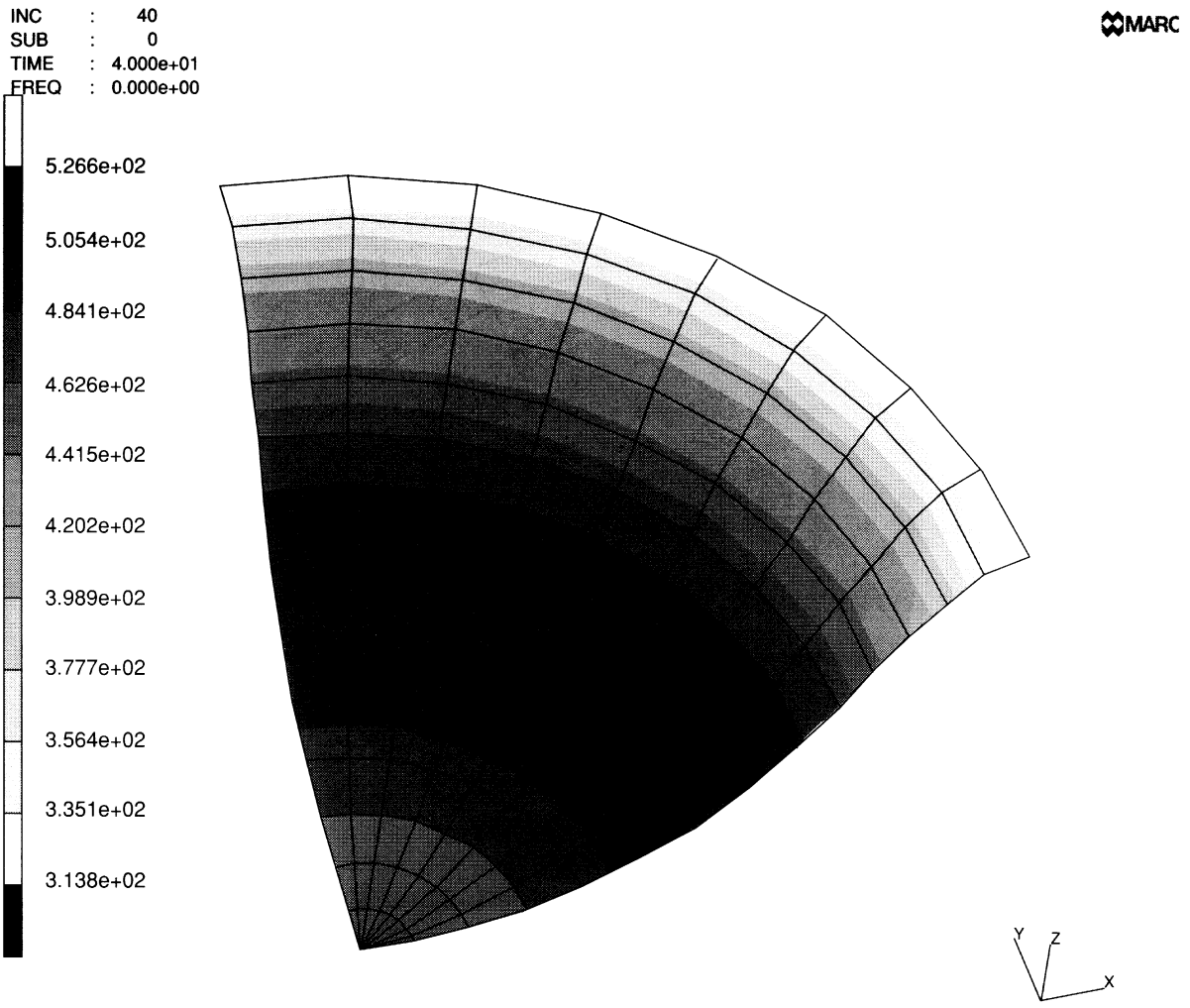

Figure E 3.30-4 Equivalent Stresses in Membrane

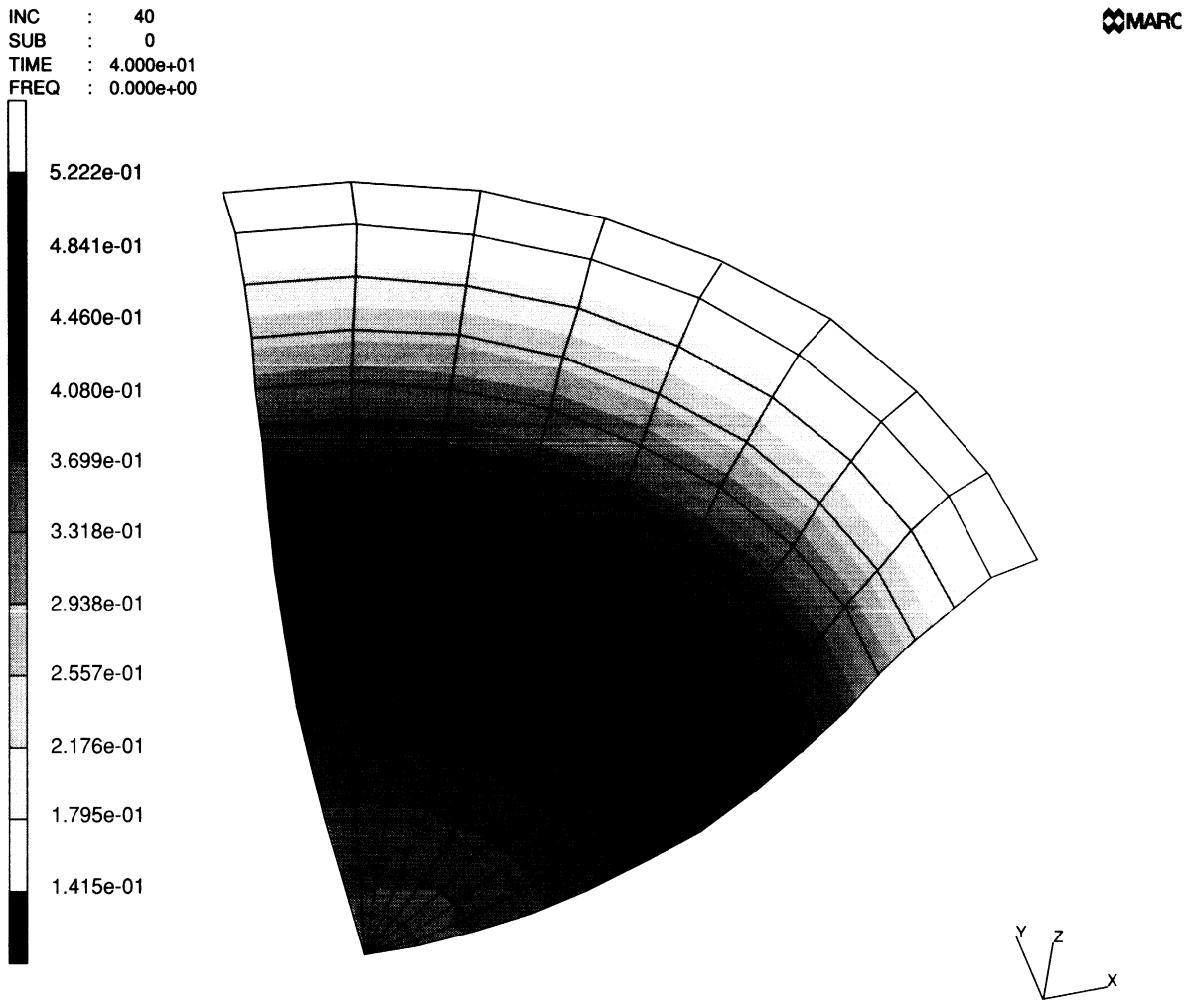

Figure E 3.30-5 Equivalent Plastic Strains at Midlayer of Shell

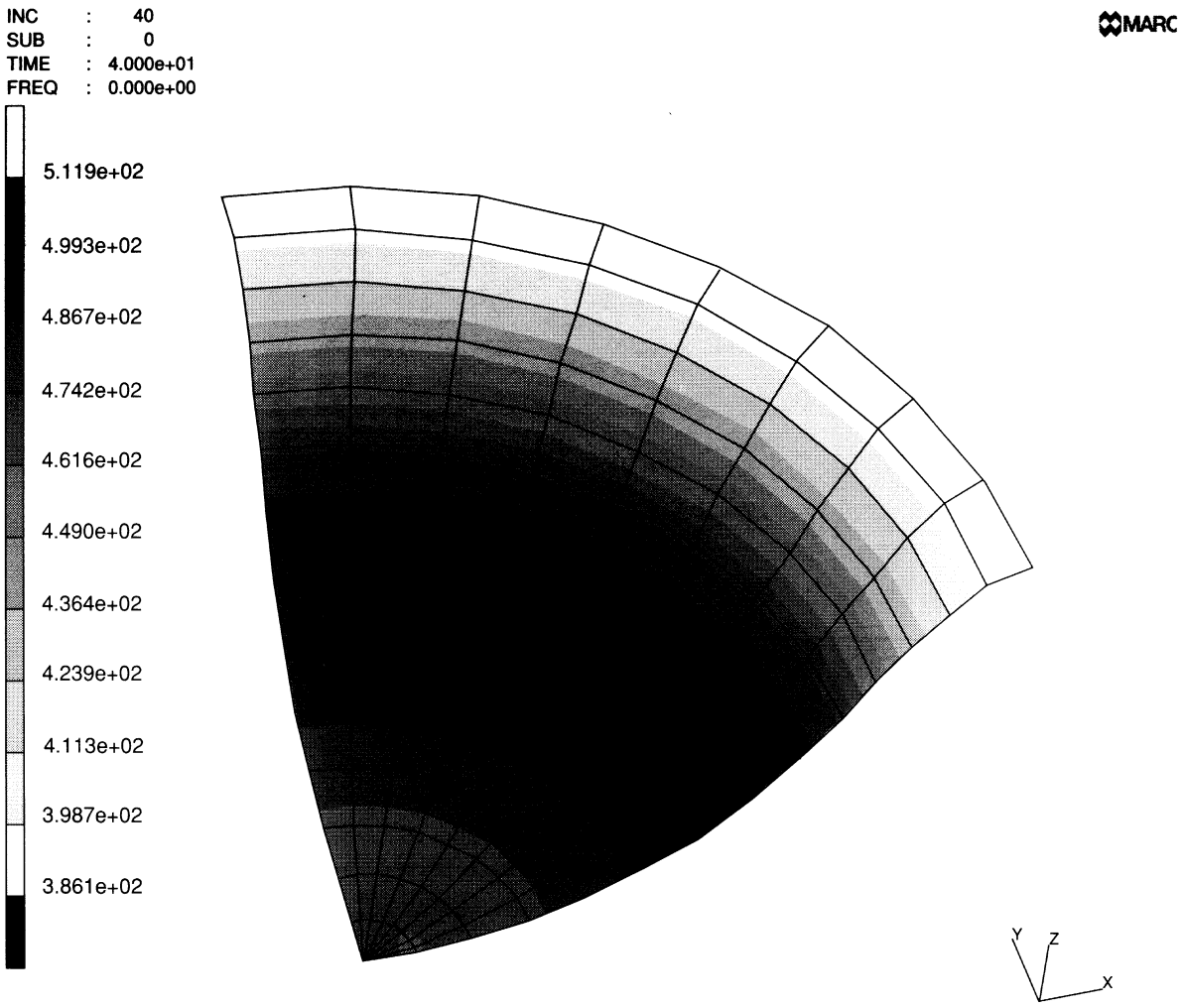

Figure E 3.30-6 Equivalent Stresses at Midlayer of Shell

E 3.31 Formation of Geological Series

This problem demonstrates the capability of the MARC program to analyze the sliding of geological strata along fault planes, until reaching a partial overlap.

In this case, there are two strata separated by an inclined fault. The upper stratum is pushed in the horizontal direction to move against the fault. It will slide along the fault overlapping the lower stratum. The stratum is 6 Km deep and 100 Km long. The computational model is plane strain. The cross section of the strata is represented. Units [N, m].

Elements (Ref. B11.1)

Library element type 11 is a plane-strain 4-node isoparametric quadrilateral element.

Model

The geometry of the strata and their mesh is shown in Figure E 3.31-1. The model consists of 696 plane-strain, type 11, element for a total of 856 nodes. Figure E 3.31-3 shows the details of the mesh at the fault plane.

Geometry

This option is not required for a plane-strain element as a unit thickness is assumed.

Boundary Conditions

Symmetry conditions are applied at the edges 1, 2, and 3 (see Figure E 3.31-1). Automated contact is applied at the interface of the fault. No friction is assumed between the two deformable strata.

Material Properties

The material of the strata is assumed to be isotropic (no variation along the thickness) with the properties:

Young modulus	E	= 34.15 E8 N/m^2
Poisson ratio	ν	= 0.23
Mass density	ρ	= 2200 kg/m^3

The linear Mohr-Coulomb criterion is assumed for the ideal yield surface with values of the two constants (refer to *Volume A, User Information*):

$\bar{\sigma}$ = 22.25 E6 N/m^2
α = .15 N/m^2

Loading

The strata are loaded with the gravity load in ten increments. In the subsequent 25 increments, an incremental displacement of 250 m in the horizontal direction is assigned to the upper part of edge 3 (see Figure E 3.31-1).

Results

The results produced by the MARC program are shown in the following figures:

Figure E 3.31-3	The deformed shape of the strata after a slide of the upper stratum of 6250 m. Notice the growth of a hill of 1019 m in the neighboring of the fault.
Figure E 3.31-4	The distribution across the strata of the σ_{xx} stress components (referred to the global axes) at the final step.
Figure E 3.31-5	The distribution across the strata of the σ_{yy} stress components (referred to the global axes) at the final step.

Summary of Options Used

Listed below are the options used in example e3x31.dat:

Parameter Options

ELEMENT
END
FINITE
LARGE DISP
PRINT
SETNAME
SIZING
TITLE
UPDATE

Model Definition Options

CONNECTIVITY
CONTACT
CONTACT TABLE
CONTROL
COORDINATE
DEFINE
DIST LOADS
END OPTION
FIXED DISP
ISOTROPIC
NO PRINT
POST
RESTART LAST

Load Incrementation Options

AUTO LOAD
CONTINUE
DISP CHANGE
DIST LOADS
NO PRINT
POST INCREMENT
TIME STEP

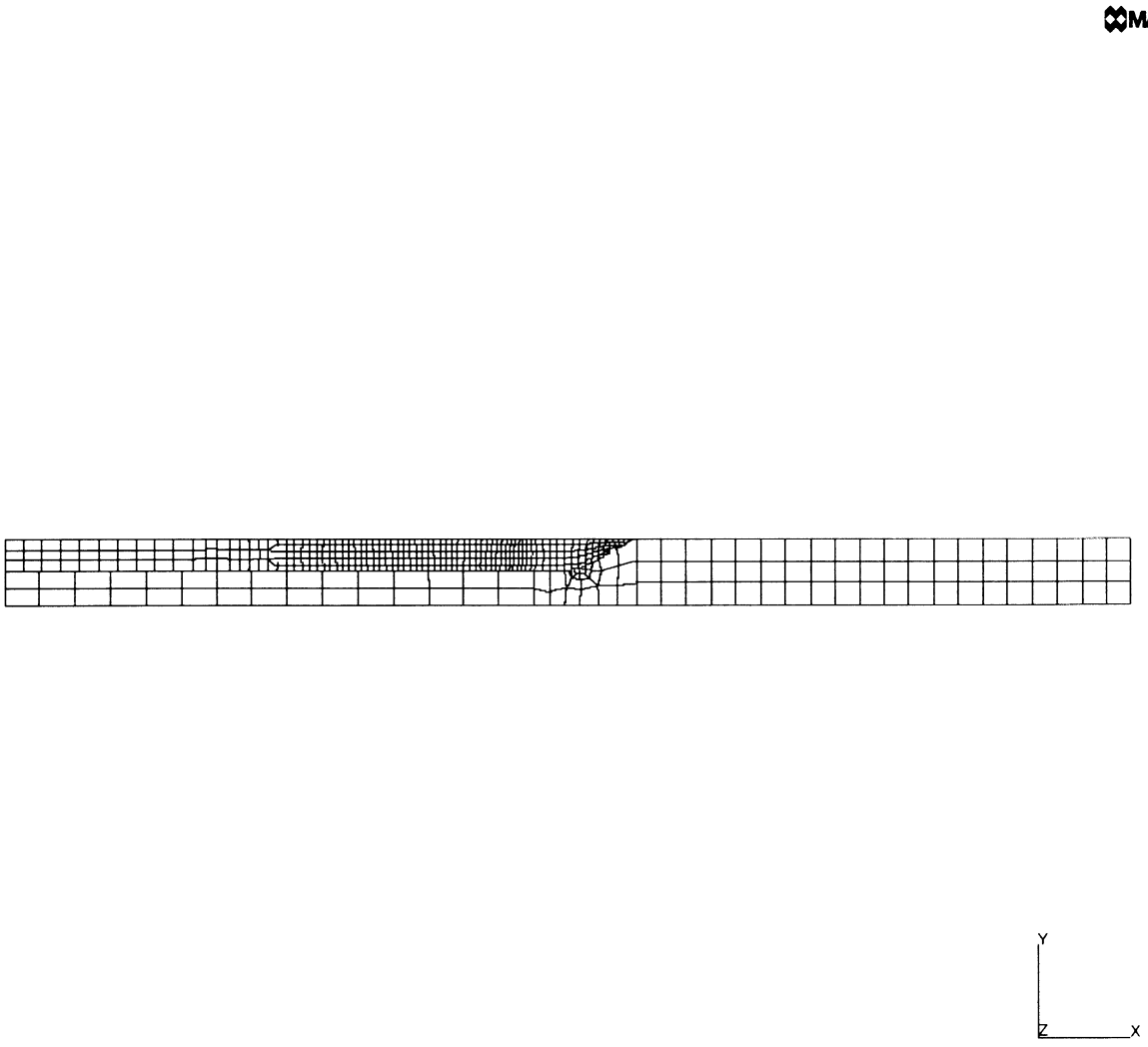

Figure E 3.31-1 FEM Model of the Geological Strata

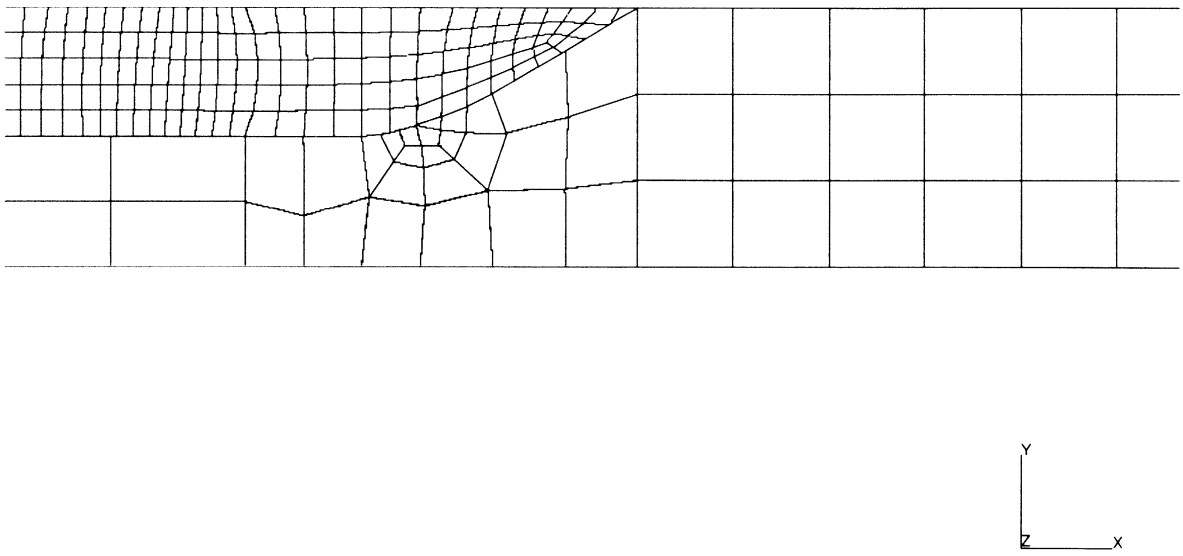

Figure E 3.31-2 Detailed Mesh at the Fault Plane

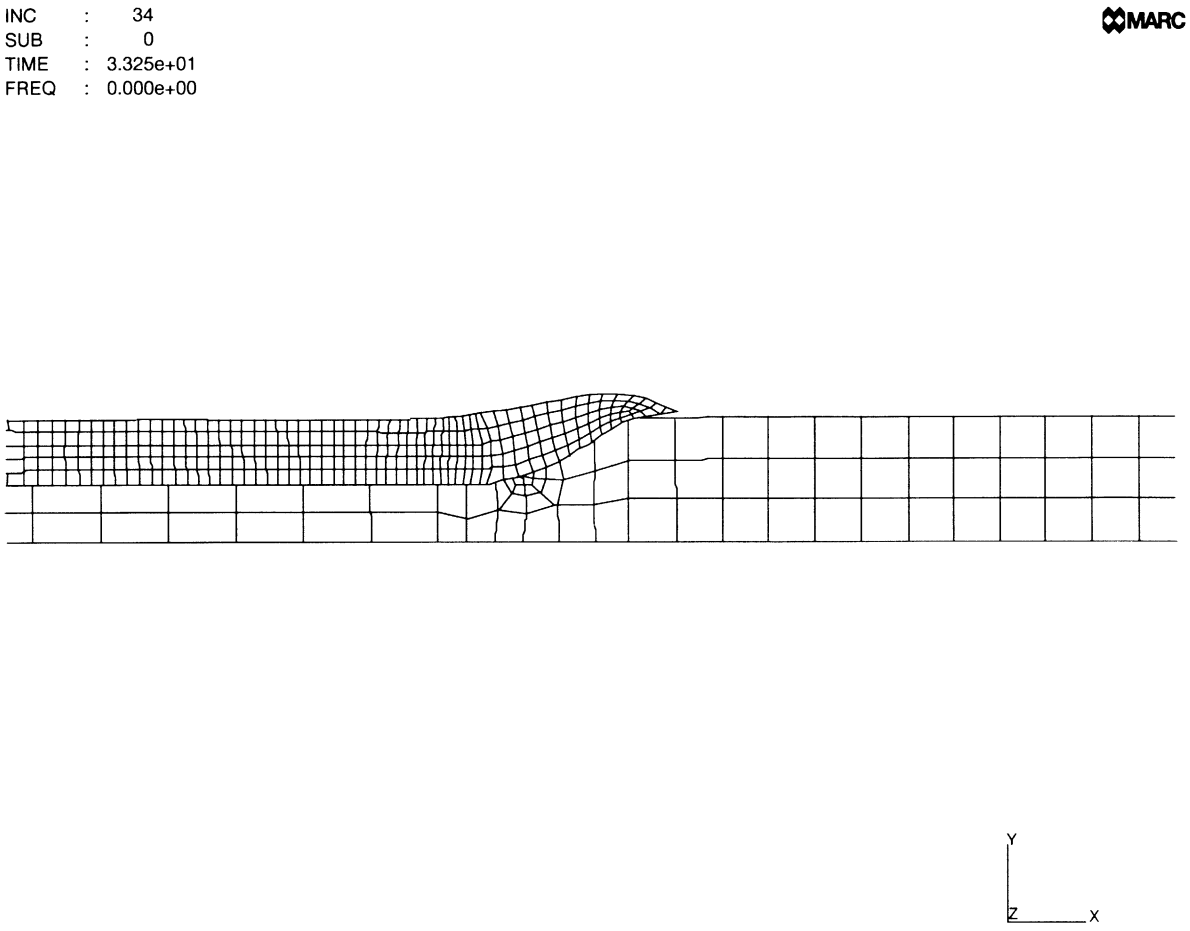

Figure E 3.31-3 Overlap of the Geological Strata

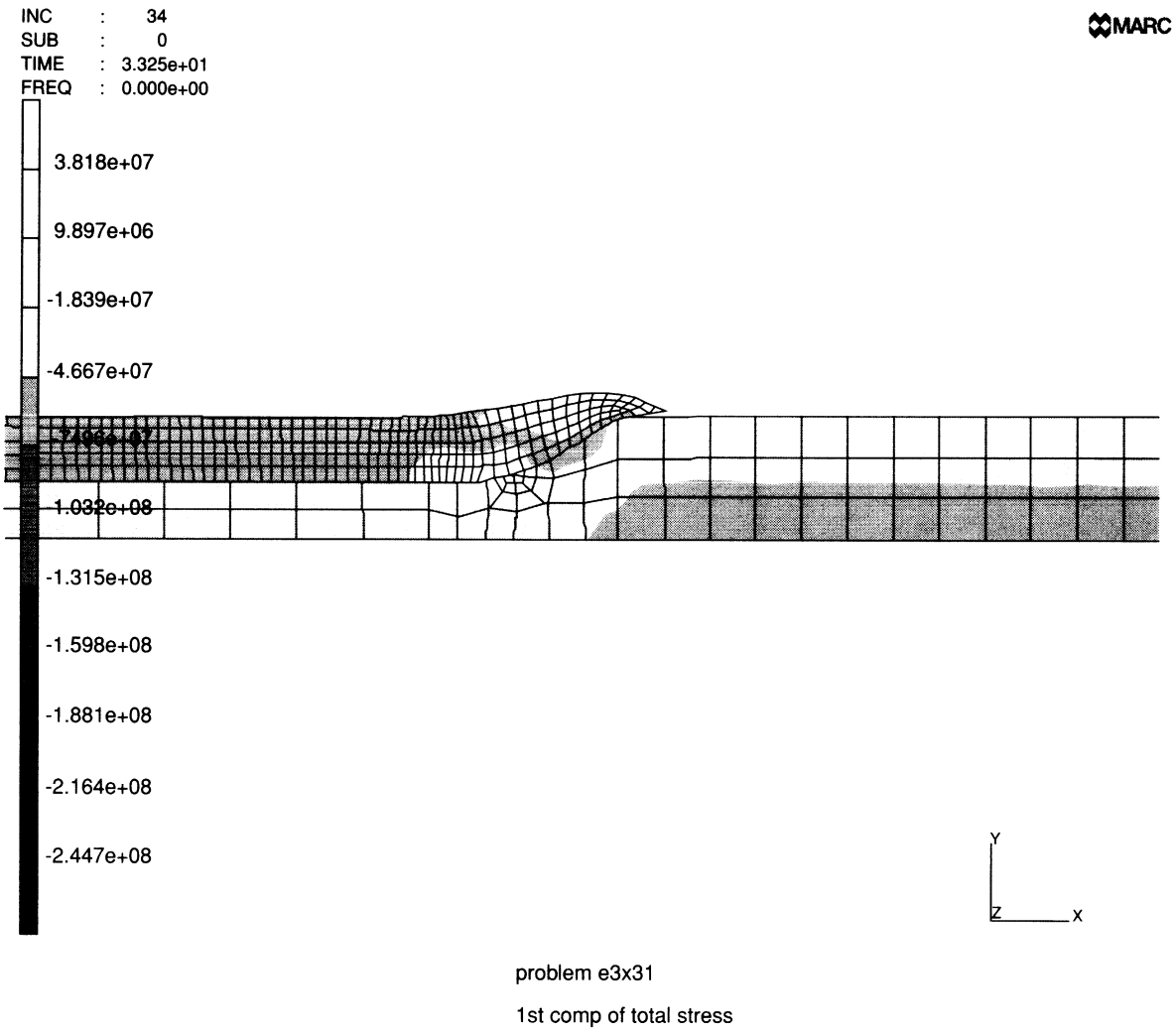

Figure E 3.31-4 Distribution of the σ_{xx} Stress Component (Global Axes)

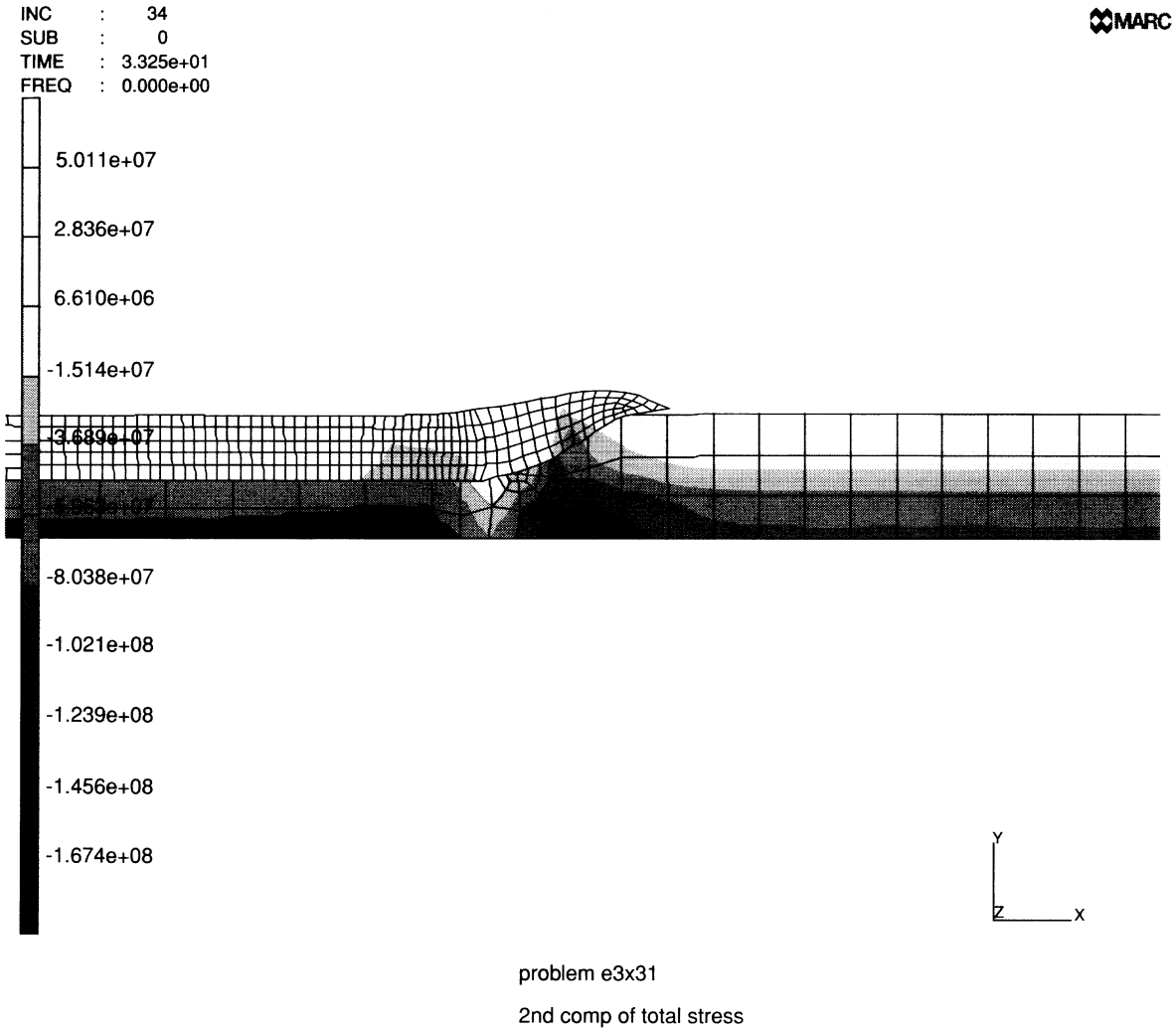

Figure E 3.31-5 Distribution of the σ_{yy} Stress Component (Global Axes)

Volume E
Demonstration Problems

Chapter 4
Large Displacement

Chapter 4 Large Displacement

MARC contains an extensive large displacement analysis capability. A discussion of the use of this capability can be found in *Volume A, User Information* and a summary of the features is give below.

Selection of elements

- Available in all stress elements

Choice of operators

- Newton-Raphson
- Strain-Correction
- Modified Newton-Raphson

Estimation of buckling loads

- Elastic-, plastic-, static- and dynamic-buckling

Choice of procedures

- Total Lagrangian
- Updated Lagrangian
- Eulerian

Large strain elastic analysis

Hyperelastic material (Mooney) behavior

Large strain elastic-plastic analysis

Distributed loads calculated based on deformed structure

Compiled in this chapter are a number of solved problems. These problems illustrate the use of LARGE DISP option for various types of analyses. Table E 4.0-1 shows MARC elements and options used in these demonstration problems.

Table E 4.0-1 Nonlinear Material Demonstration Problems

Problem Number (E)	Element Type	Parameter Options	Model Definition	Load Incrementation	User Subroutines	Problem Description
4.1	15	LARGE DISP BUCKLE	UFXORD CONTROL TRANSFORMATION	BUCKLE PROPORTIONAL AUTO LOAD AUTO INCREMENT	UFXORD	Elastic, large displacement, buckling analysis of a thin shallow, spherical cap, point load, eigenvalue extraction and load incrementation.
4.2	49 50 22	LARGE DISP ELSTO	CONTROL PRINT CHOICE	AUTO LOAD DIST LOADS	—	Elastic-plastic, large displacement analysis of a square plate, simply supported, distributed load.
4.3	25	LARGE DISP ELSTO UPDATE	CONTROL	AUTO LOAD	—	Elastic, large displacement analysis of a cantilever beam subjected to a tip load.
4.4	15	LARGE DISP BUCKLE	CONN GENER NODE FILL	AUTO LOAD BUCKLE	—	Elastic buckling of a cylinder, axial compression, buckling loads and modal shapes.
4.5	22	LARGE DISP	UFXORD OPTIMIZE POST	AUTO LOAD	UFXORD	Large displacement analysis of a pinched cylinder.
4.6	9	LARGE DISP	SPRINGS CONTROL	AUTO LOAD	—	Large displacement of an elastic truss-spring.
4.7	16	PRINT, 3 UPDATE LARGE DISP SHELL SECT	TRANSFORMATION CONN GENER UDUMP UFXORD	AUTO INCREMENT	UFXORD	Postbuckling of a deep arch.
4.8	51	PRINT, 3 FOLLOW FORCE LARGE DISP	DIST LOADS	AUTO LOAD	—	Analysis of a cable network.
4.9	90	SHELL SECT BUCKLE	—	BUCKLE	—	Buckling of a radially loaded ring.

Table E 4.0-1 Nonlinear Material Demonstration Problems (Continued)

Problem Number (E)	Element Type	Parameter Options	Model Definition	Load Incrementation	User Subroutines	Problem Description
4.10	90	SHELL SECT BUCKLE	—	DISP CHANGE BUCKLE	—	Nonsymmetric buckling modes of a circular cylinder.
4.11	49	LARGE DISP	FIXED DISP POINT LOAD	AUTO LOAD POINT LOAD	—	Large displacement analysis of a tapered plate.
4.12	3	LARGE DISP BUCKLE	FIXED DISP POINT LOAD BUCKLE INCREMENT	BUCKLE	—	Buckling of a strut using perturbation method.

E 4.11 Geometrically Nonlinear Analysis of a Tapered Plate

A tapered plate is clamped at one edge and loaded by a bending moment at the opposite edge (see Figure E 4.11-1). By means of this problems, the capability of a finite element to represent inextensional bending in the geometrically nonlinear regime can be investigated.

Element (Ref. B49.1)

Library element type 49 – a 6-node triangular thin shell element – is used. This element allows finite rotational increments so that large load steps can be chosen.

Model

The dimensions of the plate and the finite element mesh are shown in Figure E 4.11-1. Based on symmetry considerations, only one-half of the plate is modeled. The mesh is composed of 80 elements and 243 nodes.

Geometry

A uniform thickness of 0.5 mm is assumed. In thickness direction, three layers are chosen using the SHELL SECT parameter option. Although initially the mesh consists of flat elements, the coupling between the changes of curvature and the membrane deformations becomes important during the loading process. This means that the default setting for the fifth geometry field must be used.

Material Properties

The material is elastic with a Young's modulus of 2.1×10^5 N/mm^2 and a Poisson's ratio of 0.0.

Loading

The loading consists of a bending moment at the edge opposite to the clamped edge. The magnitude of this bending moment is written as f * 365.284 Nmm, where the maximum value of the scalar multiplier f equals 1.5. The total load is applied in 15 equally sized increments.

Boundary Conditions

Symmetry conditions are imposed on the edge $y = 0$ ($u_y = 0$, $\varphi = 0$). Clamped conditions are applied to the edge $x = 0$ ($u_x = 0$, $u_y = 0$, and $\varphi = 0$). Notice that the rotation constraints only apply for the midside nodes.

Results

The final deformed configuration is outlines in Figure E 4.11-5. Since this state has been reached in 15 equally sized increments, a finite rotation formulation is necessary. The horizontal and vertical tip displacements as a function of the load factor f (notice that this factor corresponds to the time) are given in Figure E 4.11-3. An analytical solution for this problem can be found in Y. Ding, *Finite-Rotations-Elements zur geometrisch nichtlinearen Analyse algemeiner Flachentragwerke*, Thesis Insititut für Statik und Dynamik, Ruhr-Univ Rochum, Germany (1989). The analytical solution for the above mentioned displacements components is given in Figure E 4.11-4 and Figure E 4.11-5. The finite element and the analytical solutions are in good agreement.

Summary of Options Used

Listed below are the options used in example e4x11.dat:

Parameter Options

ALL POINTS
DIST LOADS
ELEMENTS
END
LARGE DISP
SETNAME
SHELL SECT
SIZING
TITLE

Model Definition Options

CONNECTIVITY
COORDINATE
DEFINE
END OPTION
FIXED DISP
GEOMETRY
ISOTROPIC
NO PRINT
OPTIMIZE
POST
SOLVER

Load Incrementation

ACTIVATE
AUTO LOAD
CONTINUE
DISP CHANGE
POINT LOAD
TIME STEP

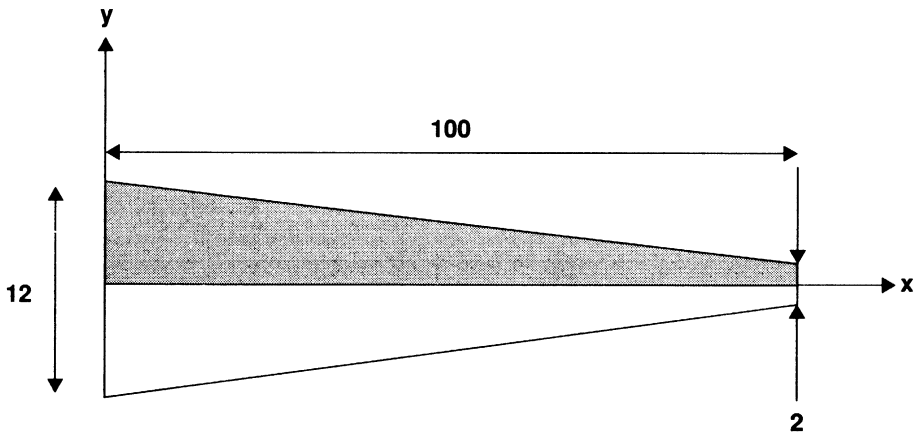

MARC

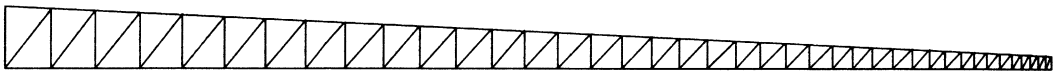

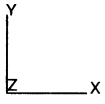

Figure E 4.11-1 Clamped Tapered Plate, Geometry, and Finite Element Mesh

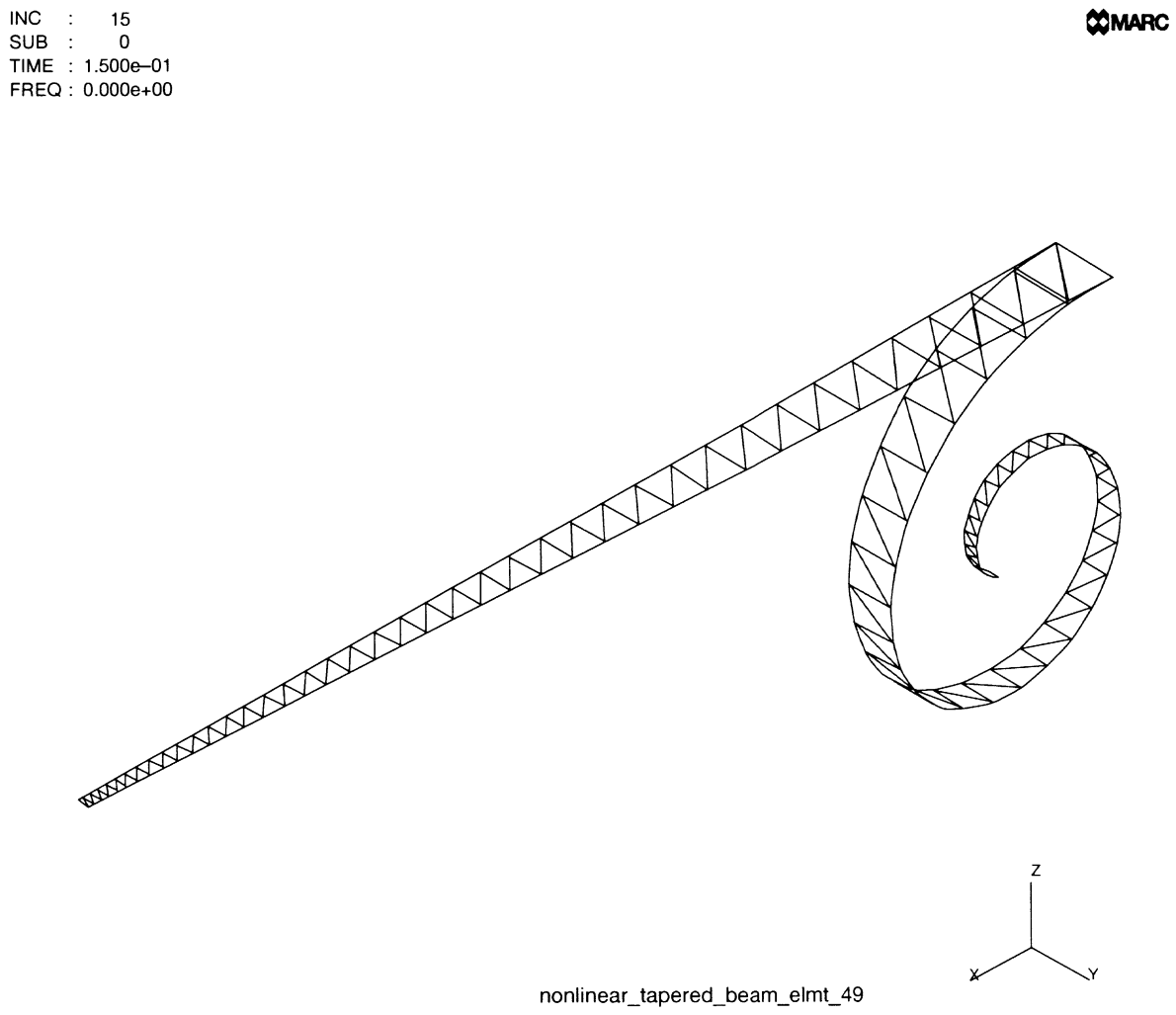

Figure E 4.11-2 Undeformed and Final Deformed Configuration

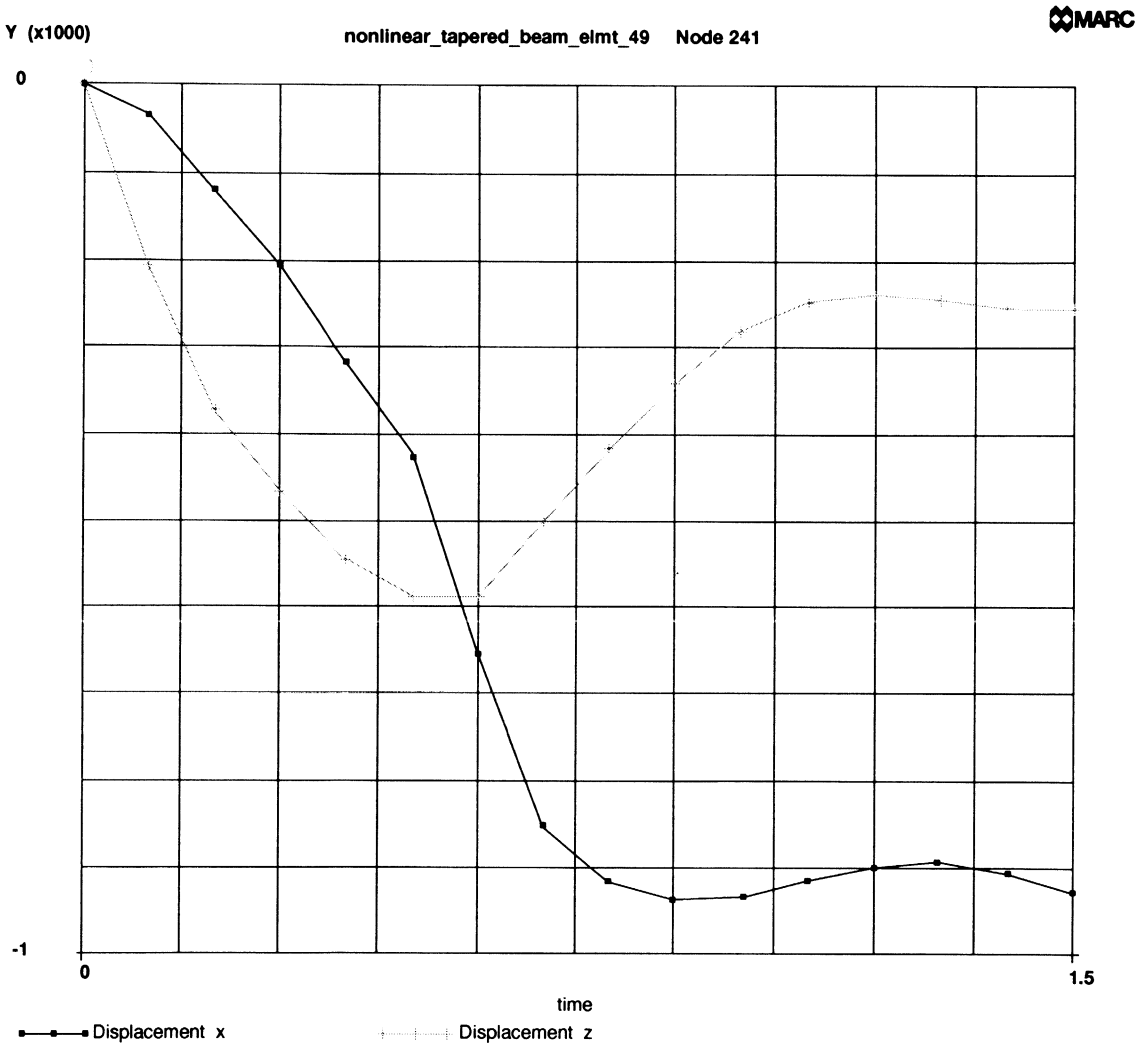

Figure E 4.11-3 Finite Element Solution Horizontal and Vertical Tip Displacement

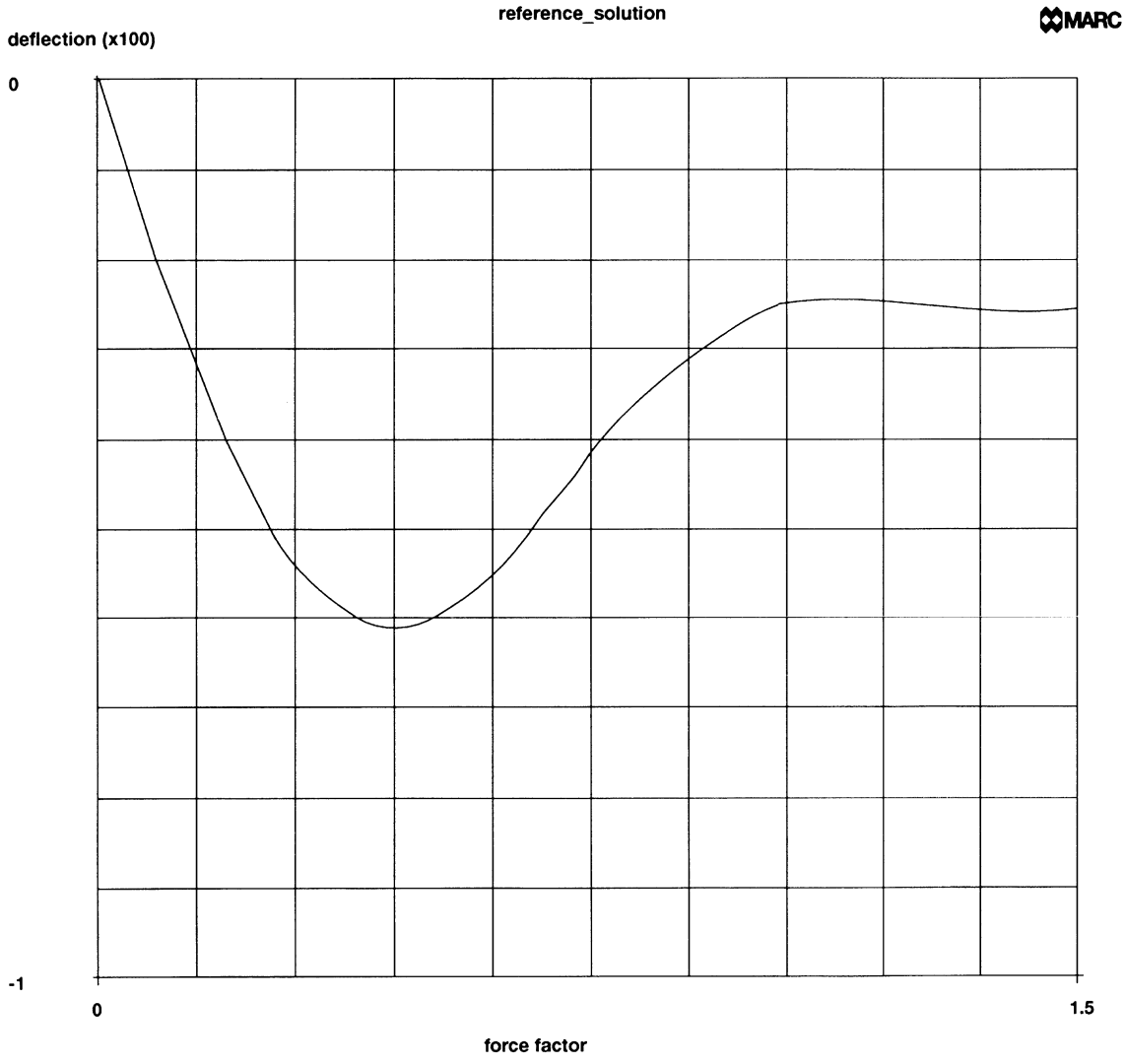

Figure E 4.11-4 Reference Solution Tip Deflection

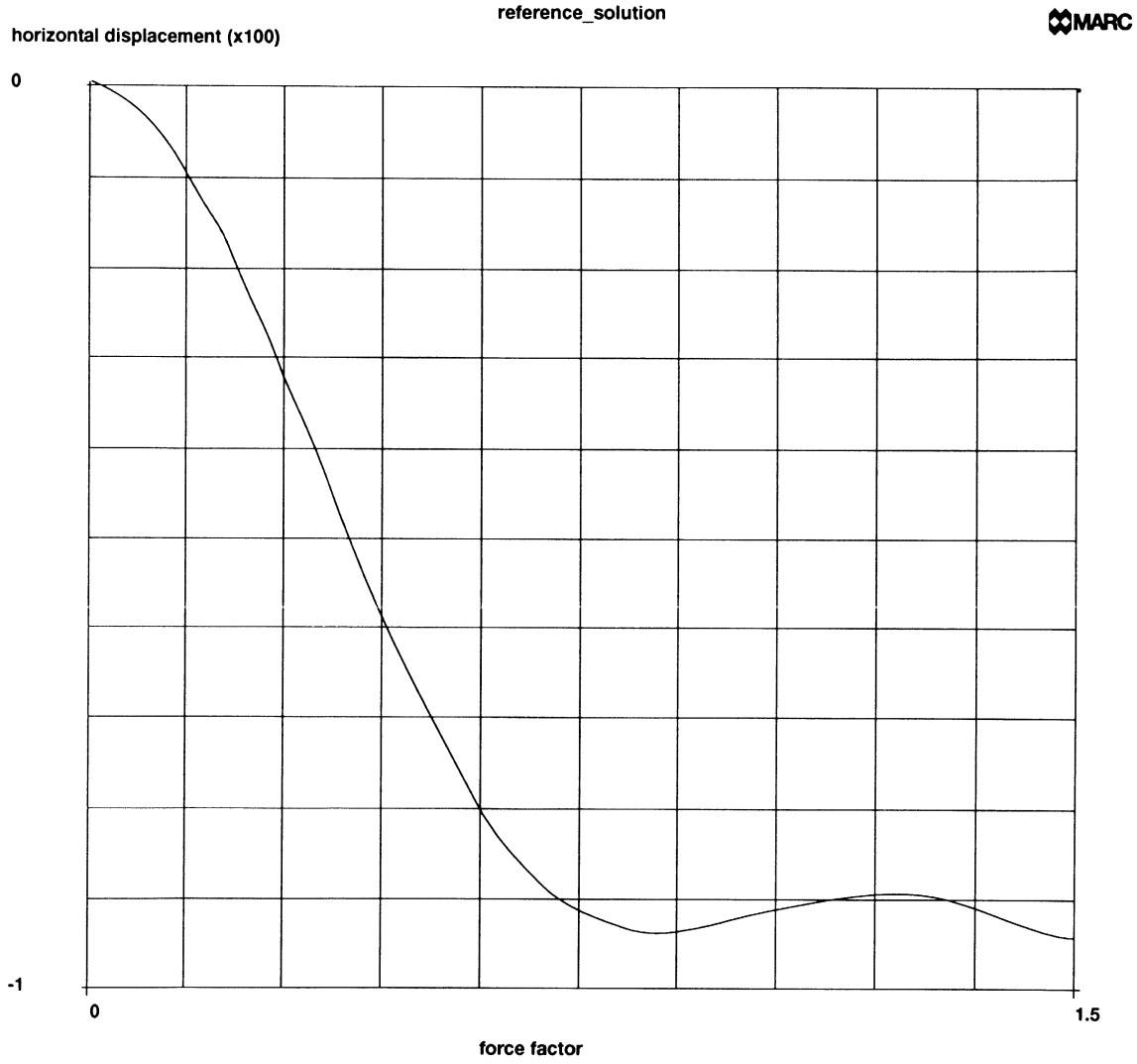

Figure E 4.11-5 Reference Solution Horizontal Tip Displacement

E 4.12 Perturbation Buckling of a Strut

An elastic post buckling analysis is conducted on an initially straight strut. The perturbation buckling technique will be demonstrated.

Model/Element

The model consists of 20 plane stress element, type 3, as shown in Figure E 4.12-1. The length is 2.0 meters and the width is 0.1.

The LARGE DISP option is used to indicate that the total Lagrange large displacement formulation will be used. The BUCKLE option indicates how many buckling modes are to be extracted.

Material Properties

The material has a Young's modulus of 1×10^9 N/m^2 and the Poisson's ratio is 0.3.

Geometry

The strut has a uniform thickness of 1 cm.

Boundary Conditions

The bottom of the strut is clamped, and, at the top, no motion is allowed in the x-direction.

Loading

This analysis is performed using four different procedures:

In the first analysis, a load is applied of magnitude 6000 (3000 at nodes 1 and 4) in increment 1, followed by 200. A buckle eigenmode is extracted and then a perturbation is applied, and then a load of 1800 is applied over nine increments. The first perturbation buckling mode is selected through the BUCKLE load incrementation option.

In the second analysis, a load is applied of magnitude 10,000 in increment 1, followed by 200. A buckle eigenmode is extracted and then a perturbation is applied, and then a load of 9000 is applied over nine increments. The second perturbation buckling mode is selected through the BUCKLE load incrementation option.

In the third analysis, a load is applied of magnitude 6000, followed by a load of 2000 over ten increments. Hence, the total load is the same as in the first analysis. In this analysis, the BUCKLE INCREMENT mode definition option is used to add the first buckle perturbation mode at the end of increment 2.

The fourth analysis is identical to the third analysis, except that the increment at which the perturbation is applied will be determined by the program automatically. The perturbation will be applied in the increment after the increment where a nonpositive definite system occurs.

In all problems, the perturbation has a scaled magnitude of 0.001.

Control

The CONTROL option is used to specify that displacement testing is to be performed with a tolerance of one percent. The solution of nonpositive definite systems will be forced.

Results

The linear collapse load of this strut is 6050 N. Figure E 4.12-2 shows the resultant deformation from the first analysis when the first mode is used. Figure E 4.12-3 shows the resultant deformation from the second analysis when the second mode is used. The results of the third analysis are identical to the first analysis. When the fully automatic perturbation procedure is used in the fourth analysis, the MARC program senses the nonpositive definite system in increment 2, and then automatically extracts the buckle mode. This gives the same results as before. Note that after the perturbation is applied and there is some lateral deflection, you again have a stable physical system and no longer have a nonpositive definite numerical problem.

Summary of Options Used

Listed below are the options used in example e4x12a.dat and e4x12b.dat:

Parameter Options

BUCKLE
ELEMENTS
END
LARGE DISP
SIZING

Model Definition Options

CONTROL
CONNECTIVITY
COORDINATES
DEFINE
END OPTION
FIXED DISP
GEOMETRY
ISOTROPIC
OPTIMIZE
POINT LOAD
POST
SOLVER

Load Incrementation

AUTO LOAD
BUCKLE
CONTINUE
POINT LOAD

Listed below are the options used in example e4x12c.datand e4x11d.dat:

Parameter Options

BUCKLE
ELEMENTS
END
LARGE DISP
SIZING

Model Definition Options

BUCKLE INCREMENT
CONTROL
CONNECTIVITY
COORDINATES
DEFINE
END OPTION
FIXED DISP
GEOMETRY
ISOTROPIC
OPTIMIZE
POINT LOAD
POST
SOLVER

Load Incrementation

AUTO LOAD
CONTINUE
POINT LOAD

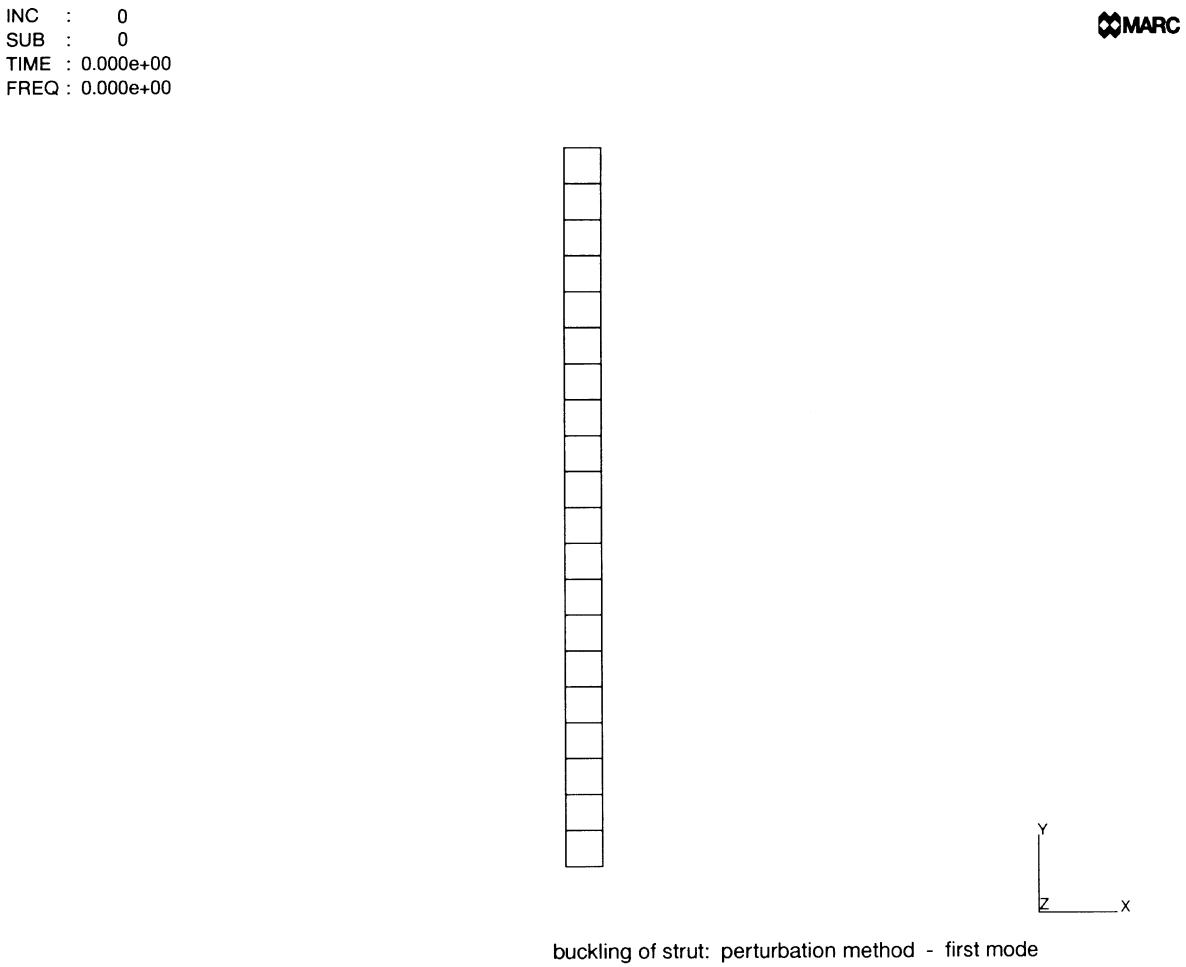

Figure E 4.12-1 Mesh of Strut

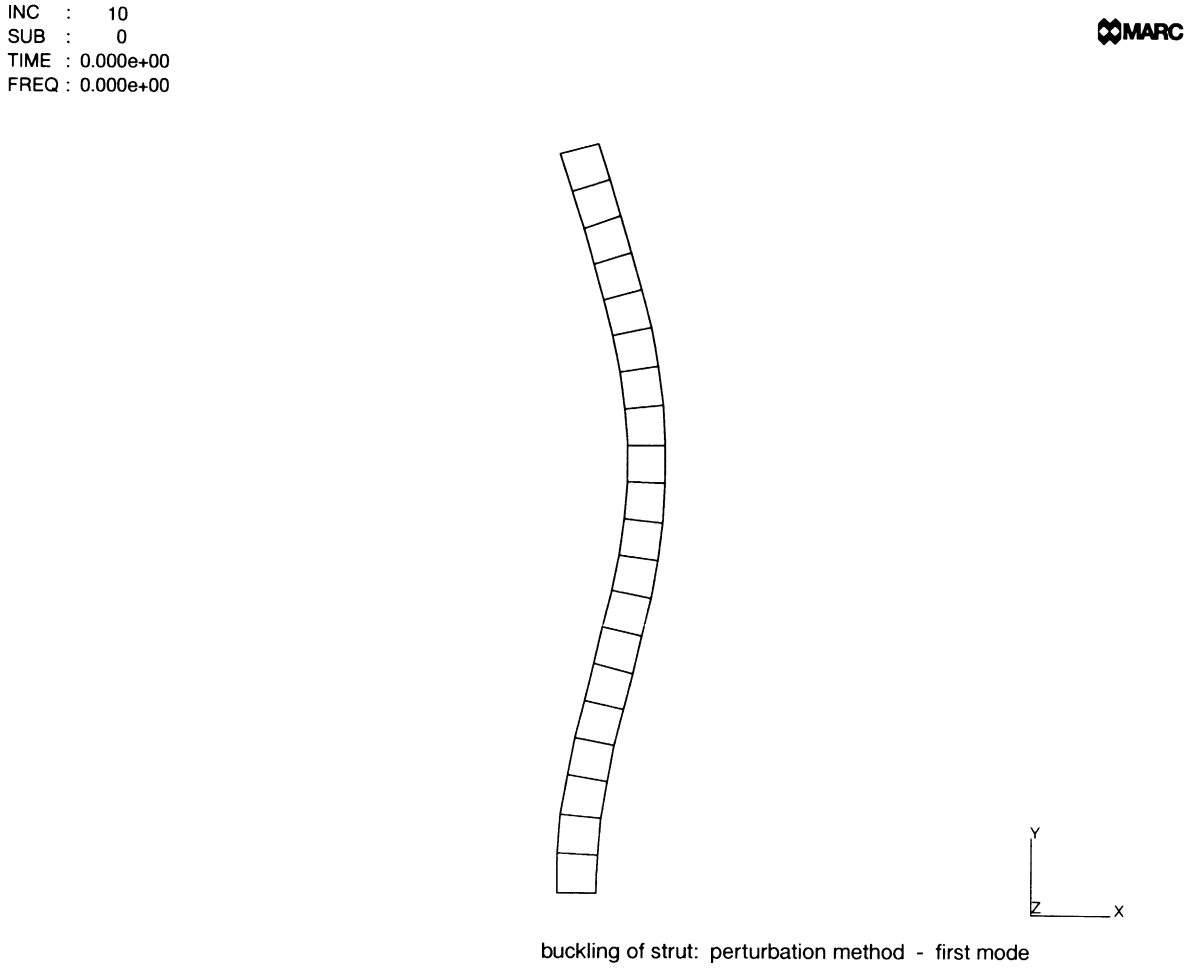

Figure E 4.12-2 Displacements Using First Mode

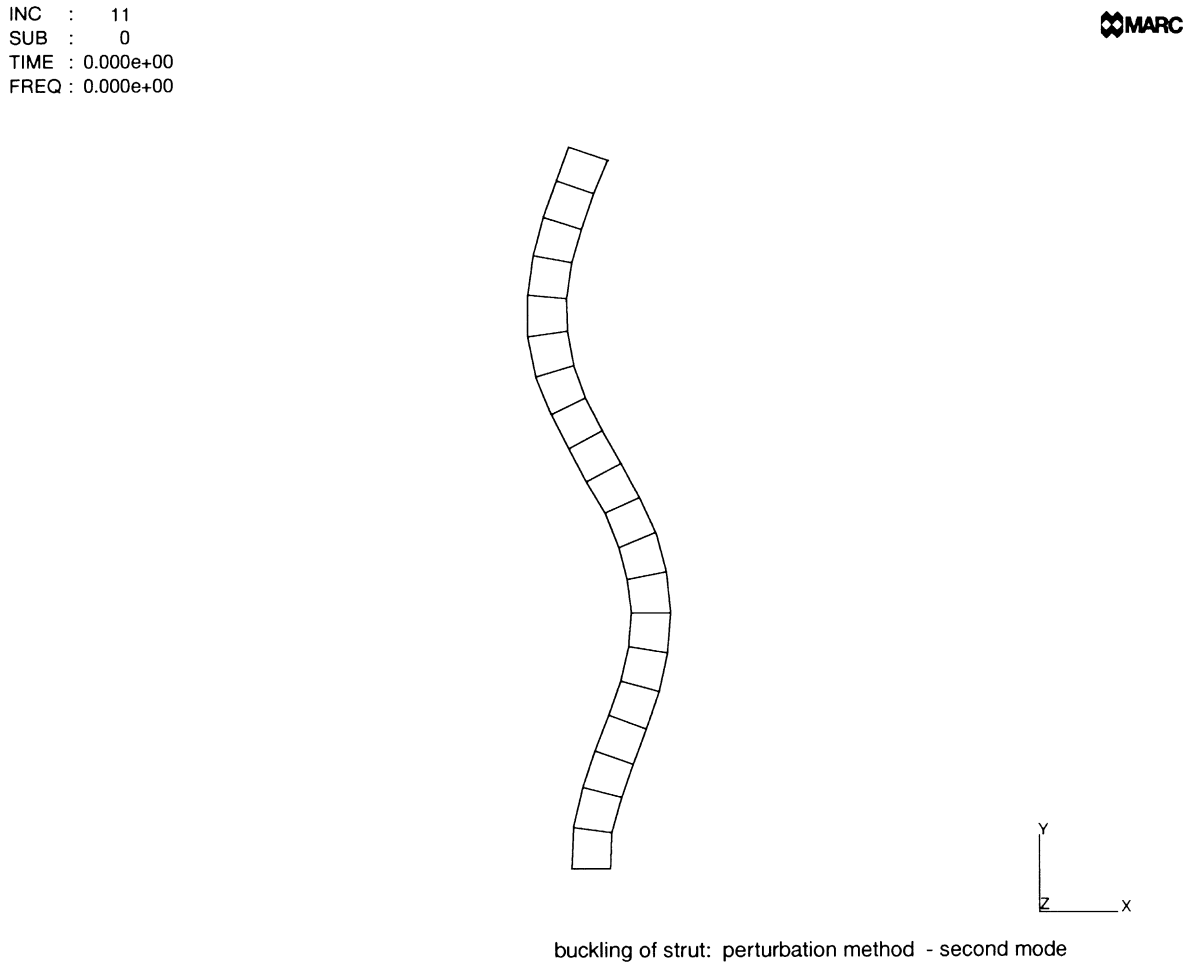

Figure E 4.12-3 Displacements Using Second Mode

Volume E
Demonstration Problems

Chapter 5
Heat Transfer

Chapter 5 Heat Transfer

MARC contains a solid body heat transfer capability for one-, two- and three-dimensional, steady-state and transient analyses. A discussion of the use of this capability can be found in *Volume A, User Information* and a summary of the features is given below.

Selection of elements:

- 1-D: Three-dimensional links (2-, 3-node)
- 2-D: Planar and axisymmetric elements (3-, 4-, 6-, and 8-node)
- 3-D: Brick elements (8- and 20-node)
- Reduced integration elements with hourglass control

Time integration operator:

- Backward difference – unconditionally stable for linear problems; automatic time-step choice; in-core and out-of-core solutions.

Temperature dependent materials (including latent heat effects); anisotropic thermal conductivity.

Extrapolated averaging for the evaluation of temperature-dependent properties.

Non-uniform initial conditions.

Temperature, time-dependent boundary conditions: prescribed temperature history, volumetric flux, surface flux, film coefficients, radiation; change of prescribed temperature boundary conditions during analysis.

Tying constraints on nodal temperatures.

Two- and three-dimensional mesh generation; bandwidth optimization.

Contour or temperature time history plots; mesh plots.

Ability to restart the analysis.

Selective print of nodal and/or element temperatures; consistent nodal fluxes.

Direct interface with stress analysis.

User subroutines.

A number of solved problems are compiled in this chapter. These problems illustrate the use of various MARC heat transfer elements and demonstrate the selection of different options. Table E 5.0-1 shows MARC elements and options used in these demonstration problems.

Table E 5.0-1 Heat Transfer Analysis Demonstration Problems

Problem Number (E)	Element Type	Parameter Options	Model Definition	Load Incrementation	User Subroutines	Problem Description
5.1	36	HEAT	—	TRANSIENT NON AUTO	—	One-dimensional steady-state heat conduction, constant properties, prescribed temperature boundary conditions, 2-node link element.
5.2	65	HEAT FORCDT	FORCDT INITIAL TEMP	TRANSIENT NON AUTO	FORCDT	One-dimensional transient heat conduction, constant properties, prescribed temperature boundary conditions, 3-node link element.
5.3	41 69 39 37 121 131	HEAT FILMS ALIAS	INITIAL TEMP FILMS CONTROL OPTIMIZE	TRANSIENT NON AUTO	—	Two-dimensional transient heat conduction, constant properties, prescribed temperature and convective boundary conditions, 3-, 4-, and 8-node reduced integration planar elements.
5.4	43 44 71 123	HEAT	INITIAL TEMP CONTROL PRINT CHOICE UDUMP	TRANSIENT NON AUTO	—	Three-dimensional transient heat conduction, constant properties, prescribed temperature and insulated boundary conditions, 8-, 20-node and reduced integration elements.
5.5	42 70	HEAT FILMS ALIAS	INITIAL TEMP CONTROL FILMS	TRANSIENT	FILM	Axisymmetric transient heat conduction, constant properties, convective boundary conditions, 8-node axisymmetric and reduced integration elements.
5.6	41	HEAT FILMS	INITIAL TEMP CONTROL FILMS	TRANSIENT	FILM	Same as problem 5.5, except using 8-node planar element.

Table E 5.0-1 Heat Transfer Analysis Demonstration Problems (Continued)

Problem Number (E)	Element Type	Parameter Options	Model Definition	Load Incrementation	User Subroutines	Problem Description
5.7	39	HEAT	ANISOTROPIC	TRANSIENT NON AUTO	ANKOND	Two-dimensional heat conduction, constant properties, anisotropic conductivity, prescribed conditions, 4-node planar element.
5.8	41	HEAT MESH PLOT	FILMS FLUXES INITIAL TEMP CONTROL TEMP EFFECTS RESTART OPTIMIZE	TRANSIENT	FILM FLUX	Nonlinear heat conduction, temperature dependent properties, prescribed temperature, convective, and radiative boundary conditions, 8-node planar element.
5.9	40 122 132	HEAT	TEMP EFFECTS INITIAL TEMP CONTROL FILMS PRINT CHOICE UDUMP	TRANSIENT NON AUTO	—	Latent heat effect, temperature dependent properties, convective boundary condition 4-node axisymmetric element.
5.10	40	HEAT JOULE	JOULE DIST CURRENT VOLTAGE FILMS	TRANSIENT NON AUTO	—	Evaluate temperatures in a wire due to current.
5.11	42 28	HEAT MARC.PLOT THERMAL T-T-T	TEMP EFFECTS FILMS TIME-TEMP CHANGE STATE INITIAL TEMP	TRANSIENT AUTO THERM CHANGE STATE	—	Evaluate transient temperature response due quenching process. Evaluate thermally-induced stresses.
5.12	39	ALIAS JOULE HEAT	VOLTAGE POST JOULE	TRANSIENT	—	Electro static planar analysis.

Summary of Options used

Listed below are the options used in example e5x17a.dat:

Parameter Options

ALL POINTS
COMMENT
DIST LOADS
END
HEAT
PRINT
SETNAME
SIZING
TITLE

Model Definition Options

CONNECTIVITY
CONTROL
COORDINATE
DEFINE
END OPTION
FIXED TEMPERATURE
INITIAL TEMPERATURE
ISOTROPIC
NO PRINT
POST
VELOCITY

Load Incrementation Options

CONTINUE
TRANSIENT NON AUTO

Listed below are the options used in example e5x17b.dat:

Parameter Options

ALL POINTS
COMMENT
DIST LOADS
END
HEAT
PRINT
SETNAME
SIZING
TITLE

Model Definition Options

CONNECTIVITY
CONTROL
COORDINATE
DEFINE
END OPTION
FIXED TEMPERATURE
INITIAL TEMPERATURE
ISOTROPIC
NO PRINT
POST
VELOCITY

Load Incrementation Options

CONTINUE
TRANSIENT NON AUTO

MARC

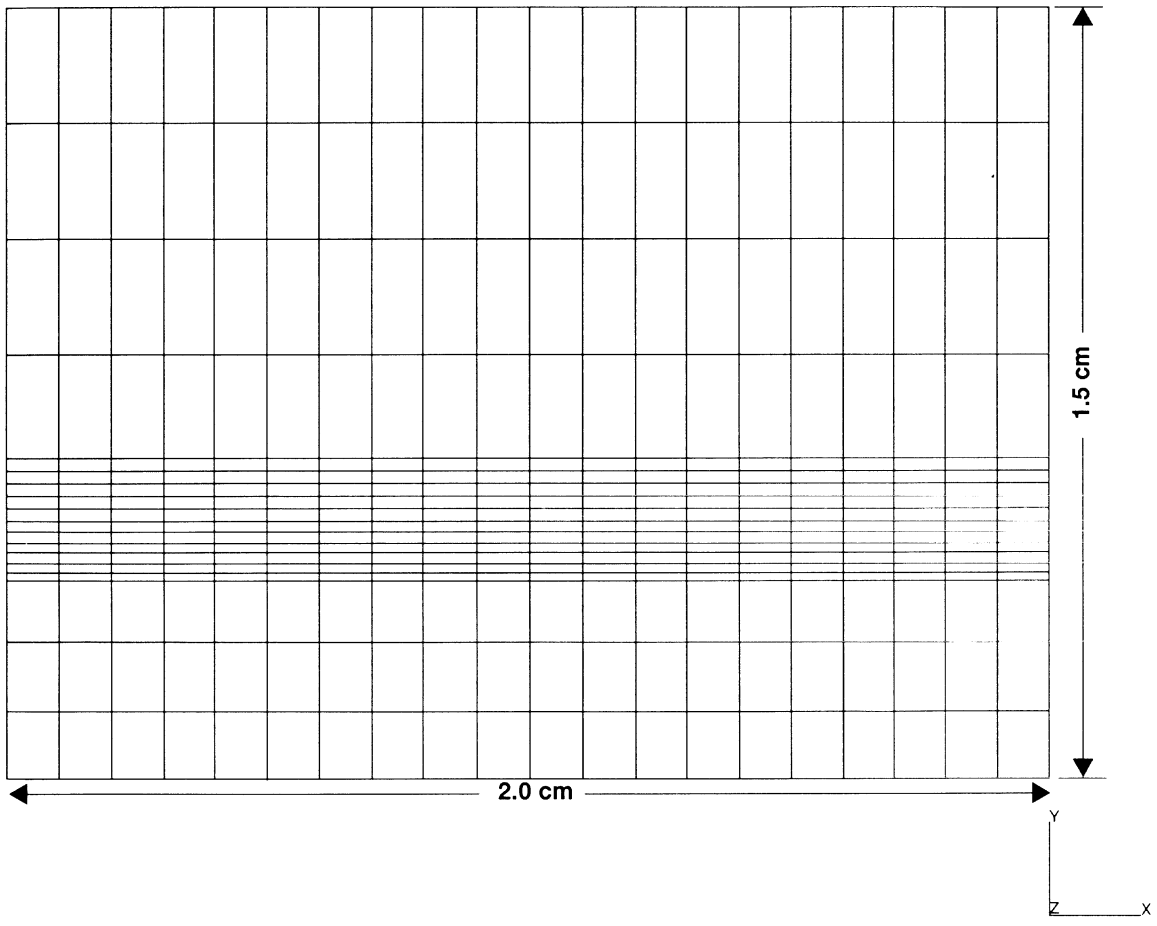

Figure E 5.17-1 Complete Finite Element Mesh

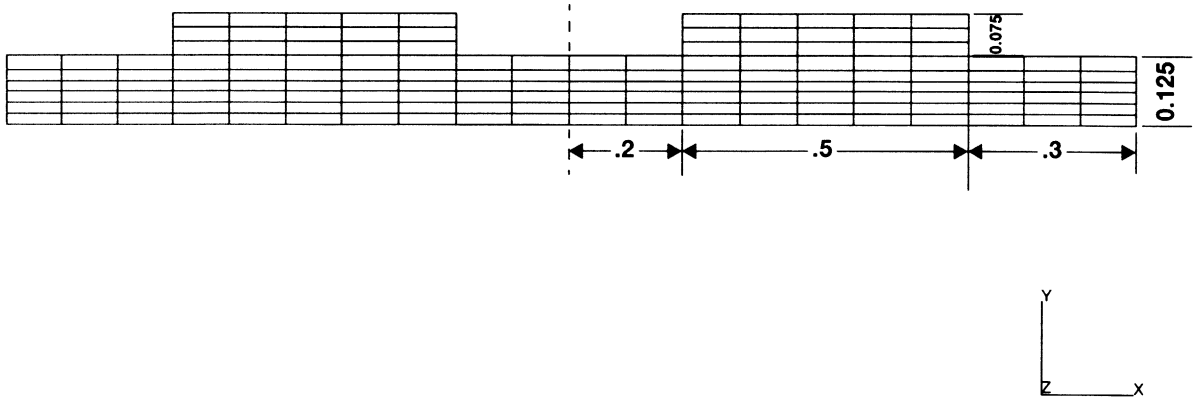

Figure E 5.17-2 Finite Element Mesh of Chips and Board

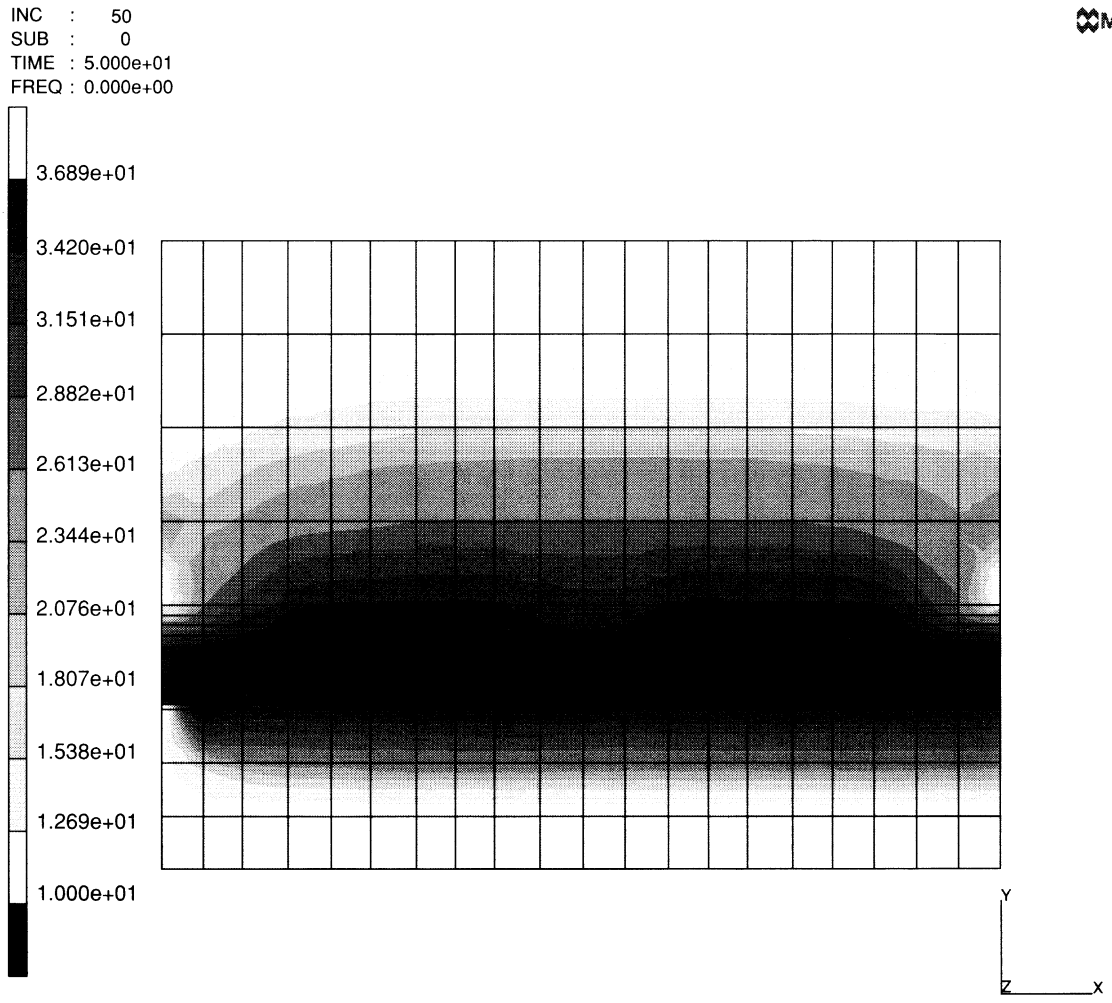

Figure E 5.17-3 Temperature Distribution Excluding Heat Convection

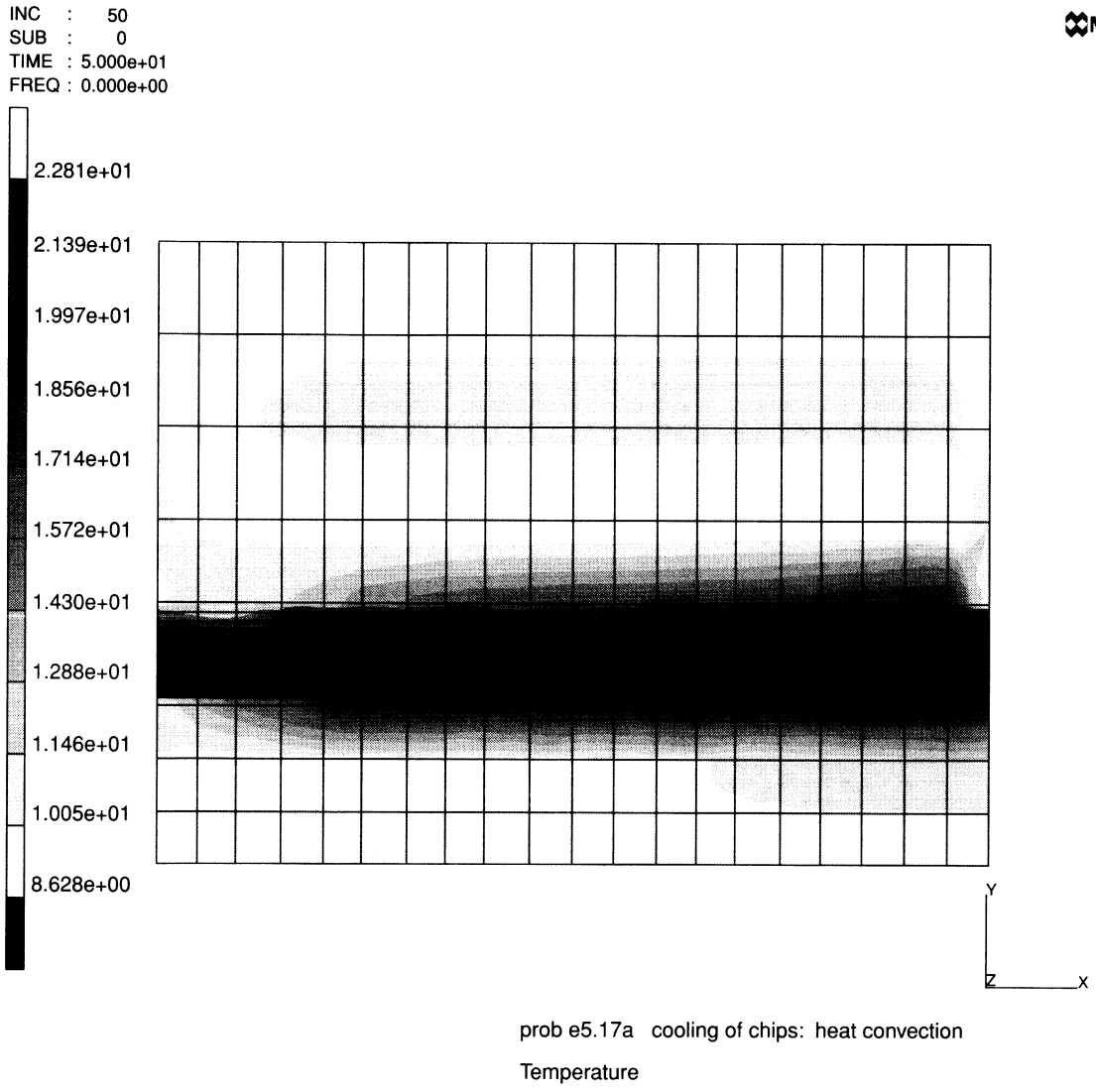

Figure E 5.17-4 Temperature Distribution Including Heat Convection

E 5.18 Square Plate Heated at a Center Portion

A square plate with an initial temperature of 20°C is heated at the upper side of a square center portion (see Figure E 5.18-1). The temperature at the outer edges is kept constant.

Element (Ref. B50.1)

Library element type 50, a 3-node triangular heat transfer shell element, is used.

Model

The dimensions of the plate and the finite element mesh are shown in Figure E 5.18-1. Based on symmetry considerations, only one quarter of the plate is modeled. The mesh is composed of 128 elements and 81 nodes.

Material Properties

The material is orthotropic with the following material constants:

Conductivity: $\lambda_{11} = 50$ W/m°C, $\lambda_{22} = 5000$ W/m°C, $\lambda_{33} = 500$ W/m°C
Density: $\rho = 7000$ kg/m^3
Specific Heat: $c = 450$ J/kg°C

Since, by default, the properties are applied with respect to element directions, the orientation option is used to specify an offset of 0 to the zx-plane (see Figure E 5.18-1).

Geometry

A uniform thickness of 0.5 m is assumed. In thickness direction, a parabolic temperature distribution is selected using the HEAT parameter option. The number of layers is set equal to 3 using the SHELL SECT parameter option.

Loading

The loading consists of a distributed flux of 800 W/m2 on the upper side of a square center portion. Two analyses are carried out. The first one (a) is a steady-state analysis; the second one (b) is a transient analysis.

Boundary Conditions

Symmetry conditions are imposed on the edges x = 0 and y = 0. Fixed temperatures are applied on the outer edges. Notice that this involves three degrees of freedom since, in thickness direction, a parabolic temperature distribution has been chosen.

Results

The steady-state temperature distribution of the top layer is shown in Figure E 5.18-2. Due to the orthotropic material properties, the temperature distribution is nonsymmetric with respect to a diagonal of the plate. As a result of the transient analysis, the temperature distribution of the top and bottom layer along the line x = 0 are shown in Figure E 5.18-3 and Figure E 5.18-4, where Figure E 5.18-3 refers to increment 1 and Figure E 5.18-4 refers to increment 15. The situation of increment 15 corresponds to the steady-state solution.

Summary of Options used

Listed below are the options used in example e5x18a.dat:

Parameter Options

ALL POINTS
DIST LOADS
ELEMENTS
END
HEAT
LUMP
SETNAME
SHELL SECT
SIZING
TITLE

Model Definition Options

CONNECTIVITY
COORDINATE
DEFINE
DIST FLUXE
END OPTION
FIXED TEMPERATURE
GEOMETRY
INITIAL TE
NO PRINT
OPTIMIZE
ORIENTATION
ORTHOTROPIC
POST
SOLVER

Load Incrementation Options

ACTIVATE
CONTINUE
CONTROL
DIST FLUXE
STEADY STATE
TEMP CHANGE

Listed below are the options used in example e5x18b.dat:

Parameter Options

ALL POINTS
DIST LOADS
ELEMENTS
END
HEAT
LUMP
SETNAME
SHELL SECT
SIZING
TITLE

Model Definition Options

CONNECTIVITY
COORDINATE
DEFINE
DIST FLUXE
END OPTION
FIXED TEMPERATURE
GEOMETRY
INITIAL TE
NO PRINT
OPTIMIZE
ORIENTATION
ORTHOTROPIC
POST
SOLVER

Load Incrementation Options

ACTIVATE
CONTINUE
CONTROL
DIST FLUXE
STEADY STATE
TEMP CHANGE

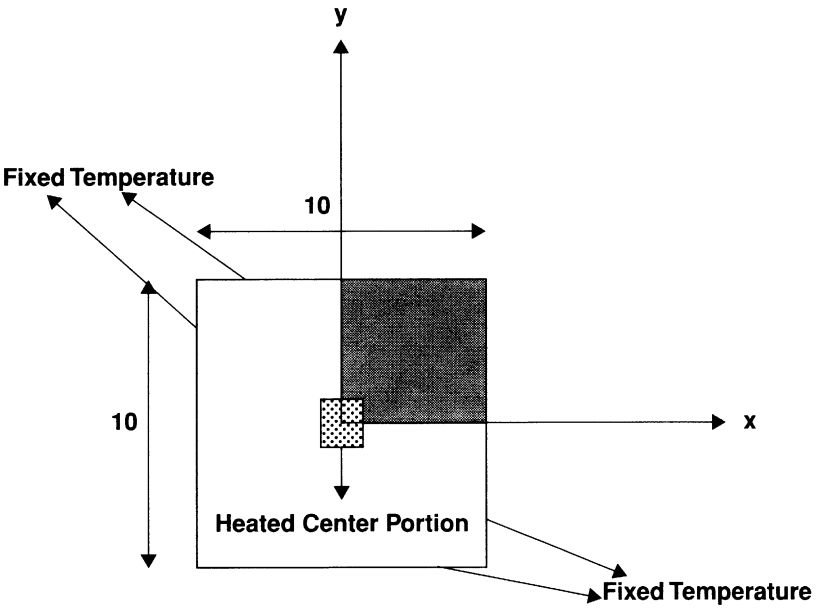

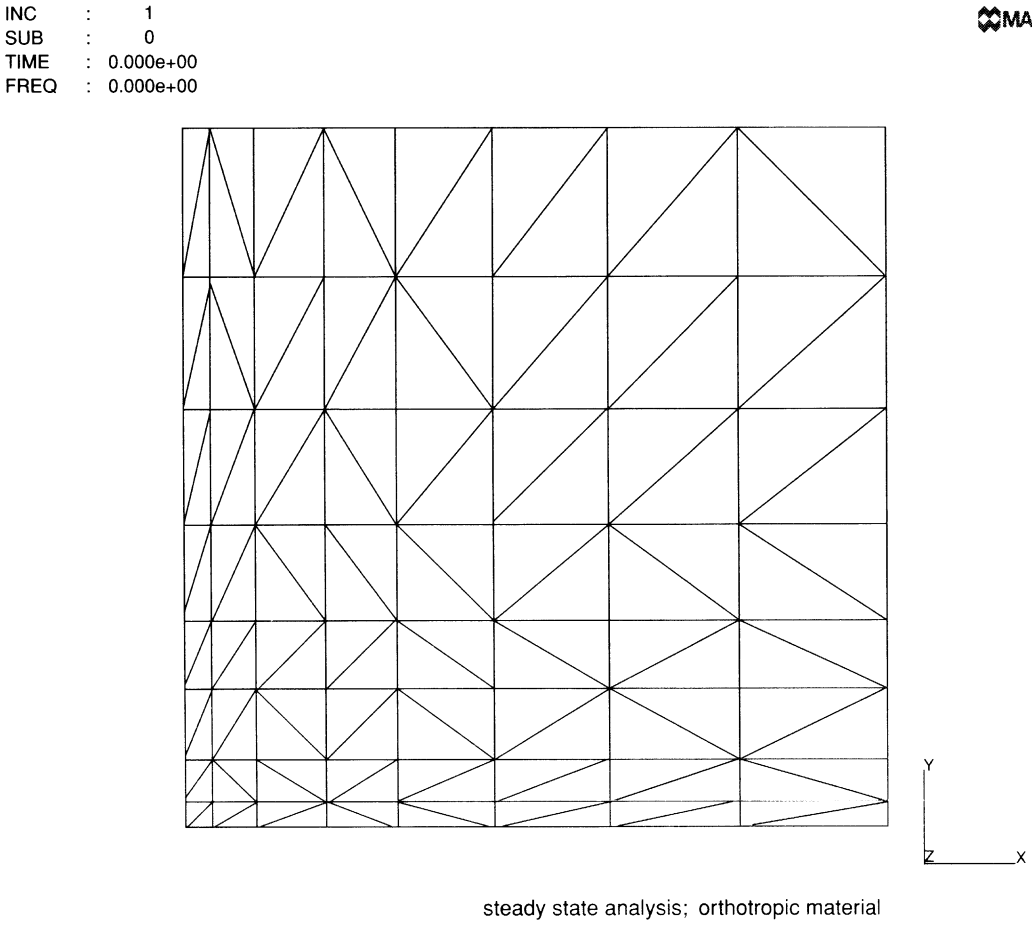

Figure E 5.18-1 Heated Square Plate, Geometry, and Finite Element Mesh

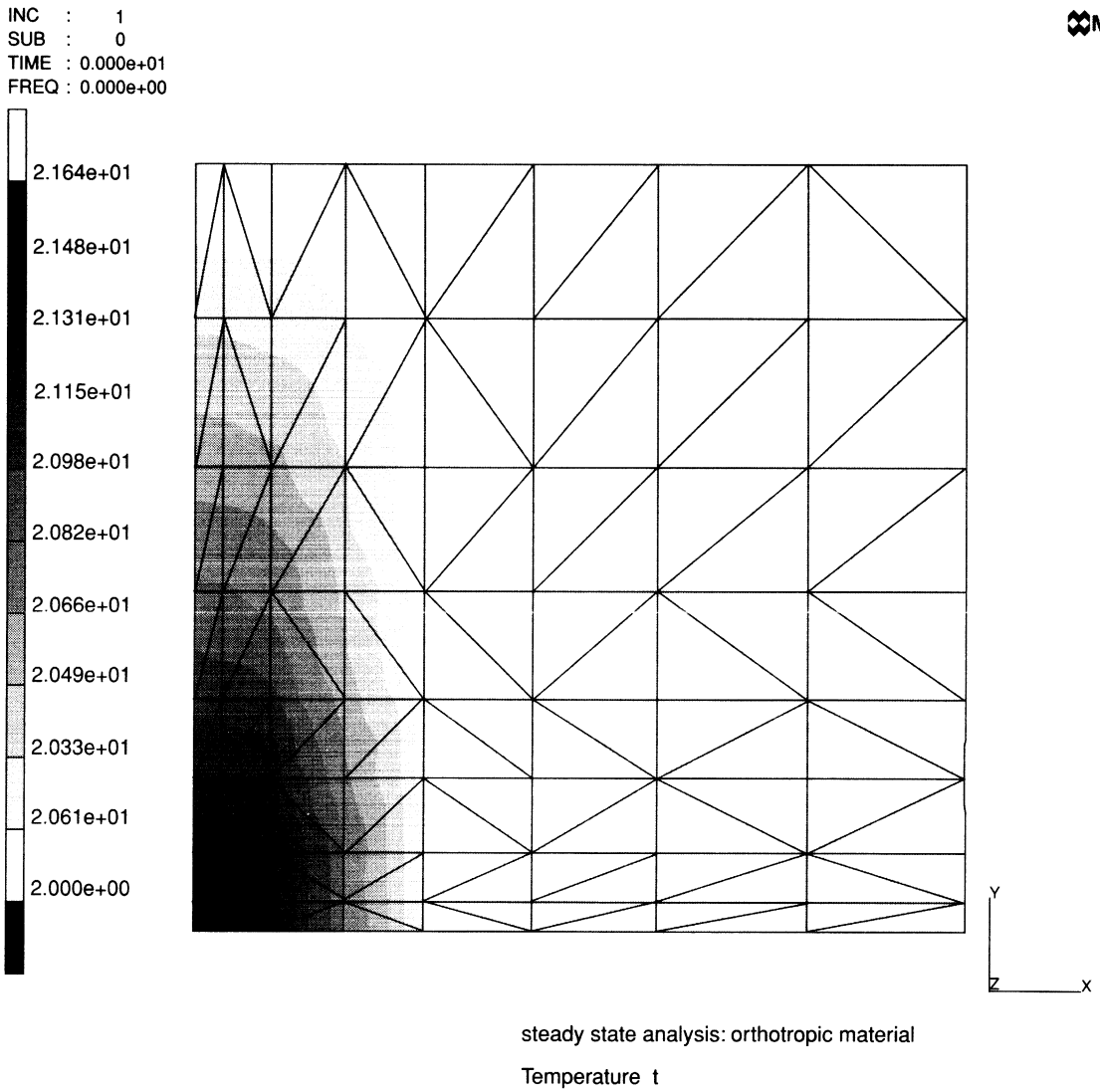

Figure E 5.18-2 Temperature Distribution Steady-state Analysis

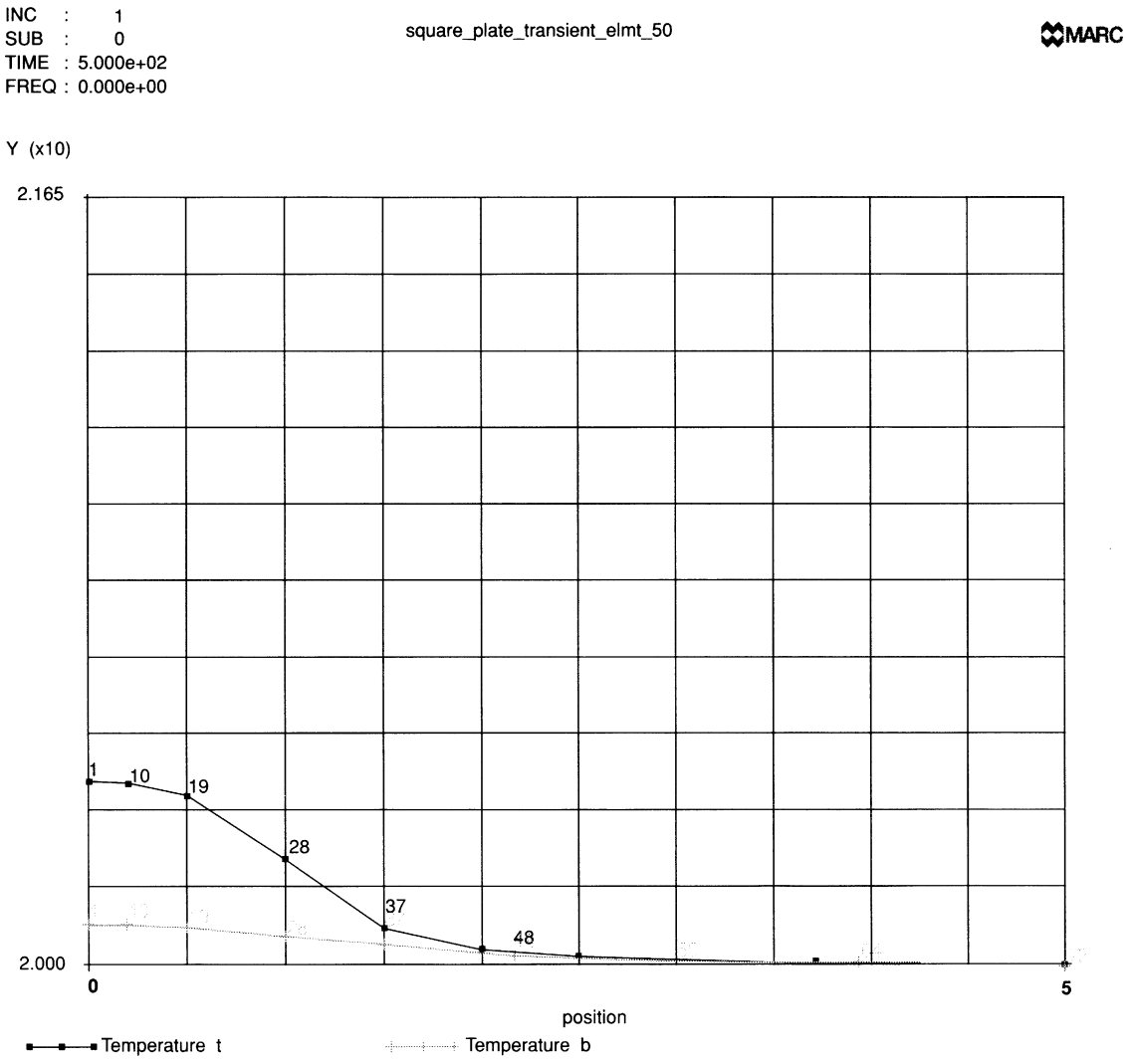

Figure E 5.18-3 Path Plots for Upper and Lower Temperature at x = 0 (inc = 1)

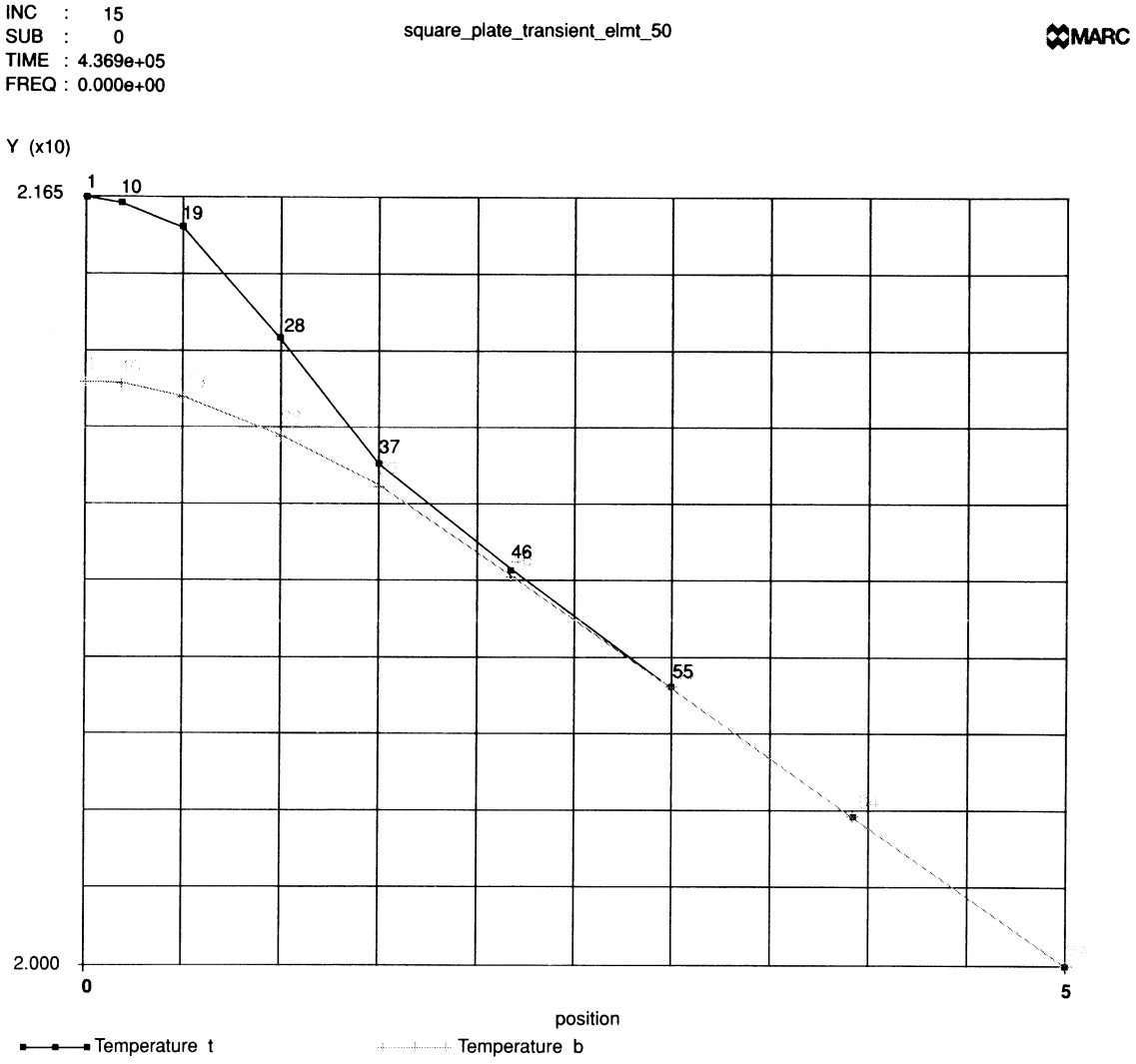

Figure E 5.18-4 Path Plots for Upper and Lower Temperature at x = 0 (inc = 15)

Volume E
Demonstration
Problems

Chapter 6
Dynamics

Chapter 6 Dynamics

MARC K.6 contains both the modal superposition and direct integration capabilities for the analysis of dynamic problems. A discussion on the use of these capabilities can be found in *Volume A, User Information* and a summary of the feature is given below.

Modal Analysis (inverse power sweep or Lanczos)

Direct Integration

- Newmark-beta operator
- Houbolt operator
- Central difference operator
- Modal superposition

Consistent and lumped mass matrices

Damping

- Modal damping
- Stiffness and/or mass damping
- Numerical damping

Initial conditions

- Nodal displacement
- Nodal velocity

Boundary conditions

- Nodal displacement history
- Nodal velocity history
- Nodal acceleration history

Nonlinear effects

- Material nonlinearity (i.e., plasticity)
- Geometric nonlinearity (i.e., large displacement)
- Boundary nonlinearity (i.e., gap-friction)

Variable time steps

- Newmark-beta operator

Compiled in this chapter are a number of solved problems. These problems illustrate the use of dynamic analysis options in the MARC program. Table E 6.0-1 shows the MARC elements and options used in these demonstration problems.

Table E 6.0-1 Dynamic Analysis Demonstration Problems

Problem Number (E)	Element Type	Parameter Options	Model Definition	Load Incrementation	User Subroutines	Problem Description
6.1	5 45	DYNAMIC	CONTROL PRINT CHOICE	DYNAMIC CHANGE DIST LOADS	—	Dynamic response of a simply supported beam subjected to a uniformly distributed load.
6.2	45	DYNAMIC	—	MODAL SHAPE RECOVER	—	Frequencies and modal shapes of a Timoshenko beam.
6.3	4 8	DYNAMIC	CONTROL UFXORD FXORD INITIAL CONDITIONS	MODAL SHAPE DYNAMIC CHANGE DIST LOADS	UFXORD	Dynamic analysis of a cantilever plate using the modal procedure. Both inverse power sweep and Lanczos method.
6.4	10	DYNAMIC LARGE DISP FOLLOW FOR	ROTATION A CONTROL	MODAL SHAPE DIST LOADS	—	Frequencies of a rotating disk (centrifugal loading effect).
6.5	27 41	DYNAMIC FLU LOAD	FLUID SOLID	MODAL SHAPE	—	Frequencies of fluid-solid coupled (dam/water) system.
6.6	9	LARGE DISP DYNAMIC RESPONSE	RESPONSE SPECTRUM	MODAL SHAPE SPECTRUM	—	Evaluate eigenvalues for a space frame and perform spectrum response calculation.
6.7	28 33	LARGE DISP HARMONIC	TYING PHI-COEFI MOONEY	HARMONIC DISP CHANGE	—	Evaluate the response of a rubber mount subjected to several frequencies.
6.8	35	LARGE DISP HARMONIC	PHI-COEFI MOONEY	HARMONIC DISP CHANGE	—	Evaluate the response of a rubber block subjected to several frequencies at different amounts of deformation.

Table E 6.0-1 Dynamic Analysis Demonstration Problems (Continued)

Problem Number (E)	Element Type	Parameter Options	Model Definition	Load Incrementation	User Subroutines	Problem Description
6.9	9	PRINT DAMPING LUMP DYNAMIC	POST INITIAL VEL DAMPING MASSES GAP DATA	DYNAMIC CHANGE	—	Elastic impact of a bar.
6.10	52	DYNAMIC	POST TYING MASSES	MODAL SHAPE RECOVER	—	Frequencies of an alternator mount.
6.11	30	DYNAMIC LINEAR	POINT LOADS	MODAL SHAPE	—	Modal analysis of a wing caisson.
6.12	9	DYNAMIC UPDATE LARGE DISP	POINT LOADS	PROPORTIONAL MODAL SHAPE	—	Vibration of a cable.
6.13	16	DYNAMIC LARGE DISP	INITIAL VELOCITY RESTART	AUTO TIME	—	Elastic-perfectly plastic beam explosively loaded.
6.14	27	DYNAMIC	DEFINE LORENZI	DYNAMIC CHANGE DIST LOADS	—	Impact loading of a center cracked rectangular plate. DeLorenzi method used to evaluate K.
6.15	7	LUMP DYNAMIC PRINT, 3	FIXED DISP	MODAL SHAPE RECOVER	—	Modal shape calculations using assumed strain element.
6.16	7	PRINT, 5 LARGE DISP DYNAMIC LUMP	INITIAL VELOCITY FIXED DISP DAMPING CONTACT	DYNAMIC CHANGE	—	Dynamic impact between deformable body and a rigid surface.

Table E 6.0-1 Dynamic Analysis Demonstration Problems (Continued)

Problem Number (E)	Element Type	Parameter Options	Model Definition	Load Incrementation	User Subroutines	Problem Description
6.17	7	PRINT, 5 DYNAMIC LUMP LARGE DISP	DAMPING FIXED DISP INITIAL VELOCITY CONTACT	DYNAMIC CHANGE	—	Dynamic contact between two deformable bodies.
6.18	52	DYNAMIC RESPONSE	CONN GENER NODE FILL	MODAL SHAPE RECOVER SPECTRUM	—	Spectral response of a pipe.
6.19	11	DYNAMIC LUMP	INITIAL VELOCITY CONTACT CONTACT TABLE	DYNAMIC CHANGE	—	Dynamic impact using explicit dynamics.
6.20	98	DYNAMIC	DIST LOADS FLUID DRAG	DYNAMIC CHANGE	—	Beam subjected to fluid loads.
6.21	72	DYNAMIC FOLLOW FOR LARGE DISP	DIST LOADS	DIST LOADS DISP CHANGE MODAL SHAPE RECOVER	—	Eigenvalues of structure with rigid body modes.

E 6.18 Spectral Response of a Pipe

This problem illustrates the spectrum response capabilities of the MARC program. The spectral displacements of a cantilever are computed and compared with analytical results.

Model

The structure is shown in Figure E 6.18-1. The mesh consists of 21 type 52 elements and 22 nodes.

Geometry

The pipe has a cross-sectional area of 5.34 E-3 square meters. The moments of inertia of the section are 1.936 E-5m^4 about the local x-axis and 1.936 E-5 m^4 about the local y-axis.

Boundary Conditions

The pipe is clamped at the left end. Node 1 is assumed to be fixed.

Material Properties

Young's modulus is 1.58 E11 Newton/m^2. The mass density is 21138 kg/m^3.

Displacement Spectral Density

A displacement spectral density function is entered through user subroutine USSD and is assigned in both the x- and y-directions. The spectral values are obtained from the spectral accelerations shown in Table E 6.18-2 via linear interpolation in a semilogarithmic plane.

Spectral Response

Four eigenvalues and the related eigenmodes were extracted using the inverse power sweep method. The response was calculated based on the extracted modes. The spectral displacements, both analytical and computed by the MARC program, are given in Table E 6.18-2. The eigenvalues are given in Table E 6.18-3.

Notice that the analytical values do not include the rotational inertia effects.

Table E 6.18-1 Spectral Accelerations [m/sec^2]

Frequencies (Hz)	Accelerations (g)
0.0001	0.03
0.1	0.03
0.85	0.98
1.15	0.98
3.21	0.35
3.83	0.44
5.18	0.44
13.	0.24
1000.	0.24

Table E 6.18-2 Displacements [m] in x and y Direction

z	Analytical	MARC Program
0.8	3.77 E-4	3.78 E-4
1.2	8.08 E-4	8.10 E-4
1.8	1.68 E-3	1.69 E-3
2.2	2.39 E-3	2.39 E-3
2.8	3.56 E-3	3.56 E-3
3.4	4.81 E-3	4.82 E-3
4.0	6.10 E-3	6.11 E-3
4.265	6.67 E-3	6.68 E-3

Table E 6.18-3 Eigenvalues [Hz]

N	Analytical	MARC Program
1	5.066	5.059
2	5.066	5.059
3	31.986	31.61
4	31.986	31.61

Summary of Options Used

Listed below are the options used in example e6x18.dat:

Parameter Options

DYNAMIC
ELEMENTS
END
RESPONSE
SIZING
TITLE

Model Definition Options

CON GENER
CONNECTIVITY
COORDINATE
END OPTION
FIXED DISP
GEOMETRY
ISOTROPIC
NODE FILL
POST

Load Incrementation Options

CONTINUE
MODAL SHAPE
RECOVER
SPECTRUM

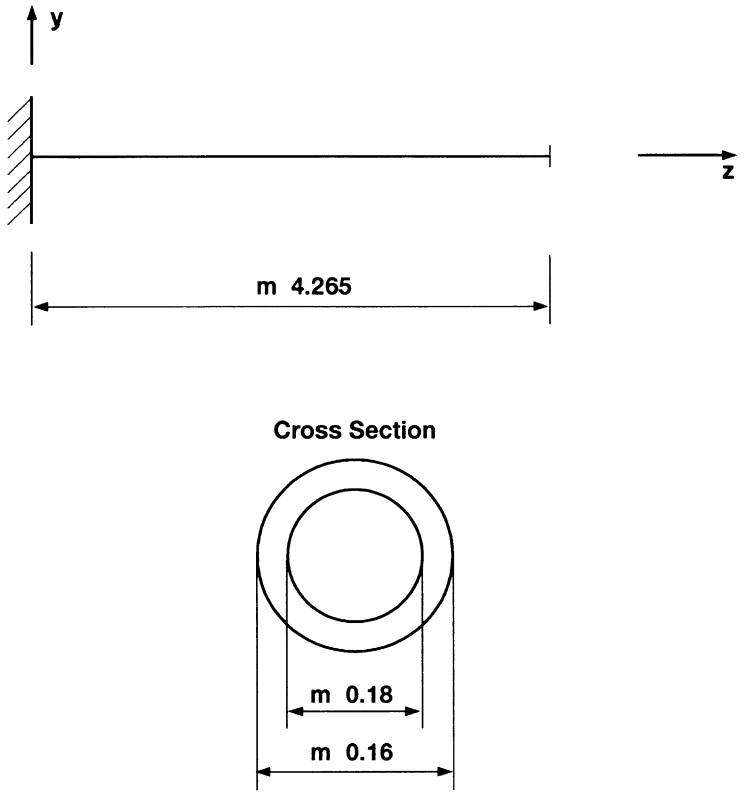

Figure E 6.18-1 Cantilever Pipe and its Cross Section

E 6.19 Dynamic Impact of Two Bars

This problem demonstrates the dynamic impact of a bar hitting against another bar fixed in space using the explicit method. The DYNAMIC, 5 option is used in this example.

Element

Element type 11, a plane-strain element has been used to model both bars. Both bars are 10 cm x 1 cm and are modeled by 10 beam elements, respectively. There is a 0.5 cm gap between the two bars as shown in Figure E 6.19-1.

Model

The structure is shown in Figure E 6.19-1. The mesh consists of 20 type 10 elements and 44 nodes.

Material Properties

The material properties of both bars are:

Young's modulus is E = 1000.0 N/cm^2
Poisson's ratio is ν = 0.0
Mass density is rho = 1.0 kg/cm^3

Boundary Conditions

Only the displacement along x-direction is free. The bar at the right is fixed at the right end.

Dynamics

The body has an initial velocity of 1.0 cm/second. The case has been studied for 12.0 seconds using a time step of 0.04 second through the DYNAMIC CHANGE option.

Results

Figure E 6.19-2 illustrates contact occurring at increment 13 and separation occurring approximately at increment 125. Figure E 6.19-3 and Figure E 6.19-4 show the velocity and acceleration histories. The reaction force at the wall is shown in Figure E 6.19-5.

Summary of Options Used

Listed below are the options used in example 6x19.dat:

Parameter Options

SIZING
ELEMENTS
DYNAMIC
PRINT
LUMP

Model Definition Options

CONNECTIVITY
OPTIMIZE
COORDINATES
ISOTROPIC
INITIAL VELOCITY
CONTACT
CONTACT TABLE
FIXED DISPLACEMENT
POST
PRINT ELEMENT
PRINT NODE
END OPTION

Load Incrementation Options

DYNAMIC CHANGE
CONTINUE

MARC

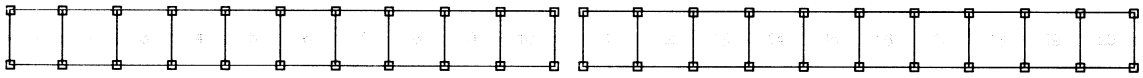

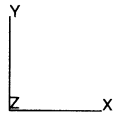

Figure E 6.19-1 Finite Element Mesh of Two Bars

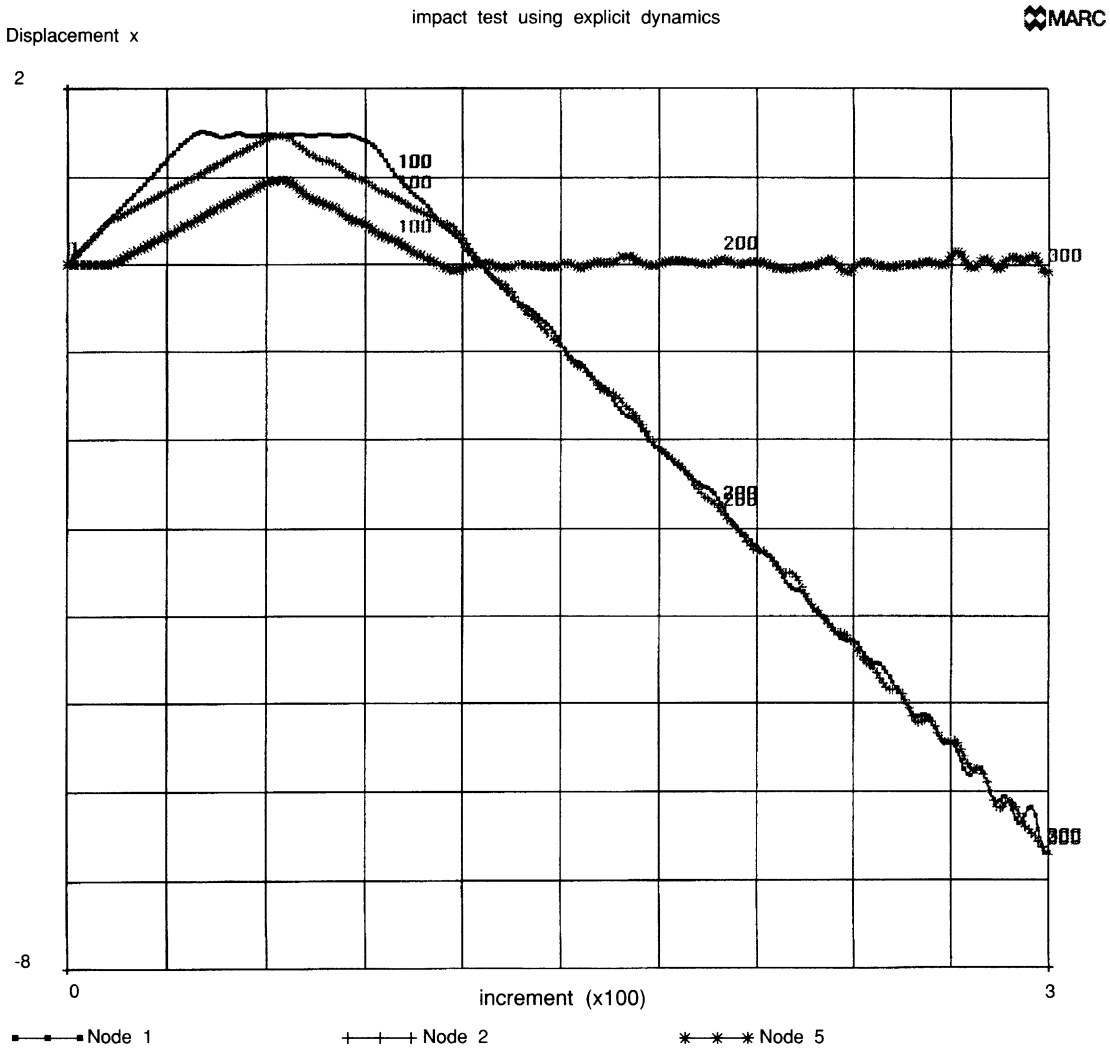

Figure E 6.19-2 Displacement History of Selected Nodes

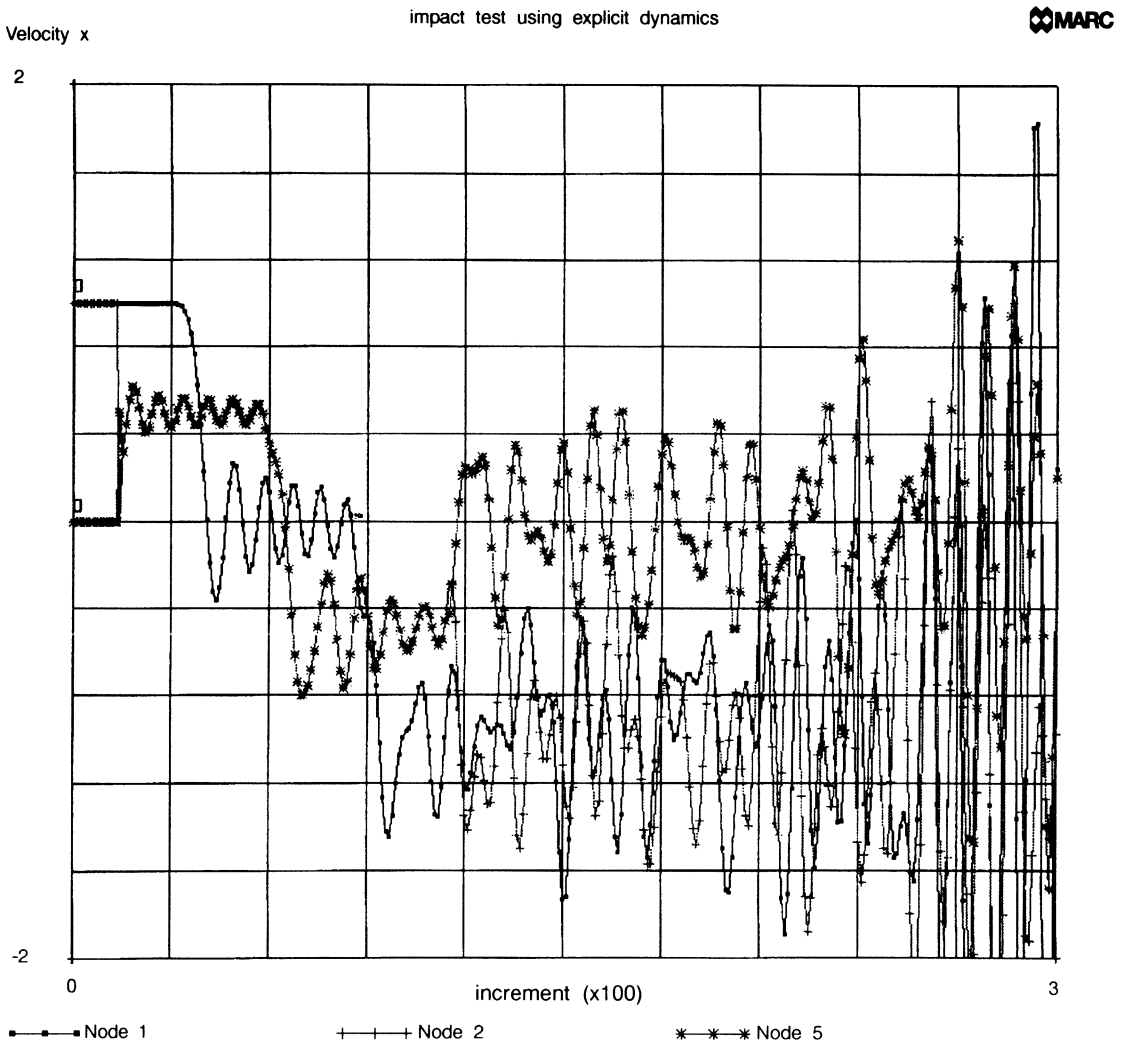

Figure E 6.19-3 Velocity History of Selected Nodes

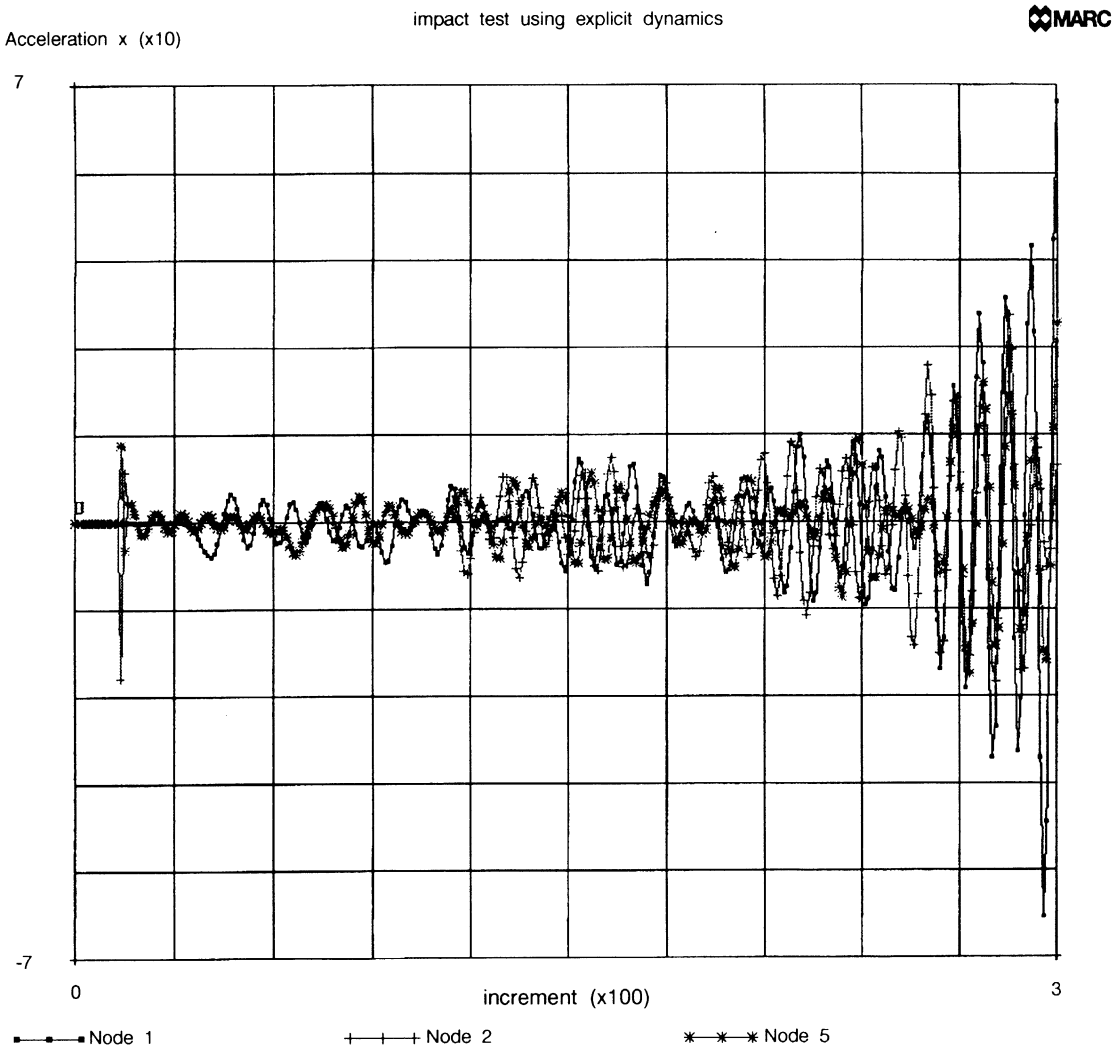

Figure E 6.19-4 Acceleration History of Selected Node

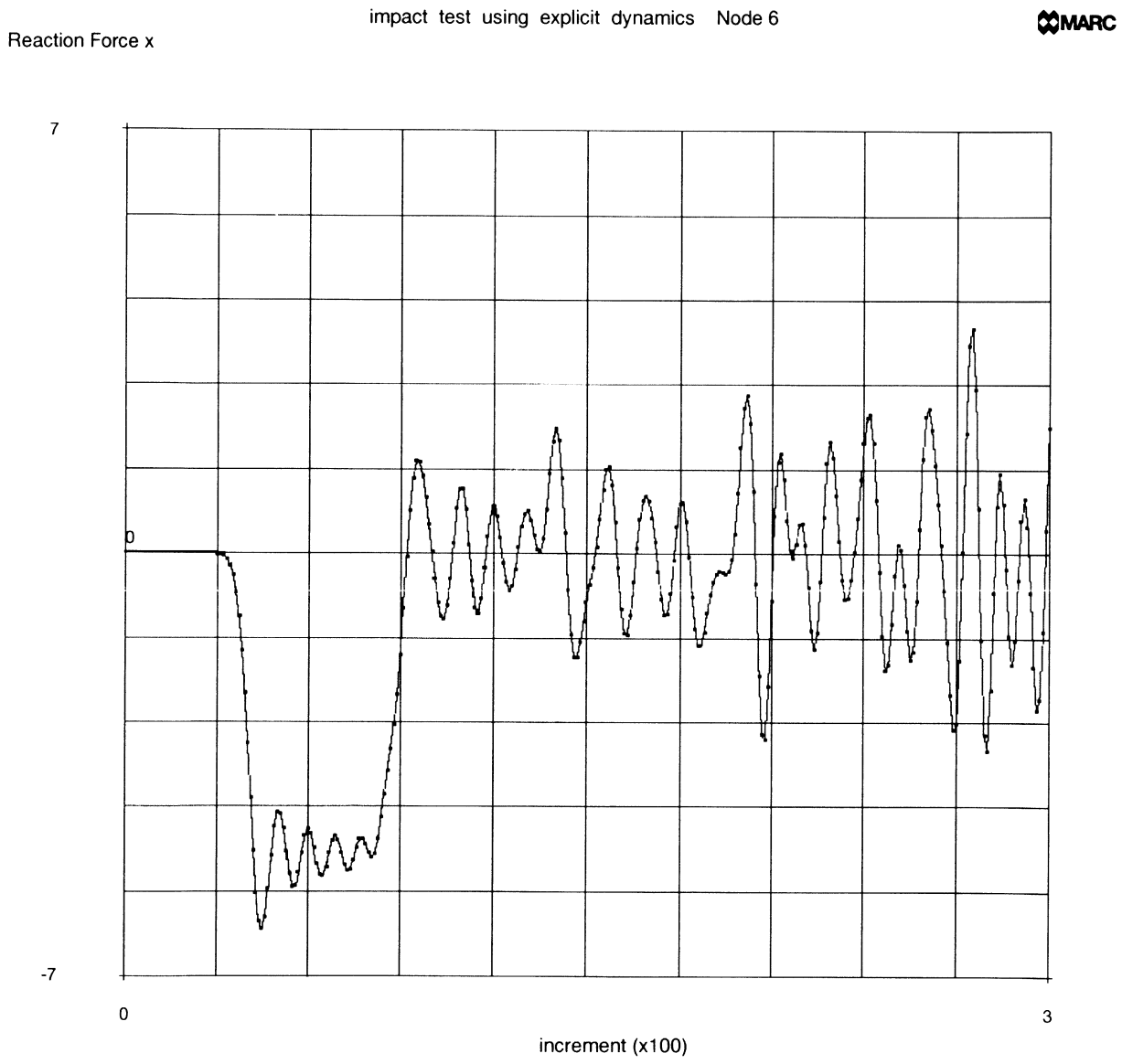

Figure E 6.19-5 Reaction Force at Wall

E 6.20 Elastic Beam Subjected to Fluid-Drag Loading

This problem demonstrates an elastic beam partially submerged under a flowing fluid being analyzed for static analysis. In addition, a dynamic analysis is performed in which wave loading is also considered.

Element

Element type 98, a 2-node straight elastic beam with the transverse shear effect in its formulation, is used.

Model

An elastic beam of length 115.47 m which lies at an angle of 60° is partially submerged under some fluid (Figure E 6.20-1). The depth of the fluid of 50 m. The beam is modeled using 10 elements and 11 nodes.

Geometry

The GEOMETRY block is used for inputting beam section properties. The beam has a cross-section area of 0.1935 m^2 and moments of inertia (I_{xx} and I_{yy}) equaling 0.00321 m^4.

Material Properties

The material of the beam is assumed to have a Young's modulus of 2.6e+07 $N/m^2$and a Possion's ratio of 0.3. The beam has a mass density of 8.0e+4 Kg/m^3.

Loading

Elements 1 to 5 are subjected to fluid drag loading. The mass density of the fluid inside the pipe is assumed to be 0.8 Kg/m^3 and the fluid outside of the pipe is assumed to be 1 Kg/m^3. The gravity constant is assumed to be 10 m/sec^2. The drag coefficient is assumed to be 0.05, and the inertia coefficient is assumed to be 0.05. The fluid outside of the pipe is flowing with a velocity of 1 m/sec in the x-direction. It has a velocity gradient of 0.04 per second. For the dynamic analysis case, the beam is subjected to wave loading in addition to the fluid-drag loading. The wave height is assumed to be 2 and the wave period is assumed to be 5. The wave phase is taken to be 0. The wave front is assumed to be moving in the x-direction.

Boundary Conditions

Nodes 1 and 11 are assumed to be hinged ($u_x = u_y = u_z = \theta_x = \theta_z = 0$).

Results

The displacements of the beam due to fluid drag loading are given in Table E 6.20-1.

Table E 6.20-1 Displacements of the Beam (m)

Node	u_x (m)	u_z (m)	θ_y (rad)
1	0	0	-7.96×10^{-2}
2	-0.767	0.443	-7.40×10^{-2}
3	-1.432	0.827	-5.89×10^{-2}
4	-1.916	1.106	-3.78×10^{-2}
5	-2.176	1.256	-1.41×10^{-2}
6	-2.204	1.272	8.60×10^{-3}
7	-2.021	1.167	2.79×10^{-2}
8	-1.666	0.962	4.3×10^{-2}
9	-1.183	0.683	5.37×10^{-2}
10	-0.613	0.354	6.02×10^{-2}
11	0	0	6.23×10^{-2}

Summary of Options Used

Listed below are the options used in example 6x20a.dat:

Parameter Options

ALIAS
ELEMENT
END
SIZING
TITLE

Model Definition Options

CONNECTIVITY
COORDINATES
DIST LOADS
END OPTIONS
FIXED DISP
FLUID DRAG
GEOMETRY
ISOTROPIC

Load Incrementation Options

DYNAMIC CHANGE
CONTINUE

Listed below are the options used in example 6x20b.dat:

Parameter Options

ALIAS
DYNAMIC
ELEMENT
END
SIZING
TITLE

Model Definition Options

CONNECTIVITY
COORDINATES
DIST LOADS
END OPTION
FIXED DISP
FLUID DRAG
GEOMETRY
ISOTROPIC

History Definition Options

CONTINUE
DIST LOADS
DYNAMIC CHANGE

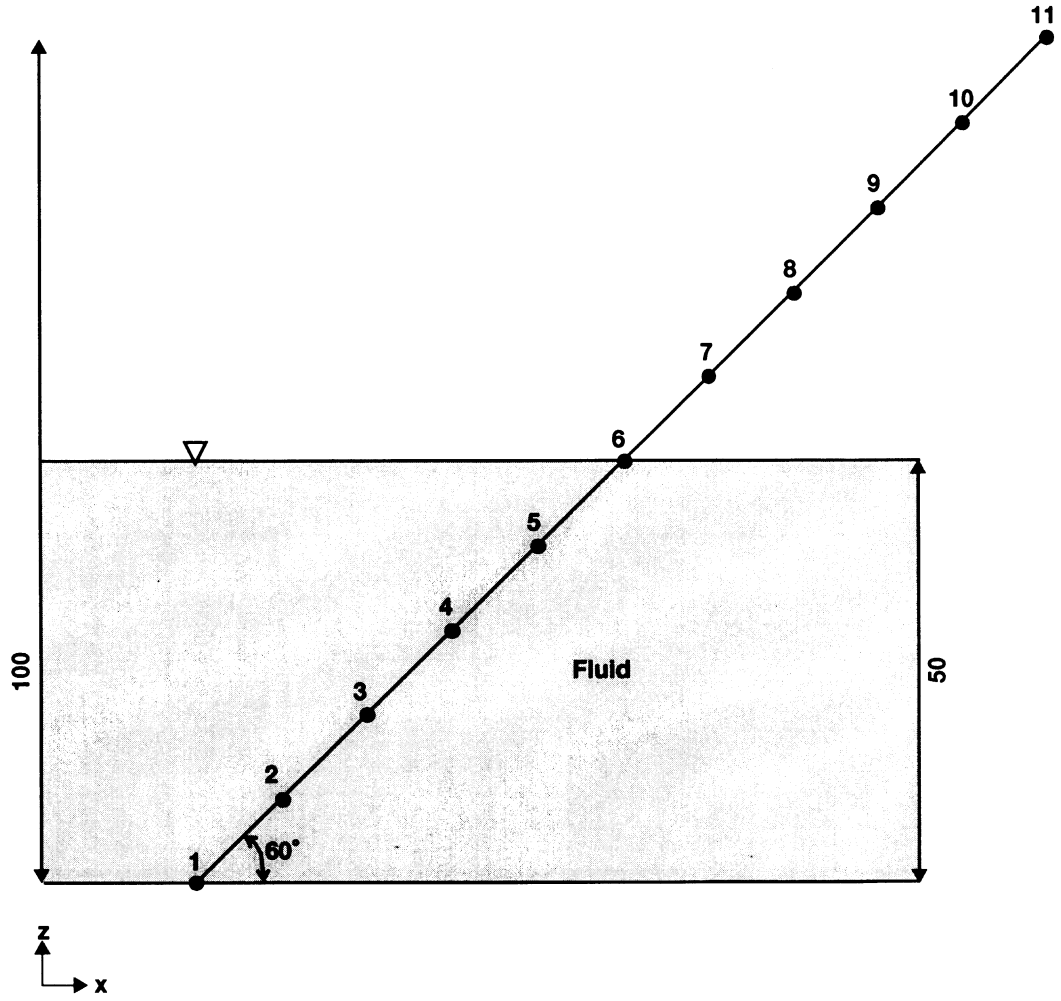

Figure E 6.20-1 Beam Partially Submerged in Fluid

E 6.21 Eigenvalue Analysis of Cubic Box

This example demonstrates the use of follower force stiffness for the eigenvalue analysis of a preloaded cubic box.

Element

Library element type 72, a thin shell, is used for this analysis. There are 96 elements and 290 nodes in the model as shown in Figure E 6.21-1. the box, 10 cm x 10 cm x 10 cm, is fixed in space to prevent rigid body motion and preloaded with uniform pressure of 10.0 N/cm^2. The rigid body constraint is then released and the eigenvalue analysis is preformed. The FOLLOW FOR option is used to insure that the load is applied on the deformed geometry.

Material Properties

The material is elastic and its properties are:

Young's modulus is	E	= 10000.0 N/cm^2
Poisson's ratio is	ν	= 0.45
Mass density is	ρ	= 7.0e-5 kg/cm^3

Geometry

The thickness of the shell is 0.5 cm.

Boundary Conditions

The model is fixed at three corners of the box. The constraints are then released to demonstrate the extraction of rigid body modes.

Control

The full Newton-Raphson iterative method is used with a convergence tolerance of 0.0001% on residuals requested.

Results

The modal shapes are shown in Figure E 6.21-2 andFigure E 6.21-2. The six eigenvalues for rigid body are:

Eigenvalue	With Follower Force Stiffness (Cycles/s)	Without Follower Force Stiffness (Cycles/s)
1	1.29857e-4	3.38527e-6
2	9.55539e-6	5.83730e-6
3	1.75523e-5	1.94645e-4
4	5.2039e+0	30.1477e+0
5	5.20390e+0	30.1573e+0
6	5.20390e+0	30.1478e+0

You can observe that the inclusion of the follower force stiffness results in a more accurate representation.

Summary of Options Used

Listed below are the options used in example e6x21.dat:

Parameter Options

ELEMENT
DYNAMIC
FOLLOW FOR
END
LARGE DISP
SIZING
TITLE

Model Definition Options

CONNECTIVITY
CONTROL
COORDINATES
GEOMETRY
ISOTROPIC
FIXED DISP
DEFINE
DIST LOADS
END OPTION
OPTIMIZE
POST

Load Incrementation Options

DIST LOADS
AUTO LOAD
CONTINUE
TIME STEP
DISP CHANGE
MODAL SHAPE
RECOVER

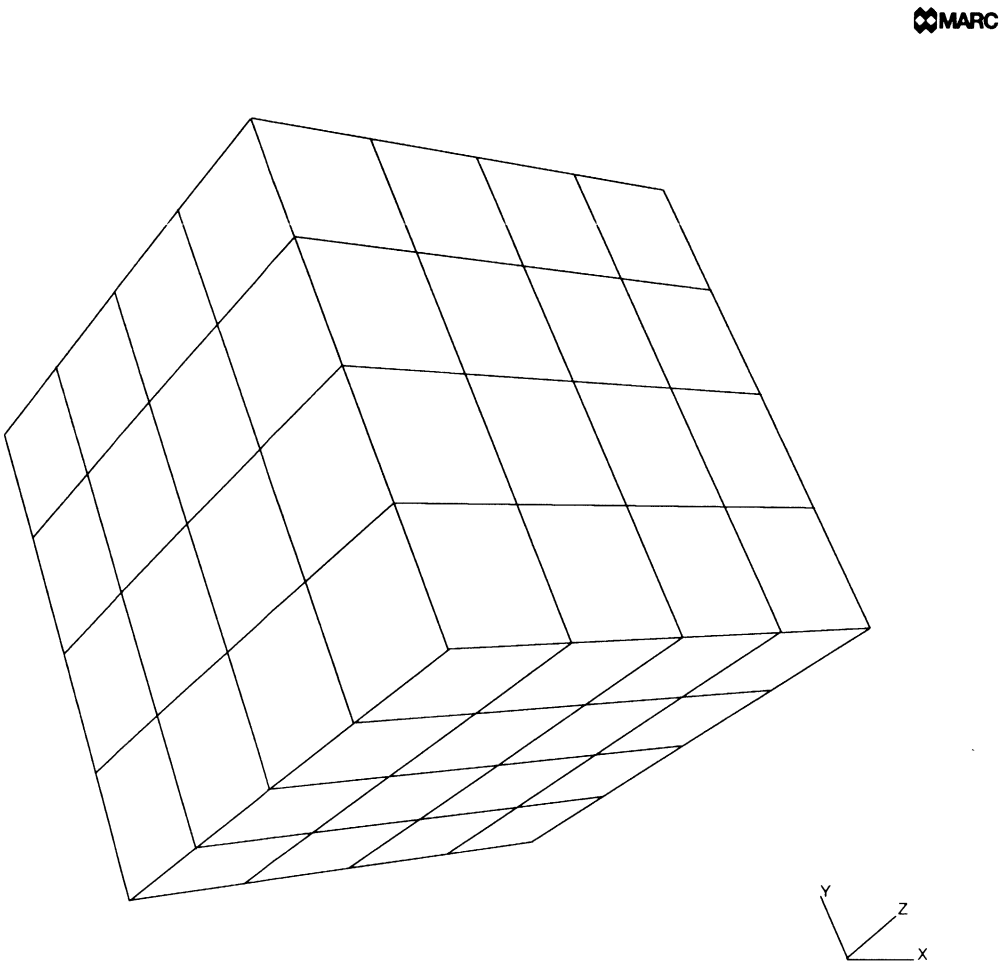

Figure E 6.21-1 Mesh of Box

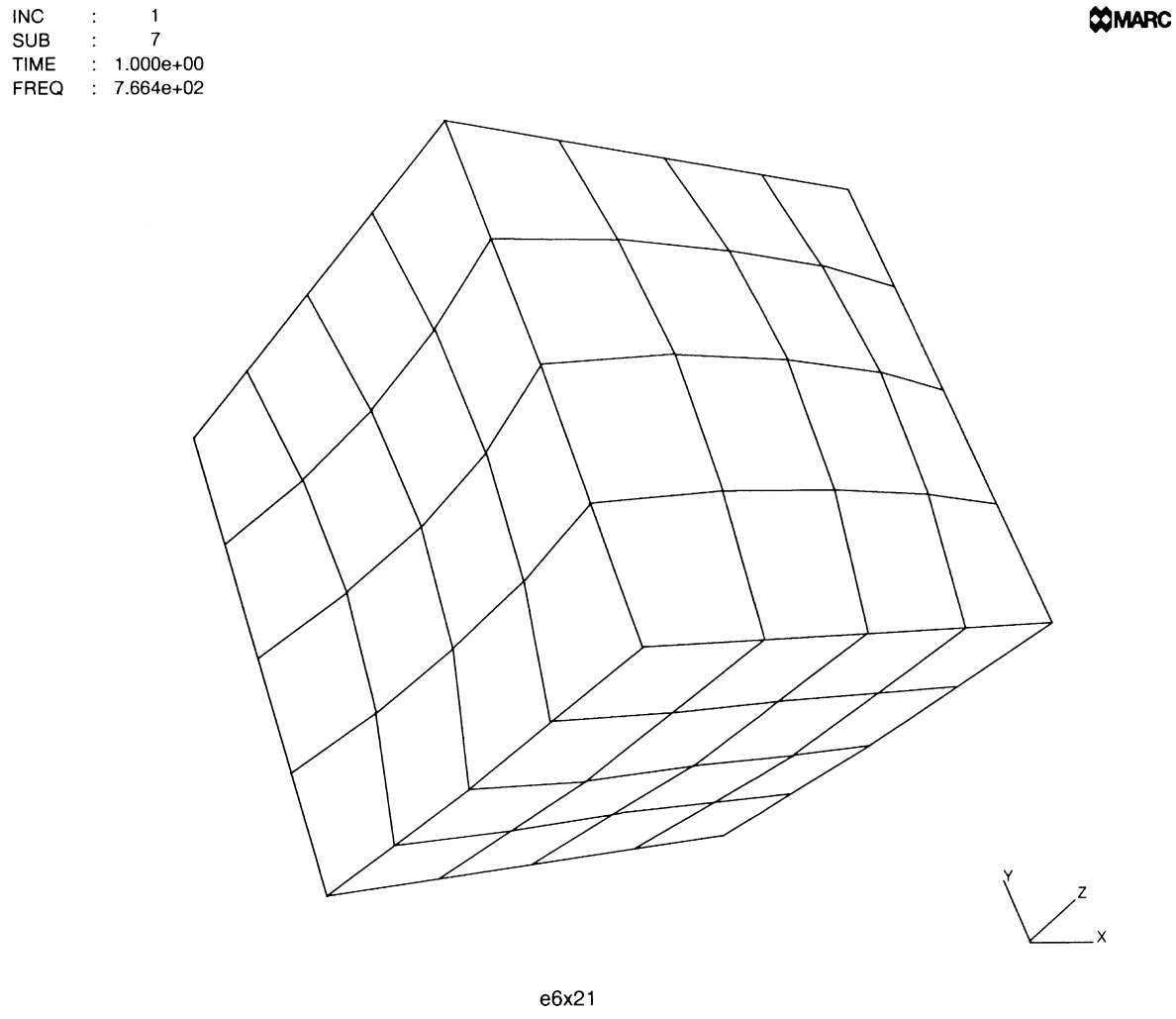

Figure E 6.21-2 Seventh Eigenmode

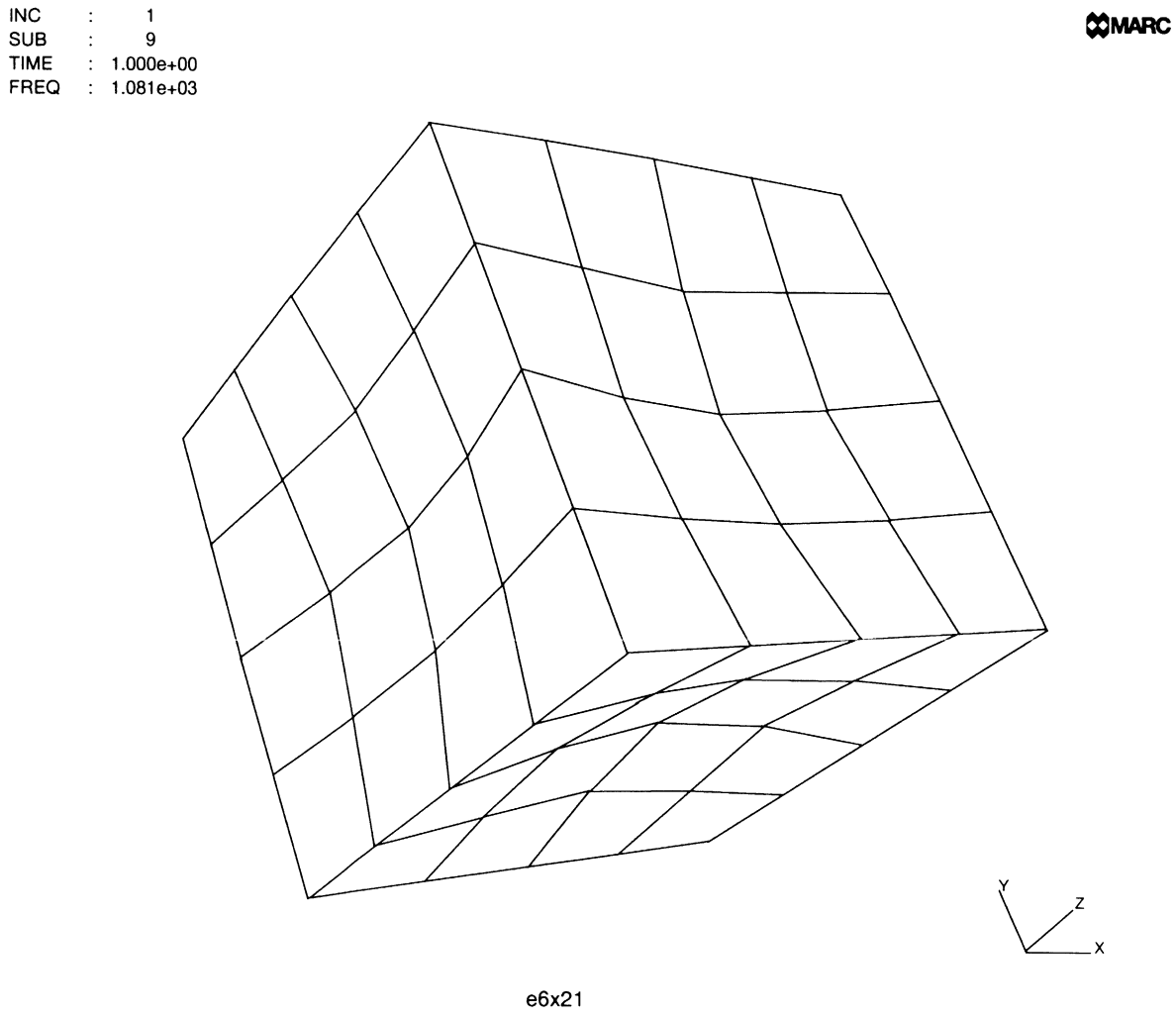

Figure E 6.21-3 Ninth Eigenmode

Volume E
Demonstration Problems

Chapter 7
Contact

Chapter 7 Contact

Special Analysis Capabilities in the MARC Program

In addition to the various analysis capabilities discussed in previous chapters concerned with problems of linear elasticity, plasticity and creep, large displacement, heat transfer as well as dynamics, this chapter contains demonstration problems for the illustration of additional analysis capabilities in the MARC problem. Detailed discussions of these capabilities can be found in *Volume A, User Information* and a summary of the various capabilities illustrated is given below.

- Steady, creeping flow of rigid, perfectly plastic material (R-P Flow).
- The use of gap-friction element (Element Type 12 and Type 97).
- Analysis of concrete (CRACKING) structures.
- Analysis of rubber structures (MOONEY, OGDEN, and FOAM).
- Simulation of composite material (COMPOSITE).
- Simulation of viscoelastic material.
- Axisymmetric structure under nonsymmetric loading (FOURIER Analysis).
- Study of mesh refinement (QUALIFY).
- Analysis of hydrodynamic bearings.
- Use of the rezoning technique for large deformation analysis.

Compiled in this chapter are a number of solved problems. Table E 7.0-1 shows the MARC elements and options used in these demonstration problems.

Table E 7.0-1 Special Topics Demonstration Problems

Problem Number (E)	Element Type	Parameter Options	Model Definition	Load Incrementation	User Subroutines	Problem Description
7.1	32	ELSTO R-P FLOW	CONTROL	AUTO LOAD	—	Steady, creeping flow of rigid, perfectly plastic material (R-P Flow).
7.2	10 12	—	OPTIMIZE CONTROL ISOTROPIC GAP DATA	POINT LOADS DIST LOADS AUTO LOAD	—	The use of gap-friction element in the analysis of a man-hole cover in a pressure vessel.
7.3	75	SHELL SECT	UFXORD CONTROL CRACK DATA ISOTROPIC	AUTO INCREMENT	UFXORD	Analysis of a concrete barrel vault shell subjected to self-weight.
7.4	12 32	LARGE DISP	RESTART CONTROL MOONEY GAP DATA	PROPORTIONAL AUTO LOAD	—	Side pressing of a hollow rubber cylinder.
7.5	33 82 119	LARGE DISP FOLLOW FOR	NODE FILL CONTROL MOONEY	DIST LOADS	—	Analysis of a thick rubber cylinder.
7.6	75	SHELL SECT	DEFINE COMPOSITE ORIENTATION ORTHOTROPIC PRINT ELEM	—	—	Elastic analysis of a multilayered square plate under uniform pressure (composite material).
7.7	75	SHELL SECT	DEFINE COMPOSITE ORTHOTROPIC PRINT ELEM ORIENTATION INITIAL STATE CHANGE STATE	—	—	Elastic analysis of a multilayered square plate subjected to uniform pressure and thermal loading (composite material).

Table E 7.0-1 Special Topics Demonstration Problems (Continued)

Problem Number (E)	Element Type	Parameter Options	Model Definition	Load Incrementation	User Subroutines	Problem Description
7.8	62	FOURIER	CONTROL FOURIER RESTART	—	UFOUR	Fourier analysis of a cylinder under external pressure.
7.9	62	FOURIER	CONTROL FOURIER RESTART CASE COMBIN	—	UFOUR	Fourier analysis of a cylinder in plane strain subjected to a line load.
7.10	27	MESH PLOT QUALIFY	POST	—	—	Use of the QUALIFY option for the study of mesh refinement.
7.11	3 9	—	CONTROL CRACK DATA ISOTROPIC RESTART	POINT LOAD	—	Analysis of a simply supported concrete beam subjected to concentrated loads.
7.12	27	—	TYING PRINT CHOICE ISOTROPIC VISCELPROP	AUTO LOAD TIME STEP	—	Analysis of a simply supported concrete beam subjected to concentrated loads.
7.13	14 17	SCALE ELSTO	TYING	AUTO LOAD PROPORTIONAL INC	—	Analysis of pipeline structure using element type 14 and 17, and the pipeline mesh generator MARCPIPE.
7.14	28	—	ISOTROPIC VISCELPROP PRINT CHOICE	AUTO LOAD TIME STEP	—	Internal pressurization of an externally reinforced long, thick walled, viscoelastic cylinder.
7.15	37	BEARING	THICKNESS VELOCITY TYING	—	UFXORD UFCONN UTHICK UVELOC UGROOV	Calculation of the pressure distribution in a spiral groove thrust bearing including grooves.

Table E 7.0-1 Special Topics Demonstration Problems (Continued)

Problem Number (E)	Element Type	Parameter Options	Model Definition	Load Incrementation	User Subroutines	Problem Description
7.16	39	BEARING	CONN GENER NODE FILL THICKNESS VELOCITY	DAMPING COMPONENTS STIFFNESS COMPONENTS THICKNESS CHANGE	UTHICK UBEAR	Analysis of a journal bearing. Determine the load carrying capacity of the bearing.
7.17	10	UPDATE FINITE LARGE DISP REZONE	FORCDT WORK HARD	AUTO LOAD COORDINATE CHANGE REZONE	FORCDT	Analysis of a thick-walled cylinder under internal pressure. Demonstration of rezoning capability.
7.18	32 12	LARGE DISP	MOONEY GAP DATA VISCELMOONEY	AUTO LOAD TIME STEP	—	Side pressing of a hollow viscoelastic rubber cylinder.
7.19	26	—	MOONEY TYING	AUTO LOAD	—	Plane stress stretching of a rubber sheet with a hole.
7.20	82	FOLLOW FOR PRINT, 5	DEFINE CONTACT CONTROL OGDEN	MOTION CHANGE AUTO LOAD DIST LOADS TIME STEP	—	Compression of an O-ring.
7.21	26	—	OGDEN	DISP CHANGE AUTO LOAD		Plane stress stretching of a rubber sheet with a hole.
7.22	75	LARGE DISP SHELL SECT	OGDEN DIST LOADS DAMAGE VISCELOGDEN	AUTO LOAD DIST LOADS TIME STEP	—	Loading of a rubber plate including damage and rate effects.
7.23	11	LARGE DISP	FOAM CONTACT	AUTO LOAD TIME STEP	—	Compression of a foam tube.

Table E 7.0-1 Special Topics Demonstration Problems (Continued)

Problem Number (E)	Element Type	Parameter Options	Model Definition	Load Incrementation	User Subroutines	Problem Description
7.24	75	—	ORIENTATION ORTHOTROPIC COMPOSITE	—	—	Demonstrate composites.
7.25	22	LARGE DISP	ORIENTATION ORTHOTROPIC FAIL DATA COMPOSITE	POINT LOAD POST INCREMENT AUTO LOAD PROPORTIONAL INC	—	Progressive failure of fiber reinforced composite.
7.26	95 97	—	GAP DATA WORK HARD DIST LOAD	DIST LOADS	—	Pipe collars in contact.

E 7.23 Compression of a Foam Tube

This example demonstrates the use of the generalized Ogden rubber foam model for the high compression of a tube.

Element

Library element 11, the plane strain, is used for this analysis. There are 140 elements and 175 nodes in the model as shown in Figure E 7.23-1. Two rigid plates are moving toward the tube. The tube has an inner radius of 20 cm and an outer radius of 10 cm. Because of symmetry, only half of the tube of modelled.

Material Properties

The foam tube can be described using the foam material model using a two term series. The data was fixed such that:

Term	μ (N/cm)	α	β
1	0.0	2.0	-1.0
2	-32.0	-2.0	1.0

Contact/Boundary Conditions

All of the kinematic constrains are provided using rigid contact surfaces. The contact tolerance and the bias factor are set to 0.2 cm and 0.99 cm, respectively.

The rigid surface at the bottom and top move at a speed of 1.5 cm/second in a period of 8.15 seconds toward the tube.

Control

The full New-Raphson iterative method is used with a convergence tolerance of 1% on residuals requested.

Results

The deformed mesh at increments 10, 16, and 29 are shown in Figure E 7.23-2 through Figure E 7.23-4. The shear strain distribution is shown in Figure E 7.23-5. Using Mentat, you can determine that the initial area is 469.90 cm^2 and the final area is 421.05 cm^2; hence, there is a 10% reduction in volume.

Summary of Options Used

Listed below are the options used in example e7x23.dat:

Parameter Options

ALL POINTS
ELEMENTS
END
LARGE DISP
PRINT
SETNAME
SIZING
TITLE

Model Definition Options

CONNECTIVITY
CONTACT
CONTROL
COORDINATE
DEFINE
END OPTION
FIXED DISP
FOAM
NO PRINT
OPTIMIZE
POST
SOLVER

Load Incrementation Options

AUTO LOAD
CONTINUE
TIME STEP

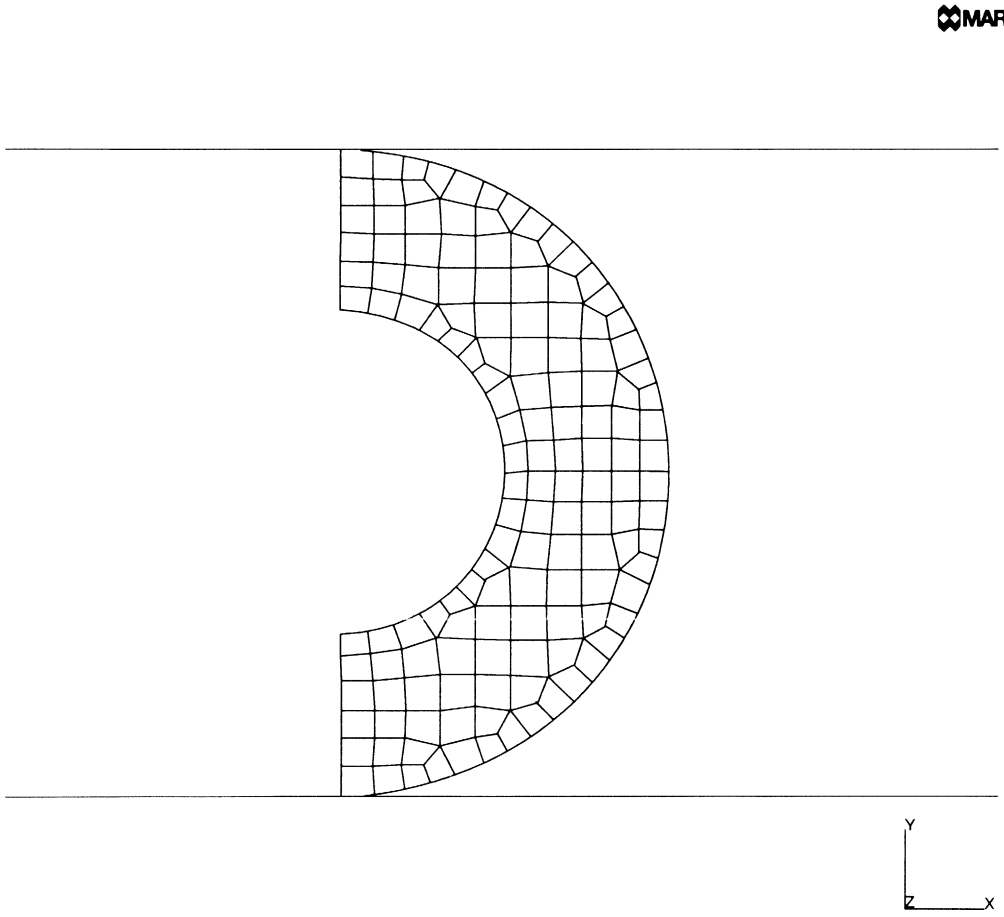

Figure E 7.23-1 Finite Element Mesh of Tube

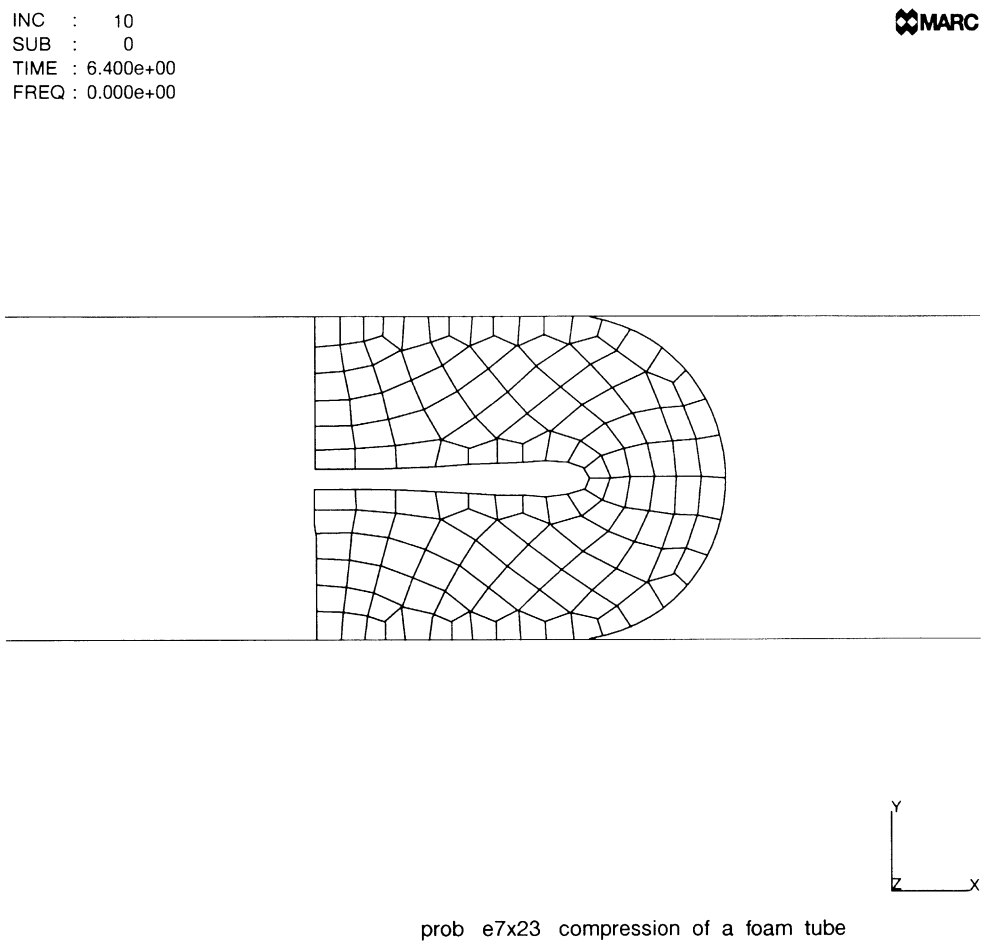

Figure E 7.23-2 Deformed Mesh at Increment 10

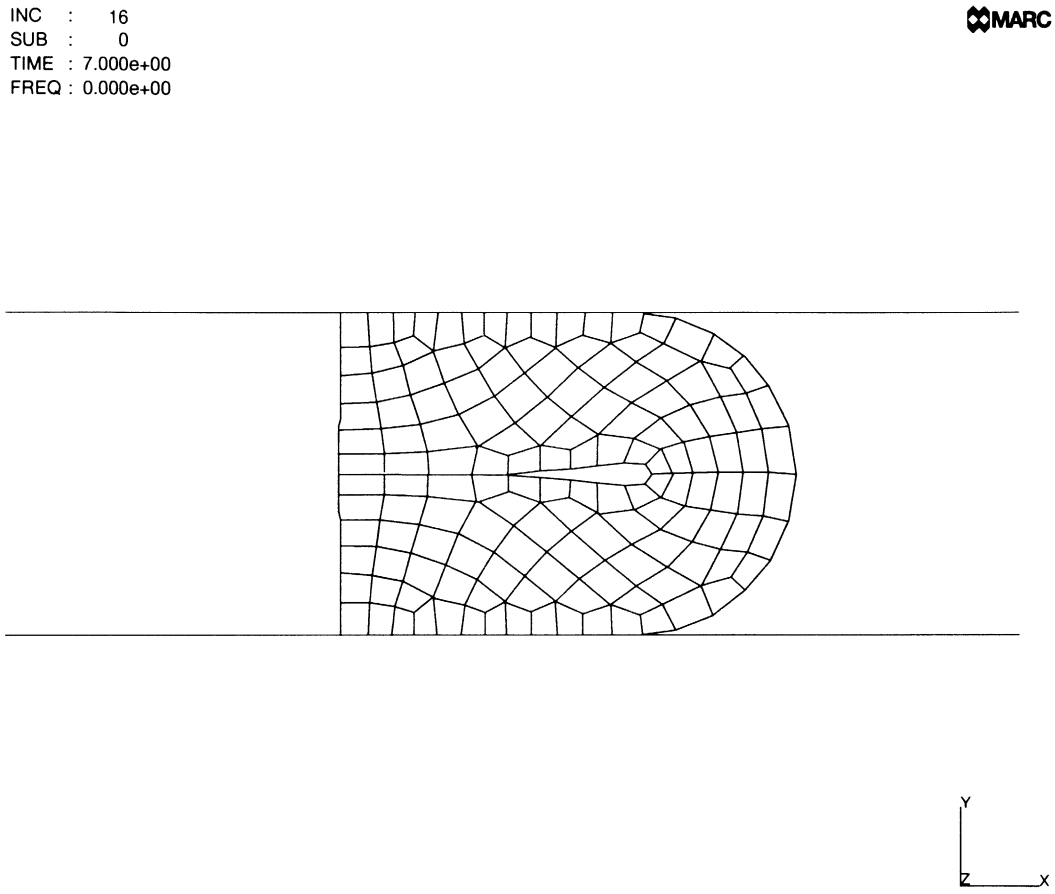

Figure E 7.23-3 Deformed Mesh at Increment 16

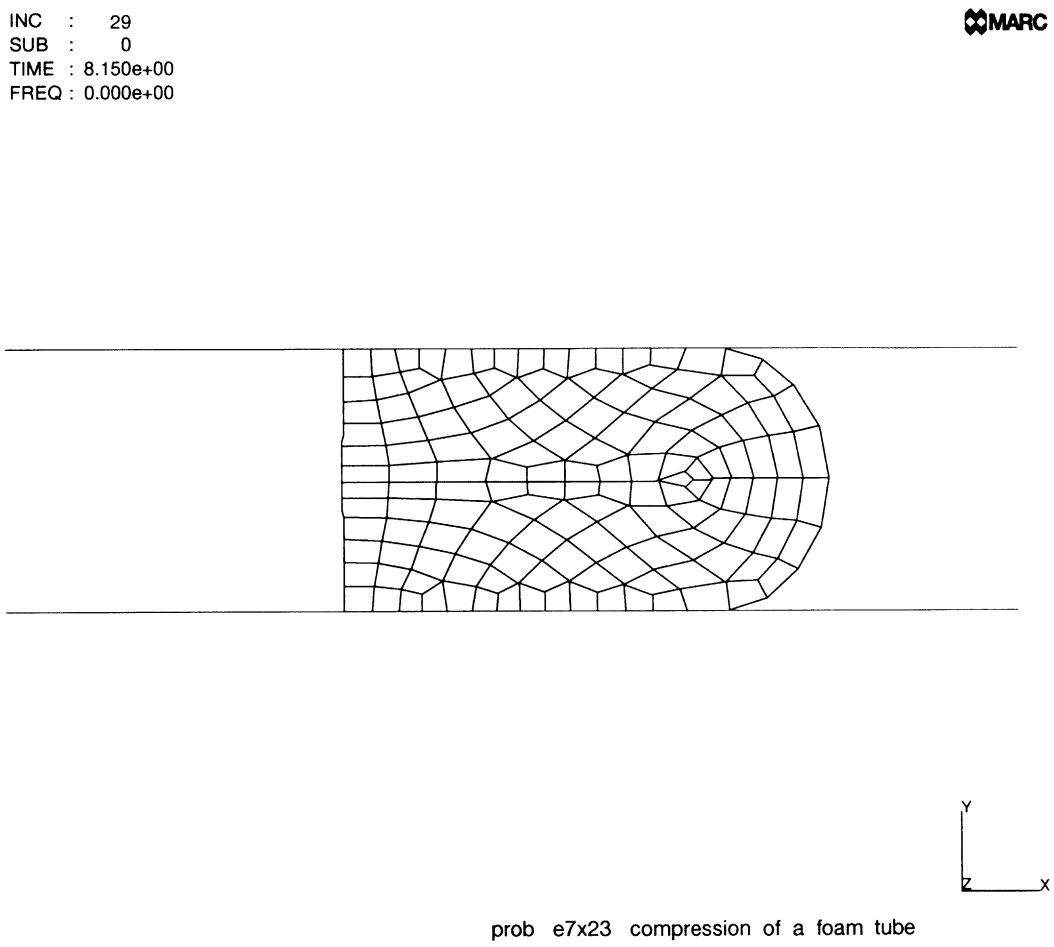

Figure E 7.23-4 Deformed Mesh at Increment 29

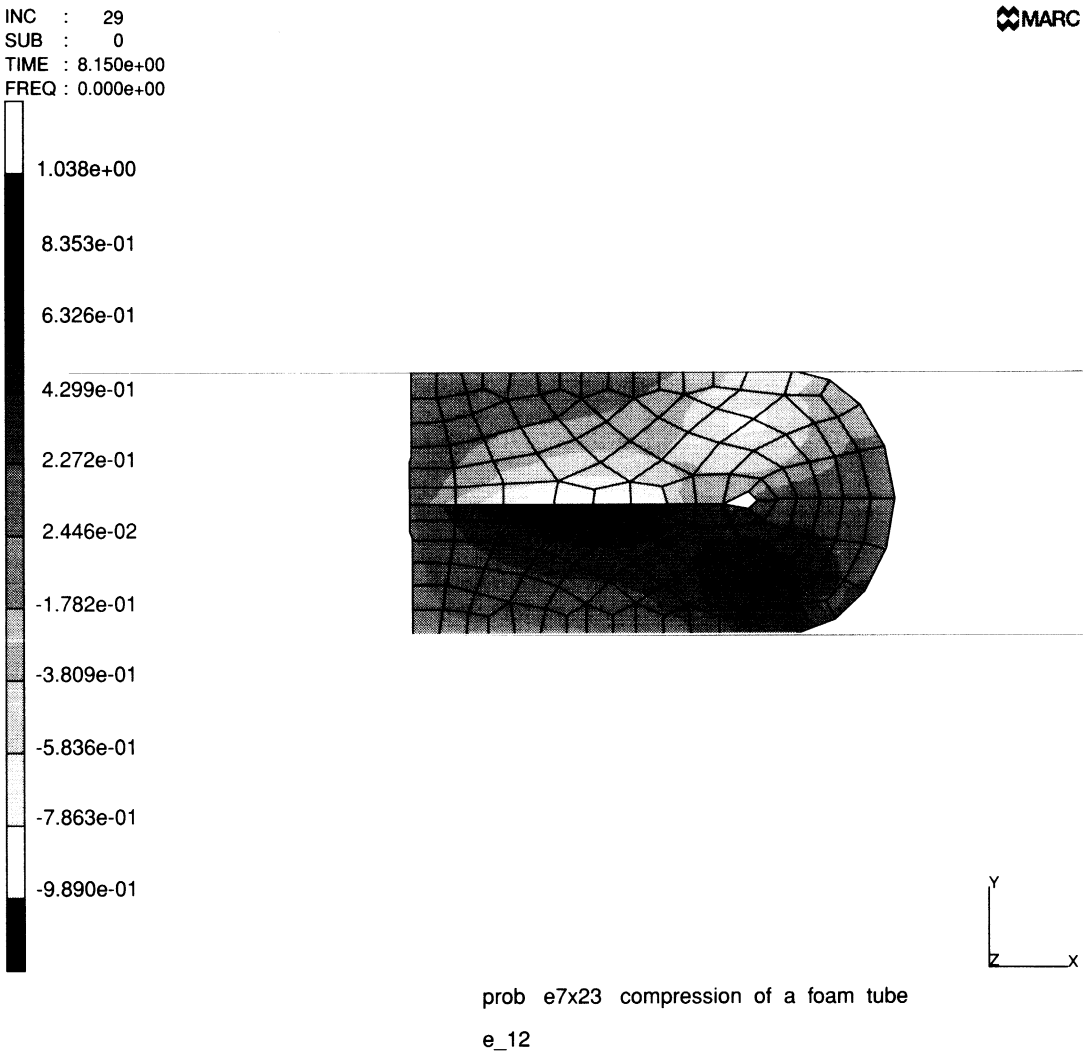

Figure E 7.23-5 Shear Strain in Compressed Tube

E 7.24 Constitutive Law for a Composite Plate

This example provides an analytic qualification of the constitutive law existing in a composite laminated plate. The model is made of a single finite element.

Model

The plate is made of a single shell element (element 75 in the MARC program). The element has four nodes with bilinear interpolation of displacement and rotation components.

Material Properties

The plate is made of eight laminae of boron-epoxy set to produce an equilibrated and symmetric laminate with the angles:

/+45/-45/+45/-45/S

Each lamina in boron-epoxy has the following properties of orthotropic material:

E_{11} = 29.7 E6 psi
E_{22} = 2.97 E6 psi
ν_{12} = 0.33
G_{12} = 1. E psi

Geometry

The plate has total thickness THT = 0.4 inches. The thickness in every lamina is thus THL = 0.05 inches.

Orientation

The orientation of the lamina is given by assigning the reference axis E_1 to be side 1-2 of the element (see Figure E 7.24-1) The angles assigned to the fibers imply rotations of +45° or -45° with respect to the normal E_3 to the plate. The rotation starts from E_1, positive if counter-clockwise.

Boundary Conditions

The plate is loaded with a constant membrane strain in the x-direction. $\varepsilon_{mx} = 1$ is obtained by assigning to nodes 1 and 3 displacements $u_x = 2$, $u_y = 0$. While this would produce large strains, small strain theory is used here so you can easily compare the calculations with the analytical solution.

Results

By assigning a displacement $u_x = 2$ to a plate with H = B = 2 inches, you obtain for all laminae:

$$\varepsilon_x = 1$$
$$\varepsilon_y = \gamma_{xy} = 0$$

The strains and stresses in a lamina at +45° are computed as:

$$\varepsilon'_{45} = T_{45} \cdot \varepsilon = \begin{bmatrix} 0.5 & 0.5 & 0.5 \\ 0.5 & 0.5 & -0.5 \\ -1. & 1. & 0 \end{bmatrix} \cdot \begin{Bmatrix} 1 \\ 0 \\ 0 \end{Bmatrix} = \begin{Bmatrix} 0.5 \\ 0.5 \\ -1. \end{Bmatrix}$$

$$\sigma'_{45} = D \cdot \varepsilon'_{45} = 10^6 \begin{bmatrix} 30 & 1 & 0 \\ 1 & 3 & 0 \\ 0 & 0 & 1 \end{bmatrix} \cdot \begin{Bmatrix} 0.5 \\ 0.5 \\ -1. \end{Bmatrix} = 10^6 \begin{Bmatrix} 15.5 \\ 2. \\ -1. \end{Bmatrix}$$

Shear

The plate is loaded with membrane shear by assigning to nodes 2 and 3 the displacements $u_x = 0, u_y = 2$.

Results

By assigning displacements $u_x = 0$ and $u_y = 2$ to a plate with H = B = 2 inches, you obtain for all the laminae:

$$\nu_{xy} = 1.$$
$$\varepsilon_y = \varepsilon_y = 0$$

The strains and stresses in a laminae are computed as:

$$\varepsilon'_{45} = T_{45} \cdot \varepsilon = \begin{bmatrix} 0.5 & 0.5 & 0.5 \\ 0.5 & 0.5 & -0.5 \\ -1. & 1. & 0 \end{bmatrix} \cdot \begin{Bmatrix} 0 \\ 0 \\ 1 \end{Bmatrix} = \begin{Bmatrix} 0.5 \\ -0.5 \\ 0. \end{Bmatrix}$$

$$\sigma'_{45} = D \cdot \varepsilon'_{45} = 10^6 \begin{bmatrix} 30 & 1 & 0 \\ 1 & 3 & 0 \\ 0 & 0 & 1 \end{bmatrix} \cdot \begin{Bmatrix} 0.5 \\ -0.5 \\ 0. \end{Bmatrix} = 10^6 \begin{Bmatrix} 14.5 \\ -1. \\ 0. \end{Bmatrix}$$

Bending

The plate is loaded in bending by assigning to nodes 2 and 3 a rotation $\phi_y = 2$. You obtain a constant curvature $\chi_x = 1$.

Nodes 1 and 4 are clamped. Nodes 2 and 3 are free in the remaining degree of freedom.

Results

Assigning a rotation $\phi_y = 2$ to a plate with H = B = 2 inches, you obtain:

$\chi_x = 1.$
$\chi_y = \chi_y = 0$

The first lamina, at z = 0.175 from midspan, has $\varepsilon_x = z \cdot \chi_x = 0.175$ in local axes.

The strains and stresses in the first lamina at +45° are computed as:

$$\varepsilon'_{45} = T_{45} \cdot \varepsilon = \begin{bmatrix} 0.5 & 0.5 & 0.5 \\ 0.5 & 0.5 & -0.5 \\ -1. & 1. & 0 \end{bmatrix} \cdot \begin{Bmatrix} 0.175 \\ 0 \\ 0 \end{Bmatrix} = \begin{Bmatrix} 0.875 \\ -0.875 \\ 0.175 \end{Bmatrix}$$

$$\sigma'_{45} = D \cdot \varepsilon'_{45} = 10^6 \begin{bmatrix} 30 & 1 & 0 \\ 1 & 3 & 0 \\ 0 & 0 & 1 \end{bmatrix} \cdot \begin{Bmatrix} 0.875 \\ -0.875 \\ 0.175 \end{Bmatrix} = 10^6 \begin{Bmatrix} 2.175 \\ 0.35 \\ 0.175 \end{Bmatrix}$$

Summary of Options Used

Listed below are the options used in example e7x24a.dat:

Parameter Options

ELEMENTS
END
SHELL SECT
SIZING
TITLE

Model Definition Options

COMPOSITE
CONNECTIVITY
COORDINATE
END OPTION
FIXED DISP
ORIENTATION
ORTHOTROPIC
PRINT ELEMENT

Listed below are the options used in example e7x24b.dat:

Parameter Options

ELEMENTS
END
SHELL SECT
SIZING
TITLE

Model Definition Options

COMPOSITE

CONNECTIVITY
COORDINATE
END OPTION
FIXED DISP
ORIENTATION
ORTHOTROPIC
PRINT ELEMENT

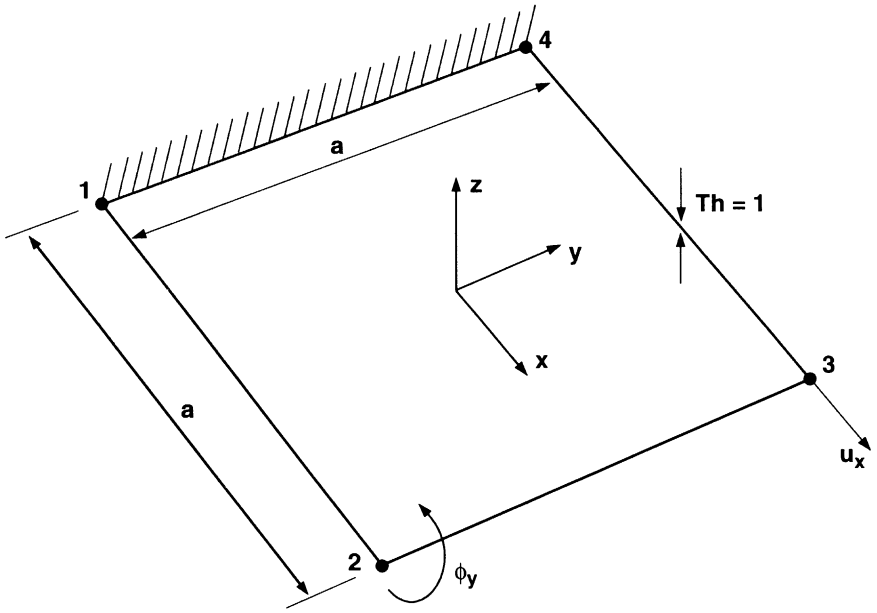

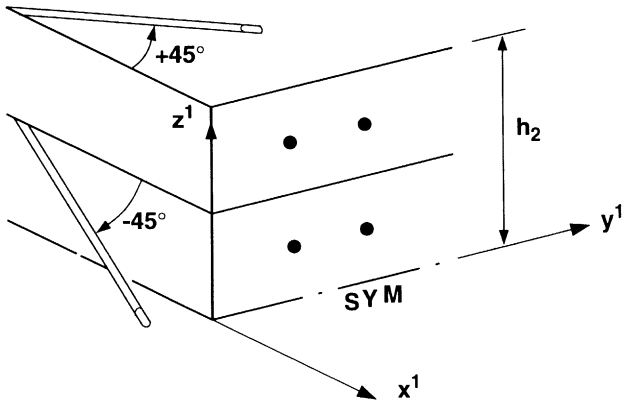

Figure E 7.24-1 Geometry and Lamination of a Composite Plate

E 7.25 Progressive Failure of a Composite Strip

This problem tests the capability of the MARC program to performing progressive failure of composite structures. The test structure modelled here is a strip with a rectangular cross section clamped at both ends and loaded by concentrated forces at midspan.

The material is a laminate, with eight laminae alternating the fiber direction between 0° and 90°. The fiber failure stress in tension is taken here to be the same as in compression.

Under linear elastic behavior, the strip behaves like a beam clamped at both ends. The largest (bending) stresses occur at midspan and at the supports. The load is increased in 126 increments until the fibers are broken and only the matrix bears the load. Correspondingly, the deformed shape of the strip moves from that of a beam to a 3-hinged arch.

Model

Due to symmetry, only half of the strip is modeled. The FEM mesh includes 30 elements and 153 nodes. Element 22, (8-noded shell) is used. LARGE DISP and UPDATE are active for geometrically nonlinear analysis. The strip has length l = 200 mm, width b = 10mm, and thickness t = 1 mm. The mesh is shown in Figure E 7.25-1.

Material Properties

The material is a laminated carbon-epoxy. Two outer skins, with a thickness of 0.25 mm, have the fibers in the longitudinal direction (global X axis). They confine a "core", thick 0.5 mm, with fibers in the transverse direction. The laminae have 0.125 mm thickness. Therefore, eight laminae make up the strip.

E_{11} = 2140000 N/mm^2
E_{22} = 9700 N/mm^2
ν_{12} = 0.28
G_{12} = 5400 N/mm^2
G_{23} = 3600 N/mm^2
G_{31} = 5400 N/mm^2

A lamina fails for maximum stress with the following limit values:

σ_1 = 1020 N/mm^2 in the direction of the fibers, tension or compression

σ_2 = 59 N/mm^2 in the direction orthogonal to the fibers, tension or compression

τ = 95 N/mm^2 shear

Supports

Nodes 1, 2, and 3 at the strip end are clamped allowing for transverse dilation.

Nodes 151, 152, and 153 at midspan have symmetry conditions.

All midspan nodes undergo the same vertical deflection.

Loads

A concentrated load is applied at midspan. The magnitude is increased to p = 3000 N in 125 load increments.

Results

The time history of the tip deflection is shown in Figure E 7.25-2. You can easily observe when plys failed in the system by the jump in the deflection. The first failure occurs in increment 10.

Figure E 7.25-3 and Figure E 7.25-4 show the time history of the stresses in layers 1 and 5. The final figure, Figure E 7.25-5, shows the axial reaction force at the clamped end. Notice the sudden decrease in stress level. The strip deformation has already moved to that of a three-hinged arch.

Summary of Options Used

Listed below are the options used in example e7x25.dat:

Parameter Options

ELEMENTS
END
LARGE DISP
SHELL SECT
SIZING
TITLE
UPDATE

Model Definition Options

COMPOSITE
CONNECTIVITY
CONTROL
COORDINATE
END OPTION
FAIL DATA
FIXED DISP
ORIENTATION
ORTHOTROPIC
POST
TYING

Load Incrementation Options

AUTO LOAD
CONTINUE
NO PRINT
POINT LOAD
POST INCREMENT
PRINT ELEMENT
PROPORTIONAL INCREMENT

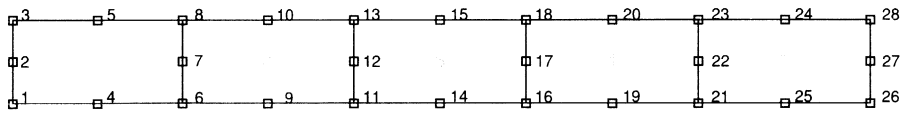

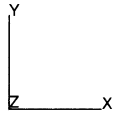

Figure E 7.25-1 Finite Element Mesh of Strip

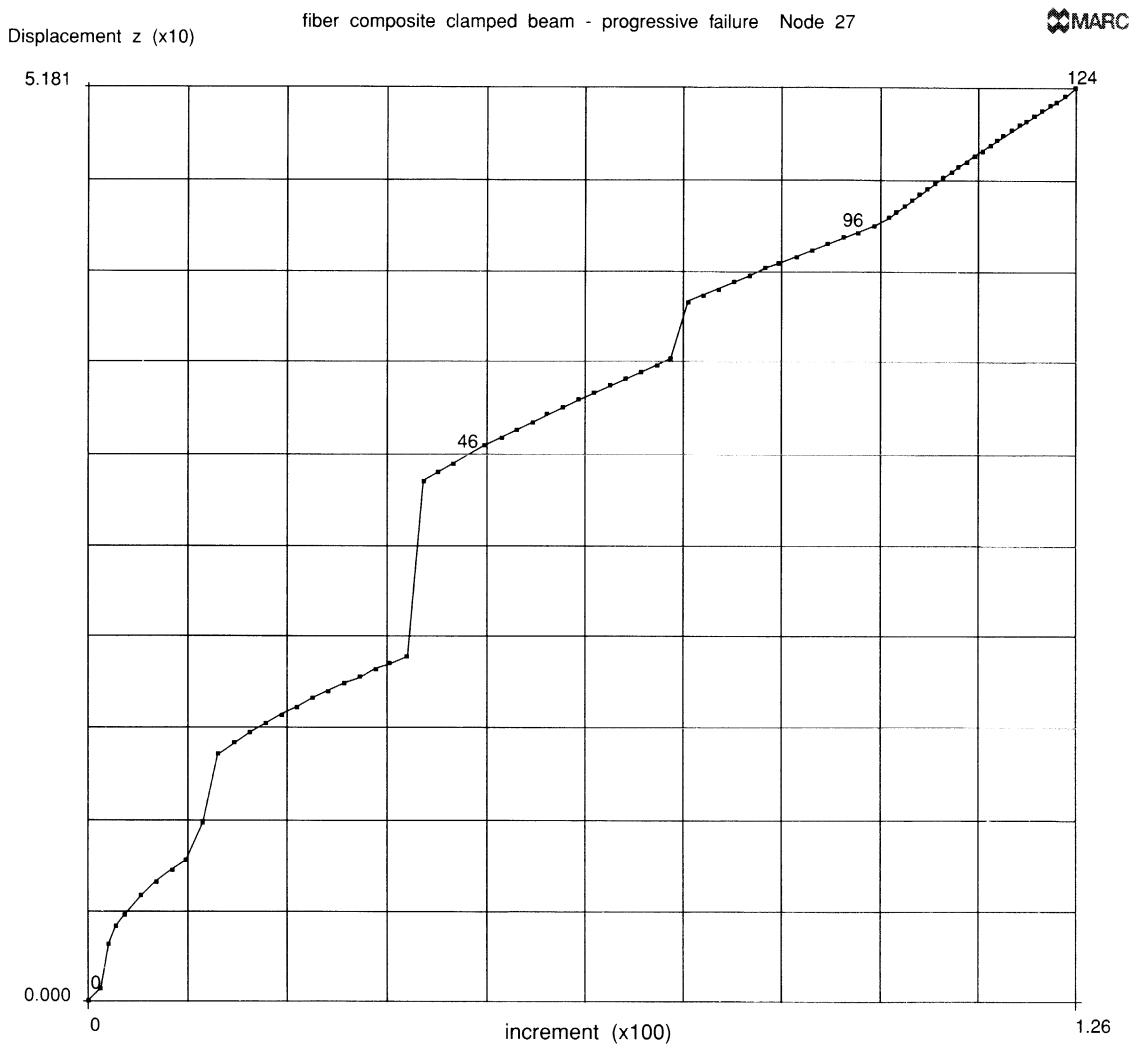

Figure E 7.25-2 History of Deflection of the Tip

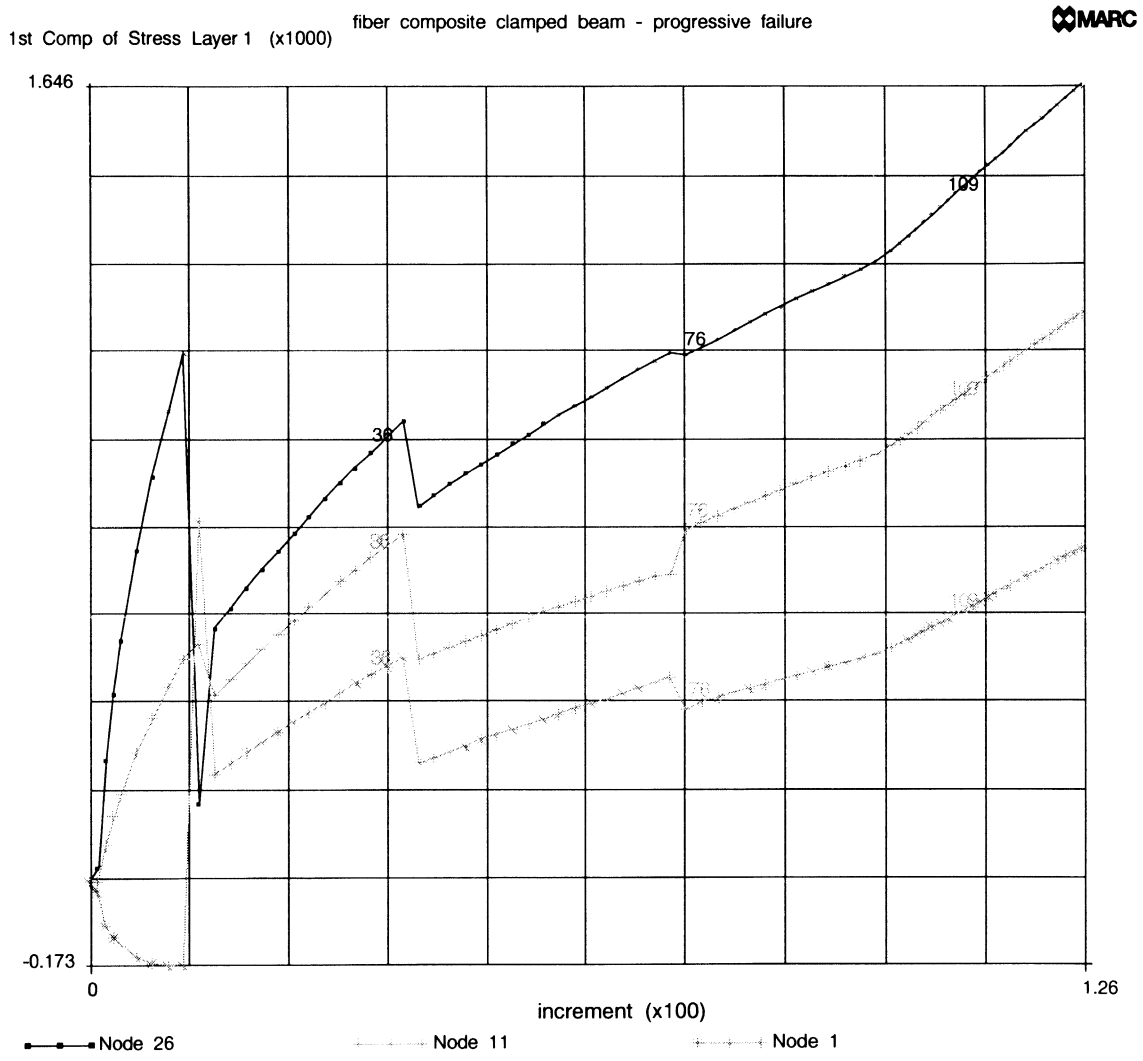

Figure E 7.25-3 History of First Component of Stress in Layer 1

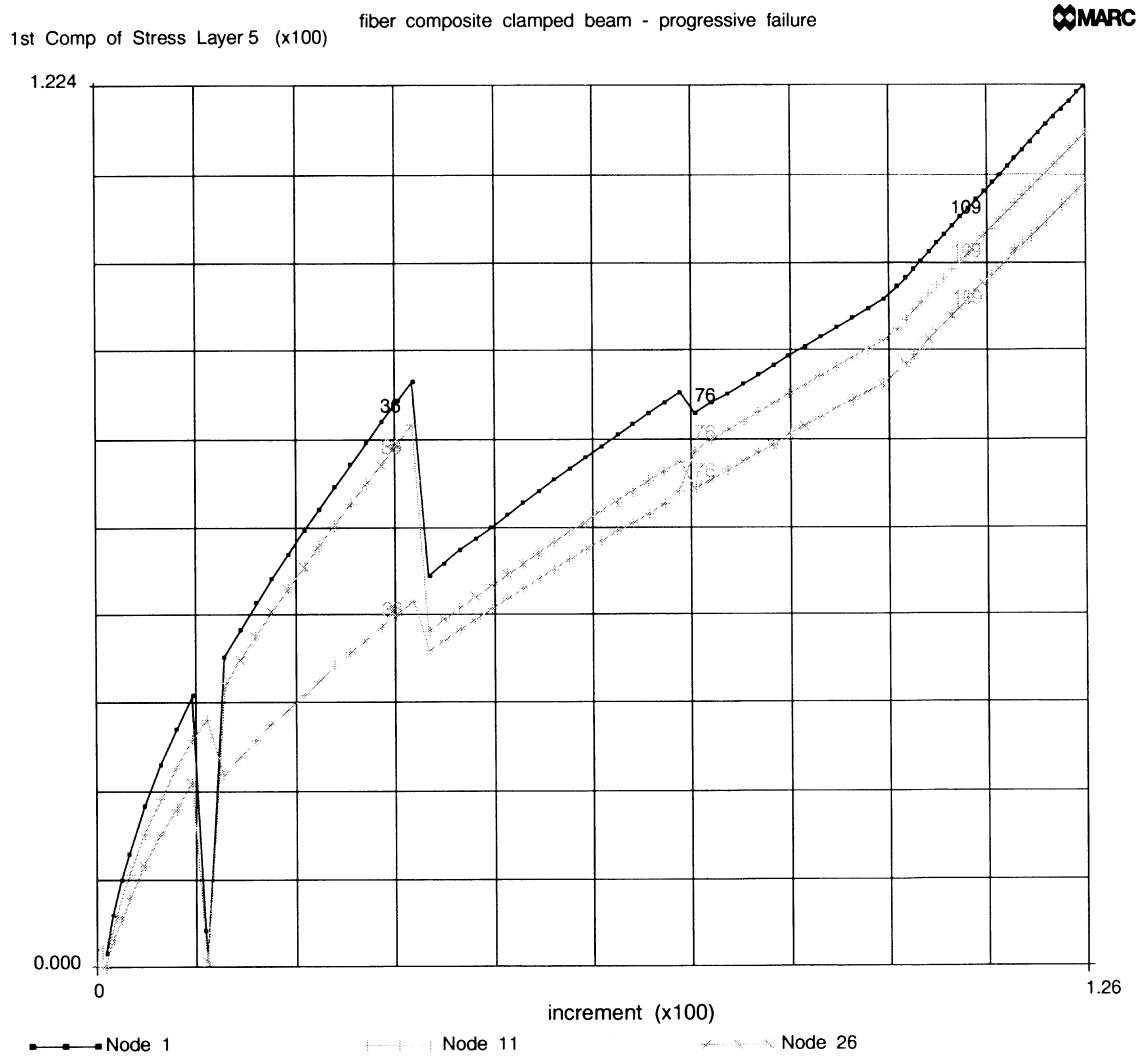

Figure E 7.25-4 History of First Component of Stress in Layer 5

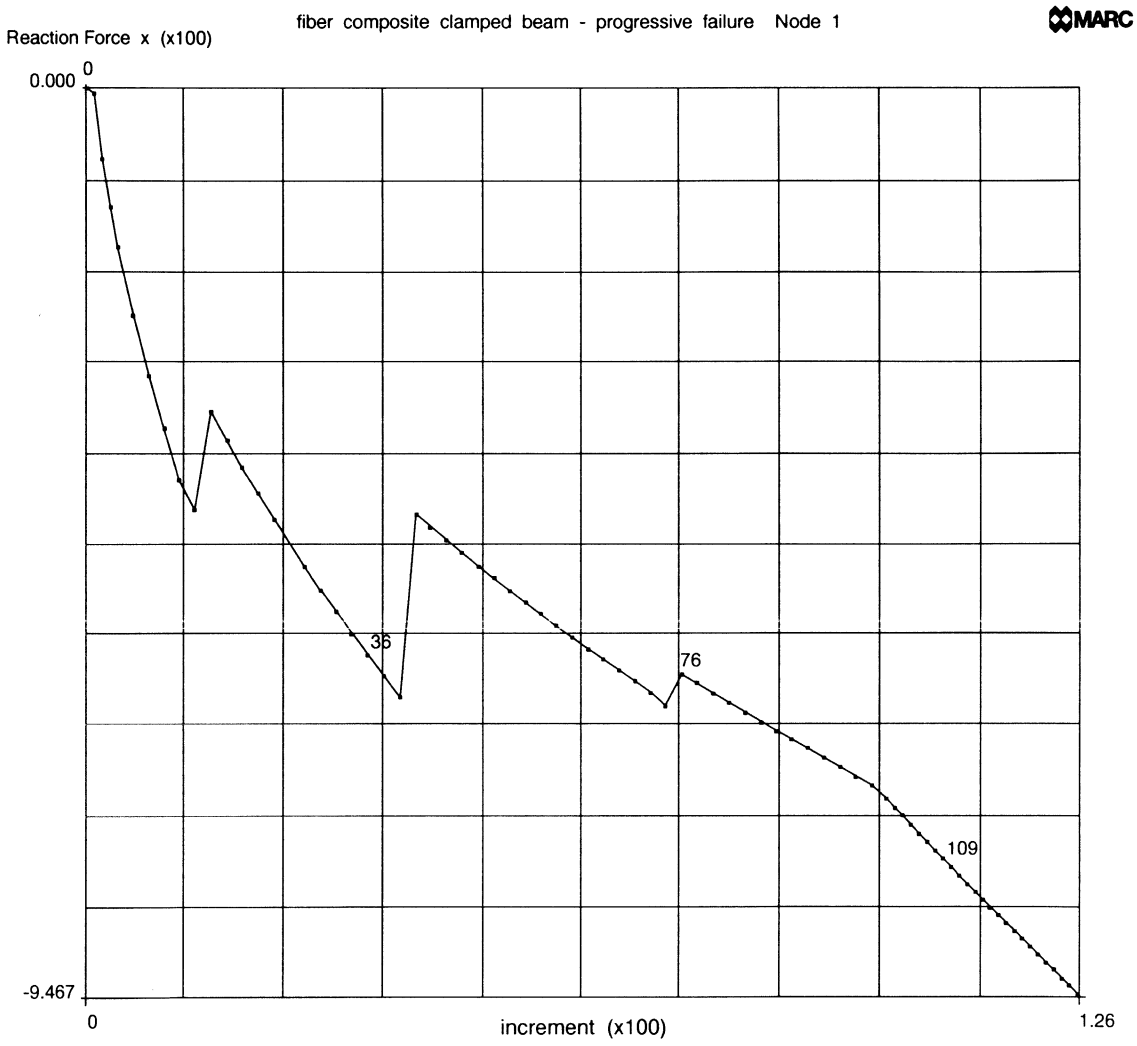

Figure E 7.25-5 History of the Reaction Force at Clamped End

E 7.26 Pipe Collars in Contact

This problem demonstrates the plastic strain capability of the axisymmetric element 95 together with the non-axisymmetric gap element 97. Two pipes are connected under bending loads.

The quadrilateral element 95 represents the cross-section of a ring in the z,r symmetry plane at $\theta = 0°$. A pure axisymmetric deformation induces displacements u,v in the z,r plane. These remain constant for θ ranging from 0° to 360°. A flexural deformation in the z,r plane induces different displacements u,v at opposite sections, $\theta = 0°$ and $\theta = 180°$, along the ring. A twist in the ring induces a circumferential displacement w, equal at every θ, and assigned to the position $\theta = 90°$.

The gap element 97 works in the flexural mode. Extra degrees of freedom have been included to account for independent contact and friction between facing sides of element 95 (q = 0° - 180°). Motion can only occur in the z,r plane.

Element (Ref. B95.1 and B97.1)

In element 95, five degrees of freedom are associated with each node:

u,v displacements at 0° and 180°, respectively
w circumferential displacement at 90° angle

Element 95 is integrated numerically in the circumferential direction. The number of integration points (odd number) is given in the SHELL SECT parameter option. The points are equidistant on the half circumference (see Figure E 7.26-1 and Figure E 7.26-2)

Here, nine integration points along the half circumference are chosen via the SHELL SECT parameter option.

Element 97 is a 4-node gap and friction link with double contact and friction (0° - 180°). It is designed to be used with element type 95.

Model

The FEM model represents the longitudinal section of the pipe junction in the z,r plane. The mesh consists of 248 elements, type 95 and 9 elements type 97 for a total of 330 nodes. The mesh is shown in Figure E 7.26-2.

Material Properties

The two pipes are made with the same material:

E (Young modulus) = 2E5 N/mm^2
ν (Poisson ratio) = .3
σ_y = 200. N/mm^2

A work-hardening curve is assigned as follows:

σ [N/mm^2]	ε_p
200.	0
250.	.3
300.	.6

Loads

The bending load is applied as shown in Figure E 7.26-1. The loads acts in the longitudinal direction (z-direction)

Results

The results produces by the MARC program for the pipe junction with gaps can be seen in the following figures.

Figure E 7.26-3	The deformed section at 0°.
Figure E 7.26-4 and Figure E 7.26-5	The von Mises stress at 0° and 180° (layer 1 and 9, respectively)
Figure E 7.26-6	The plastic strain at 0°. No plastic strain appears at 180°.

NOTE: Only the deformed shape at 0° can be visualized with the Mentat graphics program even if all the element variables can be visualized. The displacements and all the nodal quantities referring to 180° can be seen on the output file.

Summary of Options Used

Listed below are the options used in example e7x25.dat:

Parameter Options

ELEMENTS
END
LARGE DISP
SHELL SECT
SIZING
TITLE
UPDATE

Model Definition Options

CONNECTIVITY
CONTROL
COORDINATES
END OPTION
FIXED DISP
GAP DATA
ISOTROPIC
OPTIMIZE
POST

Load Incrementation Options

CONTINUE
DIST LOADS

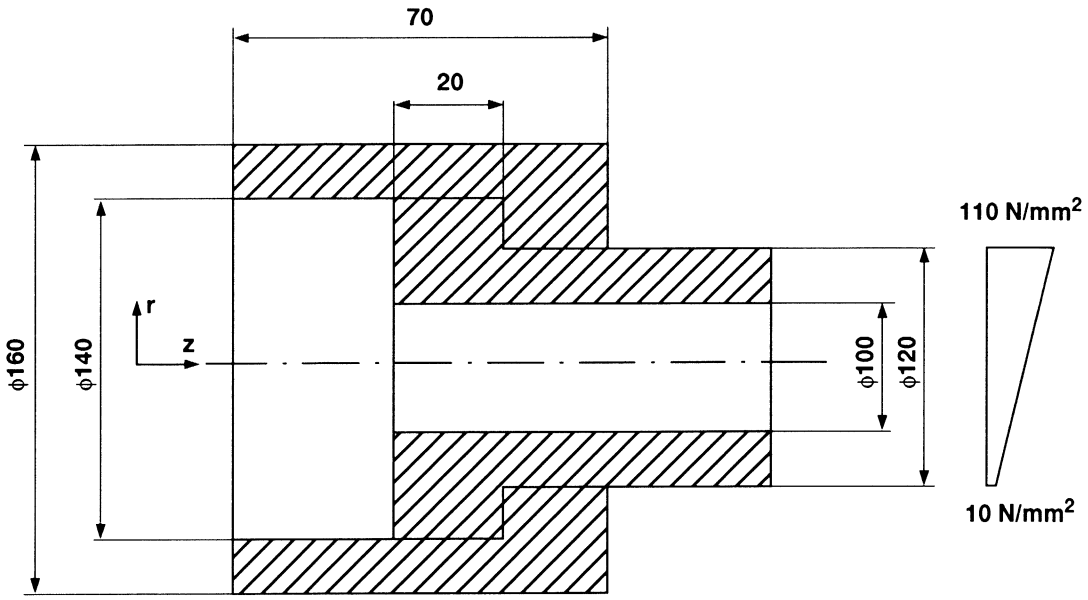

Figure E 7.26-1 Geometric Dimension and Bending Loads

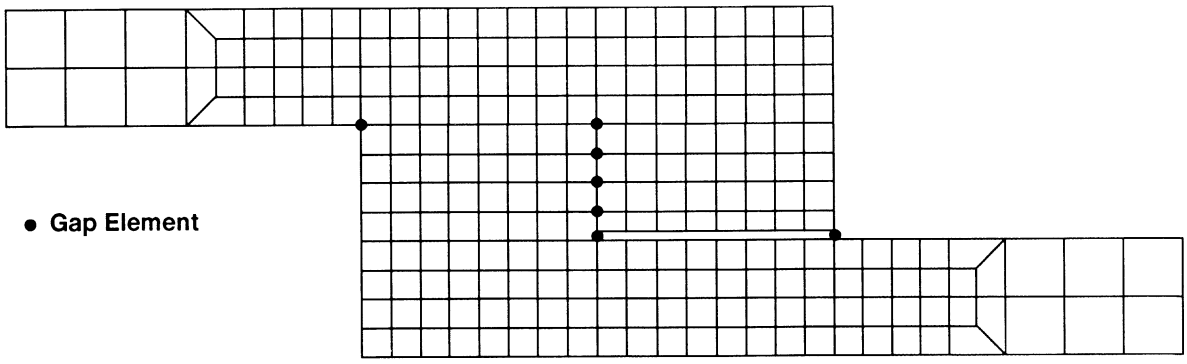

Figure E 7.26-2 FEM Model

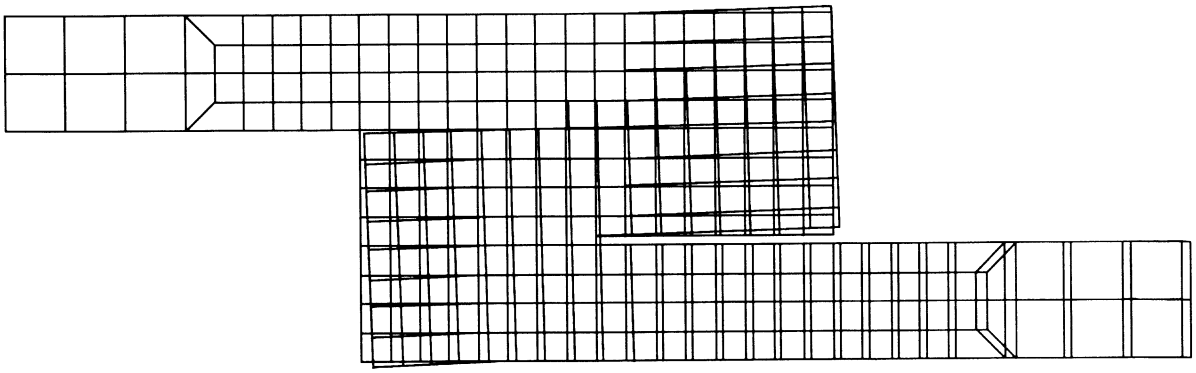

Figure E 7.26-3 Deformed Shape at 0°

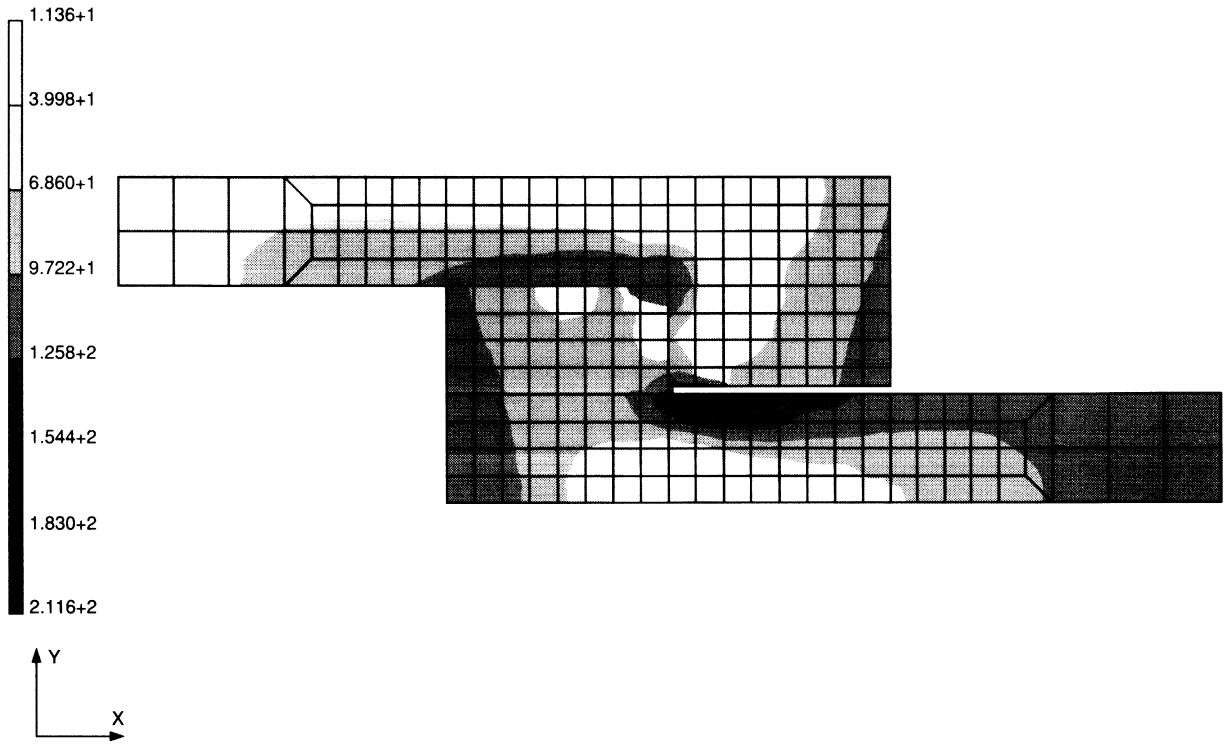

Figure E 7.26-4 von Mises Stress Contour at 0˚, Layer 1

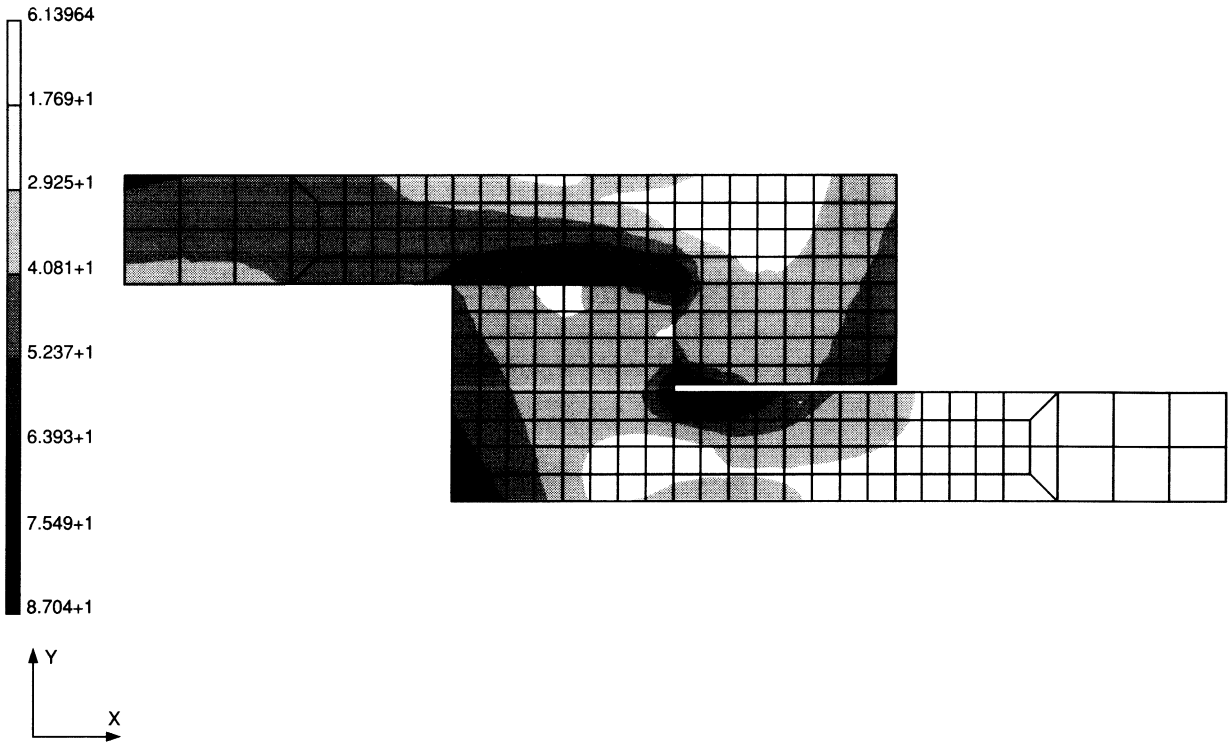

Figure E 7.26-5 von Mises Stress Contour at 180˚, Layer 9

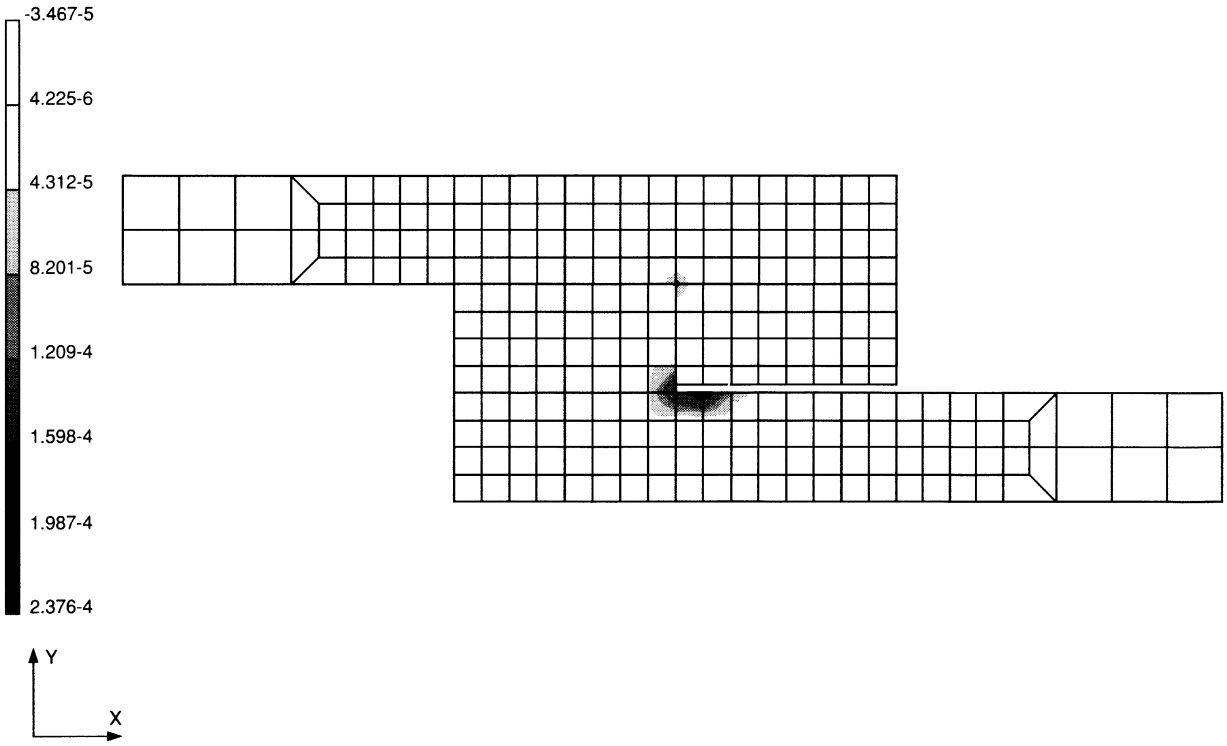

Figure E 7.26-6 Plastic Strain Contour at 0˚, Layer 1

Volume E
Demonstration
Problems

Chapter 8
Advanced Topics

Chapter 8 Advanced Topics

This chapter demonstrates capabilities that have been added to the MARC program in the last few releases. These capabilities include substructures, cracking, composites, contact, electrostatics, magnetostatics, and acoustics capabilities among others. Discussions of these capabilities can be found in *Volume A, User Information* and a summary of the various capabilities is given below:

Substructures

- Linear analysis
- Nonlinear analysis
- Cracking analysis

Thermal-mechanical coupled analysis

Composite analysis

- Failure criteria
- Progressive failure

Activate and deactivate

Contact analysis

- Two-dimensional
- Three-dimensional
- Springback
- Friction

Electrostatic analysis

Magnetostatic analysis

Acoustic analysis

Adaptive Meshing

- Linear analysis
- Nonlinear analysis

Compiled in this chapter are a number of solved problems. Table E 8.0-1 shows the MARC elements and options used in these demonstration problems.

Table E 8.0-1 Recent Analysis Capabilities in MARC

Problem Number (E)	Element Type	Parameter Options	Model Definition	Load Incrementation	User Subroutines	Problem Description
8.1	26	ELASTIC SUBSTRUCT NEWDB SUPER	SUBSTRUCTURE DIST LOAD SUPERINPUT RESTART	BACK TO SUBS	SSTRAN	Hole in plate. Generate substructure (1-1) and 1-2). Combine substructures, perform analysis. Read RESTART tape, Go back to substructures to obtain results.
8.2	27	SUBSTRUCT NEWDB SUPER J-INT SCALE	SUBSTRUCTURE DIST LOADS SUPERINPUT J-INTEGRAL WORK HARD	AUTO LOAD PROPORTIONAL INC	WKSLP	Double-edge notch specimen using substructure. Elastic region away from the crack is treated as a substructure.
8.3	10 12	SUBSTRUCT NEWDB SUPER	SUBSTRUCTURE SUPERINPUT POINT LOADS GAP DATA	POINT LOADS AUTO LOAD BACK TO SUBS	—	End plate aperture breakaway problem. The rate is treated as a substructure leaving the contact elements to be at highest level.
8.4	26	—	ISOTROPIC CRACK DATA TYING	PROPORTIONAL INC AUTO LOAD	—	Collapse of a notched concrete beam.
8.5	75	PRINT	CONN GENER COMPOSITE ISOTROPIC ORTHOTROPIC	POINT LOADS AUTO INCREMENT	—	Cracking of a plate one-way reinforced using shell elements.
8.6	27 46	PRINT	CONN GENER NODE FILL CRACK DATA ISOTROPIC	POINT LOADS AUTO INCREMENT	REBAR	Cracking of a one-way reinforced plate using rebar elements.

Table E 8.0-1 Recent Analysis Capabilities in MARC (Continued)

Problem Number (E)	Element Type	Parameter Options	Model Definition	Load Incrementation	User Subroutines	Problem Description
8.7	11 12 39	FINITE UPDATE LARGE DISP COUPLE MESH PLOT	CONTROL FIXED DISP FIXED TEMP INITIAL TEMP ISOTROPIC GAP DATA CONVERT WORK HARD TEMP EFFECTS RESTART DIST FLUXES	TRANSIENT	—	Thermal-mechanically coupled analysis of the compression of a block.
8.8	21	—	ORTHOTROPIC DIST LOADS	—	HOOKLW ANELAS	Bending of a thick anisotropic plate.
8.9	3	—	DEFINE ORTHOTROPIC ORIENTATION FALL DATA PRINT ELEM	—	—	Failure criteria calculation of an orthotropic plate.
8.10	52	—	HYPOELASTIC	—	UBEAM	Nonlinear beam bending.
8.11	26	—	ERROR ESTIMATE	DEACTIVATE ACTIVATE	—	Example of Activate, Deactivate and error estimates.

Table E 8.0-1 Recent Analysis Capabilities in MARC (Continued)

Problem Number (E)	Element Type	Parameter Options	Model Definition	Load Incrementation	User Subroutines	Problem Description
8.17	7	REZONING UPDATE FINITE LARGE DISP PRINT,8	CONTACT RESTART LAST	AUTO LOAD TIME STEP	—	Metal extrusion analysis using the CONTACT option. Coulomb friction.
8.18	75	SHELL SET,7 LARGE DISP UPDATE FINITE PRINT,8	CONTACT	AUTO LOAD TIME STEP MOTION CHANGE	WKSLP	Stretch forming of a circular sheet. Coulomb friction between sheet and punch.
8.19	7	UPDATE FINITE LARGE DISP PRINT,8 SIZING	CONTACT UMOTION	AUTO LOAD TIME STEP	MOTION	Three dimensional indentation rolling of elastic-perfectly plastic material.
8.20	39	SIZING ELECTRO	POINT CHARGE FIXED POTENTIAL	STEADY STATE	—	Point charge in a circular region.
8.21	43	SIZING ELECTRO	FIXED POTENTIAL POINT CHARGE	STEADY STATE	—	Point charge in a circular cylinder.
8.22	39	SIZING\ MAGNET	POINT CURRENT FIXED POTENTIAL	STEADY STATE	—	Point current in a circular region.
8.23	109	MAGNET	FIXED POTENTIAL POINT CURRENT	STEADY STATE	—	3D analysis of a magnetic field in a coil.
8.24	39	MAGNET	ISOTROPIC FIXED POTENTIAL POINT CURRENT B-H RELATION	STEADY STATE	—	2D nonlinear magnetostatic analysis.

Table E 8.0-1 Recent Analysis Capabilities in MARC (Continued)

Problem Number (E)	Element Type	Parameter Options	Model Definition	Load Incrementation	User Subroutines	Problem Description
8.25	39	ACOUSTIC PRINT,3	ISOTROPIC	DYNAMIC CHANGE	—	2D acoustic problem demonstrating the eigenvalue analysis in a circular cavity with barrier.
8.26	39	ACOUSTIC	ISOTROPIC FIXED PRESSURE	DYNAMIC CHANGE	FORCDT	2D acoustic problem demonstrating the eigenvalue analysis of a rectangular cavity.
8.27	26	INPUT TAPE	FIXED DISP ORTHOTROPIC	AUTO LOAD PROPORTIONAL CONTROL	—	Progressive failure of a plate with a hole.
8.28	41 103	ELECTRO	POINT CHARGE FIXED POTENTIAL	STEADY STATE	—	Linear distribution of dipoles.
8.29	41 103	MAGNET	POINT CHARGE FIXED POTENTIAL	STEADY STATE	—	Magnetic field around two wires carrying opposite currents.
8.30	111	EL-MA HARMONIC PRINT, 3	DIST CURRENT FIXED POTENTIAL	DIST CURRENT HARMONIC POINT CURRENT	—	Harmonic electromagnetic analysis of a waveguide.
8.31	112	EL-MA PRINT, 3	FIXED POTENTIAL	DYNAMIC CHANGE POTENTIAL CHANGE	—	Transient electromagnetic analysis around a conducting sphere.
8.32	113	EL-MA HARMONIC	FIXED POTENTIAL	DIST CURRENT HARMONIC	—	Calculate the resonance in a cavity.
8.33	111	EL-MA HARMONIC	FIXED POTENTIAL	POINT CURRENT CURRENT DYNAMIC CHANGE HARMONIC	—	Steady state analysis of an infinitely long wire using both harmonic and transient analysis.

Table E 8.0-1 Recent Analysis Capabilities in MARC (Continued)

Problem Number (E)	Element Type	Parameter Options	Model Definition	Load Incrementation	User Subroutines	Problem Description
8.34	28	PORE UPDATE ISTRESS	SOIL INITIAL PC INITIAL VOID INITIAL STRESS DIST LOADS	DIST LOADS TIME STEP DISP CHANGE AUTO LOAD	—	Drained triaxial test on normally consolidated clay.
8.35	32	PORE ISTRESS	SOIL SOLVER INITIAL PC INITIAL STRESS INITIAL VOID DIST LOADS DEFINE	DIST LOADS TIME STEP AUTO TIME CONTROL	—	Coupled pore-pressure calculation of stratified soil embankment.
8.36	116	PRINT, 5	SPRINGS CONTACT DEFINE	CONTACT TABLE AUTO LOAD TIME STEP	—	Interference fit of two cylinders.
8.37	11	PRINT, 8	CONTACT SPRINGS DEFINE	CONTACT TABLE AUTO LOAD TIME STEP	—	Interference fit between sectors of two cylinders. Demonstrates symmetry surfaces.
8.38	75	LARGE DISP UPDATE FINITE	CONTACT WORK HARD CONTACT TABLE	AUTO LOAD TIME STEP	—	Deep drawing of a box using rigid punch described as NURBS.
8.39	5	LARGE DISP	CONTACT POINT LOAD	AUTO INCREMENT POINT LOAD	—	Contact of two beams by a point load.
8.40	11	ADAPT ELASTIC	ADAPTIVE ATTACH NODES SURFACE POINT LOAD	—	—	Adaptive meshing of a disk subjected to point loads.
8.41	3	ADAPT ELASTIC	ADAPTIVE ERROR ESTIMATES	—	—	Adaptive meshing of a stress concentration.

Table E 8.0-1 Recent Analysis Capabilities in MARC (Continued)

Problem Number (E)	Element Type	Parameter Options	Model Definition	Load Incrementation	User Subroutines	Problem Description
8.42	11	ADAPT LARGE DISP FOLLOW FOR	CONTACT ATTACH NODE SURFACE DIST LOADS	MOTION CHANGE AUTO LOAD TIME STEP	—	Double-sided contact analysis with adaptive meshing.
8.43	119	LARGE DISP FOLLOW FOR ADAPT	ADAPTIVE MOONEY CONTACT	AUTO LOAD TIME STEP DISP CHANGE	—	Modeling a rubber seal with adaptive meshing.
8.44	11	UPDATE LARGE DISP FINITE ADAPT	WORK HARD ADAPTIVE CONTACT CONTACT TABLE	MOTION CHANGE TIME STEP AUTO LOAD	—	Rolling example with adaptive meshing.

E 8.38 Deep Drawing of a Box Using NURB Surfaces

This example demonstrates the deep drawing of a box modeled with shell elements. The punch and holder are modeled with NURBS using the CONTACT option. The improvement in computational performance is demonstrated by the use of the sparse direct solver.

Geometry

The sheet is made up of 636 element type 75 with dimensions of 225 cm by 220 cm. Element type 75 is a thick shell element which may also be used to simulate thin shells. The shell thickness (1.2 cm) is specified through the GEOMETRY option in the first field (EGEOM1).

Loading

The punch is given a constant velocity of 3 cm/second. The AUTO LOAD option with 112 step sizes is specified with each step size (0.25 seconds) specified through the TIME STEP option. The total motion is 84 cm.

Material Properties

The material is treated as elastic-plastic with a Young's modulus of 2.1e5 N/cm^2, a Poisson's ratio of 0.3, and an initial yield stress of 188.66 N/cm^2. The yield stress is given through the WORK HARD DATA model definition option.

Boundary Conditions

One-quarter of the geometry is used due to symmetry. The appropriate nodal constraints are applied in the global x,y directions to impose symmetry. The box is deep-drawn by a punch having a constant velocity of 3 cm/sec.

Contact

This option had three bodies. The first body is a rectangle of 626 shell elements. The second body is a rigid die which is made up of 7 different NURBS. The third body is the rigid holder which has two major parts – a flat holder and a curved shoulder with 12 NURBS to describe the complete shoulder. The workpiece is firmly held by the rigid dies with 0.02 contact tolerance and high separation force entered to simulate the condition. To avoid unnecessary self contact check, the contact table is used.

Control

Displacement control was used with a convergence tolerance of 10%. No more than 20 recycles per increment is specified.

Results

Three bodies are declared in e8x38a.dat with nonanalytical form for NURBS used for the analysis. All surface defined as NURBS are discretized into 4-node patches.

The difference in e8x38b.dat is that the rigid dies are using the analytical form of NURBS to implement contact conditions. Computational performance is improved 10% by use of the analytical NURBS when comparing CPU time for e8x38a.dat and e8x38b.dat. Because an exact representation of the surface is made, the results are better.

Four bodies are declared in e8x38c.dat with the shoulder in the third rigid die in e8x38b.dat becoming the fourth body.

Figure E 8.38-1 shows the geometry configuration for the deep-drawing analysis. Figure E 8.38-4 shows the 7 NURBS rigid punch. Figure E 8.38-5 shows the 12 NURBS rigid holder. The deformation of the sheet is shown at increments 20, 50, 80, and 110 in Figure E 8.38-4 through Figure E 8.38-7. The equivalent stress is shown in Figure E 8.38-8. The equivalent plastic strain is shown in Figure E 8.38-9. You can observe that the maximum plastic strain is 70%.

Summary of Options Used

Listed below are the options used in example e8x38a.dat:

Parameter Options

ELEMENTS
END
FINITE
LARGE DISP
PRINT
SHELL SECT
SIZING
TITLE
UPDATE

Model Definition Options

CONNECTIVITY
CONTACT
CONTACT TABLE
CONTROL
COORDINATES
END OPTION
FIXED DISP
GEOMETRY
ISOTROPIC
NO PRINT
OPTIMIZE
POST

Load Incrementation Options

AUTO LOAD
CONTINUE
TIME STEP

Listed below are the options used in example e8x38b.dat:

Parameter Options

ELEMENTS
END
FINITE
LARGE DISP
PRINT
SHELL SECT
SIZING
TITLE
UPDATE

Model Definition Options

CONNECTIVITY
CONTACT
CONTACT TABLE
CONTROL
COORDINATES
END OPTION
FIXED DISP
GEOMETRY
ISOTROPIC
NO PRINT
POST
SOLVER

Load Incrementation Options

AUTO LOAD
CONTINUE
TIME STEP

Listed below are the options used in example e8x38c.dat:

Parameter Options

ELEMENTS
END
FINITE
LARGE DISP
PRINT
SHELL SECT
SIZING
TITLE
UPDATE

Model Definition Options

CONNECTIVITY
CONTACT
CONTACT TABLE
CONTROL
COORDINATES
END OPTION
FIXED DISP
GEOMETRY
ISOTROPIC
NO PRINT
POST
SOLVER

Load Incrementation Options

AUTO LOAD
CONTINUE
TIME STEP

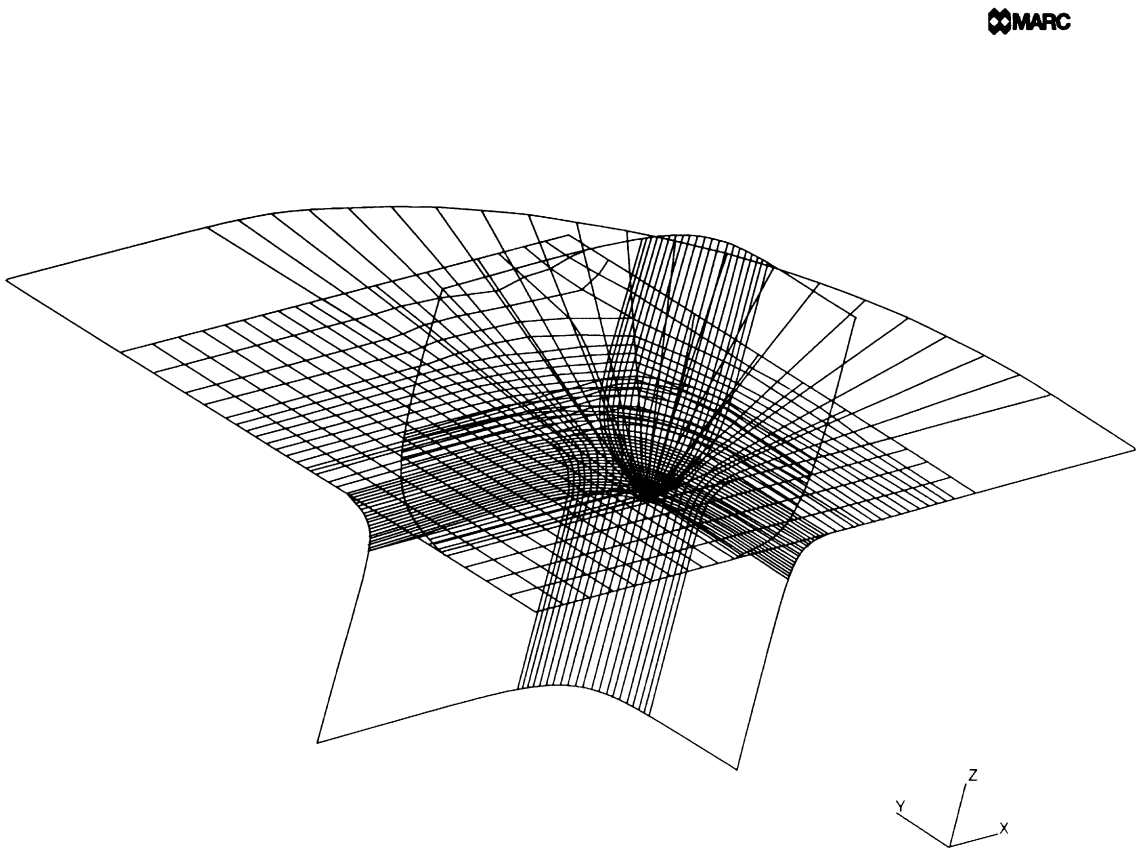

Figure E 8.38-1 Plate with Rigid Surfaces

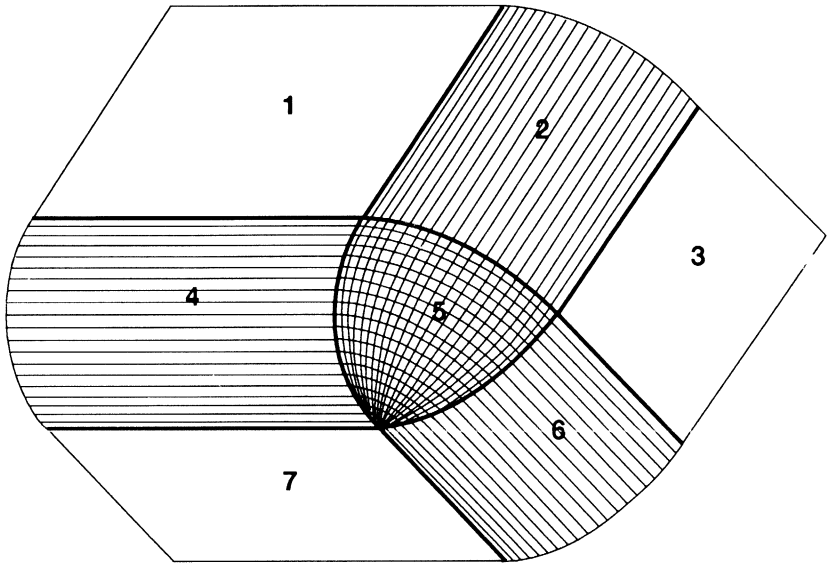

Figure E 8.38-2 Male Punch Consisting of Seven NURBS

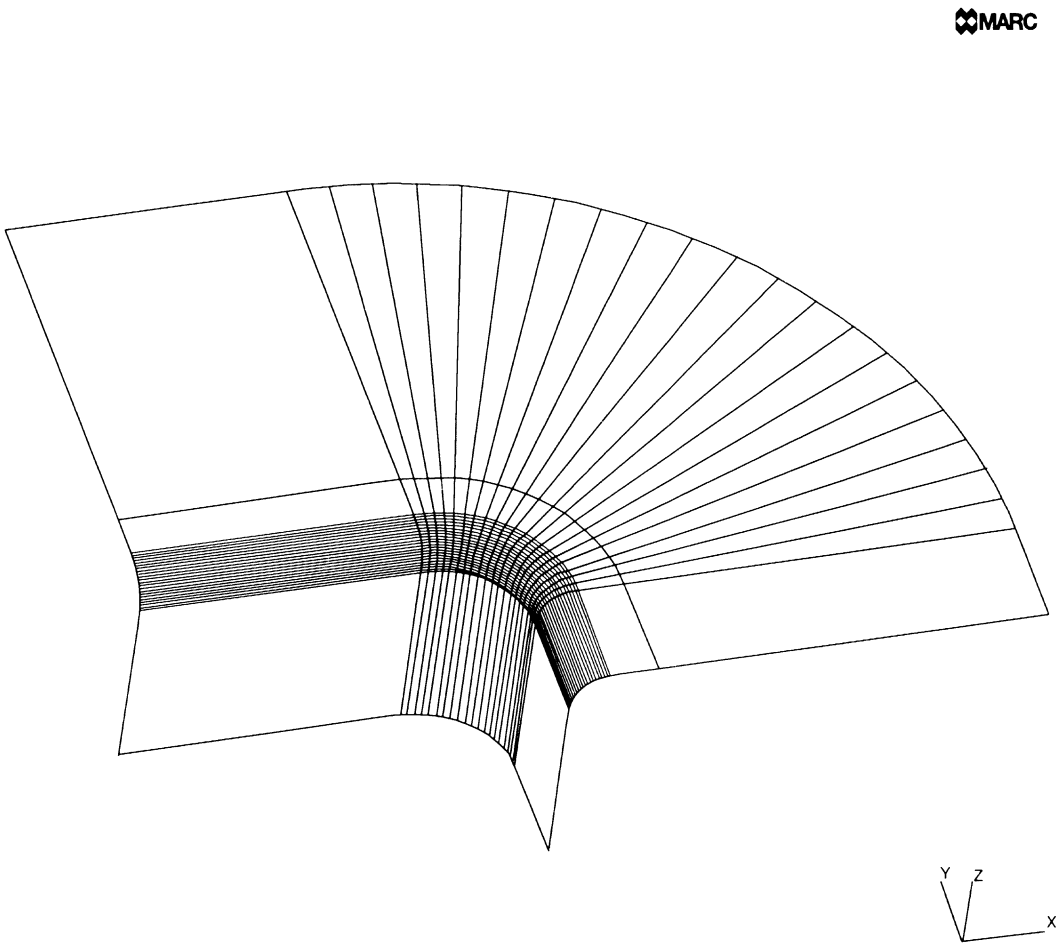

Figure E 8.38-3 Blank Holder

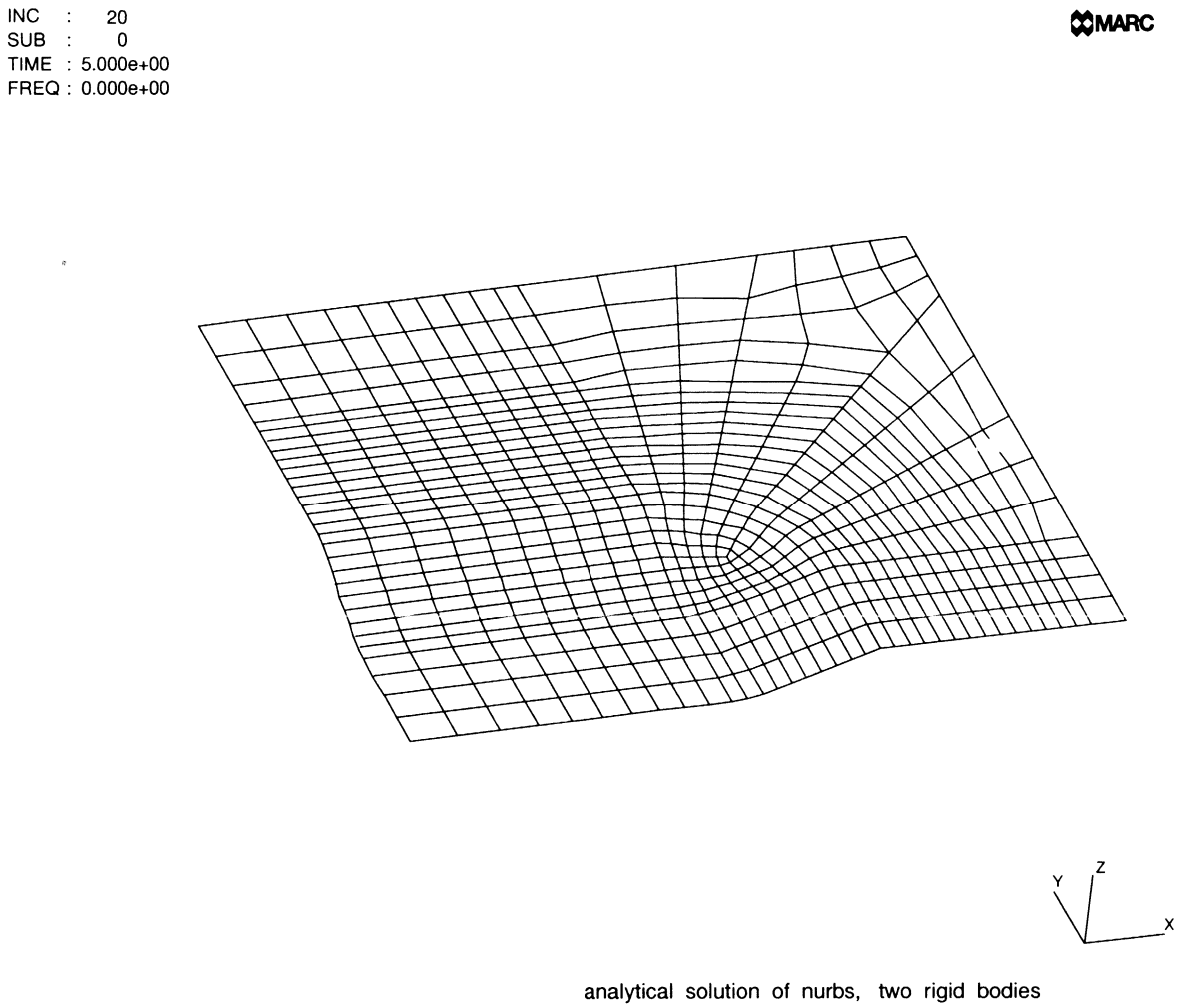

Figure E 8.38-4 Deformed Plate at Increment 20

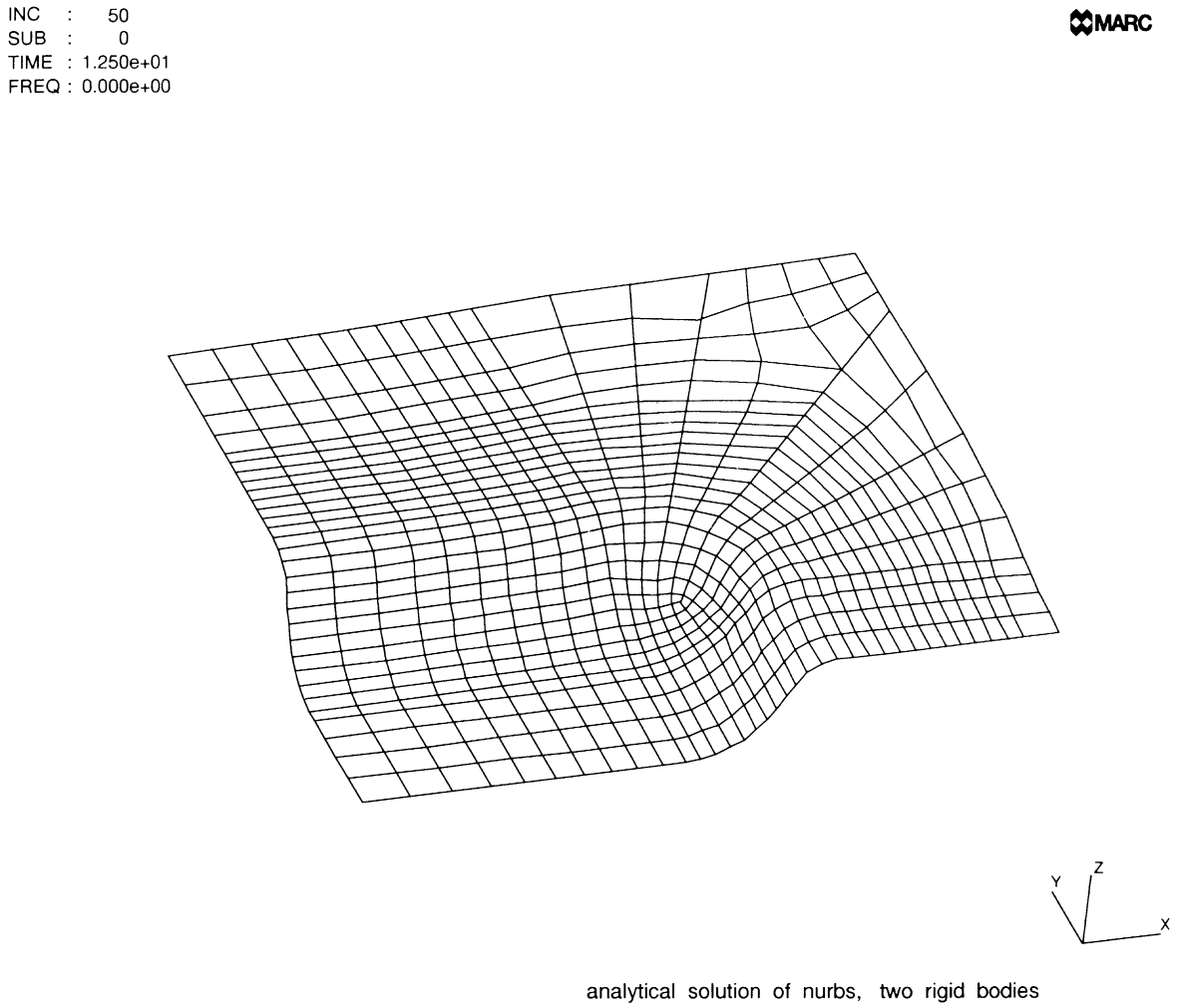

Figure E 8.38-5 Deformed Plate at Increment 50

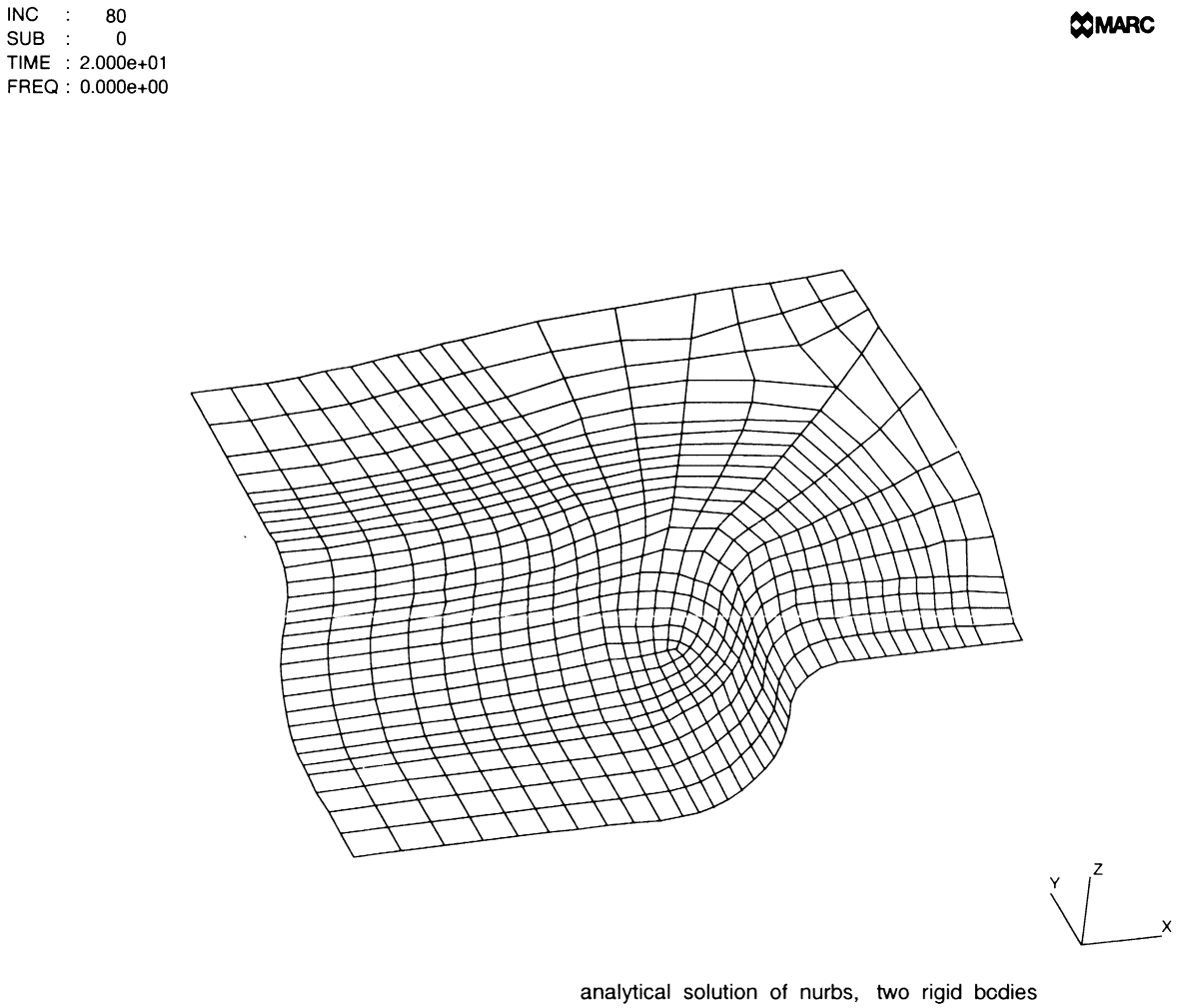

Figure E 8.38-6 Deformed Plate at Increment 80

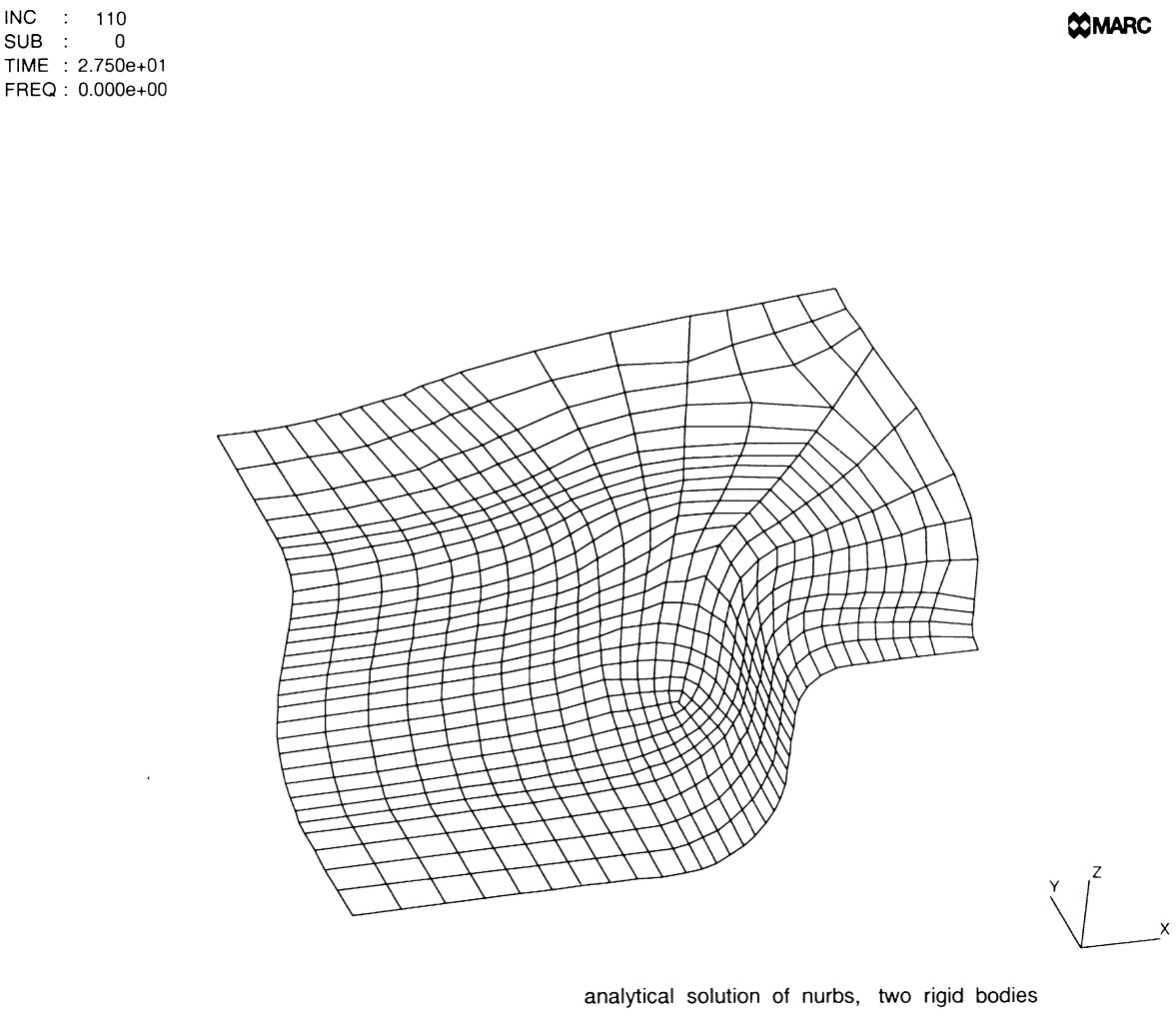

Figure E 8.38-7 Deformed Plate at Increment 110

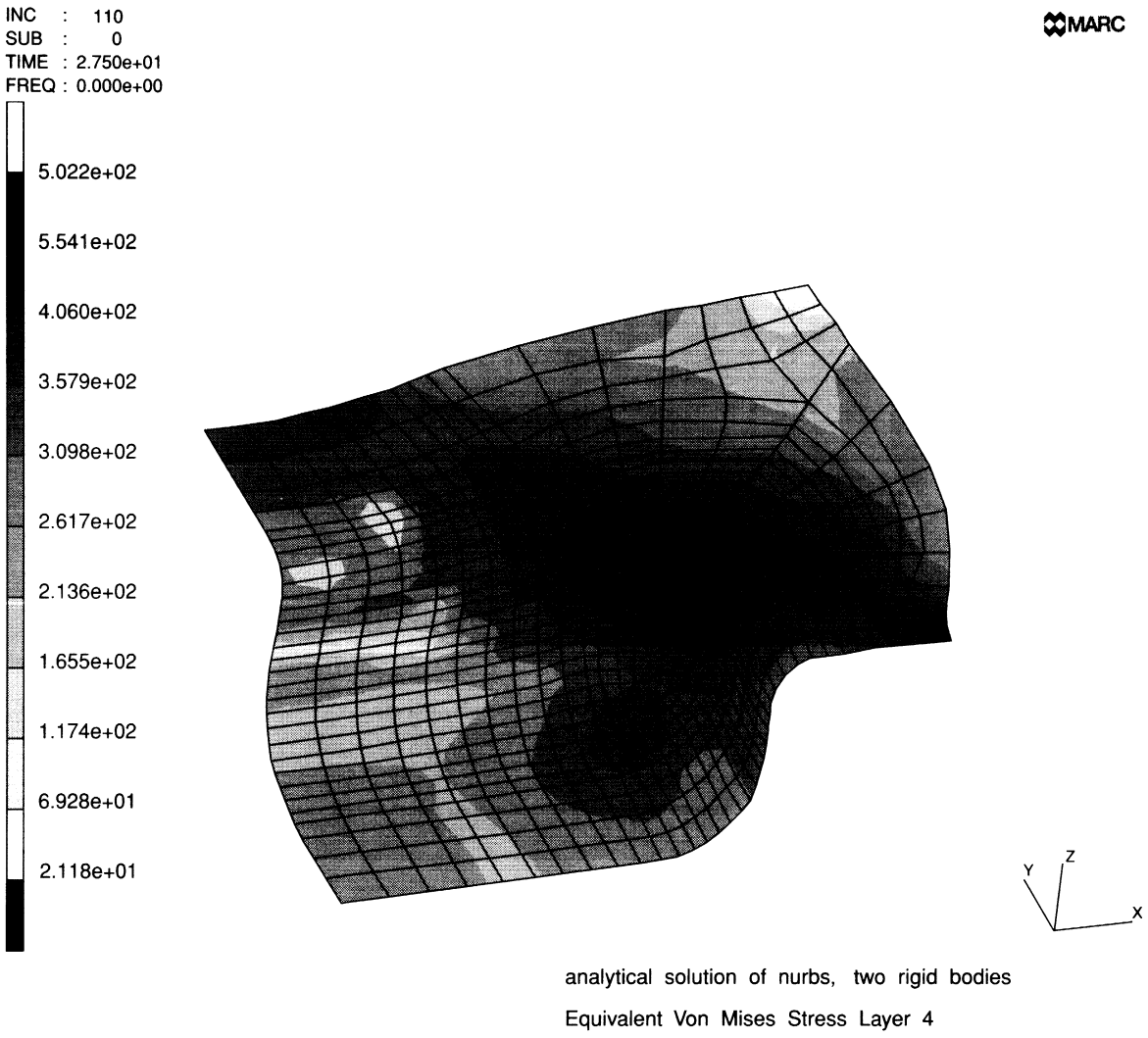

Figure E 8.38-8 Equivalent Stress at Midsurface at Increment 110

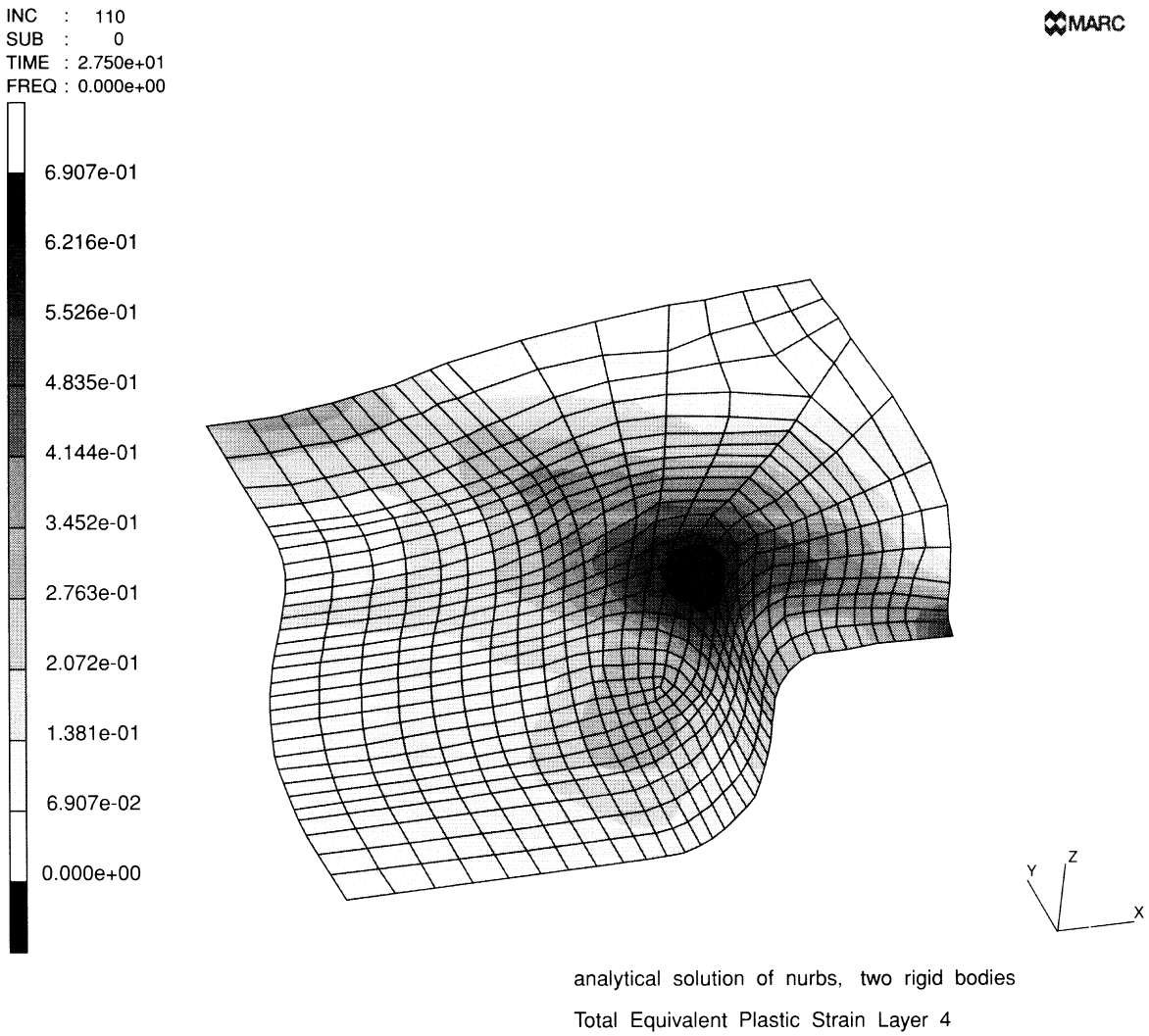

Figure E 8.38-9 Equivalent Plastic Strain at Midsurface at Increment 110

E 8.39 Contact of Two Beams Using AUTO INCREMENT

This problem demonstrates bringing two beams into contact as an example of large deflection which exhibits inelastic response. The AUTO INCREMENT option is used to control the magnitude of the load increment. A beam acted on by a point load eventually comes into contact with a second beam (Figure E 8.39-1). The geometrically nonlinear problem is solved adaptively by the arc-length method. The procedure stops at the step before the upper beam slips from the lower beam (Figure E 8.39-5).

Element (Ref. B5.1)

Element type 5 is 2-node rectangular-section beam-column with three global degrees of freedom per node.

Geometry

The beams are 80 inches in length with a distance of 20 inches separating the beams. The height of 2.5 is input in the first data field of GEOMETRY option. The cross-sectional area of 1 is input in the second data field (EGEOM2).

Material Properties

Linear elastic properties are specified in the ISOTROPIC option – Young's modulus = 1,000,000 psi and Poisson's ratio is 0.3333.

Boundary Conditions

Fully clamped conditions are applied to one end of each beam.

Geometric Nonlinearity

The LARGE DISP parameter option indicates that geometric nonlinear analysis will be performed.

Control

Residual-force control is used with a relative error of 10%. No more than 20 recycles per increment is specified.

Loading

The POINT LOAD option is used to enter the total applied load of 585 pounds at node 29 along the global Y-direction. The initial load is 1% of the total load in the first increment and subsequent loading will be adjusted adaptively based on arc-length method.

Contact

This option declares that there are 2 flexible bodies. Each is made of 20 beam elements. Contact tolerance distance is 0.01.

Results

The deformed beams are shown in Figure E 8.39-2 through Figure E 8.39-5. The load deflection curve is shown in Figure E 8.39-6. After the beams contact, the upper beam comes into contact with the lower beam at point A. The effect of stiffening due to the additional stiffness of the lower beam is observed until point B, as the contact node, slips onto the lower beam. At that moment, the pure bending dominates the response and corresponds to another type of instability until point C, at which time the upper beam will slip away the lower beam.

Summary of Options used

Listed below are the options used in example e8x39.dat:

Parameter Options

ELEMENTS
END
LARGE DISP
PRINT
SIZING
TITLE

Model Definition Options

CONNECTIVITY
CONTACT
CONTROL
COORDINATE
END OPTION
FIXED DISP
GEOMETRY
ISOTROPIC
POINT LOAD
POST
PRINT ELEMENT
PRINT NODE

Load Incrementation Options

AUTO INCREMENT
CONTINUE
POINT LOAD

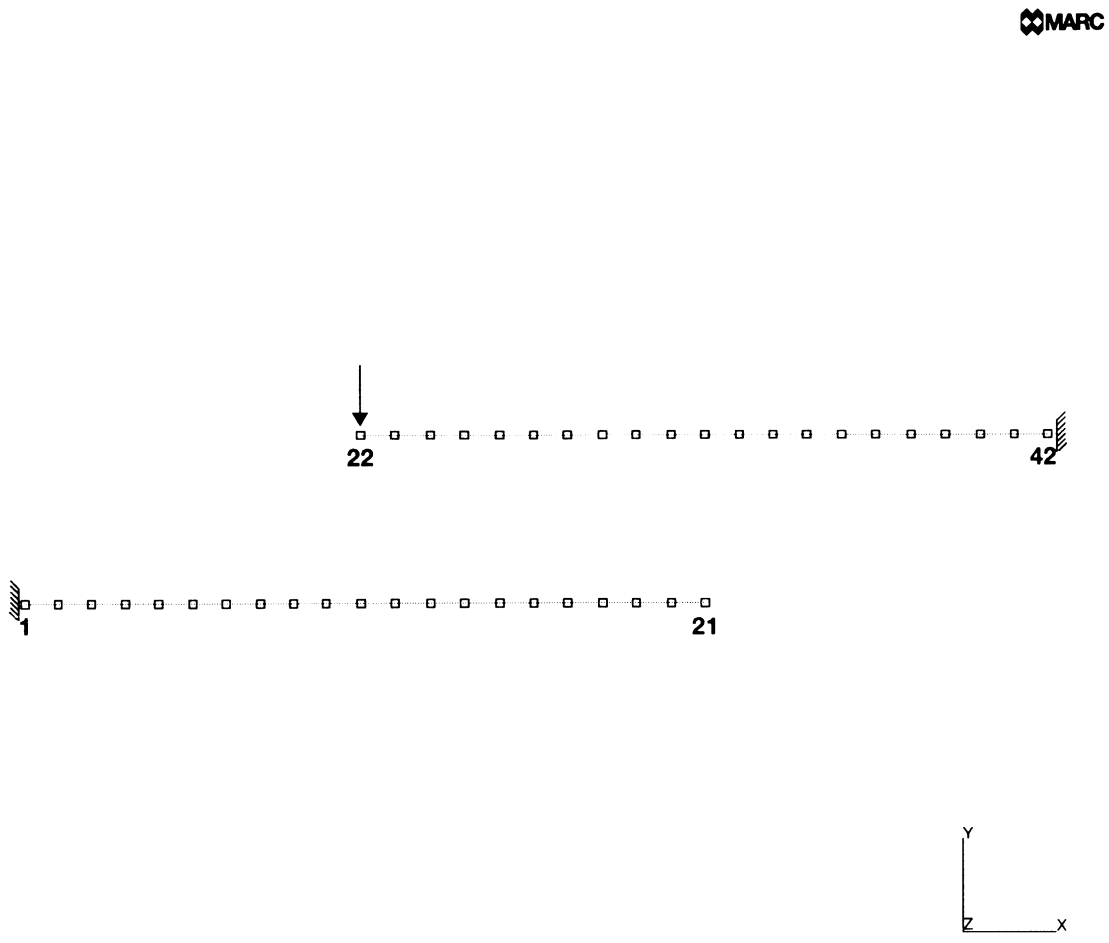

Figure E 8.39-1 Mesh of Two Beams

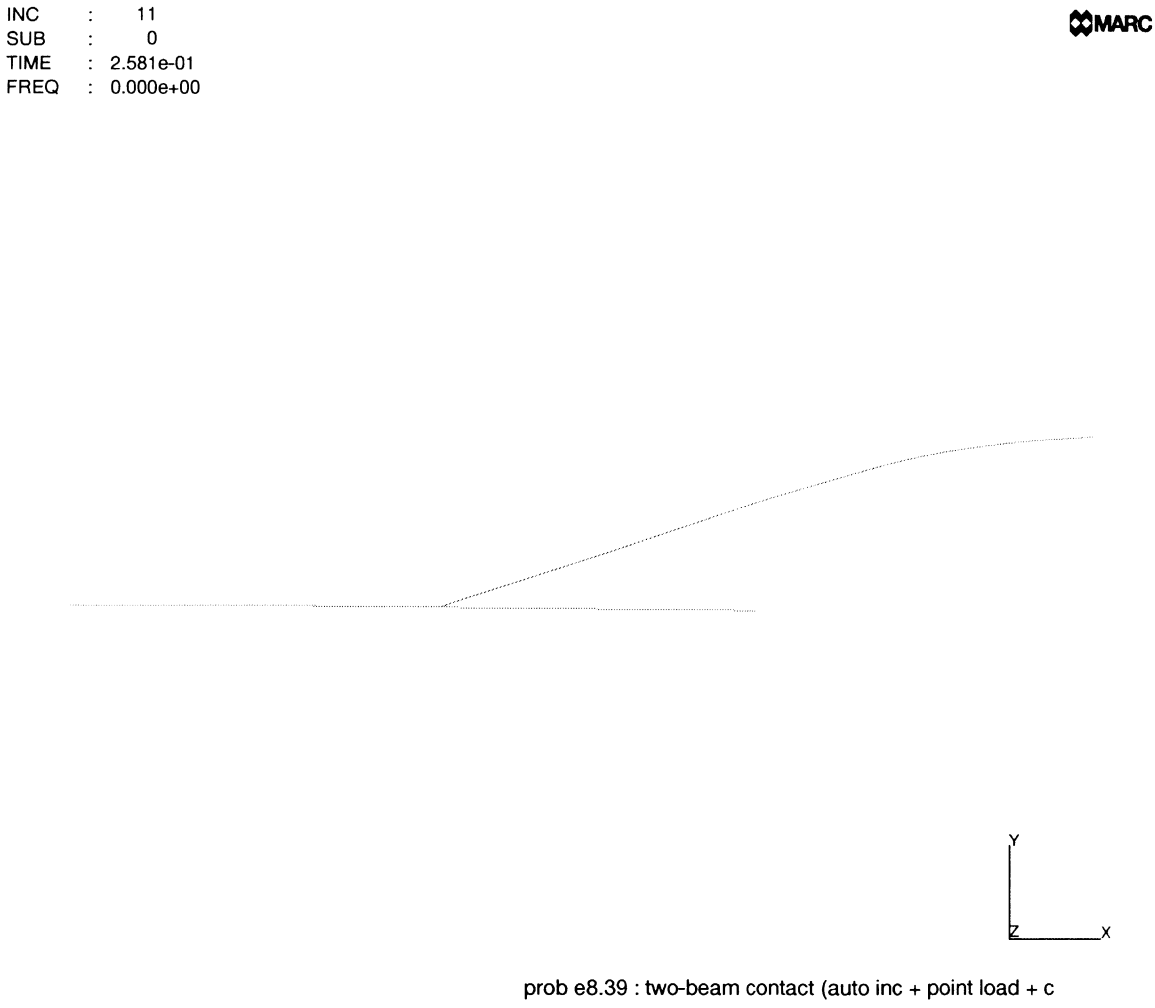

Figure E 8.39-2 Initial Contact of Beams

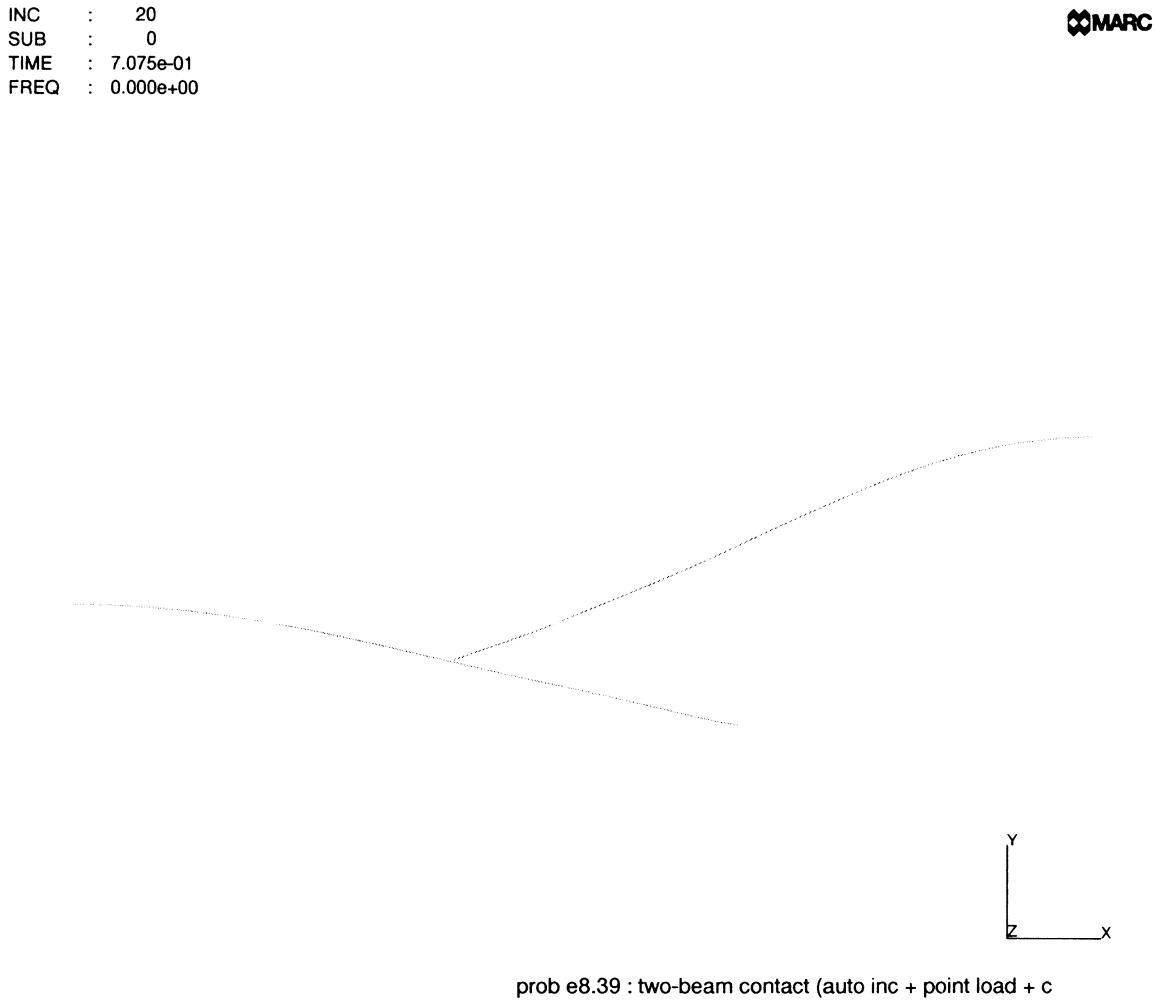

Figure E 8.39-3 Deformed Mesh at Increment 20

Figure E 8.39-4 Deformed Mesh at Increment 30

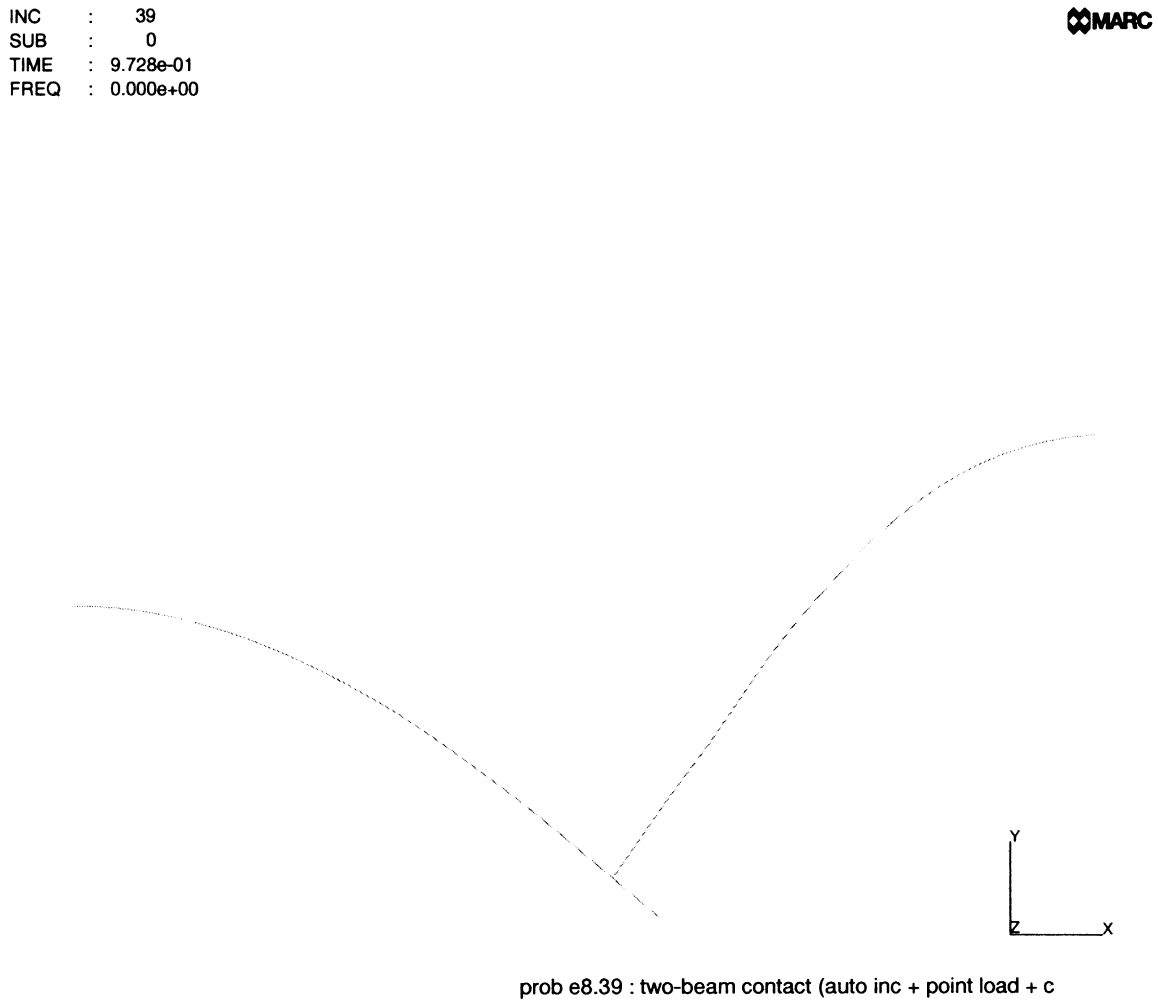

Figure E 8.39-5 Deformed Mesh at Increment 39

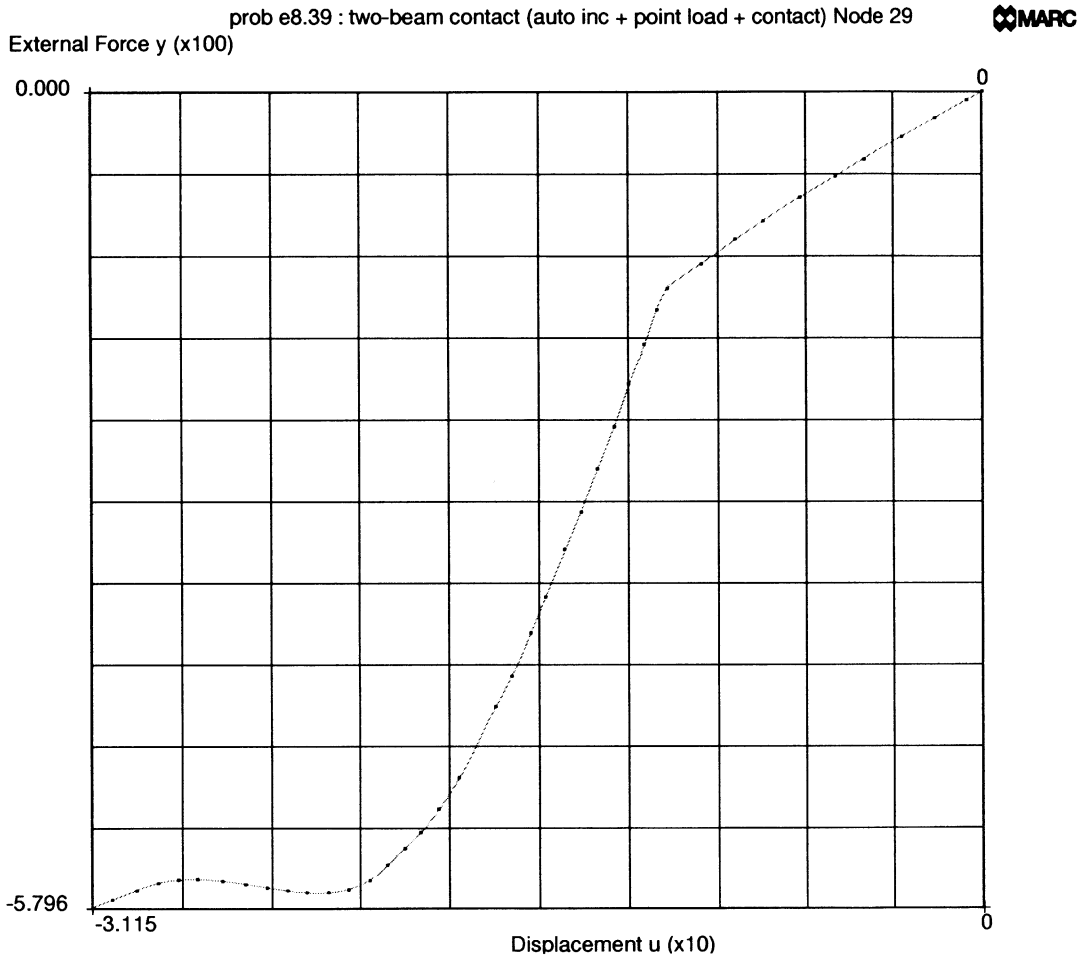

Figure E 8.39-6 Load Deflection Curve

E 8.40 Circular Disk Under Point Loads Using Adaptive Meshing

This problem illustrates the use of adaptive meshing for a simple geometry. A circular disk is crudely modeled, and the program improves the finite element model.

Element

Element type 11, a 4-node linear isoparametric plane-strain element is used in the model.

Model

The original coarse mesh containing only four elements is shown in Figure E 8.40-1. The disk has a radius of 1 mm and a unit thickness. The SURFACE option is used to define a circular curve which has this geometry. The ATTACH NODES option is used to specify that the boundary nodes are located on the curve. When new boundary nodes are created, they will automatically be placed on the curve.

Geometry

No geometry is necessary as the default is used.

Material Properties

Young's modules is 2. 1x 10^5 N/mm^2, and Poisson's ratio is 0.3. As new elements are created, they will be given these material properties.

Boundary Conditions

The bottom point, node 9, is constrained in both directions. The top point, node 1, is constrained in the x-direction to insure no rigid body motion. Additionally, it is given a point load of 0.1 N vertically.

Adaptive Meshing

The ADAPTIVE parameter option is used to indicate the maximum number of elements and nodes allowed. The ELASTIC parameter option is used to indicate that the analysis is to be repeated until the adaptive criteria is satisfied. Only the loads applied in increment 0 will be considered.The ADAPTIVE model definition option is used to indicate that an element should be refined if the stress is greater than 75% of the maximum stress. A limit of 4 levels of subdivisions is allowed. In theory, the maximum number of elements would be 4 x 4^4 = 1024; this is less than given on the parameter option.

Results

The progression of meshes is shown in Figure E 8.40-2 through Figure E 8.40-5. You can observe the concentration of elements in the vicinity of the point loads. Furthermore, the nodes on the boundary take on the shape of the circle. As the mesh is improved, the solution converges to the correct results. Looking at the maximum y displacement, you can observe that the original solution is substantially incorrect.

Level	Maximum Displacement $*10^{-6}$
0	.9070
1	.9054
2	1.067
3	1.331
4	1.548
5	1.549

Summary of Options used

Listed below are the options used in example e8x40.dat:

Parameter Options

ADAPTIVE
ELASTIC
ELEMENTS
END
PRINT
SIZING
TITLE

Model Definition Options

ADAPTIVE
ATTACH NODE
CONNECTIVITY
COORDINATE
END OPTION
FIXED DISP
ISOTROPIC
NO PRINT
POINT LOAD
POST
SOLVER
SURFACE

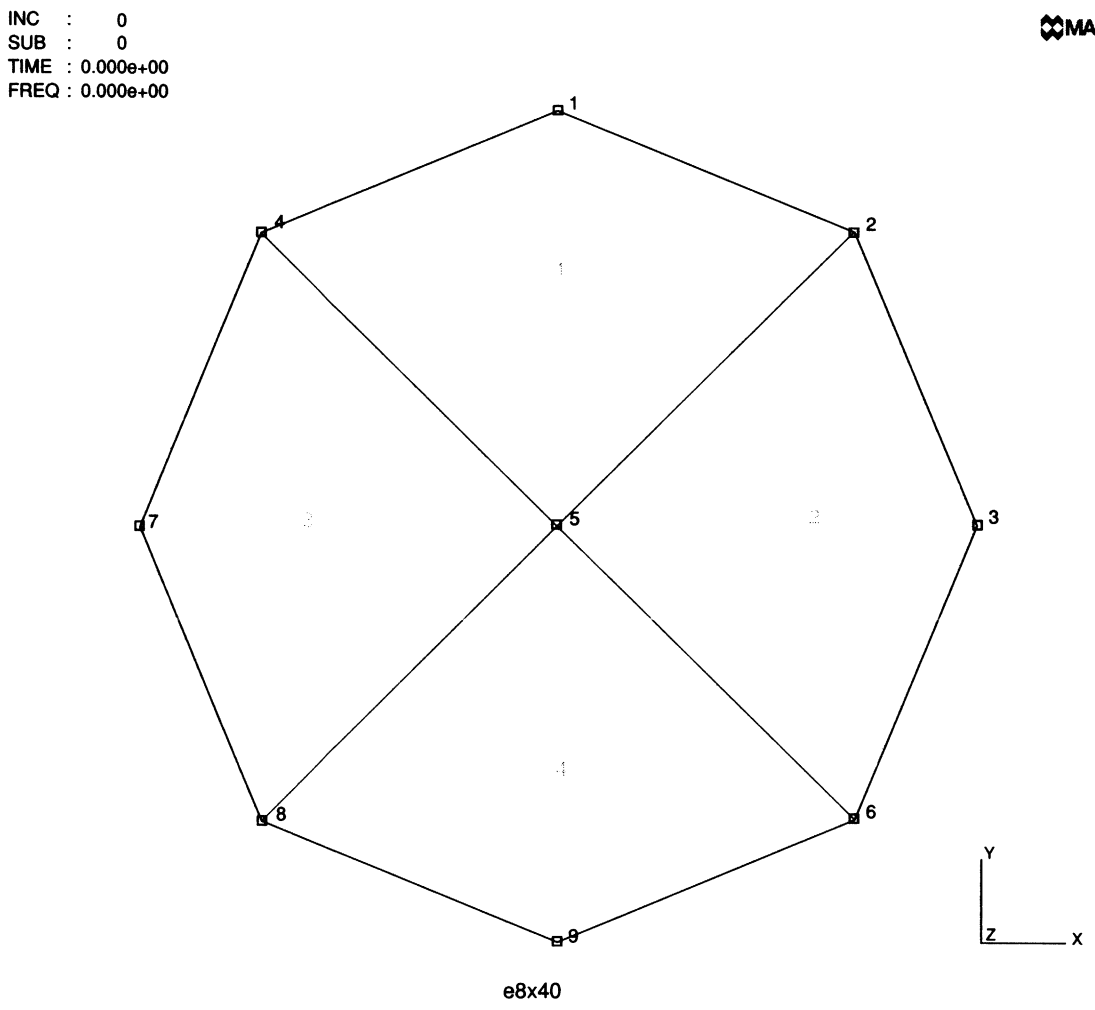

Figure E 8.40-1 Original Mesh

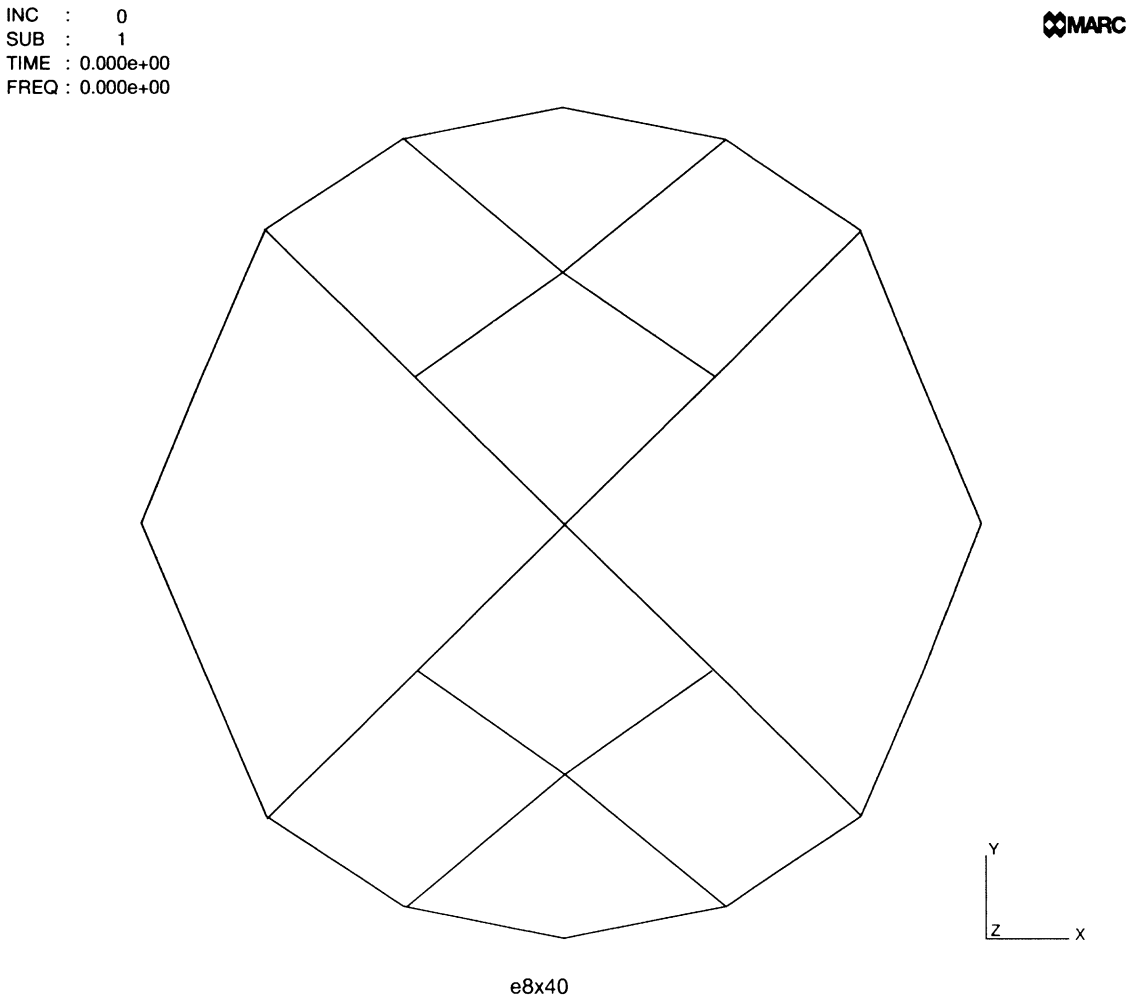

Figure E 8.40-2 First Adaptive Mesh

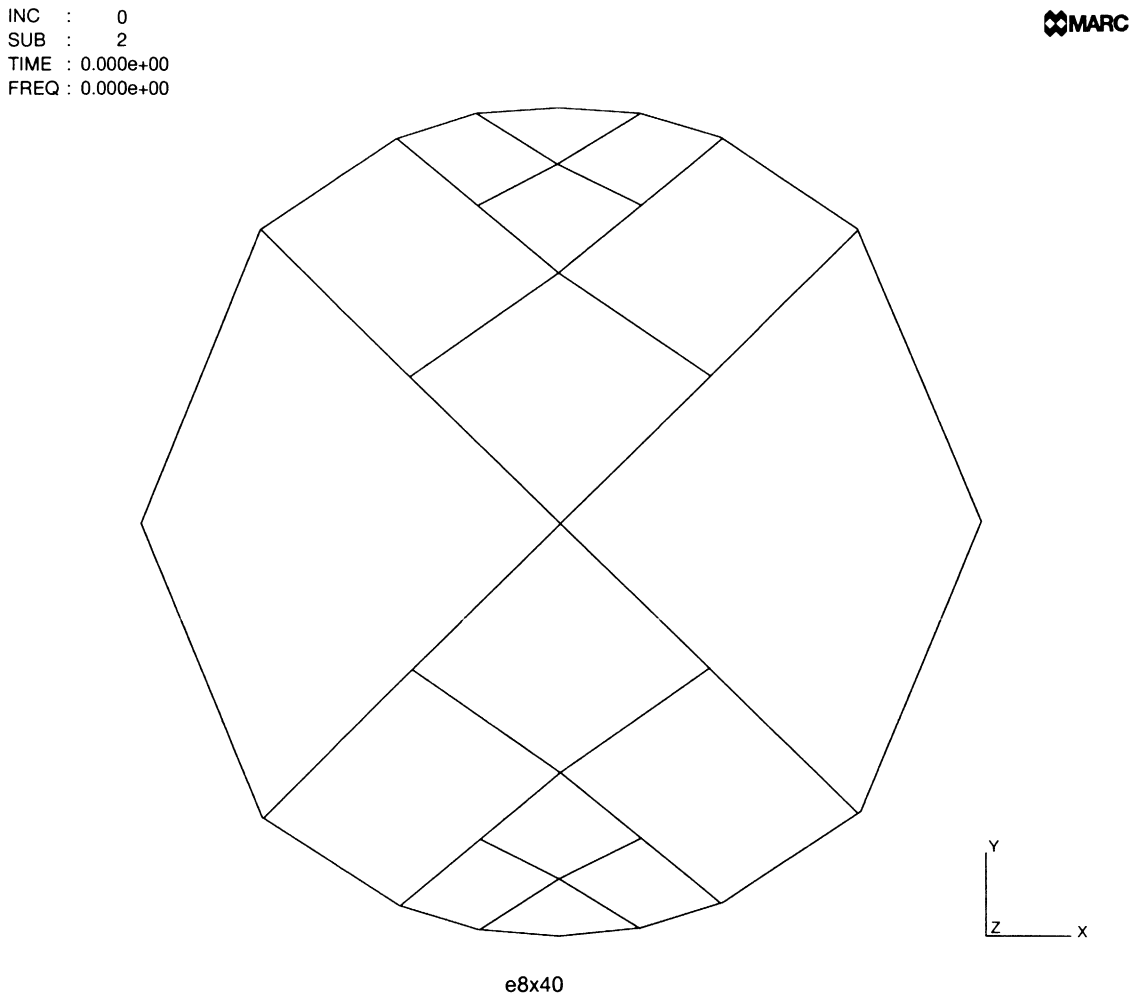

Figure E 8.40-3 Second Adaptive Mesh

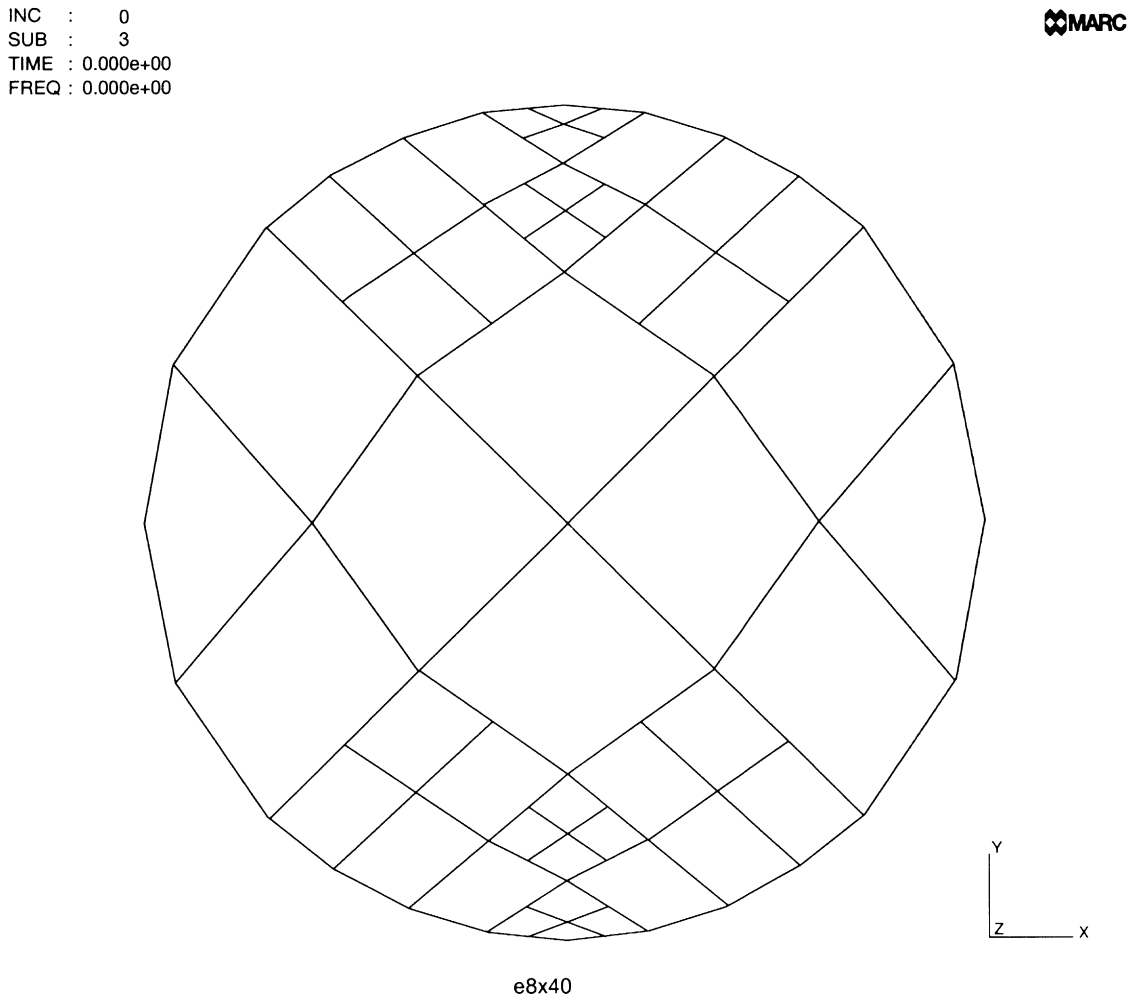

Figure E 8.40-4 Third Adaptive Mesh

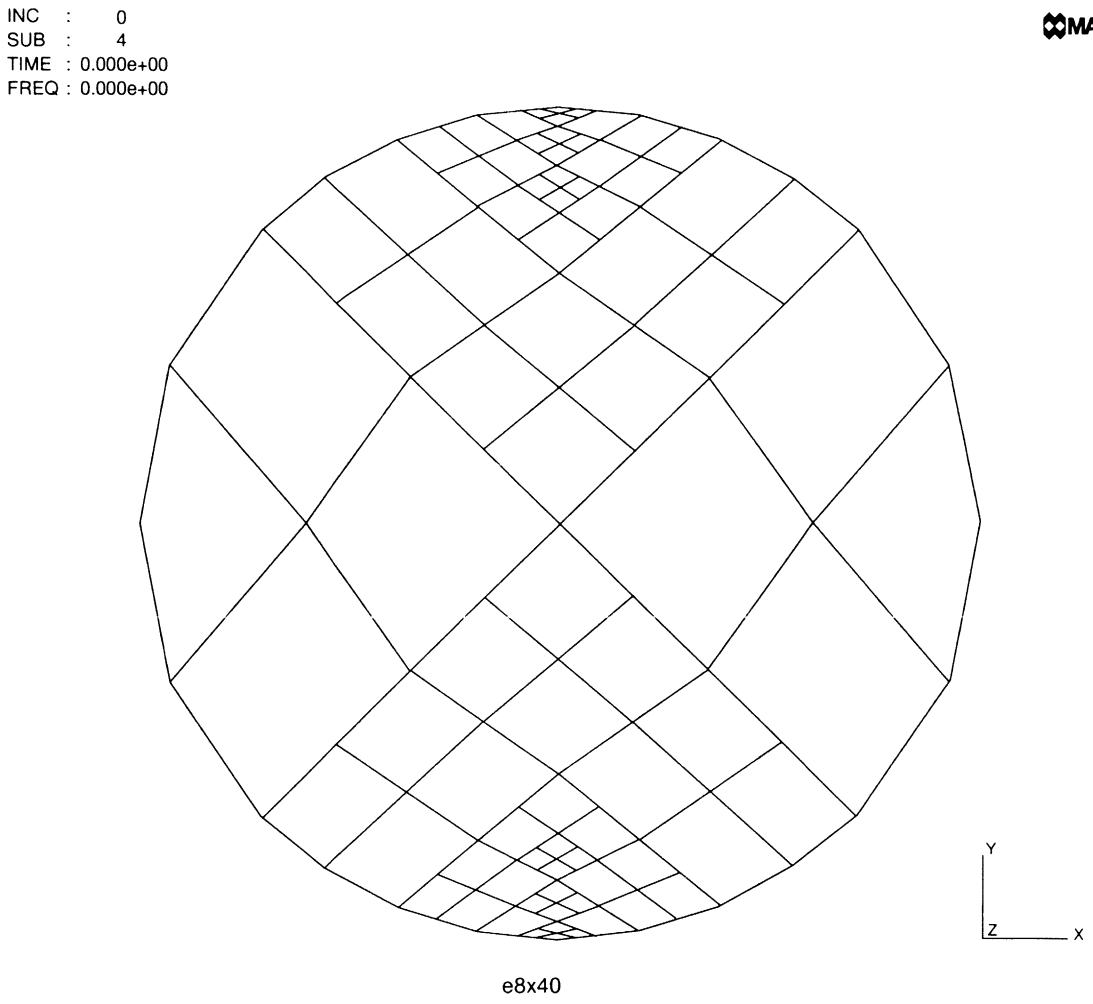

Figure E 8.40-5 Fourth Adaptive Mesh

E 8.41 Stress Singularity Analysis Using Adaptive Meshing

This problem demonstrates the use of adaptive meshing for the analysis of a stress singularity. The adaptive meshing will increase the number of elements in the region of high stresses and/or high stress gradients.

Element

Element type 3, a 4-node plane-stress element, is used in this analysis.

Model

The plate is a square of dimensions of 100 inches with one-quarter cutout. The initial model, consisting of three elements and eight nodes is shown in Figure E 8.41-1. A singular stress develops at node 5 because of the sharp corner.

Geometry

The plates are given a unit thickness.

Material Properties

The material is elastic with a Young's modulus of 30×10^6 psi and a Poisson's ratio of 0.3.

Boundary Conditions

Nodes 7 and 8 have constraints on y-motion while nodes 3 and 6 have constraints on x-motion. Nodes 1, 4, and 7 have a prescribed displacement in the negative x-direction of 0.01 inch. As new elements are created, displacement constraints will automatically be generated as required.

Adaptive Meshing

The Zienkiewicz-Zhu error criteria is used with a very tight tolerance of 0.001. A limit of four levels of subdivisions is requested. In theory, the maximum number of elements that could exist at the end is $3 * 4^4 = 768$. The ELASTIC parameter option is used to indicate that the analysis is to be repeated until the results satisfy the adaptive meshing error criteria. Additionally, the ERROR ESTIMATES option is used to evaluate the quality of the mesh.

Results

Figure E 8.41-2 through Figure E 8.41-6 show a progression of the created meshes. The stress at the corner node is shown below:

Iteration	σ_{xx} x 10^2 psi	σ_{xy} x 10^2 psi
0	2.33	3.469
1	2.376	4.825
2	2.892	6.535
3	3.229	9.615
4	4.271	13.56
5	4.498	14.80
6	4.583	14.56
7	4.577	14.53
8	4.583	14.53
9	4.583	14.54
10	4.583	14.54

Note that at higher iterations, the mesh refinement is propagating through the region. Because the number of levels is restricted to 4, the mesh is no longer being enriched at the corner. By iteration 7, the results do not substantially change. If the number of levels is allowed to increase, the solution will continue to change. The ERROR ESTIMATES option informs you that the aspect ratios and warpage is 1.0 and that the largest stress jump occurs at node 5.

Summary of Options used

Listed below are the options used in example e8x41.dat:

Parameter Options

ADAPTIVE
ALL POINTS
ELASTIC
ELEMENTS
END
PRINT
SIZING
TITLE

Model Definition Options

ADAPTIVE

CONNECTIVITY
CONTROL
COORDINATE
END OPTION
ERROR ESTIMATE
FIXED DISP
GEOMETRY
ISOTROPIC
POST

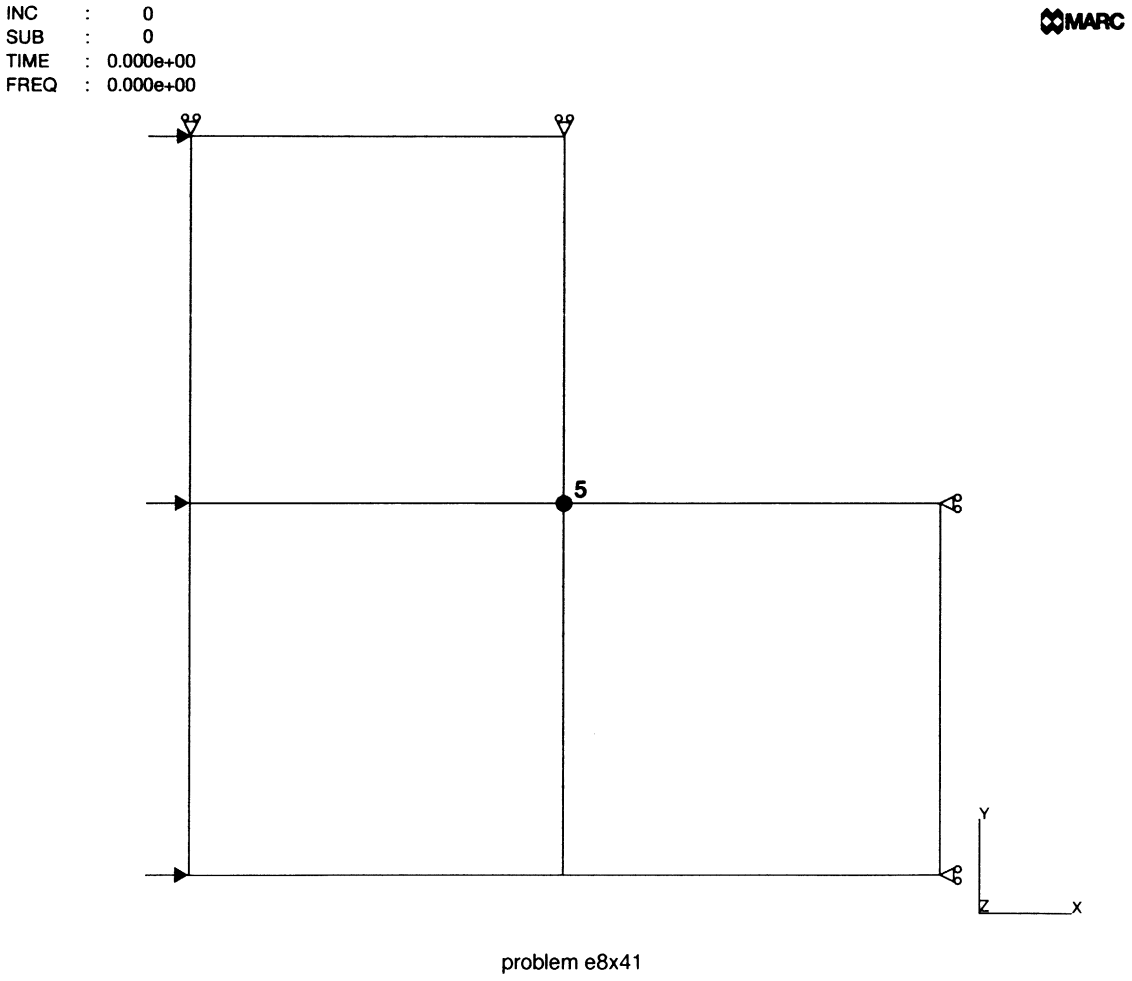

Figure E 8.41-1 Original Finite Element Mesh

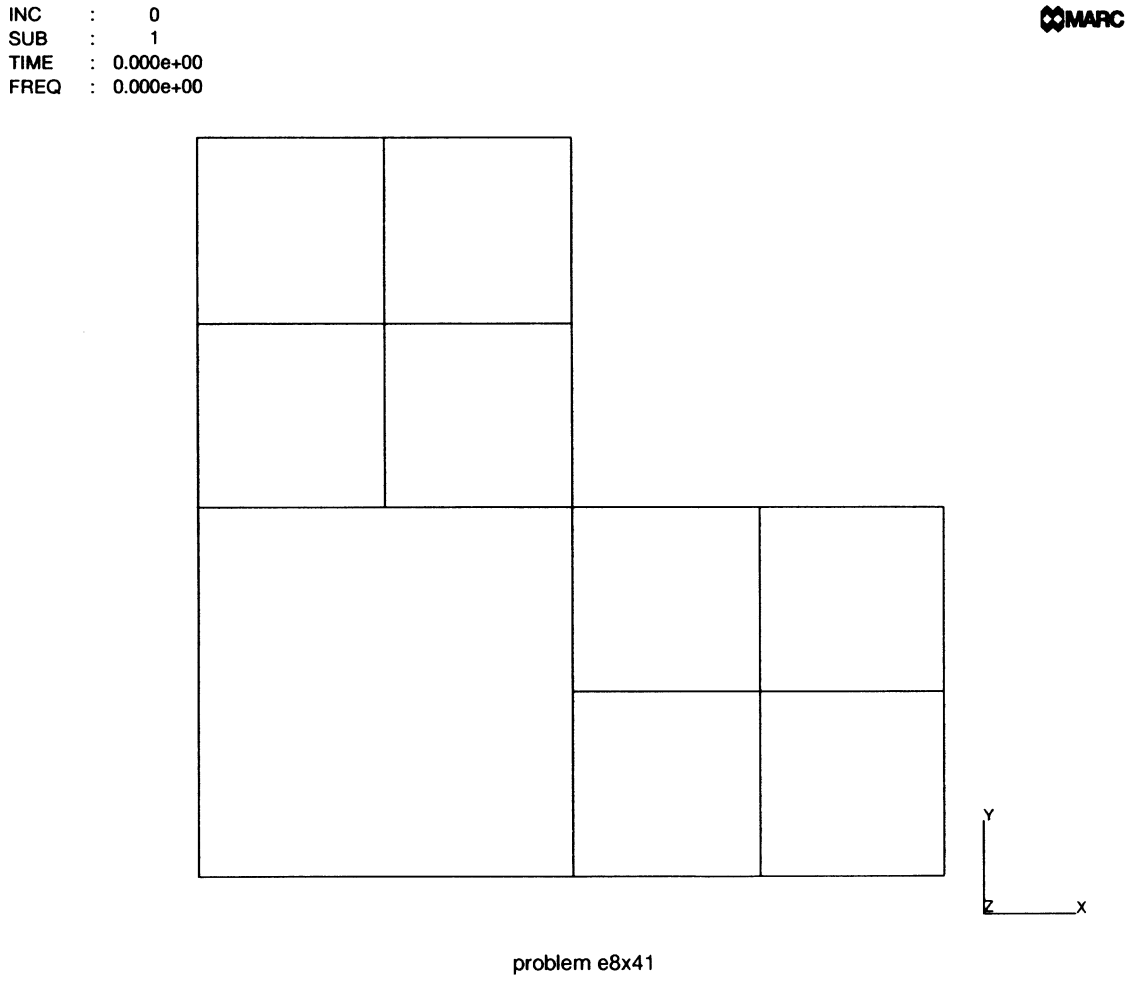

Figure E 8.41-2 First Adaptive Mesh

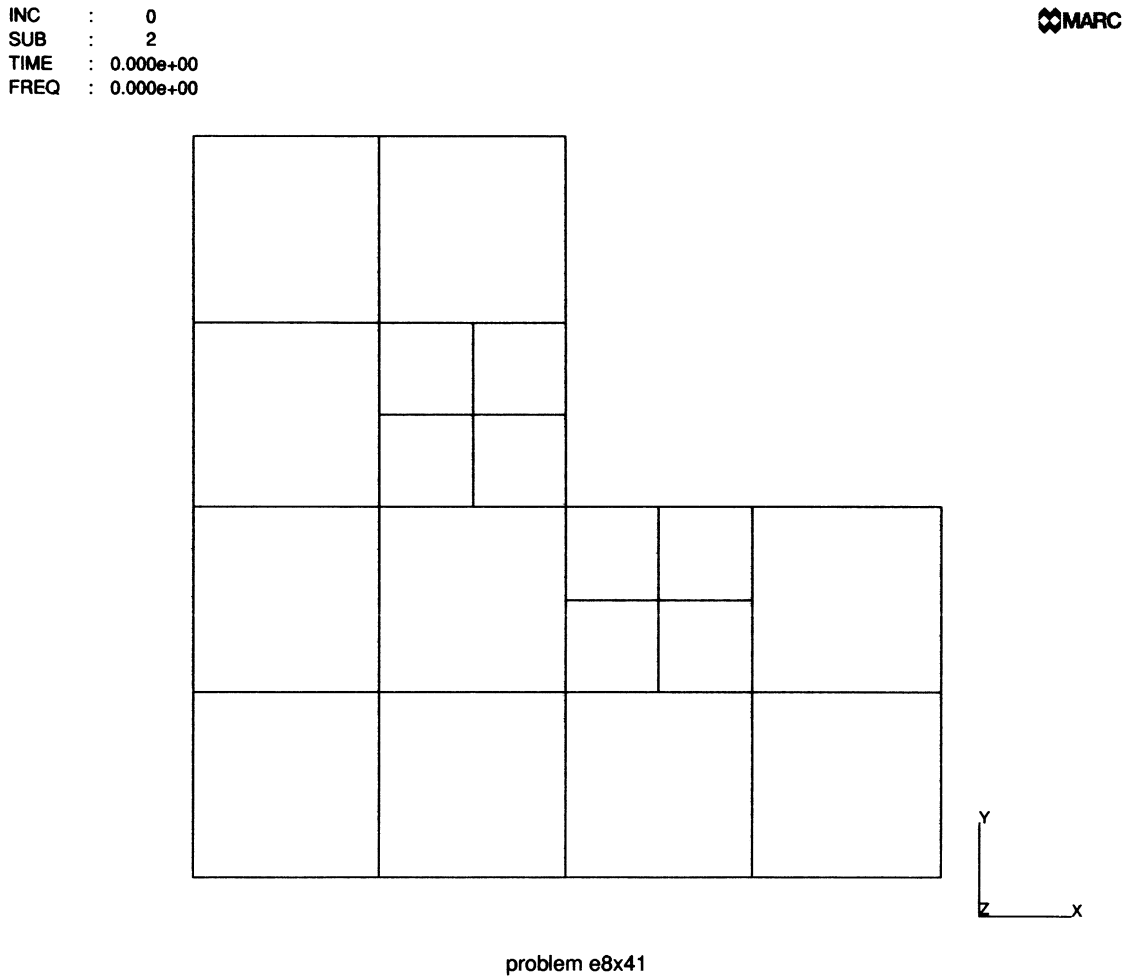

Figure E 8.41-3 Second Adaptive Mesh

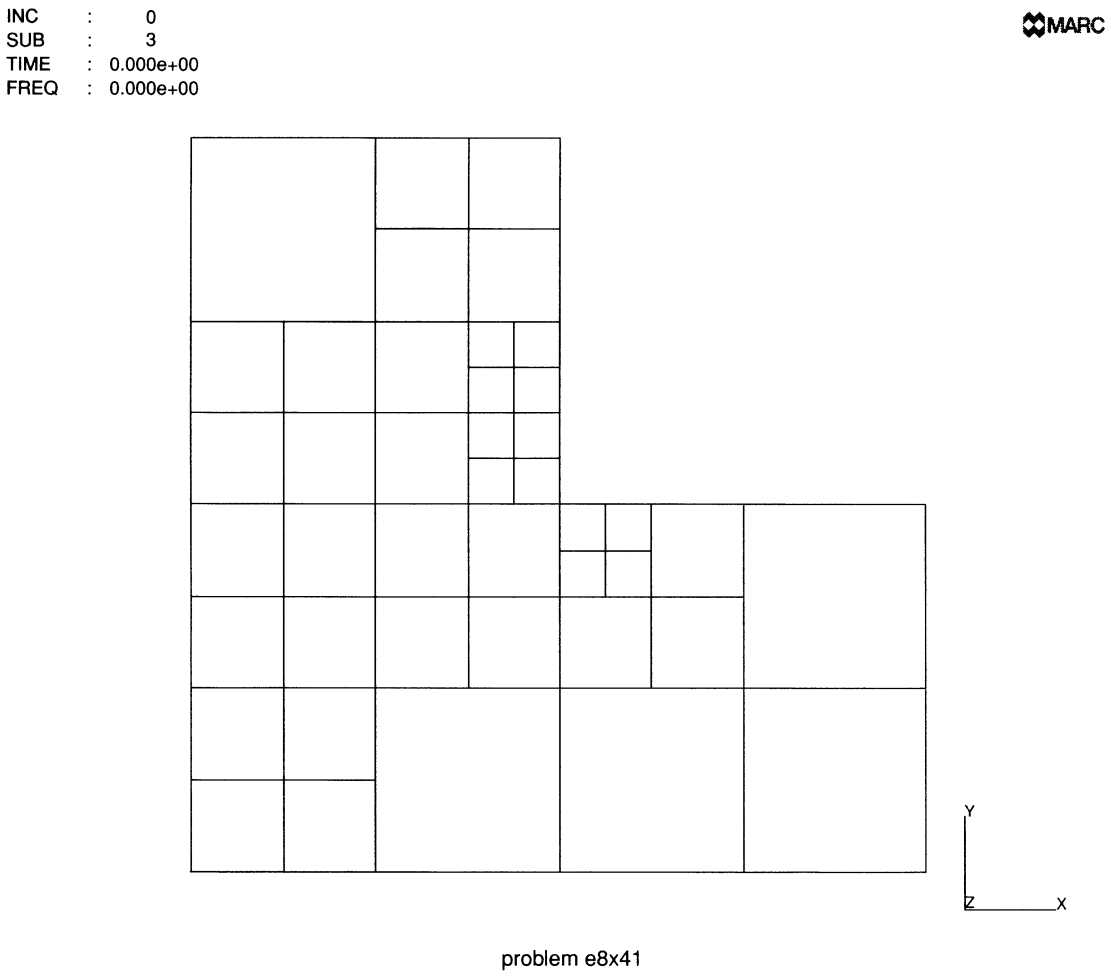

Figure E 8.41-4 Third Adaptive Meshing

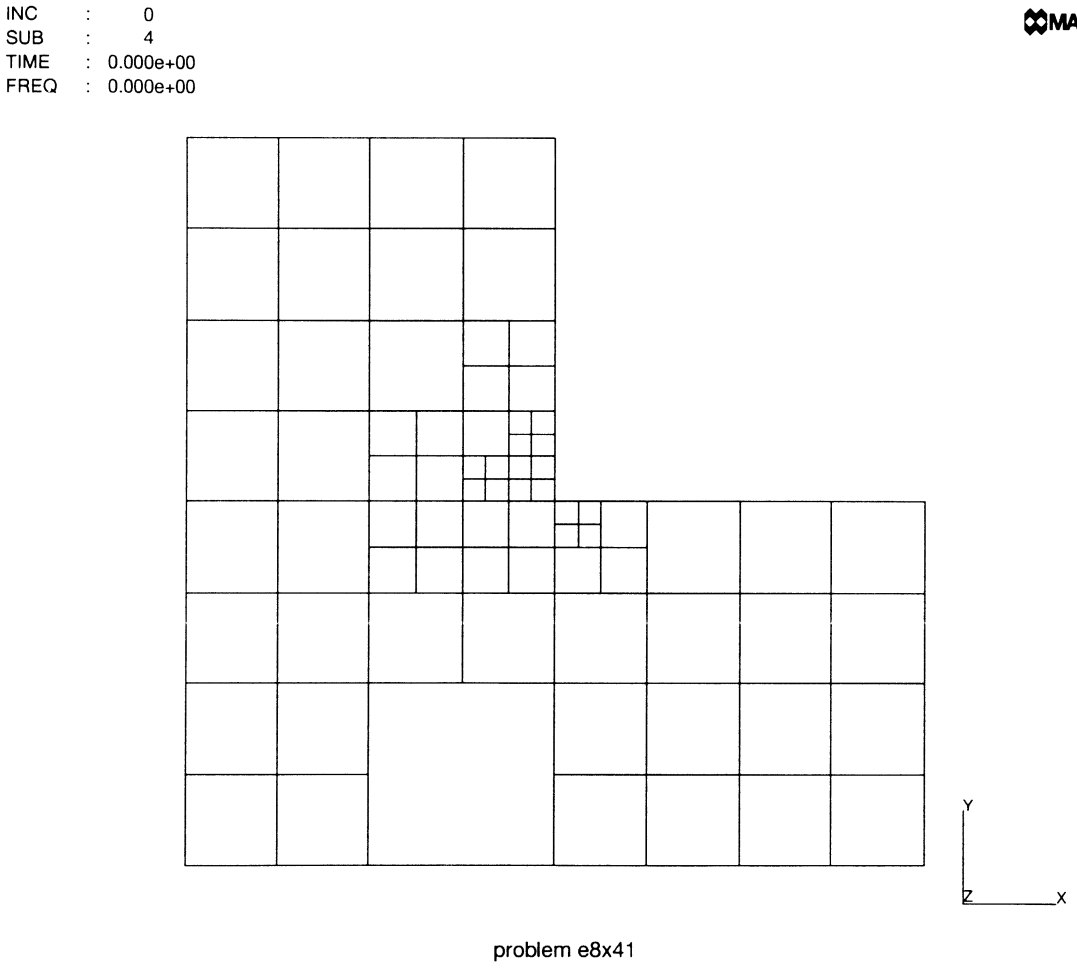

Figure E 8.41-5 Fourth Adaptive Mesh

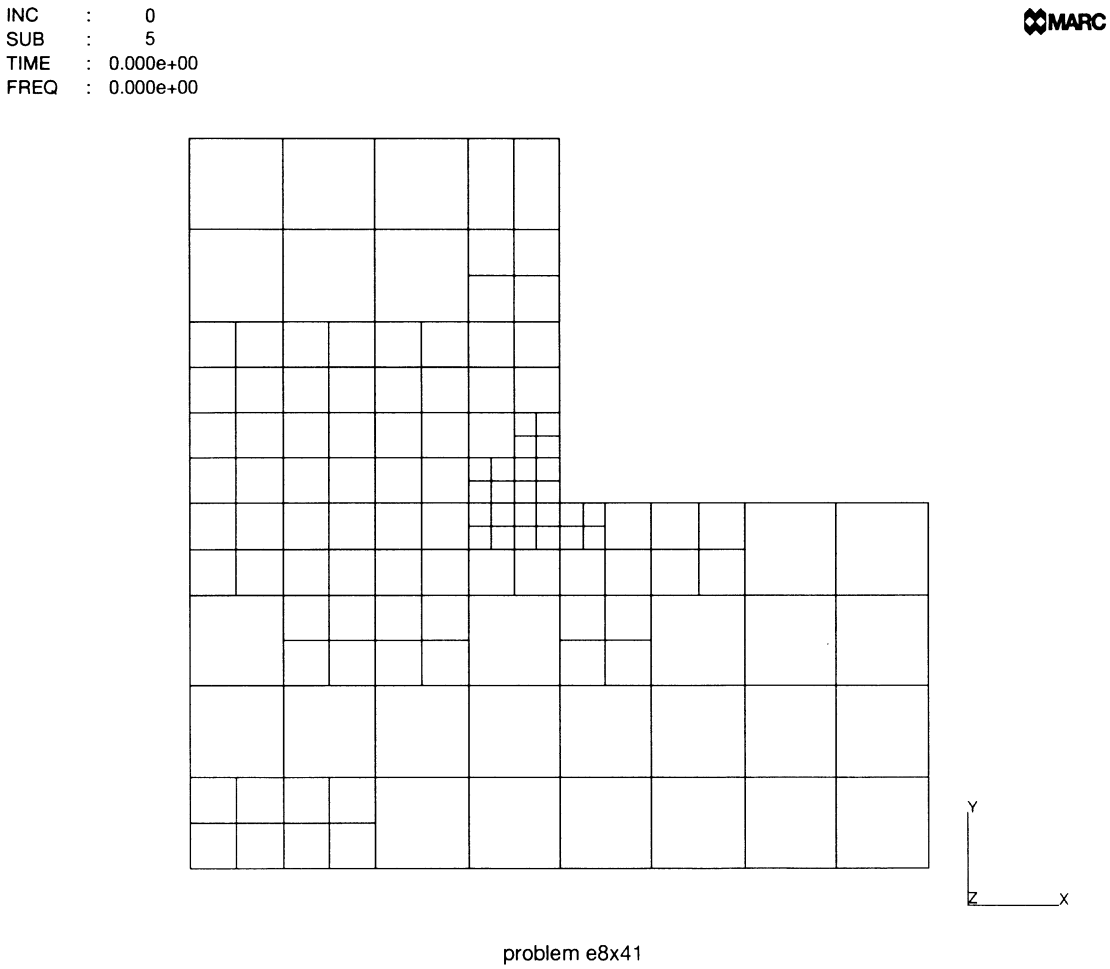

Figure E 8.41-6 Fifth Adaptive Mesh

E 8.42 Contact Analysis with Adaptive Meshing

This problem demonstrates the capability of adaptive meshing analysis during a contact process. A rod is bent about a deformable roll by a rigid punch (Figure E 8.42-1).

Geometry

The rod has a length of 0.28 m and a thickness of 0.02 m. The rigid roll has a radius of 0.31.

Material Properties

The material for all elements is treated as an elastic material with a Young's modulus of 1.5e7 N/m^2 and a Poisson's ratio 0.3.

Boundary Conditions

The upper end of the rod is firmly fixed. To avoid the rigid body mode, the center of the roller is fixed.

Control

Residual-force control is used with a relative error of 10%. A maximum of 15 iterations is used per load step.

Contact

This option declares three flexible bodies. The first is a one-layer rod and the second is a roller. The third body is a rigid punch moving with .005 cm/second along the global x-direction. Contact tolerance distance is 1.e-4 m. The ATTACH NODE option, in conjunction with the SURFACE option in an adaptive mesh analysis, allows new created nodes to attach to the surface. The surface the nodes are attached to is a circle with the center located at .037,2.6795 with a radius of .031. A list of nodes attached to this surface is the boundary nodes along the deformable roll.

Results

Initially, one element is placed through the thickness of the rod. As contact occurs between the punch and the rod, you observe the mesh refinement. Similarly, where the rod contacts the deformable roll, both bodies show local mesh refinement. As the nonlinear process continues, adaptivity occurs when new regions come into contact. Finally, you can observe that the rod has been bent around and that the refinement has occurred on the rod through the thickness in the direction where contact has occurred. Two levels of refinement are allowed in this analysis. The deformed shape is shown in Figure E 8.42-2 through Figure E 8.42-5.

Summary of Options Used

Listed below are the options used in example e8x42.dat:

Parameter Options

ADAPTIVE
DIST LOADS
ELEMENTS
END
FOLLOW FOR
LARGE DISP
PRINT
SETNAME
SIZING
TITLE

Model Definition Options

ADAPTIVE
ATTACH NODE
CONNECTIVITY
CONTACT
CONTROL
COORDINATE
DEFINE
DIST LOADS
END OPTION
FIXED DISP
GEOMETRY
ISOTROPIC
NO PRINT
OPTIMIZE
POINT LOAD
POST
RESTART
SOLVER
SURFACE

Load Incrementation Options

AUTO LOAD
CONTINUE
DIST LOADS
MOTION CHANGE
TIME STEP

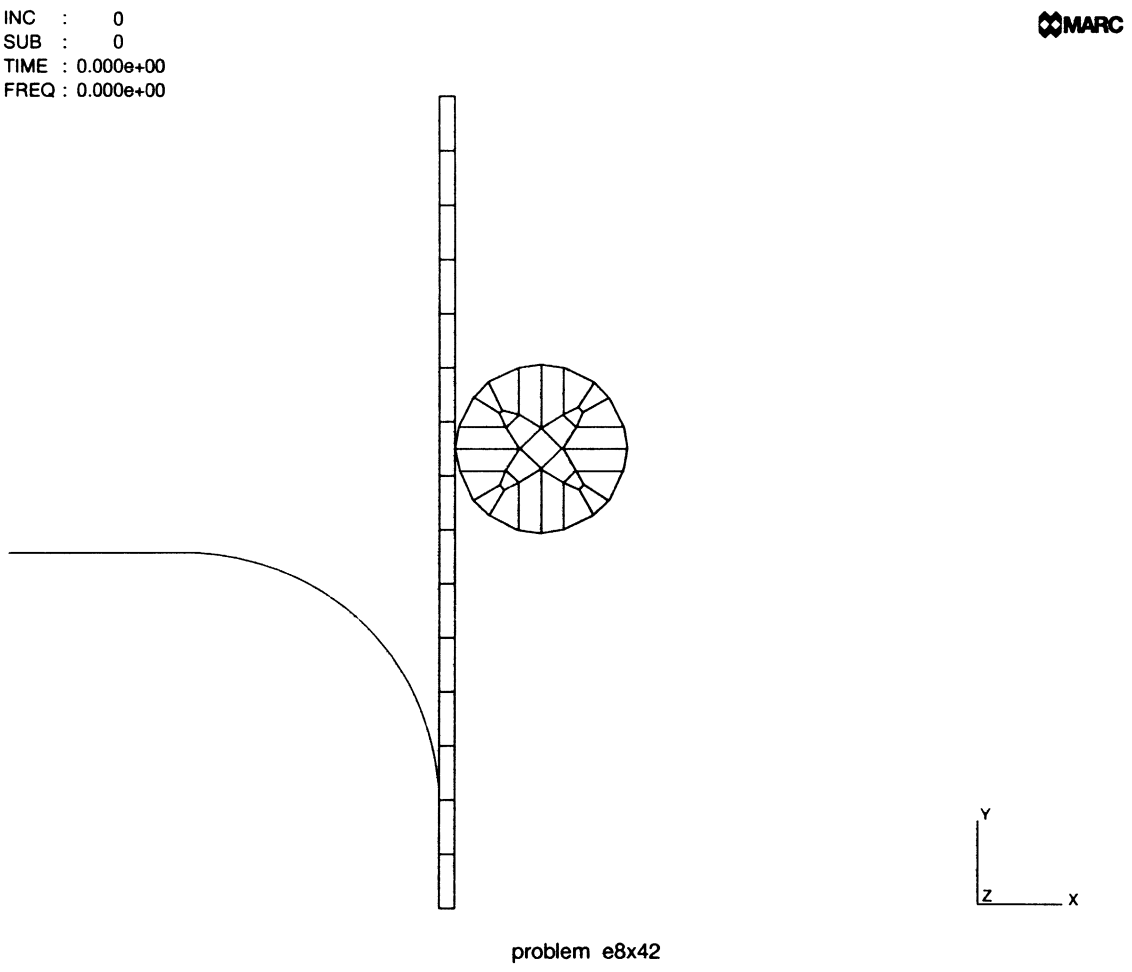

Figure E 8.42-1 Original Mesh

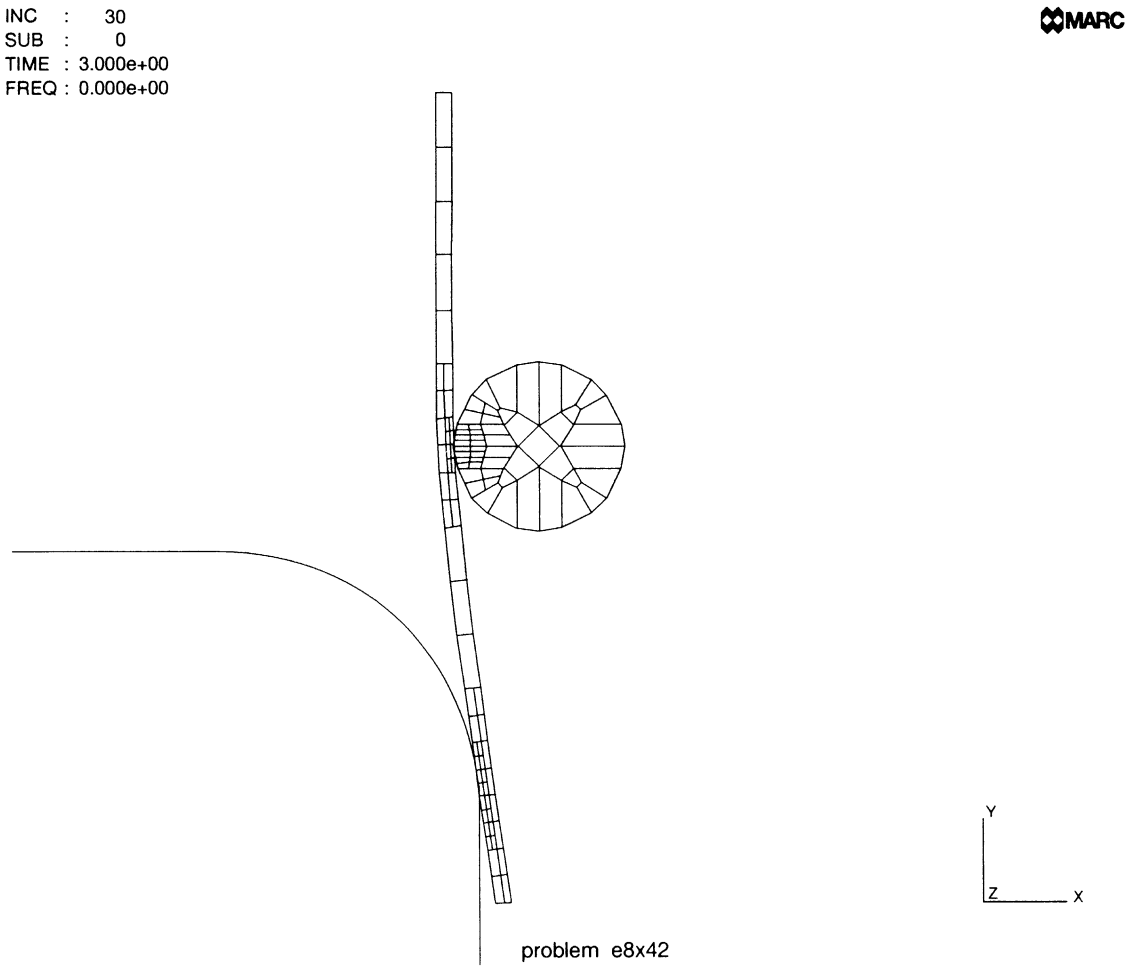

Figure E 8.42-2 Deformed New Mesh at Increment 30

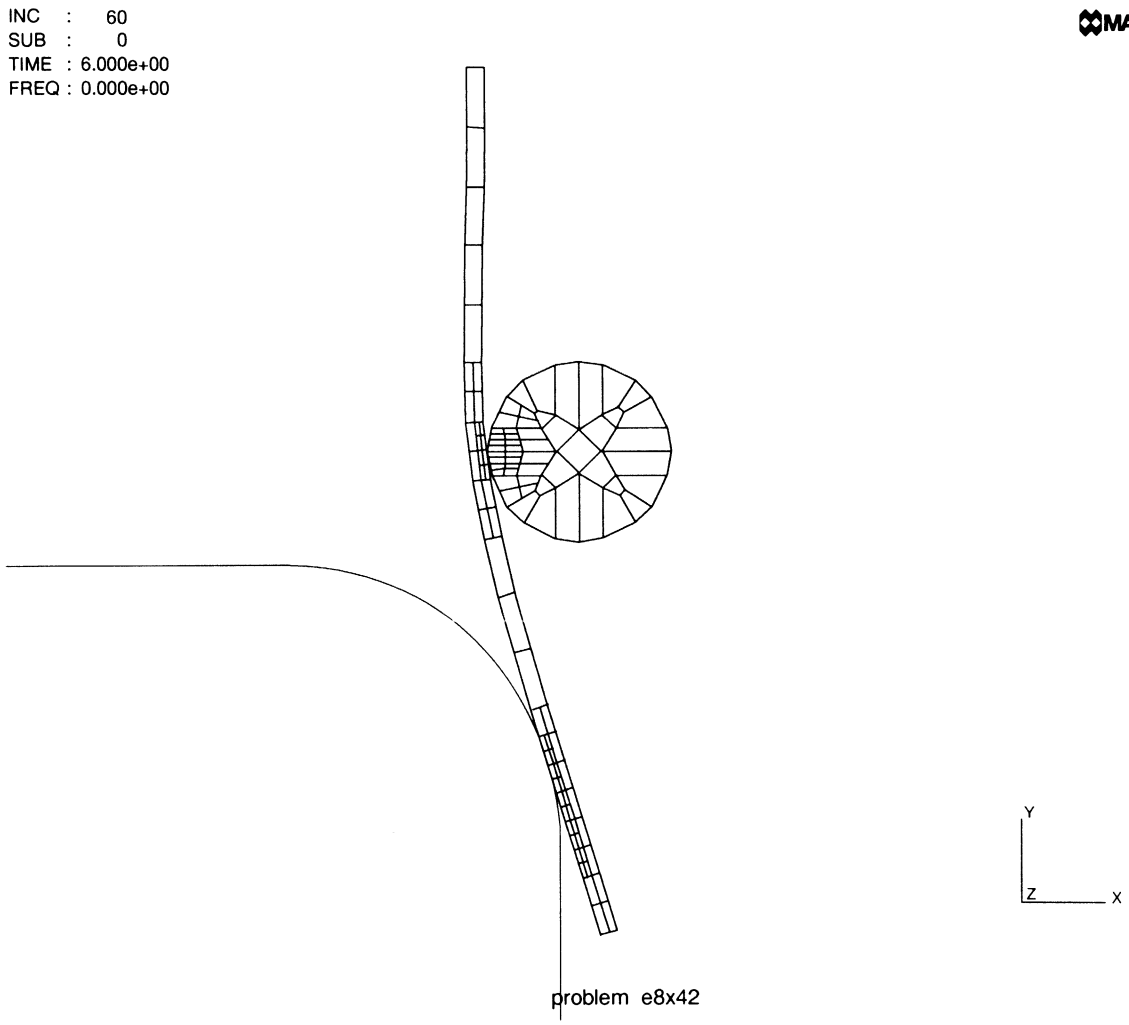

Figure E 8.42-3 Deformed New Mesh at Increment 60

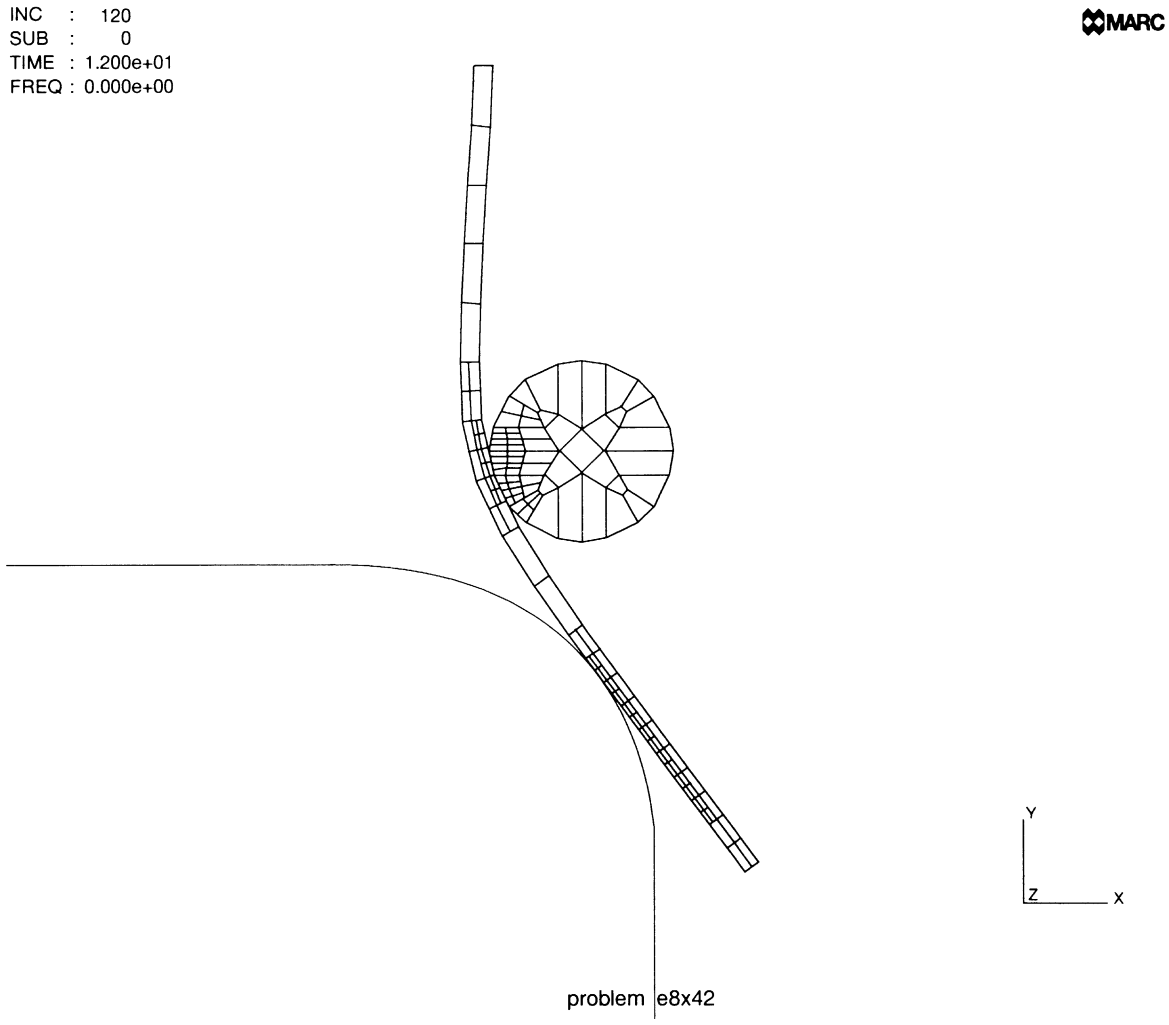

Figure E 8.42-4 Deformed New Mesh at Increment 120

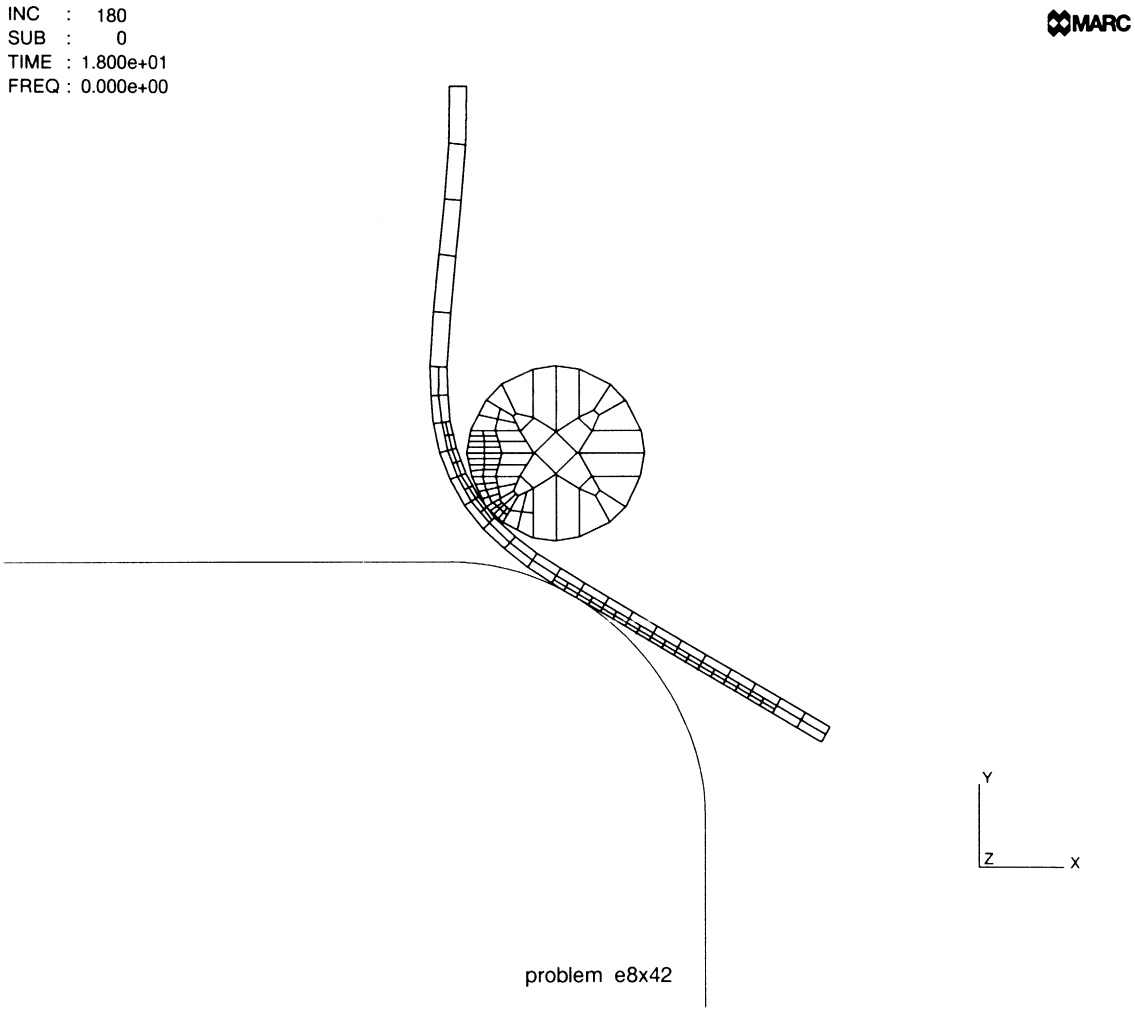

Figure E 8.42-5 Deformed New Mesh at Increment 180

E 8.43 Rubber Seal Analysis Using Adaptive Meshing

This problem demonstrates the use adaptive meshing in a nonlinear rubber analysis of a seal. In a nonlinear analysis, the mesh quality is checked at the end of each converged increment. If the mesh needs to be refined, this is performed before the beginning of the next increment. This model uses the Mooney material model.

Element

This example uses element type 119, a lower-order isoparametric axisymmetric element, using the modified Herrmann formulation. This element uses reduced integration with hourglass control. The four corner nodes have conventional displacement degrees of freedom with an additional degree of freedom representing the hydrostatic pressure. The original mesh was created using element type 82. The ALIAS option was used to convert element type 82 to element type 119.

Model

The original model is shown in Figure E 8.43-1 and consists of 560 elements and 644 nodes.

Material Properties

A two-term Mooney-Rivlin model is used with $C_{10} = 0.3$ N/cm^2 ; $C_{01} = 0.04$ N/cm^2.

Boundary Conditions

The region indicated in Figure E 8.43-2 has prescribed displacement boundary conditions. In the first 8 increments, the tip of the seal is deflected 2 cm. In the next 12 increments, the tip is deflected an additional 3.0 cm. Additionally, a pressure load is placed on the region indicated which has a total magnitude of 0.25 N/cm^2. The AUTO LOAD option is used to specify that fixed increment sizes are to be used. The time step used by the contact procedure is 1 second.

Control

The PRINT, 5, 8 parameter option is used to obtain additional information regarding the progress of contact. The Cuthill-McKee optimizer is used. The bandwidth will be re-optimized when new elements are created due to the adaptive procedure or when self contact occurs in the seal. The CONTROL option specifies the maximum number of elements is 100 and the number of iterations is 10. Displacement convergence checking is used with a 10% tolerance. The initial stress stiffness terms are subjected to compressive behavior and neglecting these terms may prevent a non-positive definite matrix from occurring.

Adaptive

Two adaptive criteria are used. The first indicates that elements should be refined when they come into contact. In this problem, the seal will come into self contact and elements on both surfaces will be refined. The second criteria is based on the stress levels in the element. It implies subdivision of those elements whose stress is greater than 75% of maximum stress. This results in the subdivision of elements in the bend region.

Contact

There is one deformable body that may go into self contact. If contact occurs, the surfaces will use a Coulomb friction with a coefficient of 0.3. To improve convergence, the body is not allowed to separate unless the force is greater than 100 N. Based on the size of the element, the program will choose its own contact tolerance.

Results

Figure E 8.43-3 shows the deformation after ten increments. The initial mesh refinement is due to the stress level. Figure E 8.43-4 shows the deformation just as contact is to occur. The results at increment 19 (Figure E 8.43-5) show that mesh refinement has occurred due to contact. At the end of the analysis, the number of elements is 560 and the number of nodes is 716.

Summary of Options Used

Listed below are the options used in example e8x43.dat:

Parameter Options

ADAPTIVE
ALIAS
DIST LOADS
ELEMENTS
END
FOLLOW FOR
LARGE DISP
PRINT
SIZING
TITLE

Model Definition Options

ADAPTIVE
CONNECTIVITY
CONTACT
COORDINATE
DIST LOADS
END OPTION
FIXED DISP
MOONEY
NO PRINT
OPTIMIZE
POINT LOAD
POST

Load Incrementation Options

AUTO LOAD
CONTINUE
CONTROL
DISP CHANGE
DIST LOADS
TIME STEP

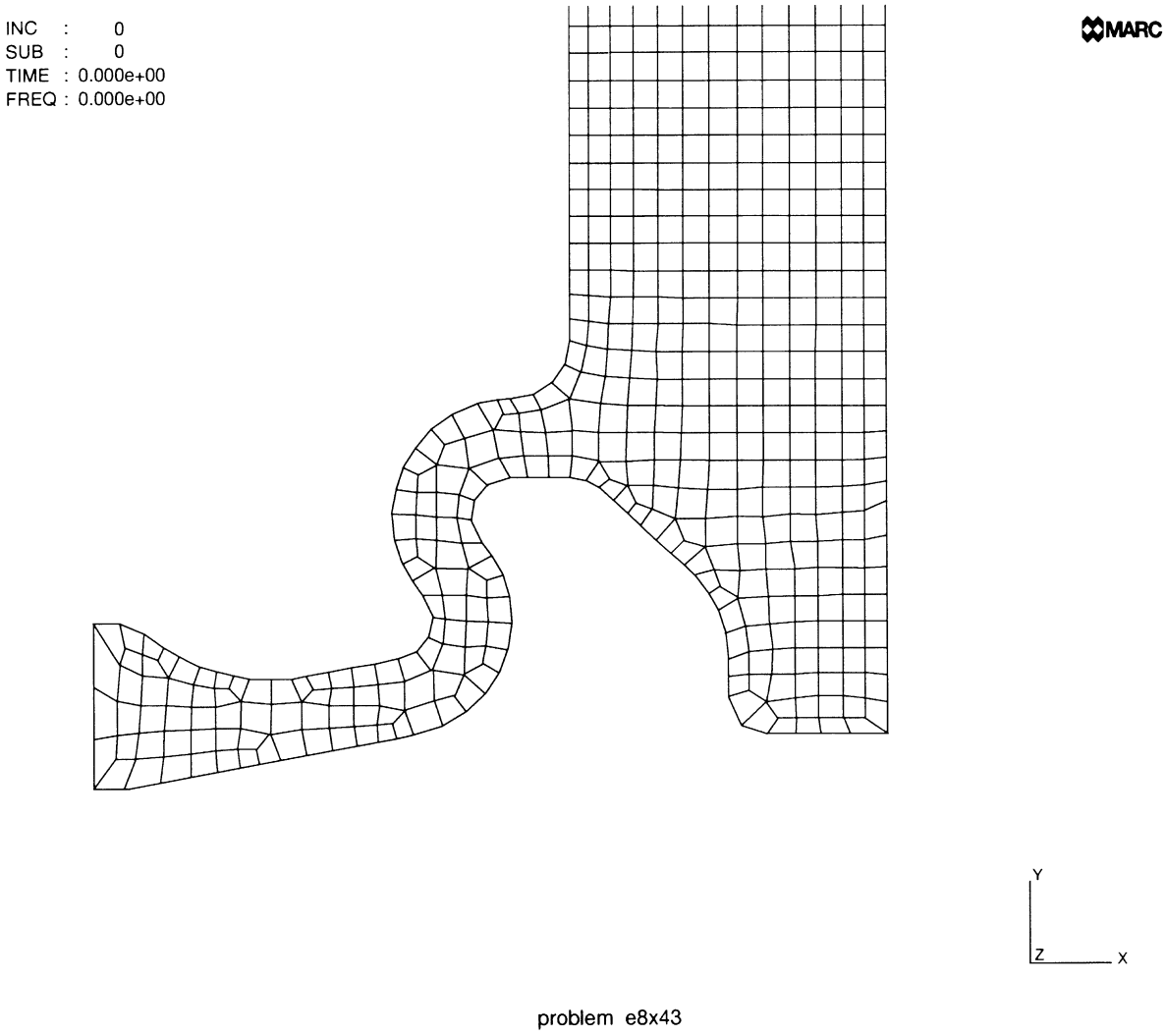

Figure E 8.43-1 Close-up of Original Finite Element Mesh

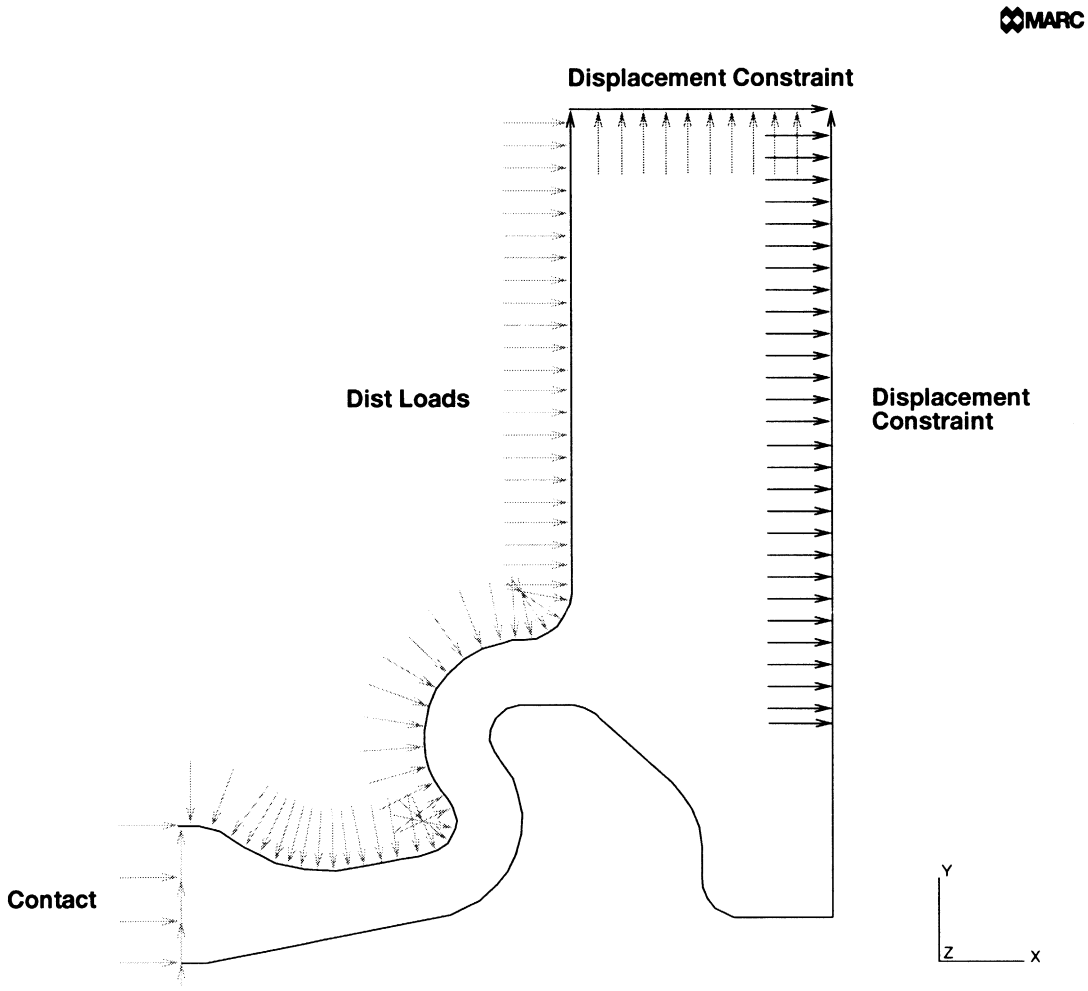

Figure E 8.43-2 Seal with Prescribed Boundary Conditions

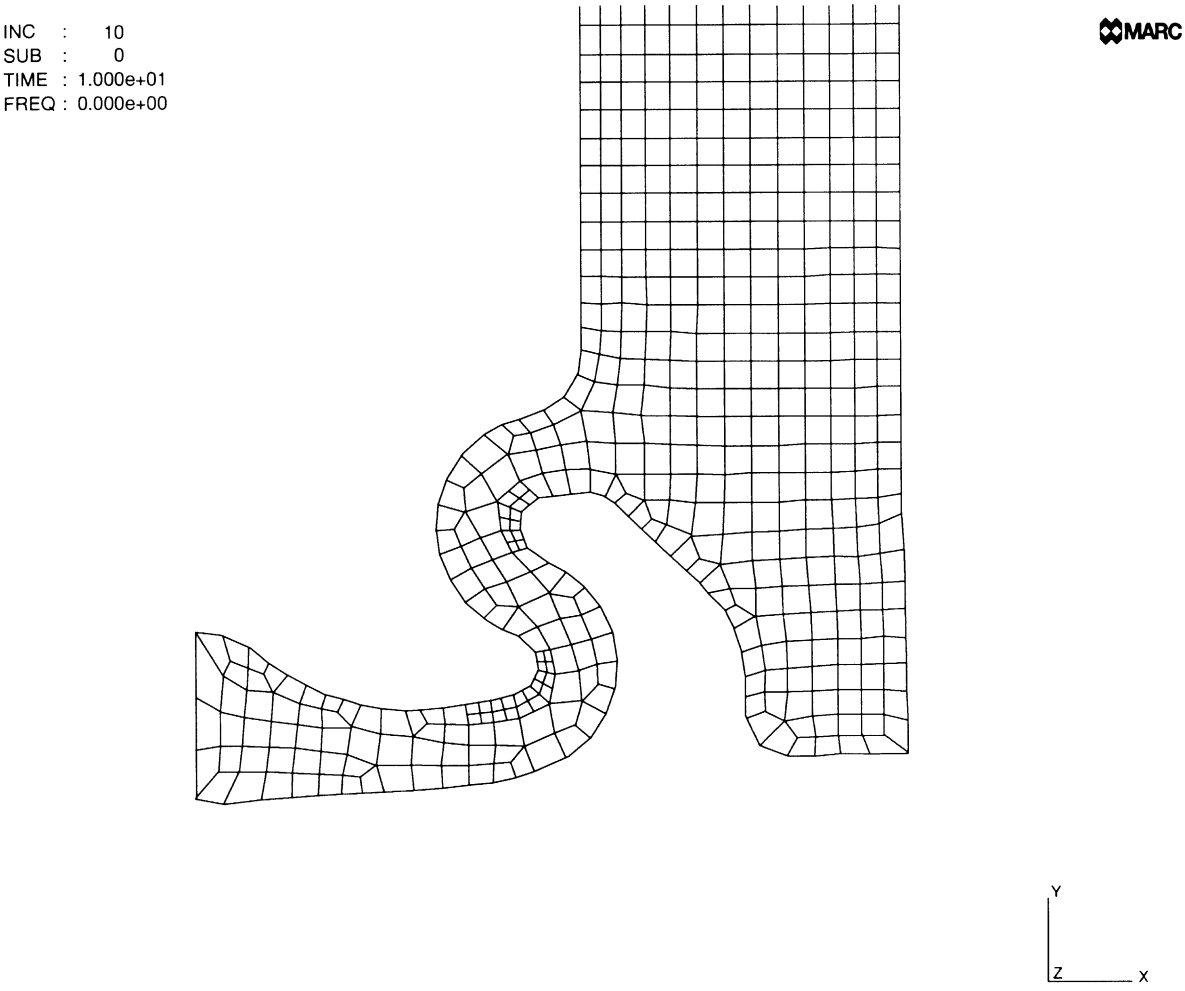

Figure E 8.43-3 Deformed Mesh Showing New Elements

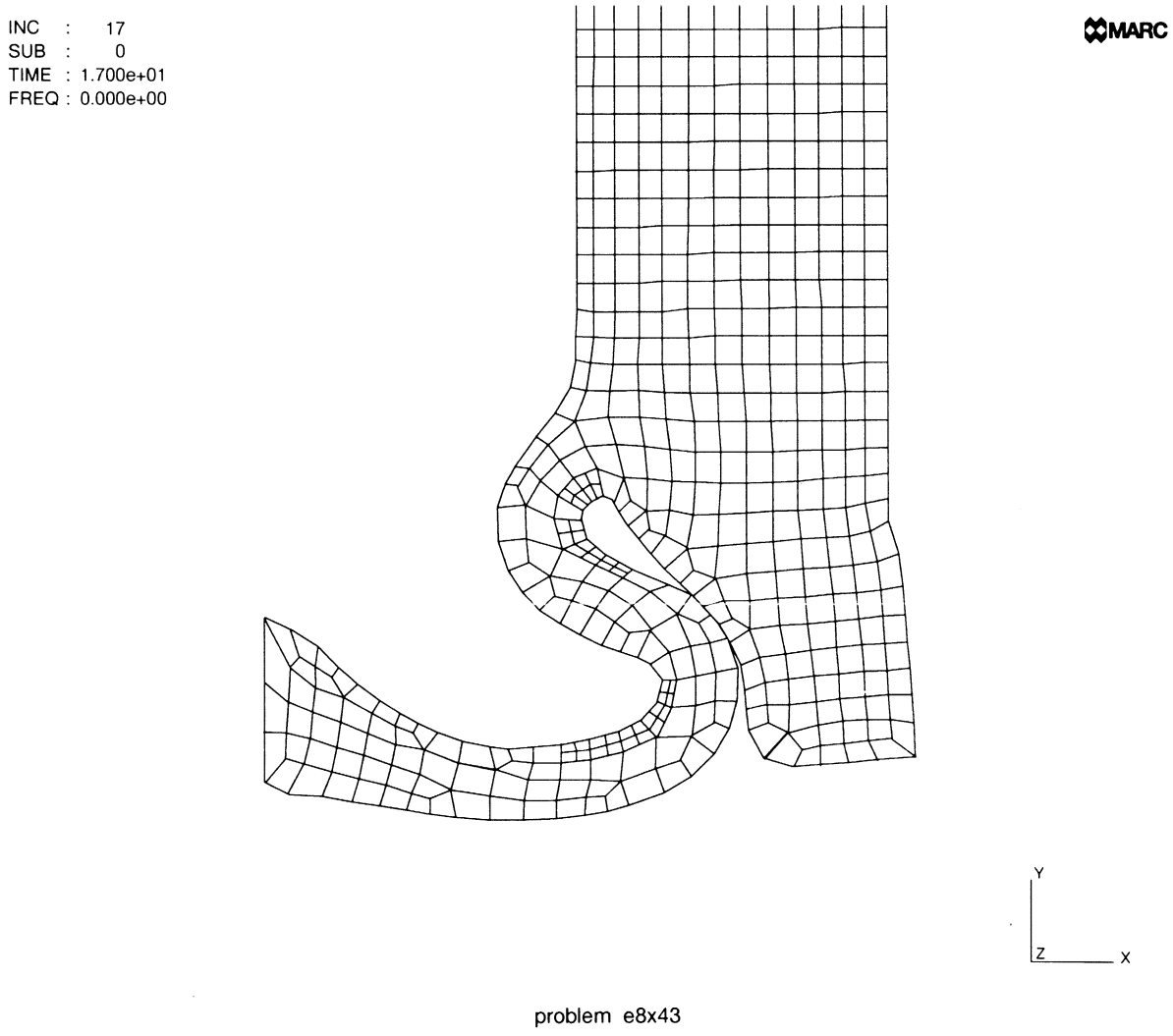

Figure E 8.43-4 Deformed Mesh at Initial Contact

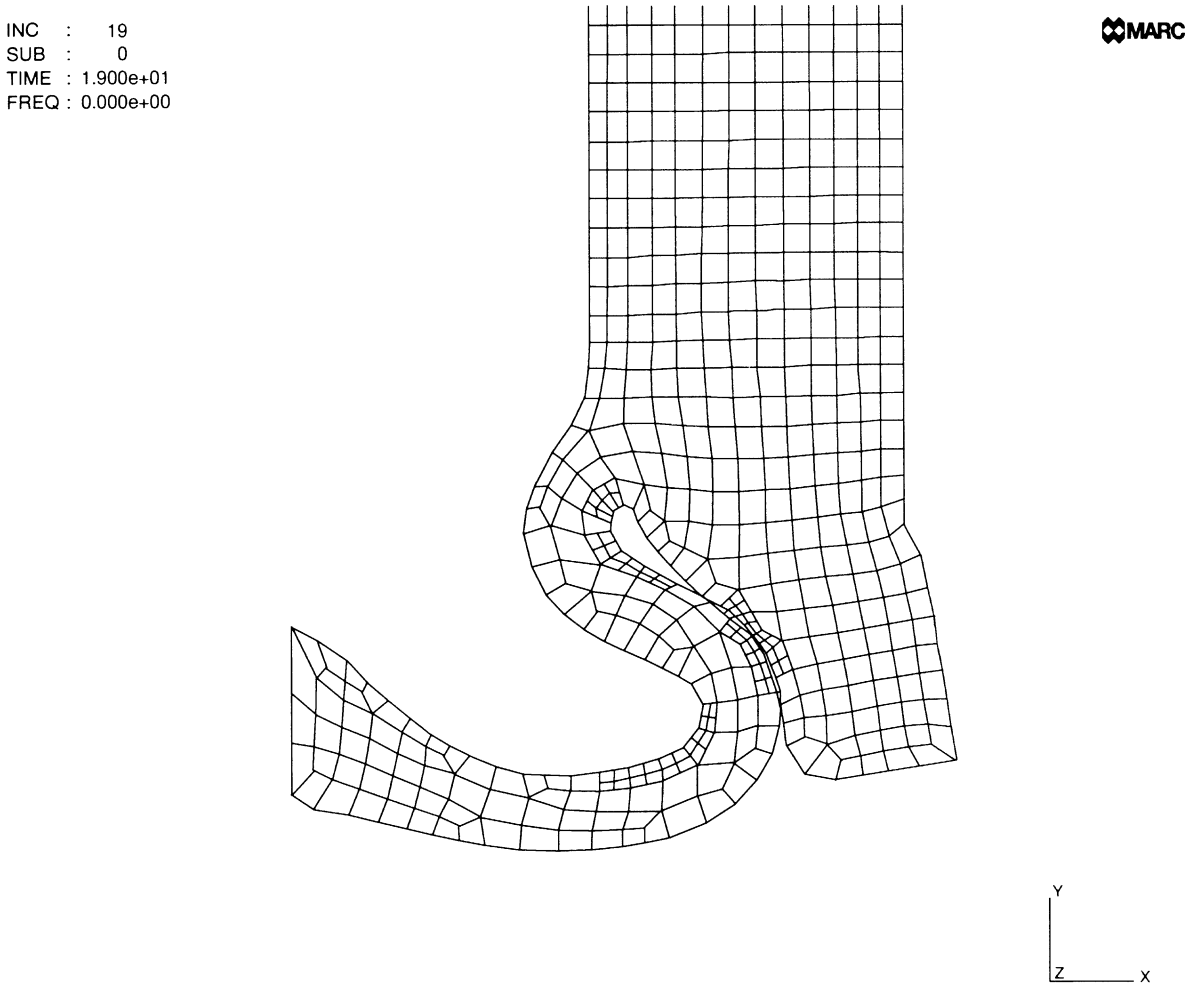

Figure E 8.43-5 Adaptivity Due to Contact

E 8.44 Simplified Rolling Example with Adaptive Meshing

This problem demonstrates the use of contact and adaptive meshing for performing a simplified rolling of a sheet.

Element

Element type 11, the 4-node isoparametric element, is used in this model. The constant dilatation formulation is selected through the GEOMETRY option.

Model

The initial model of the workpiece is shown in Figure E 8.44-1. A single row of elements is used in the thickness direction. The adaptive meshing procedure will be used to increase the number of elements when the material approaches the roll. The workpiece is 28.0 cm long and 1.025 cm thick. The radius of the roll is 64 cm.

Material Properties

The sheet is a high-strength steel with a Young's modulus of 2.1×10^5 N/cm^2, a Poisson's ratio of 0.3, and an initial yield stress of 200 N/cm^2. The material has a work-hardening curve shown in Figure E 8.44-2

Geometry

The unit thickness is one. The constant dilatation option is set in the GEOMETRY option.

Boundary Conditions

The nodes along the line y = 0 are constrained such that there is no y deflection. This represents a symmetry condition. The CONTACT option is used to prescribe the motion of the roller.

Contact

There are three bodies in the model. The first is the deformable workpiece, the second is the roller, and the third is the ram.

The first body consists of the original 20 elements. As the adaptive meshing procedure adds more elements to the system, the additional elements will be included in the first body. The CONTACT TABLE option is used to indicate that body 1 contacts only bodies 2 and 3 and not itself.

The second body has its center of rotation at -5.9, 64.775 and has a friction coefficient of 0.1. It is created from a circular arc (type 2) using method 1 (enter starting point, end point, center, and radius) with 60 divisions used along the arc.

The ram (the third body) is modeled as a single line segment.

In the first 15 increments, the roll is given a motion of -1 radians/second or 57.295°/seconds. The ram is given a motion of $r \bullet \omega = -64$ cm/sec. This is done to insure that the workpiece does not initially slip. The time step is 0.004. So, effectively, the roll turns 0.004 radian = 0.229 degrees. The ram is removed from the system by using the RELEASE option and given a large velocity in the opposite direction. An additional 140 increments are taken.

The contact surfaces were given their velocity through the MOTION CHANGE option.

In this example, the Coulomb friction for a rolling model was used with a coefficient of friction of 0.1. The friction forces were based upon the nodal contact forces as opposed to the default extrapolated stress model.

The relative sliding velocity was chosen as 0.1 which is a small number compared to the roll's tangential velocity at the interface = 64 rad/sec * 1 cm = 64 cm/sec.

The contact tolerance is 0.10 cm.

Control

This analysis used displacement control with a tolerance of 10%. A maximum number of iterations was chosen as 25. In general, fewer iterations were required for convergence.

Adaptive Meshing

The adaptive meshing procedure was used with the box option (type 4) with a maximum number of two subdivisions. When using the box option, when an element is fully within the volume in space defined by the box, it will be refined. In this problem, we know that the region under the roller is of interest, so we define a box in this area. The box is defined to cover a region from $-3 < x \leq 3$ for all y and z as shown in Figure E 8.44-2.

Results

The deformed mesh at increments 48, 75, and 100 are shown in Figure E 8.44-3 through Figure E 8.44-4.

Summary of Options Used

Listed below are the options used in example e8x43.dat:

Parameter Options

ADAPTIVE
ELEMENTS
END
FINITE
LARGE DISP
PRINT
SIZING
TITLE
UPDATA

Model Definition Options

ADAPTIVE
CONNECTIVITY
CONTACT
CONTACT TABEL
CONTROL
COORDINATE
END OPTION
FIXED DISP
GEOMETRY
ISOTROPIC
NO PRINT
POST
RESTART
WORK HARD

Load Incrementation Options

AUTO LOAD
CONTACT TABLE
CONTINUE
CONTROL
MOTION CHANGE
RELEASE
TIME STEP

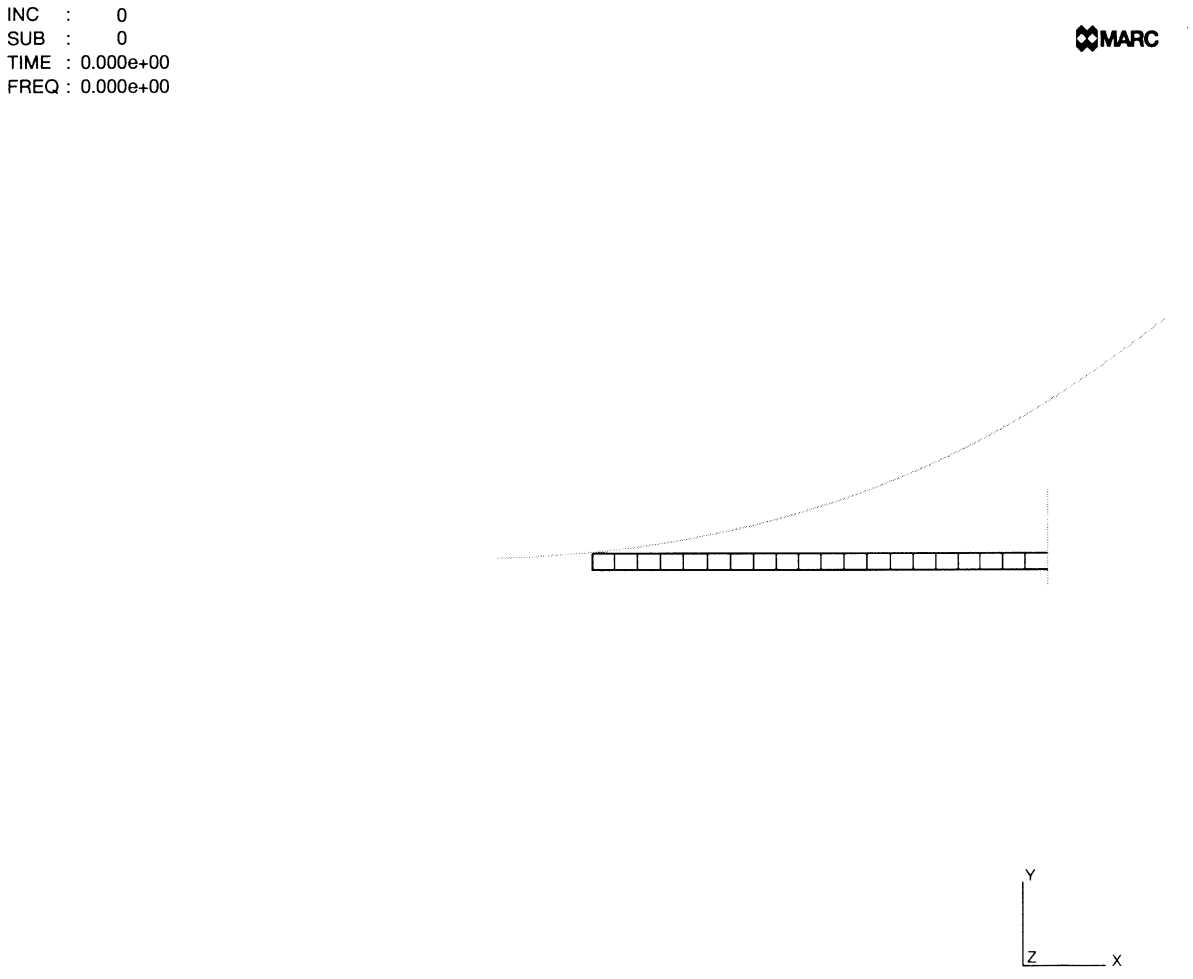

Figure E 8.44-1 Original Finite Element Mesh

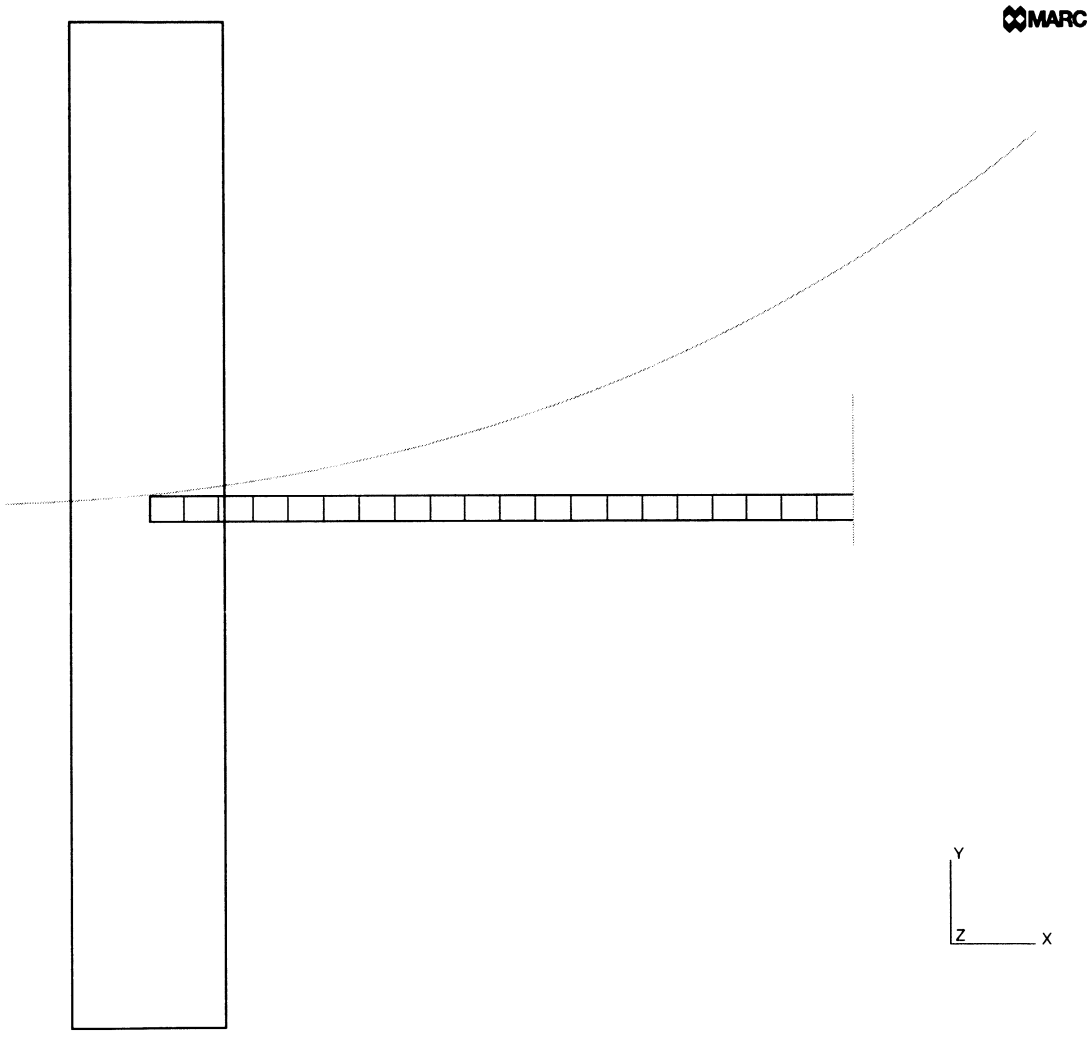

Figure E 8.44-2 Adaptive Criteria Box

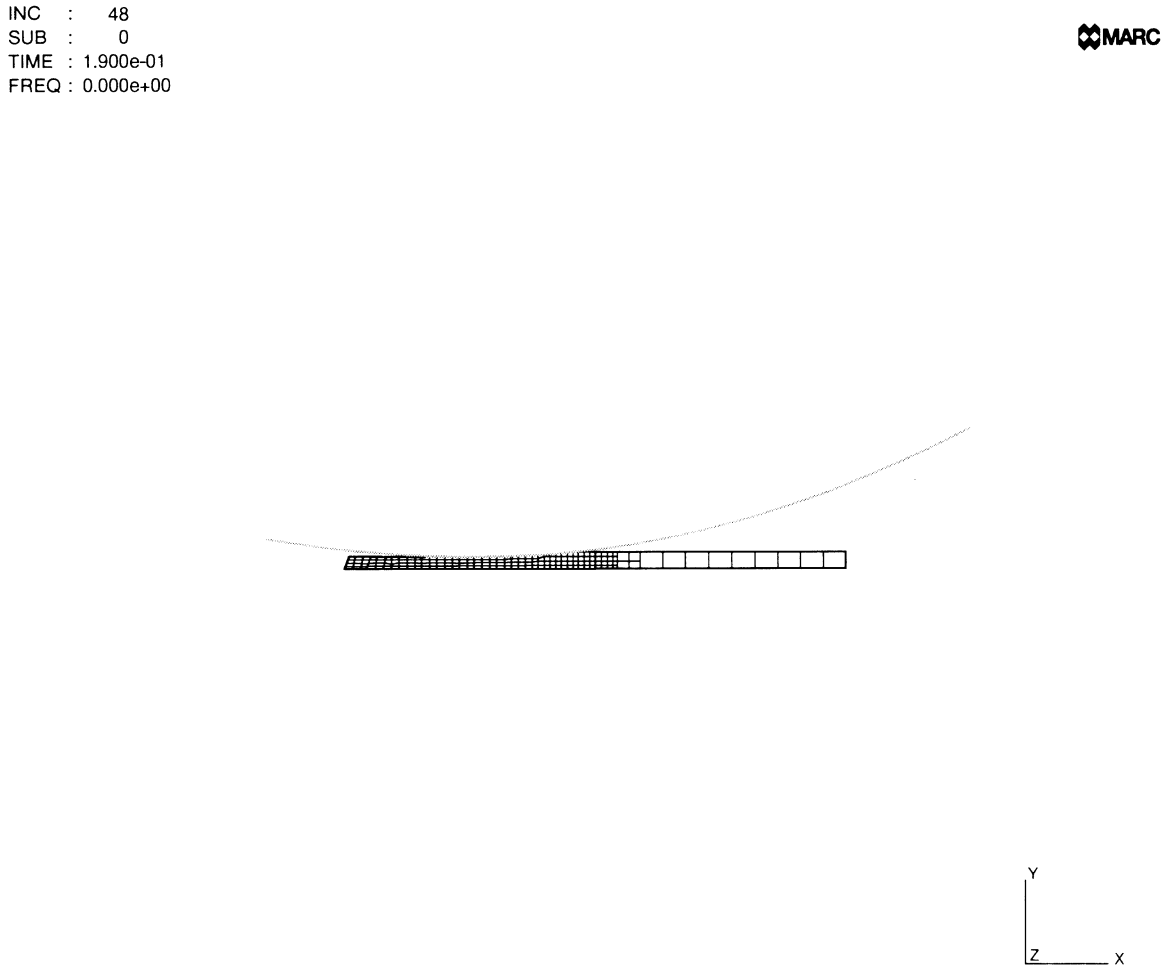

Figure E 8.44-3 Deformed Mesh at Increment 48

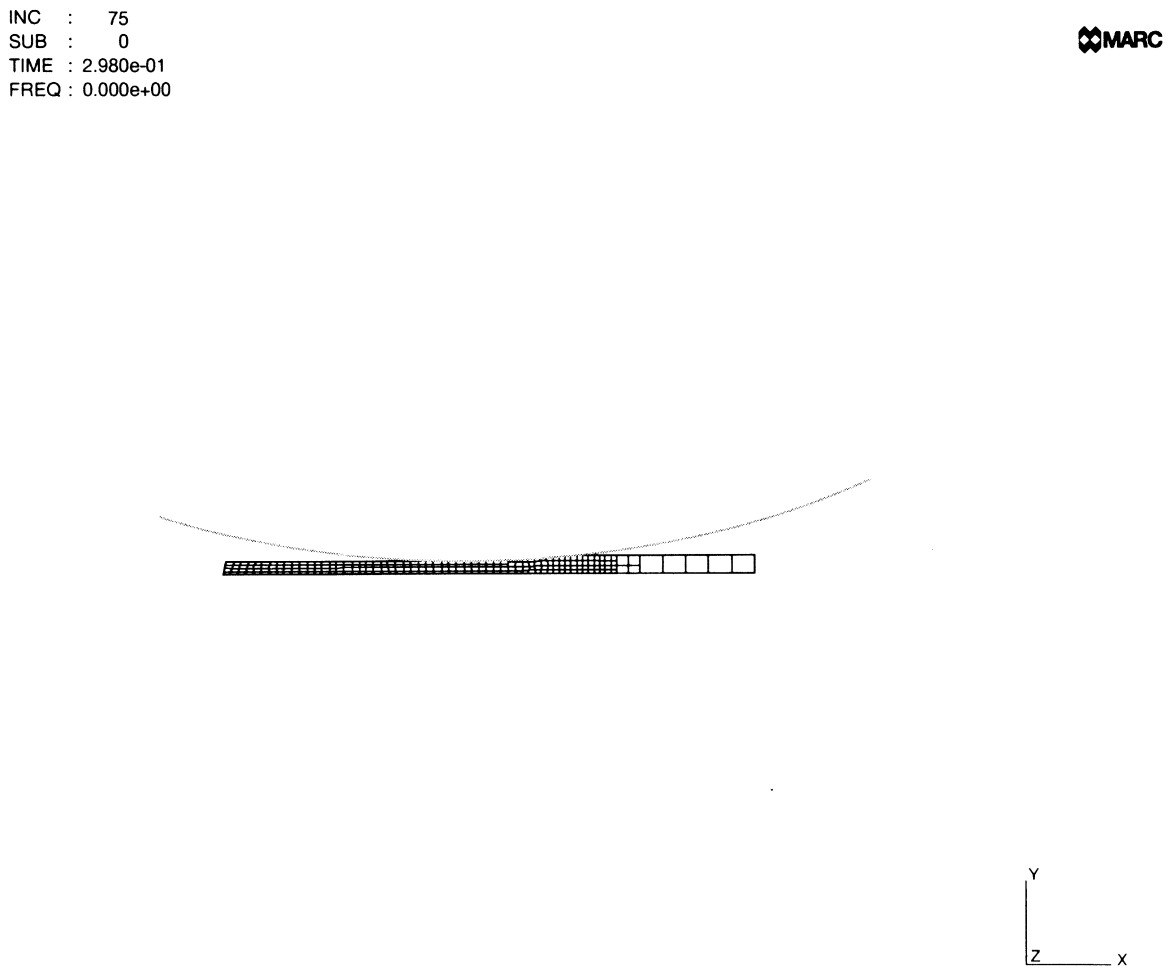

Figure E 8.44-4 Deformed Mesh at Increment 75

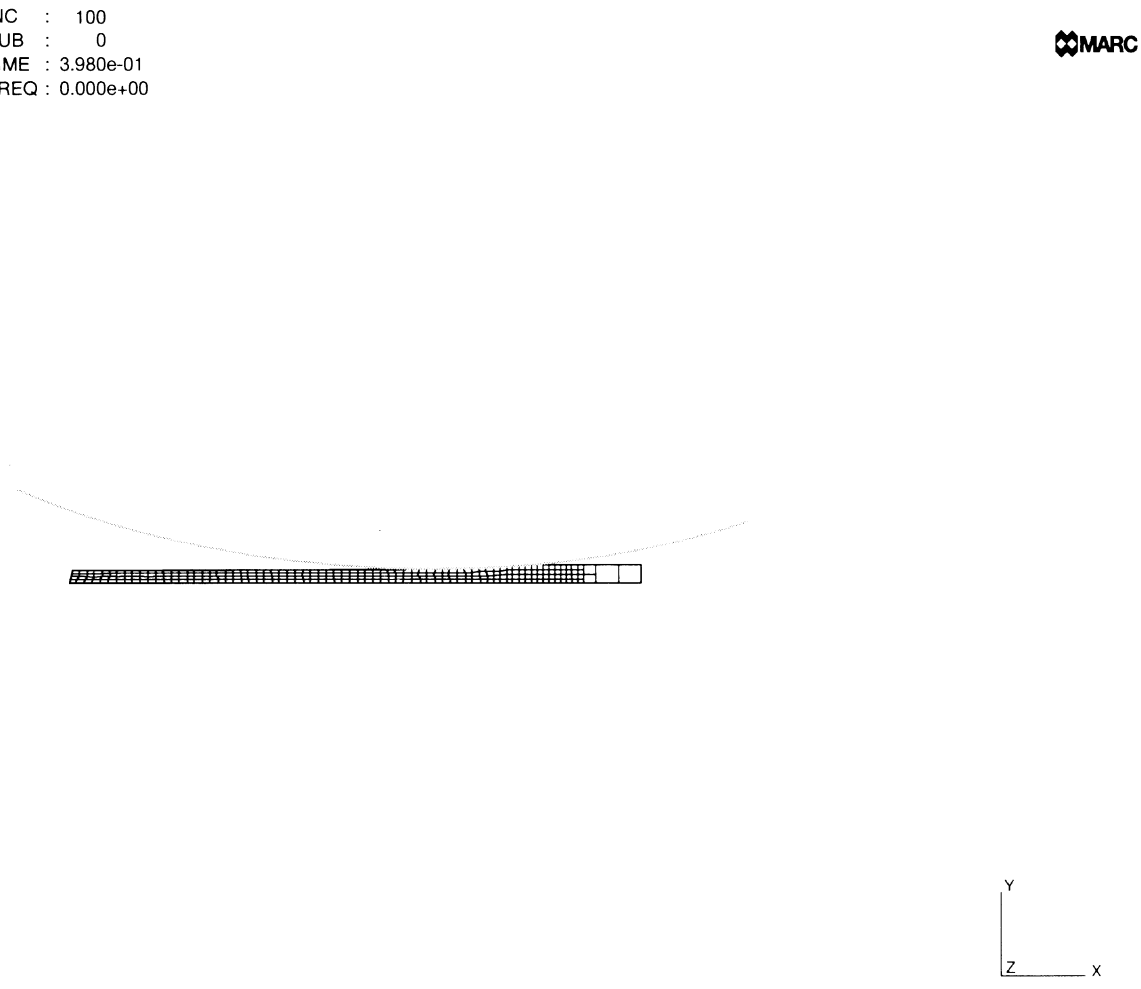

Figure E 8.44-5 Deformed Mesh at Increment 100

MARC Corporate Headquarters
260 Sheridan Avenue, Suite 309
Palo Alto, CA 94306, USA
Tel: (415) 329-6800
Fax: (415) 323-5892
Email: support@marc.com

MARC Analysis Research Corporation
Bredewater 26
2715 CA Zoetermeer
The Netherlands
Tel: 31-(0)79-510411
Fax: 31-(0)79-517560
Email: support@marc.nl

Nippon MARC Co.,Ltd.
P.O.Box 5056
Shinjuku Daiichi Seimei Bldg.
2-7-1 Nishi-Shinjuku
Shinjuku-ku, Tokyo 163, Japan
Tel: 81-(0)3-3345-0181
Fax: 81-(0)3-3345-1529
Email: system@marc.co.jp

MARC Software Deutschland GmbH
Ismaningerstrasse 9
85609 Aschheim
Germany
Tel: 49-(0)89-9045033
Fax: 49-(0)89-9030676
Email: support@marc.de

Nippon MARC Co.,Ltd.
Dai 2 Kimi Bldg.
2-11 Toyotsu-cho
Suita-city,Osaka 564, Japan
Tel: 81-(0)6-385-1101
Fax: 81-(0)6-385-4343

MARC Software Deutschland GmbH
Alte Dohrener Str. 66
D-30173 Hannover, Germany
Tel: 49-(0)511-800211
Fax: 49-(0)511-801042

MARC UK Ltd.
35, Shenley Pavilions, Chalkdell Drive
Shenley Wood
Milton Keynes, MK5 6LB, UK
Tel: 44-1908-506505
Fax: 44-1908-506522

Espri-MARC S.r.l.
Viale Brigata Bisagno 2/10
16129 Genova
Italy
Tel: 39-(0)10-585949
Fax: 39-(0)10-585949

Document Title: **Volume E, Demonstration Problems, K6 Additions**
Part Number: RF-3019-06
Revision Date: July, 1995

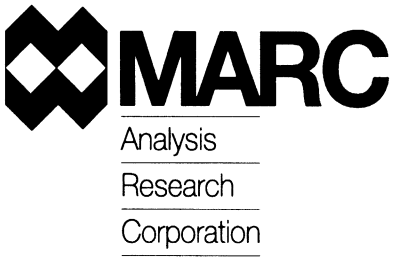

VOLUME E
Demonstration Problems

K6 Changes

Copyright © 1995 MARC Analysis Research Corporation
Printed in U. S. A.
This notice shall be marked on any reproduction of this data, in whole or in part.

MARC Analysis Research Corporation
260 Sheridan Avenue, Suite 309
Palo Alto, CA 94306 USA

Phone: (415) 329-6800
FAX: (415) 323-5892
email: techpubs@marc.com

Document Title: **Volume E, Demonstration Problems, K6 Changes**
Part Number: RF-3020-06
Revision Date: July, 1995

PROPRIETARY NOTICE

MARC Analysis Research Corporation reserves the right to make changes in specifications and other information contained in this document without prior notice.

Although due care has been taken to present accurate information, MARC Analysis Research Corporation DISCLAIMS ALL WARRANTIES WITH RESPECT TO THE CONTENTS OF THIS DOCUMENT (INCLUDING, WITHOUT LIMITATION, WARRANTIES OR MERCHANTABILITY AND FITNESS FOR A PARTICULAR PURPOSE) EITHER EXPRESSED OR IMPLIED. MARC Analysis Research Corporation SHALL NOT BE LIABLE FOR DAMAGES RESULTING FROM ANY ERROR CONTAINED HEREIN, INCLUDING, BUT NOT LIMITED TO, FOR ANY SPECIAL, INCIDENTAL OR CONSEQUENTIAL DAMAGES ARISING OUT OF, OR IN CONNECTION WITH, THE USE OF THIS DOCUMENT.

This software product and its documentation set are copyrighted and all rights are reserved by MARC Analysis Research Corporation. Usage of this product is only allowed under the terms set forth in the MARC Analysis Research Corporation License Agreement. Any reproduction or distribution of this document, in whole or in part, without the prior written consent of MARC Analysis Research Corporation is prohibited.

RESTRICTED RIGHTS NOTICE

This computer software is commercial computer software submitted with "restricted rights." Use, duplication, or disclosure by the government is subject to restrictions as set forth in subparagraph (c)(i)(ii) or the Rights in technical Data and Computer Software clause at DFARS 252.227-7013, NASA FAR Supp. Clause 1852.227-86, or FAR 52.227-19. Unpublished rights reserved under the Copyright Laws of the United States.

TRADEMARKS

All products mentioned are the trademarks, service marks, or registered trademarks of their respective holders.

Preface

This manual contains the updates to *Volume E, Demonstration Problems* for the K6 release. The *Volume E, Demonstration Problems* demonstrates most of the MARC program capabilities. The MARC program is a powerful, modern, general-purpose nonlinear finite element program for structural, thermal, and electromagnetic analyses.

In a typical finite element analysis, you will need to define the:

mesh (which is an *approximate* model of the actual structure);
material properties (Young's modulus, Poisson's ration, etc.);
applied loads (static, dynamic temperature, inertial, etc.);
boundary conditions (geometric and kinematic constraints); and
type of analysis (linear static, nonlinear, buckling, thermal, etc.).

The steps leading up to the actual finite element analysis are generally termed preprocessing; currently, many users accomplish these steps by using an interactive color graphics pre- and post-processing program such as the Mentat II graphics program. After an analysis, the results evaluation phase (post-processing) is where you check the adequacy of the design (and of the approximate finite analysis model) in terms of critical stresses, deflection, temperatures, and so forth.

This update manual is divided into two sections: the *K6 Additions* and the *K6 Changes*. This section, *K6 Changes*, highlights the changes in the MARC K6 release. It is organized similar to the complete *Volume E, Demonstration Problems*.

Volume E, Demonstration Problems is divided into four parts with each part containing two chapters. The manual has eight chapters grouped by the type of demonstration problems.

Part 1

Chapter 1, Introduction provides a general introduction to the problems demonstrated in all parts of *Volume E, Demonstration Problems*. Following the text is a set of cross reference tables showing keywords for the following:

parameter options
model definition options
mesh display options
history definition options
mesh rezoning options
element types
user subroutines

Each keyword is cross-referenced to the problem in which its use is demonstrated

Chapter 2, Linear Analysis	demonstrates most of the element types available to the user. Many linear analysis features are illustrated. The use of adaptive meshing for linear analysis is demonstrated here.
Part II	
Chapter 3, Plasticity and Creep	demonstrates the nonlinear material analysis capabilities. Both plasticity and creep phenomena are covered.
Chapter 4, Large Displacement	demonstrates the program's ability to analyze both large displacement and small strain effects.
Part III	
Chapter 5, Heat Transfer	demonstrates both steady-state and transient heat transfer capabilities.
Chapter 6, Dynamics	demonstrates many types of dynamic problems. These include analyses performed using both the modal and direct integration methods. The influences of fluid coupling and initial stresses on the calculated eigenvalues are shown. Harmonic and spectrum response analysis is also demonstrated here.
Part IV	
Chapter 7, Contact and Advanced Topics	demonstrates some of the special program capabilities of the MARC program. This includes the ability to solve rubber (incompressible), foam, viscoelastic, contact, and composite problems as well as others.

Chapter 8, Advanced Topics	demonstrates the capabilities most recently added to the MARC program. They include the ability to use substructures, in both linear and nonlinear analysis, to perform cracking analysis, analysis of contact problems, the ability to perform coupled thermal-mechanical analysis, electrostatic, magnetostatic and acoustic analysis. The use of adaptive meshing to solve nonlinear analysis is demonstrated here.

Volume E, Demonstration Problems summarizes the physics of each problem and describes the options required to define the problem. Figures are given of the mesh geometry and typical output results. The actual input and user subroutines are not included in the manual. They may be found on the distribution media associated with the MARC installation.

Each problem in *Volume E, Demonstration Problems* has a **Summary of Options Used**. Options and user subroutines are called out in the text by the use of a different type font – such as CONTINUE option, CHANGE STATE option, user subroutine UFCONN and user subroutine UFXORD.

Contents K6 Changes

Chapter 2 Linear Analysis

Chapter 3 Plasticity And Creep

Chapter 4 Large Displacement

Chapter 5 Heat Transfer

Chapter 6 Dynamics

Chapter 7 Contact

Chapter 8 Advanced Topics

Figures K6 Changes

Chapter 2 Linear Analysis

Chapter 3 Plasticity And Creep

Chapter 4 Large Displacement

Chapter 5 Heat Transfer

Chapter 6 Dynamics

Chapter 7 Contact

Chapter 8 Advanced Topics

Chapter 1 Introduction

Chapter 2 Linear Analysis

Chapter 3 Plasticity And Creep

Volume E
Demonstration Problems

Chapter 1
Introduction

Table E 1.0-1 Parameter Option Cross Reference

Delete qualify

Table E 1.0-2 Plot Option Cross Reference

continue					
e3x7c.dat	e3x16.dat	e5x8a.dat	e5x8b.dat	e6x6a.dat	e6x6b.dat
e7x13d.dat	e8x1a.dat	e8x1c.dat			

contours		
e3x7c.dat	e5x8b.dat	e7x10.dat

displaced				
e3x16.dat	e6x6a.dat	e6x6b.dat	e7x13d.dat	e8x1c.dat

elem ident	
e6x6a.dat	e6x6b.dat

end plot					
e3x7c.dat	e3x16.dat	e5x8a.dat	e5x8b.dat	e6x6a.dat	e6x6b.dat
e7x13d.dat	e8x1a.dat	e8x1c.dat			

node ident		
e6x6a.dat	e6x6b.dat	e8x1a.dat

plot type		
e6x6a.dat	e6x6b.dat	e7x13d.dat

position
e3x7c.dat

scaling				
e3x16.dat	e6x6a.dat	e6x6b.dat	e8x1a.dat	e8x1c.dat

Table E 1.0-2 Plot Option Cross Reference (Continued)

sectioning					
e7x13d.dat					
title					
e3x7c.dat	e3x16.dat	e5x8a.dat	e5x8b.dat	e6x6a.dat	e6x6b.dat
e7x10.dat	e8x1a.dat	e8x1c.dat			

Volume E
Demonstration Problems

Chapter 2
Linear Analysis

E 2.1 Hemispherical Shell Under Internal Pressure

A thin hemispherical shell is analyzed subjected to uniform internal pressure. The material behavior is considered elastic. The accuracy of element type 1 is verified.

Element (Ref. B1.1)

Library element type 1 is used. Element 1 is a 2-node axisymmetric thin shell with three degrees of freedom per node.

For this element, as for any 2-node element, it is necessary to adopt some unambiguous direction convention in order to provide the correct sign to the pressure loads. The convention adopted for this element is to define a right-handed set of local coordinates (x,y) for each element, with the positive x-direction from node 1 to node 2 of the element (see CONNECTIVITY). This gives a unique positive y-direction (90 degrees counterclockwise to local x), and with this definition the following conventions hold:

> Positive pressure always gives negative nodal load components in the positive local y-direction.

The sign convention that is adopted for the global axes should be noted. A positive rotation of 90° is assumed to transform the axis of symmetry Z to the radial axis R. Nodal points have three global displacement degrees of freedom:

1. Axial (parallel to the symmetry axis)
2. Radial (normal to symmetry axis)
3. Cross-sectional rotation (right-handed)

Model

The geometry of the middle surface of the hemisphere and the mesh are shown in Figure E 2.1-1. A 90-degree section is referenced to the Z-R global coordinate system. The shell is divided into nine elements with 10 nodes, each element subtending an angle of 10 degrees.

Geometry

The wall thickness of the shell is 0.01 in. and the radius of curvature is 1.0 in. The thickness is entered as EGEOM1 in the GEOMETRY option. EGEOM2 and EGEOM3 are not used for this element type.

Material Properties

All elements are assumed to have the same properties. Values used for Young's modulus and Poisson's ratio are 5×10^6 psi and 0.3, respectively, and are entered in the ISOTROPIC option. The material is given a high yield stress so that it will not go plastic.

Loading

A uniform internal pressure of 1.0 psi is applied to all elements.

Boundary Conditions

Node 1 is constrained to move axially, with no rotation and no translation in the R-direction. Node 10 is constrained to move radially, with no rotation and no translation in the Z-direction.

Note

Element 15 or Element 89 could also be used to model this type of problem. This higher-order element would allow a coarser mesh to be used; two element type15 would give equivalent results in this case. Element 15 or Element 89, in addition, allows the application of nonuniform loads through the use of user subroutine FORCEM.

Results

For a thin spherical shell, the solution is that the circumferential stress is equal to pr/2t, which, for this particular problem, is 50 psi. The MARC solution is given at layer 1 on the inner surface and layer 11 at the outer surface. One observes that the MARC solution is within .02% of the exact solution. A discussion of the analytic solution may be found in many elementary books on elasticity, such as *Theory of Elasticity* by Timoshenko and Goodier.

Summary of Options Used

Listed below are the options used in example e2x1.dat:

Parameter Options

ELEMENT
END
SIZING
TITLE

Model Definition Options

CONNECTIVITY
COORDINATE
DIST LOADS
END OPTION
FIXED DISP
GEOMETRY
ISOTROPIC

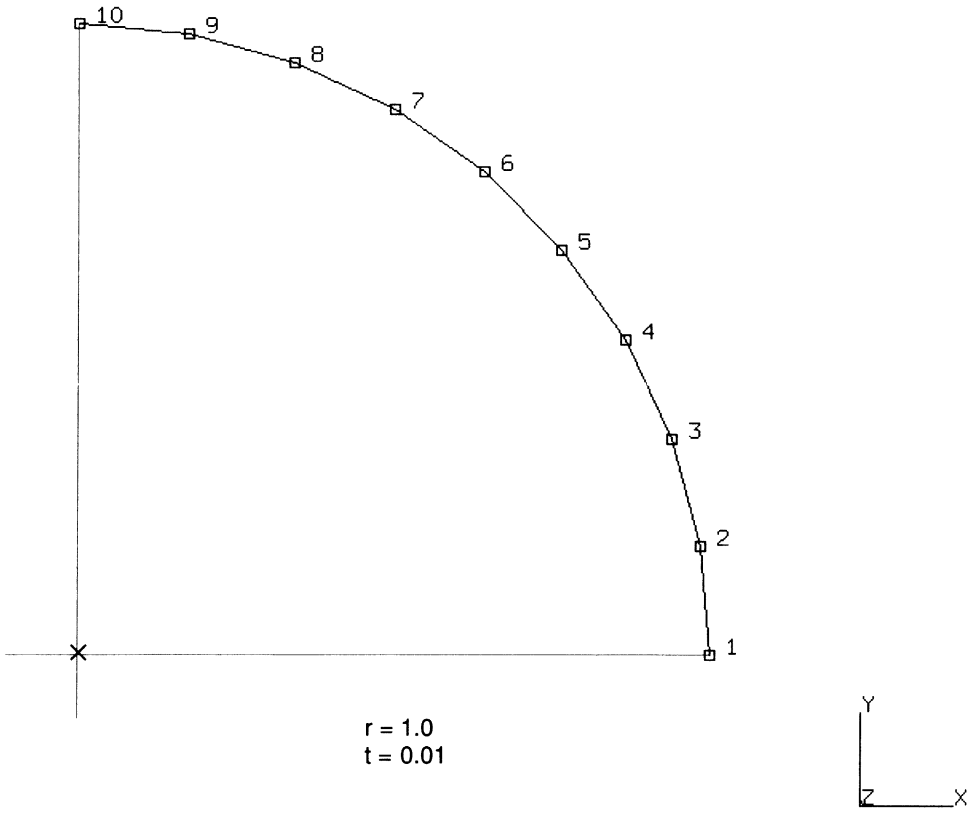

Figure E 2.1-1 Geometry and Mesh Layout for Axisymmetric Shell

E 2.5 Doubly Cantilevered Beam Loaded Uniformly

The solution of a cantilevered beam with a rectangular cross section subjected to a uniform load is obtained. This problem demonstrates the accuracy of the simple two-dimensional beam element.

Element (Ref. B5.1)

As this is a two-dimensional problem, it is possible to use element type 5, a straight, 2-node, rectangular-section, beam column. The displacement assumption is linear along the length of the beam and a cubic displacement assumption in the direction normal to the beam. The numerical integration is 3-point Gaussian quadrature along the length of the element and 11-point Simpson's rule through the thickness. The two nodes of each element have three degrees of freedom each: u, v, and right-hand rotation.

Model

Symmetry allows a model of one-half the beam to be used. Five elements and six nodes are used for a total of 18 degrees of freedom (see Figure E 2.5-1).

Geometry

The height of 1. (in-plane) is specified in the first data field, EGEOM1. The cross-sectional area of 1. is specified in the second data field, EGEOM2.

Loading

All five elements are loaded with a uniform distributed load of magnitude 10. This load is specified in the DIST LOADS option as type 0 (IBODY = 0).

Boundary Conditions

One end of the beam is rigidly fixed; $u = v = \theta = 0$ for node 1. The midbeam node (6) is fixed against axial expansion ($u = 0$) and against right-hand rotation ($\theta = 0$); this ensures the correct symmetry conditions.

Results

Deflections at nodal points shown in Figure E 2.5-2 are tabulated in Table E 2.5-1 and compared with exact answers. Correlation is very good. However, for a problem where the beam bending aspect of the model is critical, element type 16 should be used. With its higher-order integration and additional degrees of freedom per node, it will yield better answers.

Table E 2.5-1 Results

Node	MARC Computed Deflection	Analytically Calculated Deflection
1	0	0
2	2.03×10^{-5}	2.03×10^{-5}
3	6.40×10^{-5}	6.40×10^{-5}
4	1.103×10^{-4}	1.103×10^{-4}
5	1.440×10^{-4}	1.440×10^{-4}
6	1.563×10^{-4}	1.563×10^{-4}

The solution may be expressed as:

$$\sigma = \frac{My}{I}$$

$$\text{Shear force } V = p\left(\frac{l}{2} - x\right)$$

$$\text{Moment } M = \frac{pl^2}{12}\left(1 - \frac{6x}{l} + \frac{6x^2}{l^2}\right)$$

$$\text{Rotation} = \frac{Pl^3}{12EI}\left(\frac{2x}{l} - \frac{3x^2}{l^2} + \frac{2x^3}{l^3}\right)$$

$$\text{Displacement} = \frac{pl^4}{24EI}\left(\frac{x^2}{l^2} - \frac{2x^3}{l^3} + \frac{x^4}{l^4}\right)$$

Summary of Options Used

Listed below are the options used in example e2x5.dat:

Parameter Options

ELEMENT
END
SIZING
TITLE

Model Definition Options

CONNECTIVITY
COORDINATE
DIST LOADS
END OPTION
FIXED DISP
GEOMETRY
ISOTROPIC

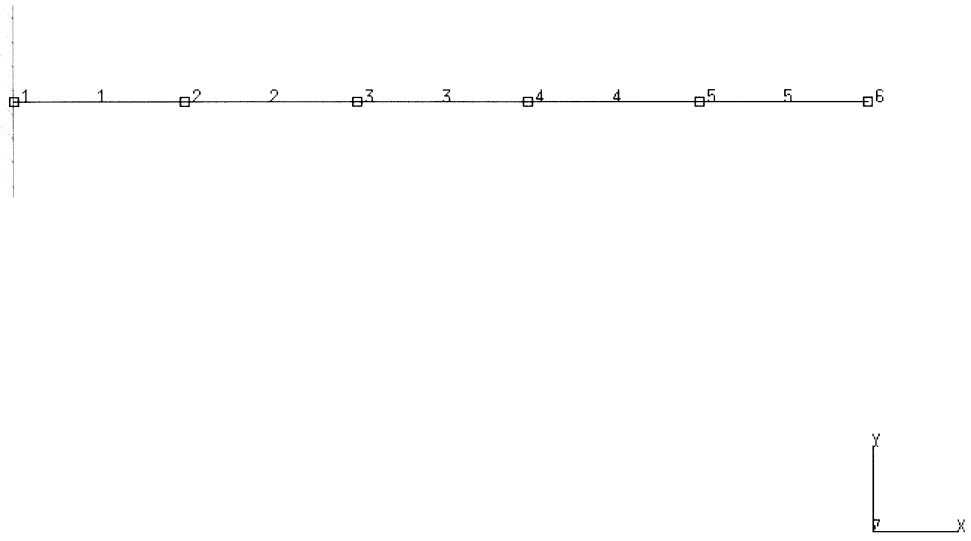

Figure E 2.5-1 Beam Model

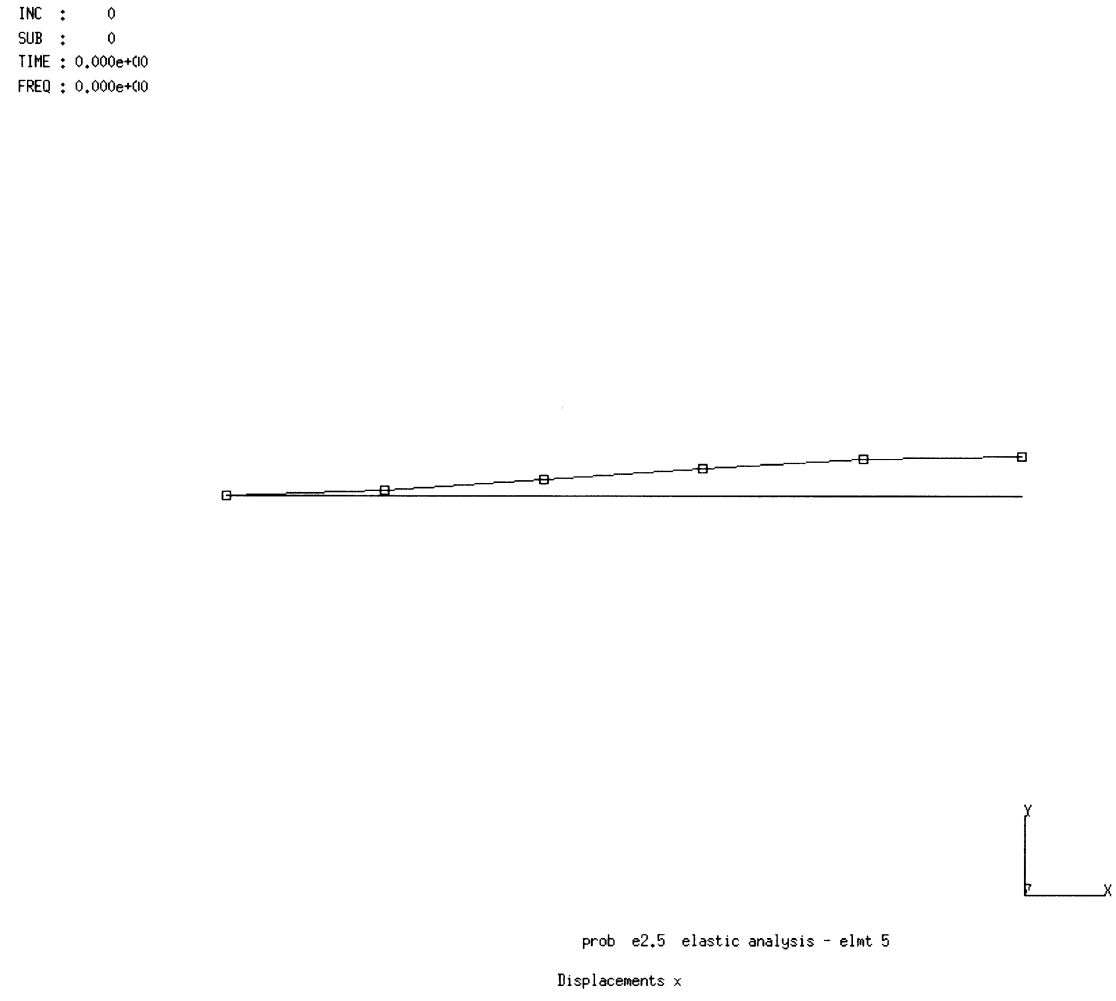

Figure E 2.5-2 Deformations

E 2.9 Plate With Hole

This problem demonstrates several ways to solve the problem of a circular hole in plate which has a known solution (Timoshenko and Goodier, *Theory of Elasticity*). The hole radius to plate size ratio is chosen to be 5, approximating an infinite plate. The second order isoparametric elements (types 26 and 124) are used first, followed by the use of the linear order type 3 using adaptive meshing.

Elements (Ref B3.1, B26.1, B124.1)

Element type 26 and 124 are second-order isoparametric elements for plane stress. Type 26 is an 8-node quadrilateral, and type 126 is a 6-node triangle. Element type 3 is a 4-node first-order isoparametric element.

Model

The dimensions of the plate are 5 inches square with a 1 inch radius. Only one quarter of the plate is modeled due to symmetry conditions. The finite element mesh for element type 26 is shown in Figure E 2.9-1, and the elements near the hole are made smaller. There are 20 elements in the quadrilateral meshes and 40 elements in the triangular meshes. The triangular mesh is made from the quadrilateral mesh by adding a node in the center of each element; then, the quadrilaterals are broken up into triangles. In problem e2x9d, the mesh initially consists of two elements as shown in Figure E 2.9-2. As the mesh adapts, the number of elements increase until there are 65 elements in the mesh.

Material Properties

The material for all elements is treated as an elastic material with Young's modulus of 30.0E+06 psi and Poisson's ratio (ν) of .3.

Geometry

The plate has a thickness of 1 inch given in the first field.

Loads and Boundary Conditions

A distributed load of -1.0 psi is applied to the top edge of the mesh. The boundary conditions are determined by the symmetry conditions and require that the nodes along $y = 0$ axis have no vertical displacement, and the nodes along the $x = 0$ axis have no horizontal displacement. The origin of the model is at the center of the hole.

Adaptive Meshing

Problem e2x9d demonstrates the use of adaptive meshing. The ADAPTIVE parameter option defines an upper bound to the number of elements and nodes. The ADAPTIVE model definition option is used to indicate that the adaptive criteria is based upon

the stress in an element which is not to exceed 75% of the maximum stress. As this would clearly refine forever, a limit of five levels is requested. This procedure is a way to add elements where a stress concentration exists. The SURFACE option defines a circle with a radius of one. When used with the ATTACH option, this will insure that the newly created nodes are places on the circle. The ATTACH nodes option indicates that nodes 1, 2, and 3 are on the circle, and any newly created nodes will also lie on the circle. Boundary conditions are generated automatically for the nodes created along y = 0.

Results

Figure E 2.9-1 and Figure E 2.9-1 contour the second component of stress (σ_{22}) over the mesh. Figure E 2.9-5 tabulates and plots values of σ_{22} for Element types 26, 124 and the exact solution along the y = 0 axis. The finite element solution is approximated by a plate of finite dimensions; there is some difference in predicting the exact solution. The results would improve if more elements were used. Figure E 2.9-7 through Figure E 2.9-10 show the progression of the mesh during the adaptive meshing process. After adaptive meshing, the stress concentration predicted is 2.86.

Summary of Options Used

Listed below are the options used in example e2x9.dat:

Parameter Options

ELEMENT
END
SIZING
TITLE

Model Definition Options

CONNECTIVITY
COORDINATE
DIST LOADS
END OPTION
FIXED DISP
GEOMETRY
ISOTROPIC
POST

Listed below are the options used in example e2x9b.dat:

Parameter Options

ELEMENT
END
SIZING
TITLE

Model Definition Options

CONNECTIVITY
COORDINATE
DIST LOADS
ELEM SORT
END OPTION
FIXED DISP
GEOMETRY
ISOTROPIC
NODE SORT
PRINT CHOICE
SUMMARY

Listed below are the options used in example e2x9c.dat:

Parameter Options

ELEMENT
END
SIZING
TITLE

Model Definition Options

CONNECTIVITY
COORDINATE
DIST LOADS
END OPTION
FIXED DISP
GEOMETRY
ISOTROPIC
NO PRINT
OPTIMIZE
POST

Listed below are the options used in example e2x9d.dat:

Parameter Options

ADAPT
ELASTIC
ELEMENT
END
SIZING
TITLE

Model Definition Options

ADAPTIVE

ATTACH NODE
CONNECTIVITY
COORDINATE
DIST LOADS
END OPTION
FIXED DISP
GEOMETRY
ISOTROPIC
OPTIMIZE
POST
SURFACE

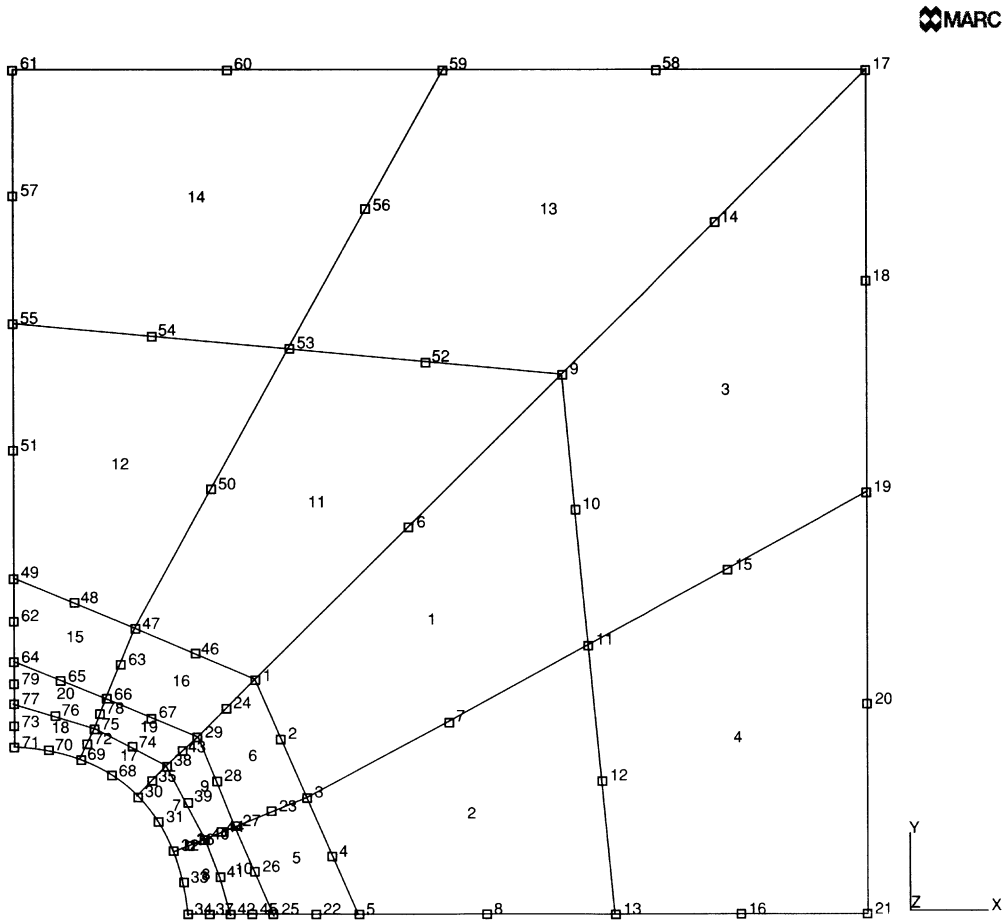

Figure E 2.9-1 Mesh Layout for Plate with Hole (Element 26)

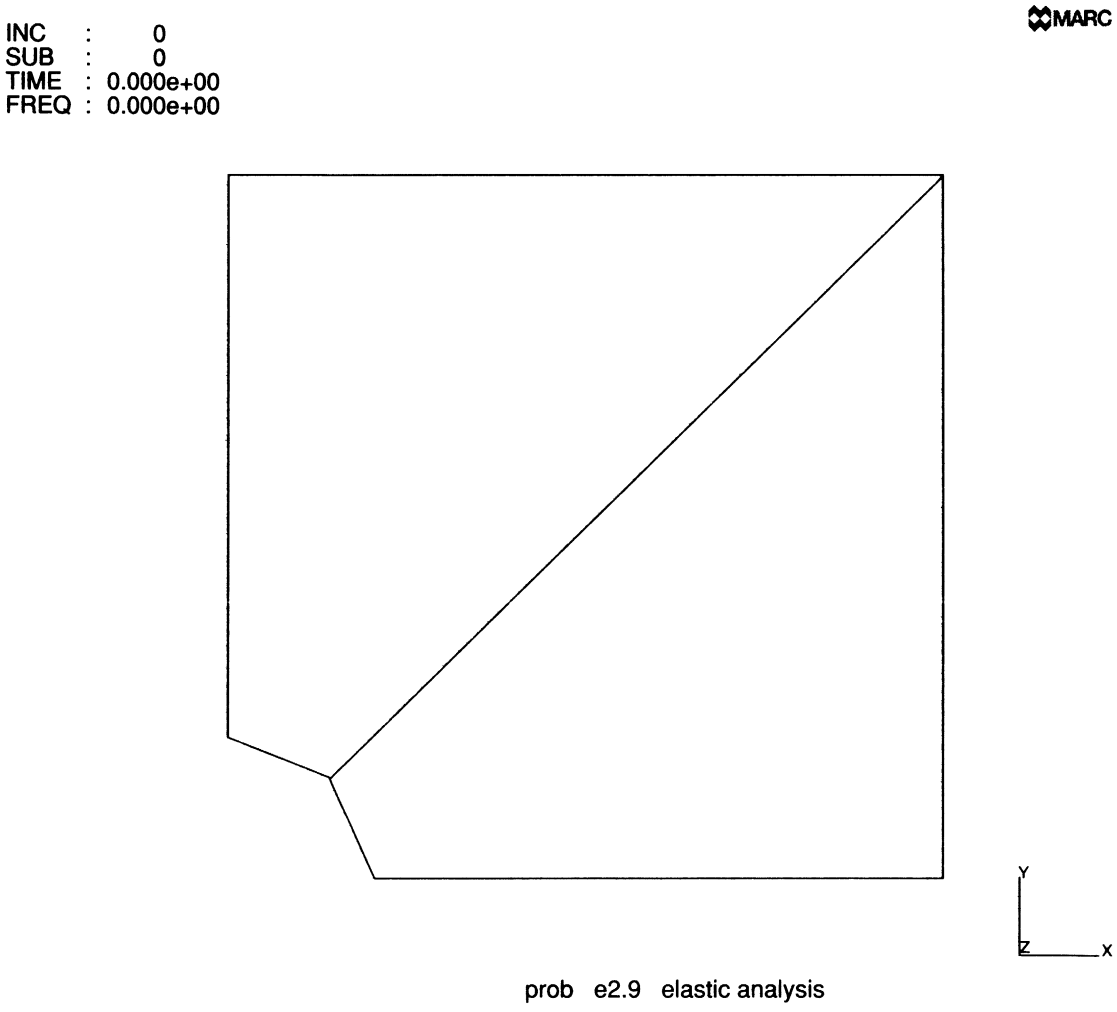

Figure E 2.9-2 Original Mesh for Plate with Hole When Using Adaptive Meshing

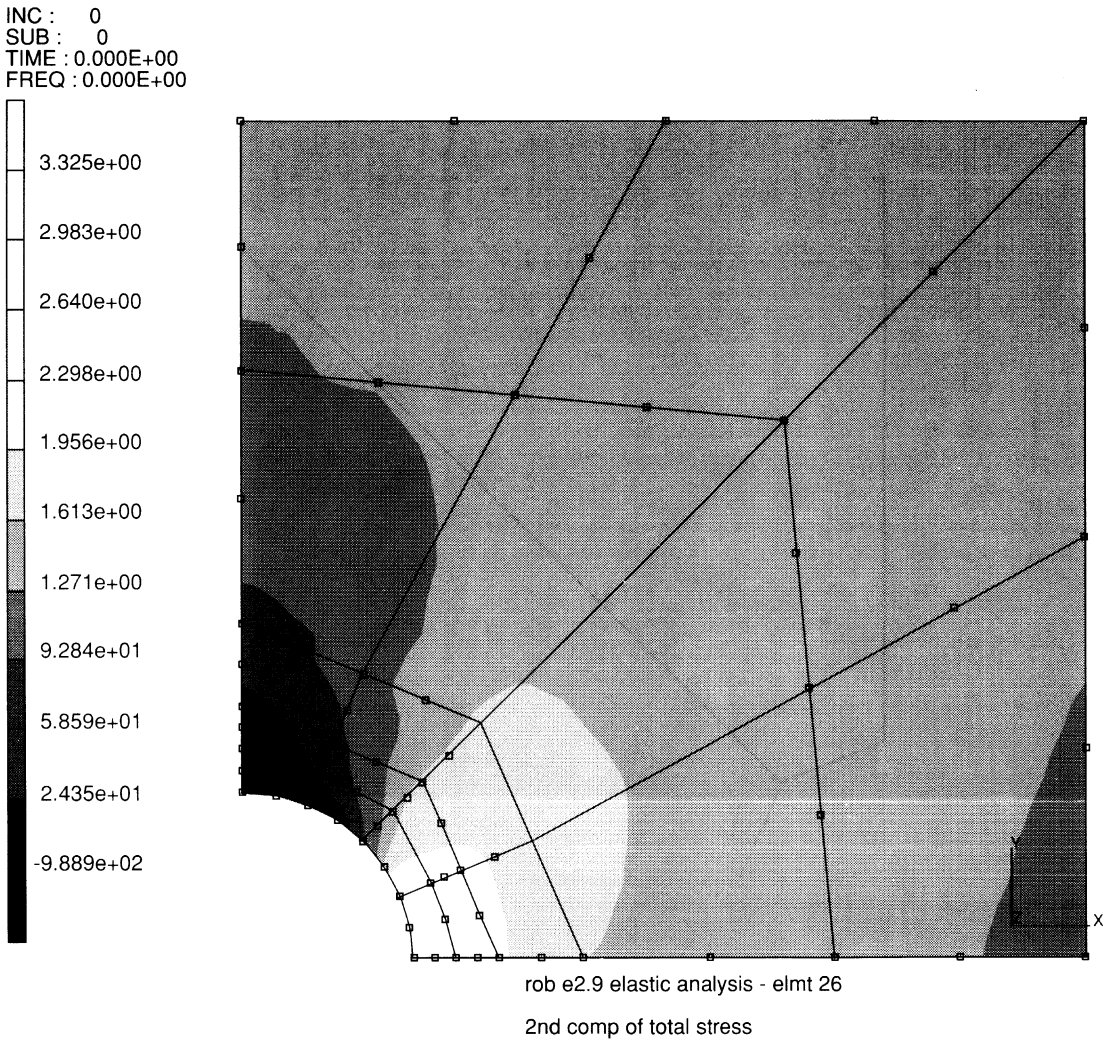

Figure E 2.9-3 Contours of $Sigma_{22}$ Element 26

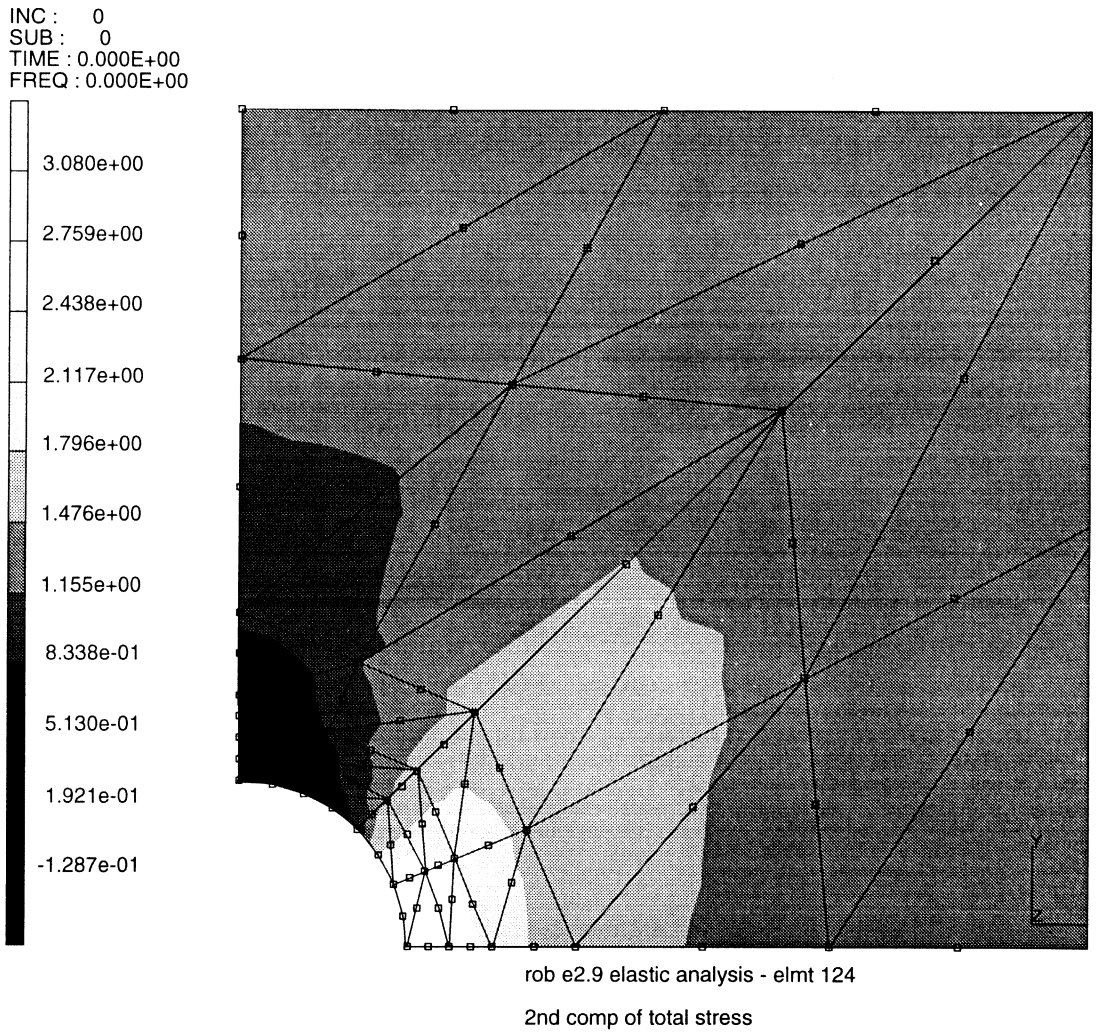

Figure E 2.9-4 Contours of Sigma$_{22}$ Element 124

Radius	Type 26	Type 124	Exact
1.00000	3.325290E+00	3.079772E+00	3.0000
1.12500	2.656915E+00	2.643165E+00	2.3315
1.25000	2.181081E+00	2.152462E+00	1.9344
1.37500	1.885873E+00	1.895210E+00	1.6841
1.50000	1.670818E+00	1.650798E+00	1.5185
1.75000	1.416509E+00	1.446365E+00	1.3232
2.00000	1.276260E+00	1.264376E+00	1.2188
2.75000	1.117434E+00	1.127211E+00	1.0923
3.50000	1.028915E+00	1.032025E+00	1.0508
4.25000	9.466122E-01	9.452355E-01	1.0323
5.00000	8.523712E-01	8.844259E-01	1.0224

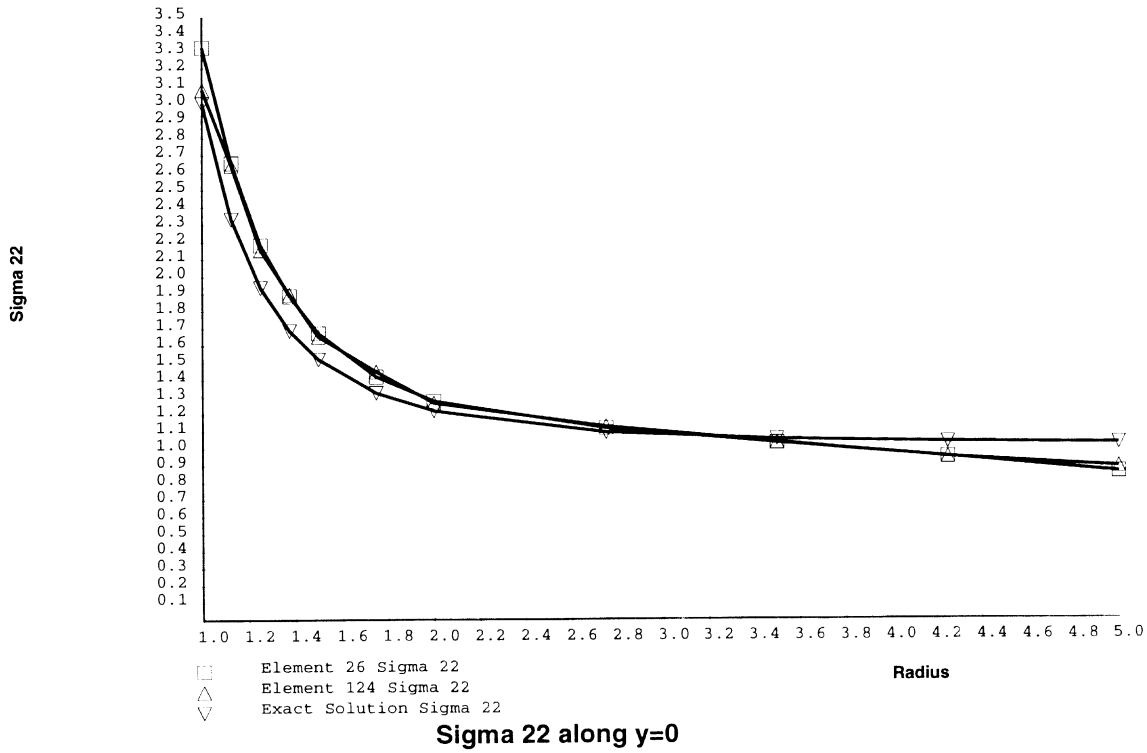

Figure E 2.9-5 $Sigma_{22}$ Along y = 0, Elements 26,124, and Exact

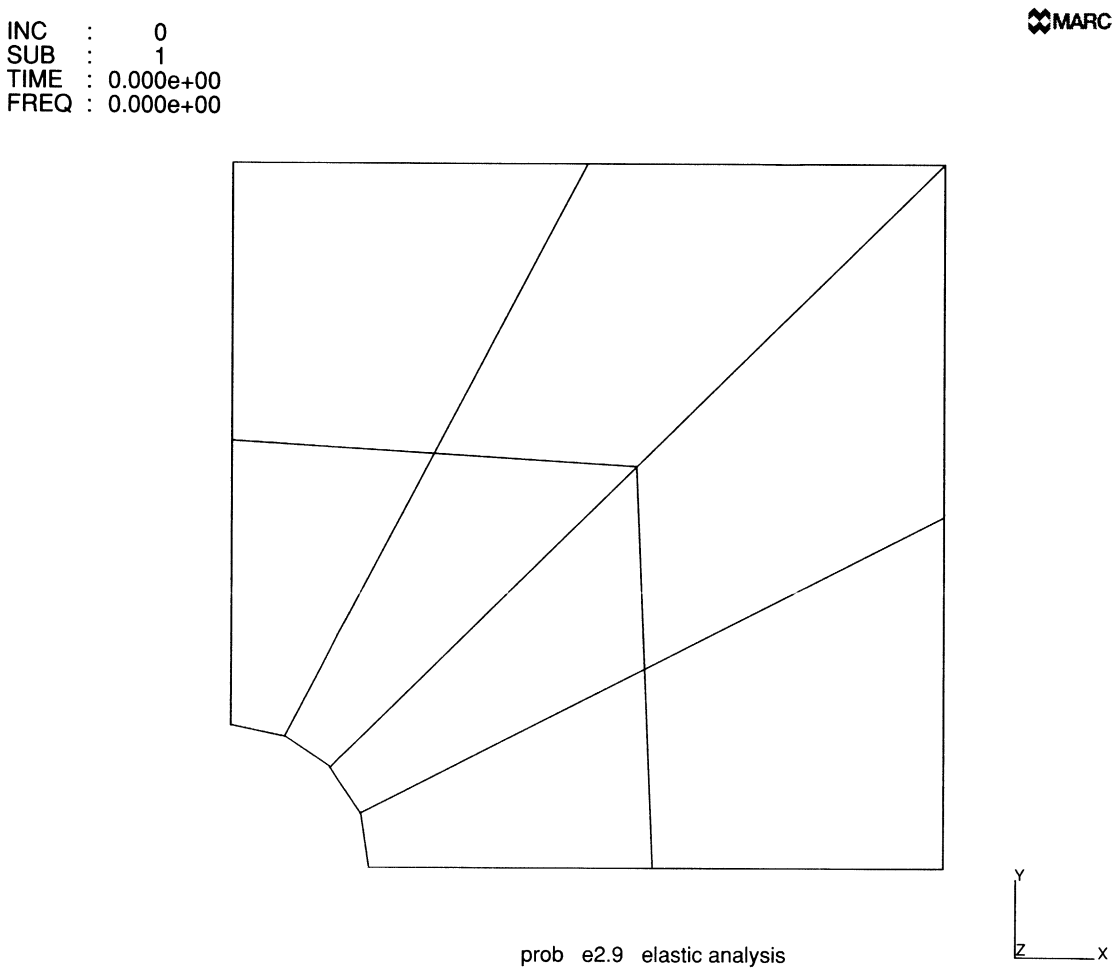

Figure E 2.9-6 Mesh After First Refinement

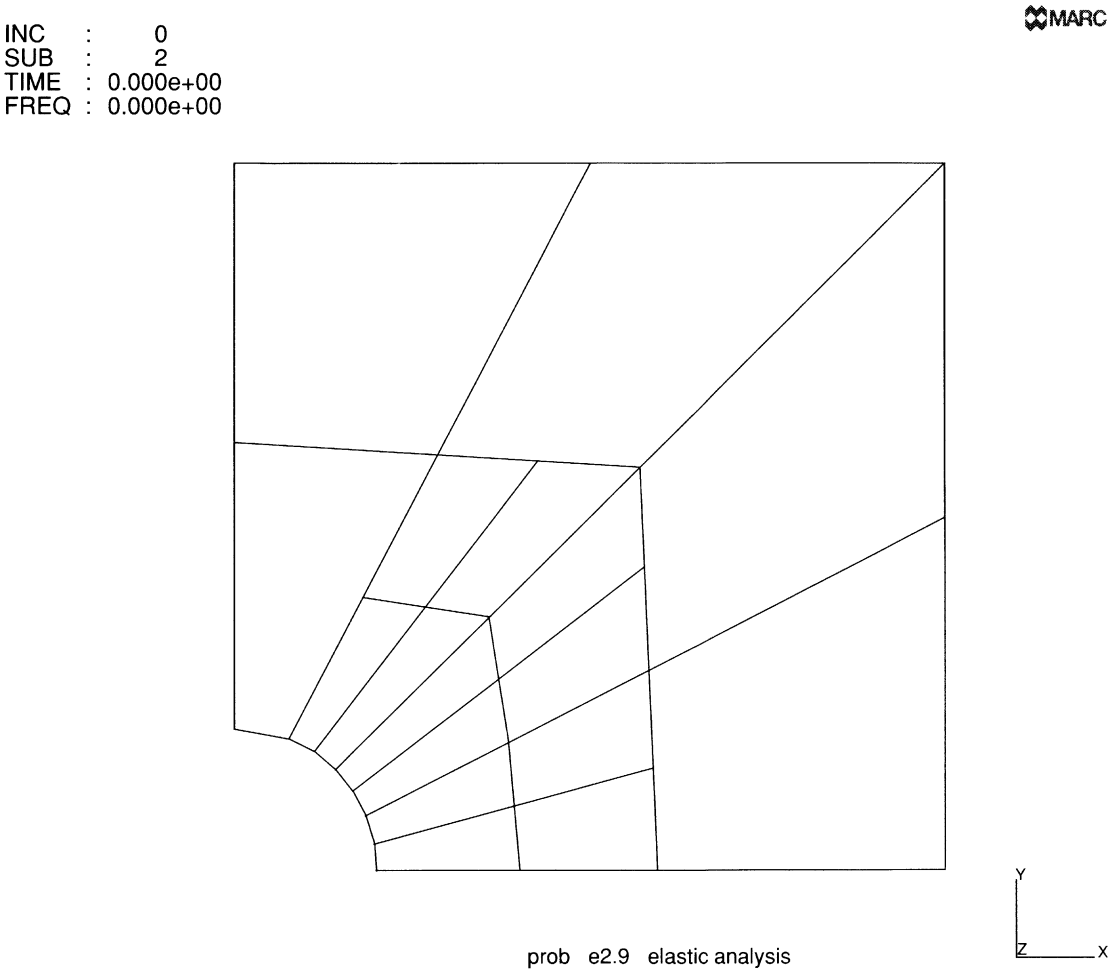

Figure E 2.9-7 Mesh After Second Refinement

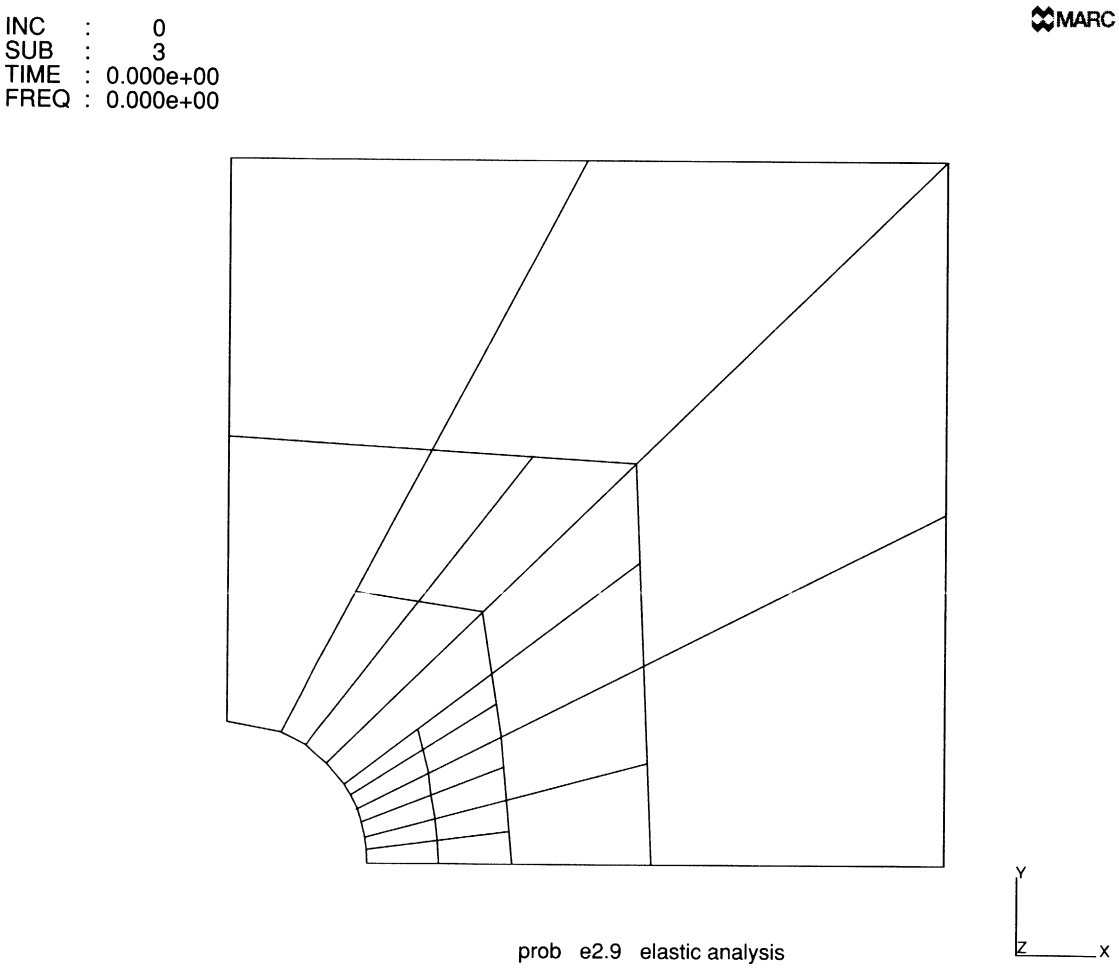

Figure E 2.9-8 Mesh After Third Refinement

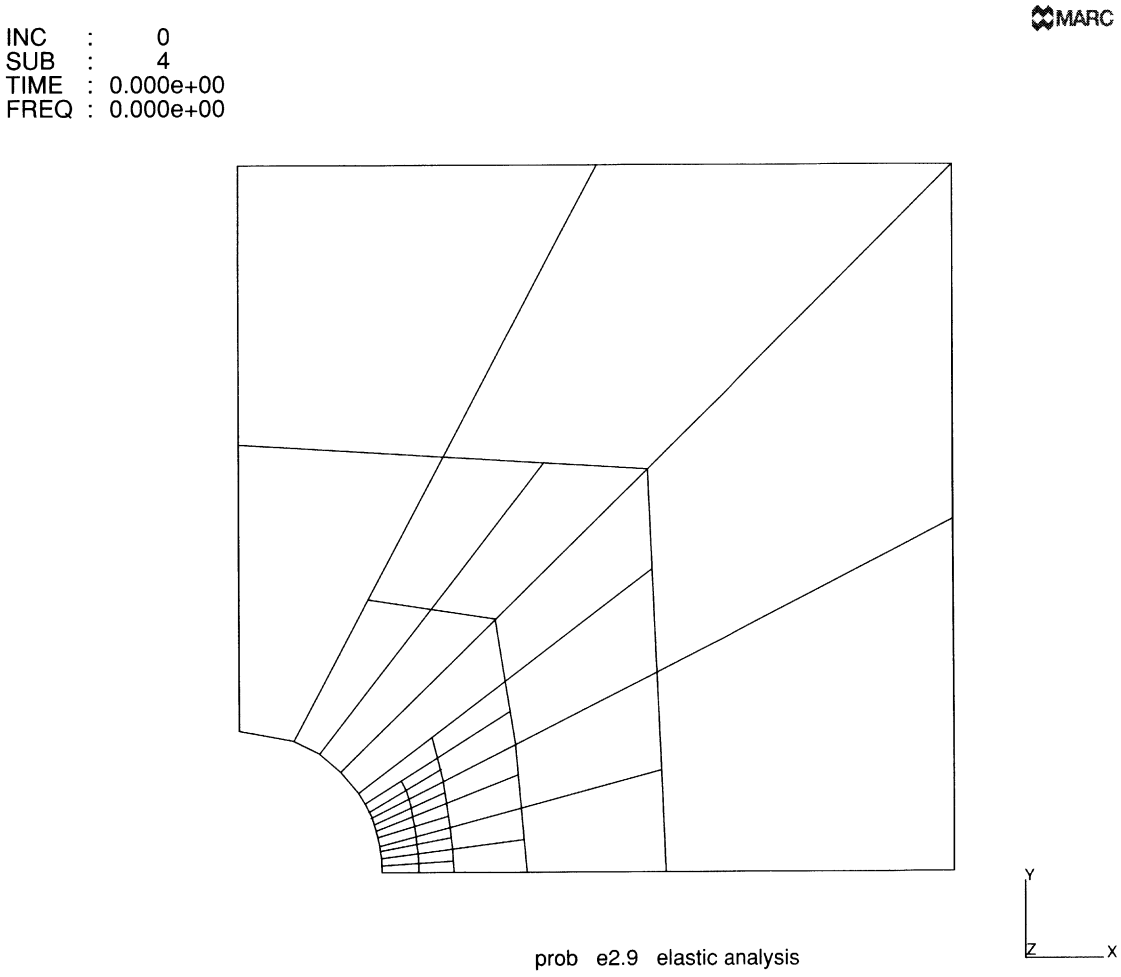

Figure E 2.9-9 Mesh After Fourth Refinement

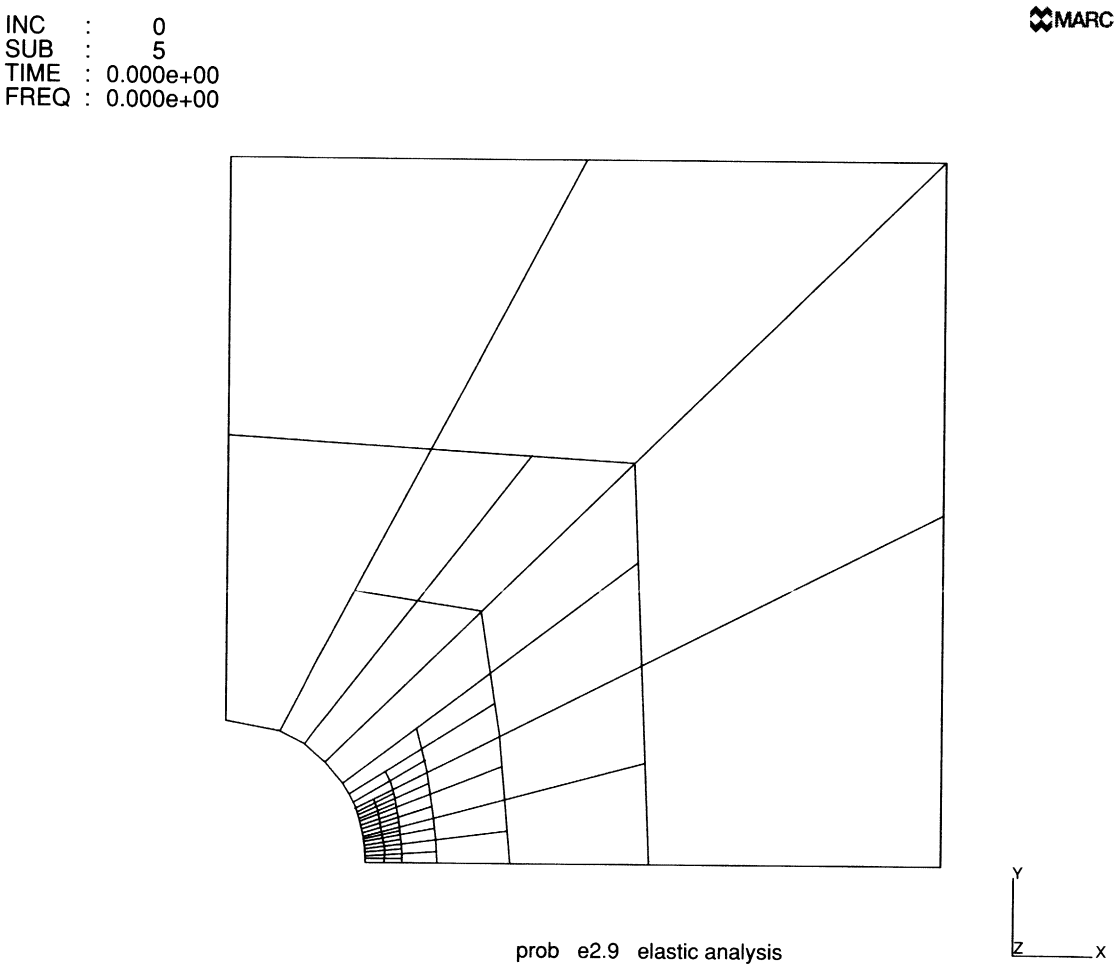

Figure E 2.9-10 Mesh After Fifth Refinement

E 2.10 Plane Stress Disk

A thin circular disk with a diameter of 12 inches is subjected to diametrically–opposed concentrated loads of 100 lbf. The disk is modeled as an elastic material using 2 different types of plane stress elements. The results are compared to the analytic solution demonstrating the accuracy of the finite element model.

This problem is also modeled using the adaptive meshing procedure.

Elements (Ref. B3.1, B114.1)

The solution is obtained using first order isoparametric quadrilateral elements for plane stress, element types 3 and 114, respectively. Type 114 is similar to type 3; however, it uses reduced integration with hourglass control.The ALIAS option is used to switch elements between the two models.

Model

The diameter of the disk is 12 inches and only one half of the disk is modeled due to symmetry conditions. The finite element mesh used for both element types is shown in Figure E 2.10-1. Initially, there are 64 elements and 82 nodes. The model origin is at the center of the disk.

Material Properties

The material for all elements is treated as an elastic material, with Young's modulus of 30.0E+04 psi, Poisson's ratio (ν) of .3, and a yield strength of 40,000 psi.

Geometry

The disk has a thickness of 1 inch given in the first field.

Loads and Boundary Conditions

A point load of -50 lbf (half of the total load) is placed on node 1 in the vertical direction. This point load is reacted by constraining the vertical displacement of the diametrically-opposed node (number 79) to zero. All nodes along the y-axis at x = 0 have their horizontal displacements constrained to zero.

Optimization

The Cuthill-McKee optimizer is used to reduce the bandwidth and hence the computational costs. Also notice that the computational costs of using element type 114 with reduced integration with hourglass control is lower than that of element type 3.

Adaptive Meshing

In problem e2x10c, the Zienkiewicz-Zhu stress error criteria is used with a tolerance of 0.05 in the third example. A maximum of three levels is allowed. The ELASTIC parameter is added to insure reanalysis until the error criteria is satisfied.

Results

The accuracy of the solution to this problem is shown in Figure E 2.10-2, where the direct stress component in the vertical direction along the y = 0 axis is plotted against its exact value given in *Theory of Elasticity*, Timoshenko and Goodier, McGraw Hill, 1970, pp 122-123 as:

$$\sigma_{yy}(x,0) = 2P\,[1 - 4d^4/(d^2 + 4x^2)^2]/\pi d$$

Both σ_{xx} and σ_{yy} are shown in Figure E 2.10-3.

The value of stress predicted by element type 114 is closer to the theoretical solution than element type 3. Also, the finite element solution cannot capture the singular behavior under the concentrated loads, and special elements and/or meshes are usually needed in order to obtain accurate solutions near such singularities. The adaptive meshing procedure is useful for these problems.

After the first solution in the third analysis, elements 1, 2, 4, 5, 58, 59, 62, and 63 are refined to satisfy the error criteria. After the second trial, original elements 8 and 53 are subdivided along with eight of the new elements. After the third trial, eight elements are subdivided. This procedure is continued until all of the elements either satisfy the error criteria or have been refined three times. A close-up of the final mesh is shown in Figure E 2.10-4.

Summary of Options Used

Listed below are the options used in example e2x10.dat:

Parameter Options

ELEMENT
END
SIZING
TITLE

Model Definition Options

CONNECTIVITY
COORDINATE
END OPTION
FIXED DISP
GEOMETRY
ISOTROPIC
OPTIMIZE
POINT LOAD
POST

Listed below are the options used in example e2x10b.dat:

Parameter Options

ALIAS
ELEMENT
END
SIZING
TITLE

Model Definition Options

CONNECTIVITY
COORDINATE
END OPTION
FIXED DISP
GEOMETRY
ISOTROPIC
OPTIMIZE
POINT LOAD
POST

Listed below are the options used in example e2x10c.dat:

Parameter Options

ADAPTIVE
ELASTIC
ELEMENT
END
SIZING
TITLE

Model Options

ADAPTIVE
CONNECTIVITY
COORDINATE
END OPTION
FIXED DISP
GEOMETRY
ISOTROPIC
OPTIMIZE
POINT LOAD
POST

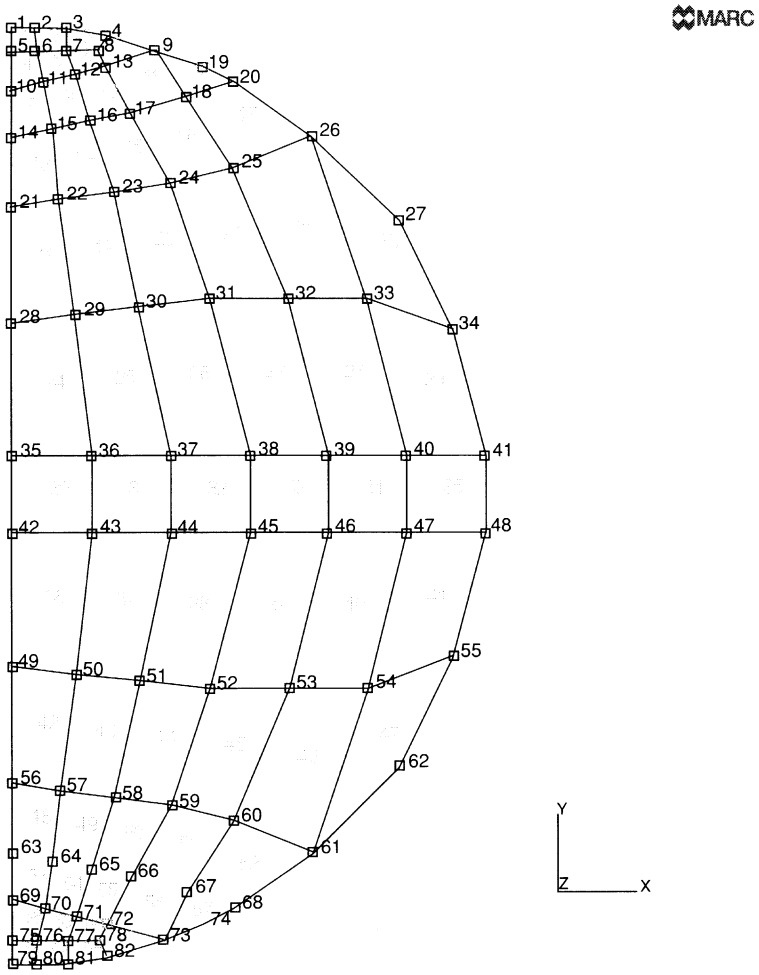

Figure E 2.10-1 Model

Radius	Type 3	Type 114	Exact
0	-1.681E+01	-1.616E+01	-1.592E+01
1	-1.571E+01	-1.508E+01	-1.478E+01
2	-1.288E+01	-1.222E+01	-1.188E+01
3	-9.108E+00	-8.615E+00	-8.276E+00
4	-5.441E+00	-5.185E+00	-4.866E+00
5	-2.489E+00	-2.174E+00	-2.086E+00
6	4.879E-01	-7.582E-01	0.000E+00

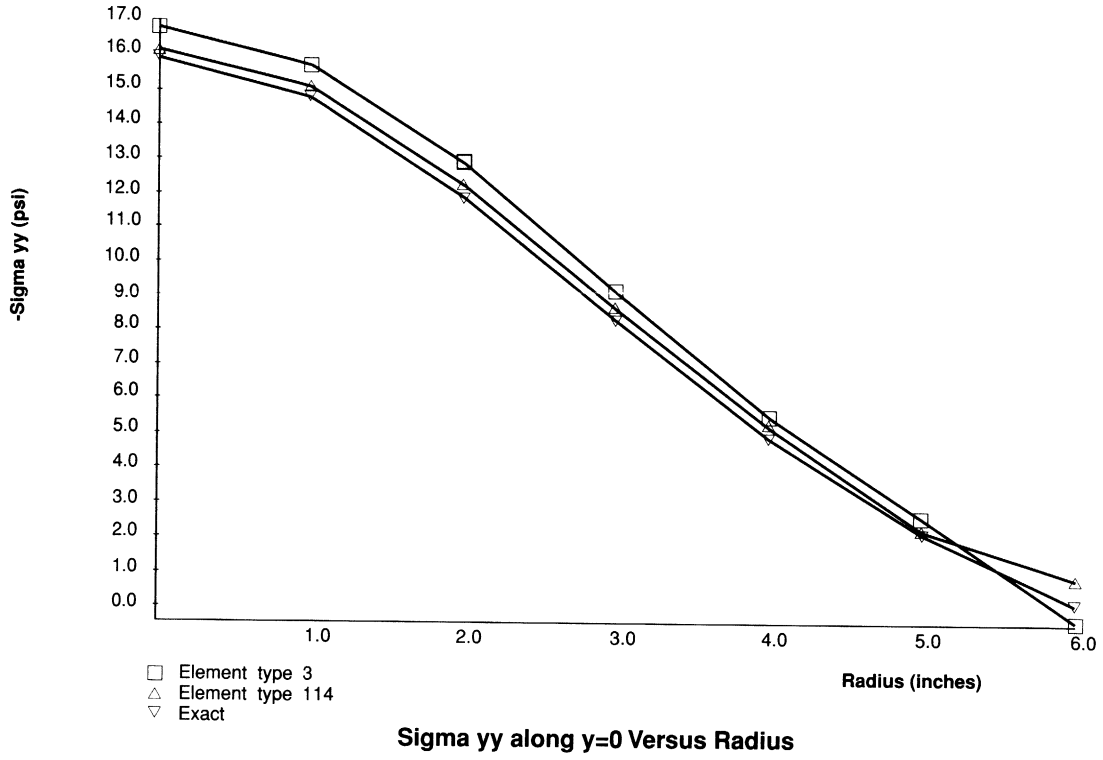

Figure E 2.10-2 $Sigma_{22}$ Along y = 0 Versus Radius

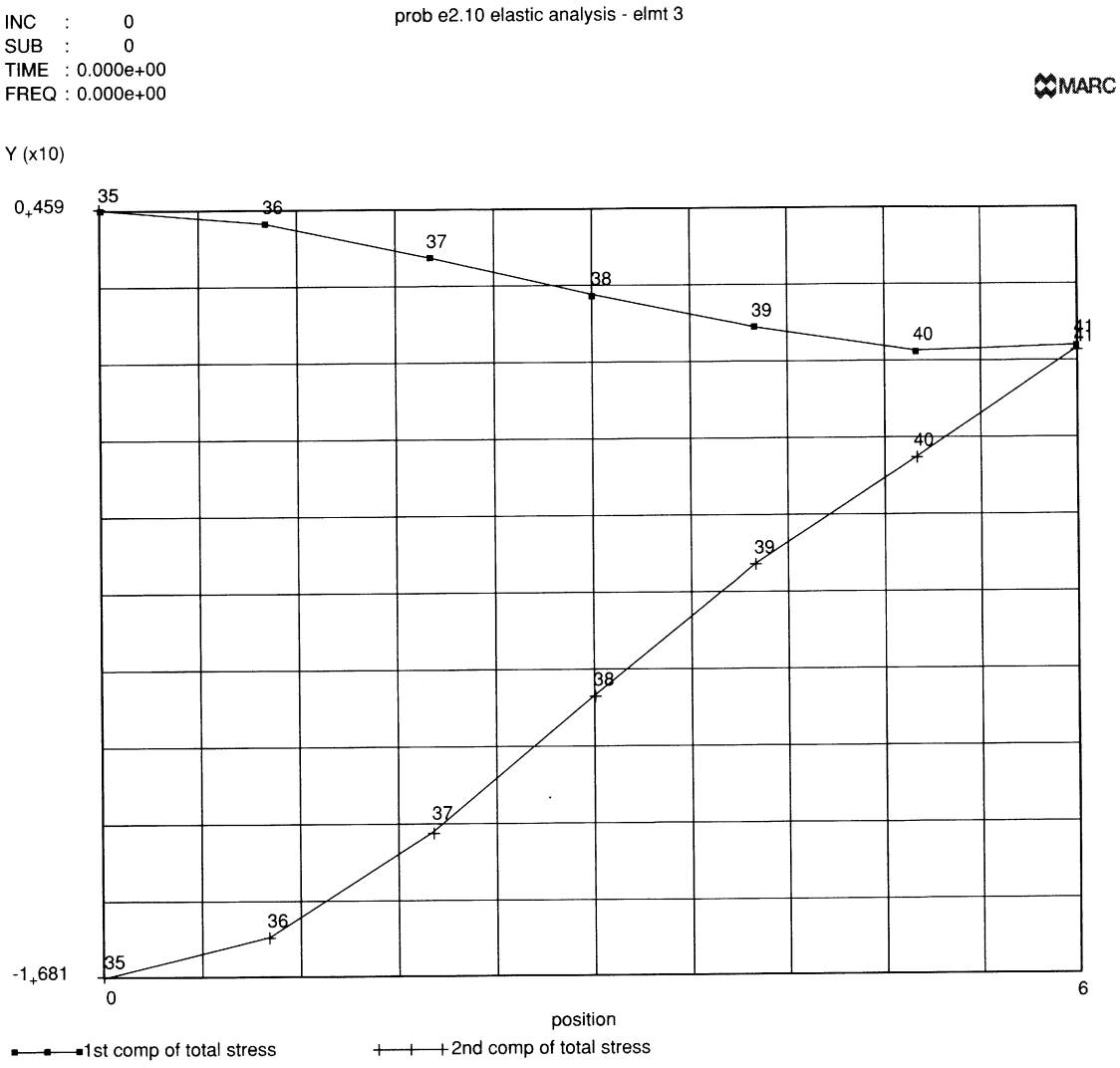

Figure E 2.10-3 Stress Component Along Nodal Path

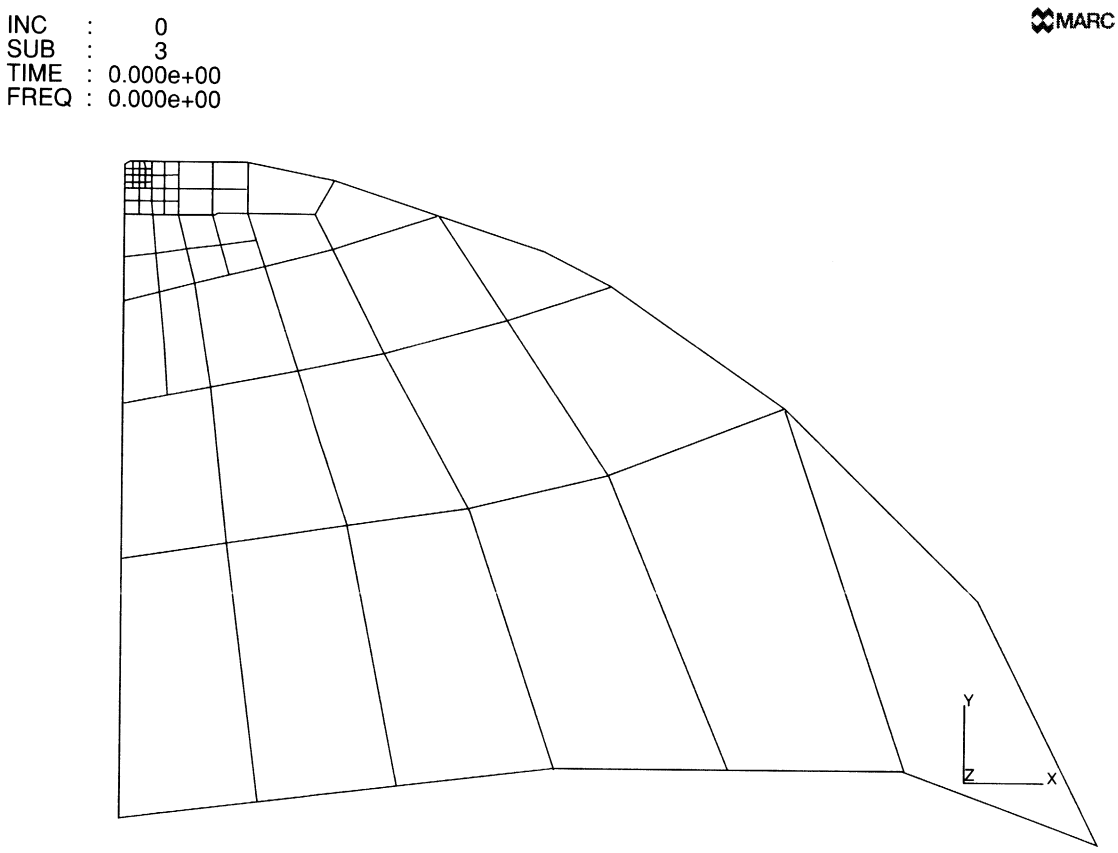

Figure E 2.10-4 Close-up of Adapted Mesh

E 2.12 Simply-Supported Thick Plate, Using Three-Dimensional Elements

A simply-supported thick plate under uniform transverse pressure is elastically analyzed. This problem is the same as E 2.11 and E 2.13; hence, the solutions can be compared showing the discrepancies due to the choice of element types. This problem is also used to demonstrate the different choices of solution procedures.

Element (Ref. B7.1and B117.1)

This example illustrates the use of element types 7 and 117, the three-dimensional isoparametric elements, details of which are given in Volume B. There are three degrees of freedom per node point for these elements:

u displacement (parallel to the x-axis)
v displacement (parallel to the y-axis)
w displacement (parallel to the z-axis)

Model

One-quarter of the plate (60 x 60 x 3 inches) is modeled since there are two planes of symmetry in this problem. The generated mesh is shown in Figure E 2.12-1. The thickness of the plate was divided into four tiers of elements. Each tier was subdivided into a five-by-five element pattern, resulting in a mesh containing 180 nodes and 100 elements.

Geometry

A nonzero number is entered in the third GEOMETRY field to indicate that the assumed strain formulation will be activated.

Material Properties

All elements are assumed to be uniform here. Values for Young's modulus, Poisson's ratio, and yield stress used are 20 x 10^6 psi, 0.3 and 20,000 psi, respectively.

Loading

The 25 elements with faces in the upper plane (z = 3 in.) are loaded by a pressure of 1.0 psi; the total load is 900 lb. in the negative z direction. Loading of this face of the elements is obtained by setting IBODY = 0 in the DIST LOAD input.

Boundary Conditions

Homogeneous boundary conditions are imposed on u for all nodes in the plane x = 30 and on v for all nodes in the plane y = 30 to account for the symmetry conditions. Simple support conditions are imposed on w for those points in the plane z = 1.5 inches that lie along the edges x = 0 and y = 0. A total of 71 degrees of freedom, out of the total of 540, are restrained.

Solvers

Problem e2x12b uses the default MARC profile solver. The SOLVER option is not included. Problem 32x12c uses the element-by-element iterative solver. A convergence criteria of $1x10^{-16}$ is specified. Problem e2x12e uses the Sparce direct solver.

Results

The six components of strain and stress for each element are referred to the global coordinate system and are computed at the element's integration points. Element type 7 has 8 integration points. Element type 117 has 1 integration point. A comparison of the maximum transverse deflection at the center of the plate shows good agreement between elements type 7, 117 and, from problem 2.11, element type 8. These are summarized below:

Type 7	1.09293E-03 inch	node	180
Type 117	1.09193E-03 inch	node	180
Type 8	1.06190E-03 inch	node	36

In addition, contour plots of von Mises stresses are shown for element types 7 and 117 on the deformed shape in Figure E 2.12-2 and Figure E 2.12-3. Maximum von Mises stresses are:

Type 7	1.035E+02 psi	Element 100	point 8
Type 117	8.553E+01 psi	Element 100	point 1
Type 8	1.300E+01 psi	Element 1	point 1

In problem 32x12b, you can observe that the half bandwidth is 44 and the:

number of profile entries including fill-in is	6414
number of profile entries excluding fill-in is	1754

total Workspace needed with in-core matrix storage is 320745 words

As this is a small problem, the ebe iterative solver actually requires more memory requiring 356875 words. To achieve the convergence requested, 175 iterations were required. Normally, a larger tolerance, such as 0.001, would have been chosen. In e2x12e, when using the sparse direct solver, the Workspace requirement is only 30,3619 words. For this problem, the computational speed is 2 to 3 times faster.

Summary of Options Used

The input for MESH3D is e2x12a.dat.

Listed below are the options used in example e2x12b.dat:

Parameter Options

ELEMENT
END
SIZING
TITLE

Model Definition Options

CONNECTIVITY
CONTROL
COORDINATE
DIST LOADS
END OPTION
FIXED DISP
ISOTROPIC
POST

Listed below are the options used in example e2x12c.dat:

Parameter Options

ELEMENT
END
PROCESS
SIZING
TITLE

Model Definition

CONNECTIVITY
CONTROL
COORDINATE
DIST LOADS
END OPTION
FIXED DISP
ISOTROPIC
POST
SOLVER

Listed below are the options used in example e2x12d.dat:

Parameter Options

ELEMENT
END
SIZING
TITLE

Model Definition Options

CONNECTIVITY
CONTROL
COORDINATE
DIST LOADS
END OPTION
FIXED DISP
ISOTROPI C
POST

Listed below are the options used in example e2x12e.dat:

Parameter Options

ELEMENT
END
SIZING
TITLE

Model Definition Options

CONNECTIVITY
CONTROL
COORDINATE
DIST LOADS
END OPTION
FIXED DISP
ISOTROPIC
POST
SOLVER

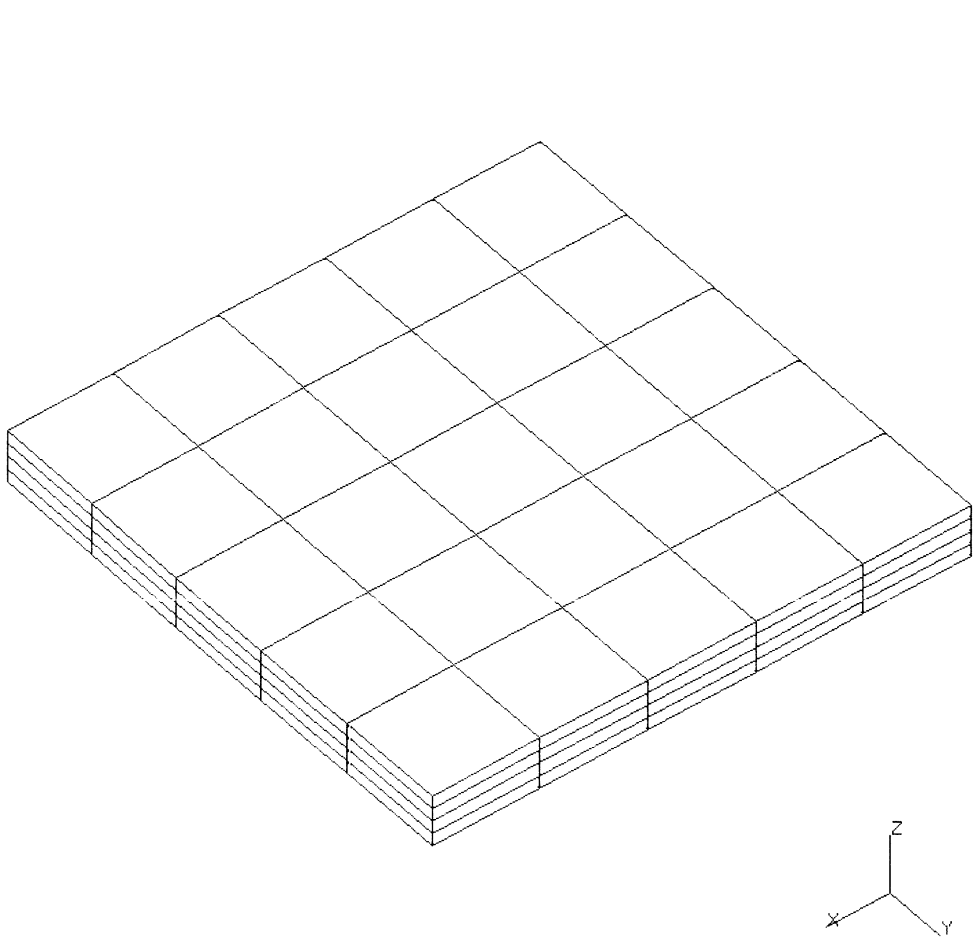

Figure E 2.12-1 Model

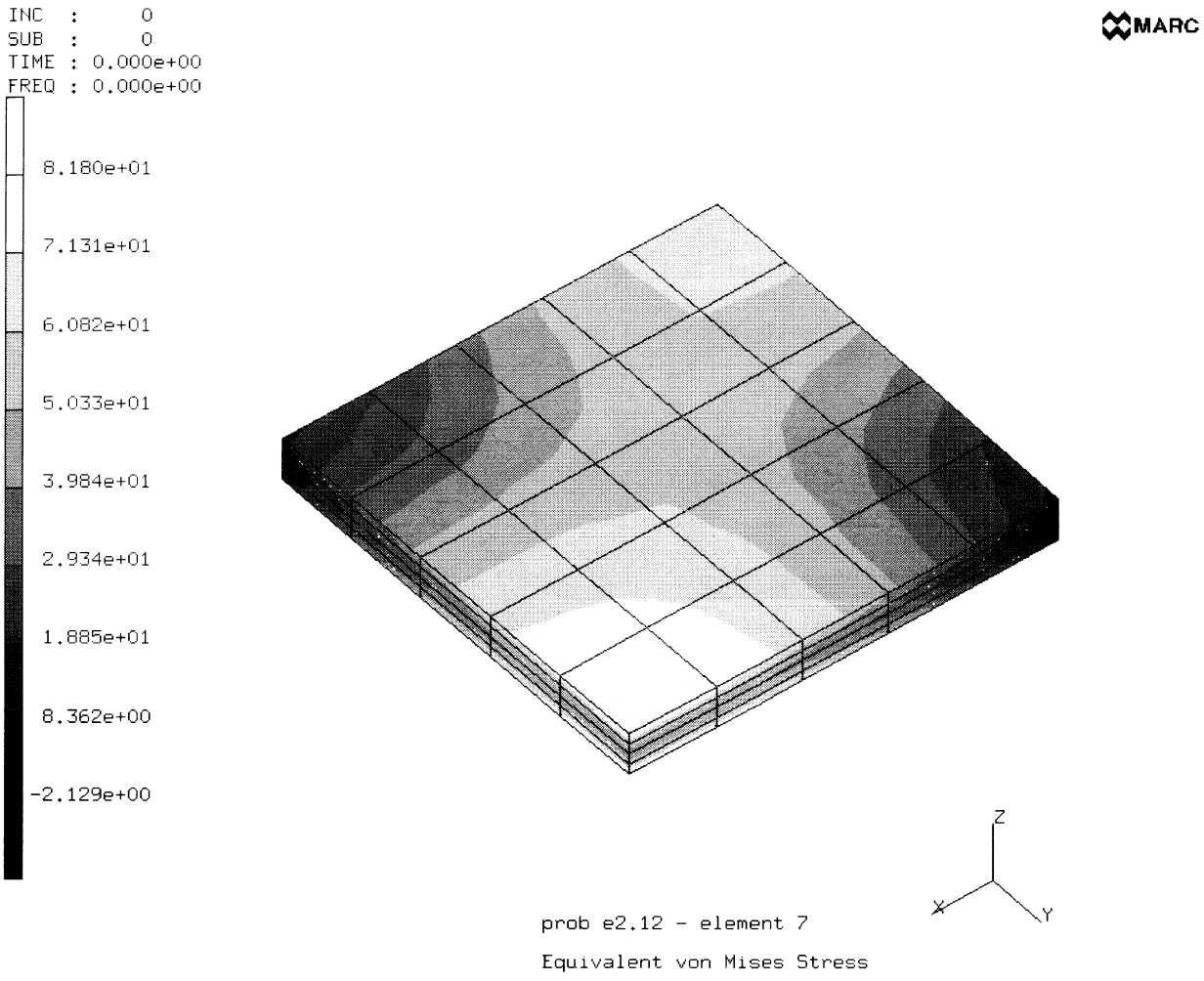

Figure E 2.12-2 Plot of von Mises Stress Element 7

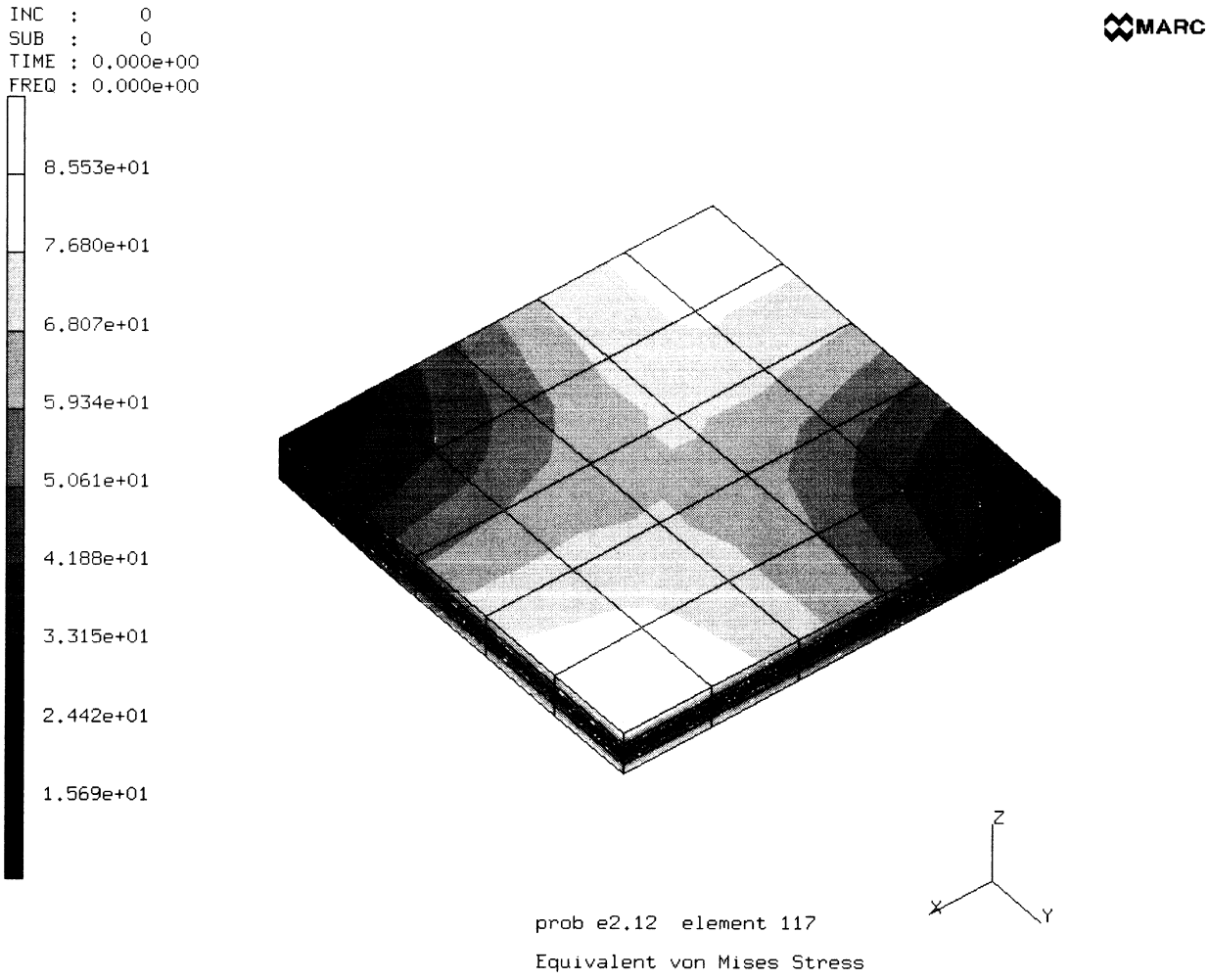

Figure E 2.12-3 Plot of von Mises Stress Element 117

E 2.18 Shell Roof Using Element 22

This problem is one of several in which a barrel-vault shell roof is loaded under its own weight. The results of these analyses are compared in Section E 2.19. This example demonstrates the use of user subroutine UFXORD to generate the coordinates for element type 22.

Element (Ref. B22.1)

Element type 22, a curved quadrilateral thick-shell element, is used. The displacements are interpolated from the values of the eight nodes on the middle shell surface. The four corner nodes and four midside nodes each have six degrees of freedom, three displacements and three rotations.

Model

The four element model takes advantage of symmetry conditions for a one-quarter section of the shell. The ends of the structure are supported by diaphragms, with two free edges. The model has a support end, two symmetry boundaries and one free edge. There are 21 nodes for a total of 126 degrees of freedom. See Figure E 2.18-1.

Geometry

The thickness is 3.0 inches.

Material Properties

Young's modulus is 3.0×10^6 psi; Poisson's ratio is taken as 0.

Loading

All four elements are loaded under self-weight, positive in the negative z-direction. This corresponds to IBODY = 1 in the DIST LOADS option.

Boundary Conditions

Three sets of boundary conditions are necessary; one on each of the symmetry edges and one on the supported edge. At the supported end, we have $u = w = 0$. On the $y = 300$ symmetry boundary, axial displacement is fixed ($v = \theta_x = 0$). On the $x = 0$ symmetry boundary, movement tangential to the shell surface is fixed ($u = \theta_y = 0$). The constraint on rotation normal to the shell is imposed only at node 15. See Figure E 2.16-2 and Figure E 2.18-1.

User Subroutines

Subroutine UFXORD is used to generate the three coordinates. The first coordinate read from the COORDINATE block is used to generate two of the three global coordinates. Notice that NCRD = 2 on the second card of the COORDINATE block, rather than the default of 3 for this element.

Results

The results from problems E 2.16, E 2.17, E 2.18, and E 2.19 are compared in problem E 2.19.

Summary of Options Used

Listed below are the options used in example e2x18.dat:

Parameter Options

ELEMENT
END
SIZING
TITLE

Model Definition Options

CONNECTIVITY
COORDINATE
DIST LOADS
END OPTION
FIXED DISP
GEOMETRY
ISOTROPIC
UFXORD

Listed below is the user subroutine found in u2x18.f:

UFXORD

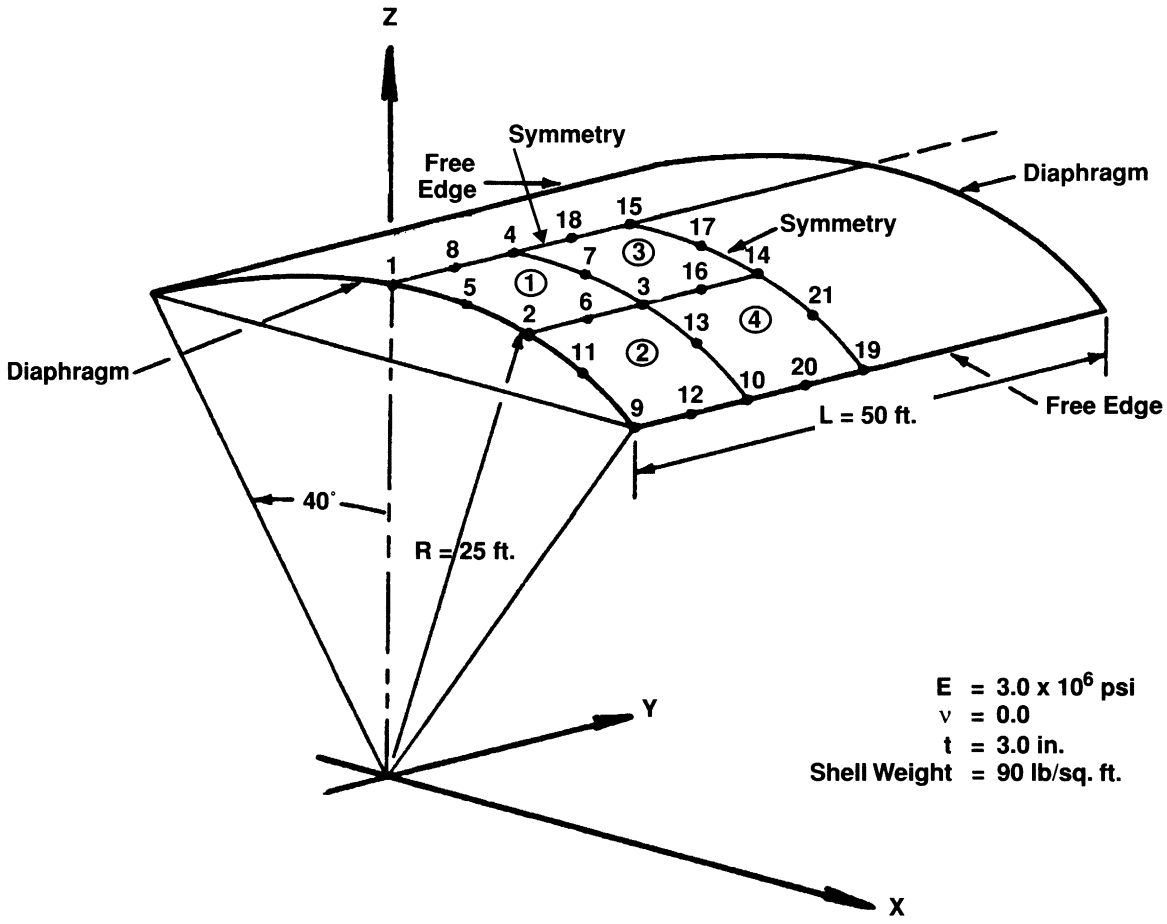

Figure E 2.18-1 Cylindrical Shell Roof Configuration, Element 22

E 2.22 J-Integral Evaluation Example

This example illustrates the use of the J-Integral evaluation procedure in MARC, as well as the 1/4-point element geometry at the crack tip. The example is that of a double-edge notch (DEN) specimen under axial tension (Mode I) (Figure E 2.22-1). This example is chosen because of the availability of an accepted value for K_I for comparison. The fundamental problem in a crack problem is the singularity in the strain field at the crack tip. For elastic response the singularity is of order $1\sqrt{r}$, where r measures distance away from the crack tip. It can be shown that the second order isoparametric elements reproduce this singularity when the side nodes are placed at the 1/4-points instead of at the midsides. This condition is achieved by merging two nodes in each element at the crack tip. Based on this consideration, a rather coarse mesh for the problem is shown in Figure E 2.22-2 and Figure E 2.22-3. The coarseness of the mesh is acceptable because the only output required is the J-integral value, and it has been shown [1] that the differential stiffness technique, as is used in the MARC program, provides good estimates of J with relatively coarse models.

Element (Ref. B27.1-1)

Element type 27 is a plane-strain quadrilateral element. There are eight nodes and two degrees of freedom at each node.

Model

Only a quadrant of the model is used because of obvious symmetries. A second COORDINATES block was used to move the side nodes of the crack tip elements to the 1/4 points (1/4 of the way along the sides from the crack tip to the opposite face of the element).

Geometry

No geometry is specified.

Material Properties

The Young's modulus is 30 x 10^6 psi and Poisson's ratio is 0.3.

Loading

The loading is shown in Figure E 2.22-1. The load is applied as a uniform negative pressure of 100 psi on the appropriate faces of the end elements.

Boundary Conditions

The boundary conditions for the model quadrant are determined by symmetry conditions. The edge along the y-direction is constrained in both degrees of freedom. The edge along the x-direction is constrained to displacement along the x-axis. Boundary conditions are illustrated in Figure E 2.22-1.

J-Integral

The J-integral is evaluated numerically by moving nodes within a certain ring of elements around the crack tip, to represent a differential crack advance, and measuring the change in strain energy. The J is the negative differential of strain energy with respect to crack advance. This mesh has three obvious "rings" of elements around the crack tip, so that three evaluations of J are available. Since the J-integral should be path independent for elastic problems, the variation in J between the three values gives some idea of the accuracy of the solution. A differential movement has to be supplied to evaluate J. Numerical experiments have indicated that setting this movement to less than 1/50 times the size of the smallest crack tip element gives a convergent solution (convergence in the sense of the numerical difference providing the differential). The use of too small a movement causes roundoff difficulties.

In this case, a value of 10^{-2} was used. The smallest element dimension is 1, so that this represents 1/100, a satisfactory value. The midside nodes are moved proportionally for each evaluation.

Results

The program provides an output of the strain energy difference. This must be normalized by the crack opening area to obtain the value of J. Since this specimen is of unit thickness, the crack opening area is $\Omega 1$, where $\Omega 1$ is the differential crack motion. The mesh used symmetry about the crack line, so that that strain energy change in the actual specimen would be twice that printed out. Finally, since this is a plane strain, Mode I problem, the J-integral may be immediately converted to K_I, the stress intensity factor, by the relation:

$$K_I = \sqrt{\frac{E}{1-\nu^2}}\ J$$

These results are summarized in Table E 2.22-1.

It is clear from these results that the path independence is well reproduced, and that the error in the solution for K_I is quite small. The user should note that such a coarse mesh will not give an accurate model of the stress field close to the cracktip.

However, because the 1/4-point technique used here includes the $1/\sqrt{r}$ singularity, a reasonable refinement of the same mesh would give excellent predictions of the near-tip elastic stress field. As a general guideline, it appears that second-order elements with the 1/4-point technique give good results for J-integral evaluation when the crack tip elements are sized about 20% of the crack depth or ligament width, whichever is smaller. For near-tip stress field prediction, the size should be reduced to about 5% of crack depth or ligament width.

Table E 2.22-1 J-Integral Evaluation Results

	Move Tip Only	Move First Ring of Elements	Move Second Ring of Elements
Strain energy change given in program (Δu)	6.7313×10^{-5}	6.693×10^{-5}	6.689×10^{-5}
J-Integral	1.324×10^{-2}	1.3386×10^{-2}	1.3378×10^{-2}
$K_I = \sqrt{\frac{E}{1-\nu^2}}\ J$	666.	664.	664.
$K_I / \sigma_{net}\sqrt{1}$	1.052	1.050	1.050
cf 1.028 [2]	+2.4%	+2.2%	+2.2%

References

1. Parks, D. M., "A Stiffness Derivative Finite Element Technique for Determination of Elastic Crack Tip Stress Intensity Factors," *Int. J. Fracture*, Vol. 10, No. 4, December 1974, pp. 487-502.
2. Bowie, I. L., "Rectangular Tensile Sheet With Symmetric Edge Cracks," *J. Applied Mechanics*, Vol. 31, 1964, pp. 208-212.

Summary of Options Used

Listed below are the options used in example e2x22.dat:

Parameter Options

ELEMENT
ELSTO
END
J-INT
SIZING
TITLE

Model Definition Options

CONNECTIVITY
COORDINATE
DIST LOADS
END OPTION
FIXED DISP
ISOTROPIC
J-INTEGRAL
PRINT CHOICE

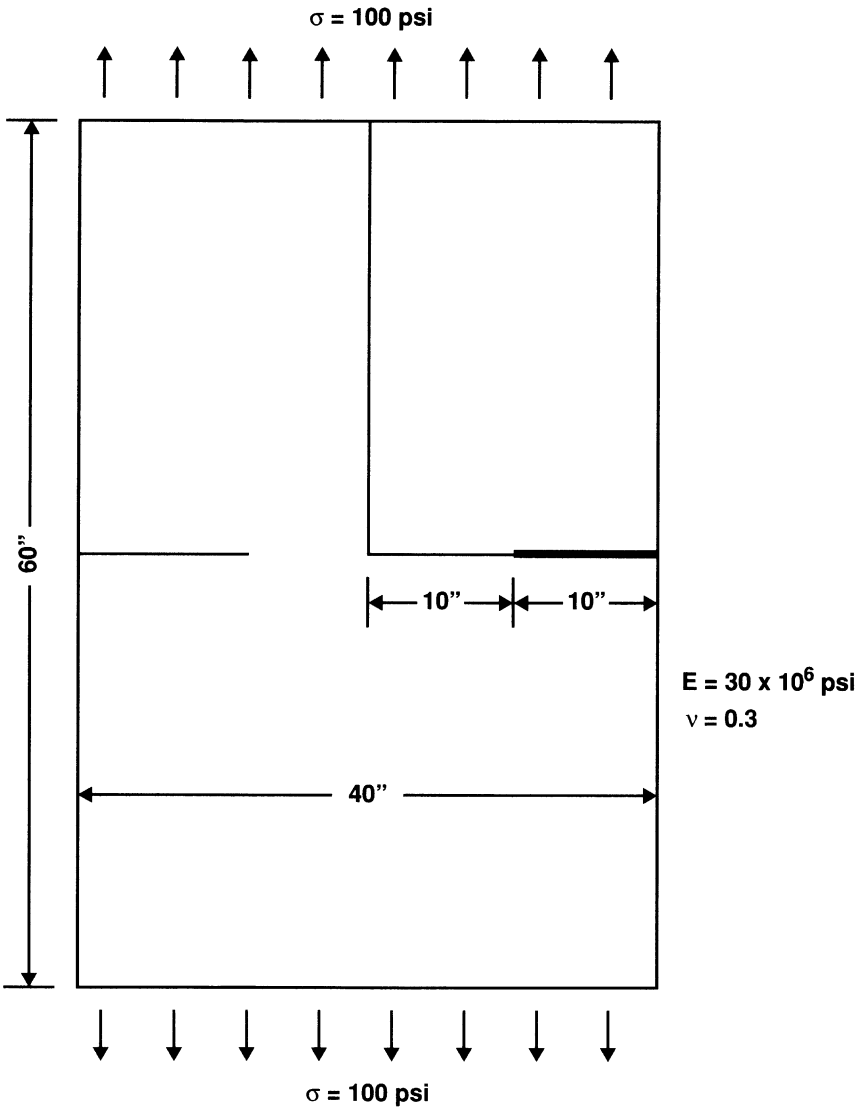

Figure E 2.22-1 Double-Edge Notch Specimen, Showing Blocks for Mesh Generation

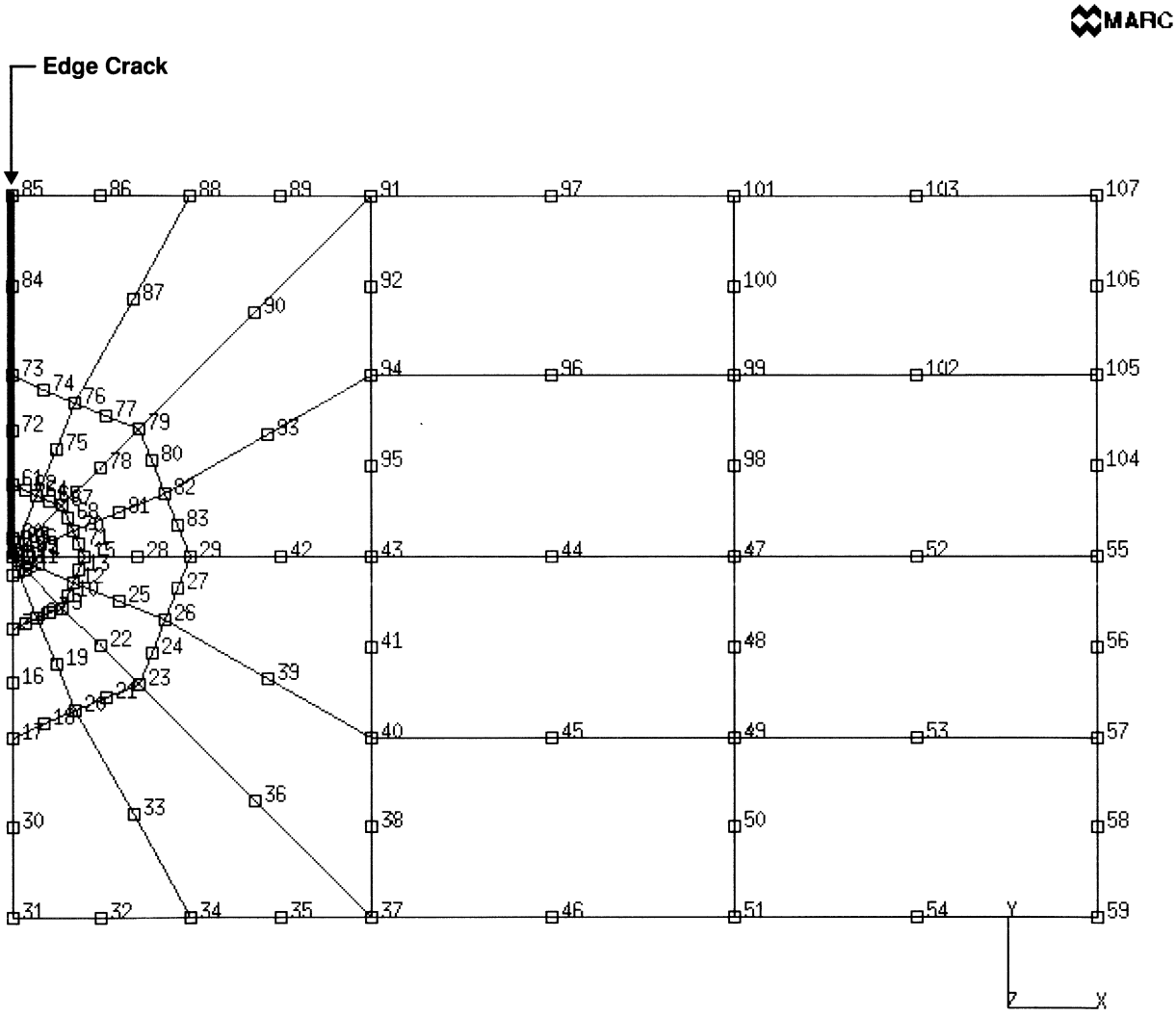

Figure E 2.22-2 Mesh for Double-Edge Notch Specimen

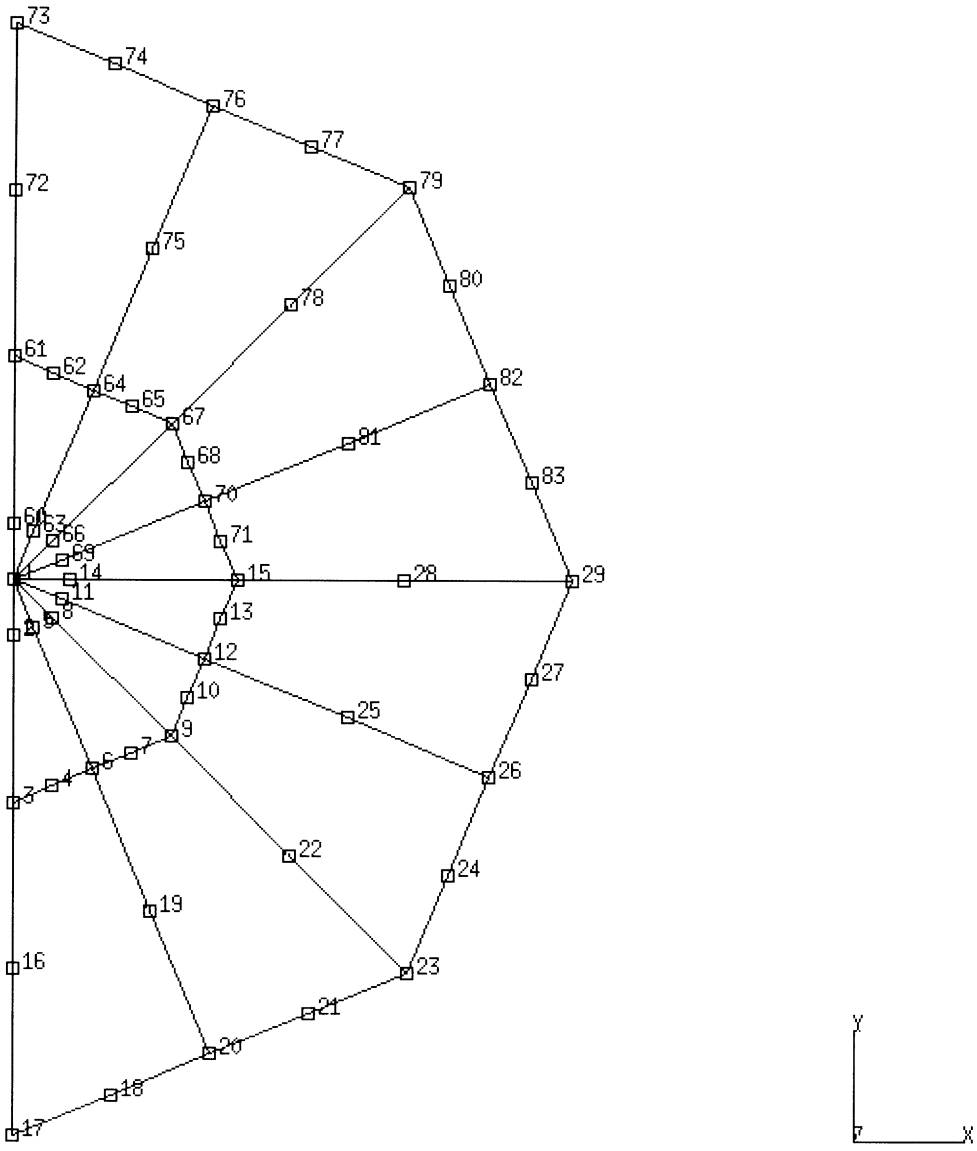

Figure E 2.22-3 Mesh Detail of Double-Edge Notch Specimen

E 2.30 Notched Circular Bar, J-Integral Evaluation

This problem illustrates the use of MARC element type 28 and the J-INT option for an elastic analysis of a notched circular bar, subjected to uniformly distributed axial forces. The J-integral evaluation is intended for the study of the stress concentration at the notch of the bar. The use of options ELSTO and ALIAS is also illustrated.

Element (Ref. B28.1)

Element type 28 is a second order distorted quadrilateral with eight nodes. Each node has two degrees of freedom. For J-integral calculations, a high-order element is required; hence, the selection of element type 28.

Model

The dimensions of the bar and the finite element mesh are shown in Figure E 2.30-1. This is the same mesh as is used in problem E 2.22. The mesh consists of 32 elements and 107 nodes. The ALIAS option is used to convert element type 27 to 28.

Material Properties

The material is elastic with a Young's modulus of 30.E6 psi and Poisson's ratio of 0.3.

Geometry

Not required for axisymmetric elements.

Boundary Conditions

The following boundary conditions are imposed: v = 0 at r = 0 (axis of symmetry) and u = 0 at uncracked portion of line z = 0.

Loading

A distributed load of 100 psi is applied on the outer edge of elements 15, 16, 31 and 32.

The midside nodes 2, 5, 8, 11, 14, 69, 66, 63 and 60 have been moved to quarter-point position for the J-integral evaluations. The quarter-point nodes more accurately reflect the singularity at the crack tip. Their coordinates are modified by inputting a new COORDINATES model definition block. The mesh is generated as if it was made of element type 27, and the ALIAS option was used so that the program would consider them to be type 28.

J-INTEGRAL

In the current analysis three rings of elements are chosen for the J-integral evaluations.

J-Integral Evaluations	Number of Nodes Moved in List Number		Nodal Movements of List Number in r Direction	
	1	2	1	2
1	1	9	-0.01	-0.0075
2	27	9	-0.01	-0.0050
3	53	9	-0.01	-0.0050

Node numbers are shown in the J-INTEGRAL model definition block.

Results

A comparison of the J-integral evaluation is tabulated in Table E 2.30-1. A deformed mesh plot and stress contours are shown in Figure E 2.30-3 and Figure E 2.30-4, respectively.

Table E 2.30-1 Comparison of J-Integral Evaluations

MARC	SED Output	J	K	Difference (K/K_I)
1	0.01131	0.0360189	1089.7	2.28%
2	0.01127	0.0358915	1087.8	2.01%
3	0.01125	0.0358278	1086.8	2.01%
NOTE: Stress intensity factor estimation for mode I cracking				

The stress intensity factor K_I for an axisymmetric bar is:

$$K_I = \sigma_n \sqrt{\pi b} \quad F_2\left(\frac{b}{R}\right)$$

$$\sigma_n = \frac{P}{\pi b} \quad ,$$

$$F_2(\xi) = \frac{1}{2}\left(1 + \frac{1}{2}\ \xi + \frac{3}{8}\ \xi^2 - 0.363\ \xi^3 + 0.731\ \xi^4\right)\sqrt{1-\xi}$$

(error < 1%)

therefore, $K_I = 1065.39$

For an axisymmetric model, plane strain assumption is assumed to exist locally, and the relation between J and K_I is:

$$K_I = \sqrt{\frac{E}{1-\nu^2}J} = \sqrt{32967033*J}$$

MARC output is the strain energy density (SED) of the area of crack tip movement. The expression of J-integral is:

$$J = \frac{SED*2}{\pi b^2 - \pi(b-\delta b)z^2} = \frac{SED*2}{\pi(10^2 - 9.99^2)} = \frac{SED}{0.3140022}$$

Summary of Options Used

Listed below are the options used in example e2x30.dat:

Parameter Options

ALIAS
ELEMENT
ELSTO
END
J-INT
SIZING
TITLE

Model Definition Options

CONNECTIVITY
COORDINATE
DIST LOADS
END OPTION
FIXED DISP
ISOTROPIC
J-INTEGRAL

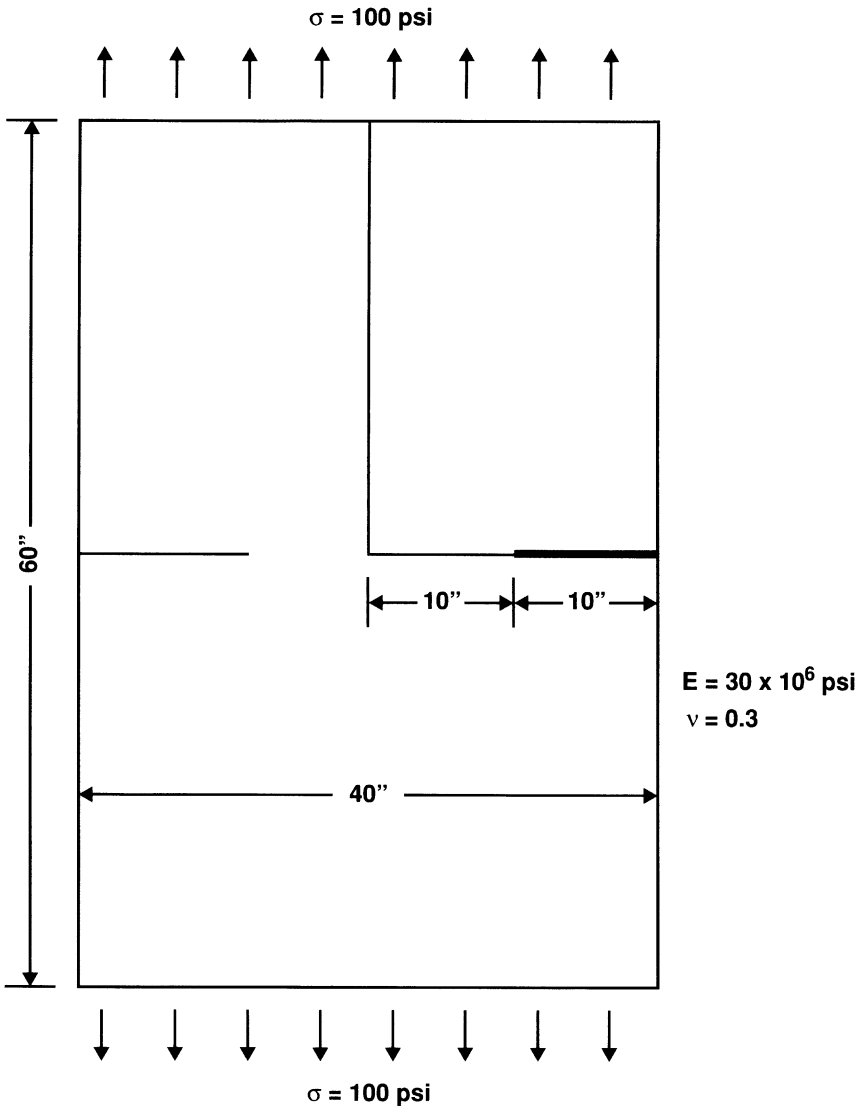

Figure E 2.30-1 Notched Circular Bar and Mesh

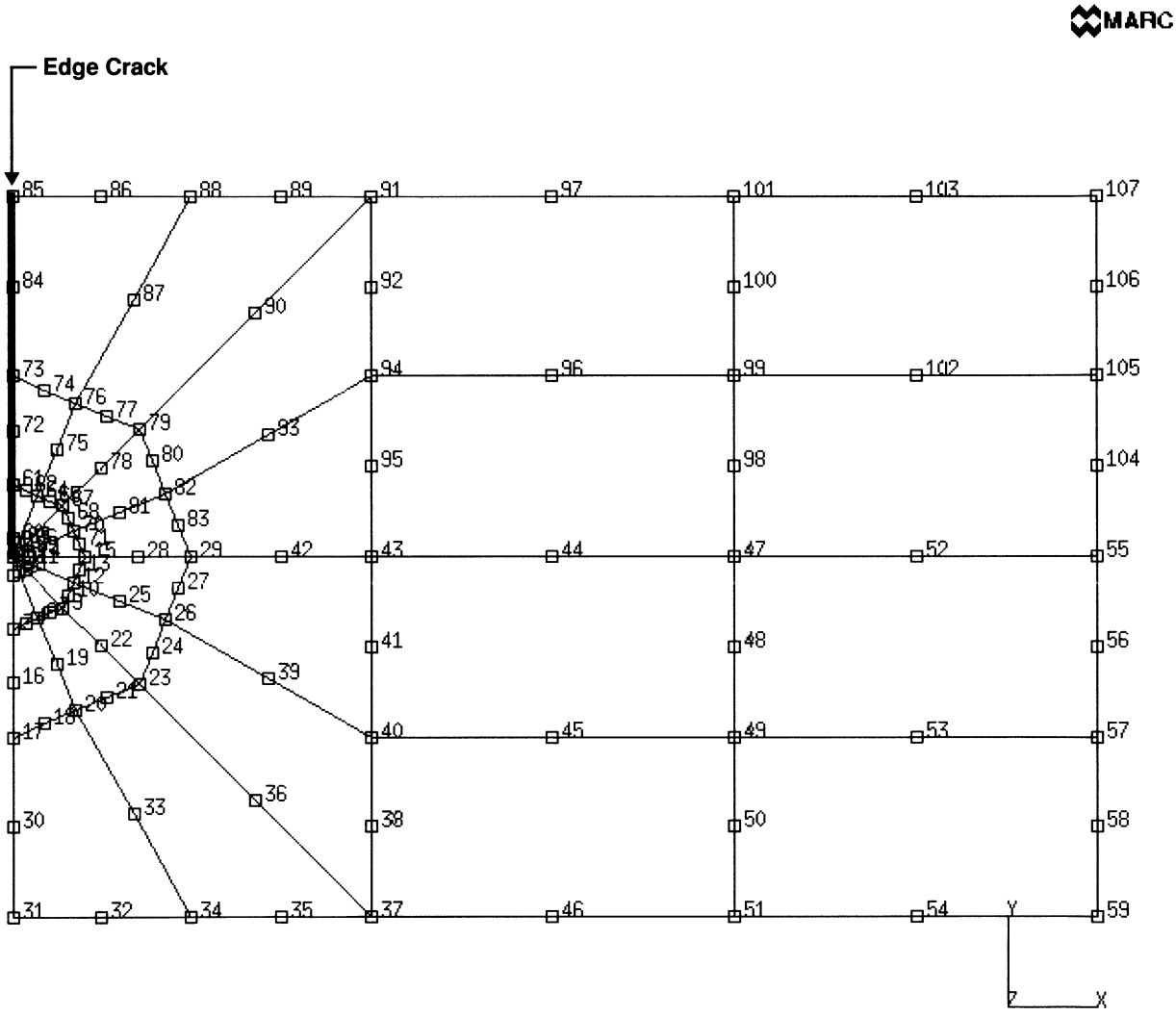

Figure E 2.30-2 Mesh for Double Edge Notch Specimen

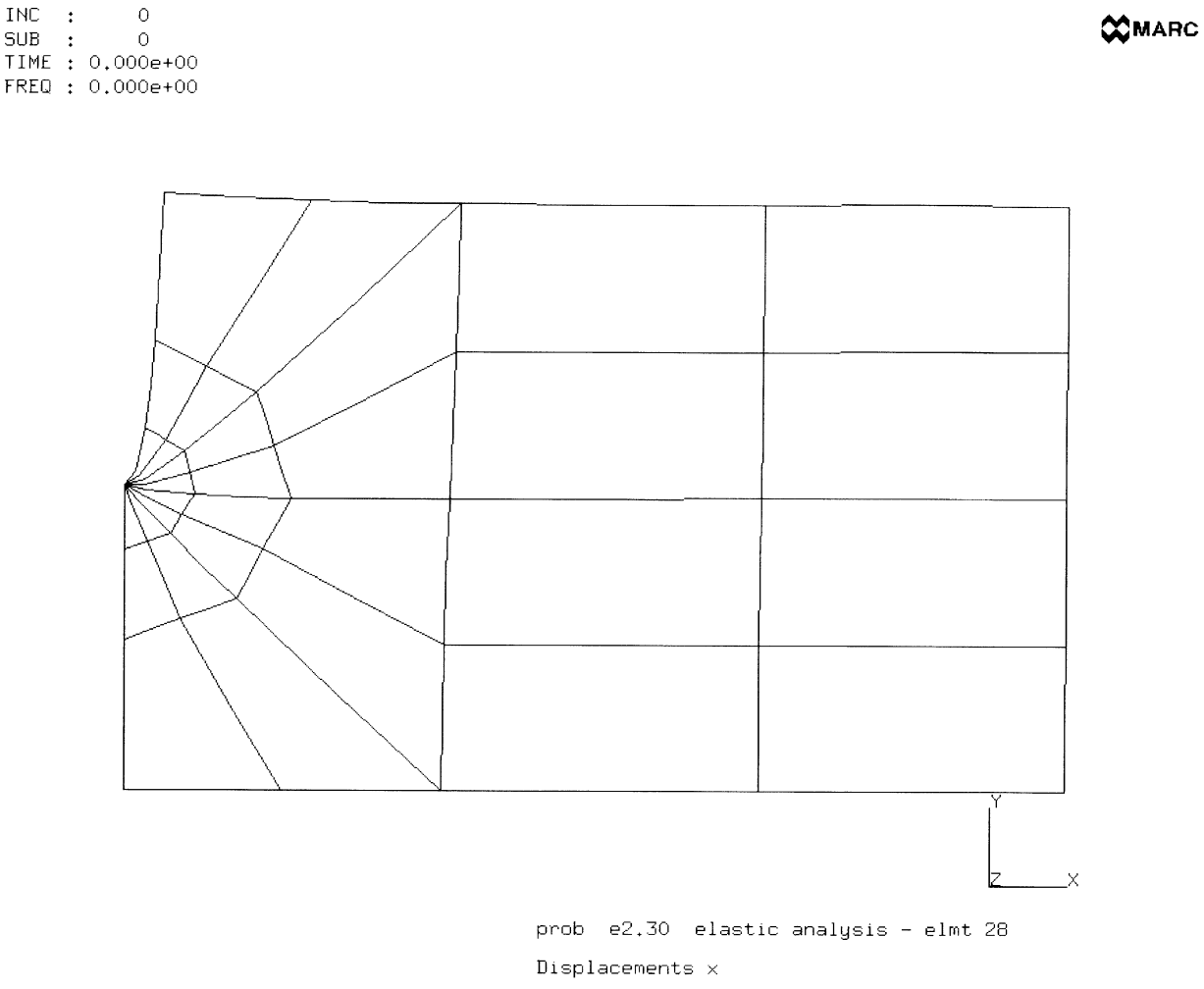

Figure E 2.30-3 Deformed Mesh

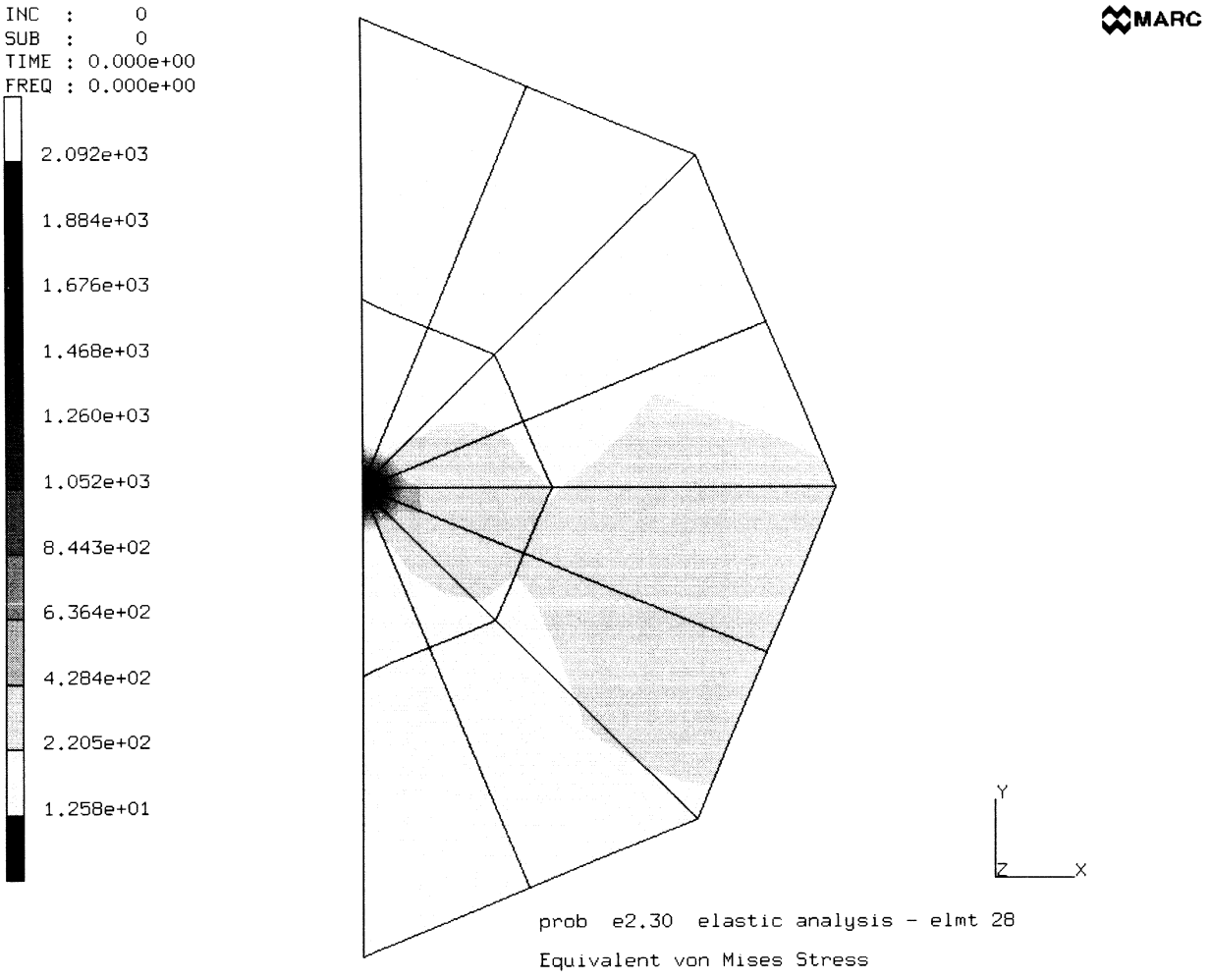

Figure E 2.30-4 Stress Contours

E 2.31 Square Section With Central Hole Using Generalized Plane Strain Element

This problem illustrates the use of MARC element types 29 and 56 (generalized plane strain, distorted quadrilateral), options OPTIMIZE and SCALE for an elastic analysis of a square plate subjected to a uniform pressure. The pressure is applied to the surface of a circular hole located at the center of the section.

Element (Ref. B29.1 and B56.1)

The analysis is performed twice: first with element type 29, which uses 9-point integration, and then with element type 56, which uses 4-point integration.

Model

The dimensions of the plate and a finite element mesh are shown in Figure E 2.31-1. The model consists of 20 elements and 81 nodes. Only one-quarter of the section is modeled due to symmetry.

Material Properties

The material behaves elastically with a Young's modulus of 50×10^4 psi and the Poisson's ratio of 0.2. The solution is scaled such that one integration point has reached the yield stress of 200 psi.

Geometry

The thickness of the section is 1.0 inch, which is given in EGEOM1.

Loading

A uniform pressure of 1000 psi is applied to the inner surface of the hole. The pressure load is scaled to the condition of first yield.

Boundary Conditions

Zero displacements are assumed to exist on the lines of symmetry: $u = 0$ at $x = 0$, and $v = 0$ at $y = 0$.

Optimization

The Sloan optimizer is used. As this is a generalized plane strain model, the bandwidth does not decrease, but the number of profile entries, including fill-in, is reduced from 1687 to 1198.

Results

A deformed mesh plot is shown in Figure E 2.31-2 and the stress contours are depicted in Figure E 2.31-3. First, one observes that the results are symmetrical about the 45-degree line. The scale factor using element type 29 (full integration) is 0.116, and the scale factor using element type 56 is 0.120 more than the factor computed for element 29. Element type 29 has integration points closer to the hole where the stress is larger, resulting in a lower scaling factor.

The results are compared with the analytically calculated (Timoshenko and Goodier, *Theory of Elasticity*) results of a hollow cylinder submitted to uniform pressure on the inner surface and are summarized below.

Displacement* (in.)		**Stress Components (psi)**	
Computed	**Calculated**	**Computed****	**Calculated*****
2.97×10^{-4}	2.80×10^{-4}	$\sigma_x = -1.08 \times 10^{-2}$	$\sigma_x = -1.16 \times 10^{-2}$ (σ_r)
		$\sigma_y = 1.18 \times 10^{-2}$	$\sigma_y = -1.16 \times 10^{-2}$ ($\sigma\theta$)
*At node point 34.		**At node point 3 in element 8	***On the inner surface

Summary of Options Used

Listed below are the options used in example e2x31a.dat:

Parameter Options

ELEMENT
END
SCALE
SIZING
TITLE

Model Definition Options

CONNECTIVITY
COORDINATE
DIST LOADS
END OPTION
FIXED DISP
GEOMETRY
ISOTROPIC
OPTIMIZE

Listed below are the options used in example e2x31b.dat:

Parameter Options

ELEMENT
END
SCALE
SIZING
TITLE

Model Definition Options

CONNECTIVITY
COORDINATE
DIST LOADS
END OPTION
FIXED DISP
GEOMETRY
ISOTROPIC
OPTIMIZE

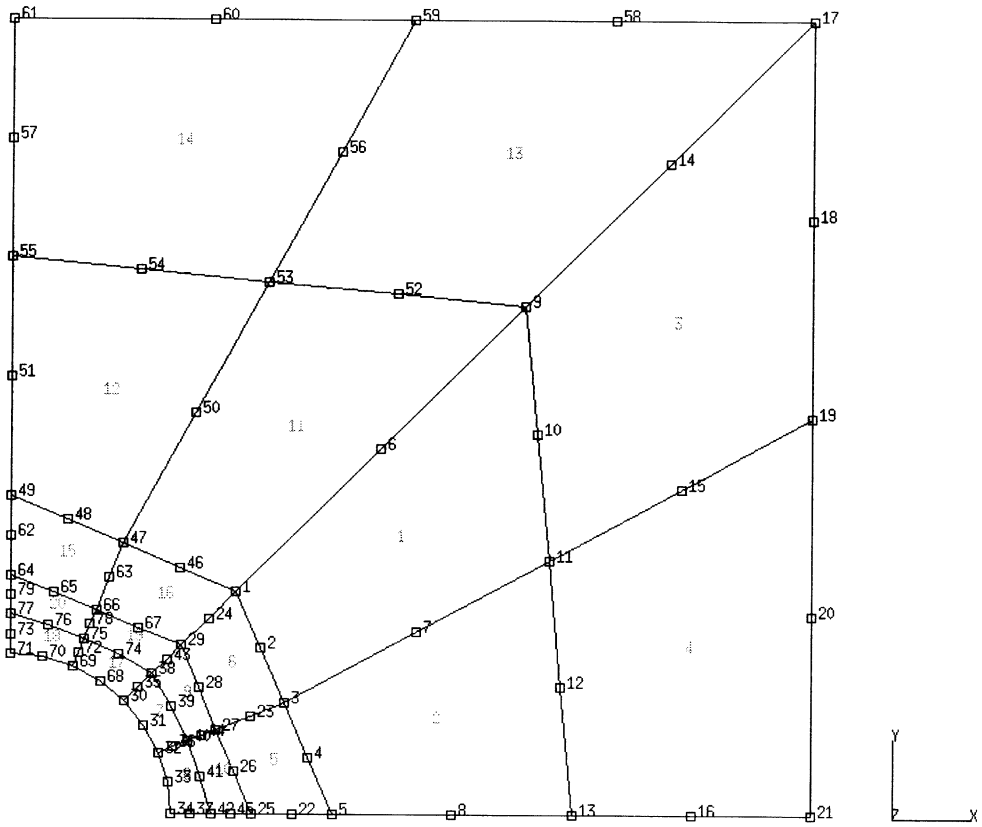

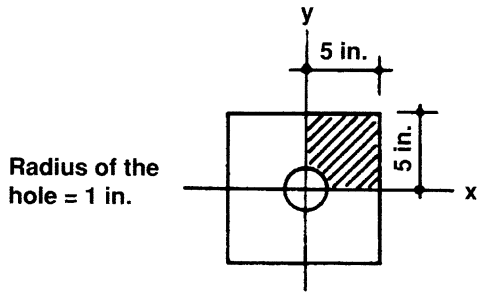

Figure E 2.31-1 Square Plate and Mesh

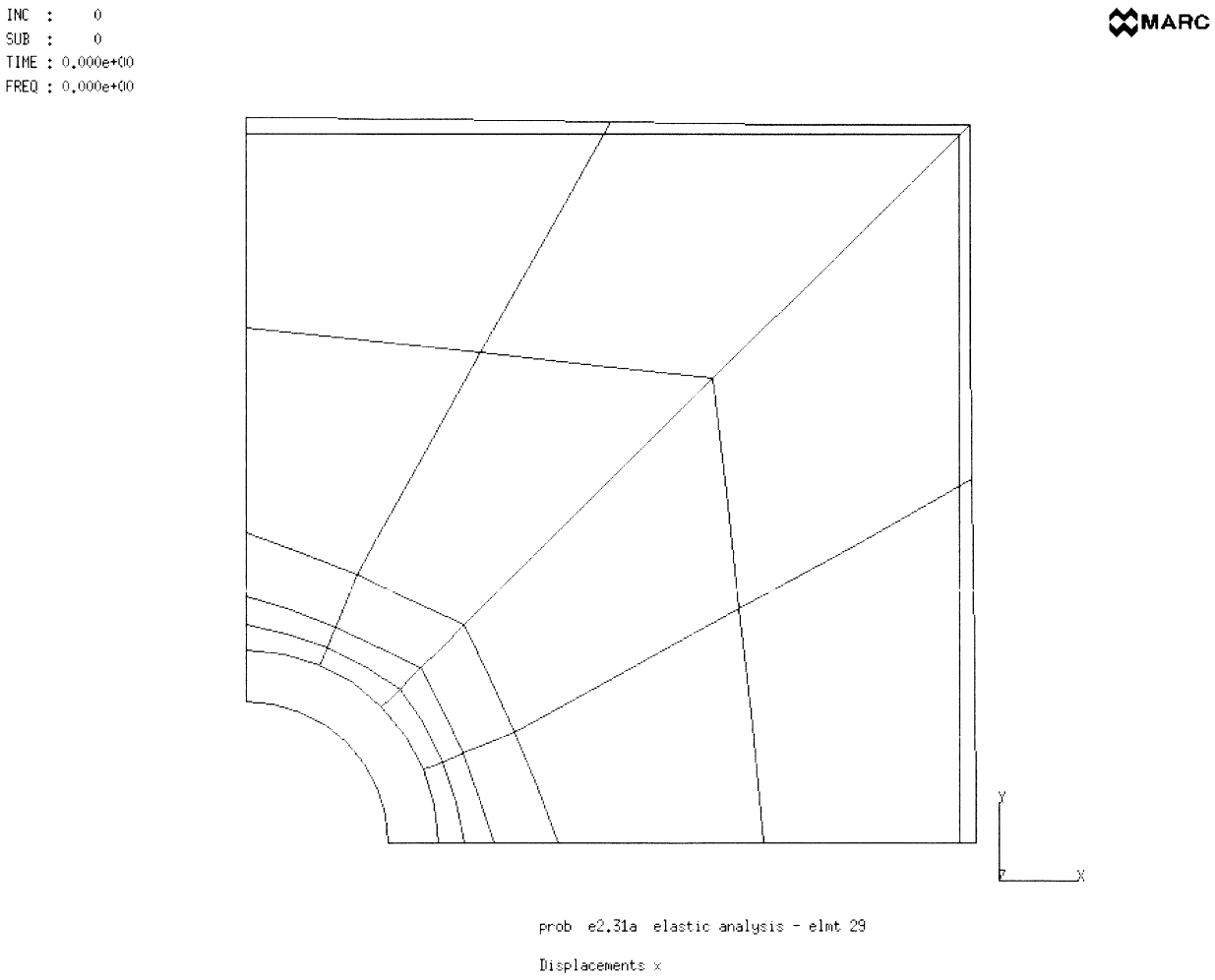

Figure E 2.31-2 Deformed Mesh Plot

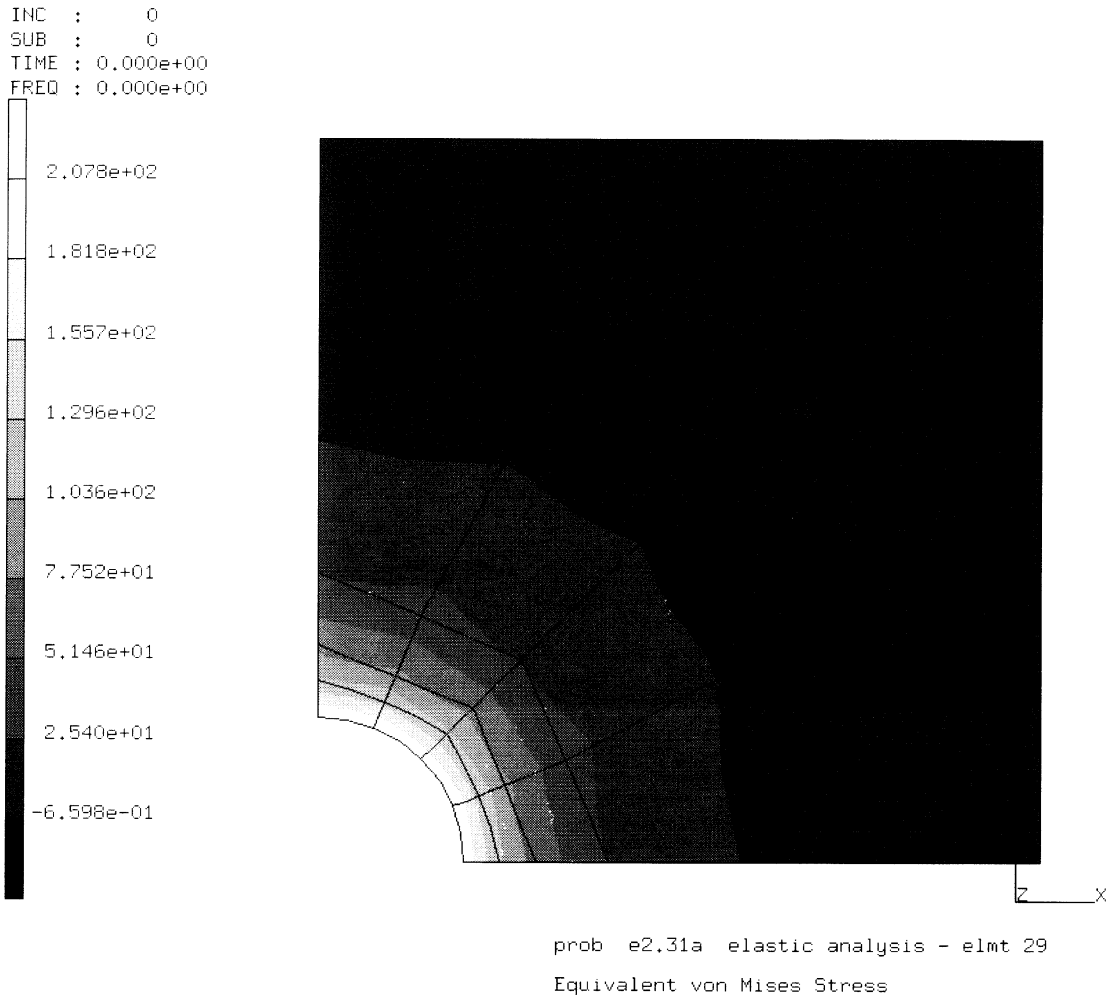

Figure E 2.31-3 Stress Contours

E 2.32 Square Plate With Central Hole Using Incompressible Element

This problem illustrates the use of MARC element type 32, options ALIAS, OPTIMIZE, and SCALE for an elastic analysis of a square plate. The plate is subjected to a uniform pressure. The pressure is applied to the surface of a circular hole located at the center of the plate.

Element (Ref. B32.1)

Element type 32, which is similar to element type 27 but modified for the Herrmann variational principle, has been developed for incompressible and nearly incompressible analysis.

Model

The dimensions of the plate and a finite element mesh are shown in Figure E 2.32-1. The mesh is the same as that used in problem E 2.31. There are 20 elements with 79 nodes in the mesh.

Material Properties

The properties are as follows: Young's modulus of 50×10^4 psi, Poisson's ratio of 0.5, and yield stress of 200 psi.

Geometry

The thickness of the plate is 1.0 inch.

Loading

A uniform pressure of 1000 psi is applied to the inner surface of the hole. The pressure load is scaled to the condition of first yield.

Boundary Conditions

Zero displacements are assumed to exist on the lines of symmetry: $u = 0$ at $x = 0$, and $v = 0$ at $y = 0$.

Optimize

The Sloan optimizer is used to reduce the bandwidth from 67 to 35.

Results

Stress contours are shown in Figure E 2.32-2 through Figure E 2.32-5.

Summary of Options Used

Listed below are the options used in example e2x32.dat:

Parameter Options

ALIAS
ELEMENT
END
SCALE
SIZING
TITLE

Model Definition Options

CONNECTIVITY
COORDINATE
DIST LOADS
END OPTION
FIXED DISP
GEOMETRY
ISOTROPIC

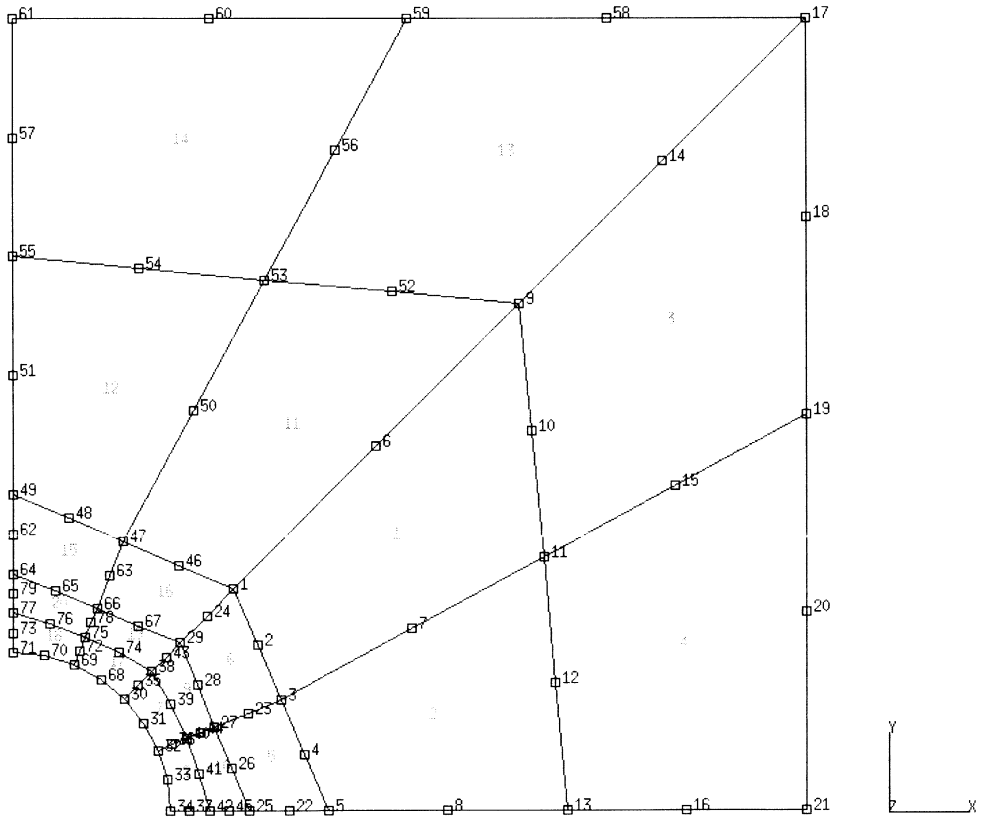

Figure E 2.32-1 Square Plate and Mesh

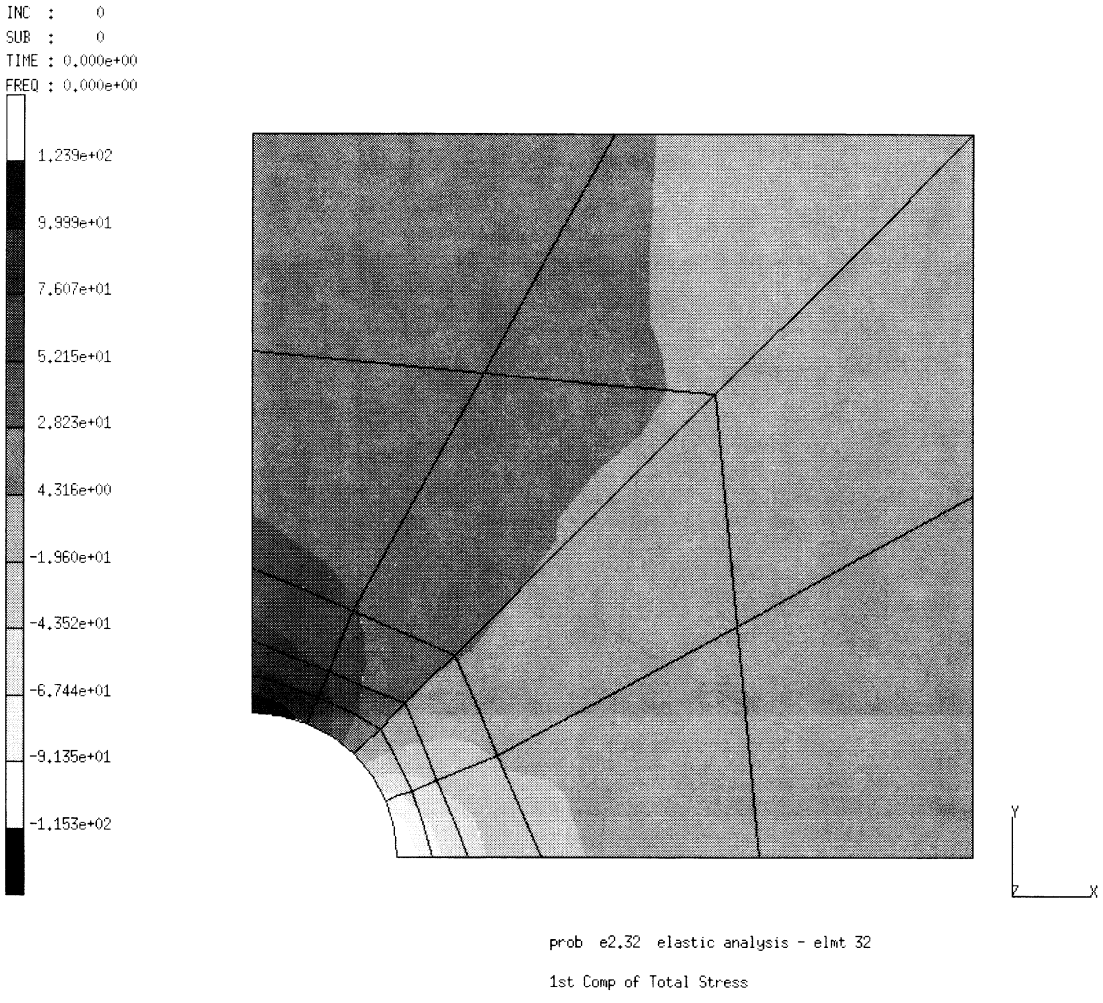

Figure E 2.32-2 Stress Contours for σ_{xx}

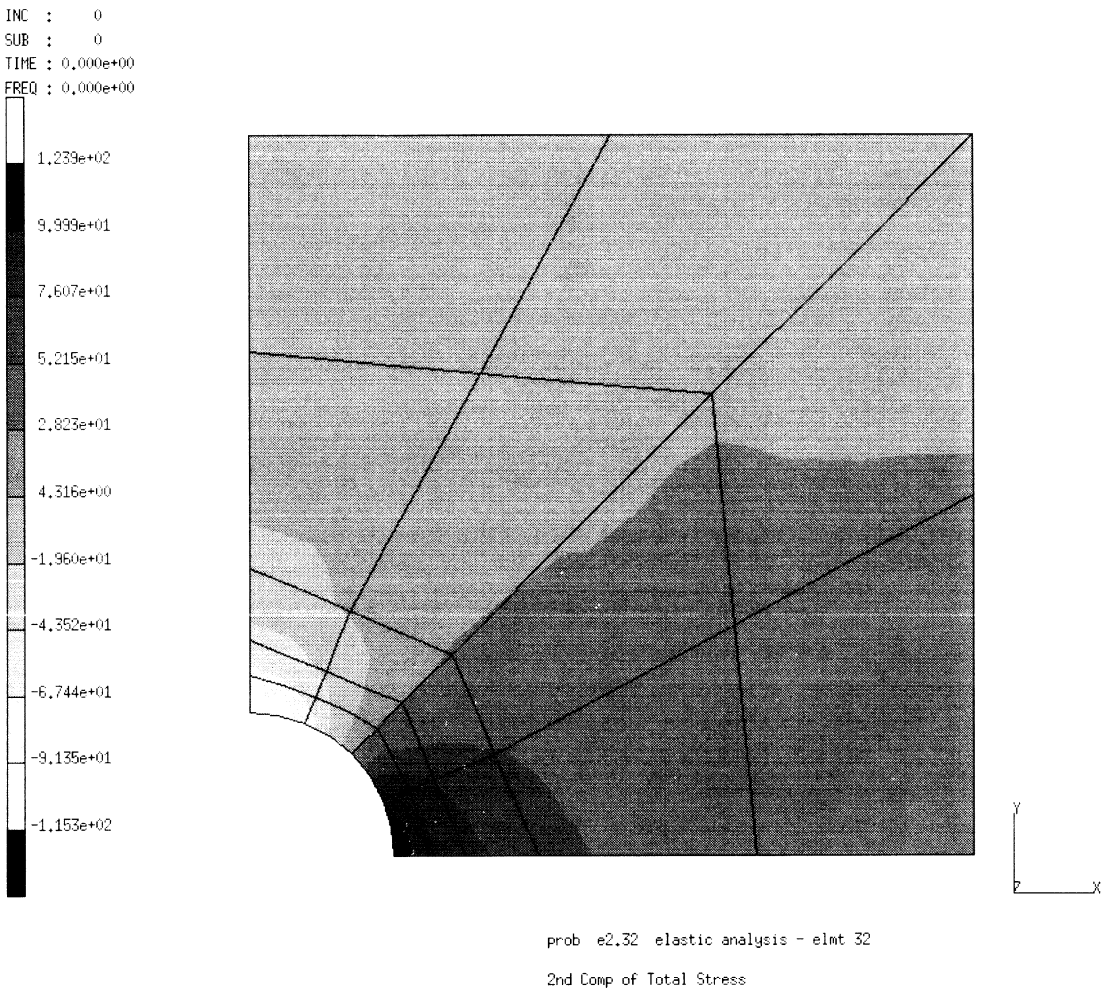

Figure E 2.32-3 Stress Contours for σ_{yy}

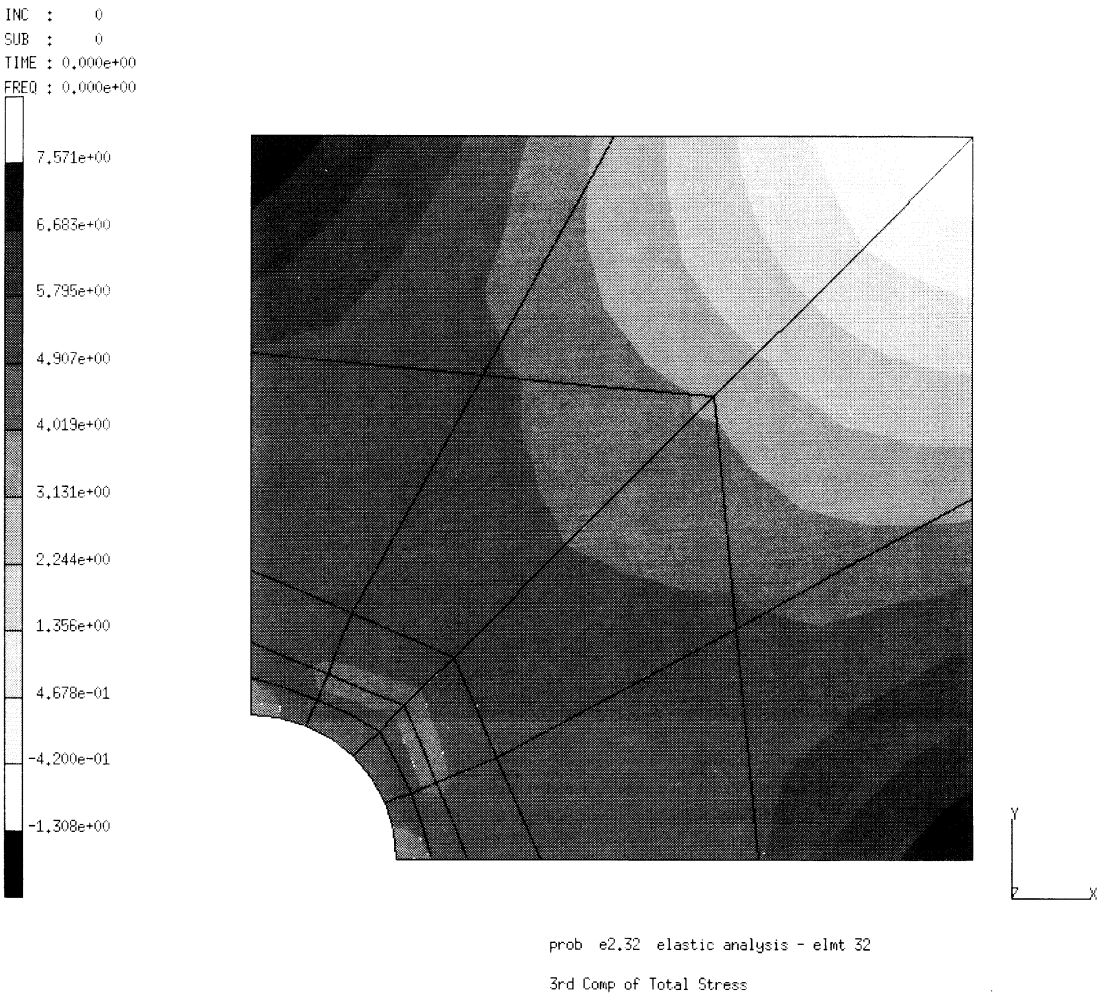

Figure E 2.32-4 Stress Contours for σ_{zz}

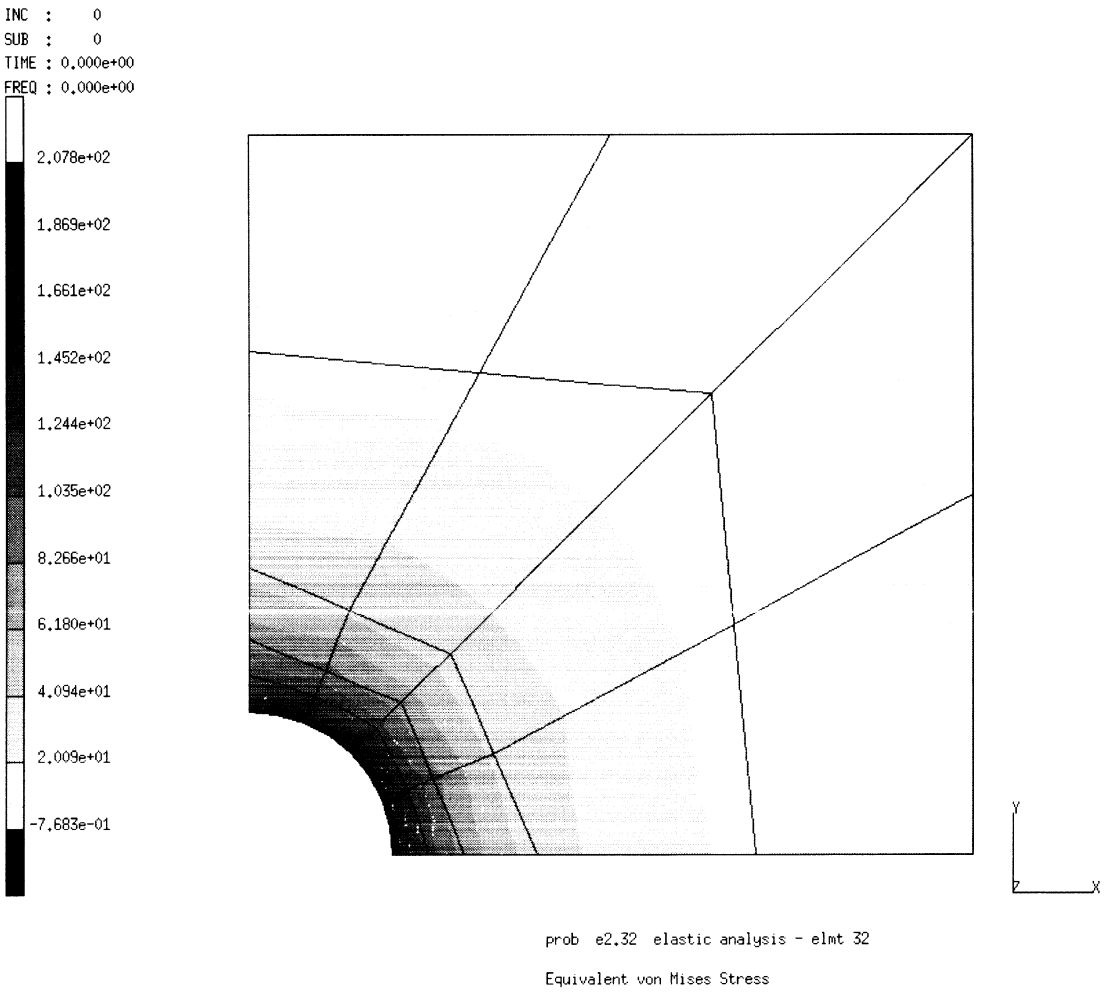

Figure E 2.32-5 Stress Contours for Equivalent Stress

E 2.34 Strip With Bonded Edges, Error Estimates

This problem illustrates the use of MARC element type 34, option CONN FILL, OPTIMIZE, and the user subroutine UFCONN for an elastic analysis of a strip. The strip is subjected to compression. This is the same problem as E 2.26, but modeled with a different element. The ERROR ESTIMATE option is used to determine mesh quality.

Element (Ref. B34.1)

Element type 34 is an 8-node, incompressible, generalized plane-strain element, Herrmann formulation. There are 10 nodes per element.

Model

The dimensions of the strip and a finite element mesh are shown in Figure E 2.34-1. There are 24 elements and 95 nodes in the mesh.

Material Properties

The elastic properties are: Young's modulus is 3×10^6 psi and Poisson's ratio is 0.4999.

Geometry

The strip has a thickness of 1 inch.

Boundary Conditions

Symmetry conditions are imposed such that $u = 0$ at $x = 0$ and $v = 0$ at $y = 0$. At the top nonzero displacement boundary condition, $v = -0.001$ inch in the y-direction. For the second extra node of elements (node 95), both degrees of freedom are constrained (no relative rotation between planes).

Optimize

The Sloan optimizer is used here. Because generalized plane strain elements are used, the bandwidth does not change, but the number of profile entries including fill-in is reduced.

Results

A deformed mesh plot is shown in Figure E 2.34-2 and a contour plot of the second component of stress is shown in Figure E 2.34-3. To increase the accuracy of the analysis, additional mesh refinement should be applied to the elements associated with the node where the largest normalized stress discontinuity occurs. In this analysis, this would be elements 23 and 24. The stress singularity exists because on one edge of element 24 shear stresses are allowed to occur, but the perpendicular side is a free edge.

Summary of Options Used

Listed below are the options used in example e2x34.dat:

Parameter Options

ELEMENT
END
QUALIFY
SIZING
TITLE

Model Definition Options

CONN FILL
CONN GENER
CONNECTIVITY
COORDINATE
END OPTION
FIXED DISP
GEOMETRY
ISOTROPIC
NODE FILL
OPTIMIZE
UFCONN

Listed below is the user subroutine found in u2x24.f:

UFCONN

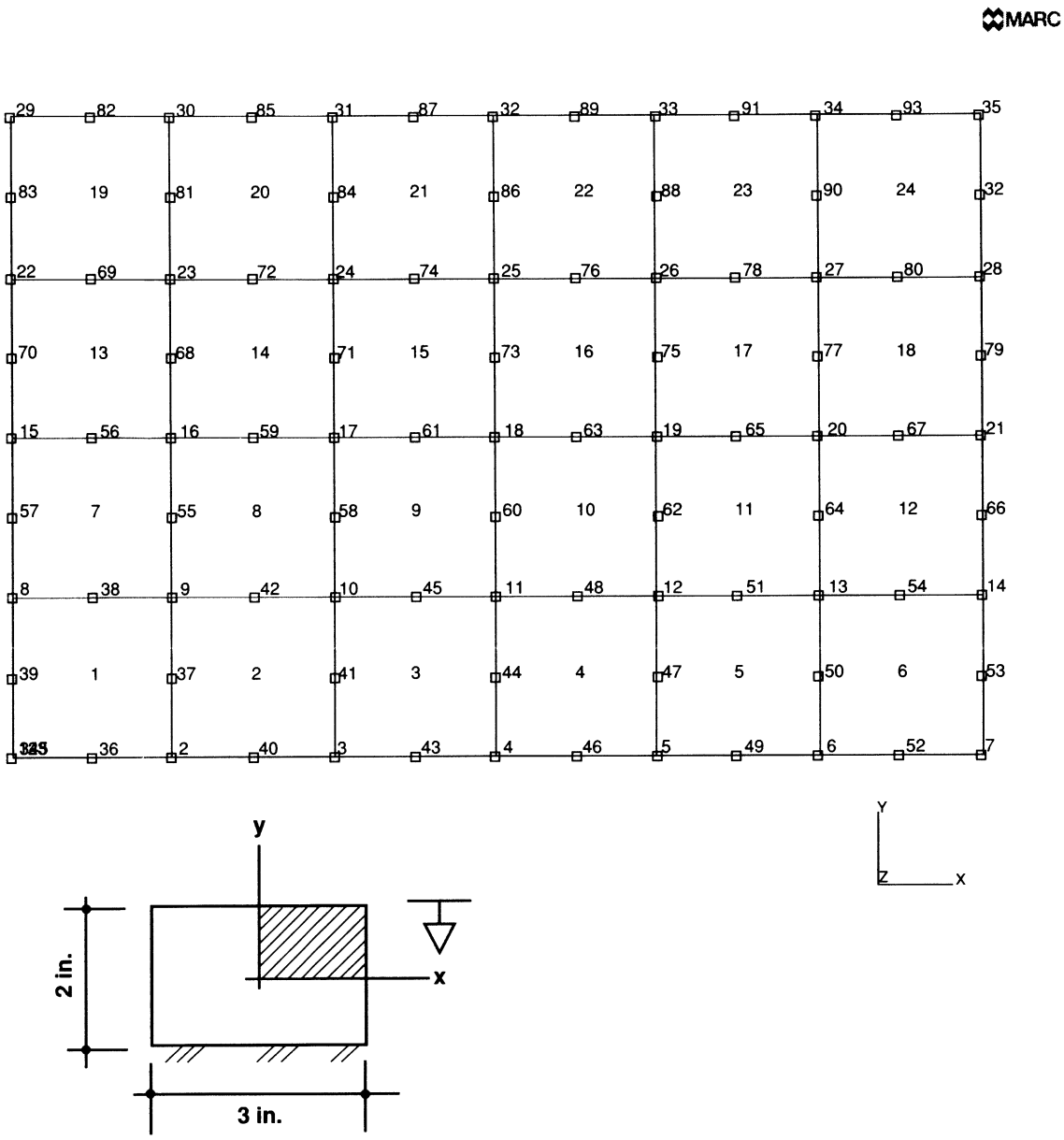

Figure E 2.34-1 Two-Dimensional Strip and Mesh

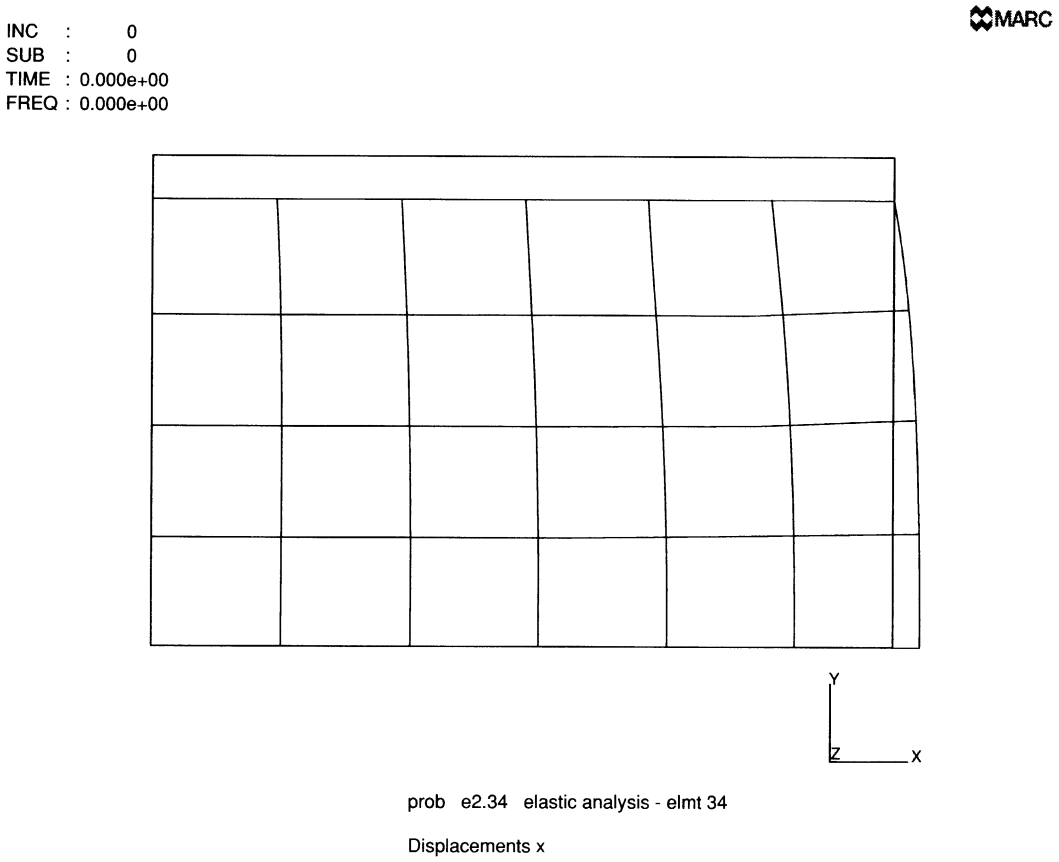

Figure E 2.34-2 Deformed Mesh Plot

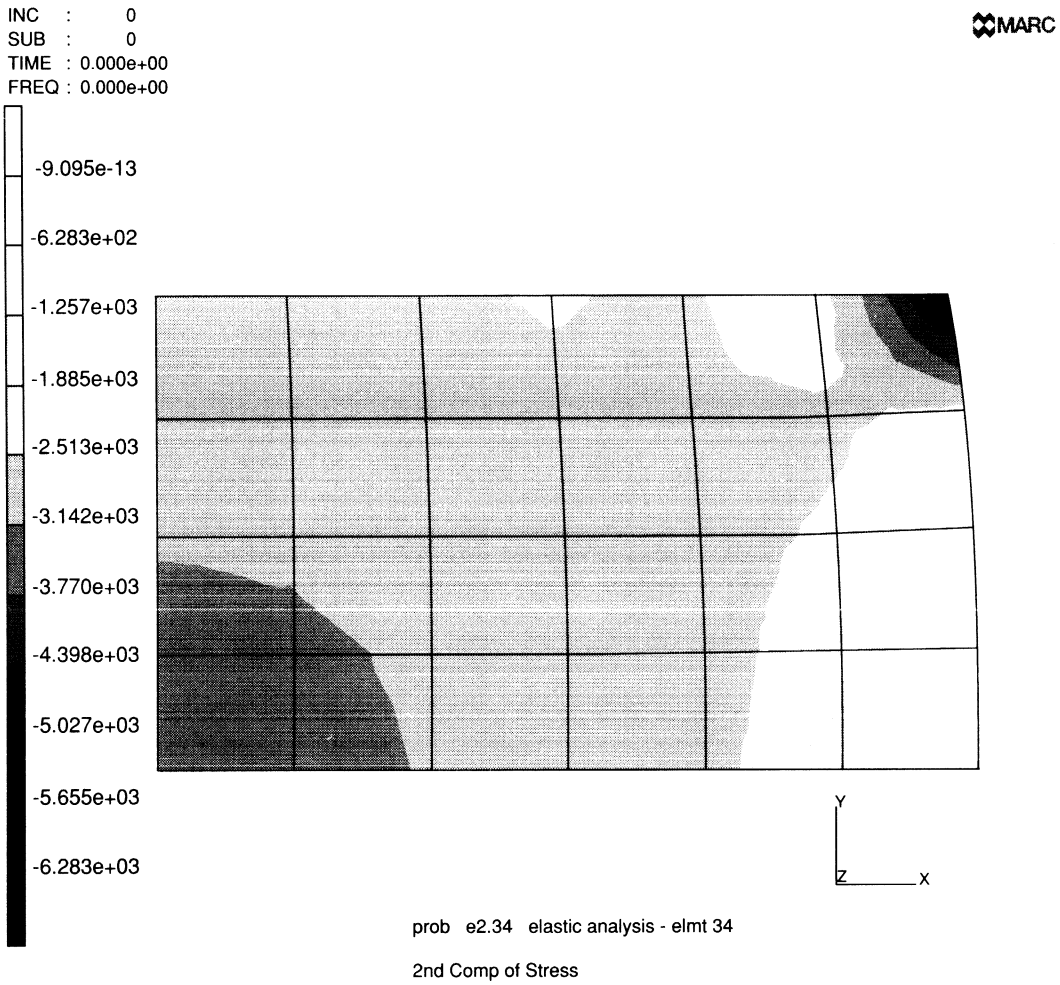

Figure E 2.34-3 σ_{yy} Contours

E 2.38 Reinforced Concrete Plate With Central Hole

This problem illustrates the use of MARC elements type 29 and type 47 and user subroutines UINSTR and REBAR for an elastic analysis of a reinforced concrete plate. The plate is subject to an initial stress in the rebars. The use of options ELSTO and SCALE is also demonstrated.

Model

The dimensions of the plate and a finite element mesh are shown in Figure E 2.38-1. The plate is modeled under conditions of generalized plane strain. The geometry is similar to problem 2.31 with the addition that reinforcements have been placed concentrically with respect to the hole. There are 28 elements and 81 nodes in the mesh. Eight of the elements are rebar elements type 47.

Material Properties

The properties of the concrete are Young's modulus is 30×10^5 psi and Poisson's ratio is 0.2.

The properties of the steel are Young's modulus is 30×10^6 psi, and Poisson's ratio is 0.3 with a yield stress of 30×10^3 psi.

Boundary Conditions

Symmetry conditions exist on the lines $x = 0$ and $y = 0$ ($u = 0$ at $x = 0$; $v = 0$ at $y = 0$). Both degrees of freedom of the second extra node of generalized plane-strain elements (element 29) are constrained, restraining the relative rotation of the top and bottom surfaces.

REBAR

Three layers of rebars are assumed to be in the plate, the cross-sectional area of which is 0.25. The direction and position of the rebar layers are shown in Figure E 2.38-2. The rebar data is defined in the user subroutine REBAR.

ELSTO allows the use of out-of-core element storage option; this reduces the amount of workspace necessary for the analysis.

ISTRESS allows the user to input initial stresses in the rebars through the user subroutines UINSTR. The rebars are given a prestress of 100 psi, which is then scaled to the yield stress of 30000 psi.

SCALE allows the stresses in the plate to be scaled to the condition of first yield.

Optimization

The bandwidth optimization is performed by using the Sloan method.

Results

In increment zero, the initial stresses are applied and scaled to the yield stress. In increment one, the structure is allowed to return to equilibrium. The resulting deformed mesh plot is shown in Figure E 2.38-3. As anticipated, the reinforcements force the plate into compression.

Summary of Options Used

Listed below are the options used in example e2x38.dat:

Parameter Options

ELEMENT
END
ISTRESS
SCALE
SIZING
TITLE

Model Definition Options

CONNECTIVITY
COORDINATE
END OPTION
FIXED DISP
GEOMETRY
ISOTROPIC
OPTIMIZE
PRINT CHOICE

Listed below are the user subroutines found in u2x28.f:

REBAR
UINSTR

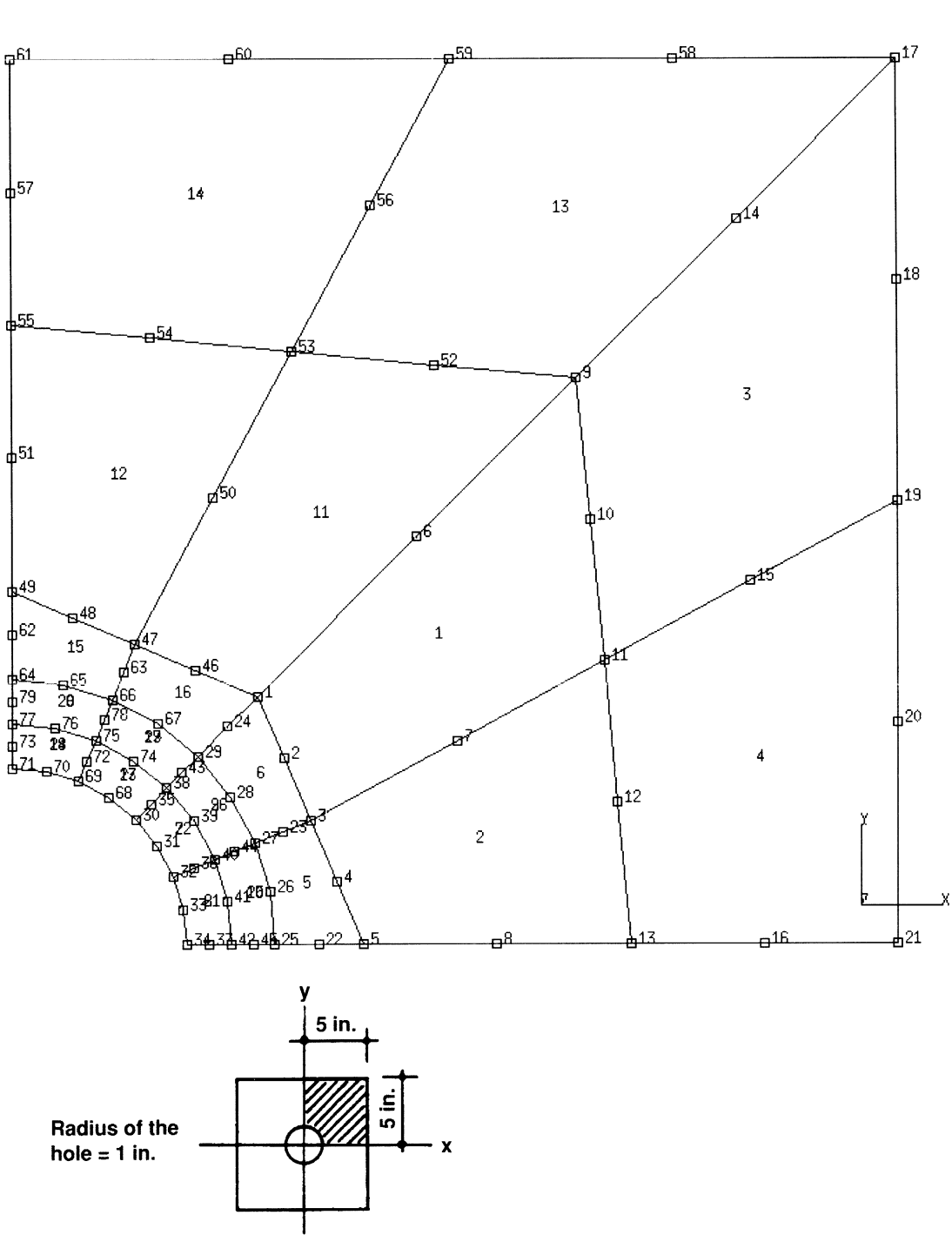

Figure E 2.38-1 Reinforced Concrete Plate and Mesh

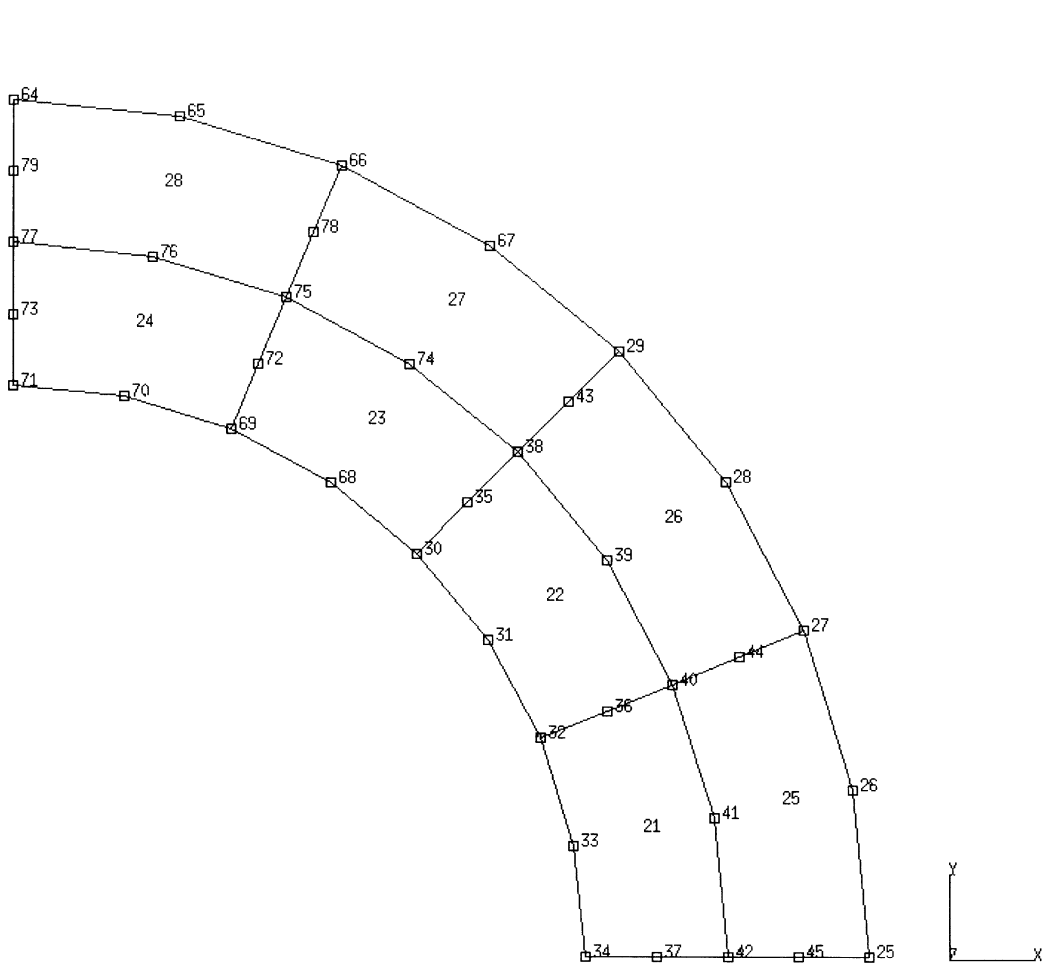

Figure E 2.38-2 Rebar Layers and Elements

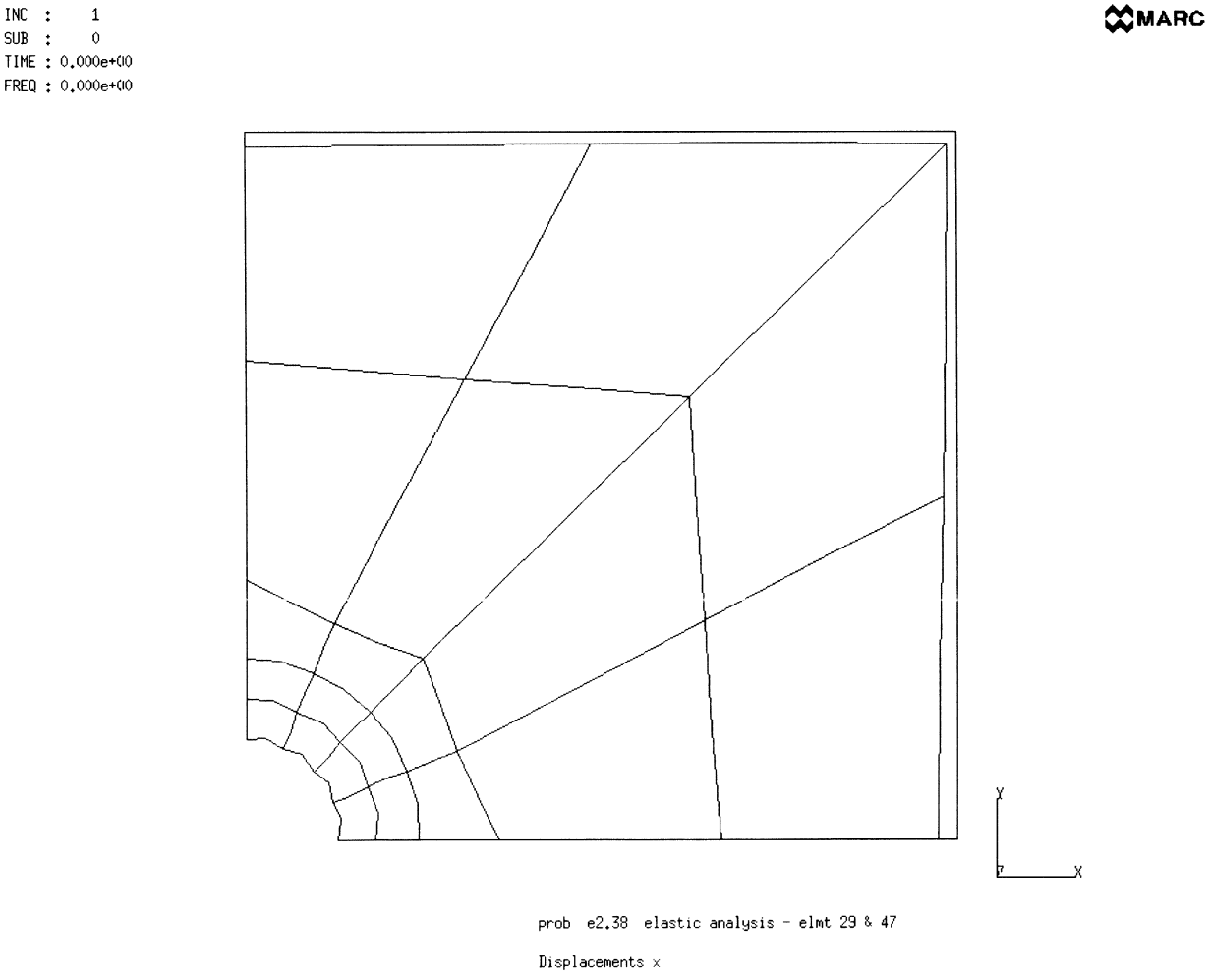

Figure E 2.38-3 Deformed Mesh Plot

E 2.40 Simply Supported Square Plate Of Variable Thickness

This problem illustrates the use of MARC element type 49 for an elastic analysis of a simply supported square plate. The plate is subjected to uniformly distributed pressure. The analysis is performed first with a constant plate thickness and then with a linearly varying thickness. This varying thickness is entered by means of user subroutine USHELL. The parameter option SHELL SECT is used for the reduction of the number of integration points through the thickness.

Element (Ref. B49.1)

Element type 49 is a nonconforming triangular shell element with arbitrary spatial orientation. There are six nodes per element, with assignable thickness at each corner node. Actually, the average thickness is used which can also be entered by means of user subroutine USHELL.

Model

The dimensions of the plate and the finite element mesh are shown in Figure E 2.40-1. The plate is analyzed using 50 elements and 121 nodes. One-quarter of the plate is modelled due to symmetry considerations.

Material Properties

The elastic analysis is performed with a Young's modulus of 2×10^5 N/mm^2 and a Poisson's ratio of 0.3.

Geometry

In the first analysis (A), the plate has a constant thickness of 3.0 mm. In the second analysis (B), the plate thickness varies in both the x- and y-directions (see Figure E 2.40-1). The length of the plate edges is 60 mm. Since a linear plate problem is solved, the elements can be considered as flat which is indicated by a 1 on the fifth geometry field. In this way, computational time is reduced.

Loading

A uniform pressure of 0.01 N/mm^2 in the negative z-direction is applied.

Boundary Conditions

Symmetry conditions are imposed on edges x = 30 ($u_x = 0$, $\phi = 0$ and y = 30 ($u_y = 0$, $\phi = 0$). Notice that the rotation constraints only apply for the midside nodes.

Simply supported conditions are imposed on edges x = 0 and y = 0 ($u_z = 0$).

Results

Stress contours are depicted in Figure E 2.40-2 and Figure E 2.40-3 for constant and varying plate thicknesses, respectively. As anticipated, the stress increases in the second analysis. The maximum stresses and deflections are:

	Constant Thickness		Varied Thickness
	MARC Solution	**Analytical Solution**	**MARC Solution**
Deflection (mm)	1.093×10^{-3}	1.065×10^{-3}	2.677×10^{-3}
Stress (N/mm^2)	1.229	1.248	2.302

The exact solution may be found in S. P. Timoshenko and S. Woinowsky-Kreiger, *Theory of Plates and Shells*.

Summary of Options Used

Listed below are the options used in example e2x40a.dat:

Parameter Options

ELEMENT
END
SHELL SECT
SIZING
TITLE

Model Definition Options

CONNECTIVITY
COORDINATE
DEFINE
DIST LOADS
END OPTION
FIXED DISP
GEOMETRY
ISOTROPIC
POST
PRINT CHOICE

Listed below are the options used in example e2x40b.dat:

Parameter Options

ELEMENT
END
SHELL SECT
SIZING
TITLE

Model Definition Options

CONNECTIVITY
COORDINATE
DEFINE
DIST LOADS
END OPTION
FIXED DISP
GEOMETRY
ISOTROPIC
POST
PRINT CHOICE

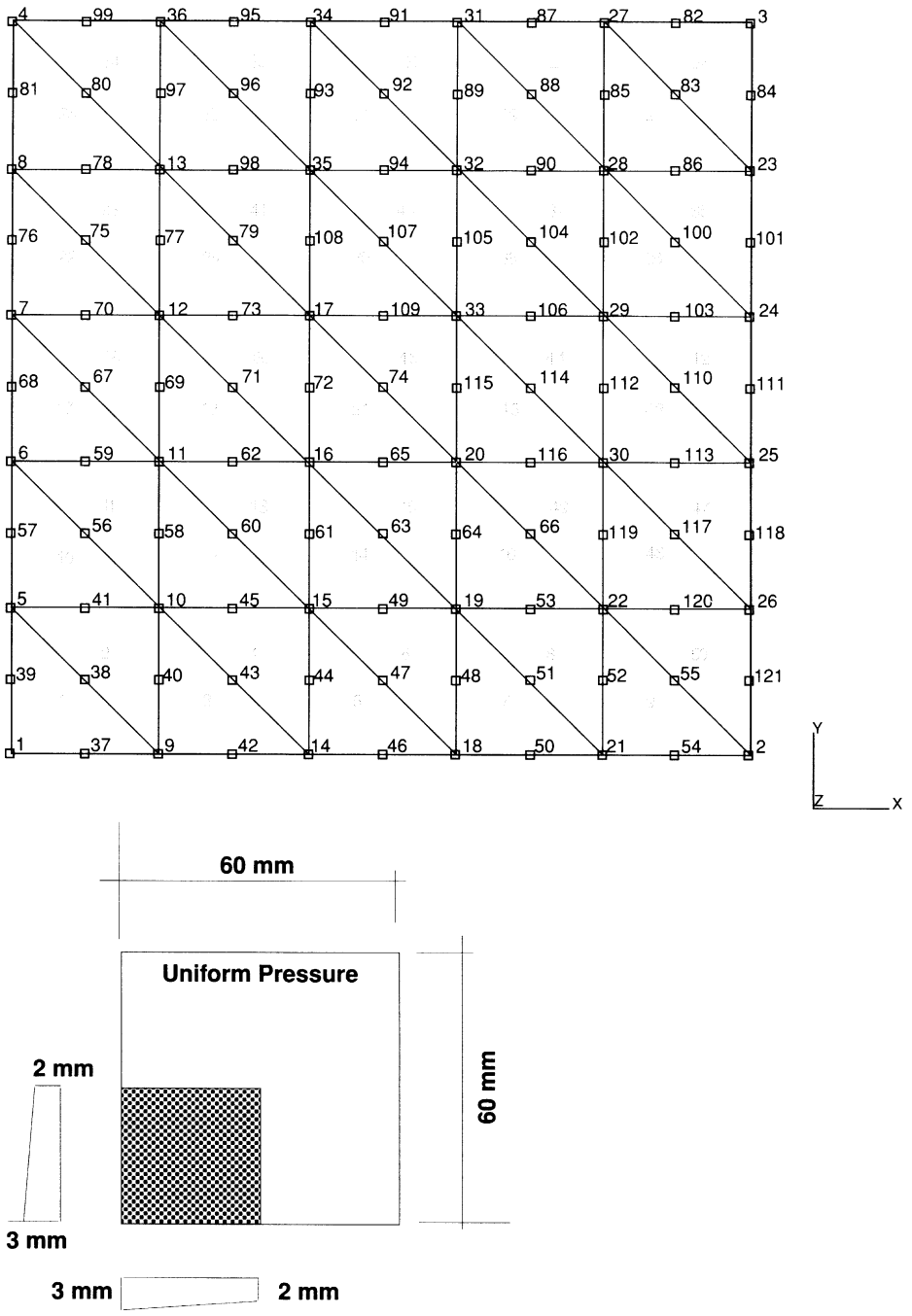

Figure E 2.40-1 Square Plate and Mesh

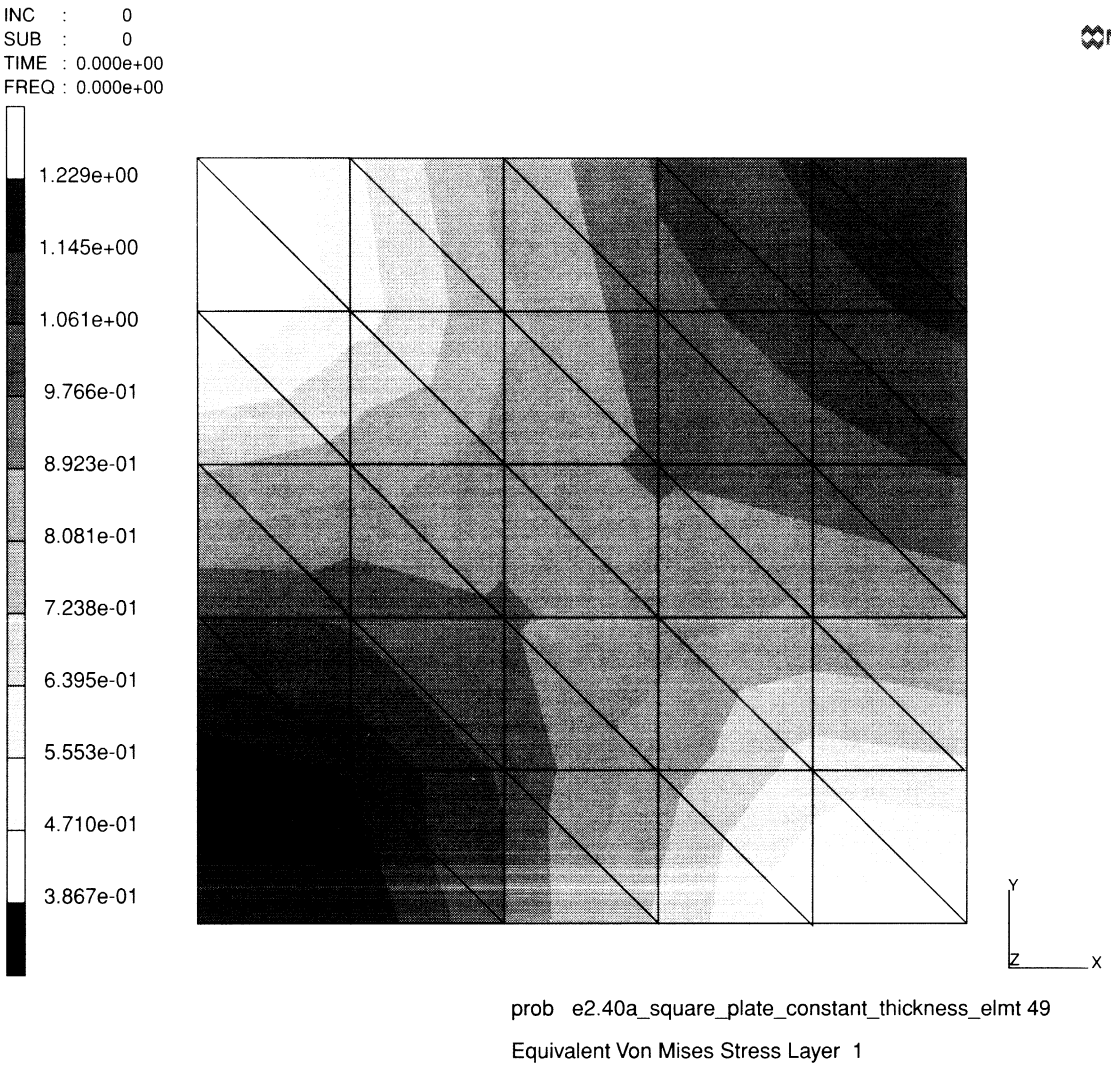

Figure E 2.40-2 Stress Contours (Constant Thickness)

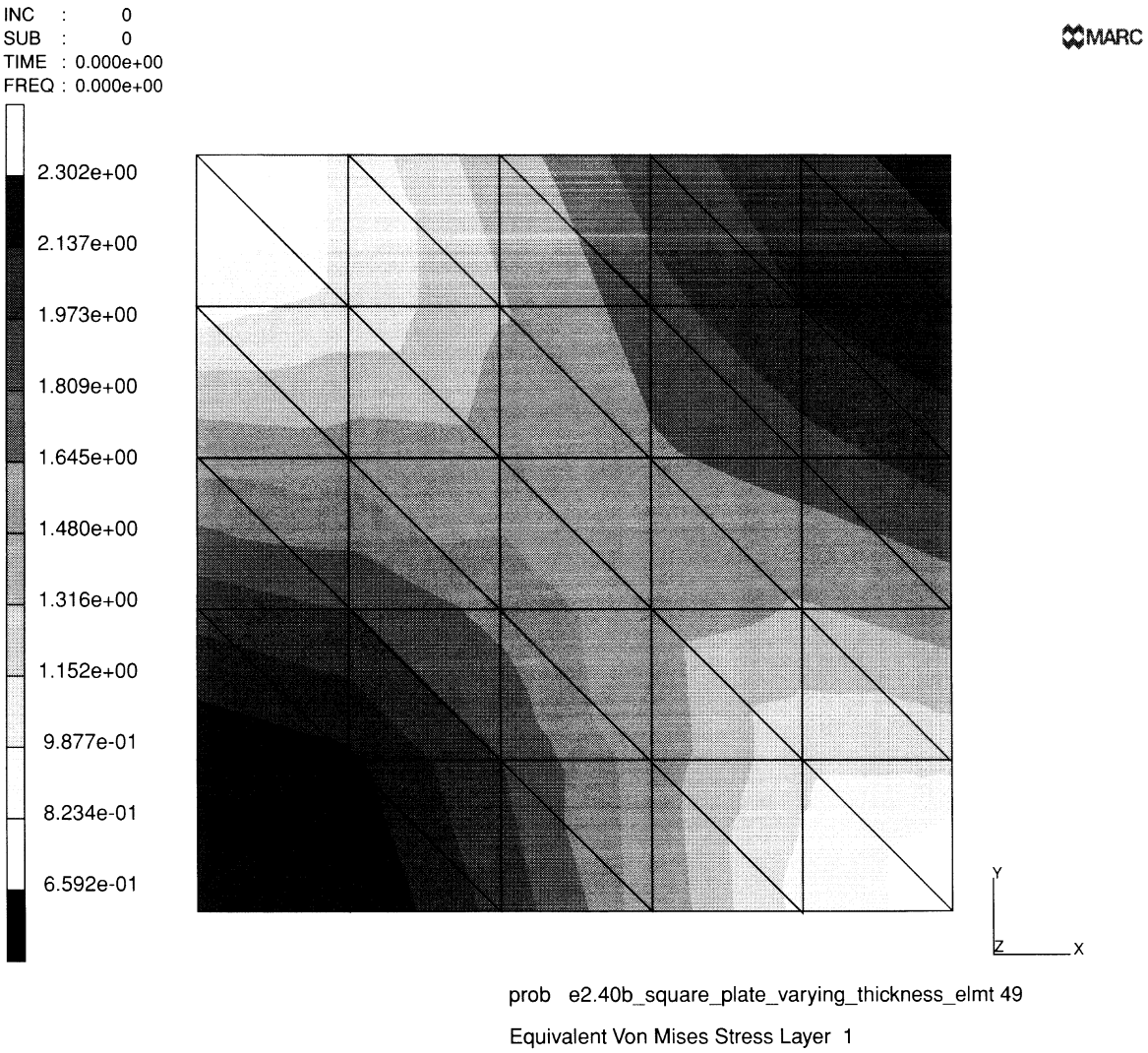

Figure E 2.40-3 Stress Contours (Variable Thickness)

E 2.41 Thermal Stresses in a Simply Supported Triangular Plate

This problem illustrates the use of MARC element type 49 for an elastic analysis of a simply supported triangular plate subjected to nonuniform heating. The temperature variation through the thickness is entered using the INITIAL STATE and CHANGE STATE model definition options. The parameter option SHELL SECT is used to reduce of the number of integration points through the thickness.

Element (Ref. B50.1)

Element 49 is a non-conforming triangular shell element with six nodes per element.

Model

The dimensions of the plate and the finite element mesh are shown in Figure E 2.41-1. Bases on symmetry considerations, only one half of the plate is modeled. The mesh is composed of 36 elements and 91 nodes.

Material Properties

The material is elastic with a Young's modulus of 2.1×10^5 N/mm^2, a Poisson's ratio of 0.3, and a coefficient of thermal expansion of 1×10^{-5}. In order to obtain layer stress components in the same direction for all elements, the ORIENTATION option is used to specify an offset of 0° with respect to the z,x-plane.

Geometry

The thickness of the equilateral triangular plate is 0.02 mm. Since a linear plate problem is solved, the elements can be considered as flat, which is indicated by a 1 on the fifth geometry field. In this way, computational time is reduced.

Loading

Initially, the temperature through the thickness is set to 10° The thermal load is applied by changing the temperature of layer 1° to 0° and of layer 3 to 20°.

Boundary Conditions

Symmetry conditions are imposed in the edge $y = 0$ ($u_y = 0$, $\phi = 0$). Notice that the rotation constraint is only applied on the midside nodes.

Simply supported conditions are imposed on the outer edges ($u_z = 0$). The remaining rigid body mode is suppressed by setting $u_x = 0$ for the node at $x = 0$, $y = 0$

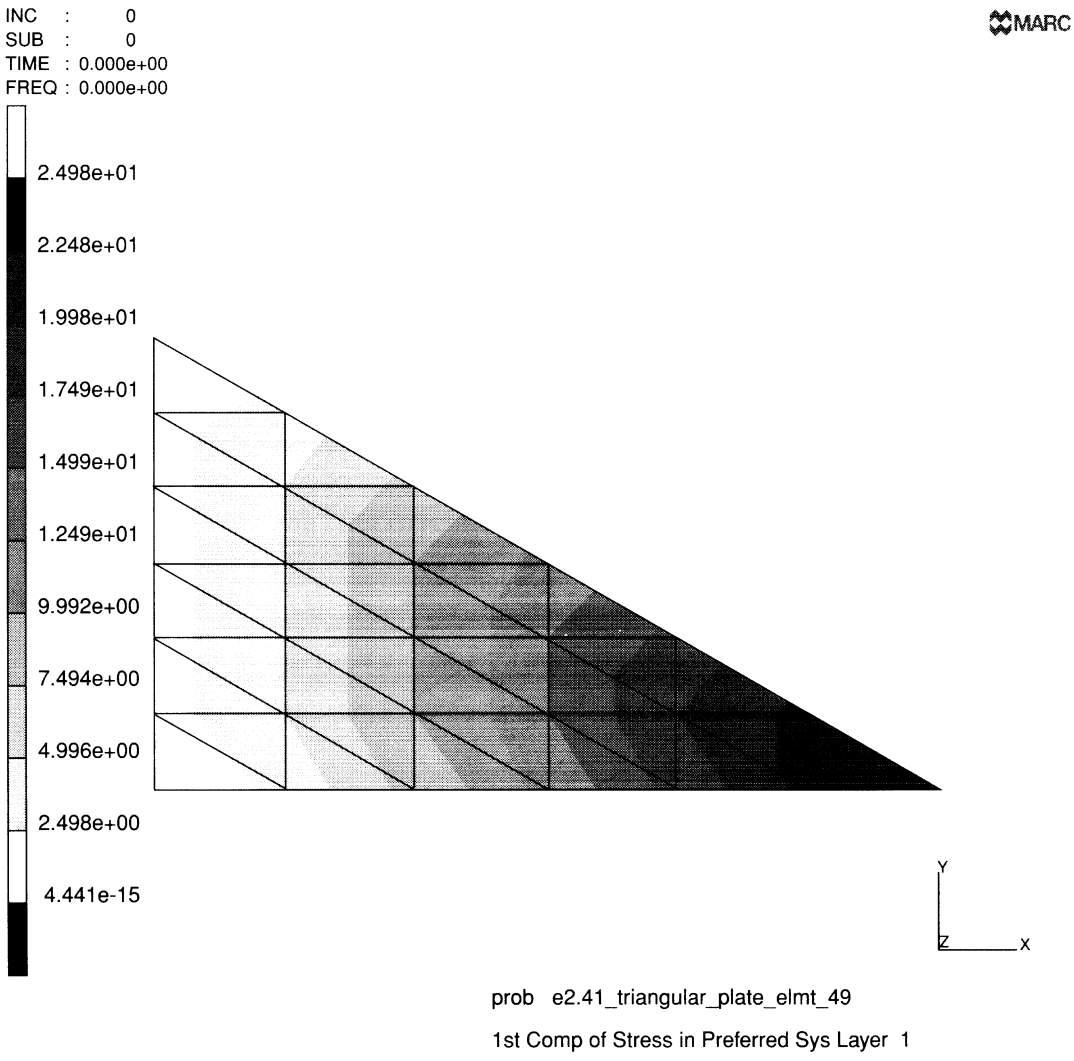

Figure E 2.41-2 Stress Contours (x-component)

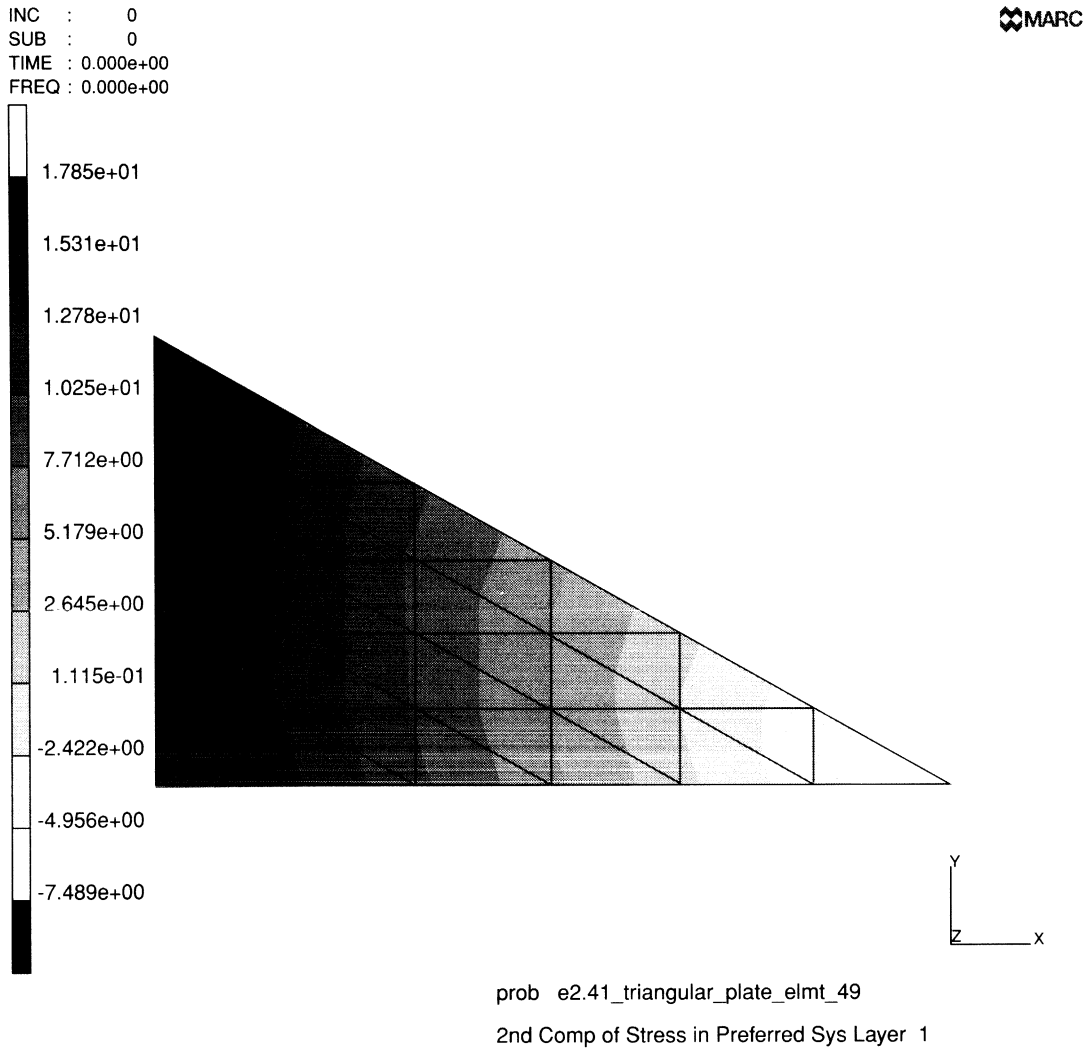

Figure E 2.41-3 Stress Contours (y-component)

E 2.46 Square Plate With Central Hole, Thermal Stresses

This problem illustrates the use of MARC element types 19, 29, and 56 for an elastic analysis of a square plate with a central hole. The hole is subjected to a linearly varying thermal load in the radial direction. The use of user subroutine CREDE is also demonstrated.

Element (Refs. B19.1, B29.1, and B56.1)

Element 19 is a 4-node, generalized plane-strain element. Element 29 is an 8-node, generalized plane-strain element, with two degrees of freedom at each node. Element type 56 has the same functionality as element 29 but uses reduced integration.

Model

The analysis is first performed using element types 29 and 56. There are 20 elements, with a total of 81 nodes. The dimensions of the plate and the finite element mesh are shown in Figure E 2.46-1. In the last model, element type 19 is used with a mesh consisting of 80 elements and 101 nodes. This mesh is shown in Figure E 2.46-2.

Material Properties

The Young's modulus is 30×10^5 psi, with Poisson's ratio of 0.3. The coefficient of thermal expansion is 12.4×10^{-7} in/in/°F. The plate is stress-free at a temperature of 0°F.

Geometry

The thickness of the plate is 1.0 inch.

Boundary Conditions

The following boundary conditions are applied along the symmetry lines:

$u = 0$ at $x = 0$
$v = 0$ at $y = 0$

At the shared node 81, rotations about both x- and y-axes are constrained:

$\theta_x = \theta_y = 0$

Thermal Load

The thermal load is caused by a linearly varying temperature in the radial direction. The temperatures are interpolated/extrapolated with:

T = 20°F at r = 1.0 inches
T = 100°F at r = 5.0 inches

The user subroutine CREDE is used for the input of thermal load at each integration point of each element. Temperatures at integration points as interpolated from the given linear distribution are specified with a DATA statement.

In problem e2x46d, the thermal loads are prescribed by specifying the temperature at the nodal points using the INITIAL TEMPERATURE and POINT TEMPERATURE options.

Optimization

The Cuthill-McKee technique is used to minimize the bandwidth.

Results

A deformed mesh plot is shown in Figure E 2.46-3 and stress contours are depicted in Figure E 2.46-4. The thermal strains created are shown in Figure E 2.46-5.

Summary of Options Used

Listed below are the options used in example e2x46a.dat:

Parameter Options

ELEMENT
END
SIZING
THERMAL
TITLE

Model Definition Options

CONNECTIVITY
COORDINATE
END OPTION
FIXED DISP
GEOMETRY
ISOTROPIC
THERMAL LOADS
UFCONN

Listed below is the user subroutine found u2x46a.f:

CREDE

Listed below are the options used in example e2x46b.dat:

Parameter Options

ELEMENT
END
SIZING
THERMAL
TITLE

Model Definition Options

CONNECTIVITY
COORDINATE
END OPTION
FIXED DISP
GEOMETRY
ISOTROPIC
THERMAL LOADS
UFCONN

Listed below are the user subroutines found in u2x46b.f:

CREDE
UFCONN

Listed below are the options used in example e2x46c.dat:

Parameter Options

ELEMENT
END
SIZING
TITLE

Model Definition Options

CONNECTIVITY
COORDINATE
DIST LOADS
END OPTION
FIXED DISP
GEOMETRY
ISOTROPIC

Listed below is the user subroutine found in u2x46c.f:

FORCEM

Listed below are the options used in example e2x46d.dat:

Parameter Options

ELEMENT
END
PROCESS
SETNAME
SIZING

Model Definition Options

CONNECTIVITY
COORDINATE
DEFINE
END OPTION
FIXED DISP
GEOMETRY
INITIAL TEMP
ISOTROPIC
OPTIMIZE
POINT TEMP
POST
PRINT ELEM
PRINT NODE
SOLVER

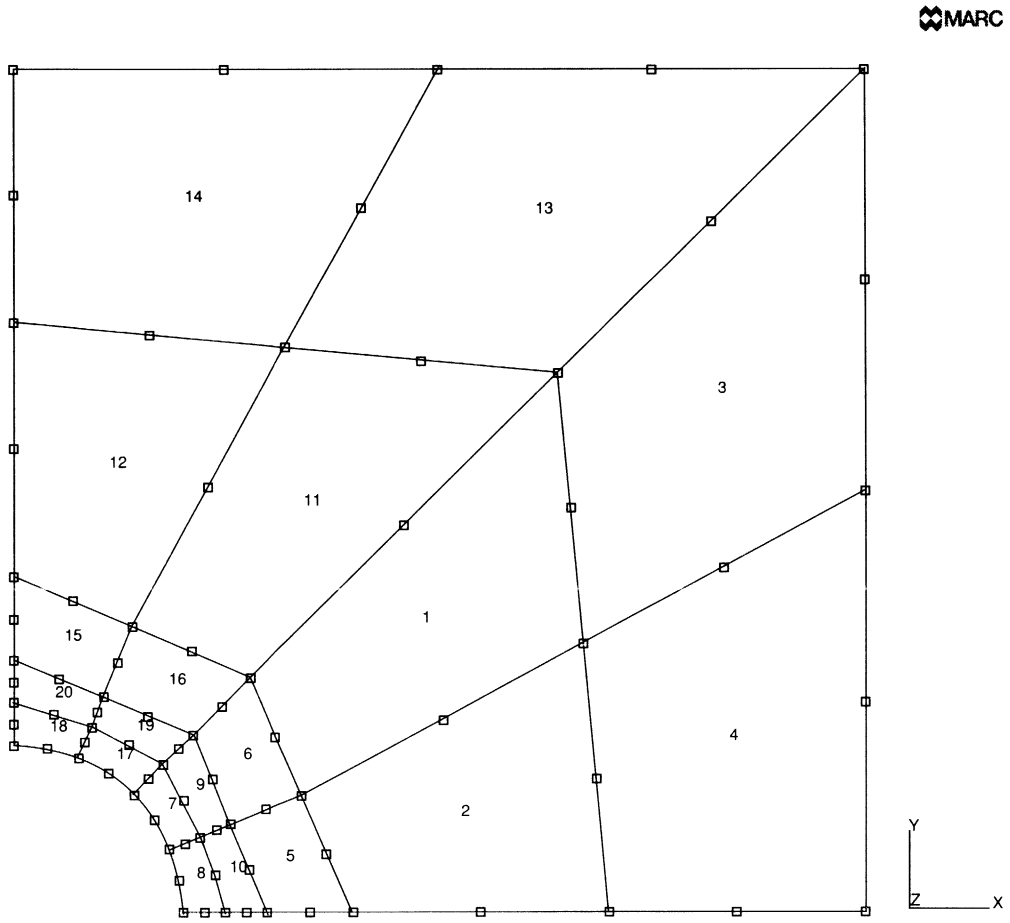

Figure E 2.46-1 Square Plate with Central Hole and Mesh

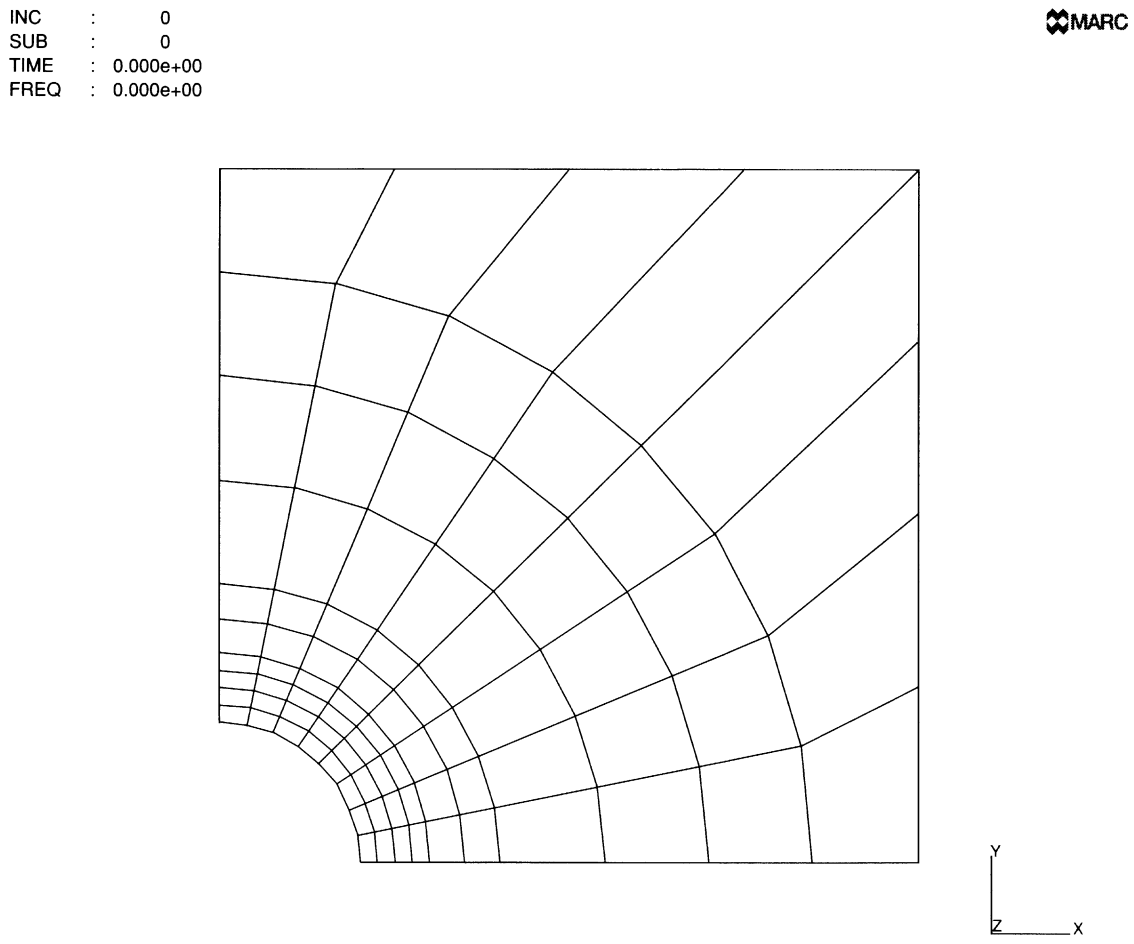

Figure E 2.46-2 Fine Element Mesh Using Element Type 19

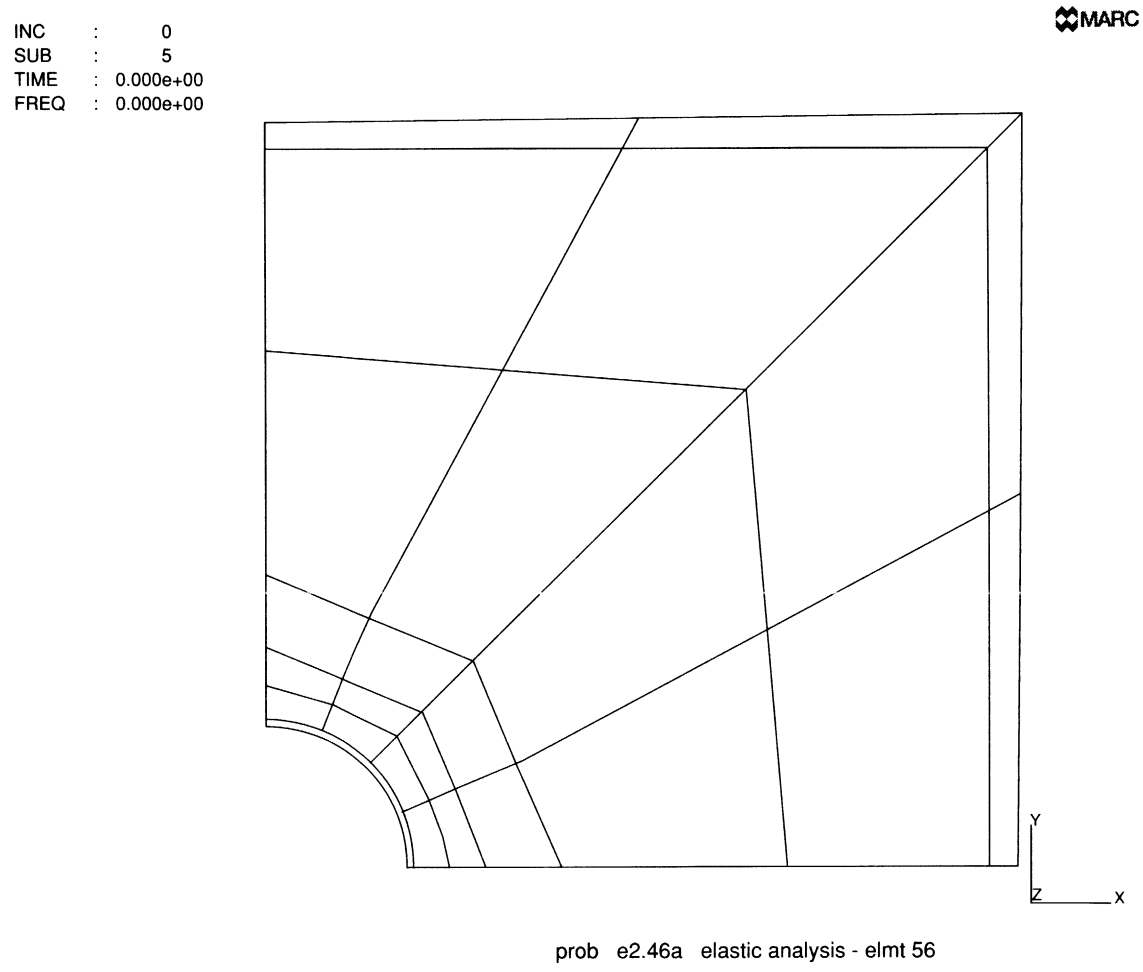

Figure E 2.46-3 Deformed Mesh Plot

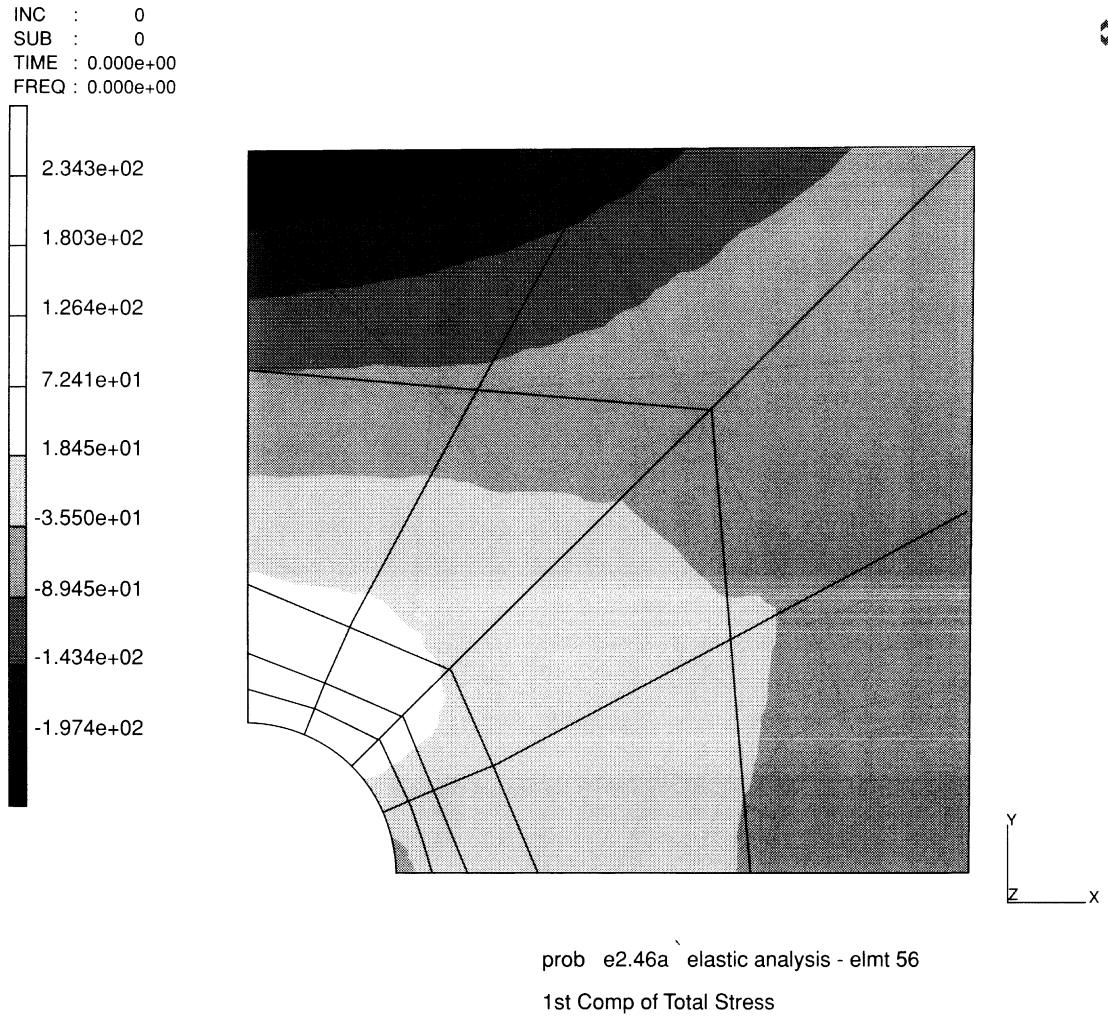

Figure E 2.46-4 Stress Contours for σ_{11}

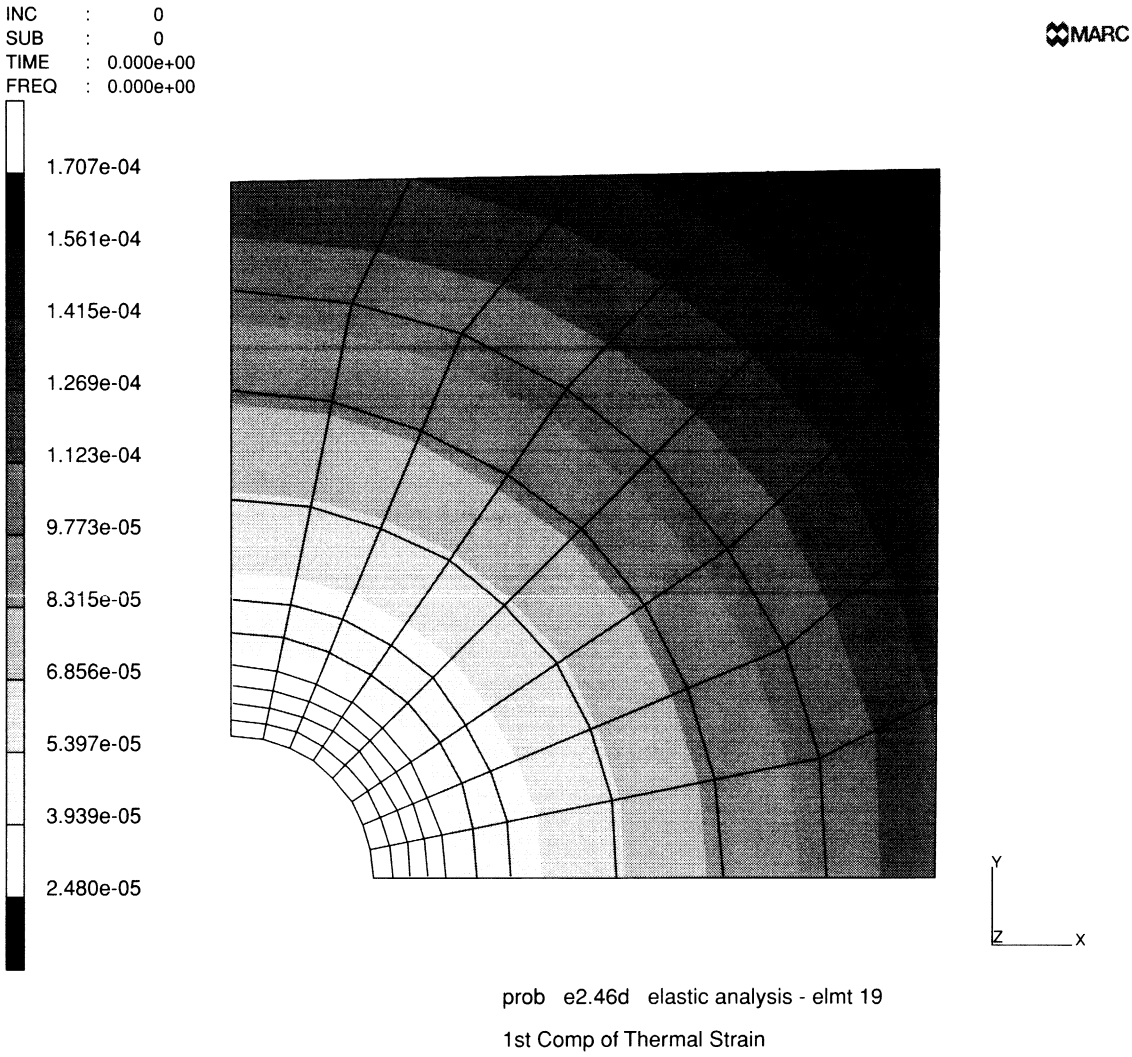

Figure E 2.46-5 Contours of Thermal Strain

E 2.59 Simply Supported Elastic Beam Under Point Load

This problem demonstrates the use of a two-node straight elastic beam for a simply supported beam structure subjected to a point load at mid-span of the beam. The effects of transverse shear are included in the formulation of the beam element.

Element (Ref. B98.1)

The element (Element 98) is a two-node straight elastic beam in space and includes the transverse shear effects in its formulation. It uses a linear interpolation in displacement along the axis of the beam and a cubic interpolation in the direction normal to the beam axis. In addition to elastic behavior, the element can also be used for hypoelastic materials. The hypoelastic behavior must be defined in the user subroutine UBEAM.

Model

As shown in Figure E 2.59-1, due to symmetry only one-half of the simply supported beam is modeled. The finite element mesh consists of five elements and six nodes. The span of the beam is 10 inches and the cross-section of the beam is assumed to be a closed, thin square section.

Geometry

The GEOMETRY block is used for entering the beam section properties. There are two options available to the user for the use of the GEOMETRY block. The section properties area = 0.0396 inches^2, $I_x = I_y = 6.4693 \times 10^{-3}$ inches^4, can be directly entered through the GEOMETRY block or through the parameter option BEAM SECT by defining area = 0.0, I_x = section number, in the GEOMETRY block. In the latter case, the user must enter the beam section properties through the BEAM SECT parameter option.

BEAM SECT

The BEAM SECT parameter option is required only if the user chooses to enter area = 0.0 and I_x = section number, in the GEOMETRY block. The beam section properties to be entered through this option area: area, I_x, I_y, torsional stiffness factor, and effective transverse shear areas.

Material Properties

The material of the beam is assumed to have a Young's modulus of 20,000 psi and Poisson's ratio of 0.3.

Loading

The beam is assumed to be subjected to a point load of 20 pounds. Due to symmetry, a 10 pound point load is applied at node 6 in the positive x-direction.

Boundary Conditions

At node 1, all translational degrees-of-freedom are constrained ($u_x = u_y = u_z = 0$) for the simulation of simply-supported conditions. At midspan (node 6), all degrees of freedom except u_x are constrained for the simulation of symmetry condition.

Results

A comparison of beam deflections is shown in Table E 2.59-1. The beam deflection at node 6 predicted by element 98 is 4% larger than that of element 52 (3.3523/ 3.2203 = 1.041). The additional beam deflection is clearly due to the effect of transverse shear allowed in element 98.

Table E 2.59-1 Comparison of Beam Deflections (in.)

Node	Element 52	Element 98
1	0.0	0.0
2	0.9532	0.9796
3	1.8291	1.8819
4	2.5505	2.6297
5	3.0399	3.1455
6	3.2203	3.3523

Summary of Options Used

Listed below are the options used in example e2x59a.dat:

Parameter Options

ELEMENT
END
SIZING
TITLE

Model Definition Options

CONNECTIVITY
COORDINATE
END OPTION
FIXED DISP
GEOMETRY
ISOTROPIC
POINT LOAD

Listed below are the options used in example e2x59b.dat:

Parameter Options

BEAM SECT
ELEMENT
END
SIZING
TITLE

Model Definition Options

CONNECTIVITY
COORDINATE
END OPTION
FIXED DISP
GEOMETRY
ISOTROPIC
POINT LOAD

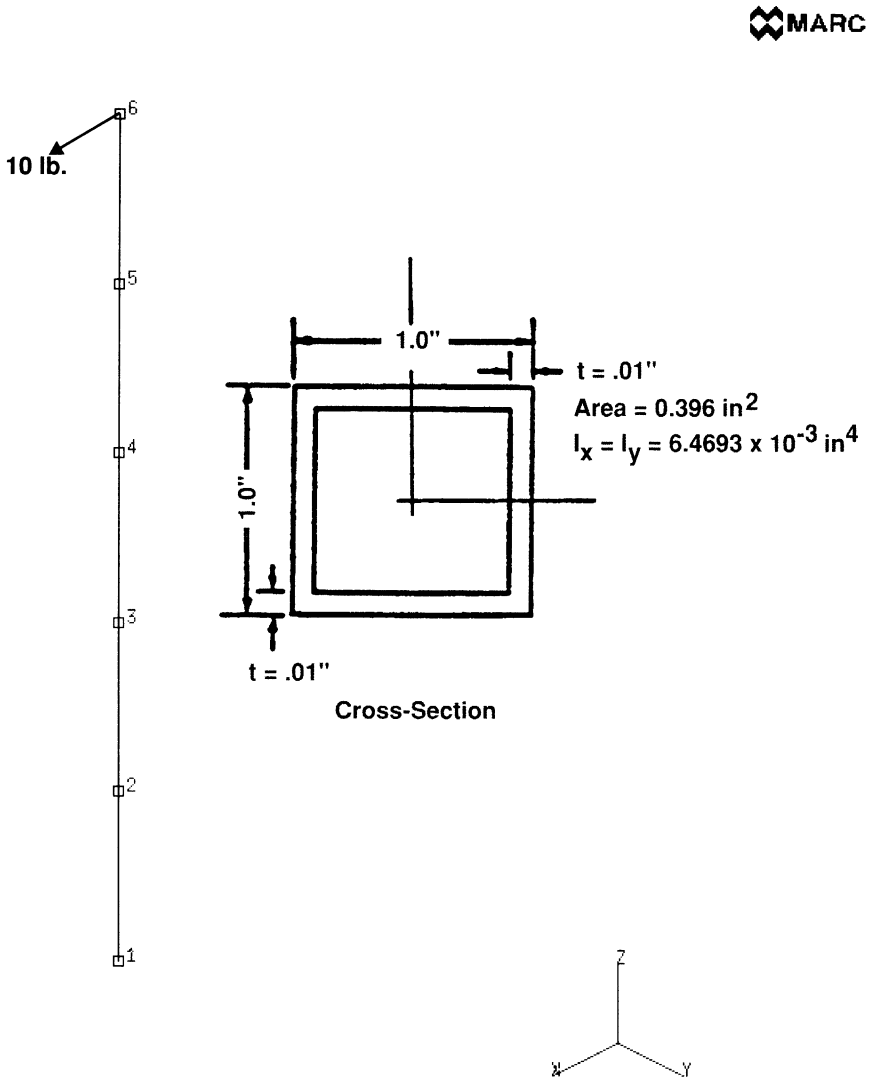

Figure E 2.59-1 Simply Supported Beam Under Point Load

Volume E
Demonstration Problems

Chapter 3
Plasticity and Creep

E 3.6 Collapse Load Of A Simply Supported Square Plate

In this problem, the maximum transverse load that a square plate of isotropic material can sustain is determined.

Element (Ref. B50.1)

Library element type 49, a 6-node triangular thin shell element, is used.

Model

The dimensions of the plate and the finite element mesh are shown in Figure E 3.6-1. Based on symmetry considerations, only one-quarter of the plate is modelled. The mesh is composed of 32 elements and 81 nodes.

Material Properties

The material is elastic with a Young's modulus of 3.0×10^4 N/mm^2, a Poisson's ratio or 0.3, and a yield stress of 30 N/mm^2.

Geometry

The thickness of the plate is specified as 0.4 mm. Since a geometrically linear plate problem is solved, the elements can be considered as flat, which is indicated by a 1 on the fifth geometry field. In this way, computational time is reduced. In order to trigger the response in thickness directions, five layers are chosen using the SHELL SECT parameter option.

Loading

A uniform pressure load of 0.02 N/mm^2 is applied. Since this load is larger than the actual collapse load, the auto increment option is used with a limited number of increments. In this way, the analysis will stop if the maximum allowed number of increments is reached.

Boundary Conditions

Symmetry conditions are imposed on the edges x = 20 ($u_x = 0, \phi = 0$) and y = 20 ($u_y = 0, \phi = 0$). Notice that the rotation constraints only apply for the midside nodes. Simply supported conditions are imposed on the edges x = 0 and y = 0 ($u_z = 0$).

Results

Figure E 3.6-2 shows the deflection of the central node as a function of the equivalent nodal load. The solution turns out to be in reasonable agreement with the reference solution taken from *Selected Benchmarks for Material Non-Linearity* by D. Linkens (published by NAFEMS, 1993). This reference solution, which is obtained using higher order elements is indicated in Figure E 3.6-3.

Summary of Options Used

Listed below are the options used in example e3x6.dat:

Parameter Options

ALL POINTS
DIST LOADS
ELEMENTS
END
SETNAME
SIZING
TITLE

Model Definition Options

CONNECTIVITY
COORDINATES
DEFINE
END OPTION
FIXED DISP
GEOMETRY
ISOTROPIC
NO PRINT
OPTIMIZE
POST
SOLVER

Load Incrementation Options

AUTO INCREMENT
CONTINUE
CONTROL
DIST LOADS

Listed below is the user subroutine found in u3x6.f:

ANPLAS

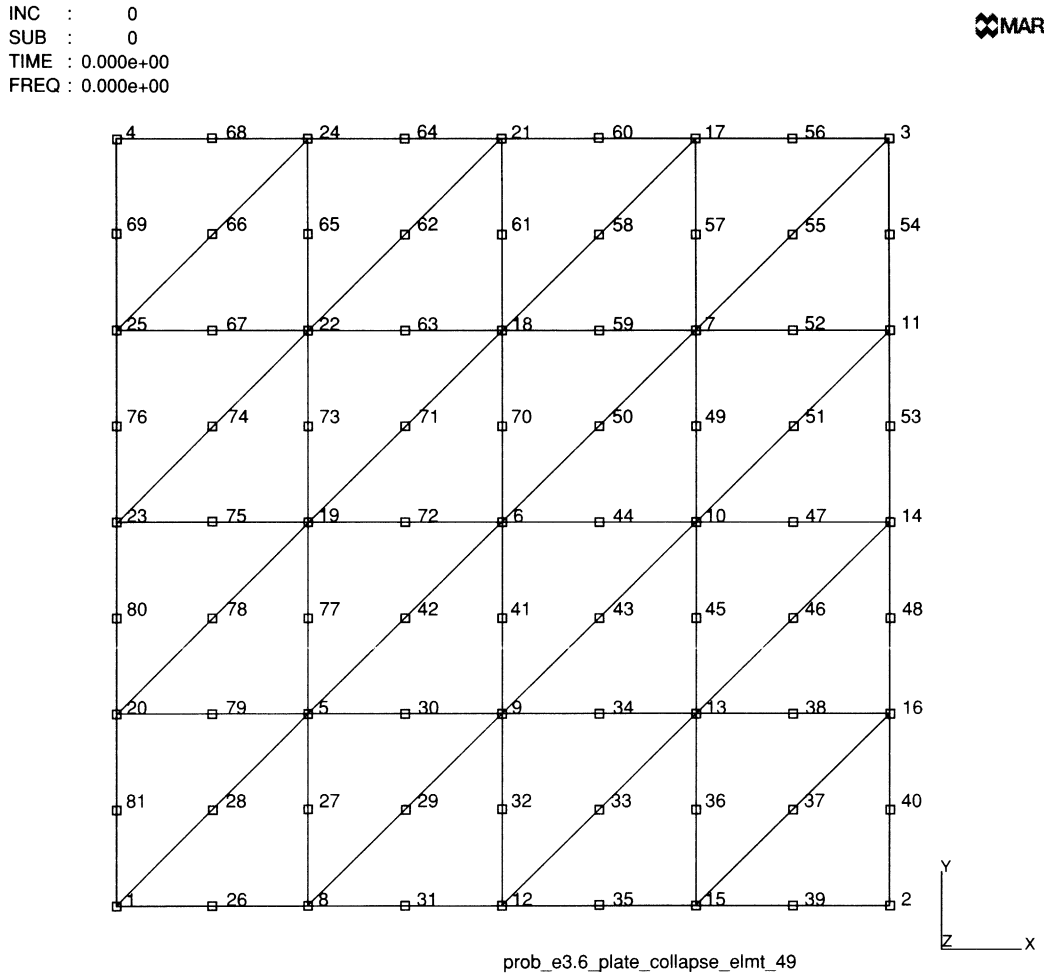

Figure E 3.6-1 Square Plate and Finite Element Mesh

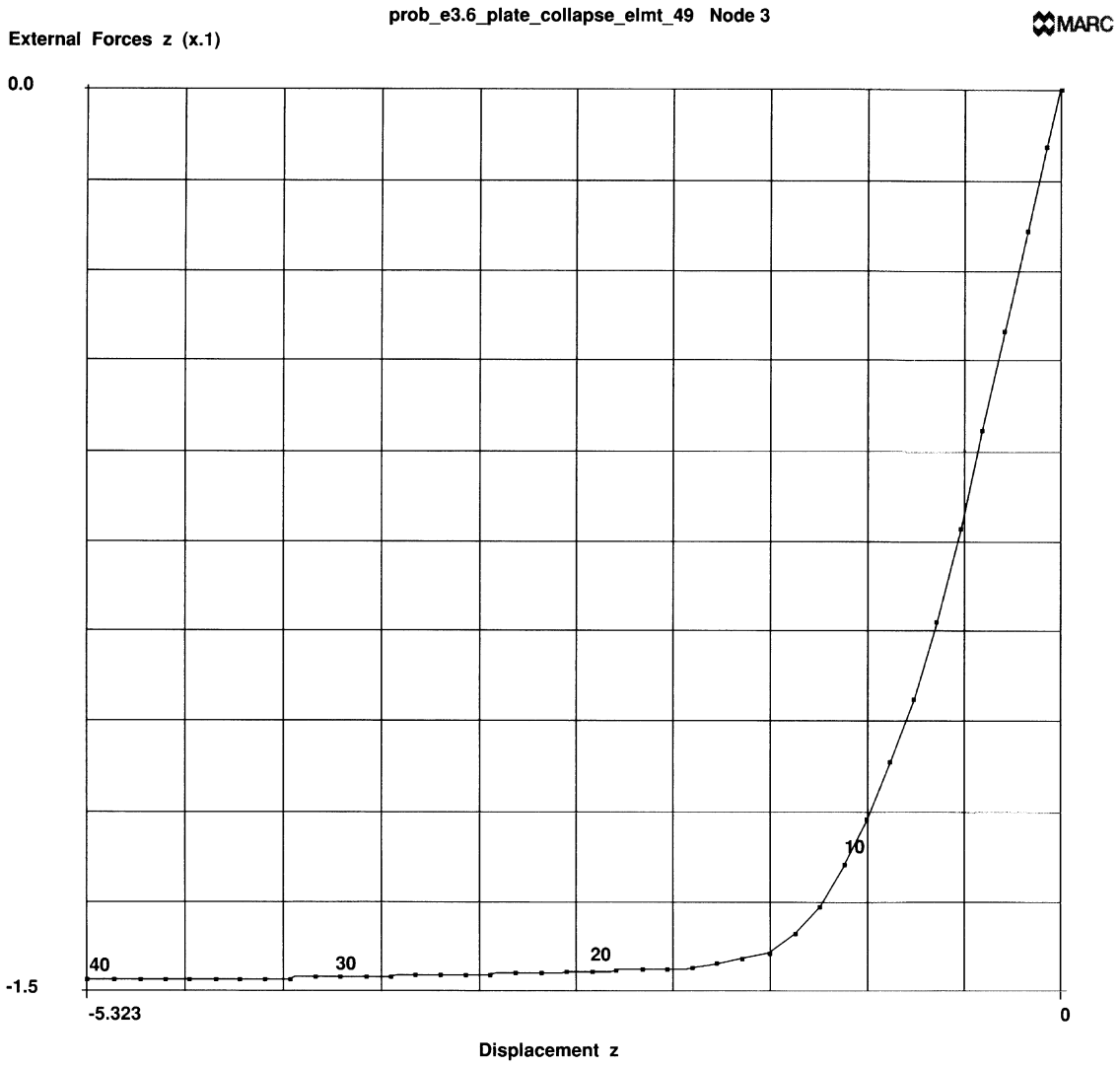

Figure E 3.6-2 Central Deflection Versus Nodal Load (MARC Solution)

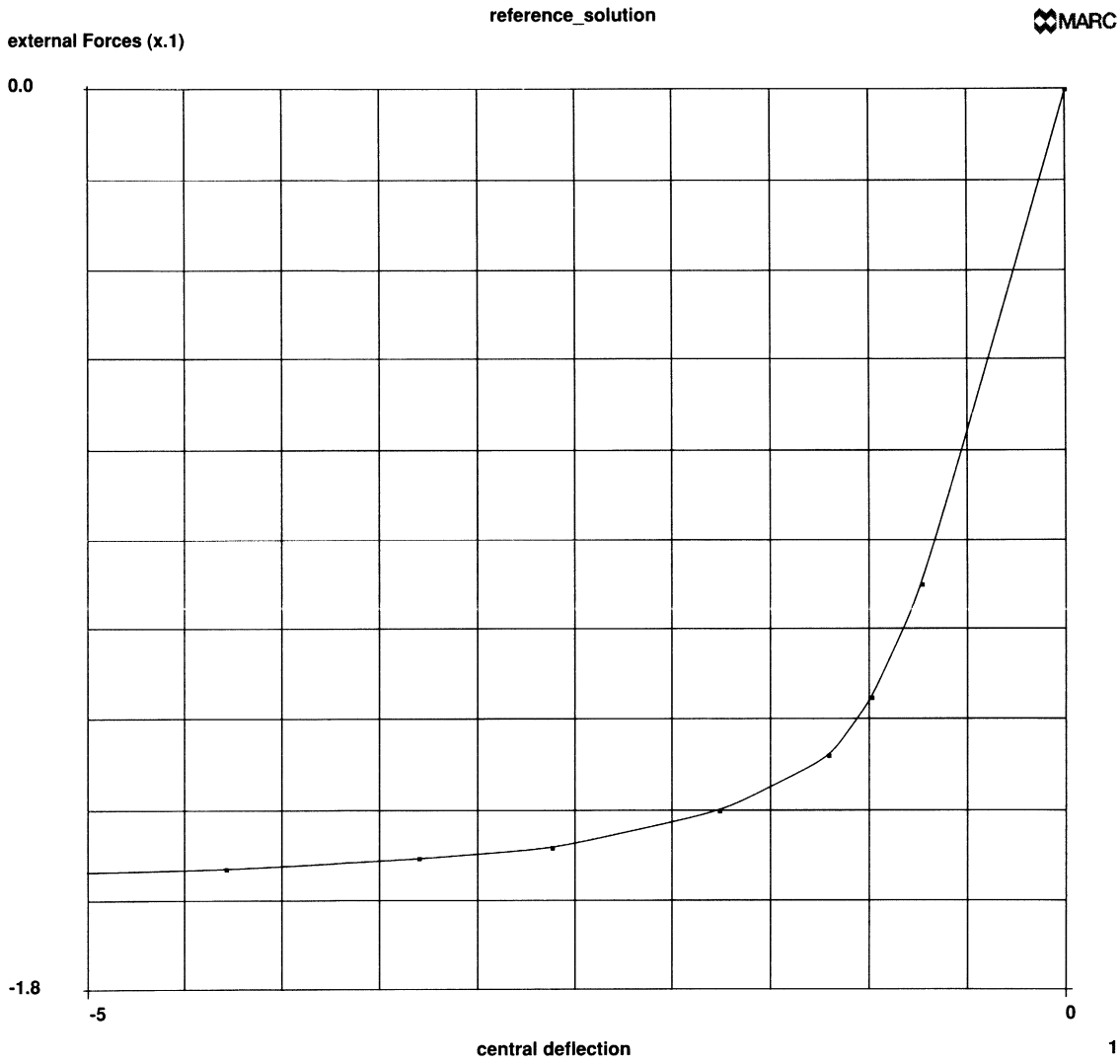

Figure E 3.6-3 Central Deflection Versus Nodal Load (Reference Solution)

E 3.12 Creep Of Thick Cylinder (Plane Strain)

A thick-walled cylinder loaded by internal pressure is analyzed using the creep analysis procedure available in the MARC program. This example provides the user with guidelines for specifying stress and strain tolerances.

Element (Ref. B10.1)

Element type 10, the axisymmetric quadrilateral, is used here.

Model

The geometry and mesh used are shown in Figure E 3.12-1. The cylinder has an outer to inner radius ratio of 2 to 1. The mesh has 20 elements, 42 nodes and 84 degrees of freedom.

Geometry

This option is not required for this element.

Material Properties

The material data assumed for this example is: Young's modulus (E) is 30.0×10^6 psi, Poisson's ratio (ν) is 0.3, and yield stress (σ_y) is 20,000 psi.

Loading

A uniform internal pressure of 1000 psi is applied to the inner wall of the cylinder using the DIST LOAD option. The inclusion of the SCALE parameter option causes this load to be automatically scaled upward to 9081.3 psi which is the pressure load which will cause the highest stress element (number 1 here) to be at a J_2 stress of 20,000 psi.

Boundary Conditions

All nodes are constrained in the axial direction such that only radial motion is allowed.

Creep

Creep analysis is flagged by use of CREEP and the conditions are set using the CREEP model definition block. The creep law used here is:

$$\dot{\varepsilon} = A\sigma^n \quad , \text{in/in-hr.}$$

where:

A is 1.075×10^{-26}

and:

n = 5.5 (where the stress is given in psi).

The exact, steady-state solution for this problem is:

$$\sigma_{zz} = \frac{p}{d}\left[\left(\frac{1}{n} - 1\right)\left(\frac{b}{r}\right)^{2/n} + 1\right]$$

$$\sigma_{rr} = \frac{p}{d}\left[\left(\frac{b}{r}\right)^{2/n} - 1\right]$$

$$\sigma_{\theta\theta} = \frac{p}{d}\left[\left(\frac{2}{n} - 1\right)\left(\frac{b}{r}\right)^{2/n} + 1\right]$$

where:

p is the internal pressure
a is the inside radius
b is the outside radius

and:

$$d = \left(\frac{b}{a}\right)^{2/n} - 1$$

The CREEP model definition option has set the fifth field to zero; therefore, the creep law has been introduced via user subroutine CRPLAW (see *Volume D, User Subroutines & Special Routines).*

Creep Control Tolerances – AUTO CREEP Option

The program runs a creep solution (under constant load conditions) via the AUTO CREEP history definition. This option chooses time steps automatically, based on a set of tolerances and controls provided by the user. These are as follows:

1. Stress Change Tolerance (AUTO CREEP Model Definition Set, Line 3, Columns 11-20). This tolerance controls the allowable stress change per time step during the creep solution, as a fraction of the total stress at a point. The stress changes during the transient creep, and the creep strain rate is usually very strongly dependent on stress (in this case, the dependence is $\sigma^{5.5}$); this tolerance governs the accuracy of the transient creep response. Due to accurate track of the transient, a tight tolerance (1% or 2% stress change per time step) should be specified. If only the steady-state solution is sought, a relatively loose tolerance (10-20%) may be assigned.

2. Creep Strain Increment Per Elastic Strain (AUTO CREEP Model Definition Set, Line 3, Columns 1-10).

   The MARC program explicitly integrates the creep rate equation, and hence requires a stability limit. This tolerance provides that stability limit. In almost all cases, the default of 50% represents that limit, and the user need not provide any entry for this value. Figure E 3.12-6 illustrates the problems that can occur if the stability limit is violated.

3. Maximum Number of Recycles for Satisfaction of Tolerances (AUTO CREEP Model Definition Set, Line 2, Columns 36-40).

   The program chooses its own time step during AUTO CREEP based on the algorithm described below. In some cases, the program may recycle in order to choose a time step to satisfy tolerances, but it is rare for the recycling to occur more than once per step. If excessive recycling occurs, it may be because of physical problems (such as creep buckling), bad coding of user subroutine CRPLAW, or excessive residual load correction. Excessive residual load correction occurs when the creep solution begins from a state which is not in equilibrium. This entry prevents wasted machine time by limiting the number of cycles to a prescribed value. The default of 5 cycles is reasonable in most normal cases.

4. Low Stress Cut-Off (AUTO CREEP Model Definition Set, Line 3, Columns 21-30.)

   This control avoids excessive iteration and small time steps caused by tolerance checks on elements with small round-off stress states. A simple example is a beam column in pure bending – the stress on the neutral axis will be a very small number; it would make no sense to base time step choice on satisfying tolerances at such points. The default here of 5% is satisfactory for most cases – the MARC program does not check those points where the stress is less than 5% of the highest stress in the structure.

5. Choice of Element For Tolerance Checking (AUTO CREEP Model Definition Set, Line 7, Columns 31-35.)

   The default option for creep tolerance checking is having all integration points in all elements checked. To save time, tolerances are checked in one selected element – this field is then used to select that element. Usually, the most highly stressed element is chosen.

Notes

All stress and strain measures used in tolerance checks are second invariants of the deviatoric state (i.e., equivalent von Mises uniaxial values).

All tolerances and controls may be reset upon restart.

When a tolerance or control may be entered in two places (i.e., on the CREEP or CONTROL Model Definition set) the values or defaults provided by the last of these options in the input deck are used.

Auto Creep

This history definition set chooses time steps according to an automatic scheme based on the tolerances described above. AUTO CREEP is designed to take advantage of diffusive characteristics of most creep solutions – rapid initial gradients which settle down with time. The algorithm is as follows:

- For a given time step Δt, a solution is obtained.
- The largest value of stress change per stress $\left|\frac{\Delta\sigma}{\sigma}\right|$ and creep strain change per elastic strain, $\left|\frac{\varepsilon^c}{\varepsilon^e}\right|$ are found. These are compared to the tolerance values set by the user, $T\sigma$ and $T\varepsilon$.

- Then the value p is calculated as the bigger of $\left|\frac{\Delta\sigma}{\sigma}\right|/T_\sigma$ or $\left|\frac{\Delta\varepsilon^c}{\varepsilon^e}\right|/T_\varepsilon$.

  a. Clearly if $p > 1$, the solution is violating one of the user's tolerances in some part of the structure. In this case, the program resets the time step as:

     $\Delta t_{new} = \Delta t_{old} * .8/p$

     i.e., as 80% of the time step which would just allow satisfaction of the tolerances. The time increment is then repeated. Such repetition continues until tolerances are successfully satisfied, or until the maximum recycle control is exceeded – in the latter case the run is ended. Clearly, the first repeat should satisfy tolerances – if it does not, the cause could be:

     excessive residual load correction
     creep buckling – creep collapse
     bad coding in subroutine CRPLAW or VSWELL

     and appropriate action should be taken before the solution is restarted.

  b. If $p<1$ the solution is satisfactory in the sense of the user supplied tolerances. In this case, the solution is stepped forward to $t+\Omega t$ and the next time step begun. The time step used in the next increment is chosen as:

     $\Delta t_{new} = \Delta t_{old}$ if $0.8 \le p \le 1.0$
     $\Delta t_{new} = 1.25 * \Delta t_{old}$ if $0.65 \le p \le 0.8$
     $\Delta t_{new} = 1.5 * \Delta t_{old}$ if $p \ge 0.65$

The diffusive nature of the creep solution is utilized to generate a series of monotonically increasing time steps.

Results

Four solutions were found and compared to the steady-state solution as shown in Table E 3.12-1 using the notation below.

1. Column A – 3% stress tolerance, 30% strain tolerance, with residual load correction.
2. Column B – 10% stress tolerance, 50% strain tolerance, with residual load correction.
3. Column C – 10% stress tolerance, 100% strain tolerance, with residual load correction.

These solutions are compared (at 20 hours) in Table E 3.12-1. Graphical comparisons are drawn in Figure E 3.12-2 through Figure E 3.12-6.

All solutions are satisfactory in the sense that monotonic convergence, with monotonic increase in time-step size, is achieved except for the strain-controlled part of the solution with 100% strain tolerance. Here the stresses oscillate. In fact, it may be shown that the strain change repeats a numerical stability criterion, and that 50% is the stability limit. The residual load correction controls the oscillation in the sense that the solution does not diverge completely. The residual load correction has little effect until a large number of steady-state increments (i.e., strain-controlled increments) have been performed. At this point, it is essential for an accurate solution. The 10% stress control allows a slightly more rapid convergence to steady-state. This control is quite satisfactory, considering that it reduces the number of increments needed by 42%.

Summary of Options Used

Listed below are the options used in example e3x12.dat:

Parameter Options

CREEP
ELEMENT
END
SCALE
SIZING
TITLE

Model Definition Options

CONNECTIVITY
CONTROL
COORDINATE
CREEP
DIST LOADS
END OPTION
FIXED DISP
ISOTROPIC
PRINT CHOICE

Load Incrementation Options

AUTO CREEP
CONTINUE
DIST LOADS

Listed below is the user subroutine used in u3x12.f:

CRPLAW

Table E 3.12-1 Creep of Thick Cylinder – Comparison of Results at 20 Hours

Stress	Location	EXACT Steady-State	A (85)†	B (48)	C (42)
σ_{zz}	inside (r=1.025)	-1372.2	-1369.2	-1375.4	-1332.8
	middle (r=1.475)	2725.1	2725.1	2725.6	2725.3
	outside (r=1.975)	5641.0	5635.9	5636.7	5638.2
σ_{rr}	inside	-8717.0	-8712.4	-8714.0	-8710.9
	middle	-3709.2	-3707.1	-3707.4	-3707.3
	outside	-145.24	-144.49	-144.56	-144.58
$\sigma\theta\theta$	inside	5972.6	5974.0	5948.3	6072.8
	middle	9159.3	9158.0	9158.9	9156.4
	outside	11427.0	11424.0	11425.0	11426.0
$\bar{\sigma}$	inside	12741.0	12719.0	12698.0	12803.0
	middle	11144.0	11141.0	11143.0	11140.0
	outside	10022.0	10019.0	10019.0	10020.0

†Number of steps required to reach 20 hours.

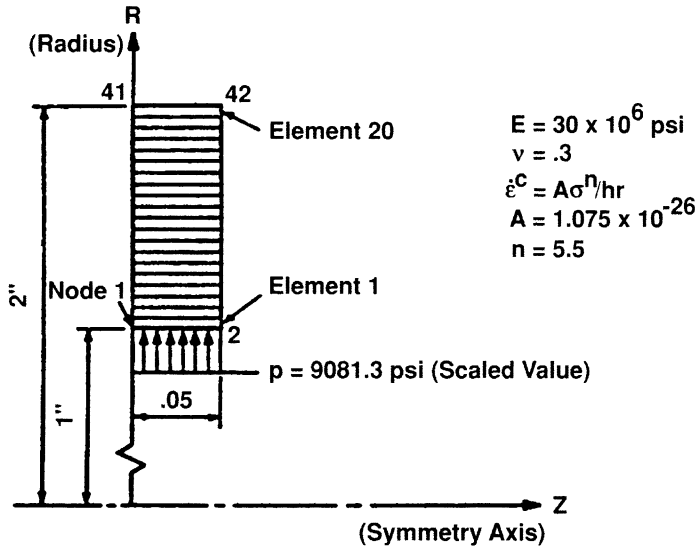

Figure E 3.12-1 Thick Cylinder Geometry and Mesh

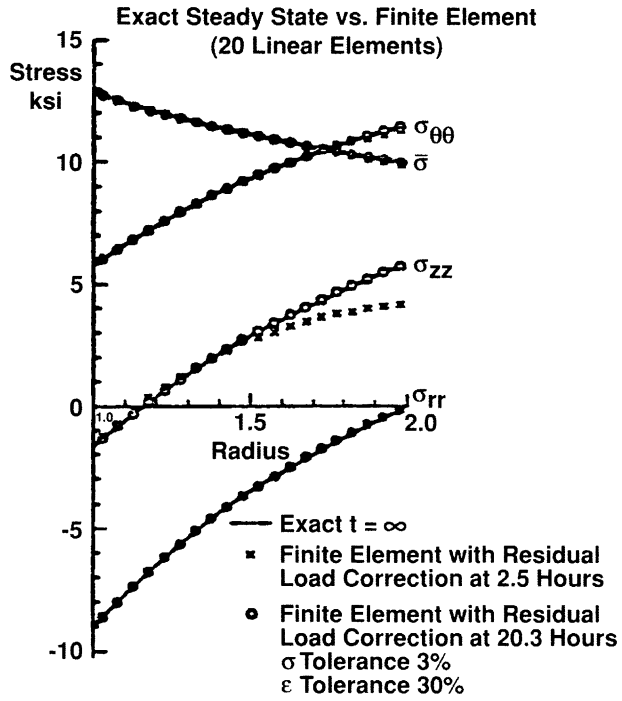

Figure E 3.12-2 Creep of Thick Cylinder, Long Time Results

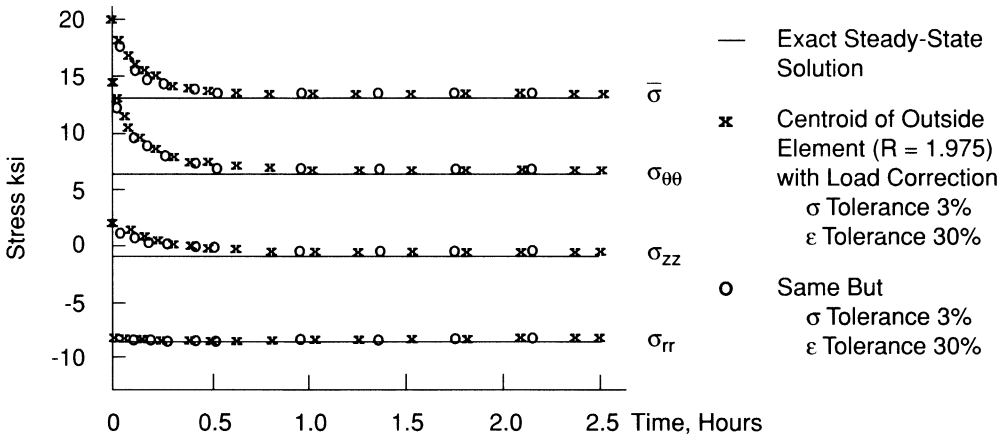

Figure E 3.12-3 Creep of Thick Cylinder – Numerical Comparisons

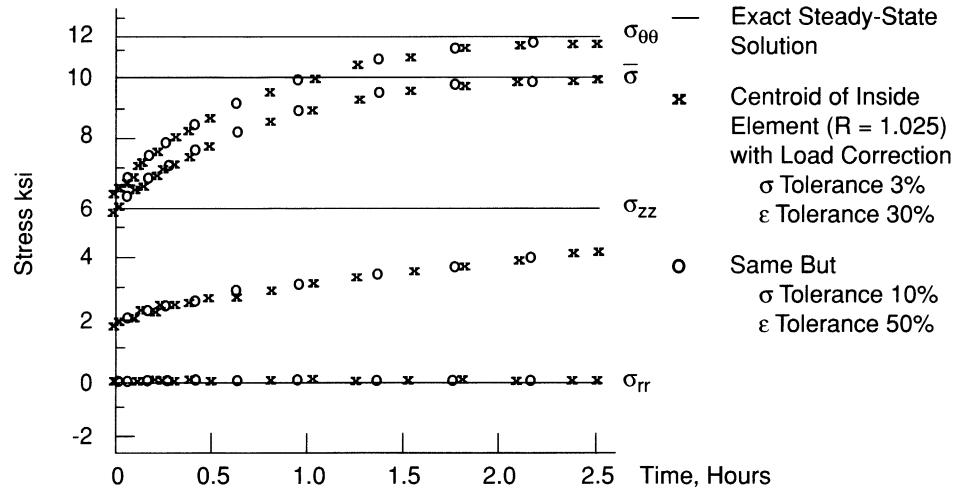

Figure E 3.12-4 Creep of Thick Cylinder – Numerical Comparisons

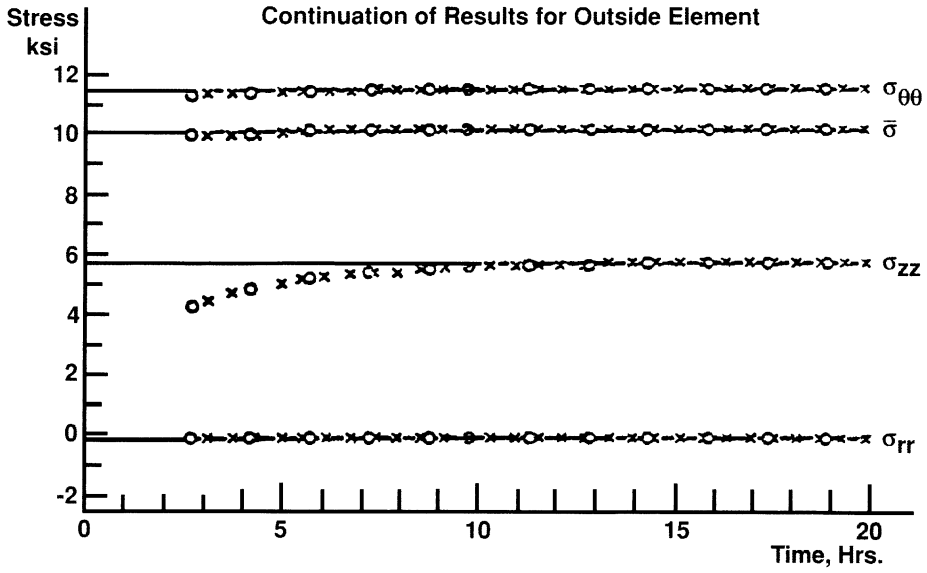

Figure E 3.12-5 Creep of Thick Cylinder – Numerical Comparisons

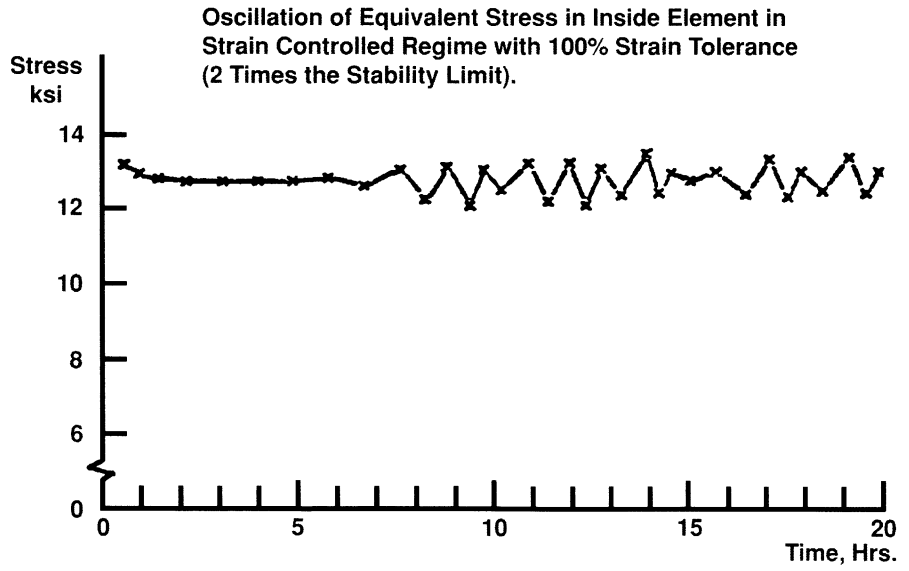

Figure E 3.12-6 Creep Ring

E 3.21 Necking Of A Cylindrical Bar

A cylindrical bar of 20 inches long and 6 inches in diameter is loaded in tension. The ends of the bar are clamped and radial motion is prevented. Away from the ends, the deformation is initially homogeneous. At a certain elongation, the deformation starts to localize. The onset of such localization will occur when the load in the bar reaches a maximum.

Elements (Ref. B10.1, B116.1)

The solution is obtained using first-order isoparametric quadrilateral elements for axisymmetric analysis with element types 10 and 116, respectively. Type 116 is similar to type 10; however, it uses reduced integration with hourglass control.

Model

Because of symmetry, only one-half of the length of the bar is modeled where the axial coordinate x ranges from 0 to 10 inches and the radial coordinate y ranges from 0 to 3 inches. More elements are placed near the middle of the bar at x = 0 and fewer are placed at the end of the bar at x=10 inches. The mesh is shown in Figure E 3.21-1 and Figure E 3.21-2 with the elements and nodes labeled, respectively. In problem e3x21d the adaptive meshing procedure is used.

Geometry

To obtain the constant volumetric strain formulation, (EGEOM2) is set to unity. This is applied to all elements of type 10. This has no effect for element type 116 because the element does not lock.

Material Properties

The material for all elements is treated as an elastic perfectly-plastic material, with a Young's modulus of 10.0E+06 psi, Poisson's ratio of 0.3, and a yield strength of 20,000 psi. The LARGE DISP, UPDATE and FINITE options are used in this analysis. The constant work-hardening rate of 30,000 psi applies to the true stress versus logarithmic strain curve.

Boundary Conditions

The symmetry conditions require that all nodes along the x = 0 axis have their x-displacements constrained to zero; all nodes along the y = 0 axis have their y-displacements constrained to zero. All nodes along the x = 10 axis have their y-displacements constrained to zero and an initial x-displacement of .01 inches.

Load History

All nodes along the x = 10 axis will continue to have their x-displacements increased by .01 inches/increment for 9 increments; then increased by 0.1 inches for 59 increments for the bar to reach a total length of 32 inches.

Analysis Control

The CONTROL option is used to specify a maximum of 80 increments and a maximum of 10 iterations. This number of iterations is specified in order to deal with sudden changes in the deformation field. The convergence checking is done on residuals with a control tolerance of 0.01. Several element variables are written onto the post file and subroutine IMPD sums the load for the load-deflection curve.

Adaptive Meshing

The adaptive meshing procedure is used based upon the Zienkiewicz-Zhu error criteria. A maximum of three levels is allowed.

Results

The value of the maximum load is readily calculated. The force, F, in the bar may be expressed in terms of the true stress σ and current cross-sectional area, A, by:

$$F = A\sigma$$

Assuming incompressibility, the current area can be related to the initial area, A_o, and the elongation, λ, by:

$$F = A_o\sigma/\lambda$$

The load reaches a maximum if the force does not change for increasing elongation. This furnishes a condition for the onset of necking, whereby:

$$dF/d\lambda = A_o\,(d\sigma/d\lambda - \sigma/\lambda)/\lambda = 0$$

With the introduction of the logarithmic strain $e = \ln \lambda$, this condition may also be expressed as:

$$h = d\sigma/de = \sigma$$

The onset of necking occurs if the true stress is equal to hardening modulus in the true stress-logarithmic strain curve. For a material with constant hardening modulus, h, this relation can be worked out in greater detail. For such a material, the true stress may be expressed in terms of the elongation by:

$$\sigma = \sigma_y + he,$$

where σ_y is the initial yield stress. Substituting yields the logarithmic strain:

$$e = 1 - \sigma_y/h.$$

In the current problem, the initial yield stress, σ_y = 20,000 psi and the hardening modulus, h = 30,000 psi, yielding a logarithmic strain of 33.33%. The onset of necking occurs at an engineering strain (the length change divided by the original length) of 39.56%, or an end point displacement of 3.956 inches.

The results from the model shown in Figure E 3.21-3 predict the onset of necking occurring earlier at about 3.0 inches. However, the load displacement curve is very flat due to the low value of the hardening modulus and an accurate value is hard to achieve. Also, the load displacement curve shows the model with element type 10, necking more than the element type 116 after the maximum load is reached. The amount of necking is also shown in the deformed plots of Figure E 3.21-4 through Figure E 3.21-7. This is because element type 116 only has one integration point (element type 10 has four) used for stress recovery and requires more elements. A finer mesh of element type 116 was made to have the same number of integration points as the element type 10 mesh. This mesh shows closer agreement with the mesh using element type 10 in Figure E 3.21-8 and Figure E 3.21-9.

When using the adaptive meshing procedure, the mesh is refined in increments 1, 11, 13, 15, 16, 18, 19, 22, 42, 47, and 50 in this nonlinear analysis. The final mesh is based upon adaptive meshing as shown in Figure E 3.21-10. At the end of the analysis, there are 704 elements and 847 nodes.

Summary of Options Used

Listed below are the options used in example e3x21a.dat:

Parameter Options

ELEMENT
END
FINITE
LARGE DISP
SIZING
TITLE
UPDATE

Model Definition Options

CONNECTIVITY
CONTROL
COORDINATE
END OPTION
FIXED DISP
GEOMETRY
ISOTROPIC
POST
PRINT CHOICE
UDUMP
WORK HARD

Load Incrementation Options

AUTO LOAD
CONTINUE
PROPORTIONAL INCREMENT

Listed below are the options used by MARC-PLOT in example e3x21b.dat:

Parameter Options

COMBINED
ELEMENT
END
PRINT
TITLE
USER

Listed below are the options used in example e3x21c.dat:

Parameter Options

ALIAS
ELEMENT
END
FINITE
LARGE DISP
SIZING
TITLE
UPDATE

Model Definition Options

CONNECTIVITY
CONTROL
COORDINATE
END OPTION
FIXED DISP
GEOMETRY
ISOTROPIC
POST
PRINT CHOICE
RESTART
WORK HARD

Load Incrementation Options

AUTO LOAD
CONTINUE
PROPORTIONAL INCREMENT

Listed below are options used in example e3x21d.dat

Parameter Options

ADAPTIVE
ELEMENT
END
FINITE
LARGE DISP
SIZING
TITLE
UPDATE

Model Definition Options

ADAPTIVE
CONNECTIVITY
CONTROL
COORDINATE
END OPTION
FIXED DISP
GEOMETRY
ISOTROPIC
POST
PRINT CHOICE
UDUMP
WORK HARD

Load Incrementation Options

AUTO LOAD
CONTINUE
PROPORTIONAL INCREMENT

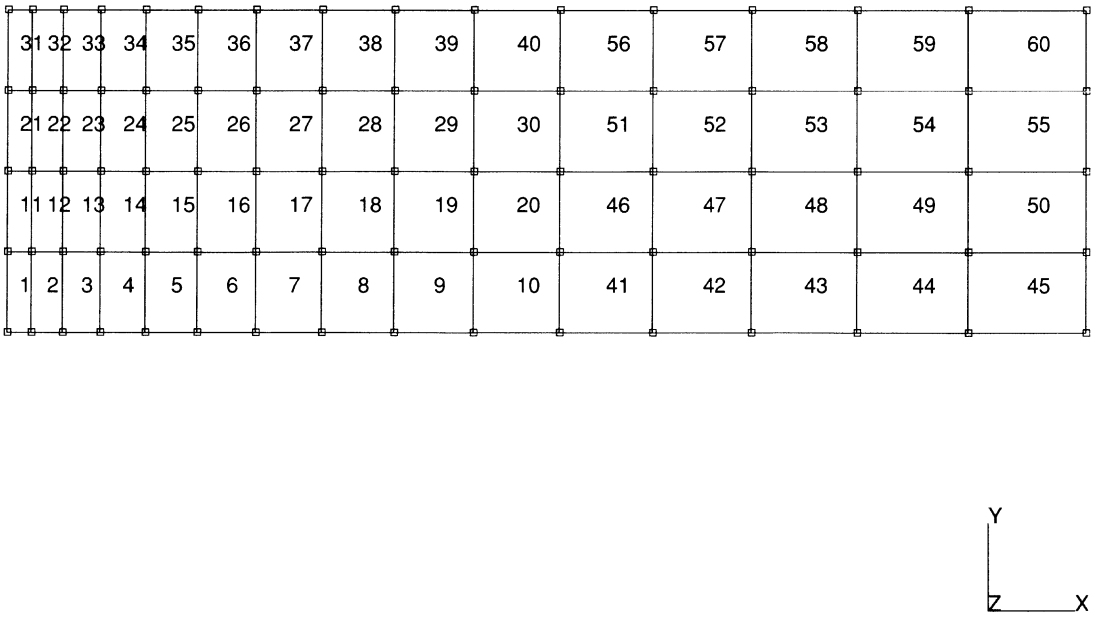

Figure E 3.21-1 Model with Elements Numbered

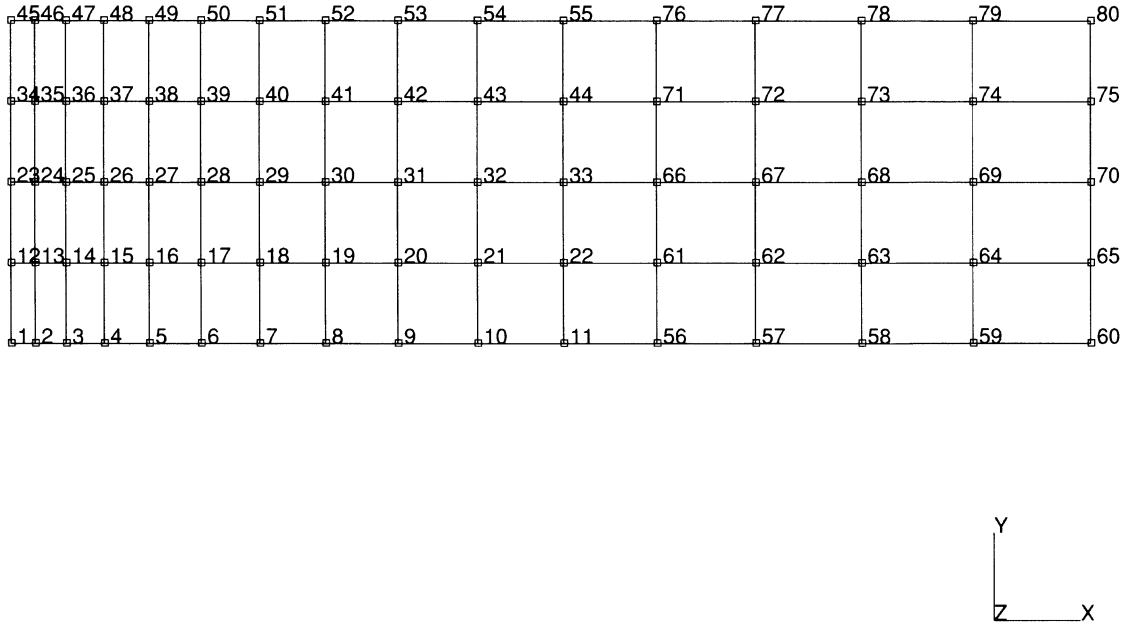

Figure E 3.21-2 Model with Nodes Labeled

Displacement	Load (x10**5 lbf)		
	Type 10	Type 116	Type 116 fine
0.0	0.0	0.0	0.0
1.00000E-02	2.86645E+00	2.87316E+00	2.86198E+00
2.00000E-02	5.64279E+00	5.65044E+00	5.65154E+00
3.00000E-02	5.65075E+00	5.65181E+00	5.65312E+oo
•	•	•	•
2.70000E+00	6.08106E+00	6.08466E+00	6.08170E+oo
2.80000E+00	6.08219E+00	6.08442E+00	6.08266E+00
2.90000E+00	6.08235E+00	6.08293E+00	6.08259E+00
•	•	•	•
3.00000E+00	6.08144E+00	6.07998E+00	6.08137E+00
3.10000E+00	6.07933E+00	6.07538E+00	6.07879E+00
3.20000E+00	6.07580E+00	6.06831E+00	6.07457E+00
3.30000E+00	6.07060E+00	6.05820E+00	6.06833E+00
3.40000E+00	6.06339E+00	6.04646E+00	6.05973E+00
•	•	•	•
4.70000E+00	5.56913E+00	5.24714E+00	5.46007E+00
4.80000E+00	5.47695E+00	5.06798E+00	5.34126E+00
4.90000E+00	5.37292E+00	4.84365E+00	5.20284E+00
5.00000E+00	5.25596E+00	4.59166E+00	5.04048E+00

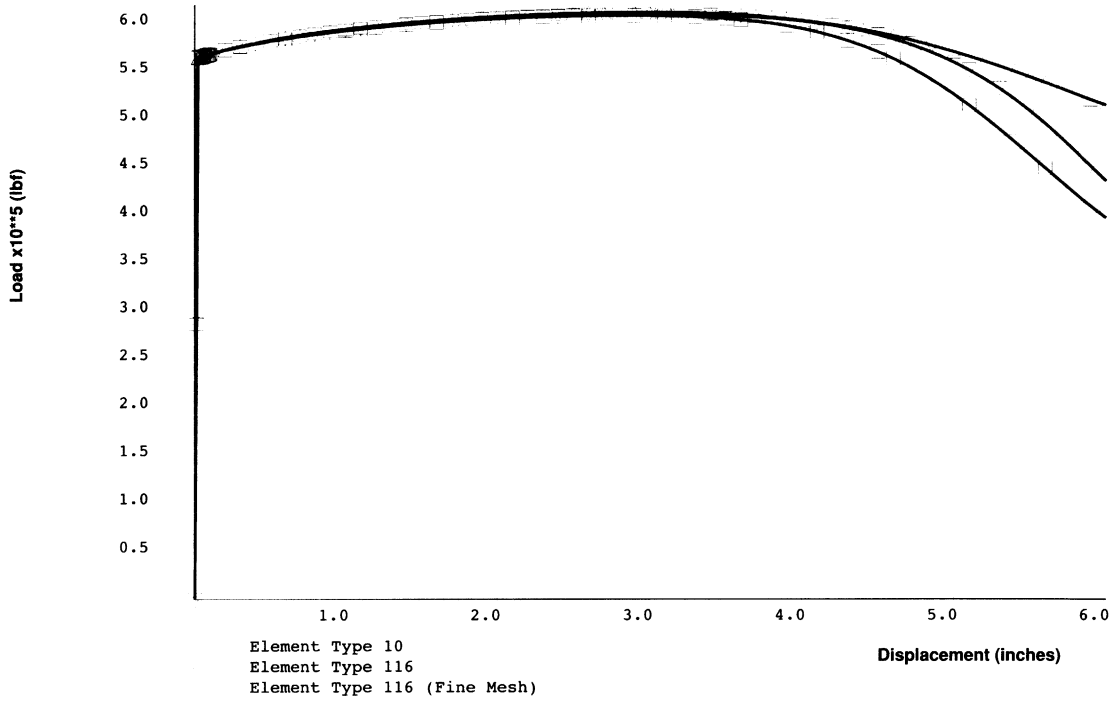

Figure E 3.21-3 Load -Displacement Curve

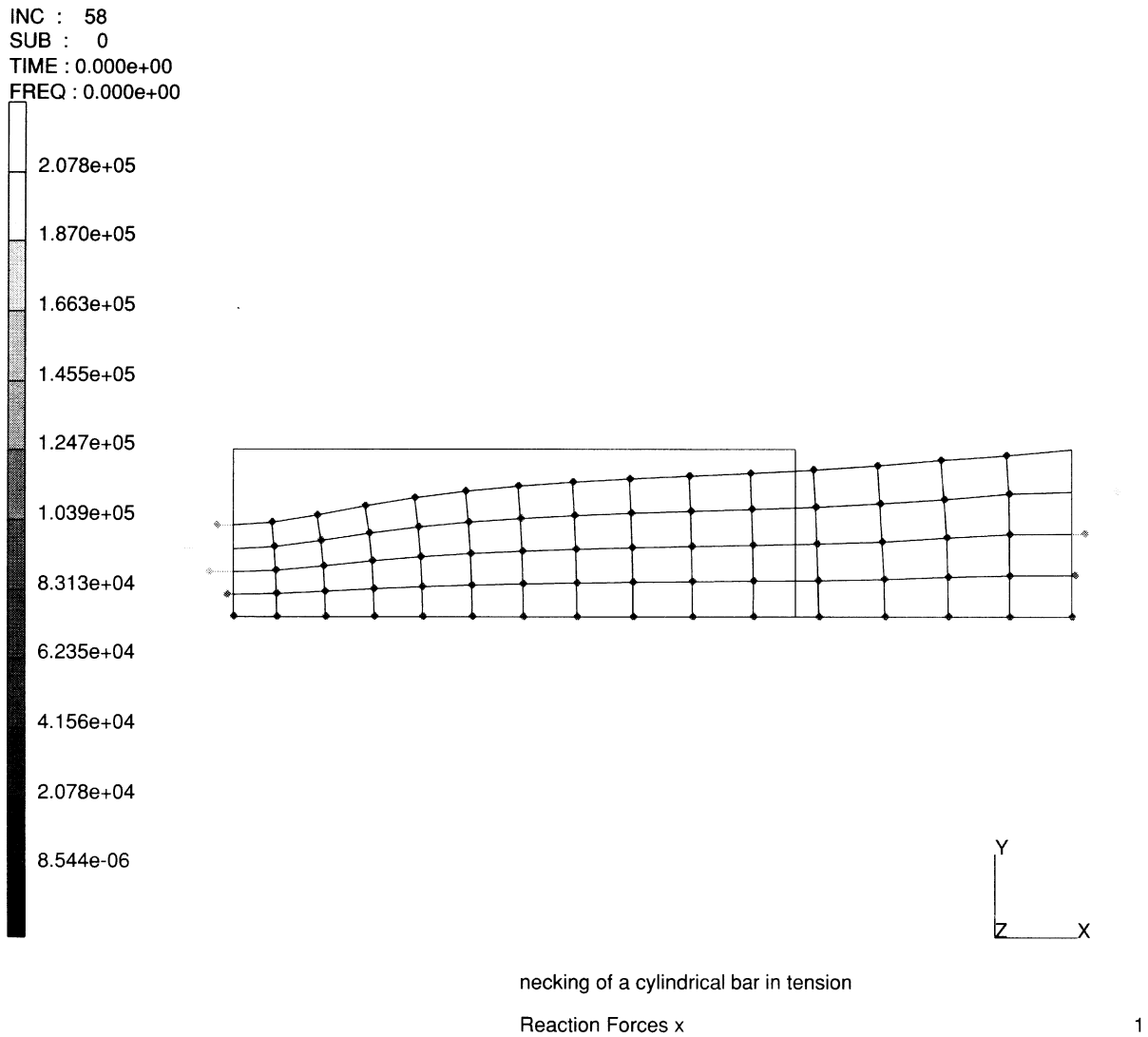

Figure E 3.21-4 Vector Plot of Reactions for Type 10

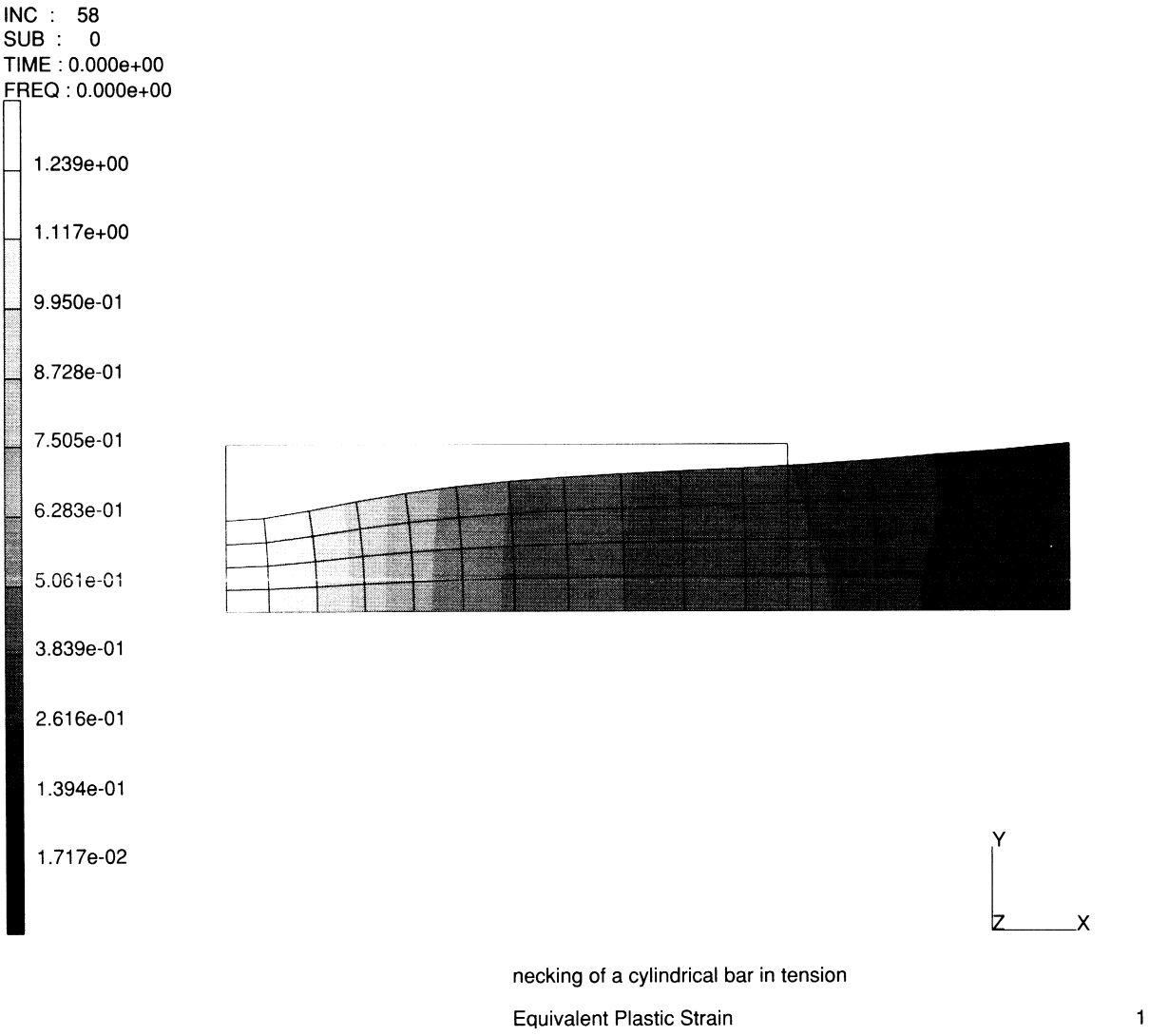

Figure E 3.21-5 Contour Plot of Equivalent Strain for Type 10

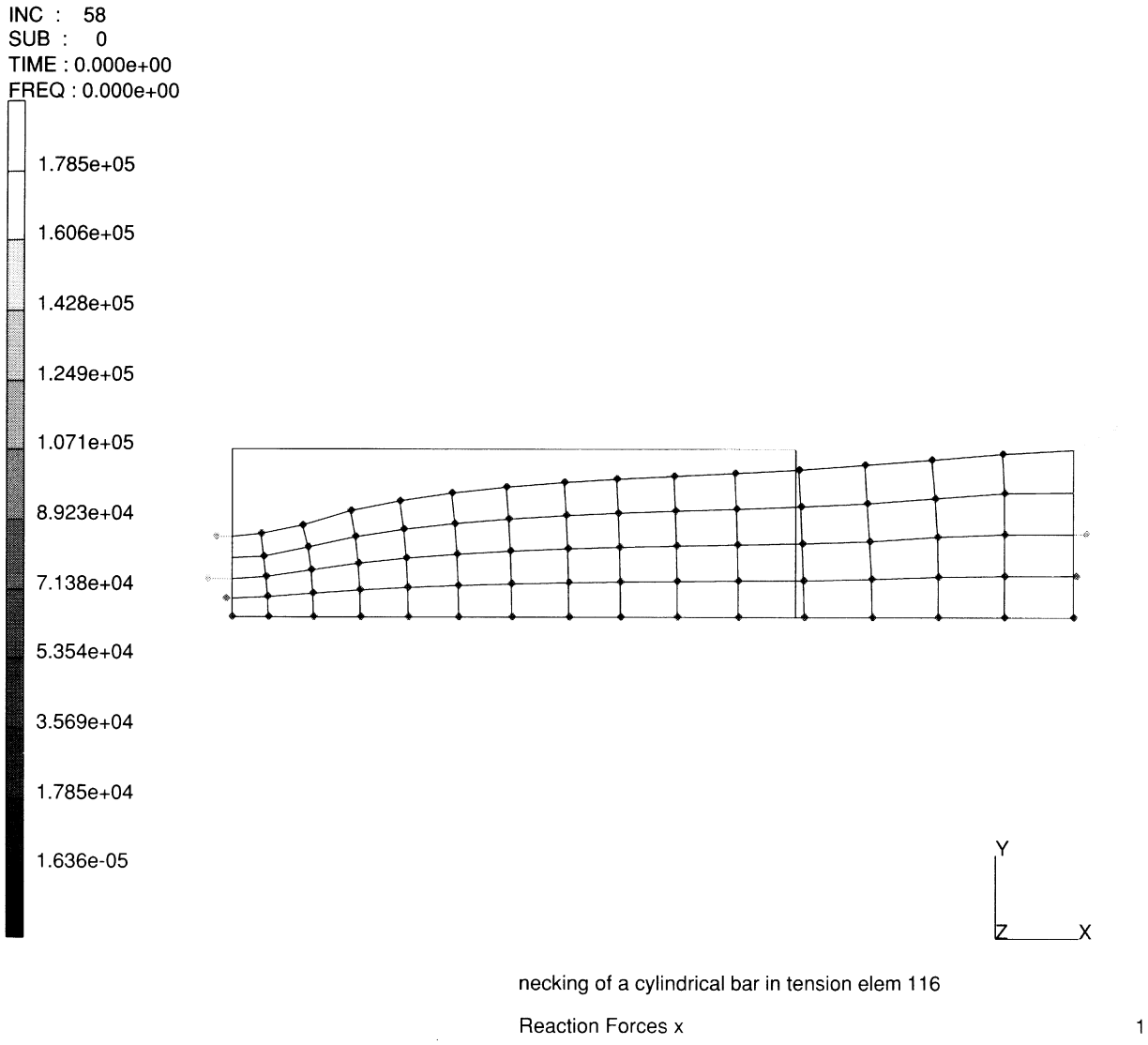

Figure E 3.21-6 Vector Plot of Reactions for Type 116 (Coarse Mesh)

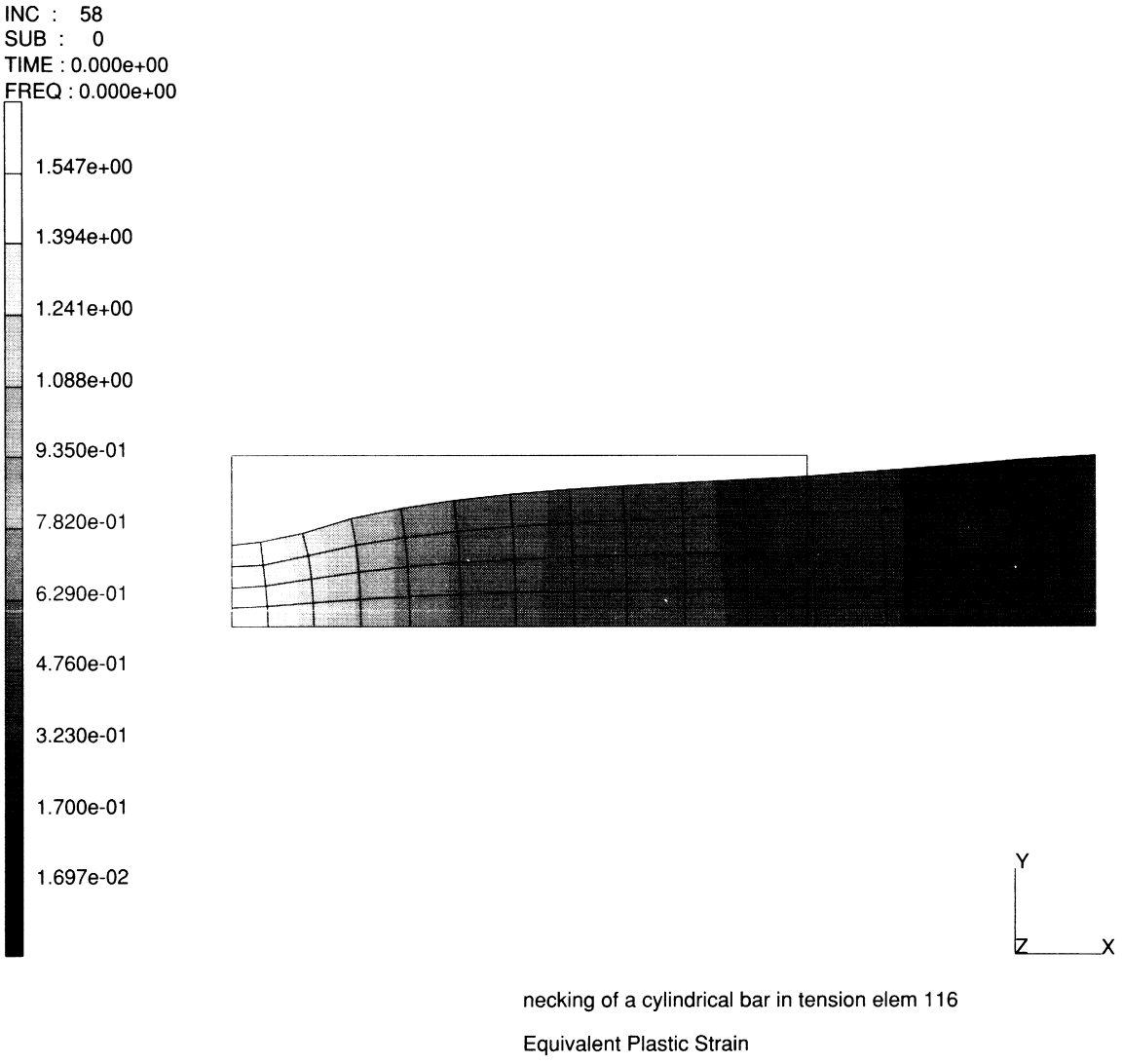

Figure E 3.21-7 Contour Plot of Equivalent Strain for Type 116 (Coarse Mesh)

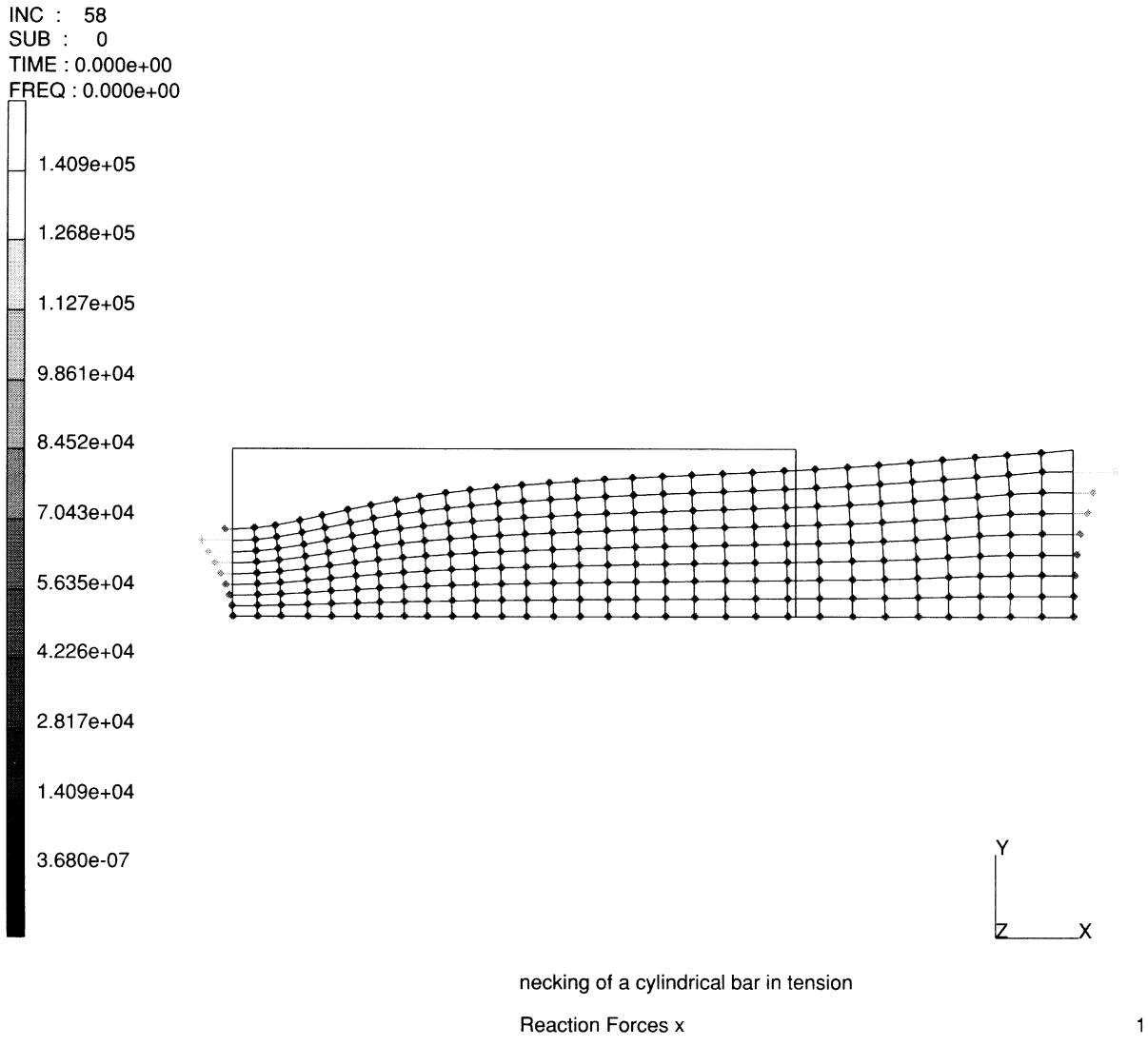

Figure E 3.21-8 Vector Plot of Reactions for Type 116 (Fine Mesh)

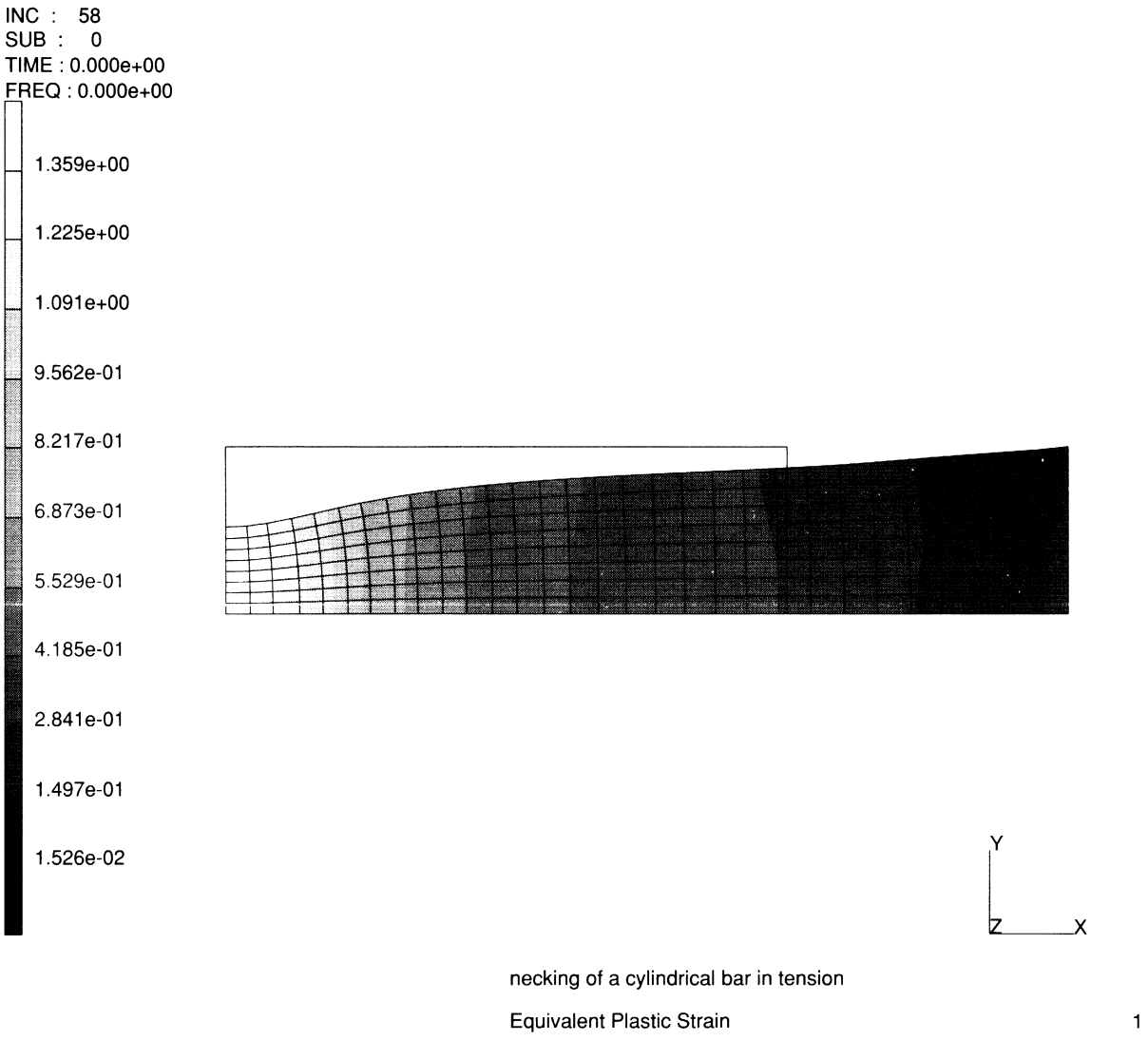

Figure E 3.21-9 Contour Plot of Equivalent Plastic Strain for Type 116 (Fine Mesh)

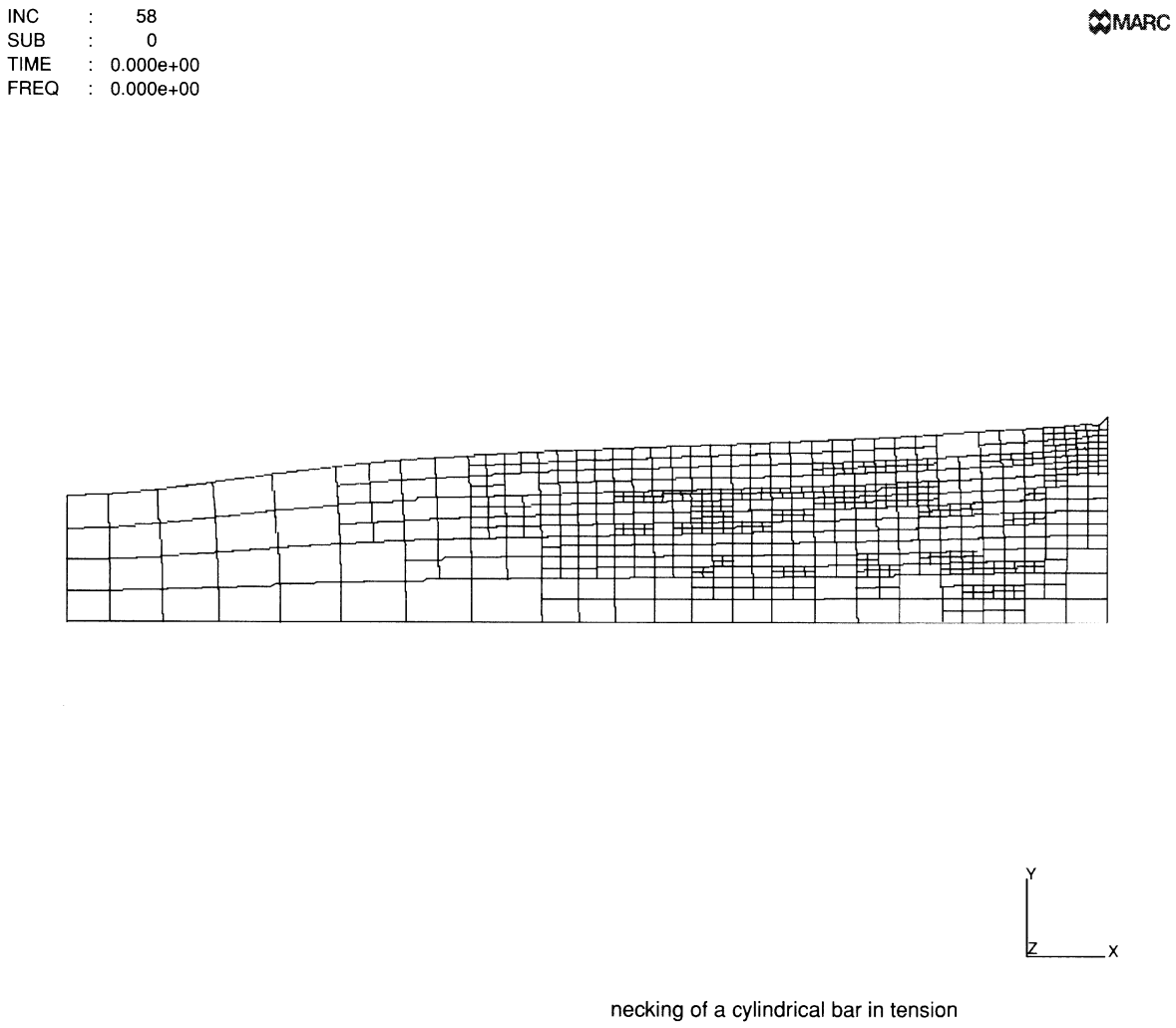

Figure E 3.21-10 Final Mesh After Adaptive Meshing

E 3.26 Hot Isostatic Pressing Of A Powder Material

This example illustrates the use of element 28 in a thermal mechanically coupled hot isostatic pressing problem. A powder material is placed into a stiffer cylindrical can which is then subjected to a pressure and thermal cycle.

Element

Element type 28, an 8-node axisymmetric element is used to model the powder and the can. Seventy elements are used to model the powder and 26 to represent the can. In a coupled analysis, element type 42 is the corresponding heat transfer element. The initial dimensions of the powder are 97 mm x 47.0 mm. The can thickness is 3 mm as shown in Figure E 3.26-1.

Loading

The loading history is shown in Figure E 3.26-3. The external pressure is ramped to 1500 MPa in 9000 seconds; it is then held constant for 10,800 seconds and then reduced to zero in 7200 seconds. The exterior temperature on the can is raised from 0° to 1440°C in the first 9000 seconds and also reduced to zero in 7200 seconds. The FORCDT option is used to prescribe the nodal temperatures. The DIST LOADS option is used to define the external pressure. Note that the FOLLOW FORCE option is used to prescribe the load on the deformed configuration.

Material Properties

As this is a coupled analysis, both mechanical and thermal properties must be prescribed. Furthermore, the material behavior is both temperature and relative density dependent. The powder is represented using the modified Shima model. The Young' modulus and Poisson's ratio are bilinear functions of the relative density and the temperature. E_o and ν_o are the initial values 20,000 MPa and 0.3, respectively. The initial yield stress is 1000 MPa.

The experimental data is:

T°(C)	$\bar{\rho}$	E (MPa)	ν	σ	E/E_o	ν/ν_o
0.0	0.7	20,000	0.3	1000.0	1.0	1.0
2000.0	0.7	2,000	0.49	100.0	0.1	1.633
0.0	1.0	30,000	0.33	Shima	1.5	1.1

The temperature-dependent properties are entered via the TEMPERATURE EFFECTS DATA option. The relative density effects for Young's modulus and Poisson's ratio are given as multiplicative factors relative to this data via the REALTIVE DENSITY option.

The values of γ and β, which are used to define the yield surfaces dependence on relative density, have initial values of 0.1406174 and 1.375. These material data are functions of the relative density:

$\gamma = (1. + \bar{\rho})^{5.5}$ and
$\beta = 6.25\ (1 - \bar{\rho})^{-0.5}$

Therefore, q_1, q_2, q_3, q_4 are entered as 1.0, 1.0, 1.0, 5.5 and b_1, b_2, b_3, b_4 are entered as 6.25, -6.25, 1.0, -0.5, respectively. The initial relative density is 0.7.

The viscosity is also a function of the temperature with a value of 50,000 at 0°C and 25,000 at 200°C.

The coefficient of thermal expansion is -1×10^{-7} mm/mm°C. The mass density is 4×10^{-6} kg/mm^3.

The thermal conductivity and the specific heat are also bilinear functions of the temperature and relative density.

The experimental data is:

T°C	$\bar{\rho}$	KW/m°C	KJ/Kg°C	K/K_o	C/Co
0	0.7	0.03	30.0	1.0	1.0
2000	0.7	0.04	50.0	1.333	1.666
0	1.0	0.042	45.0	1.4	0.9

The temperature dependent properties are entered via the TEMPERATURE EFFECTS DATA option. The relative density effects for the conductivity and specific head are defined as multiplicative factors relative to this data via the RELATIVE DENSITY option.

The can is represented as an elastic-plastic material. The properties are a function of temperature only:

T°C	E (MPa)	ν	σ_y (MPa)	K	C
0	200,000	0.3	1000	0.03	30
2000	100,000	0.4	500	0.04	50

The coefficient of thermal expansion is 1.0×10^{-6} m/m°C and the mass density is 8.0×10^{-6}. This data is defined in the ISOTROPIC and TEMPERATURE EFFECTS DATA option. The initial relative density of 0.7 is entered through the RELATIVE DENSITY option.

Control

In this problem, the convergence requirement is 10% on relative displacements with a maximum number of 20 iterations. Typically, increments required one to three iterations. The TRANSIENT NON AUTO option was used to provide fixed time steps per increment. As the exterior temperature is completely prescribed, it is not likely that large changes in temperature will occur. The third line on the CONTROL option specifies a maximum allowable temperature difference of 1000 (not used anyway because of fixed time procedure) and an error in temperature of 0.1. This will result in an accurate temperature analysis.

The RESTART option controls the restart to be written every 10 increments. The POST option insures that all the strains, stresses, equivalent plastic strain, strain rate and the relative density may be post processed. The post tape is written every 10 increments.

Results

The relative density at the end of the analysis is shown in Figure E 3.26-3 on the deformed mesh. One can observe that the material has densified to a value of 0.98 in most of the region. The area near the corners shows a reduced level of densification. The time history of relative density, inelastic strain rate, and equivalent plastic strain are shown in Figure E 3.26-4, Figure E 3.26-5, and Figure E 3.26-6, respectively.

Summary of Options Used

Listed below are the options used in example e3x26.dat:

Parameter Options

COUPLE
ELEMENTS
END
LARGE DISP
SIZING
TITLE
UPDATE

Model Definition Options

CONNECTIVITY
CONTROL
COORDINATES
DEFINE
DENSITY EFFECTS
DIST LOADS
END OPTION
FIXED DISP
FIXED TEMPERATURE
FORCDT
ISOTROPIC
POST
POWDER
RELATIVE DENSITY
RESTART
TEMPERATURE EFFECTS
WORK HARD

Load Incrementation Options

CONTINUE
DIST LOADS
TRANSIENT

Listed below is the user subroutine found in u3x26.f:

FORCDT

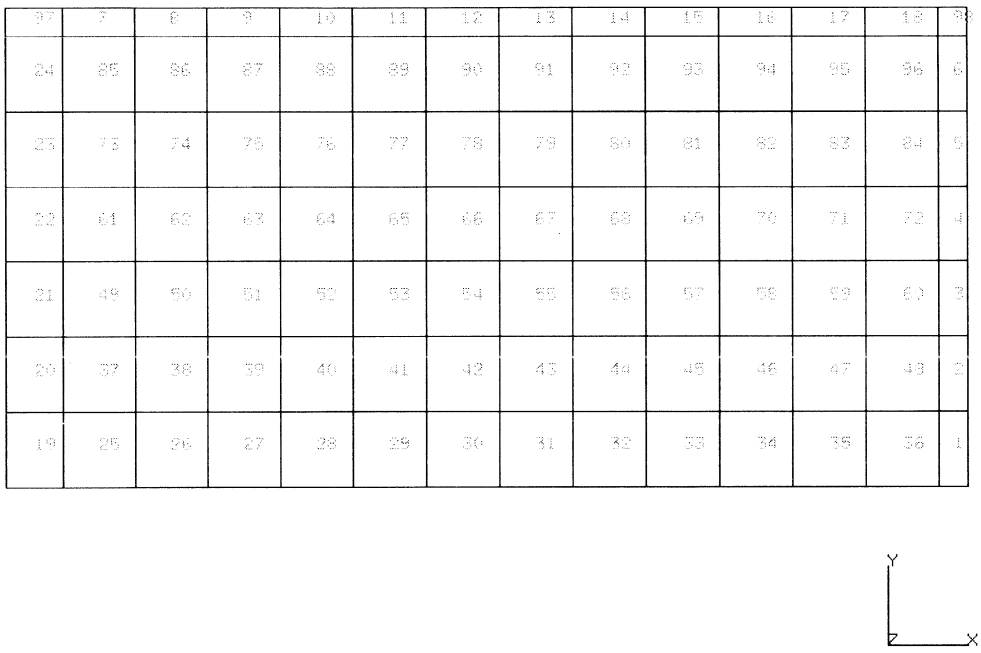

Figure E 3.26-1 Mesh

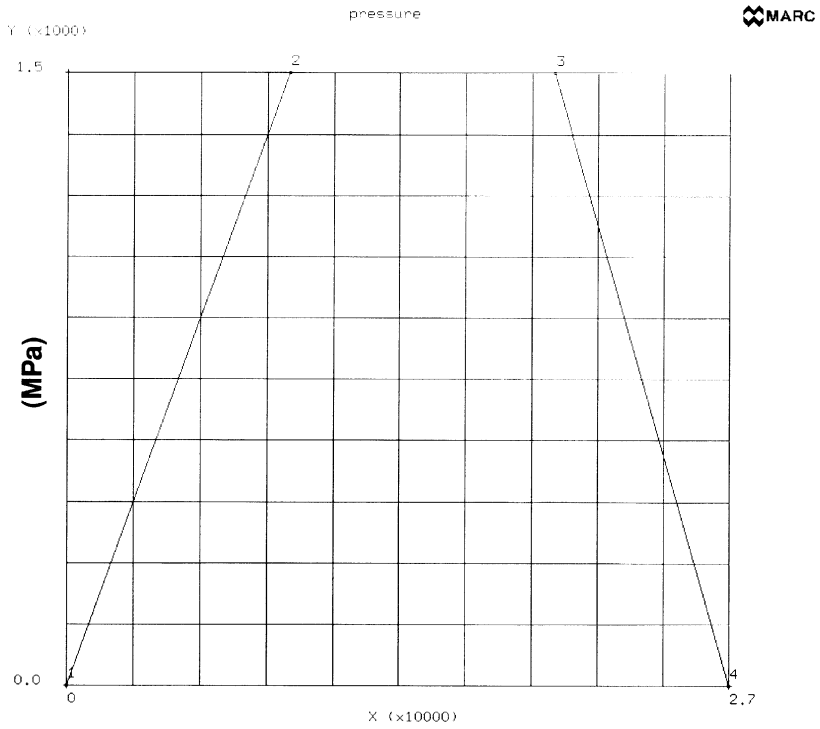

Externally Applied Pressure

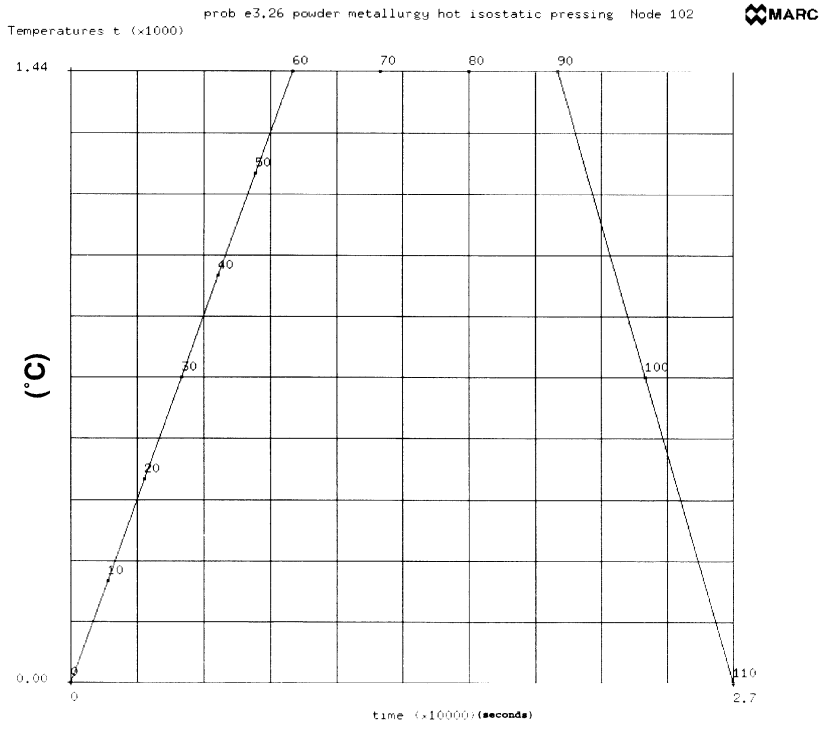

Externally Applied Temperature

Figure E 3.26-2 Time History

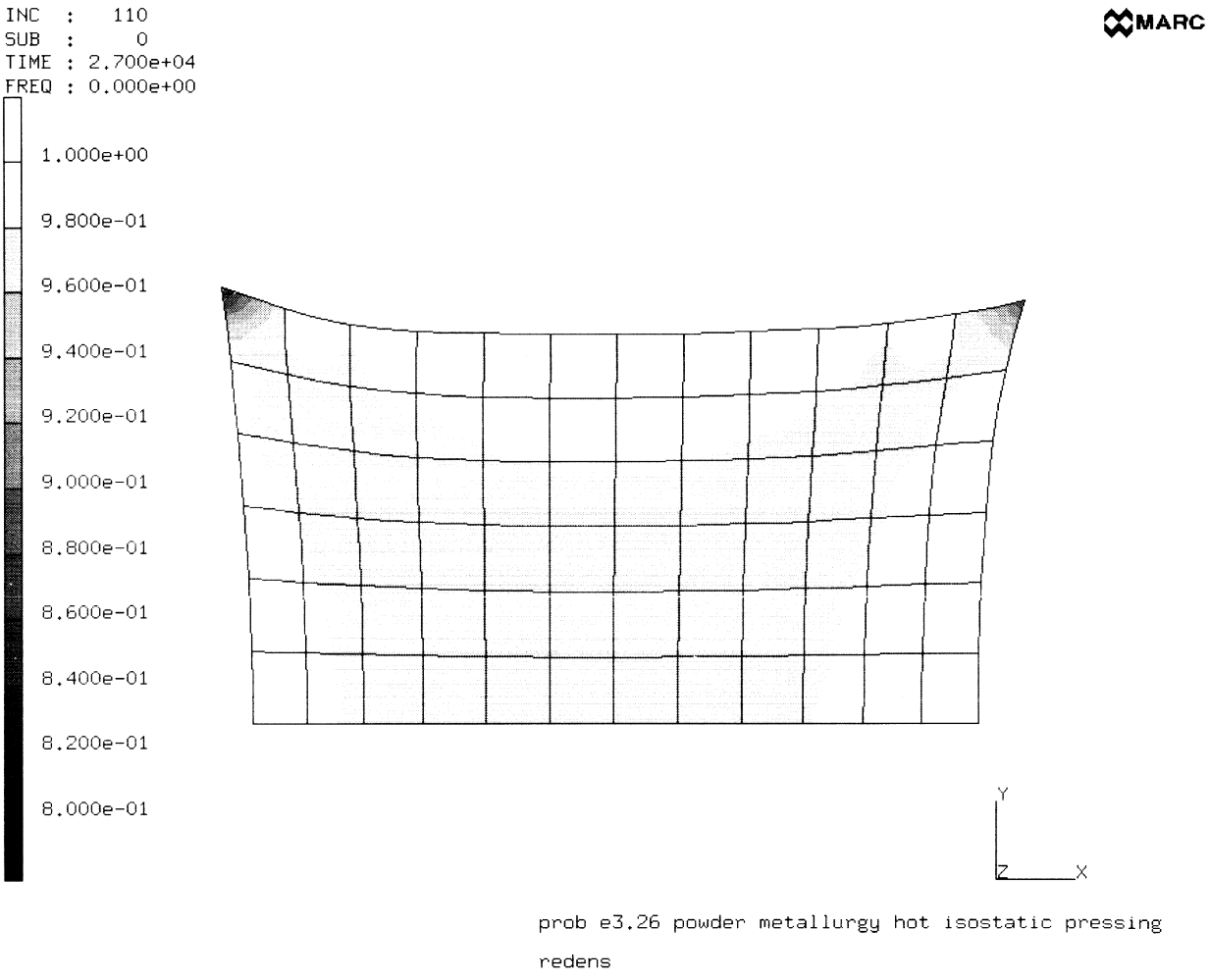

Figure E 3.26-3 Final Relative Density

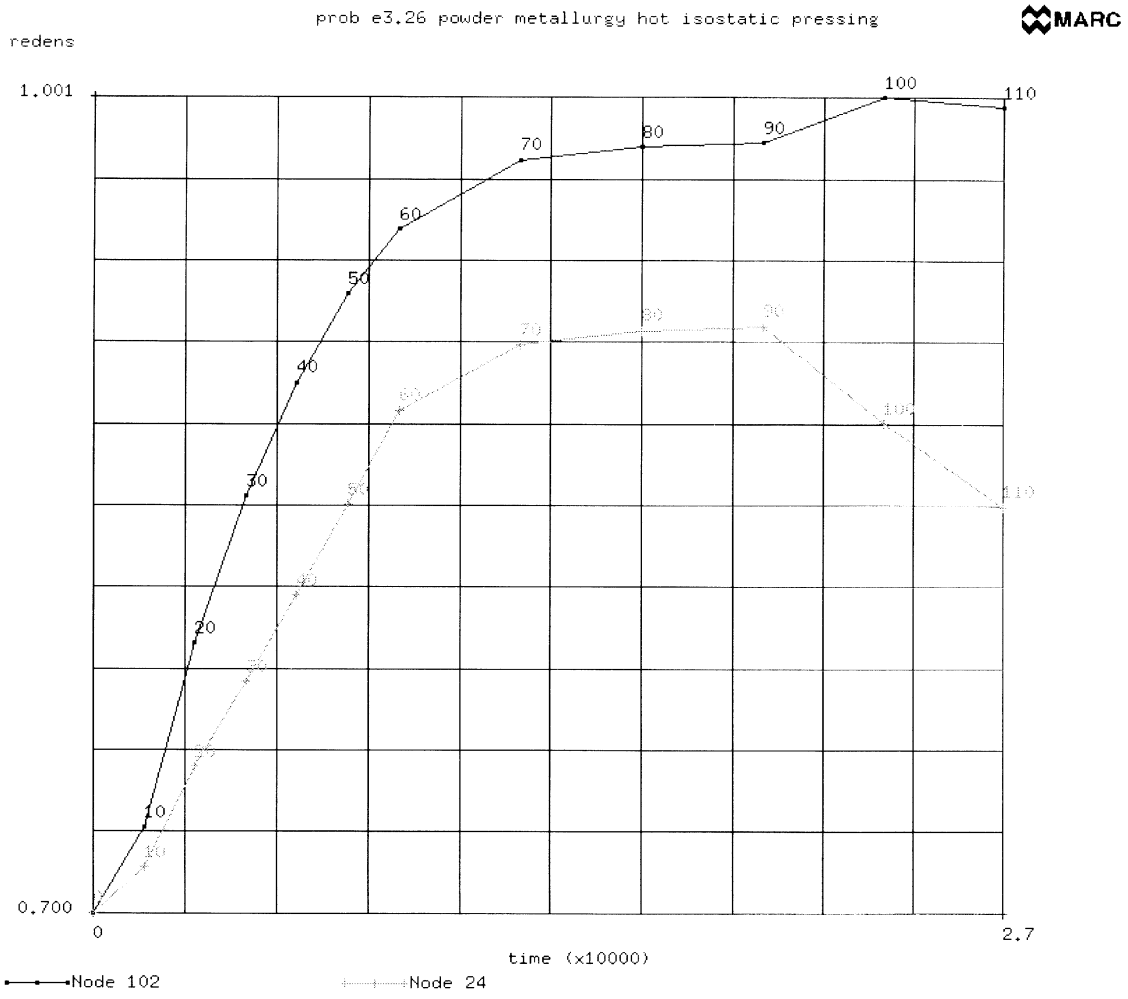

Figure E 3.26-4 Time History of Relative Density

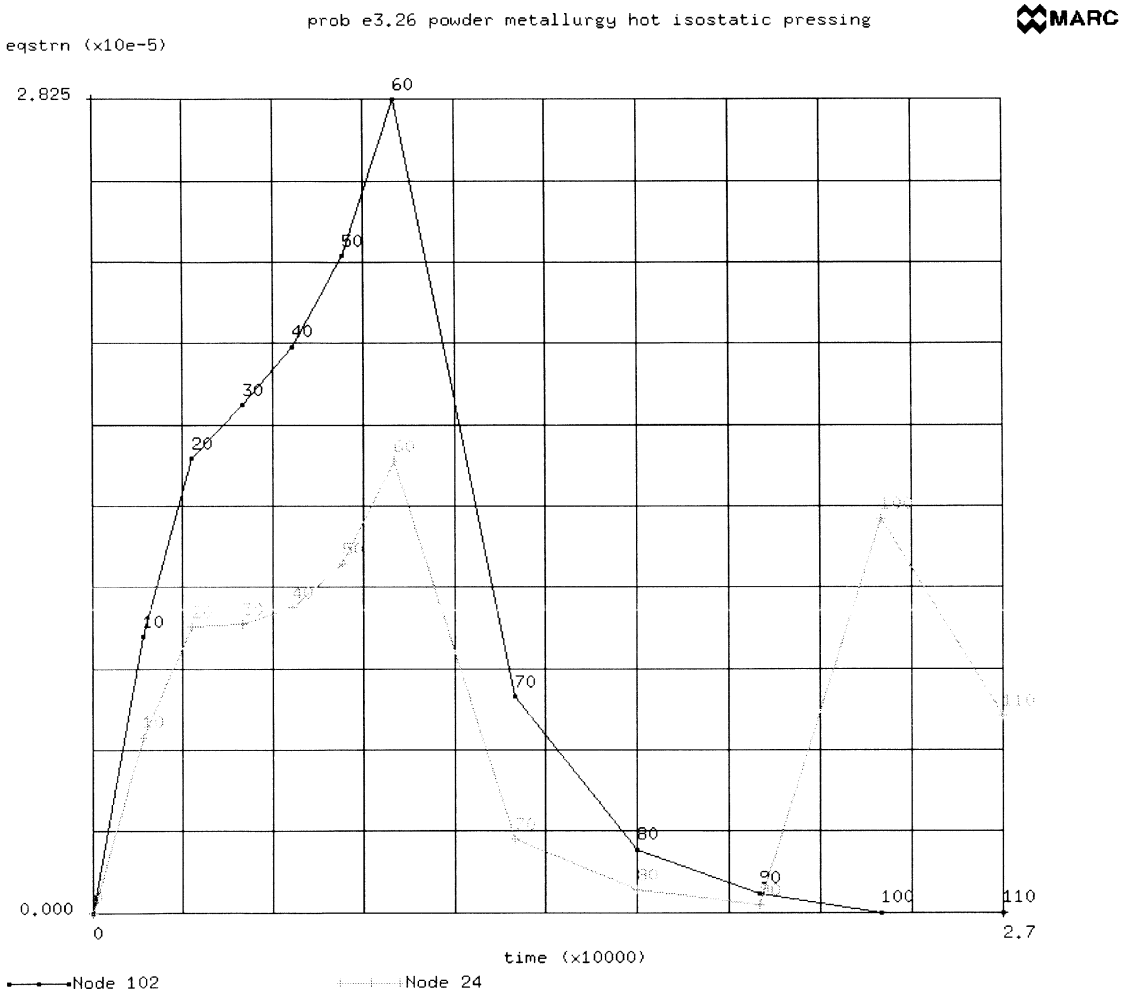

Figure E 3.26-5 Time History of Equivalent Strain Rate

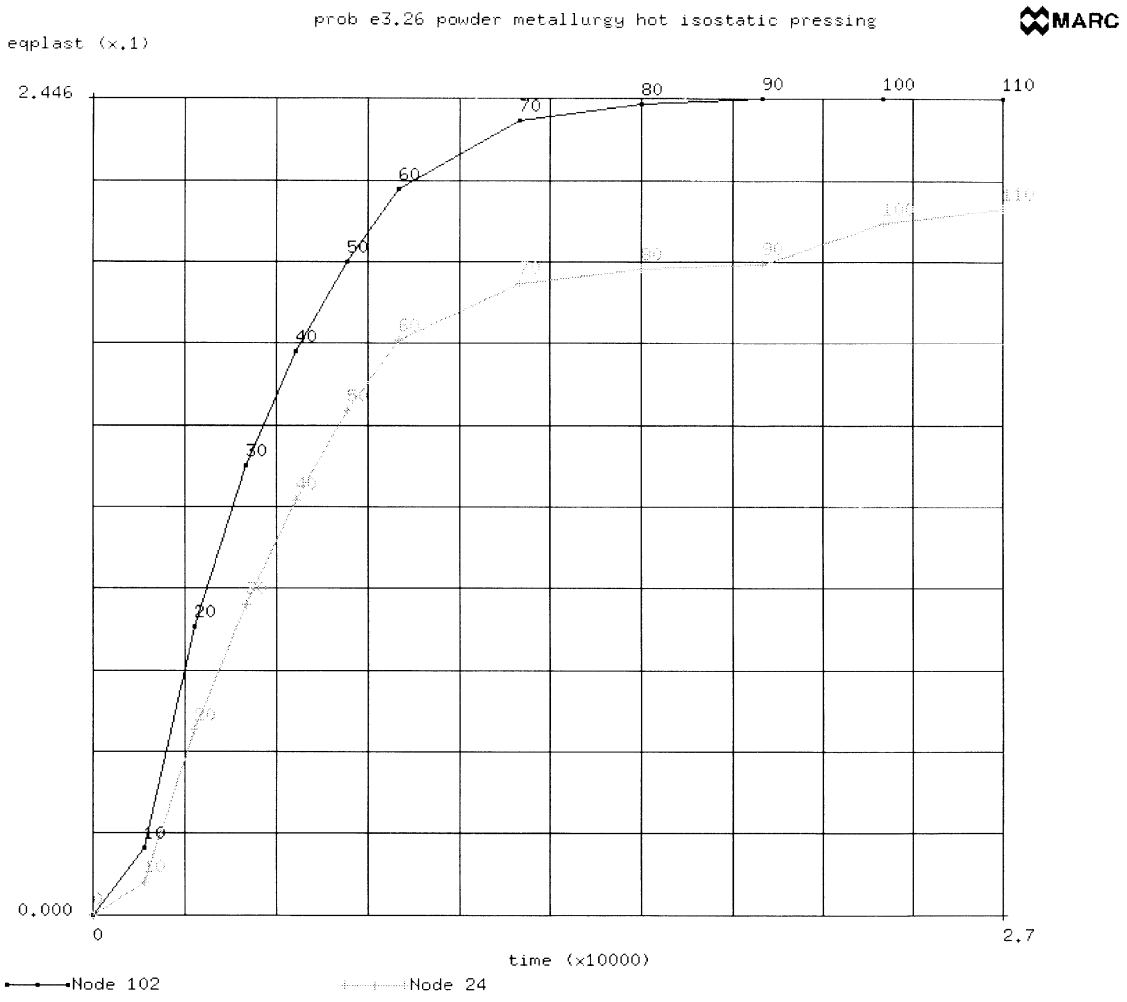

Figure E 3.26-6 Time History of Equivalent Plastic Strain

E 3.28 Void Growth In A Notched Specimen

This example illustrates the prediction of void growth in a notched specimen. This problem was first analyzed using a damage model by Sun.

Element (Ref. B 55.1)

Element type 55, an 8-node reduced integration axisymmetric element, is used in this analysis. The bar is 25 mm long, with a radius of 7mm and an elliptical notch (minor axis of 3, major of 3.873) is shown in Figure E 3.28-1. The model consists of 500 elements and 1601 nodes and is shown in Figure E 3.28-2.

Loading

Symmetry conditions are applied on the center line and the left side. The bar has an applied displacement of 1.775 applied in 230 increments using the DISP CHANGE and AUTO LOAD options.

Material Properties

The material is represented using a work hardening model. The Young's modulus is 21,000.0 N/mm^2. The work hardening data is shown in Figure E 3.28-3.

The Gurson damage model will be invoked using the strain-controlled nucleation model. The parameters used are:

First yield surface multiplier, q_1	= 1.5
Second yield surface multiplier, q_2	= 1.0
Initial void volume fraction, f_i	= 0.0057
Critical void volume fraction, f_c	= 0.3
Failure void volume fraction, f_f	= 0.15
Mean strain for nucleation	= 0.1
Standard deviation	= 0.00408

Control

The required convergence tolerance is 5% on residuals. A maximum of 15 iterations per increment is allowed. The restart tape is generated every 20 increments. The post file is generated every 10 increments. The bandwidth is minimized using the Cuthill-McKee optimizer. The AUTO LOAD option is invoked twice; the first time 80 increments of 0.1 mm are taken and then 150 more increments of 0.0025 mm are taken.

Results

The deformed geometry is shown in Figure E 3.28-4. The distribution of the void is represented in Figure E 3.28-5. Linear elastic analysis would reveal that the highest stress is at the outside radius. Due to the redistribution of the stresses and because of elastic plastic behavior, the highest triaxial stress occurs at the center and the crack initiation due to void coalescence begins here. The equivalent plastic strain is shown in Figure E 3.28-6. On subsequent loading, the cracks grow radially along the symmetry line. Figure E 3.28-7 shows the history of the void ratio at three nodes along this line.

Summary of Options Used

Listed below are the options used in example e3x28.dat:

Parameter Options

ALIAS
ELEMENT
END
FINITE
LARGE DISP
PRINT
SIZING
TITLE
UPDATE

Model Definition Options

CONNECTIVITY
CONTROL
COORDINATES
DAMAGE
DEFINE
END OPTION
FIXED DISP
ISOTROPIC
NO PRINT
OPTIMIZE
POST
RESTART
WORK HARD

Load Incrementation Options

AUTO LOAD
CONTINUE
DIST CHANGE

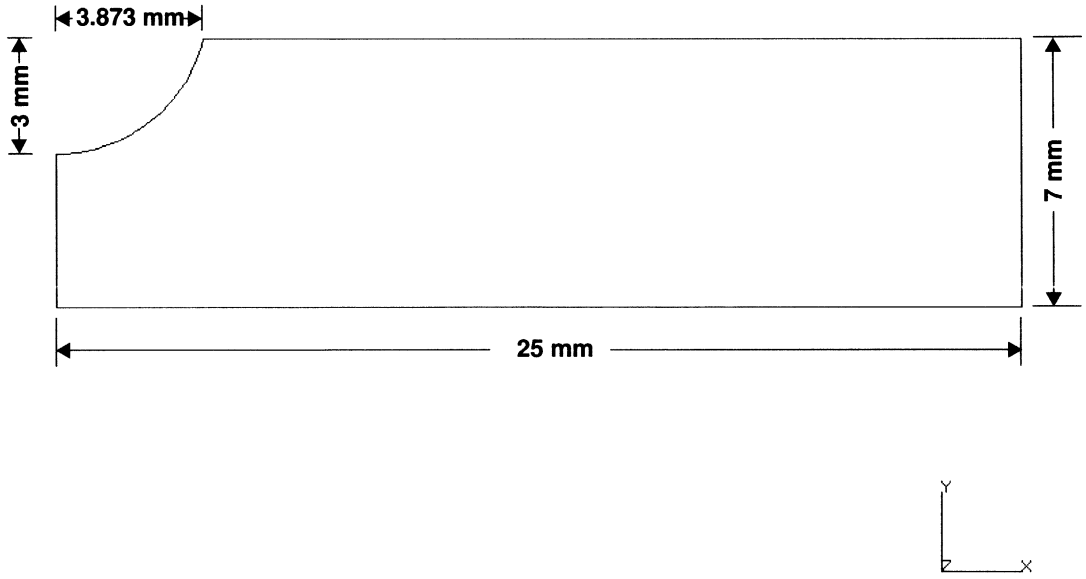

Figure E 3.28-1 Notched Specimen

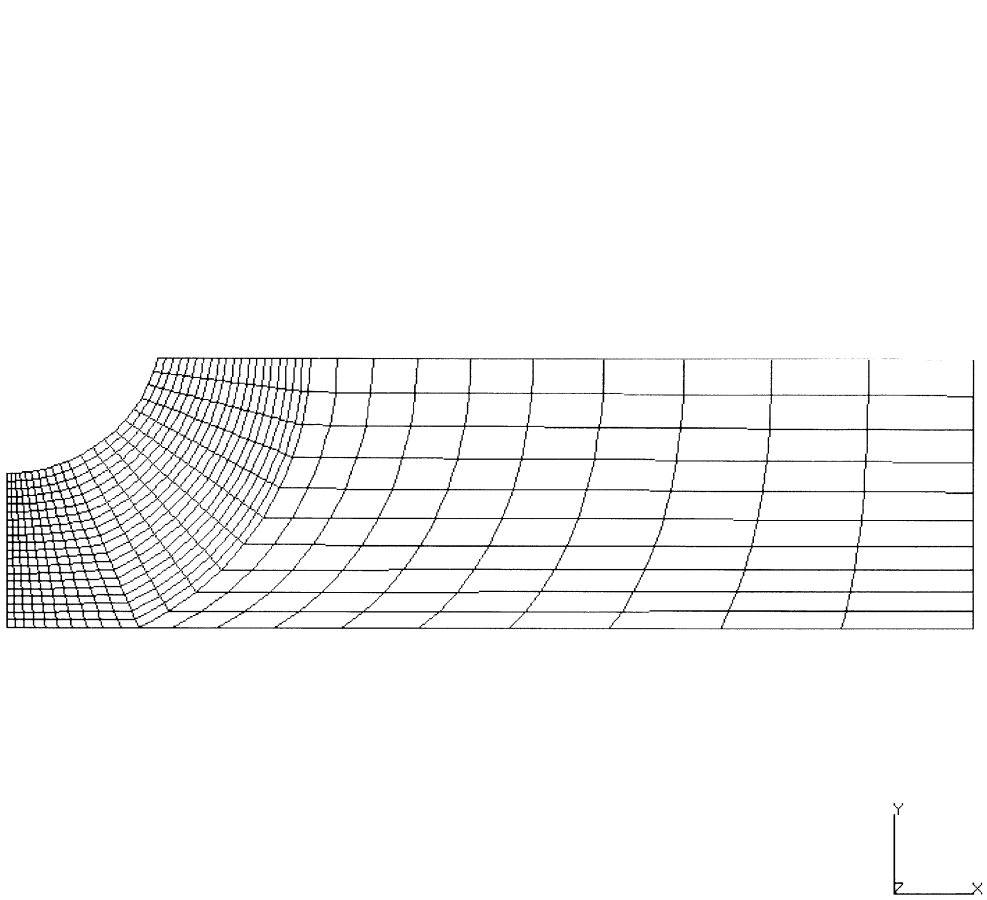

Figure E 3.28-2 Mesh

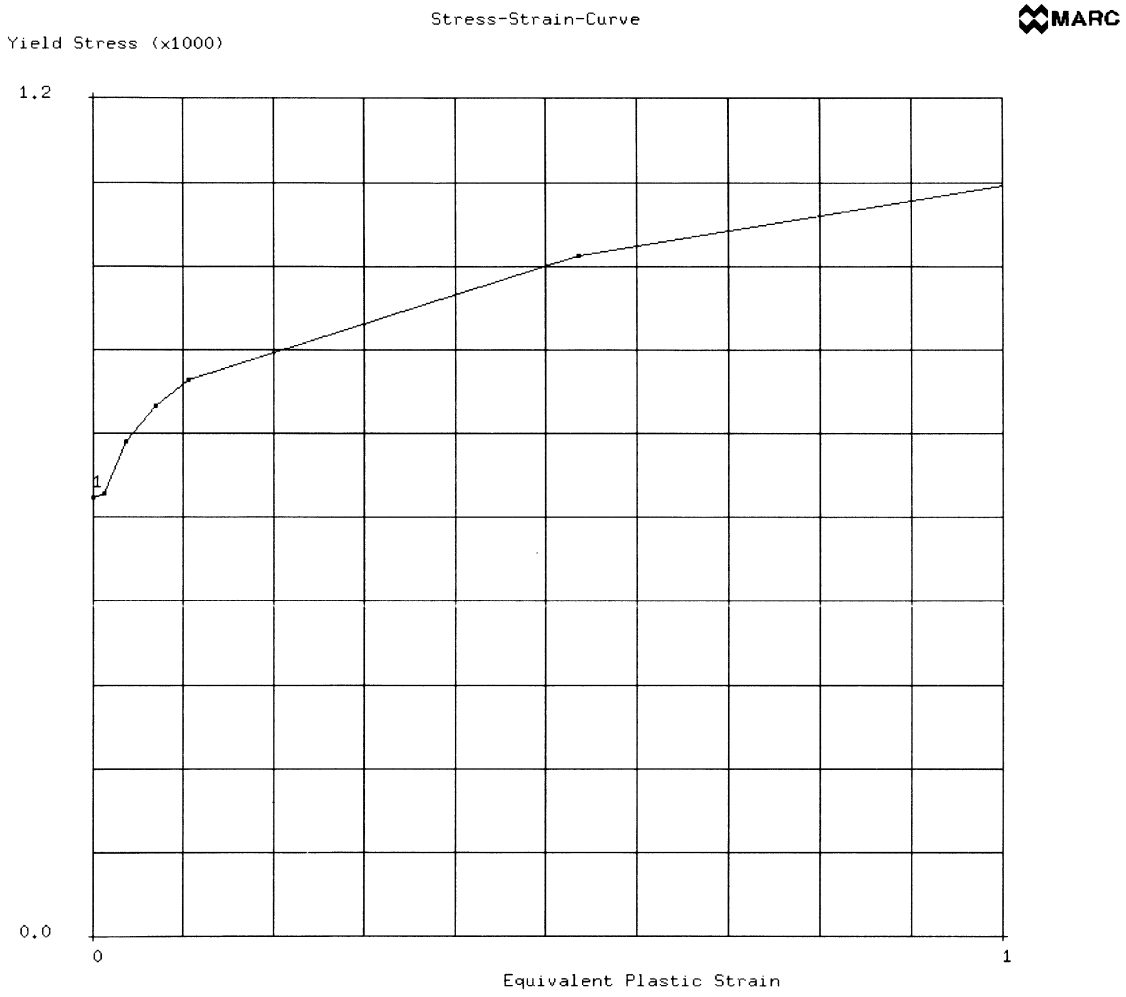

Figure E 3.28-3 Stress-Strain Curve

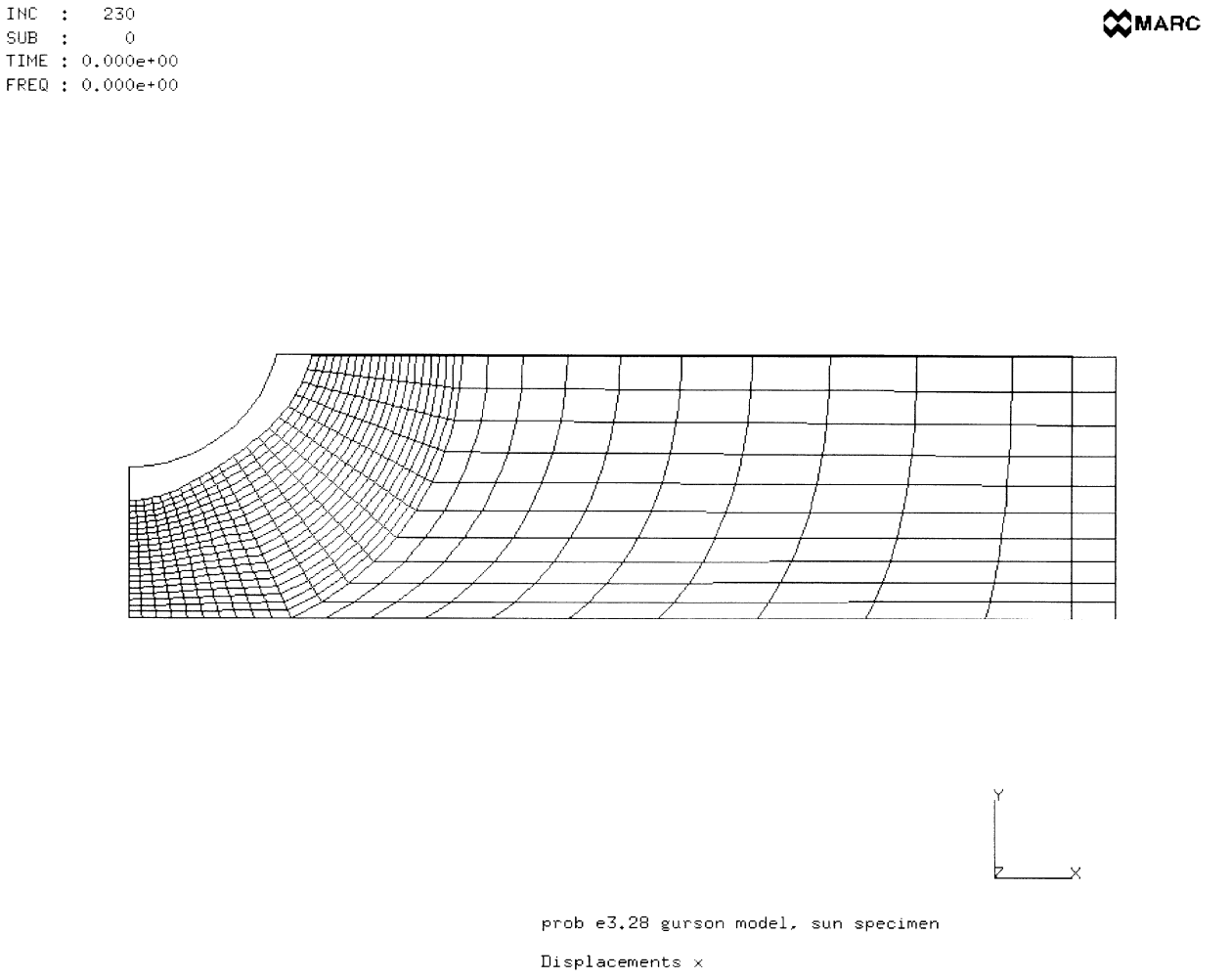

Figure E 3.28-4 Deformed Mesh

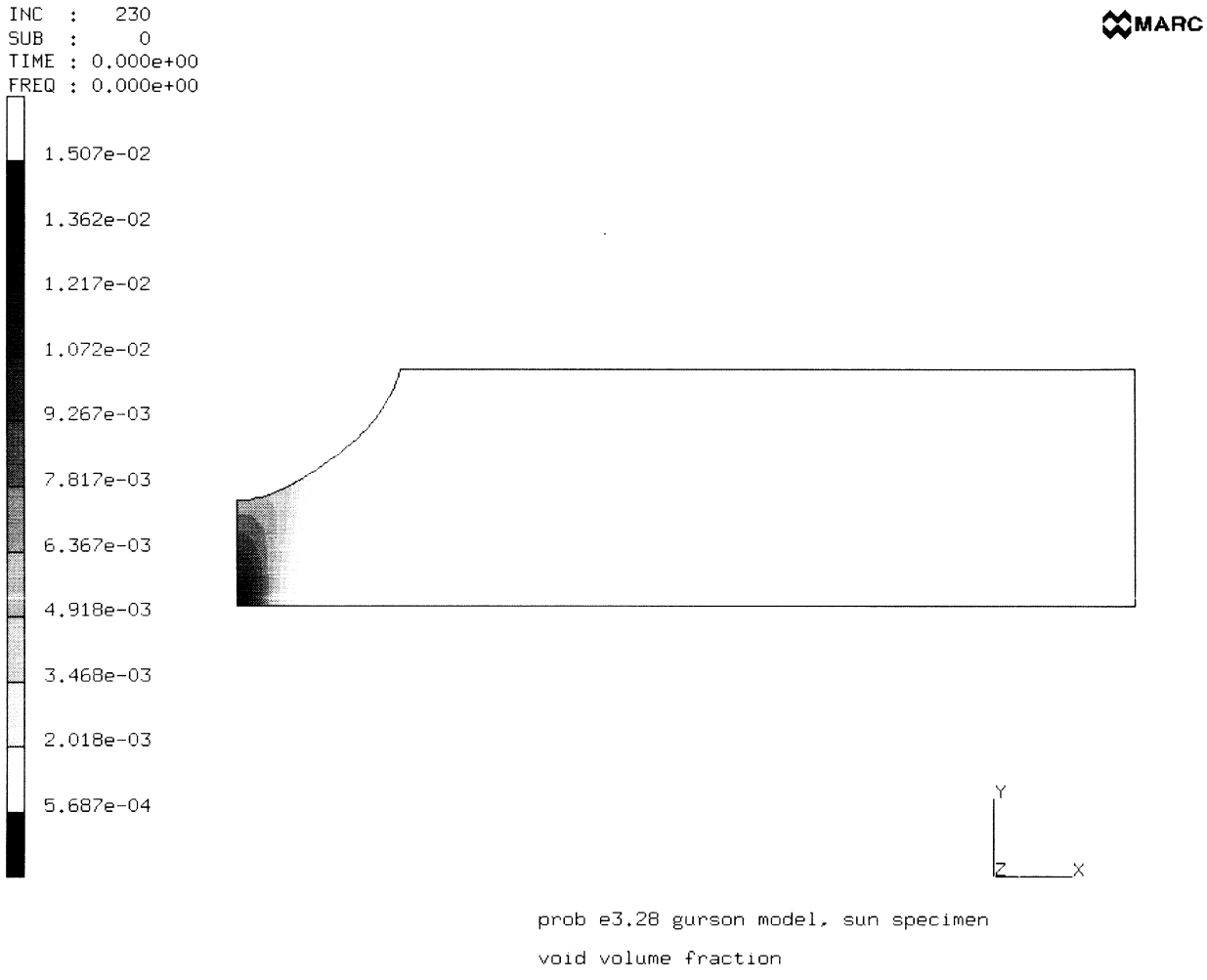

Figure E 3.28-5 Void Volume Fraction

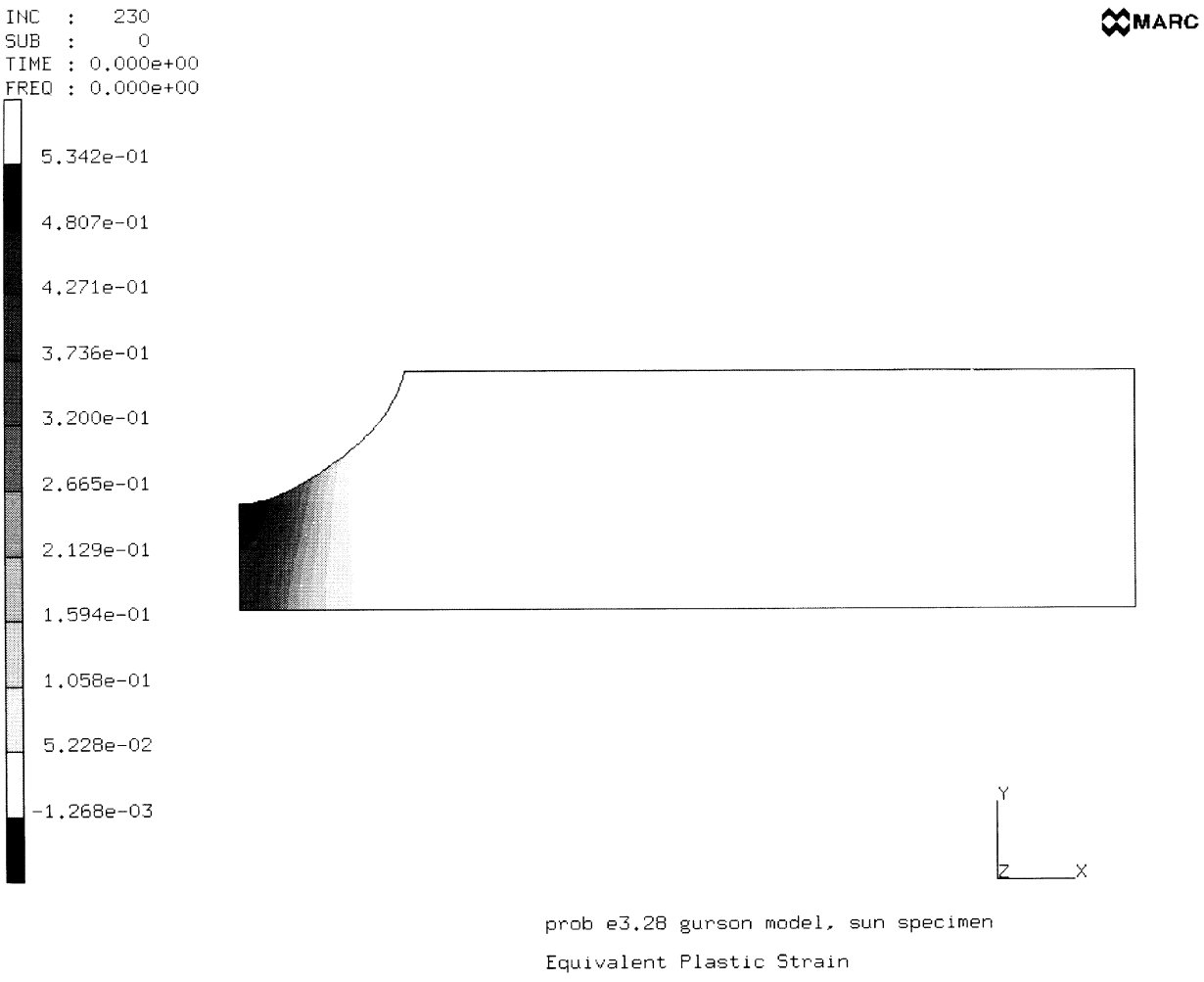

Figure E 3.28-6 Equivalent Plastic Strain

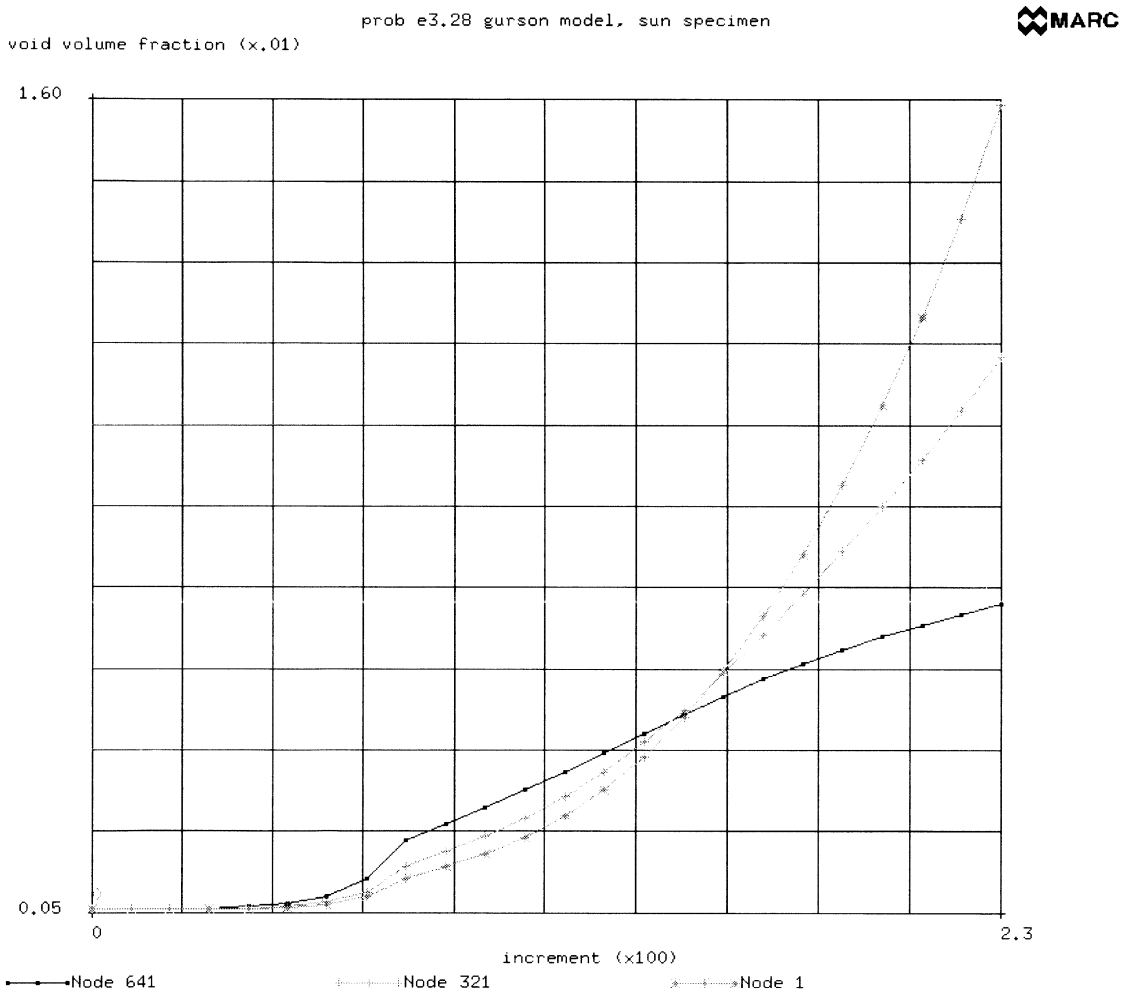

Figure E 3.28-7 Time History of Void Volume Fraction

Volume E
Demonstration Problems

Chapter 4
Large Displacement

E 4.2 Square Plate Under Distributed Load

A simply-supported square plate subjected to uniformly distributed pressure is analyzed. MARC element type 49 is utilized. In the analysis, geometrically nonlinear effects are considered. The AUTO LOAD option is used for the load incrementation. The model and input data of the problem are:

Element

Library element type 49, a 6-node triangular thin-shell element, is used.

Model

The dimensions of the plate and the finite element mesh are shown in Figure E 4.2-1. Based on symmetry considerations, only one quarter on the plate is modeled. The mesh is composed of 32 elements in 81 nodes,

Material Properties

The material is elastic with a Young's modulus of 10×10^6 N/mm^2 and a Poisson's ratio of 0.3.

Geometry

A uniform thickness of 0.25 mm is assumed. In thickness direction, three layers are chosen using the SHELL SECT parameter option.

Boundary Conditions

Symmetry conditions are imposed on the edges $x = 10$ ($u_x = 0$, $\phi = 0$) and $y = 10$ ($u_y = 0$, $\phi = 0$). Notice that the rotation constraints only apply for the midside nodes. Simply supported conditions are imposed on the edges $x = 0$ and $y = 0$ ($u_x = u_y = u_z = 0$).

Loading

A uniform pressure load of 50 N/mm^2 is applied in ten equally sized increments. The default control settings are used. Relative check on residuals with a tolerance of 0.1.

Results

The displacement history of node 1 is shown in Figure E 4.2-2. For increment 10, stress contours of the von Mises stress in the outer layers are shown in Figure E 4.2-3 and Figure E 4.2-4. Due to the geometrically nonlinear effects, the stress distribution is clearly not symmetric with respect to the midplane of the plate. The deflections at the center of the plate are given by:

Pressure (N/mm^2)	Normalized Deflection w/h	
	MARC	Reference
10	0.86	0.84
20	1.14	1.17
30	1.32	1.37
40	1.47	1.53
50	1.59	1.65

The reference solution can be found in "Bending of Rectangular Plates with Large Deflection" by S. Levy in the NACA Report 737, Washington, DC, 1942.

Summary of Options Used

Listed below are the options used in example e4x2.dat:

Parameter Options

ALL POINTS
ELEMENTS
DIST LOADS
END
SET NAME
SHELL SECT
SIZING

Model Definition Options

CONNECTIVITY
COORDINATES
DEFINE
END OPTION
FIXED DISP
GEOMETRY
ISOTROPIC
NO PRINT
OPTIMIZE
PRINT
SOLVER

Load Incrementation Options

AUTO LOAD
CONTINUE
CONTROL
DIST LOAD
TIME STEP

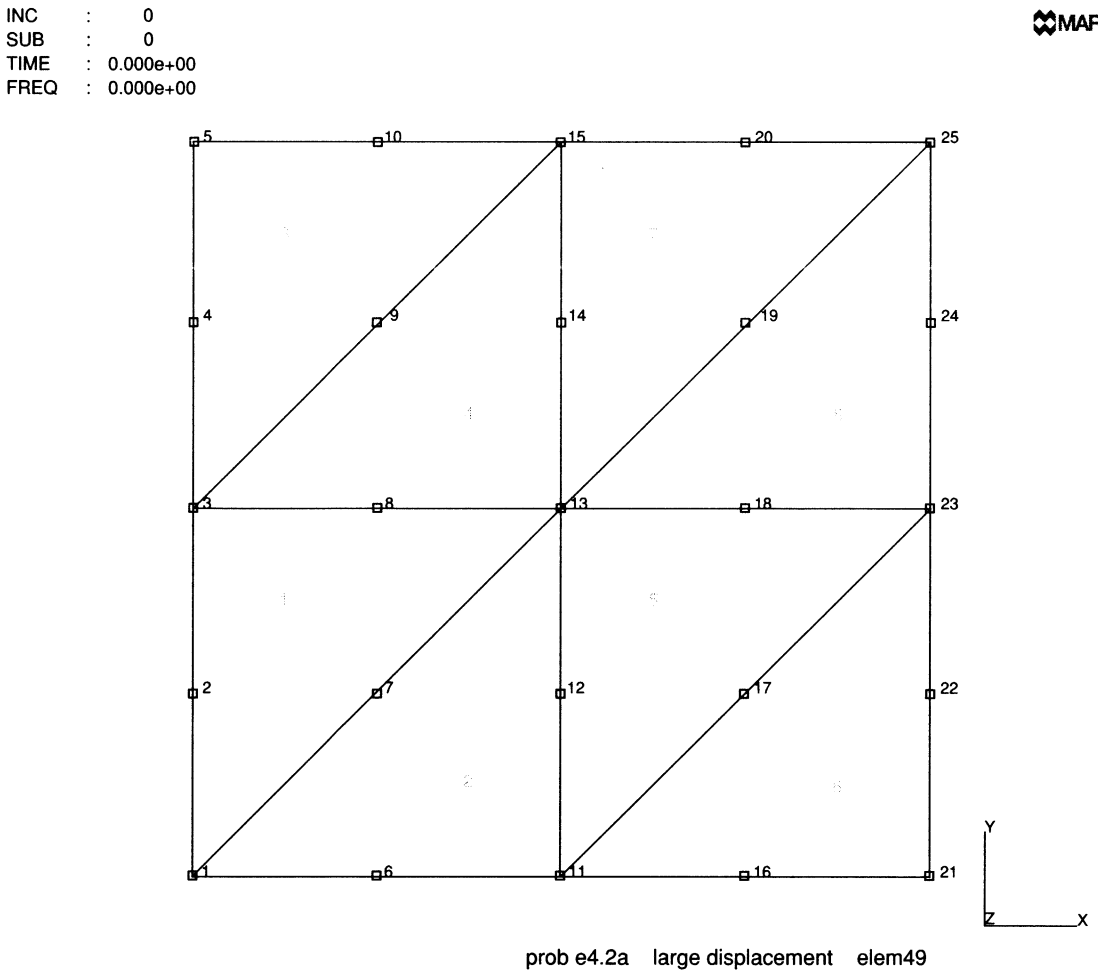

Figure E 4.2-1 Square Plate, Finite Element Mesh and Boundary Conditions

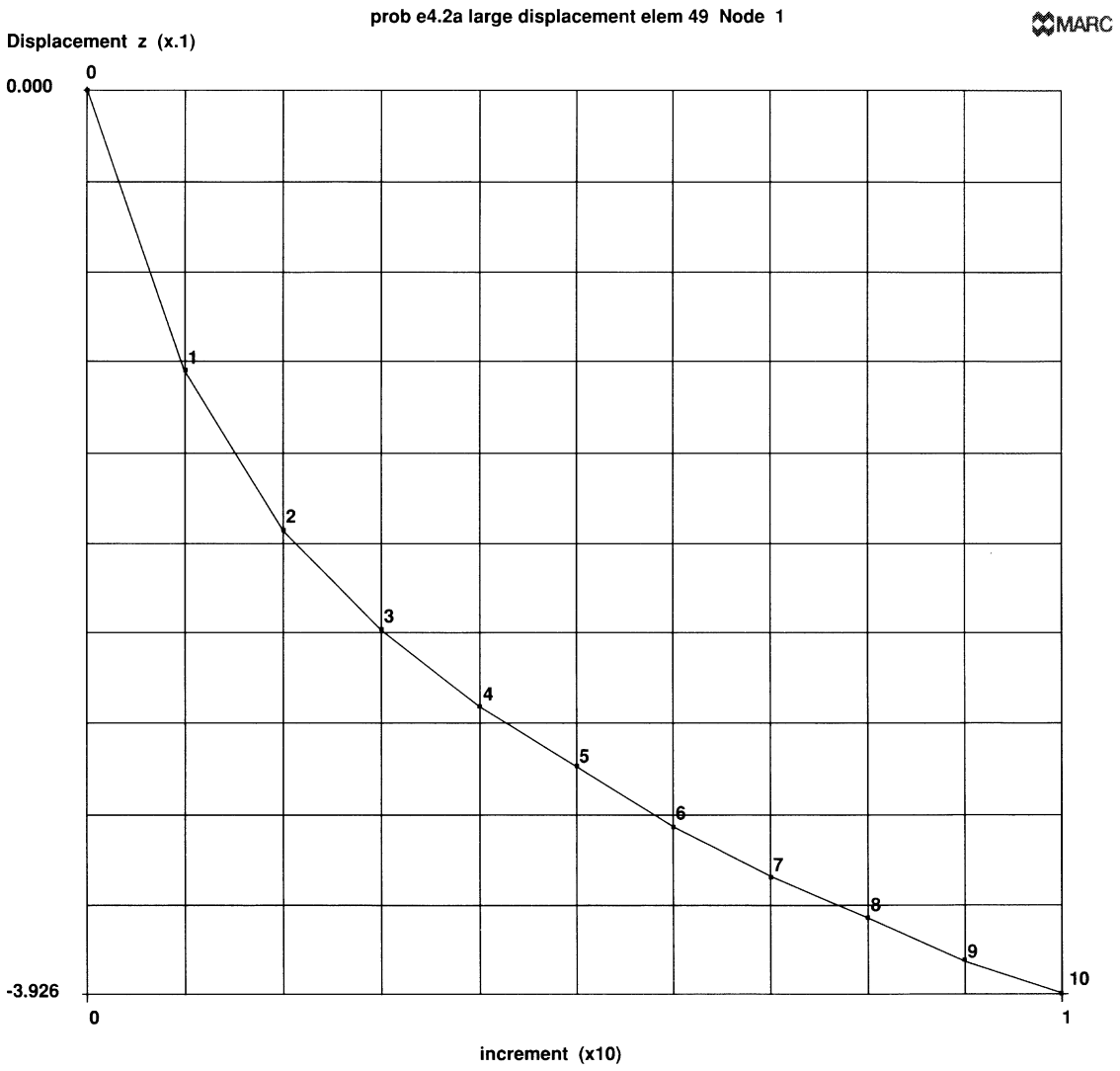

Figure E 4.2-2 Node 1 Displacement History

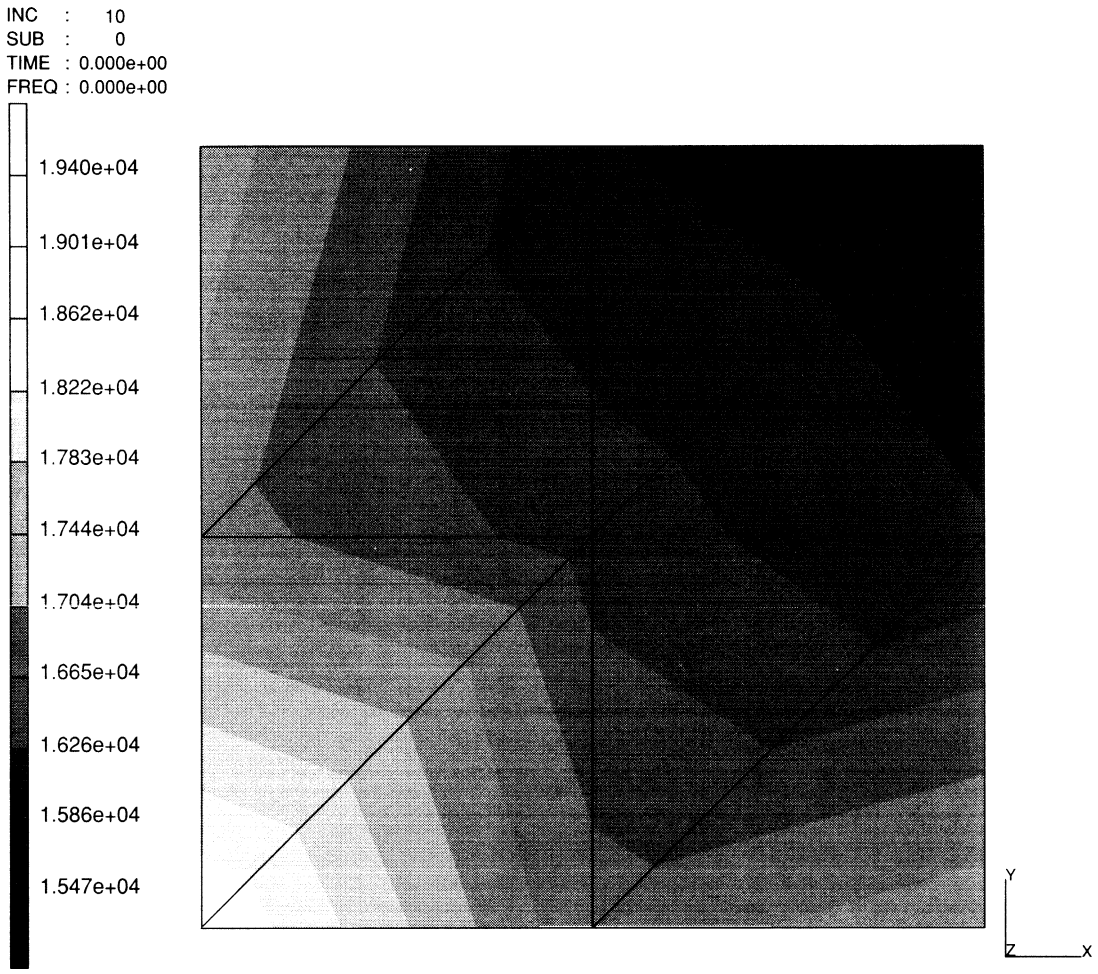

Figure E 4.2-3 Stress Contour of von Mises Stress in Layer 1 (Increment 10)

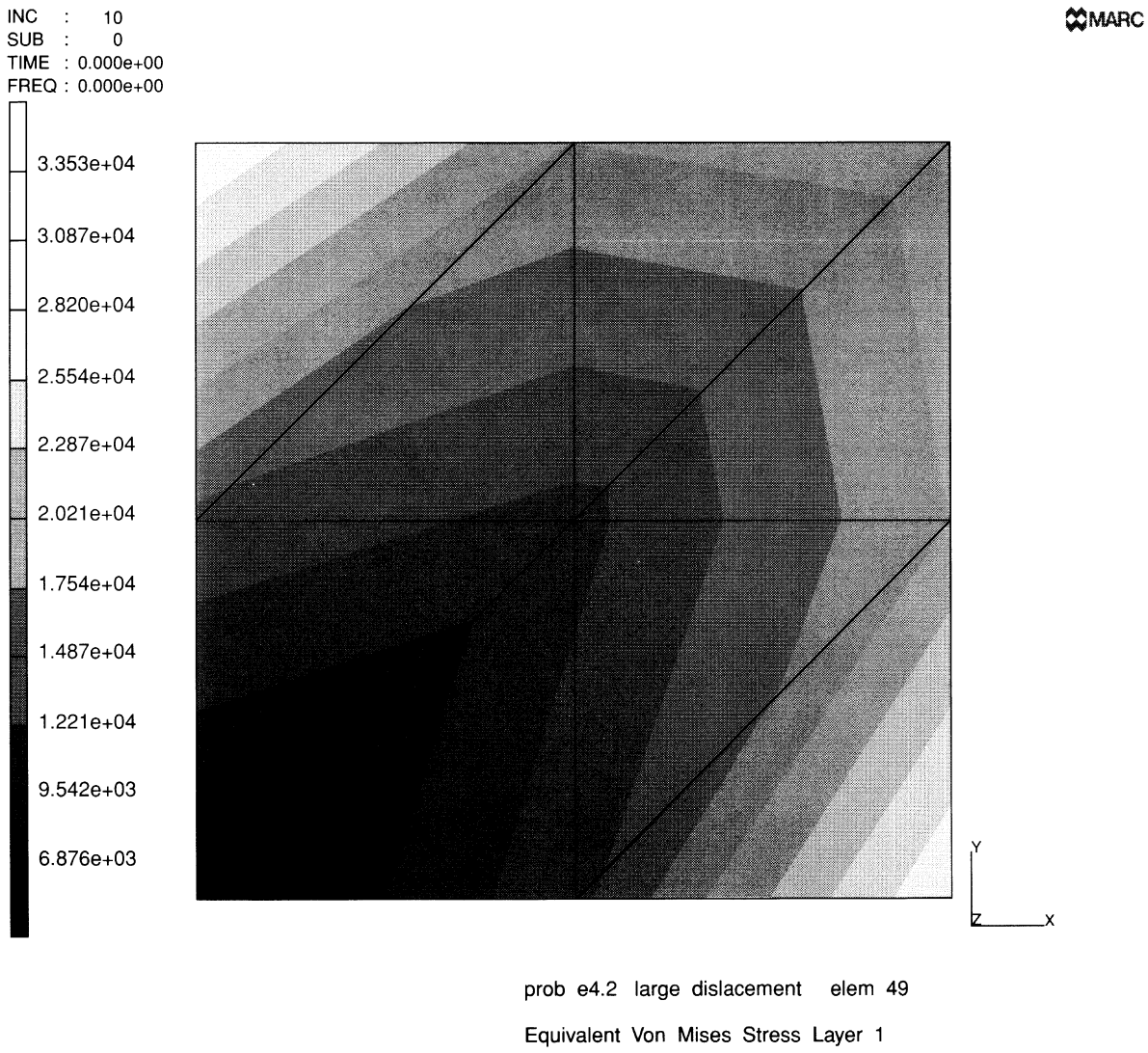

Figure E 4.2-4 Stress Contour of von Mises Stress in Layer 3 (Increment 10)

E 4.7 Post-Buckling Analysis Of A Deep Arch

A point load is applied to the apex of a semicircular arch. The arch gradually collapses as the applied load is incremented. The arch configuration after collapse is calculated and plotted. The load-displacement curve at the apex is plotted. This analysis utilizes the AUTO INCREMENT option to control the magnitude of the incremental solution and hence the magnitude of the load increment. The second analysis is the same as the first, but the arch is not allowed to penetrate itself. The analysis is performed elastically for both the pre- and post-buckling configurations.

Element

Element type 16 is a 2-node curved beam, with cubically interpolated global displacement and displacement derivatives. There are four degrees of freedom at each node. Membrane and curvature strains are output as well as axial stresses through the element thickness.

Model

The arch is modeled using 20 beam elements and 21 nodes. Only connectivity of element 1 is specified in the input. The connectivities for elements 2 through 21 are generated by option CONN GENER using element 1 as a model. The node coordinates are generated using user subroutine UFXORD. The coordinates are generated around a semicircle of radius 100 inches subtending an angle of 215 degrees. The finite element mesh is shown in Figure E 4.7-1.

Material Properties

A Young's modulus of 12.0×10^6 psi and a Poisson's ratio of 0.2 are specified in the ISOTROPIC option.

Geometry

The beam thickness is 1 inch, as specified in EGEOM1. The width of the arch elements are specified as 1 inch in EGEOM2. Omission of the third field indicates a constant beam thickness.

Loading

The total applied load is specified in the POINT LOAD block, following the END OPTION. A total load of 1200 pounds is applied at node 11, over a maximum of 300 increments. The maximum load that may be applied in the first increment is 10% of the total load, or 120 pounds. These maxima are set in the AUTO INCREMENT option.

Boundary Conditions

The arch is pinned at one support and built in at the other. Thus, the degrees of freedom at node 1 (u and v) are constrained. At node 21, a coordinate transformation is carried out such that the boundary conditions here are simply specified. So, in the transformed coordinates at node 21, degrees of freedom u′, v′ and $\partial u'/\partial s$ are constrained.

Contact

The results of the first analysis indicate that the arch would pass through itself which is physically impossible. To prevent this, the second data set uses the CONTACT option.

This option declares that here is only one flexible body which is made up of 20 elements. In order to avoid unexpected separation, the high separation forces are entered as the arch hits the left support. Contact tolerance distance is 0.02 which is 2% of thickness of shell.

Notes

A 5% residual force relative error is specified in the CONTROL OPTION.

The option SHELL SECT reduces the number of integration points through the element thickness from a default value of 11 to the specified three points.This greatly reduces computation time with no loss of accuracy in an elastic analysis.

The PRINT parameter option is set to 3. This option forces MARC to solve nonpositive definite matrices; this parameter is required for all post-buckling analyses.

The UPDATE parameter option assembles the stiffness matrix of the current deformed configuration; as well, this option writes out the stresses and strains in terms of the current deformed geometry.

The UDUMP model definition option indicates by default that all nodes and all elements will be made available for postprocessing by user subroutines IMPD and ELEVAR. In this example, the data is postprocessed to create a load-displacement curve for the arch.

Results Without CONTACT

The analysis ends in increment 75, at a load of 290.4 pounds. The total requested load is not reached due to an excessive number of recycles required for solution in the last increment. Resetting the maximum number of recycles and residual load tolerance would allow the analysis to be continued using the RESTART tape generated during the analysis. Displaced mesh plots are shown in Figure E 4.7-2 (a) through Figure E 4.7-2 (d). The displaced plots are obtained using the second data set. The POSITION option is used to access the restart tape at several different

increments. The structure actually loops through the pinned support, as there is no obstruction to this motion. A load-deflection curve is plotted for node 77 in Figure E 4.7-3.

Results With CONTACT

In example e4x7b, as the CONTACT option is used, the left support will prevent the arch from passing through and give the reasonable deformation shape. Figure E 4.7-4 through Figure E 4.7-6 show a progression of the deformation. From the load deflection curve (Figure E 4.7-7), you will observe the strong nonlinearities due to the contact which leads to a stiffening effect in the structure and a different snap-through behavior.

Summary of Options Used

Listed below are the options used in example e4x7.dat:

Parameter Options

END
LARGE DISP
PRINT
SHELL SECT
SIZING
TITLE
UPDATE

Model Definition Options

CONN GENER
CONNECTIVITY
CONTROL
END OPTION
FIXED DISP
GEOMETRY
ISOTROPIC
PRINT CHOICE
RESTART
TRANSFORMATIONS
UDUMP
UFXORD

Load Incrementation Options

AUTO INCREMENT
CONTINUE
POINT LOAD

Listed below is the user subroutine found in u4x7.f:

UFXORD

Listed below are the options used in example e4x7b.dat:

Parameter Options

END
LARGE DISP
PRINT
SHELL SECT
SIZING
TITLE
UPDATE

Model Definition Options

CONNECTIVITY
CONTACT
CONTROL
COORDINATE
END OPTION
FIXED DISP
GEOMETRY
ISOTROPIC
PRINT CHOICE
POINT LOAD
POST

Load Incrementation Options

AUTO INCREMENT
CONTINUE
POINT LOAD

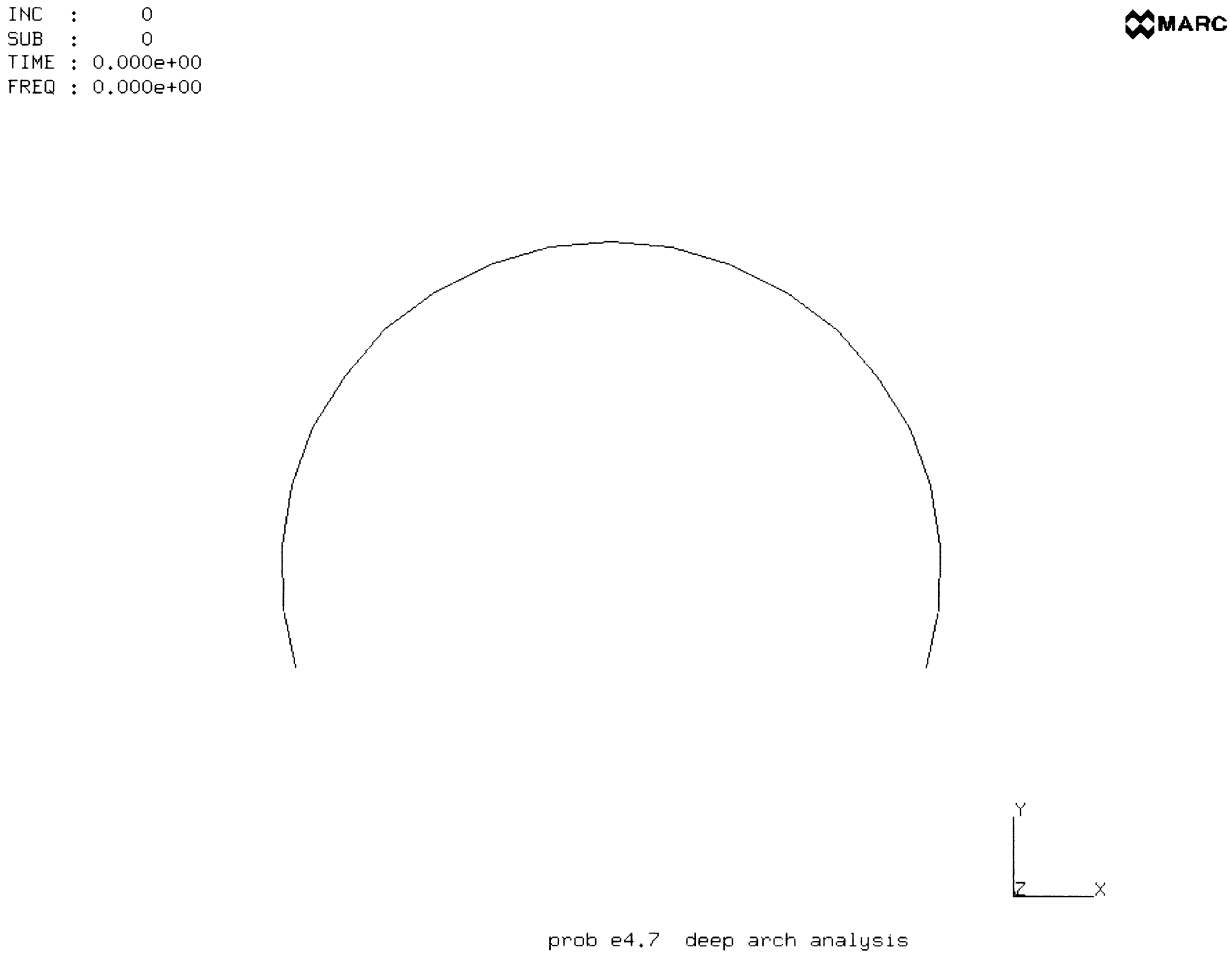

Figure E 4.7-1 Deep Arch

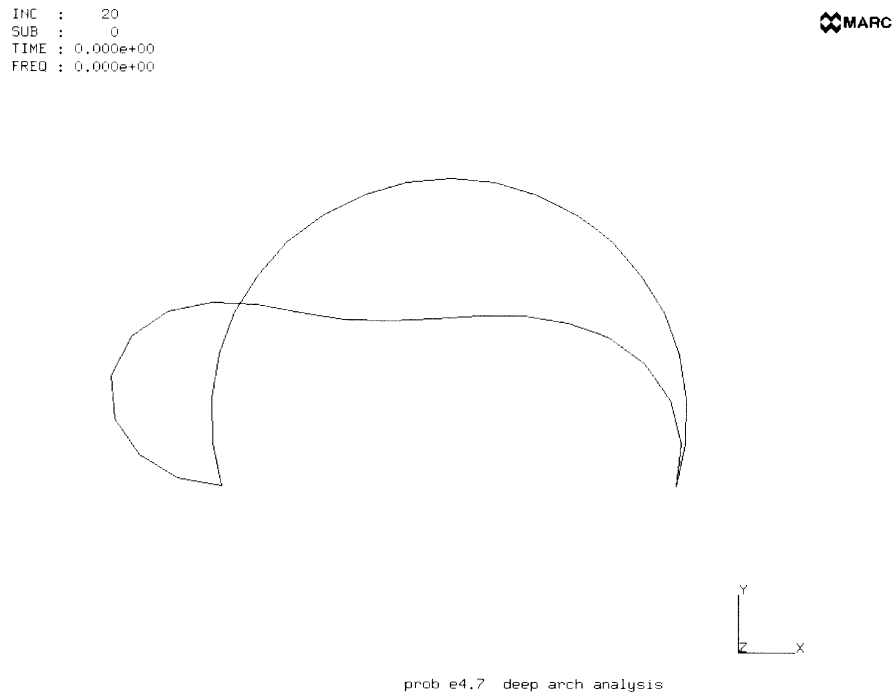

(a)

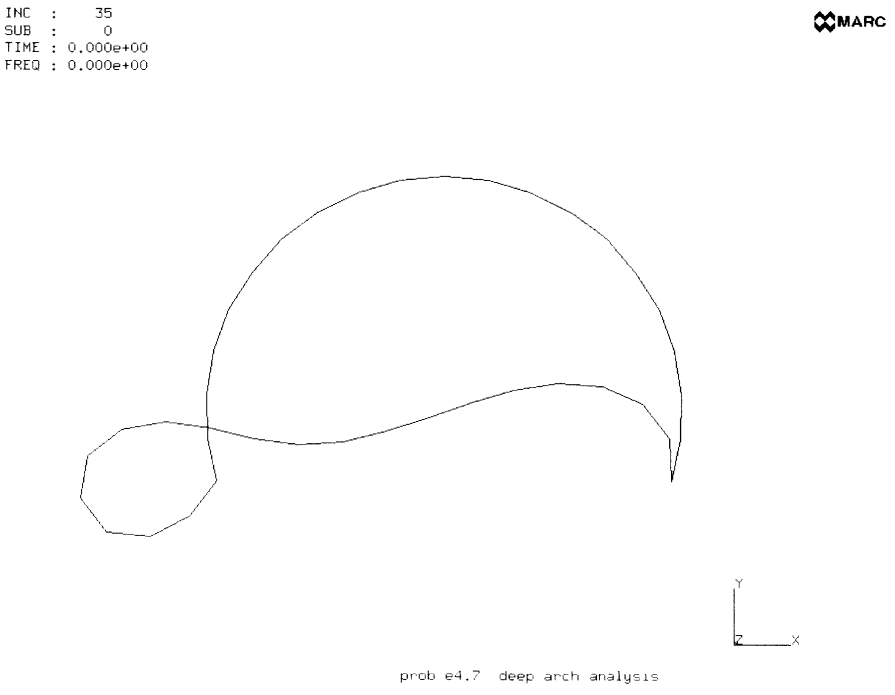

(b)

Figure E 4.7-2 Displaced Mesh

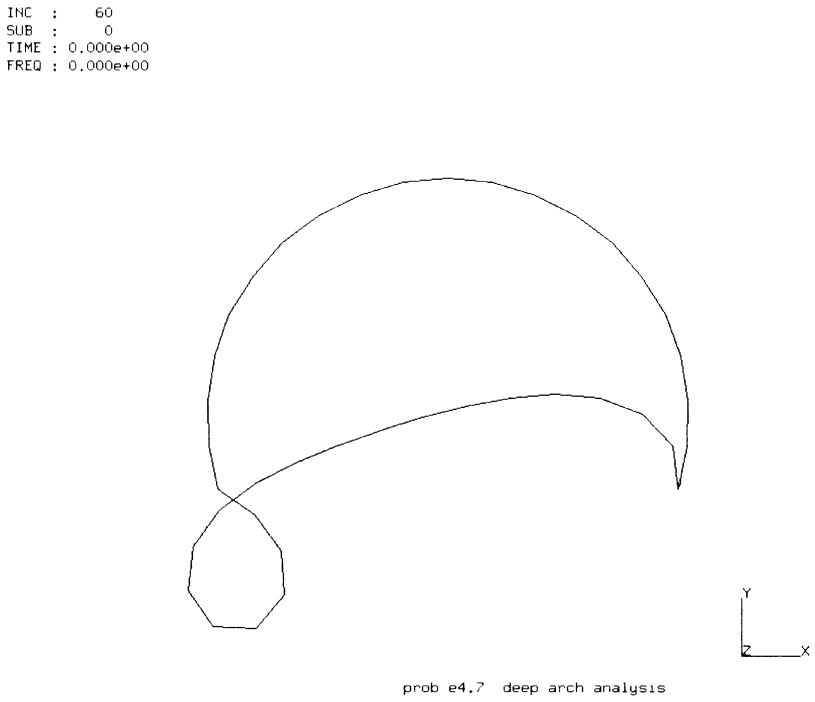

(c)

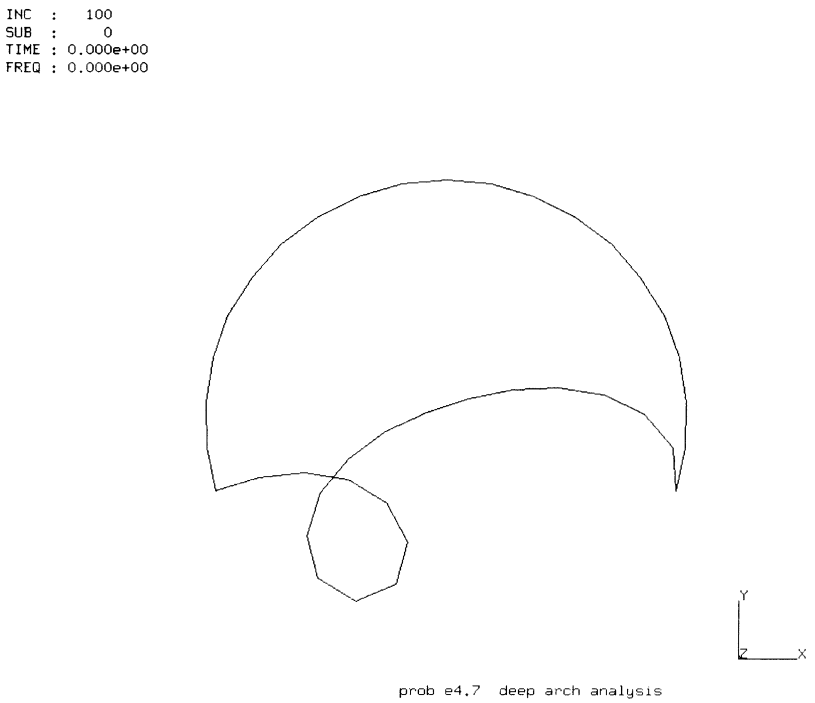

(d)

Figure E 4.7-2 Displaced Mesh (Continued)

Figure E 4.7-3 Load vs Displacement (Node 77) – No Contact

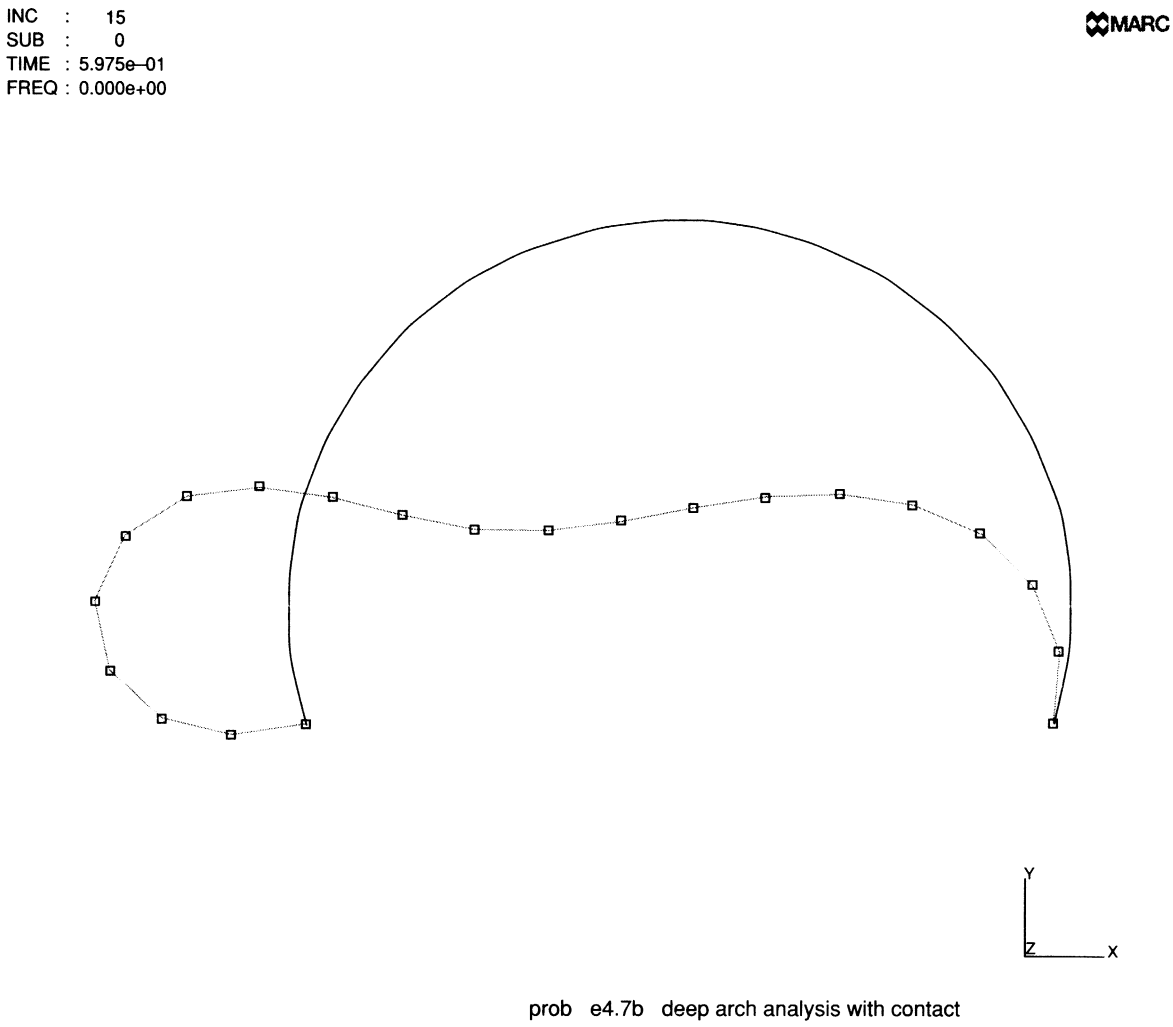

Figure E 4.7-4 Displaced Mesh with Contact at Pin

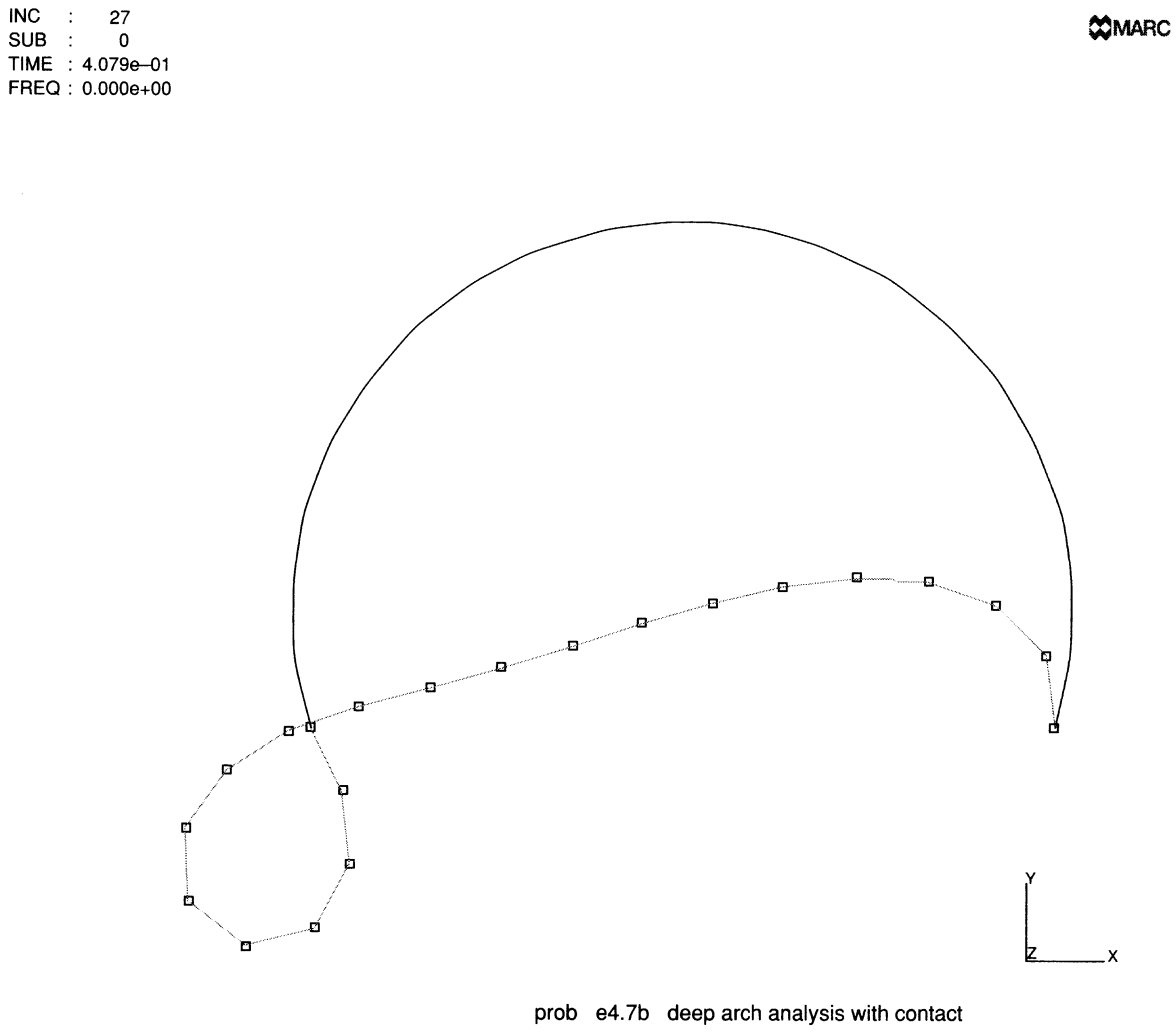

Figure E 4.7-5 Displaced Mesh With Contact at Pin

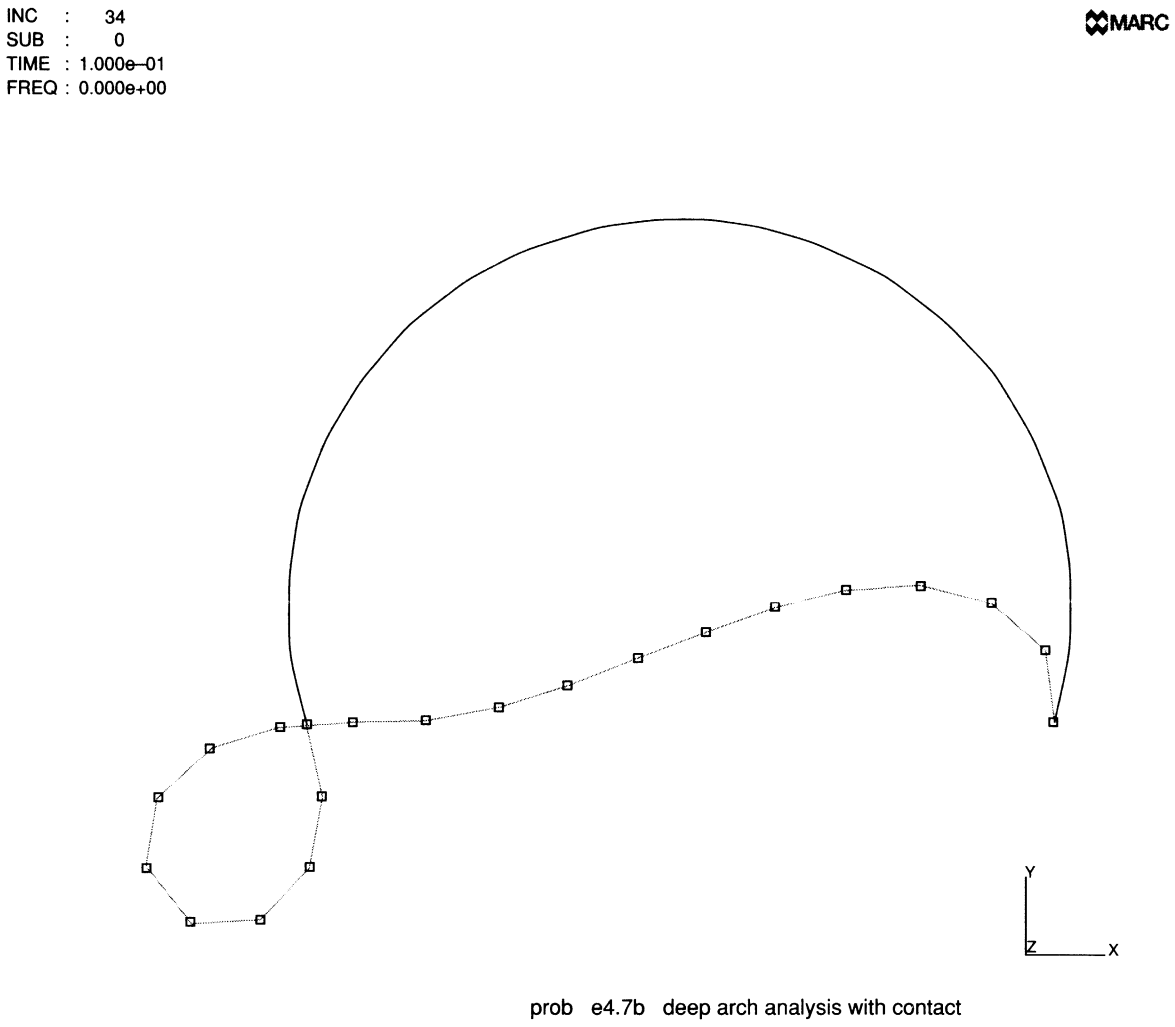

Figure E 4.7-6 Displaced Mesh With Contact at Pin

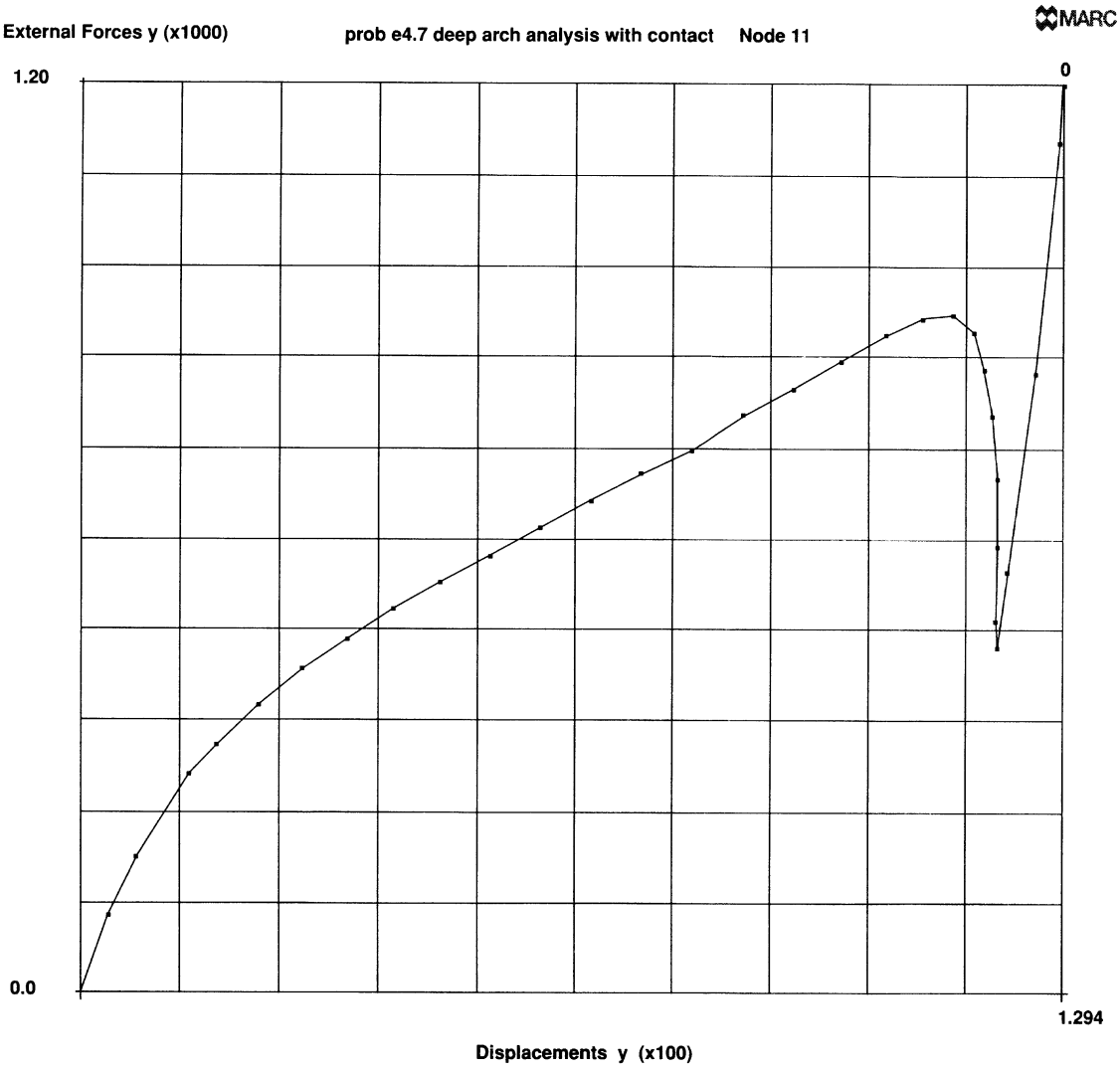

Figure E 4.7-7 Load vs Displacement (Node 77) With Contact at Pin

Volume E
Demonstration Problems

Chapter 5
Heat Transfer

E 5.16 Three Dimensional Thermal Shock

The bar of a rectangular cross section is initially at rest. At time t = 0, one end of the bar is held at a fixed temperature of 1000°F, and a transient conduction problem is solved.

Element (Ref B44.1, B123.1 and B133.1)

Element types 44 and 133 are second-order isoparametric three dimensional heat conduction elements. There are twenty nodes for brick element type 44 and 10 nodes for the tetrahedral element type 133. Element type 123 is an 8-node brick with reduced integration and hourglass control.

Model

The bar cross section is square with a thickness of one inch and a length of two inches. This transient conduction problem is performed for three meshes comprised of element types 44, 123 and 133.

Thermal Properties

The isotropic thermal conductivity value of 0.42117E-5 Btu/sec.-in.-°F. The specific heat is 0.3523E-3 Btu/lb°F. The mass density is 0.7254E-3 lb/cu.in.

Thermal Boundary Conditions

The initial temperature distribution is that all nodes have a temperature of 0.0°F. At time t = 0, the nodal temperatures of one end of the bar are fixed at 1000°F, and a transient conduction problem is solved to its completion at steady state, where all nodes will have a final temperature of 1000°F.

Control for Thermal Analysis

The maximum number of time points are fixed at 100. The maximum change in nodal temperature will be 100°F.

Thermal History

A transient thermal analysis is specified via the TRANSIENT option, with the automatic time stepping feature turned on. The initial time increment is 1.0E-2 seconds, with a final time period of 10 seconds.

Results

From the temperature history shown in Figure E 5.16-1, Figure E 5.16-3, and Figure E 5.16-5 for element types 44, 123, and 133, respectively, the automatic time stepping feature shows ever increasing time steps as the solution approaches steady state. The temperature of the free end goes slightly negative by about a tenth of a degree for element types 123 and 133. This effect has been minimized by the

inclusion of the LUMP parameter option which instructs the MARC program to lump the capacitance matrix, instead of using the consistent capacitance matrix which is the default. There is virtually no difference in the thermal history of the free end between different element types. Figure E 5.16-2, Figure E 5.16-4, and Figure E 5.16-6 are iso-thermal surfaces at a time when the free end starts to heat up significantly. These iso-thermal surfaces should be flat and perpendicular to the axis of the bar. The iso-thermal surfaces become flatter as the bar becomes hotter. Also, the iso-thermal surfaces are more irregular for the tetrahedron mesh than the brick mesh, because the brick element faces are either perpendicular or parallel to the head flow. This effect is minimized if more tetrahedron elements are used.

Summary of Options Used

Listed below are the options used in example e5x16a.dat:

Parameter Options

ELEMENT
END
HEAT
LUMP
SIZING
TITLE

Model Definition Options

CONNECTIVITY
CONTROL
COORDINATE
END OPTION
FIXED TEMPERATURE
INITIAL TEMPERATURE
ISOTROPIC
NO PRINT
POST

Load Incrementation Options

CONTINUE
TRANSIENT

Listed below are the options used in example e5x16b.dat:

Parameter Options

ALIAS
ELEMENT
END
HEAT
LUMP
SIZING
TITLE

Model Definition Options

CONNECTIVITY
CONTROL
COORDINATE
END OPTION
FIXED TEMPERATURE
INITIAL TEMPERATURE
ISOTROPIC
POST

Load Incrementation Options

CONTINUE
TRANSIENT

Time	Temperature (°F)	Time	Temperature (°F)
0.0	0.0		
1.82307E-04	7.62101E-02	8.46059E-02	4.34587E+02
3.64615E-04	2.46594E-01	1.00722E-01	5.12089E+02
5.92499E-04	5.48778E-01	1.20868E-01	5.93519E+02
8.77355E-04	9.32763E-01	1.41014E-01	6.61590E+02
1.30464E-03	1.32789E+00	1.66196E-01	7.29694E+02
1.83874E-03	1.53547E+00	1.97673E-01	7.94479E+02
2.63990E-03	1.53524E+00	2.44890E-01	8.60475E+02
3.84163E-03	1.49460E+00	3.03910E-01	9.12322E+02
5.64423E-03	2.05263E+00	3.92441E-01	9.53537E+02
7.89748E-03	4.10911E+00	5.25236E-01	9.80063E+02
1.07140E-02	9.03647E+00	7.24430E-01	9.93345E+02
1.42348E-02	1.88757E+01	1.02322E+00	9.98334E+02
1.86356E-02	3.63171E+01	1.47141E+00	9.99697E+02
2.41367E-02	6.43750E+01	2.14369E+00	9.99961E+02
3.23884E-02	1.14785E+02	3.15211E+00	9.99996E+02
4.27029E-02	1.82812E+02	4.66473E+00	1.00000E+03
5.55962E-02	2.67022E+02	6.93368E+00	1.00000E+03
6.84894E-02	3.46206E+02	1.00003E+01	1.00000E+03

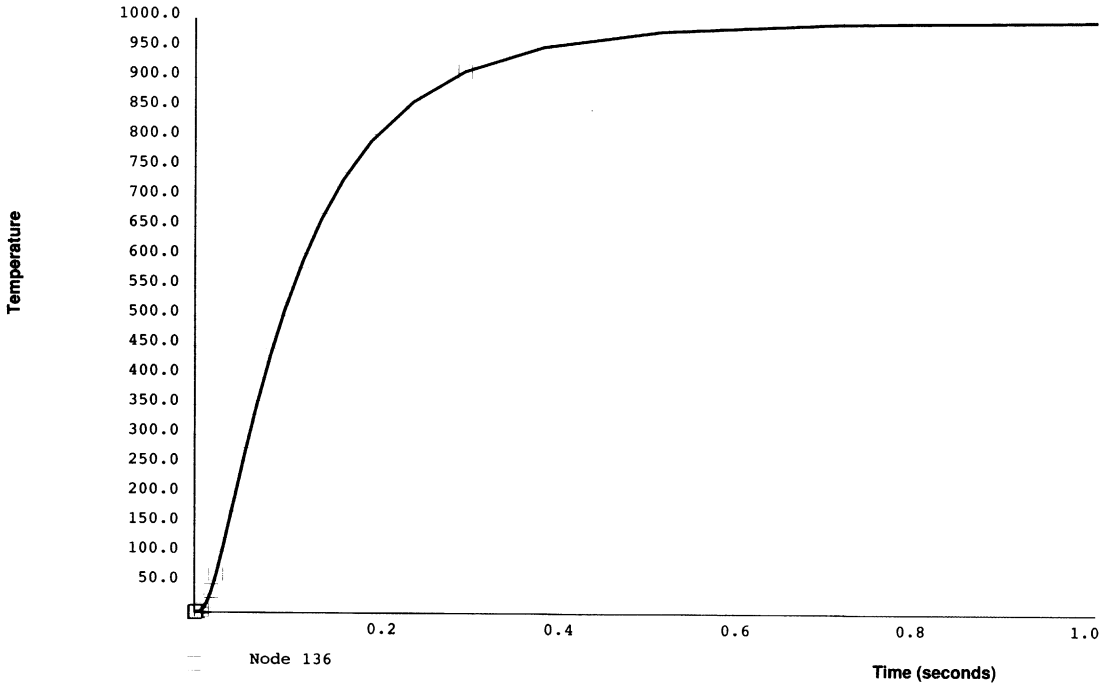

Temperature History (Element Type 44)

Figure E 5.16-1 Temperature History for Free End Node 136 Element Type 44

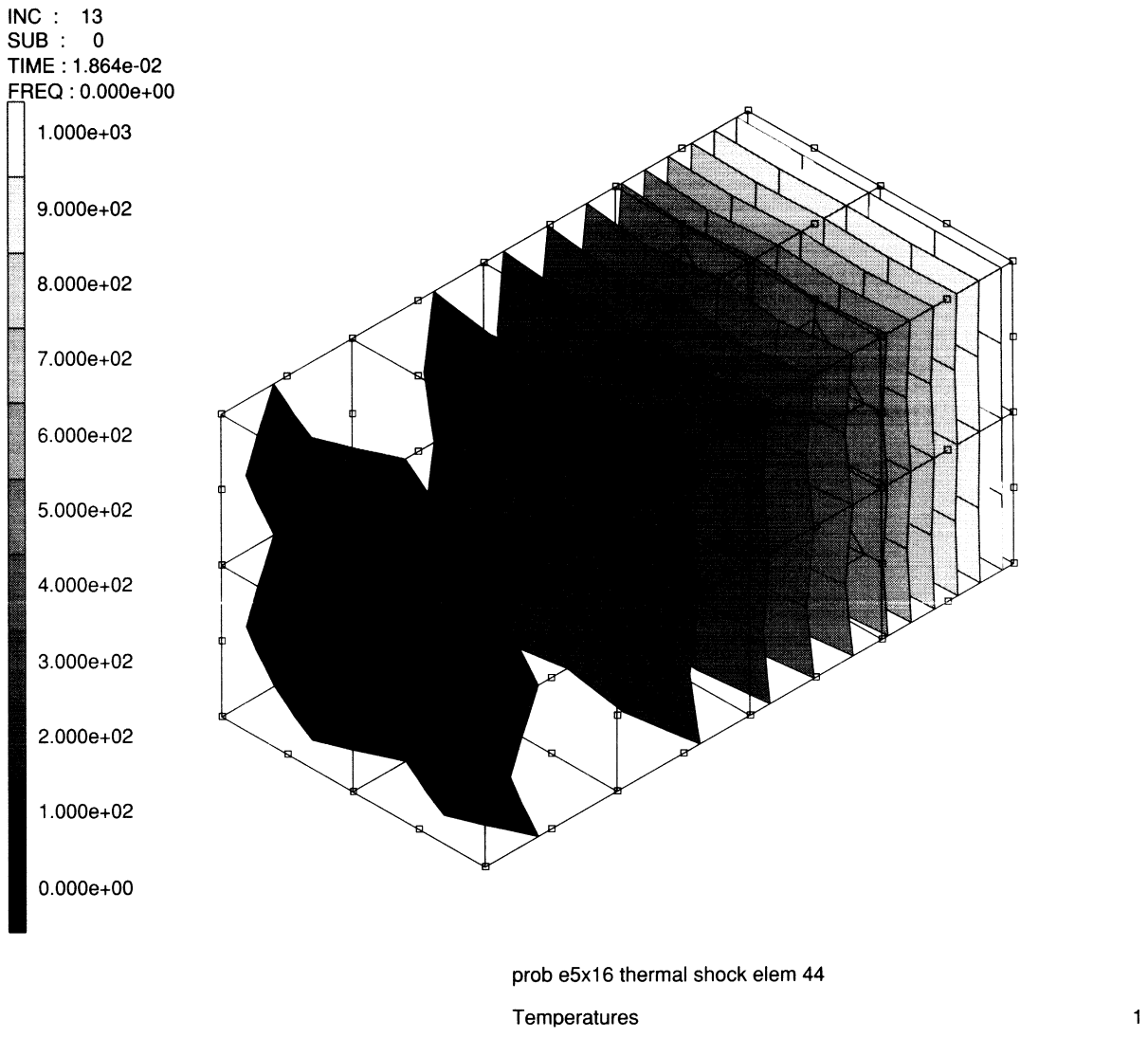

Figure E 5.16-2 Iso-thermal Surfaces at t = 0.0186 seconds (Element Type 44)

Time	Temperature (°F)	Time	Temperature (°F)
0.0	0.0		
1.99113E-04	-3.03712E-03	1.04521E-01	4.03045E+02
3.98226E-04	1.81682E-04	1.24798E-01	4.74083E+02
6.47118E-04	8.32631E-03	1.50145E-01	5.50460E+02
1.02045E-03	3.44541E-02	1.81829E-01	6.29444E+02
1.58046E-03	1.14610E-01	2.13513E-01	6.94672E+02
2.42047E-03	3.42895E-01	2.53118E-01	7.59006E+02
3.68048E-03	9.54424E-01	3.02624E-01	8.19336E+02
5.57050E-03	2.52048E+00	3.76883E-01	8.79604E+02
7.93302E-03	5.50497E+00	4.88272E-01	9.31265E+02
1.08862E-02	1.08245E+01	6.55355E-01	9.67696E+02
1.45776E-02	1.97886E+01	9.05980E-01	9.88009E+02
1.91919E-02	3.40969E+01	1.28192E+00	9.96615E+02
2.61134E-02	6.06809E+01	1.84582E+00	9.99298E+02
3.47652E-02	9.86775E+01	2.69168E+00	9.99896E+02
4.77429E-02	1.59734E+02	3.96047E+00	9.99989E+02
6.39651E-02	2.35397E+02	5.86365E+00	9.99999E+02
8.42428E-02	3.23410E+02	8.71842E+00	1.00000E+03
		1.00001E+01	1.00000E+03

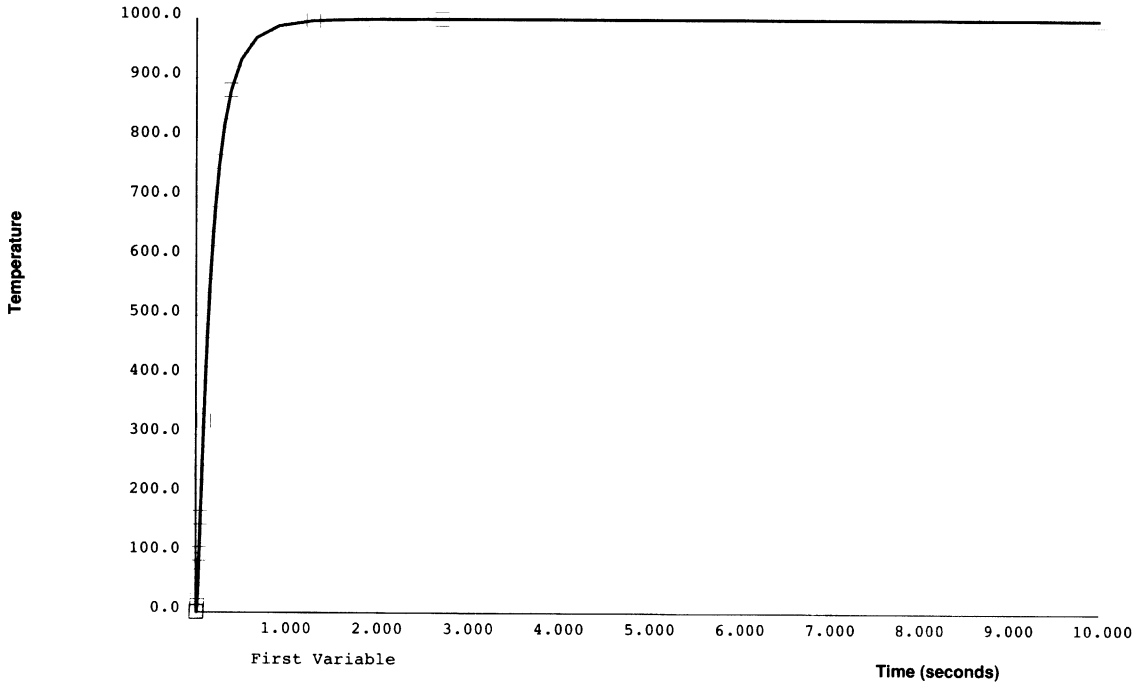

Figure E 5.16-3 Temperature History for Free End Node 126 (Element Type 123)

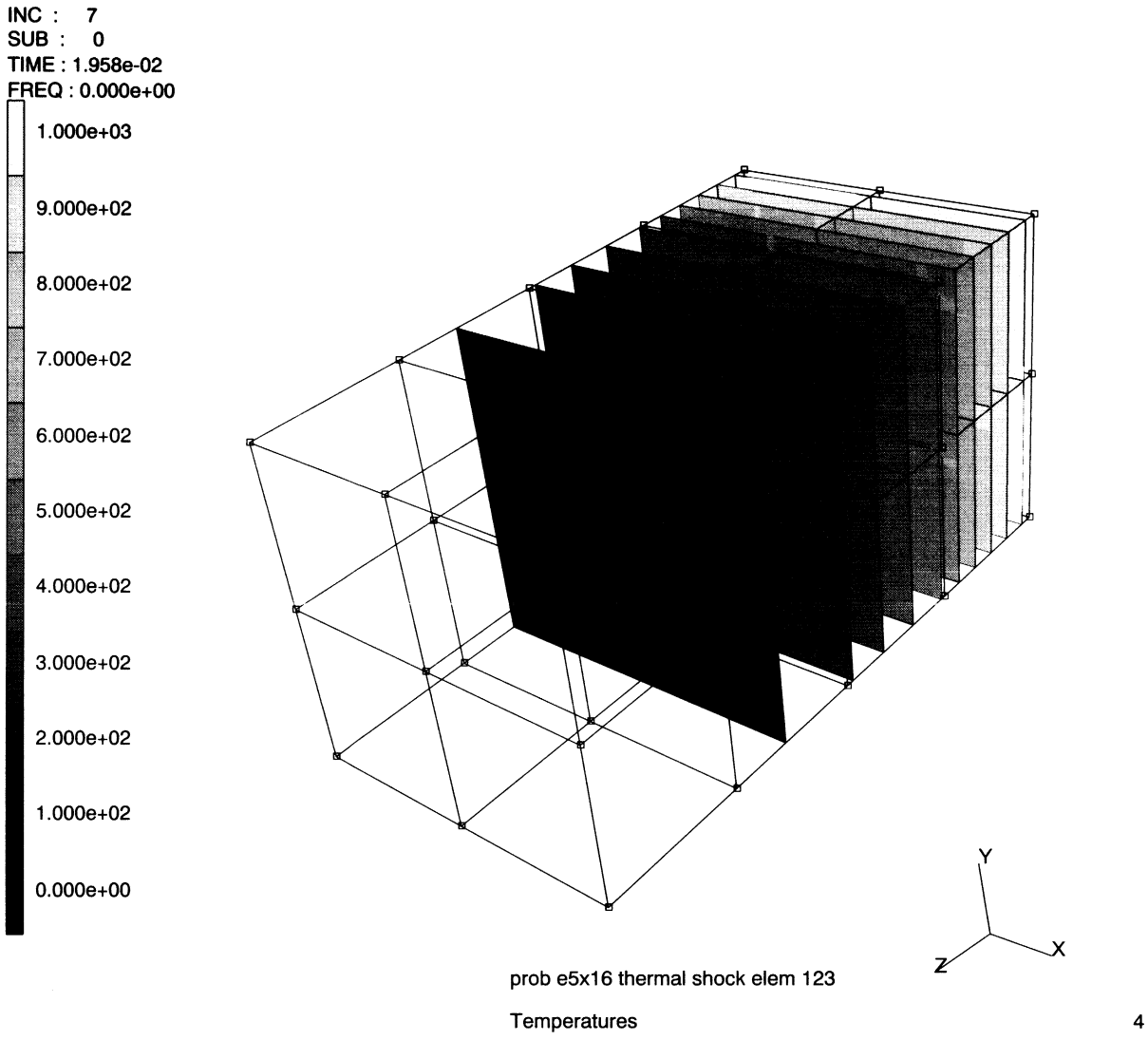

Figure E 5.16-4 Iso-thermal Surfaces at t = 0.0196 seconds (Element Type 123)

Time	Temperature (°F)	Time	Temperature (°F)
0.0	0.0		
7.10402E-04	-1.63117E-01	1.14734E-01	5.64931E+02
1.42080E-03	-3.29948E-01	1.33342E-01	6.33486E+02
2.30881E-03	-4.95783E-01	1.56602E-01	7.03065E+02
3.64081E-03	-6.80945E-01	1.85677E-01	7.70386E+02
5.30582E-03	-7.92613E-01	2.22020E-01	8.31985E+02
7.38707E-03	-4.82283E-01	2.76536E-01	8.91606E+02
1.05090E-02	2.03853E+00	3.58309E-01	9.40608E+02
1.44113E-02	9.60317E+00	4.80968E-01	9.73458E+02
1.92893E-02	2.61956E+01	6.64957E-01	9.90708E+02
2.53867E-02	5.59788E+01	9.40940E-01	9.97545E+02
3.30085E-02	1.02089E+02	1.35492E+00	9.99526E+02
4.25357E-02	1.65698E+02	1.97588E+00	9.99935E+02
5.44447E-02	2.45701E+02	2.90732E+00	9.99994E+02
6.63538E-02	3.21802E+02	4.30449E+00	1.00000E+03
8.12401E-02	4.07738E+02	6.40024E+00	1.00000E+03
9.61264E-02	4.83906E+02	9.54387E+00	1.00000E+03
		1.0000E+01	1.00000E+03

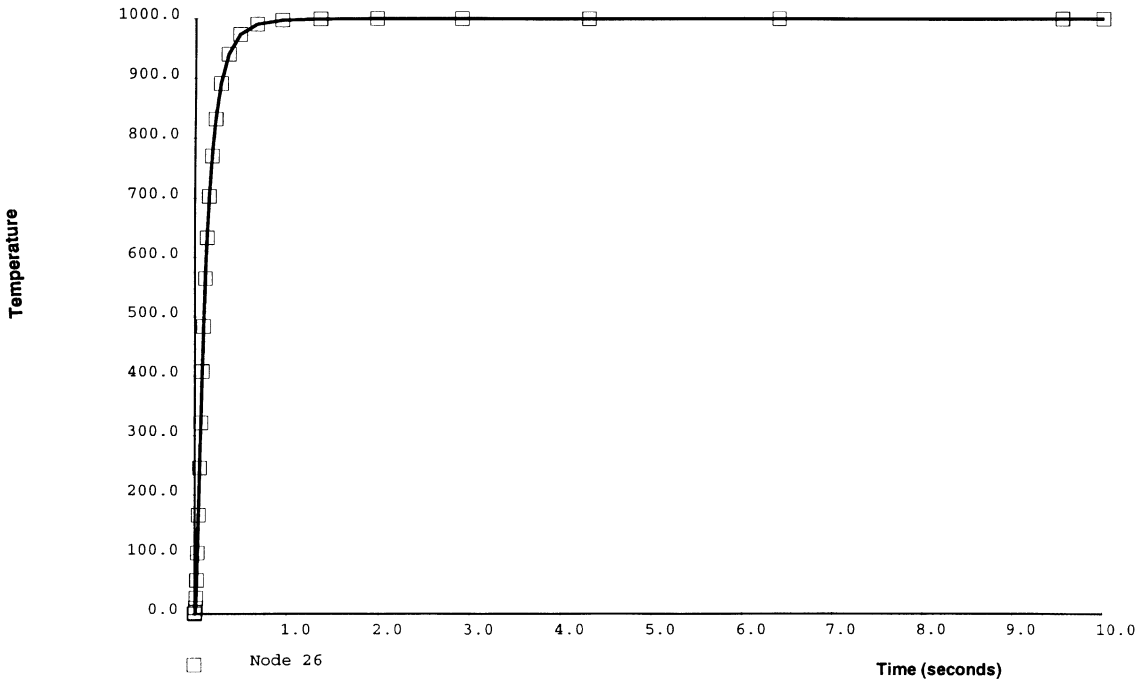

Figure E 5.16-5 Temperature History for Free End Node 26 (Element Type 133)

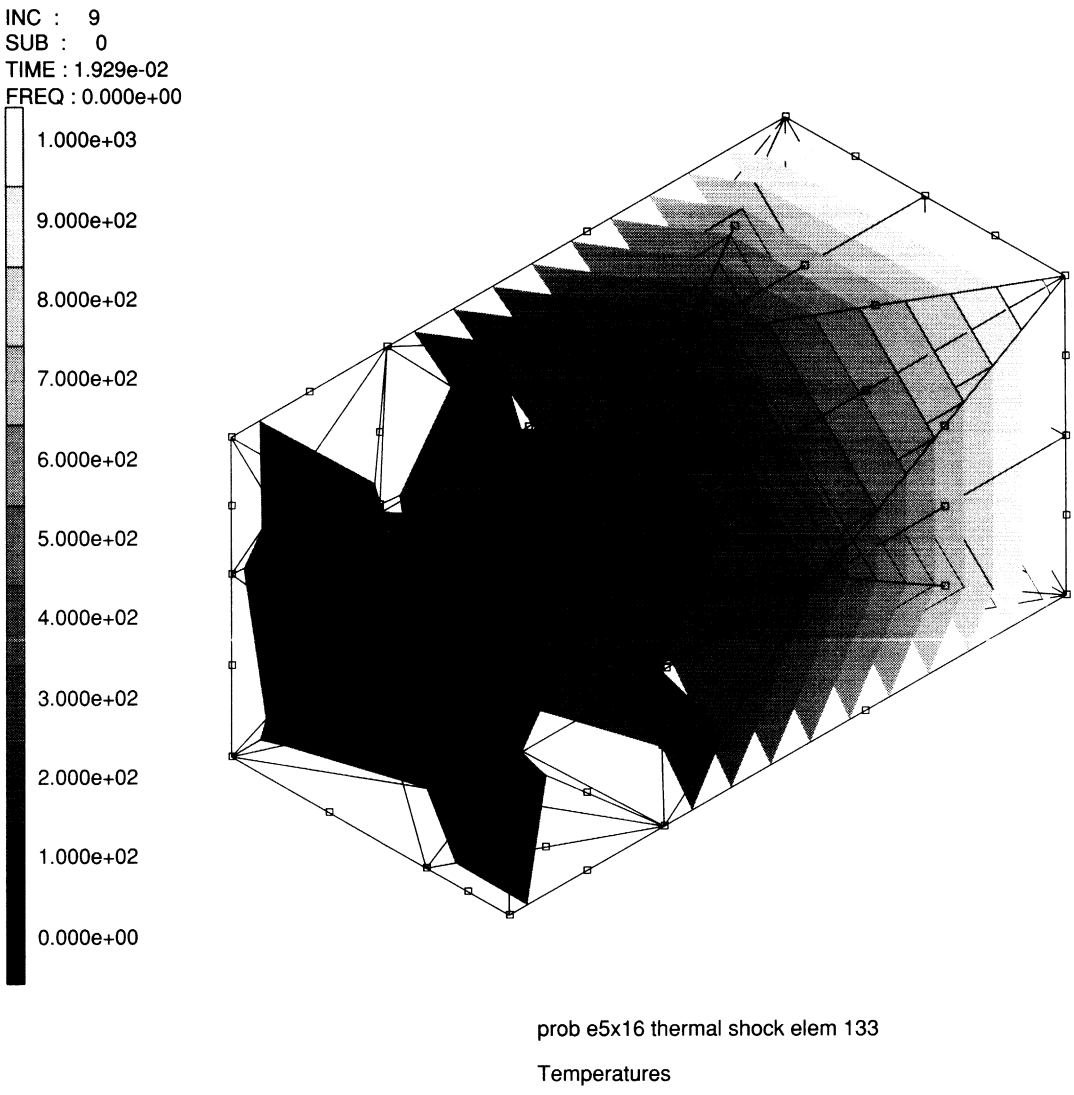

Figure E 5.16-6 Iso-thermal Surfaces at t = 0.0193 seconds (Element Type 133)

Volume E
Demonstration
Problems

Chapter 6
Dynamics

E 6.16 Dynamic Contact Between A Projectile And A Rigid Barrier

This problem demonstrates the dynamic impact between a deformable body and a rigid surface. The problem is executed using both an implicit Newmark-beta operator and the explicit central difference operator.

Model

A deformable projectile consists of nine element type 7, eight-node bricks as shown in Figure E 6.16-1. As an alternative, the analysis is also performed with element type 120 which is the reduced integration formulation. The projectile is initially 0.1 units away from the rigid surface. The DYNAMIC parameter option specifies which operator is to be chosen: a "2" indicates Newmark-beta and a "4" indicates central difference. The projectile may undergo large deformations, so a LARGE DISP parameter is included. The projectile is considered elastic and a total Lagrange analysis will be performed.

Material Properties

An artificial material was created, such that the stability limit for central difference was a large number. The Young's modulus is 10,000 psi and the mass density is 0.1 lbf-sec^2/in^4. A lumped mass matrix will be created based upon the LUMP parameter card. The projectile is given a numerical damping of 0.4. Numerical dampening is preferred over stiffness damping, because the time step can change in contact analyses, resulting in stiffness damping overdamping the system.

Given the material parameters, the elastic wave speed is $c = \sqrt{E/\rho} = 316$ in./s.

Boundary Conditions

The nodes on the xz-plane have been constrained in the y-direction. The nodes on the xy-plane have been constrained in the z-direction. The projectile has an initial velocity of -100 in/sec in the x-direction.

Controls

The maximum number of increments will be 100 with the maximum number of iterations being 3. Relative displacement error control will be used with a tolerance value of 10%. Note that when using the explicit dynamic method, iteration will not occur. A formatted post tape will be written which will contain only nodal information. The restart tape is written at every increment.

Contact

There are two bodies in this analysis. The first is the deformable projectile. The second is the rigid barrier. There is no friction between these two surfaces.

The other parameters on the second card are upper bounds to the number of surface entities and surface nodes.

The contact tolerance is 0.03 inch which is small compared to an element dimension. A very large separation force is given which effectively ensures that the projectile will stick to the barrier.

The first body is the deformable one consisting of nine elements. The second body consists of one patch. The order of the numbering ensures the correct normal direction is associated with the rigid surface.

Time Step

The time step chosen is 0.0005 second which is below the stability limit of 0.002 second. In this period, the elastic wave will travel 0.158 inch which is smaller than a typical element dimension. The total period is 0.01 second, so 20 increments will be performed.

Results

Figure E 6.16-3 and Figure E 6.16-4 show the projectile at increment two after contact first occurs, and at increment 20 at the end of the analysis. Figure E 6.16-5, Figure E 6.16-6, and Figure E 6.16-7 show the displacement, velocity, and reaction forces at selected nodes for the Newmark-beta analysis and central difference analysis. You can observe that the results are almost indistinguishable. Node 26 first comes into contact at increment 2, the displacement is .1 and remains fixed for the remainder of the analysis; velocity is zero. Node 25 comes into contact during increment 10 and remains fixed the remainder of the analysis. Nodes 31 and 32 simply decelerate during the analysis. The reactions show that spikes occur at the increments where contact occurs. The results using the reduced integration element are not substantially different.

The implicit Newmark-beta ran three times longer. This is an anomaly due to the fact that an artificial material was created such that the time steps in the two procedures were allowed to be the same.

Summary of Options Used

Listed below are the options used in example e6x16a.dat:

Parameter Options

DYNAMIC
ELEMENT
END
LARGE DISP
LUMP
PRINT
SIZING
TITLE

Model Definition Options

CONNECTIVITY
CONTACT
CONTROL
COORDINATE
END OPTION
FIXED DISP
INITIAL VELOCITY
ISOTROPIC
POST
PRINT ELEM
RESTART

Load Incrementation Options

CONTINUE
DYNAMIC CHANGE

Listed below are the options used in example e6x16b.dat:

Parameter Options

DYNAMIC
ELEMENT
END
LARGE DISP
LUMP
PRINT
SIZING
TITLE

Model Definition Options

CONNECTIVITY
CONTACT
CONTROL
COORDINATE
END OPTION
FIXED DISP
INITIAL VELOCITY
ISOTROPIC
POST
PRINT ELEM
RESTART

Load Incrementation Options

CONTINUE
DYNAMIC CHANGE

Listed below are the options used in example e6x16c.dat:

Parameter Options

ALIAS
DYNAMIC
ELEMENT
END
LARGE DISP
LUMP
PRINT
SIZING
TITLE

Model Definition Options

CONNECTIVITY
CONTACT
CONTROL
COORDINATE
END OPTION
FIXED DISP
INITIAL VELOCITY
ISOTROPIC
POST
RESTART

Load Incrementation Options

CONTINUE
DYNAMIC CHANGE

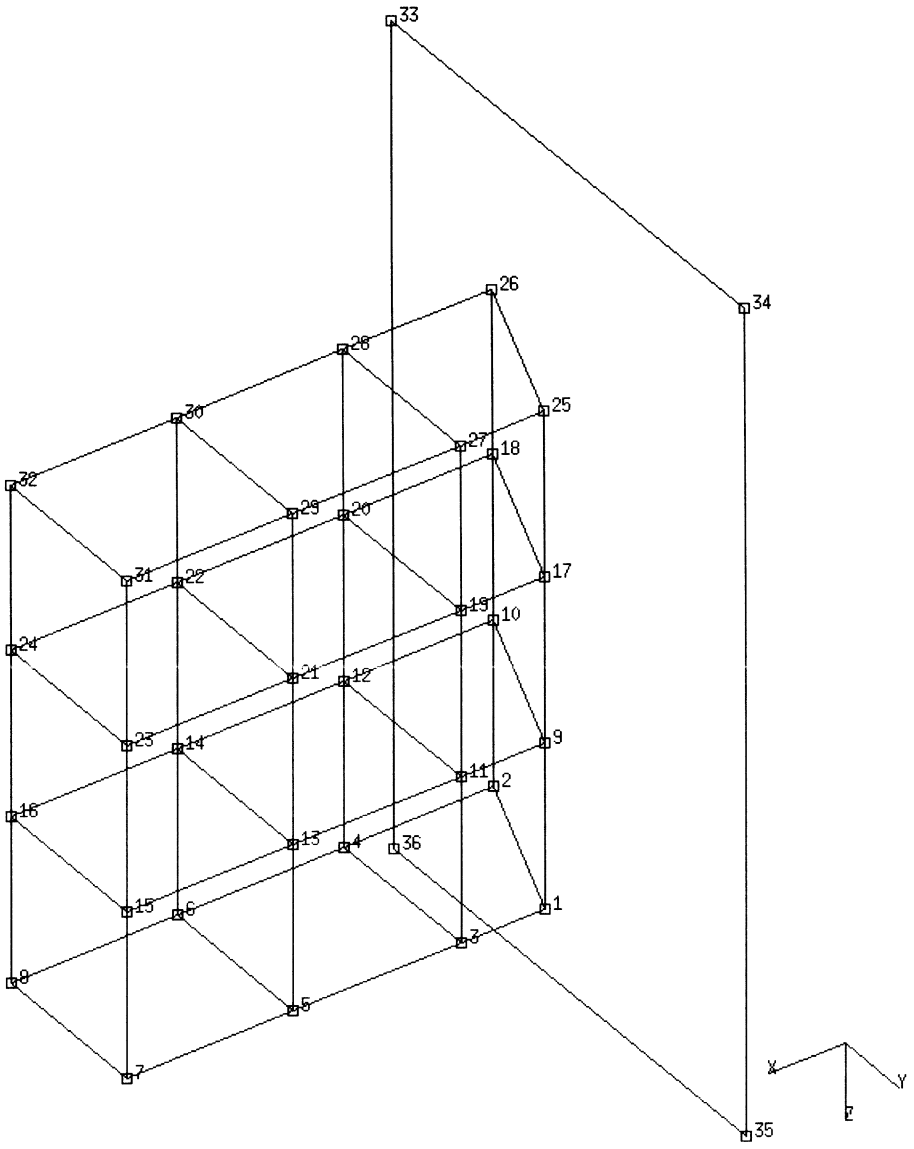

Figure E 6.16-1 Impactor and Rigid Wall

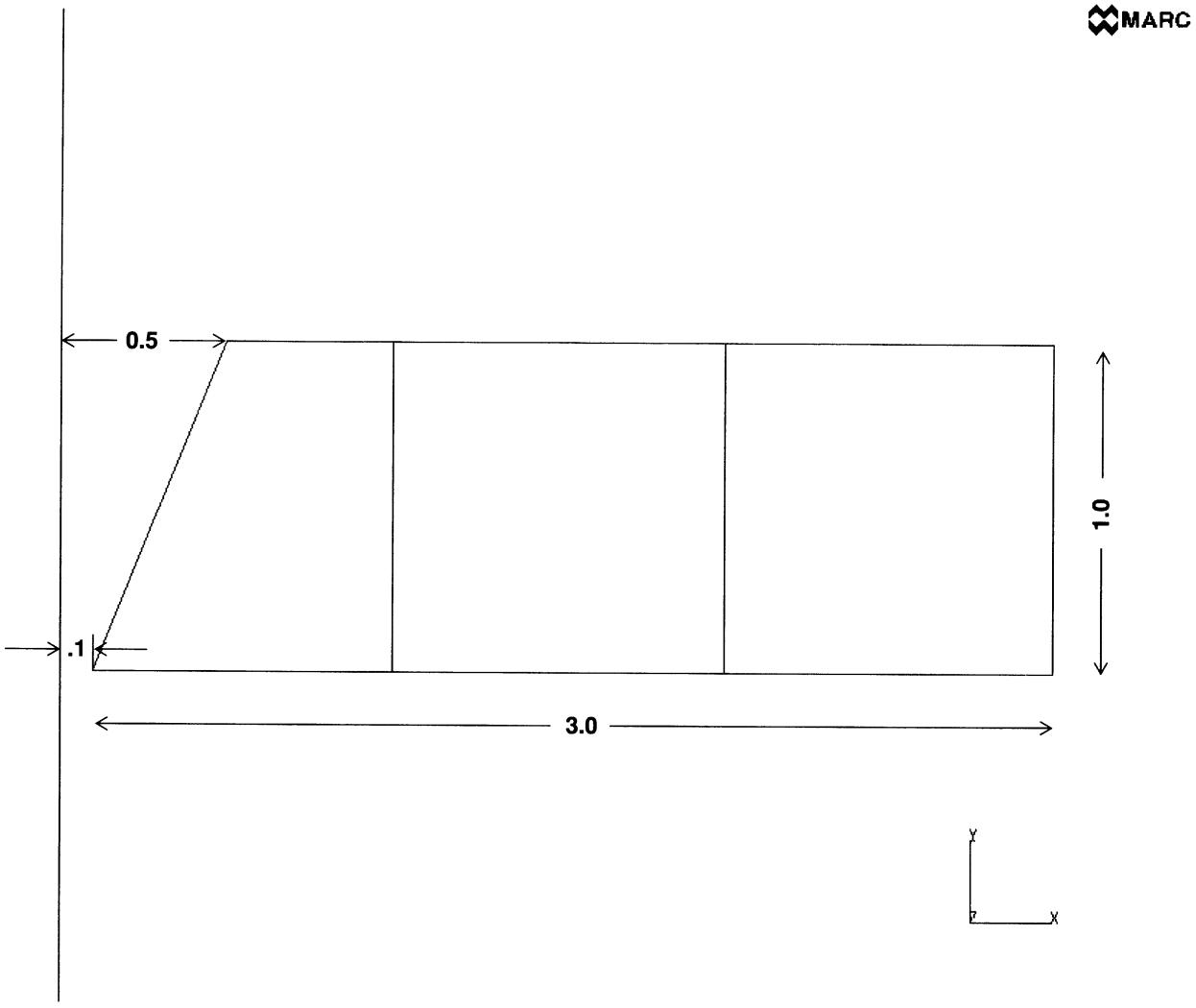

Figure E 6.16-2 Impactor Geometry

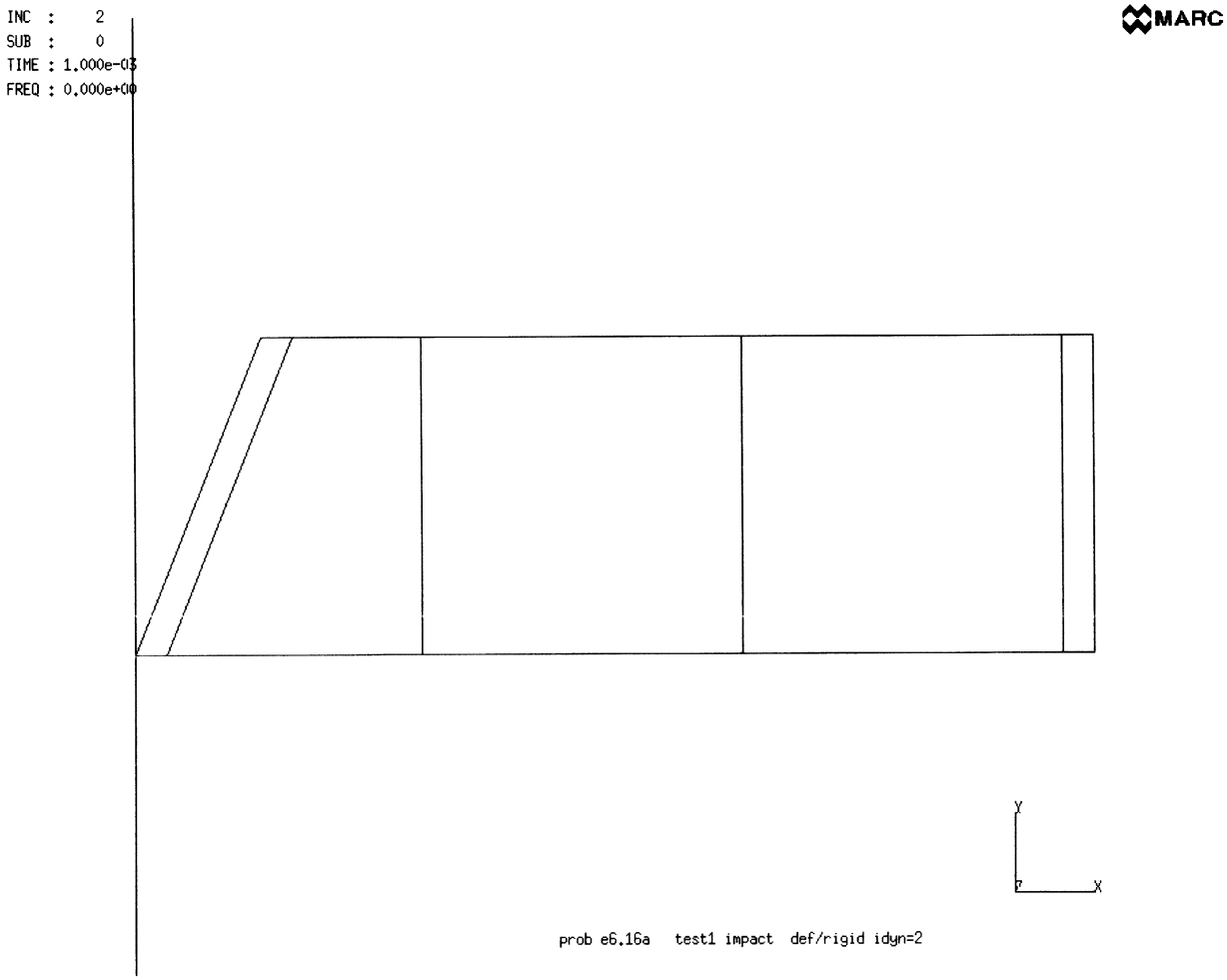

Figure E 6.16-3 Deformation at Initial Contact

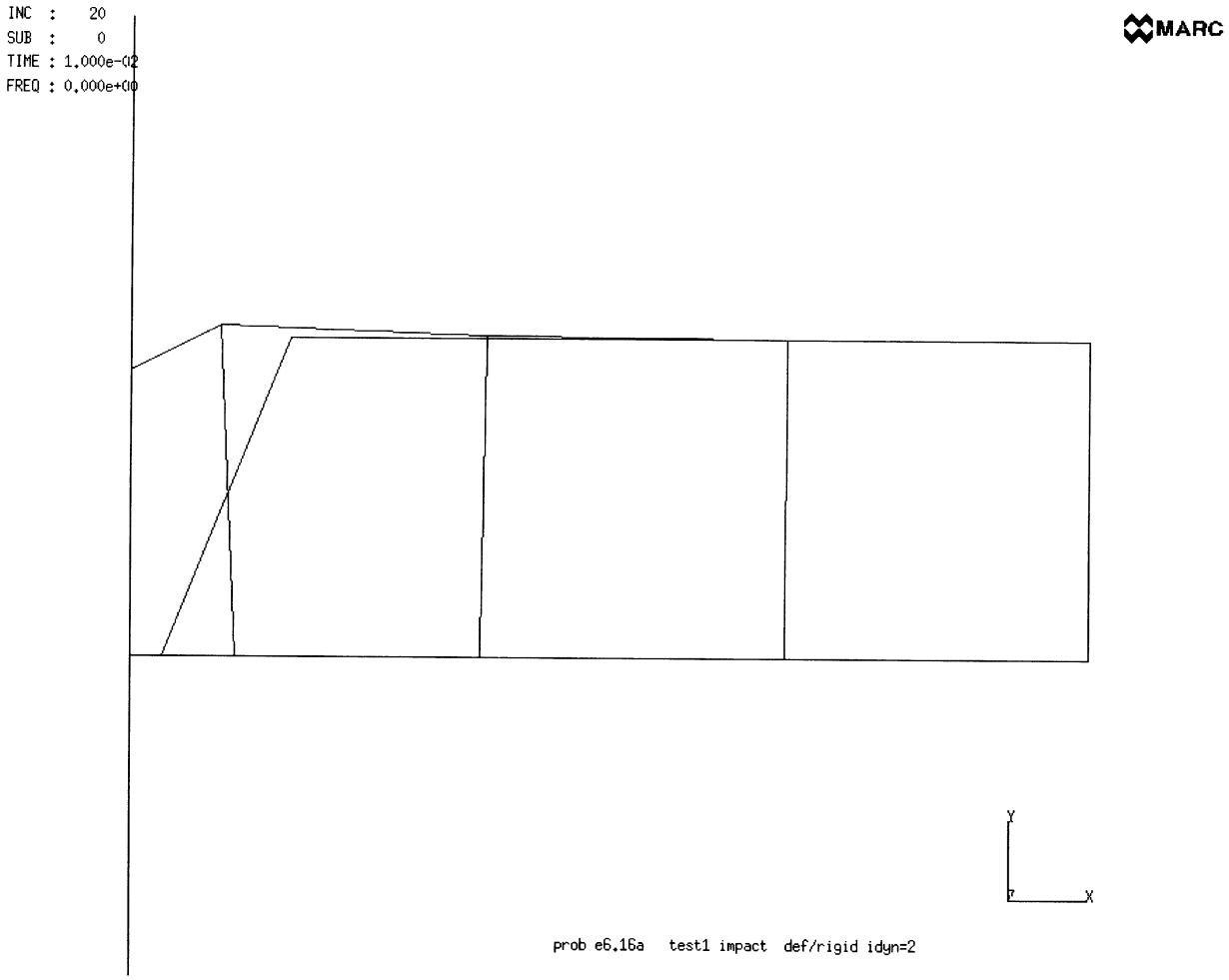

Figure E 6.16-4 Final Deformation

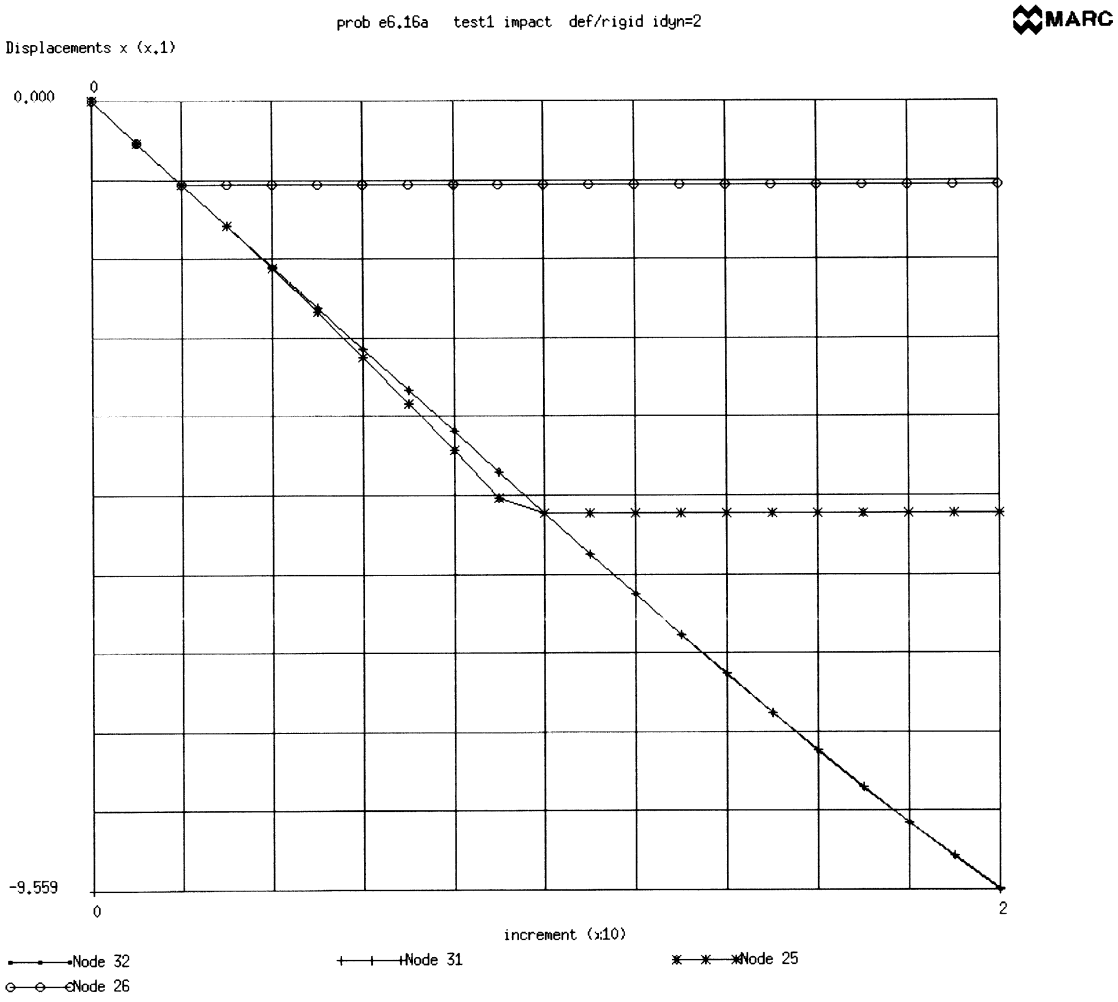

Figure E 6.16-5 (A) Displacement History (Newmark-Beta Method)

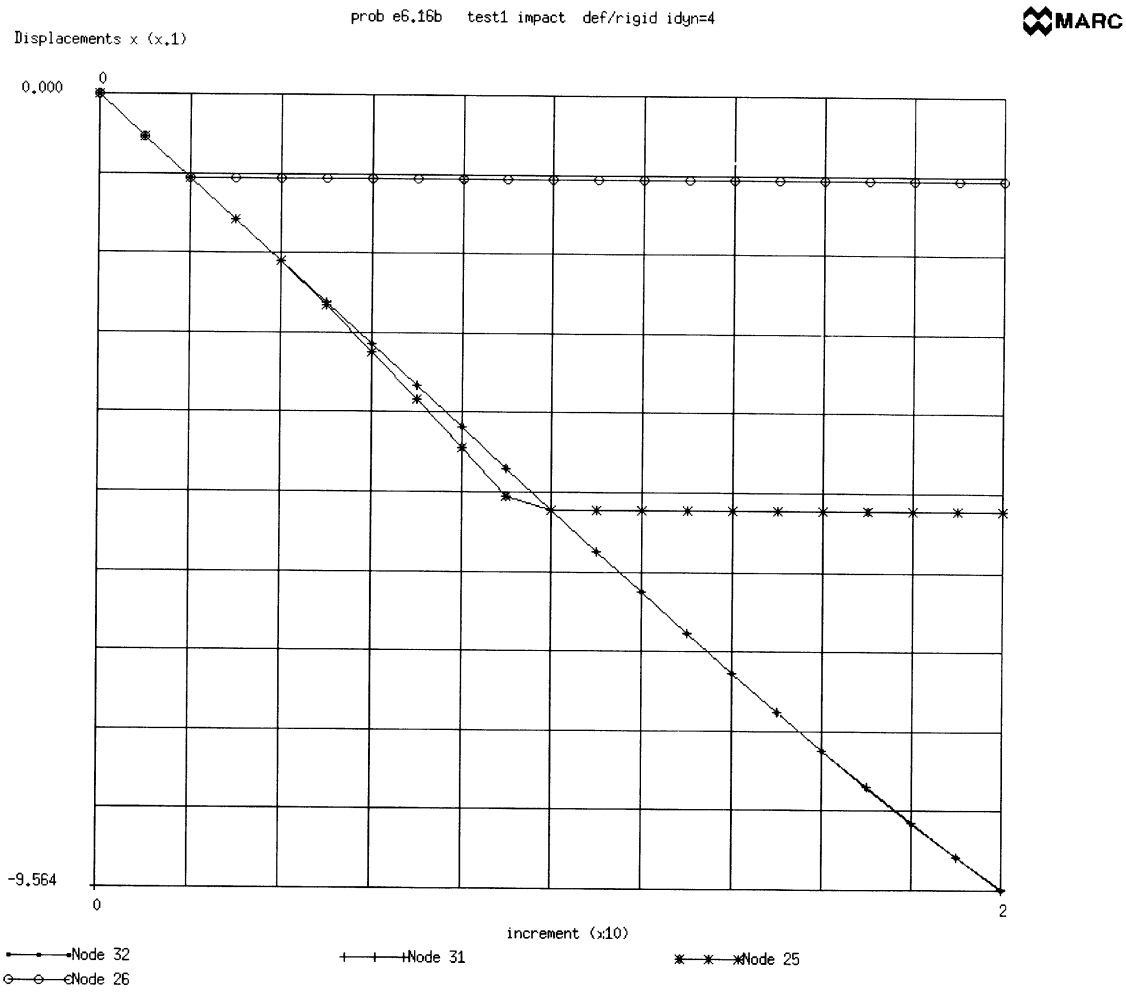

Figure E 6.16-5 (B) Displacement History (Central Difference Method)

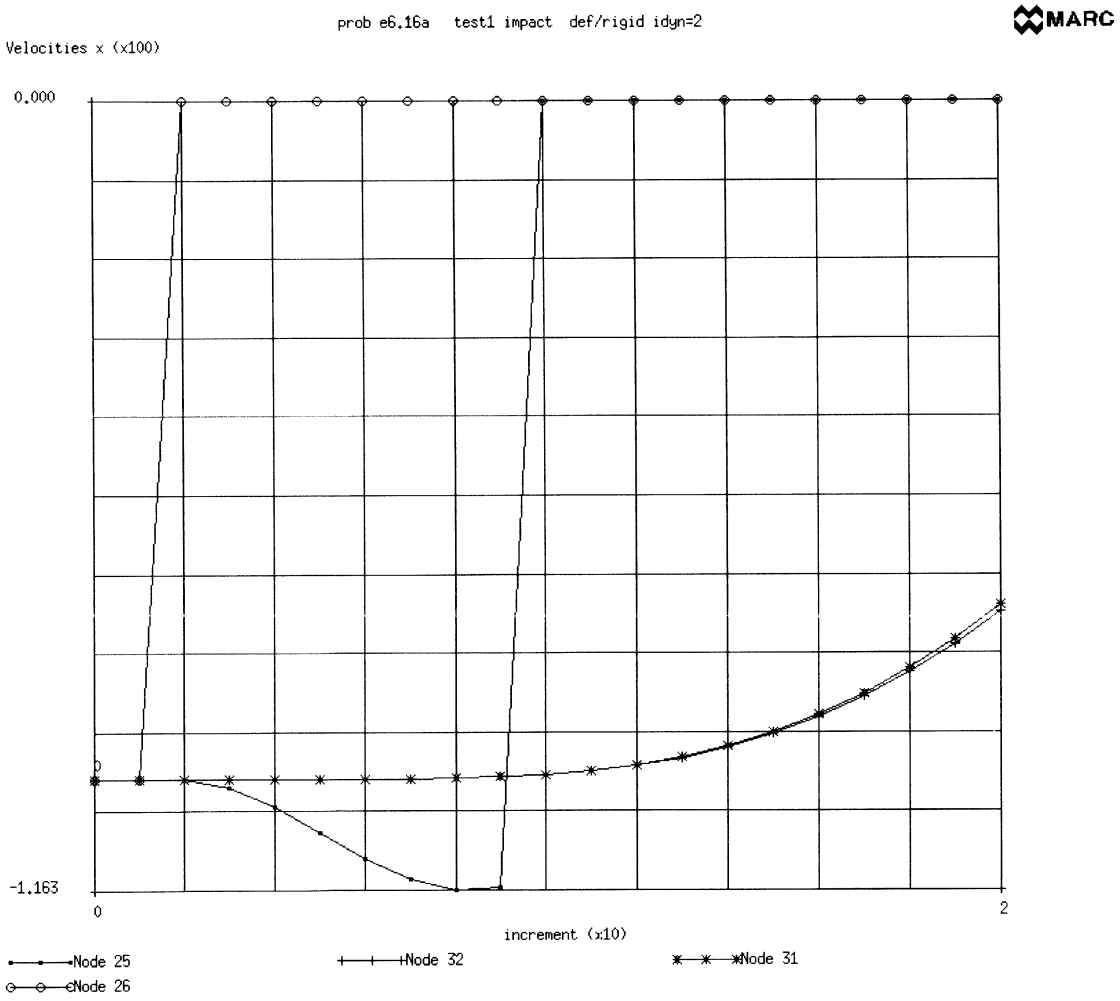

Figure E 6.16-6 (A) Velocity History (Newmark-Beta Method)

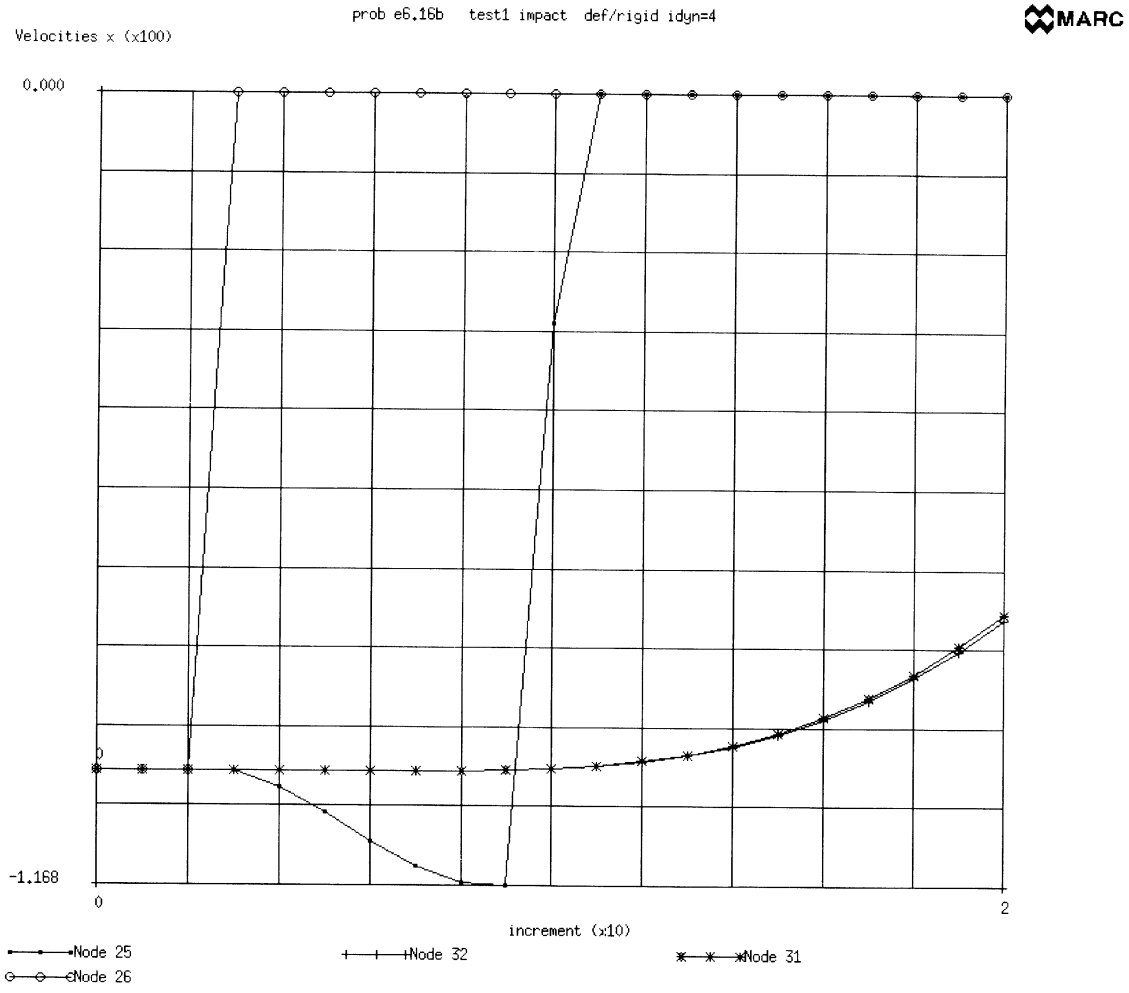

Figure E 6.16-6 (B) Velocity History (Central Difference Method)

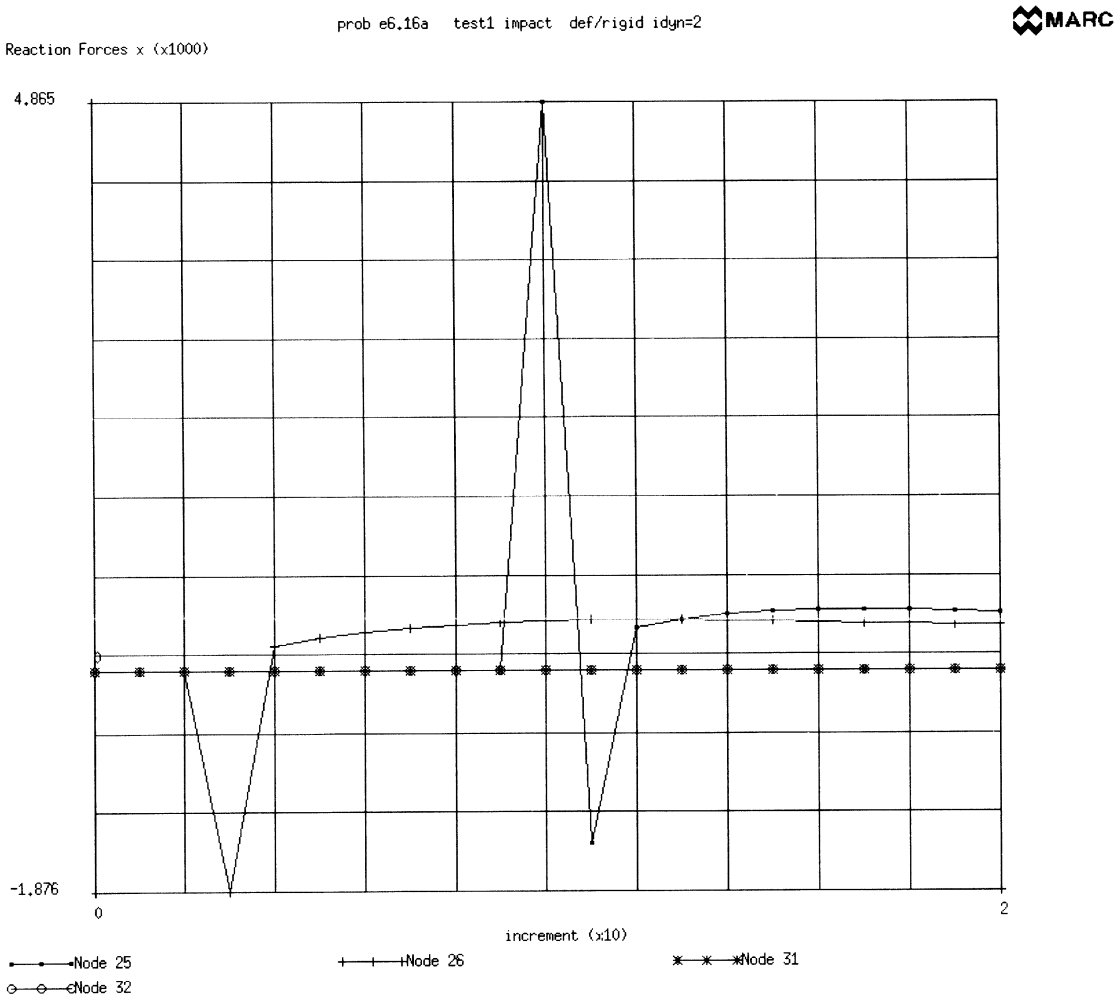

Figure E 6.16-7 (A) Reaction/Impact Force History (Newmark-Beta Method)

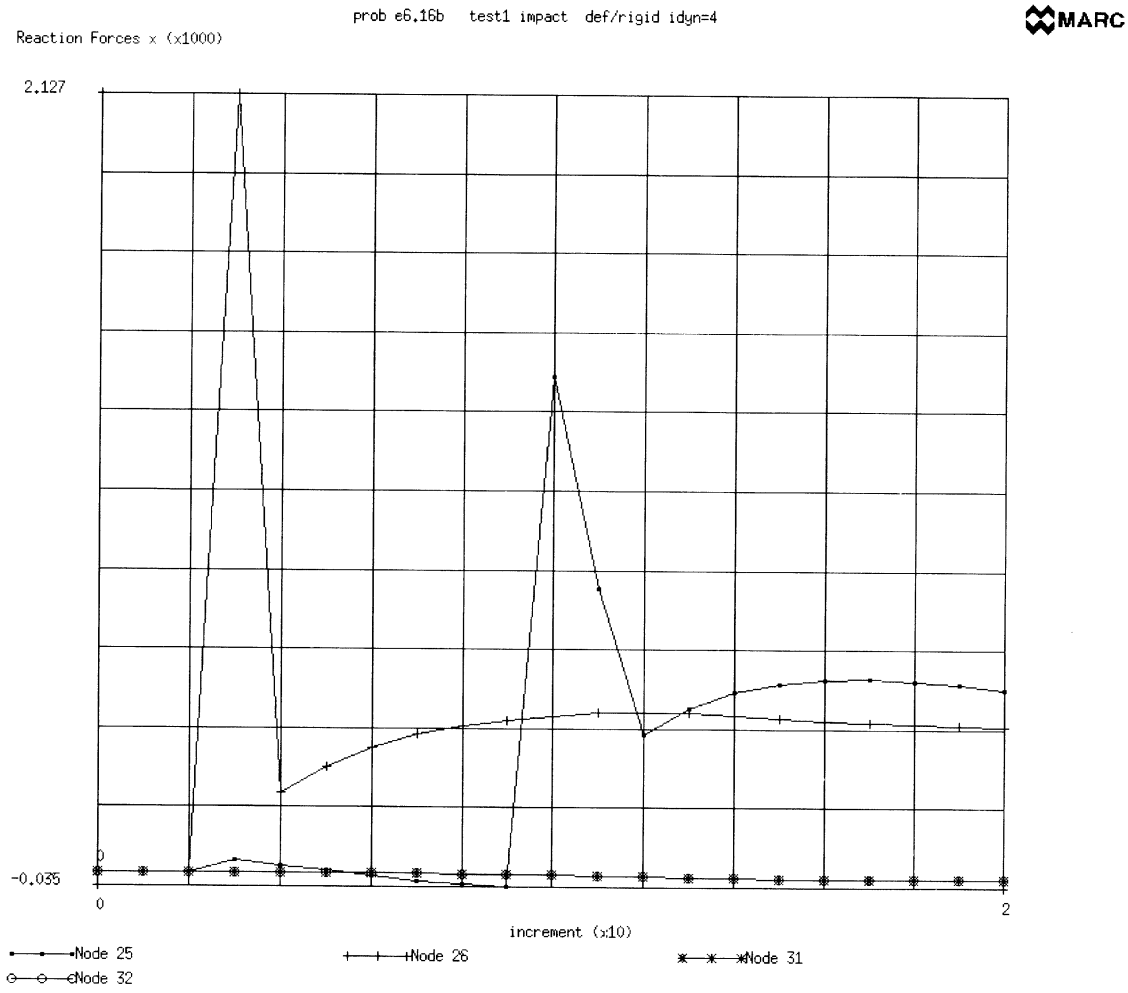

Figure E 6.16-7 (B) Reaction/Impact Force History (Central Difference Method)

E 6.17 Dynamic Contact Between Two Deformable Bodies

This problem demonstrates the dynamic impact between two deformable bodies. It is very similar to problem E 6.16, except the rigid barrier has been replaced by a deformable, yet stiff, body. Both the implicit Newmark-beta and explicit central difference procedures are demonstrated.

Model

The model is shown in Figure E 6.17-1 and Figure E 6.17-2. The project is made up of 9 brick elements type 7, where the barrier is composed of 40 brick elements. The DYNAMIC parameter option specifies which operator is to be chosen: a "2" indicates Newmark-beta and a "4" indicates central difference. The projectile may undergo elastic deformation, so the LARGE DISP parameter option is included.

Material Properties

An artificial material was created, such that the stability limit for central difference was a large number. For the projectile (elements 1 – 9), the Young's modulus is 10,000 psi and the mass density is 0.1 lbf-sec^2/in^4. The barrier is ten times stiffer with a Young's modulus of 100,000 psi. A lumped mass matrix will be created based upon the LUMP parameter option. The model is given a numerical damping of 0.4. Given the material parameters, the elastic wave speed in the projectile is

$c = \sqrt{E/\rho} = 316$ in/sec. In the barrier, it is 1000 in/sec.

Boundary Conditions

The nodes on the xz-plane have been constrained in the y-direction. The nodes on the xy-plane have been constrained in the z-direction for the projectile. The projectile has an initial velocity of -100 in/sec in the x-direction.

Controls

The maximum number of increments will be 100 with the maximum number of iterations as 25. Relative displacement error control will be used with a tolerance value of 10%. A formatted post tape will be written which will contain only nodal information. Both the restart and post tape are written every increment.

Contact

There are two bodies in this analysis. The first is the deformable projectile. The second is the deformable barrier. There is no friction between these two surfaces.

The other parameters on the second card are upper bounds to the number of surface entities and surface nodes.

The contact tolerance is 0.032 inch which is small compared to an element dimension. A very large separation force is given which effectively ensures that the projectile will stick to the barrier.

Time Step

The time step chosen is 0.0005 second which is below the stability limit of 0.0012 second. The stability limit is smaller in this problem than in E 6.16 because of the stiff barrier. The total period is 0.01 second, so 20 increments will be performed.

Results

Figure E 6.17-3 shows the deformation at increment 20. The barrier is significantly stiffer and undergoes very little deformation. The projectile is originally 0.2 inches from the barrier. You can observe in Figure E 6.17-4 that node 26 contacts the barrier in increment 3 using the implicit procedure, and increment 4 in the explicit procedure. This is due to the nature of these two different methods. There is more deformation of the barrier using the implicit procedure. Figure E 6.17-5 shows the velocity histories using the new methods. The basic correlation is good. The Newmark-beta method shows some oscillations at later increments. This could be eliminated by using more damping or decreasing the time step.

Summary of Options Used

Listed below are the options used in example e6x17a.dat:

Parameter Options

DYNAMIC
ELEMENT
END
LARGE DISP
LUMP
PRINT
SIZING
TITLE

Model Definition Options

CONNECTIVITY
CONTACT
CONTROL
COORDINATE
END OPTION
FIXED DISP
INITIAL VELOCITY
ISOTROPIC
POST
PRINT ELEM
RESTART

Load Incrementation Options

CONTINUE
DYNAMIC CHANGE

Listed below are the options used in example e6x17b.dat:

Parameter Options

DYNAMIC
ELEMENT
END
LARGE DISP
LUMP
PRINT
SIZING
TITLE

Model Definition Options

CONNECTIVITY
CONTACT
CONTROL
COORDINATE
END OPTION
FIXED DISP
INITIAL VELOCITY
ISOTROPIC
POST
PRINT ELEM
RESTART

Load Incrementation Options

CONTINUE
DYNAMIC CHANGE

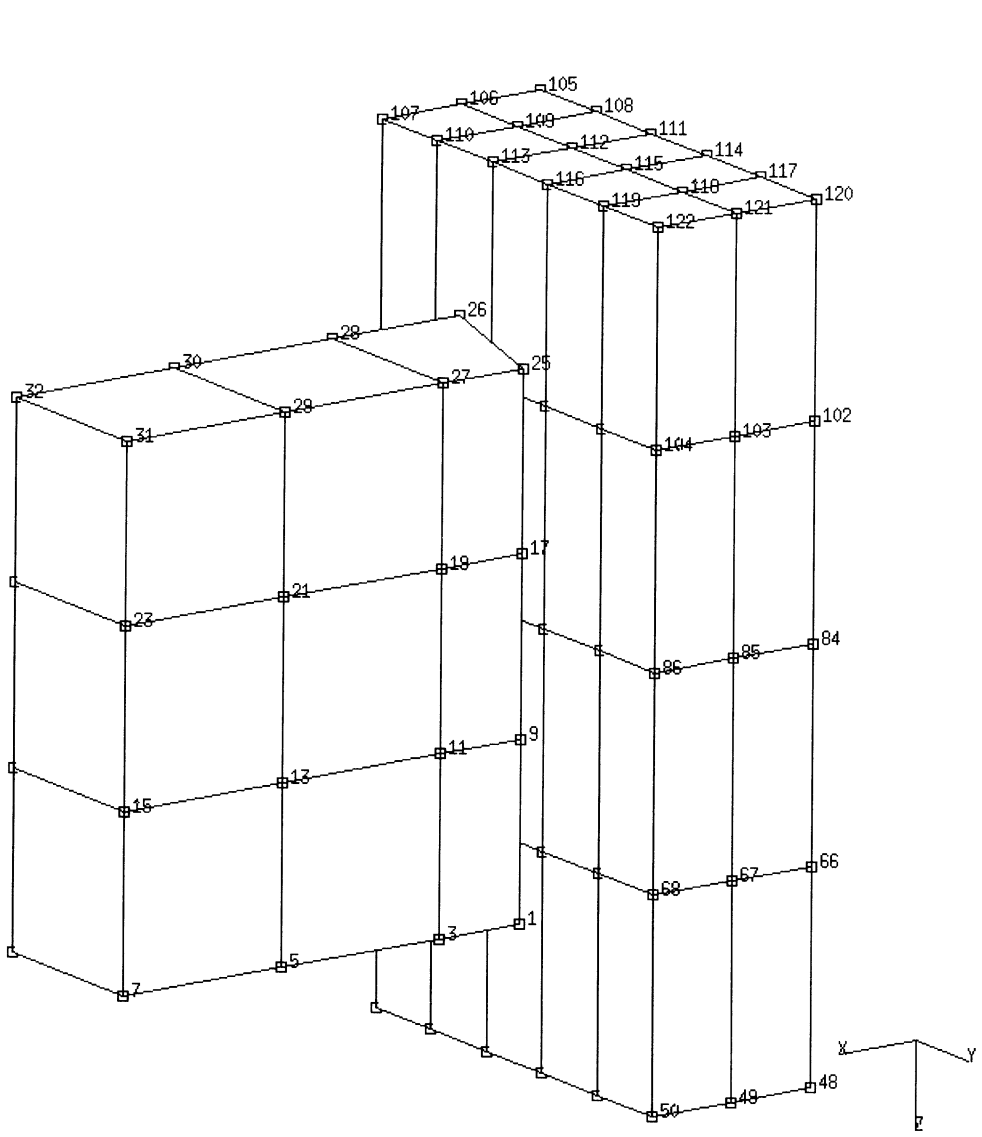

Figure E 6.17-1 Impactor and Deformable Barrier

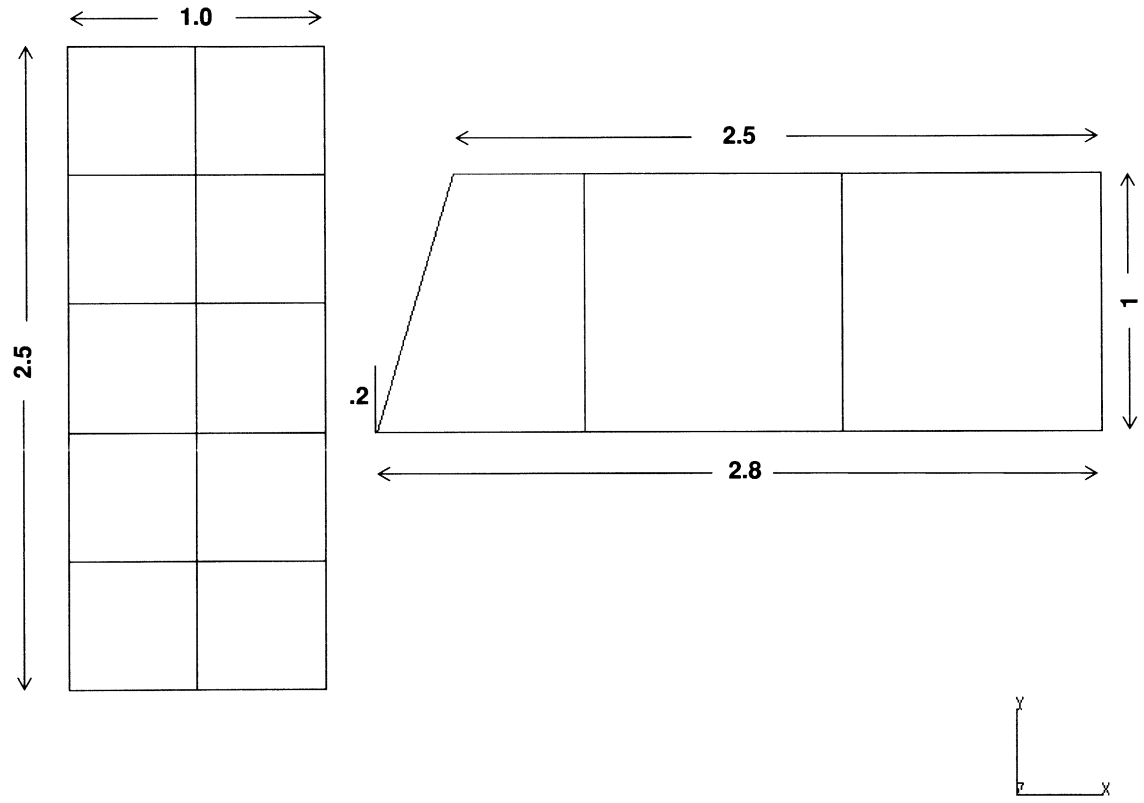

Figure E 6.17-2 Geometries

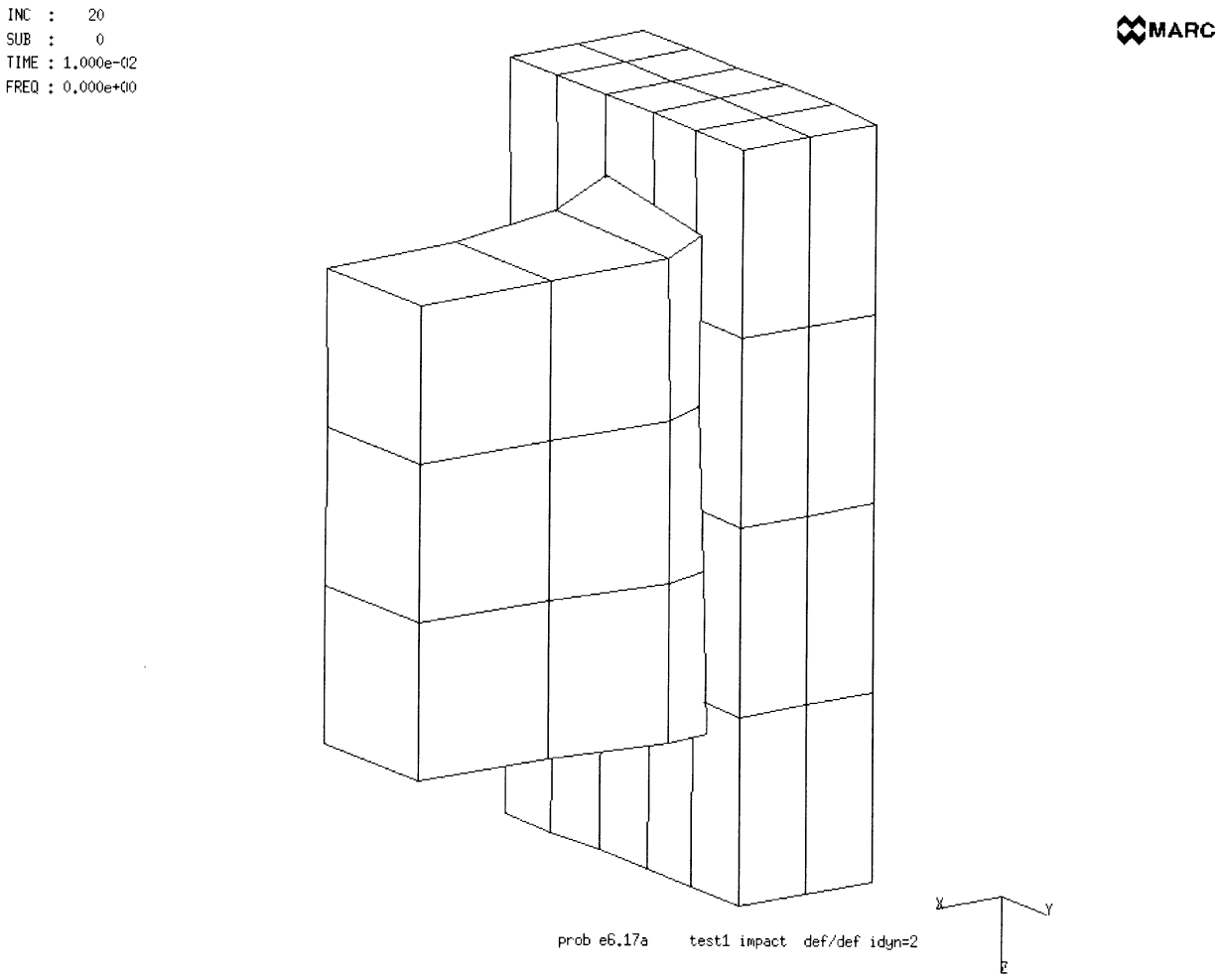

Figure E 6.17-3 Final Deformation

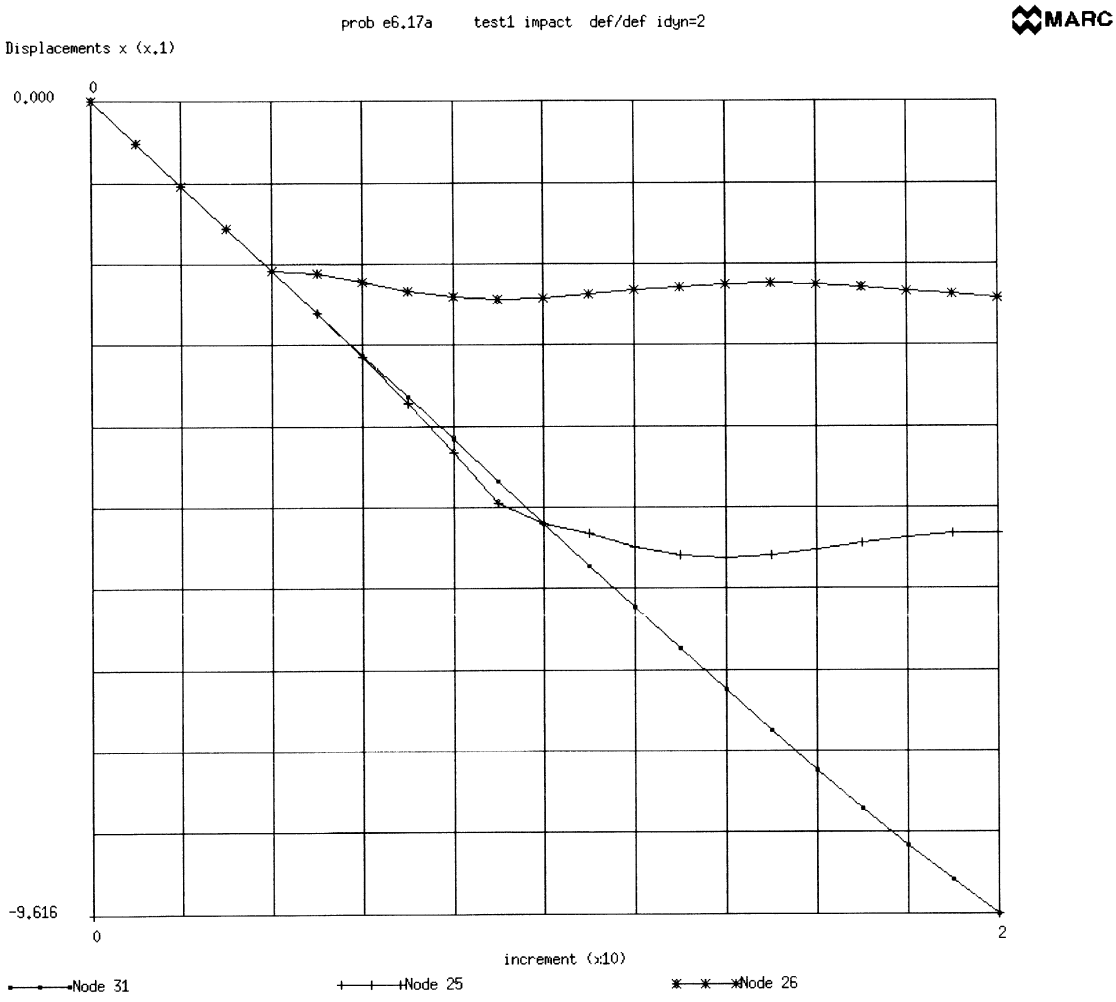

Figure E 6.17-4 (A) Displacement Histories (Newmark-beta Method)

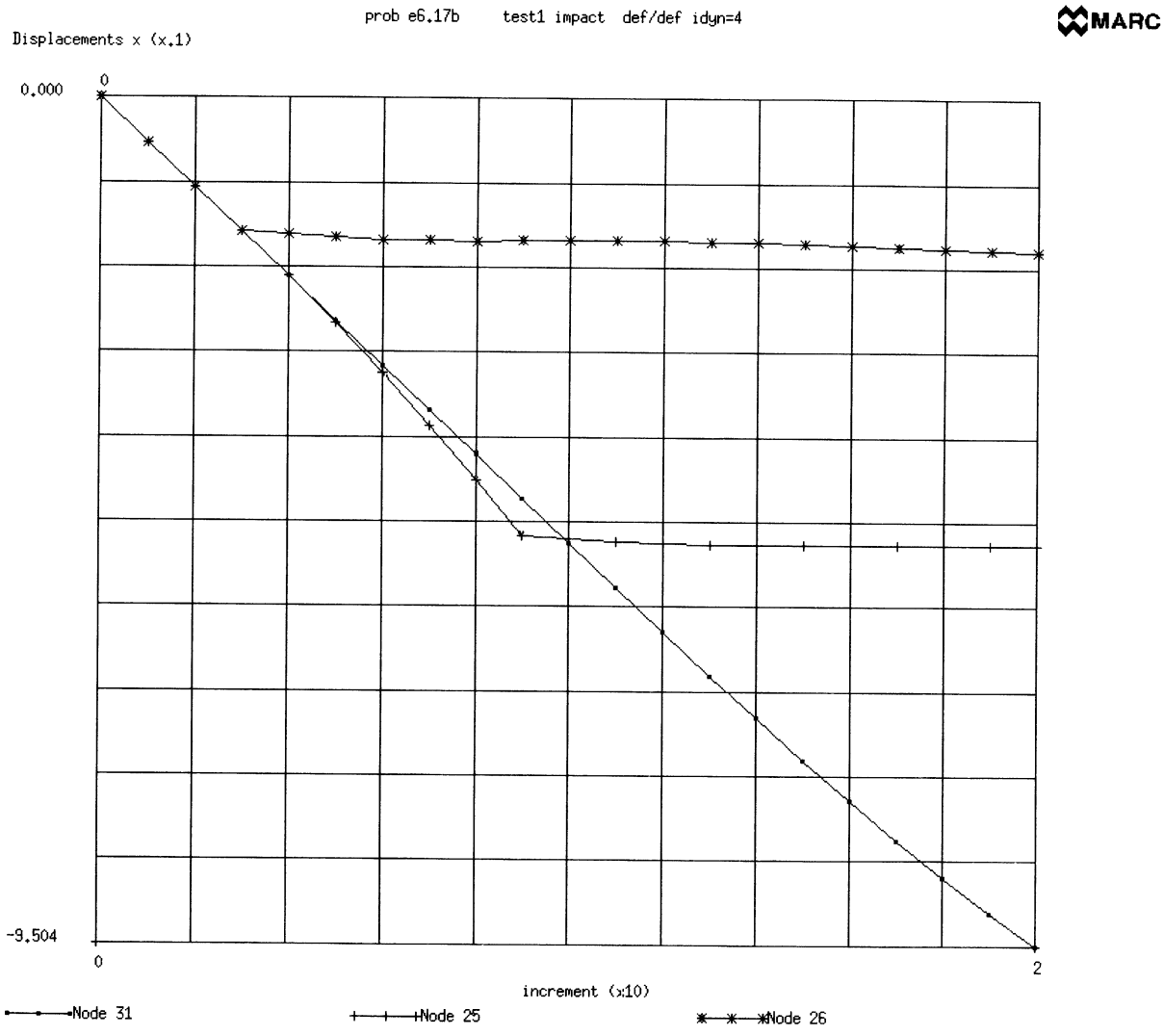

Figure E 6.17-4 (B) Displacement History (Central Difference Method)

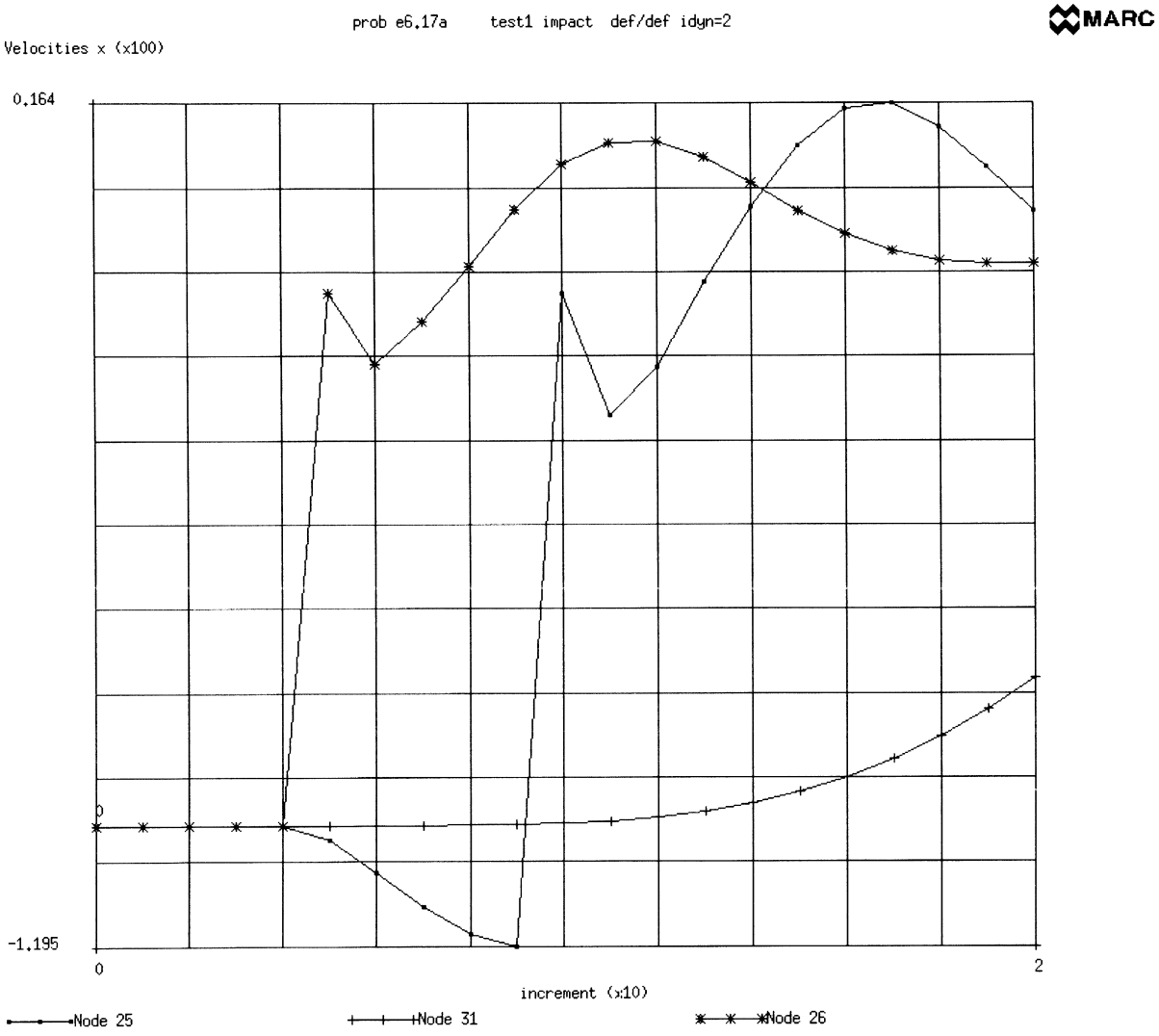

Figure E 6.17-5 (A) Velocity History (Newmark-beta Method)

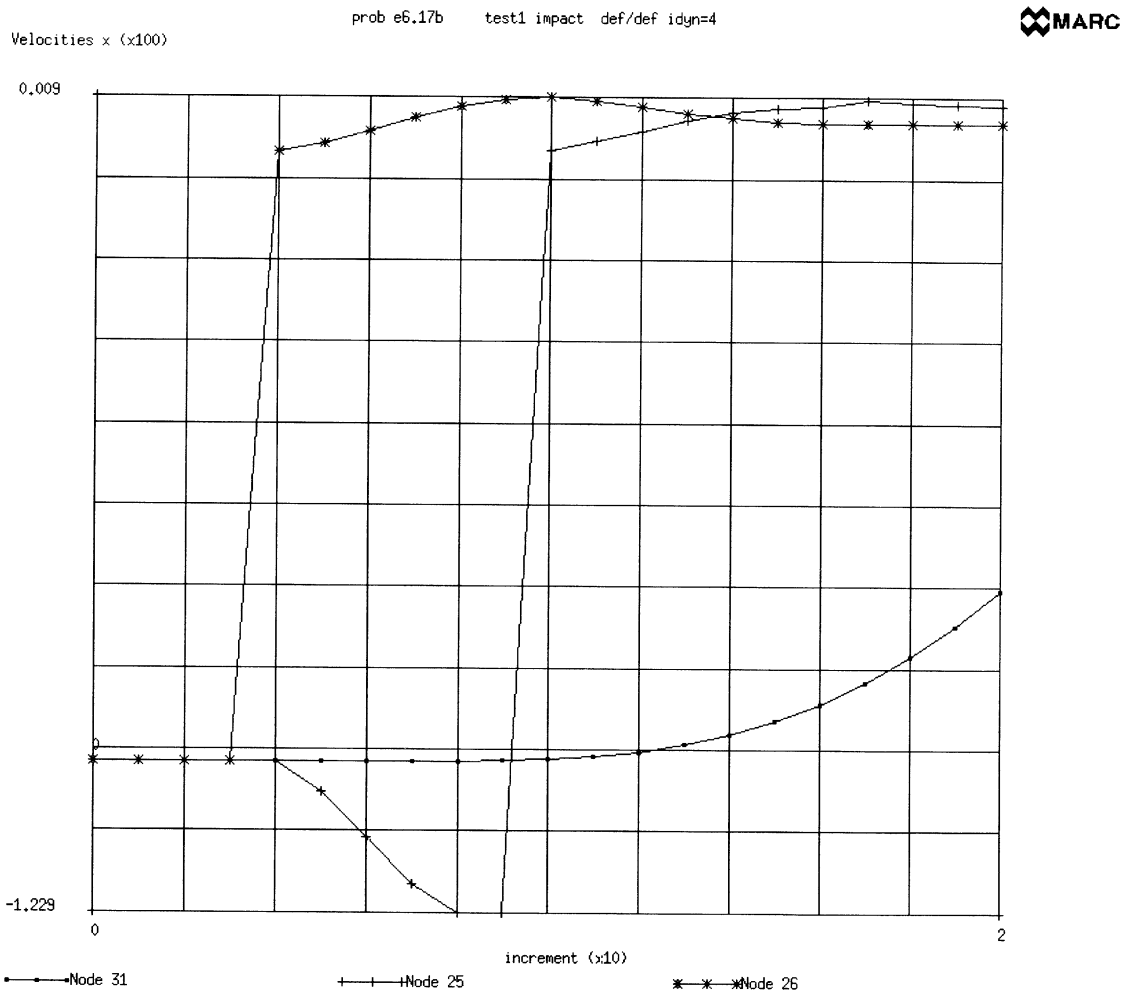

Figure E 6.17-5 (B) Velocity History (Central Difference Method)

Volume E
Demonstration Problems

Chapter 7
Contact

E 7.1 Rigid Perfectly Plastic Extrusion Isothermal and Coupled Analysis

This example illustrates the use of the R-P FLOW option in a classic plastic flow problem – the extrusion of metal in-plane strain through a 50% reduction, frictionless die. The problem is shown in Figure E 7.1-1; a uniform velocity is applied at the left-hand side. The required solution is the velocity field and extrusion force. The slip-line solution to this problem is well known [1,2].

The rigid-plastic flow option uses Herrmann incompressible elements to solve for the velocity field. The material is modeled as a non-Newtonian fluid and the program iterates for the viscosity, which is $\frac{2}{3}\frac{\bar{\sigma}}{\dot{\bar{\varepsilon}}}$, where σ is the yield stress and $\dot{\bar{\varepsilon}}$ is the equivalent plastic strain rate.

The second part of this example demonstrates the coupled analysis for steady-state rigid-plastic flow. The comparison between effect of no heat convection contribution and heat convection contribution is made in e7x1b and e7x1c. Uniform velocity and fixed temperature is applied at the left-hand side. The contribution of convection heat will be made after the solution of velocity is obtained. The nonsymmetric solver is turned on automatically when heat convection is included. The parameter option COUPLE is used to flag the coupling procedures.

Element

In this example, the plane-strain Herrmann element (element 32) is used. This element is a second-order, distorted quadrilateral (plane-strain). There are 32 elements and a total of 121 nodes.

Material Properties

The equivalent von Mises yield stress is entered as 30 x 10^3 psi in this option. The thermal properties are:

specific heat	4.2117E-2
density	0.3523E-3
thermal conductivity	0.7254E-3

The property is specified for elements 1 through 32.

Geometry

No geometry is specified.

Loading

No loading is specified.

Boundary Conditions

The material entering the die is assigned a velocity of 1 in/sec in the x-direction. The material velocities normal to the die walls are fixed as zero. In the thermal mechanically coupled analysis, the inlet temperature of the material is fixed at 800°F. The wall temperature is fixed at 500°F.

Control

A 10% tolerance on the relative residual force was chosen to determine if convergence was achieved. In a rigid plastic analysis, the computational time would have been reduced if the convergence based upon velocities was requested.

Auto Load

Because the contribution of heat convection is accounted after the solution of velocity distribution is obtained, two fixed time steps are used to simulate the coupling process. In the first increment, the heat transfer analysis is done first and subsequent stress analysis will use this new temperature distribution for material properties to obtain the solution of velocity distribution. In the next increment, the temperature distribution is obtained based on the velocity distribution result of the previous increment.

Results

The solution for the 50% reduction case chosen here is a centered fan – outside the fan the material moves as a rigid body or is stationary. The mesh is confined to the neighborhood of the fan region (Figure E 7.1-2).

Note a special consideration for the fully incompressible Herrmann formulation: since the system is semi-definite, it is only possible to solve by Gauss elimination if the first active degree of freedom is a stiffness degree of freedom and not a pressure variable (Lagrange multiplier). Thus, node 1 must have at least one unconstrained velocity component. In this case, one and two are swapped to achieve this by adding additional CONNECTIVITY and COORDINATES set by hand. The value of the input velocity is arbitrary in this case, since the yield is assumed to be rate independent. The accuracy of the solution is determined by the convergency requirements. In this analysis, nine iterations were required.

Extrusion force in 50% reduction, frictionless die. (Normalized by the tensile yield stress and input width).

Calculated at input stream	1.347
Calculated from reaction on die face	1.393
Exact (slip line) solution, $.5(1 + \pi/2)$	1.285

The predicted flow field is illustrated in Figure E 7.1-3. Velocity vectors are shown in this figure. The slip-line fan has been superimposed on this picture. The "dead" region in the corner of the die is well predicted by the finite element model, before it reaches the fan. The downstream solution also shows a little rotation of the velocity

field just below the corner of the die. This is more accurate than the upstream solution. The strain gradients on entry to the fan are very high. At this point, the slip solution shows a discontinuity in tangential velocity. A finer mesh in this region would improve this part of the solution.

The temperature distributions shown in Figure E 7.1-4 and Figure E 7.1-6 indicate the effect of heat convection on the plastic extrusion. As the contribution of heat convection is included, the heat transferred into exit from the inlet is faster and the temperature gradient between the wall and the central region is higher. The equivalent plastic strain is shown in Figure E 7.1-5. The shear bands are clearly visible.

References

1. Hill, R., *Mathematical Theory of Plasticity*, Chapter 4, (Oxford University Press, 1950.).
2. Prager, W., and Hodge, P. G., *Theory of Perfectly Plastic Solids*, Section 298 (John Wiley, 1951).

Summary of Options Used

Listed below are the options used in example e7x1.dat:

Parameter Options

ELEMENT
ELSTO
END
R-P FLOW
SIZING
TITLE

Model Definition Options

CONNECTIVITY
CONTROL
COORDINATE
END OPTION
FIXED DISP
ISOTROPIC

Load Incrementation Options

AUTO LOAD
CONTINUE

Listed below are the options used is example e7x1b.dat:

Parameter Options

COUPLE
END
ELEMENTS
HEAT
R-P FLOW
SIZING
TITLE

Model Definition Options

CONNECTIVITY
CONTROL
COORDINATE
END OPTION
FIXED DISPLACEMENT
FIXED TEMPERATURE
INITIAL TEMPERATURE
ISOTROPIC
NO PRINT
POST

Load Incrementation Options

AUTO LOAD
CONTINUE
TIME STEP

Listed below are the options used in example e7x1c.dat:

Parameter Options

COUPLE
END
ELEMENTS
HEAT
R-P FLOW
SIZING
TITLE

Model Definition Options

CONNECTIVITY
CONTROL
COORDINATE
END OPTION
FIXED DISPLACEMENT
FIXED TEMPERATURE
INITIAL TEMPERATURE
ISOTROPIC
NO PRINT
POST

Load Incrementation Options

AUTO LOAD
CONTINUE
TIME STEP

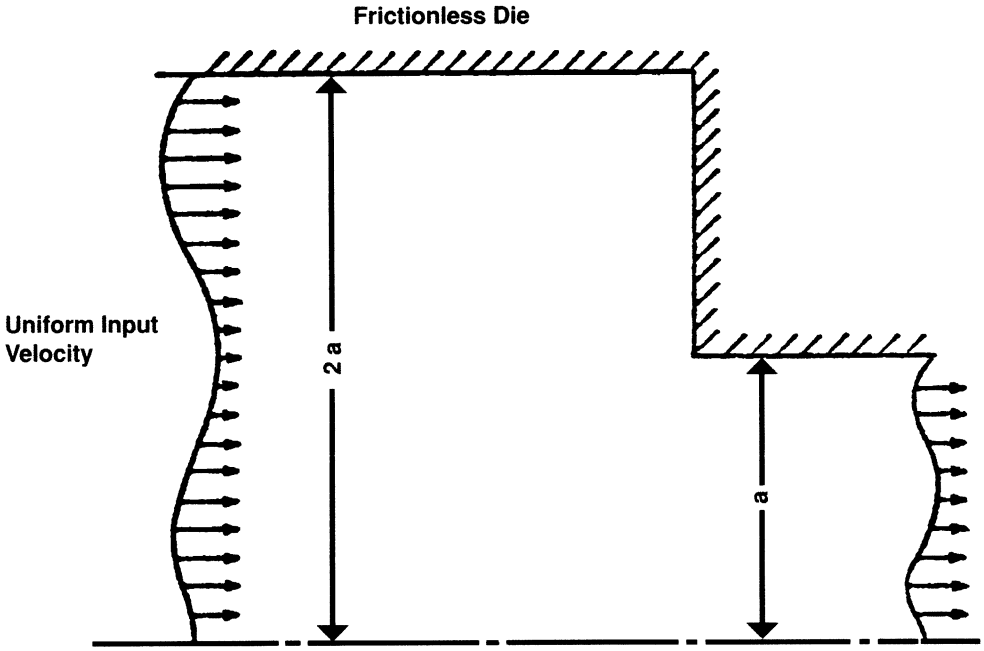

Figure E 7.1-1 50% Reduction Die Problem

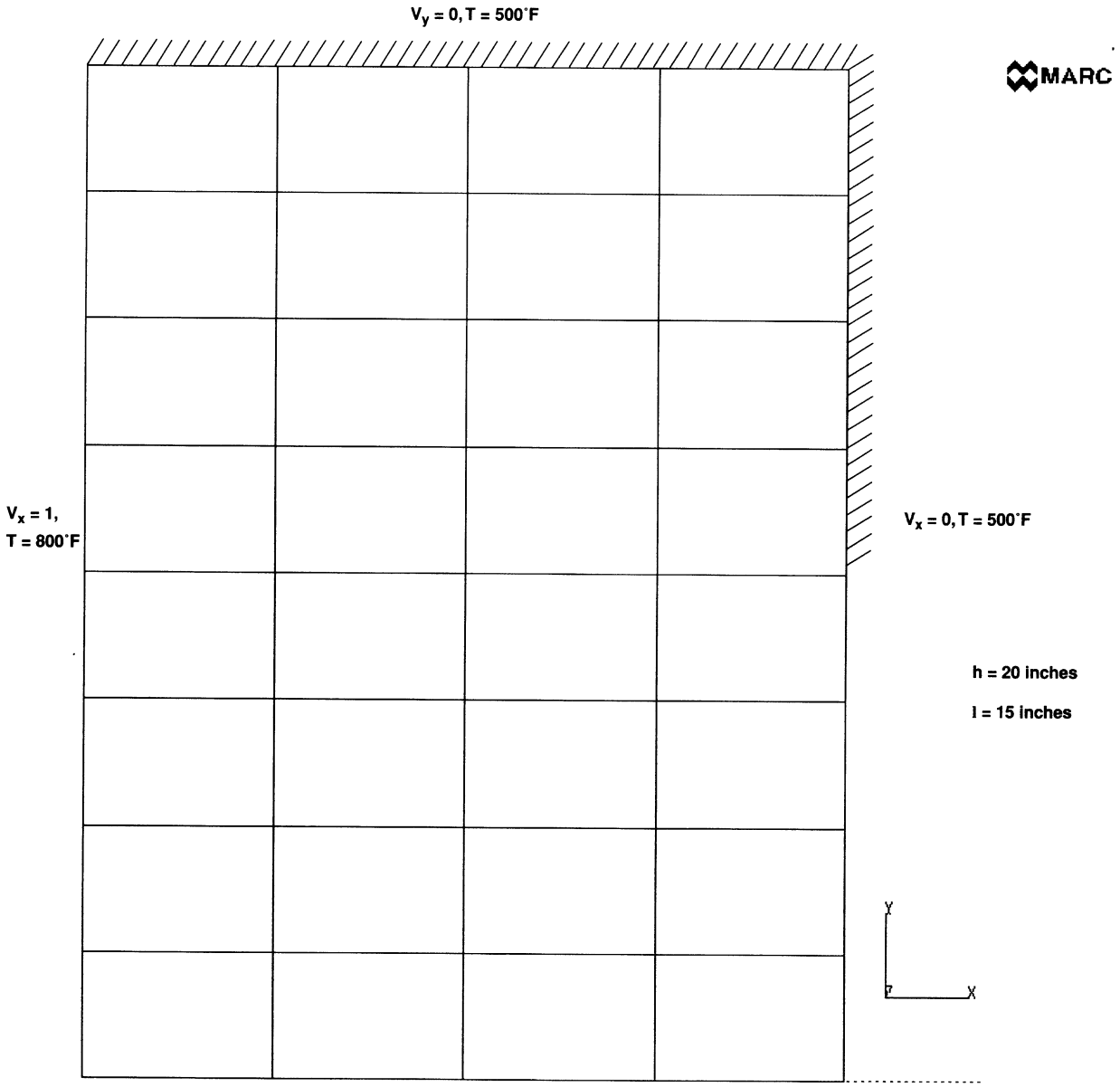

Figure E 7.1-2 Mesh and Boundary Conditions for 50% Reduction Example

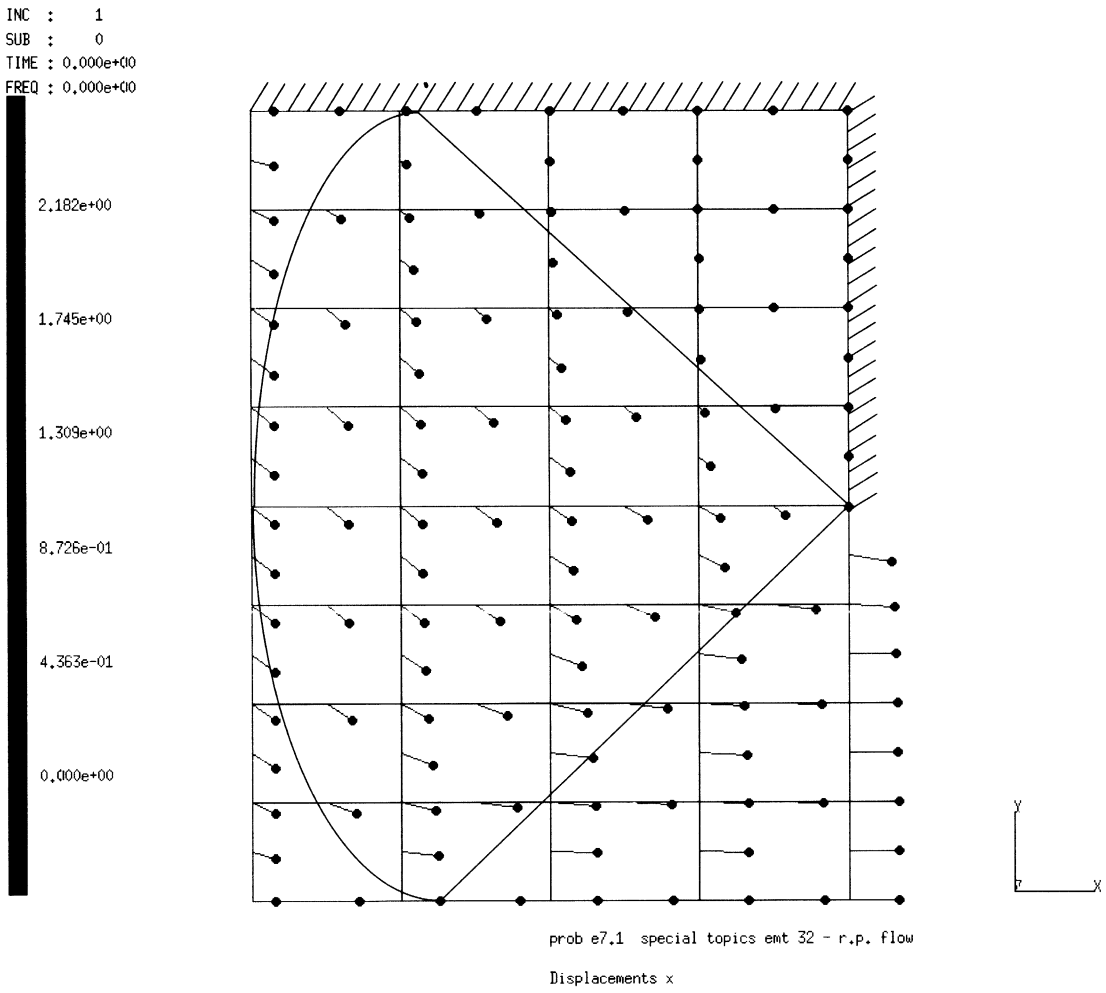

Figure E 7.1-3 50% Reduction Extrusion Velocity Field

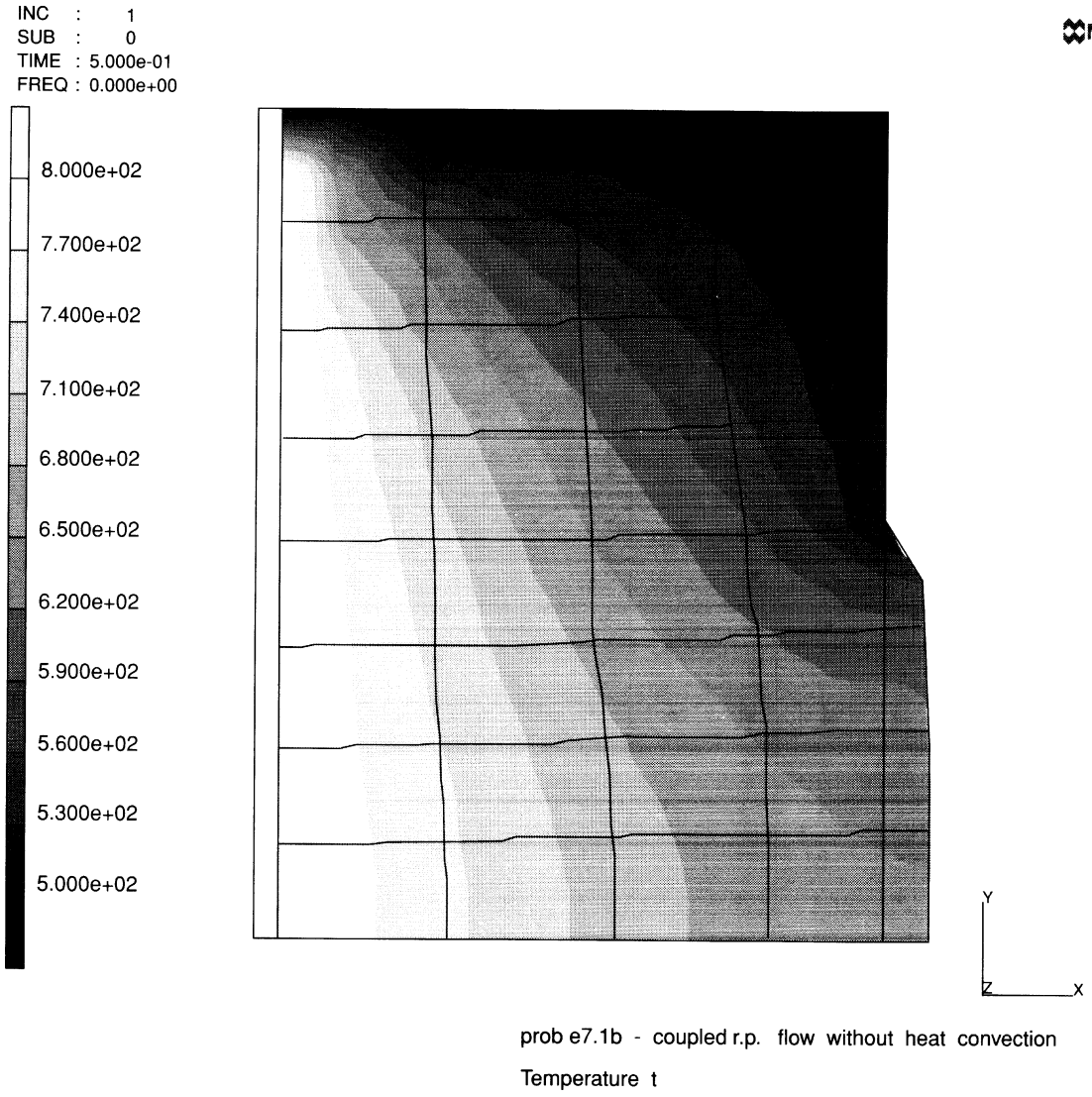

Figure E 7.1-4 Temperature Distribution in the Billet Neglecting Thermal Convection

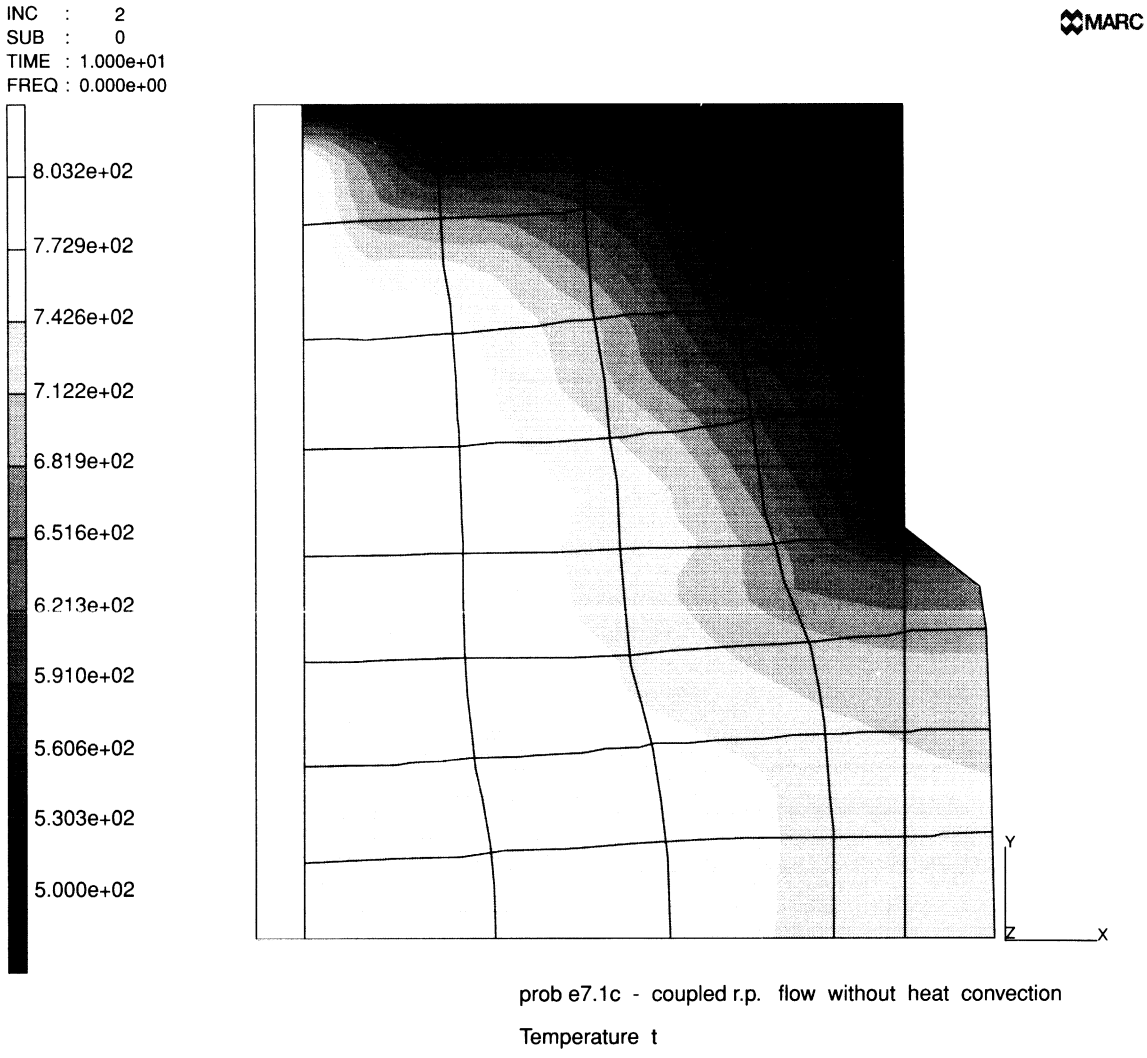

Figure E 7.1-5 Temperature Distribution in the Billet Including Convection

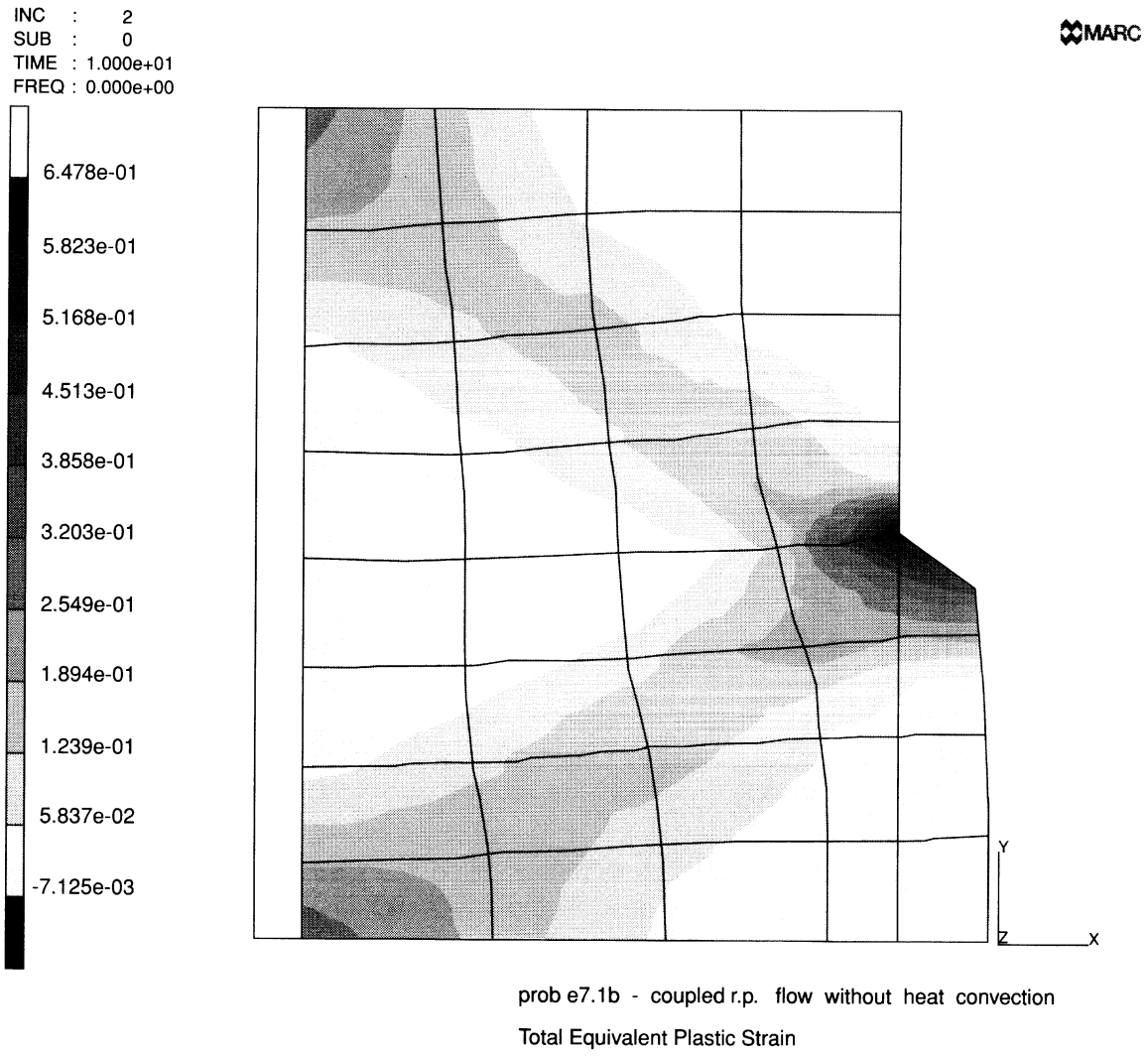

Figure E 7.1-6 Equivalent Plastic Strains in Billet Neglecting Thermal Convection

E 7.6 Biaxial Stress In A Composite Plate

This problem illustrates the analysis of a plate made of layered composite material as shown in Figure E 7.6-1. A biaxial stress field is applied and the results are compared with a textbook solution (Reference 1).

Element

Shell element 75 is used to model the plate. It is a four-node bilinear thick shell element capable of modeling the behavior of layered composite materials.

Model

A 4 x 4 mesh of shells is used for a total of 16 elements, 25 nodes and 150 degrees of freedom. (See Figure E 7.6-2.)

Material Properties

The plate consists of three layers of an orthotropic material. The top layer is 3 mm thick and is offset 45° from the middle layer. The middle layer is 4 mm thick. The bottom layer is also 3 mm thick and is offset 45° from the middle layer. This data is entered in the COMPOSITE option.

The orthotropic material properties are first entered in the ORTHOTROPIC option. The data entered here are the engineering constants E_{11}, E_{22}, E_{33}, ν_{12}, ν_{23}, ν_{31}, G_{12}, G_{22}, and G_{33} with respect to the three planes of elastic symmetry. In problem e7x6b, the anisotropic stress-strain law is entered directly through the ANISOTROPIC option. When entering the data using the ANISOTROPIC option, you must specify the values (21 values) in the symmetric triangle for a compressed form 6x6 matrix. The ply angle for the various layers is given in the COMPOSITE option.

Element type 75 has only two direct strains. Using the PRINT,11 option, you would observe the following printout:

```
layer stress-strain law in layer coords for elem 5.
```

Row \ Column	1	2	3	4	5
1	.200456E11	.70159E9	0	0	0
2	.70159E9	.200456E11	0	0	0
3	0	0	.7E9	0	0
4	0	0	0	.7E9	0
5	0	0	0	0	.7E9

The input required when using the ANISOTROPIC option is:

Row \ Column	1	2	3	4	5	6
1	.200456E11	.70159E9	0	0	0	0
2	.70159E9	.200456E11	0	0	0	0
3	0	0	.7E9	0	0	0
4	0	0	0	.7E9	0	0
5	0	0	0	0	.7E9	0
6	0	0	0	0	0	0

Loading

The biaxial stresses applied to the plate are $\sigma_x = 1. \times 10^6$ N/m^2, $\sigma_y = 2. \times 10^5$ N/m^2 and $\tau_{xy} = 0$. These distributed loads are specified in the DIST LOADS option (the units in this problem are m-kg-s). The applied load magnitudes are negative so that the applied loading is directed out of the element.

Boundary Conditions

In order to fully restrain the rigid body modes without introducing any elastic constraints, a special set of boundary conditions is used. Degrees of freedom 1 to 5 are suppressed at node 1 and degree of freedom 1 is suppressed along the entire left-hand edge. Since the layup is symmetric, only in-plane deformations are expected. The specification of additional rotational constraints at the left-hand edge is irrelevant.

Print Control

The use of the suboption PREF under PRINT ELEM allows the user to obtain printout of the layer stresses in the preferred (ply) coordinate system. The generalized shell resultant quantities are always expressed in the local shell $\tilde{v}^1$, $\tilde{v}^2$ system. Here, these coordinates are parallel to global x and y, respectively.

Results

Results for this problem are given on page 169 in the reference below. They are summarized below:

		Reference	MARC
ε_x^o		.00685	.006875
ε_y^o		.00332	.003324
ε_{xy}^o		-.00784	-.007845
Layers 1,3 x 10^6N/m^2	σ_1	29.6	29.85
	σ_2	18.8	18.87
	σ_{12}	-2.5	-2.49
Layer 2 x 10^6N/m^2	σ_1	139.3	139.8
	σ_2	11.4	11.46
	σ_{12}	-5.5	-5.49

Figure E 7.6-3 shows the deformed shape of the structure. The displacements are all planar, and there is no coupling between bending and axial extension due to the symmetry of the layup. There is, however, coupling between axial extension and in–plane shear. The results are identical, independent of the way the material is input.

Reference

Agarwal, B.D., Broutman, L., *Analysis and Performance of Fiber Composites*, Wiley, 1980.

Summary of Options Used

Listed below are the options used in example e7x6.dat:

Parameter Options

ELEMENT
END
SHELL SECT
SIZING
TITLE

Model Definition Options

COMPOSITE
CONNECTIVITY
COORDINATE
DEFINE
DIST LOADS
END OPTION
FIXED DISP
ORIENTATION
ORTHOTROPIC
POST
PRINT ELEM

Listed below are the options used in example e7x6b.dat:

Parameter Options

ELEMENT
END
SHELL SECT
SIZING
TITLE

Model Definition Options

ANISOTROPIC
COMPOSITE
COORDINATE
DEFINE
DIST LOADS
END OPTION
FIXED DISP
ORIENTATION
POST
PRINT ELEM

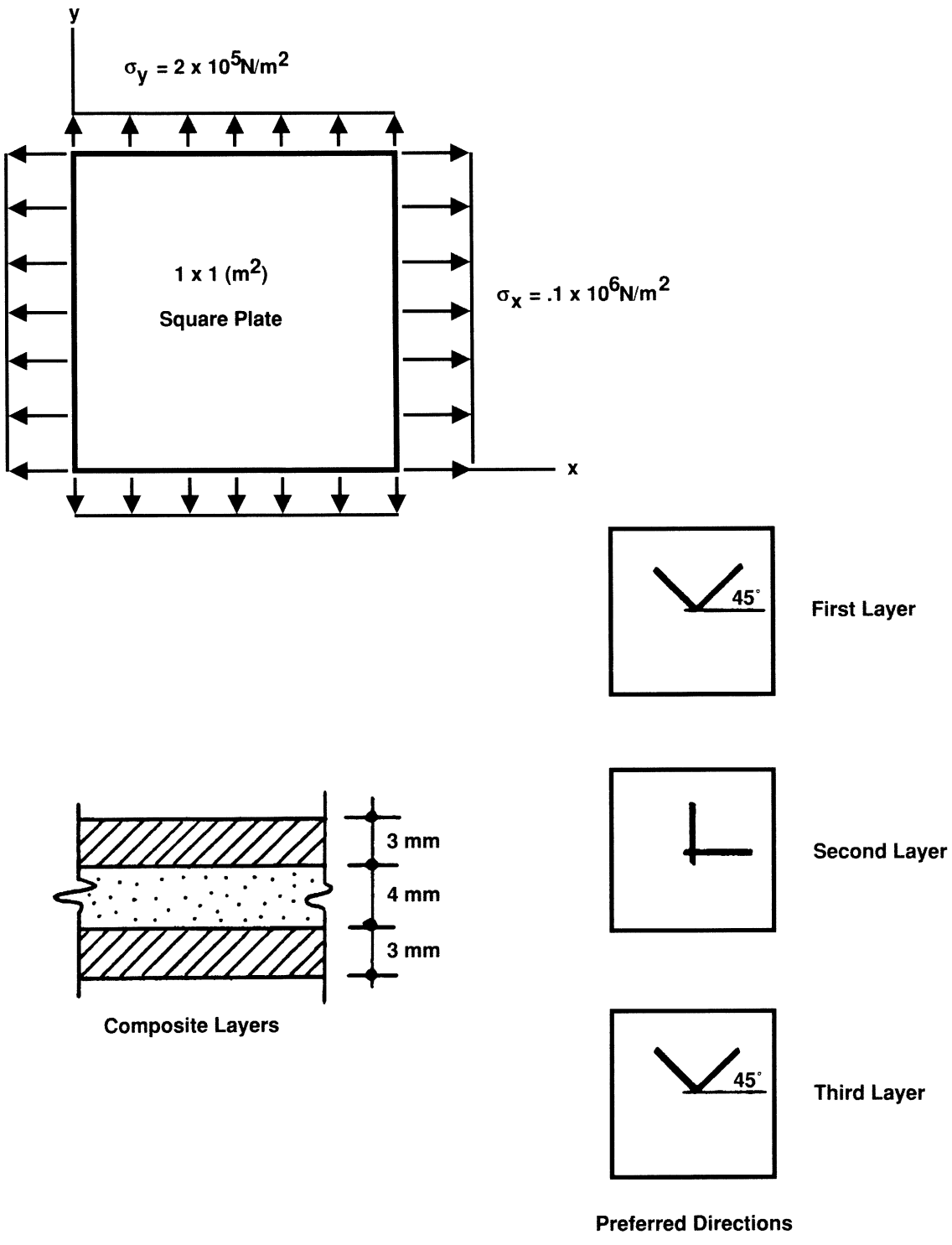

Figure E 7.6-1 Composite Plate

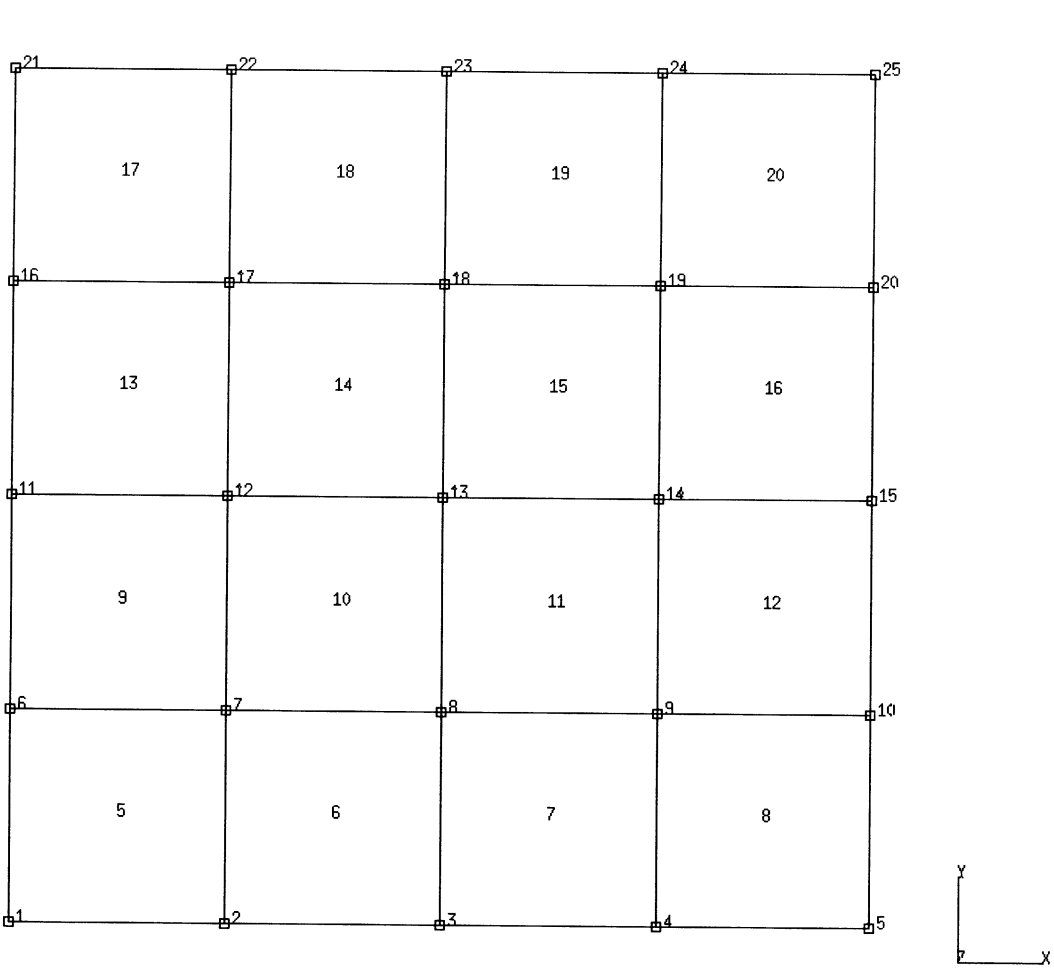

Figure E 7.6-2 Finite Element Mesh

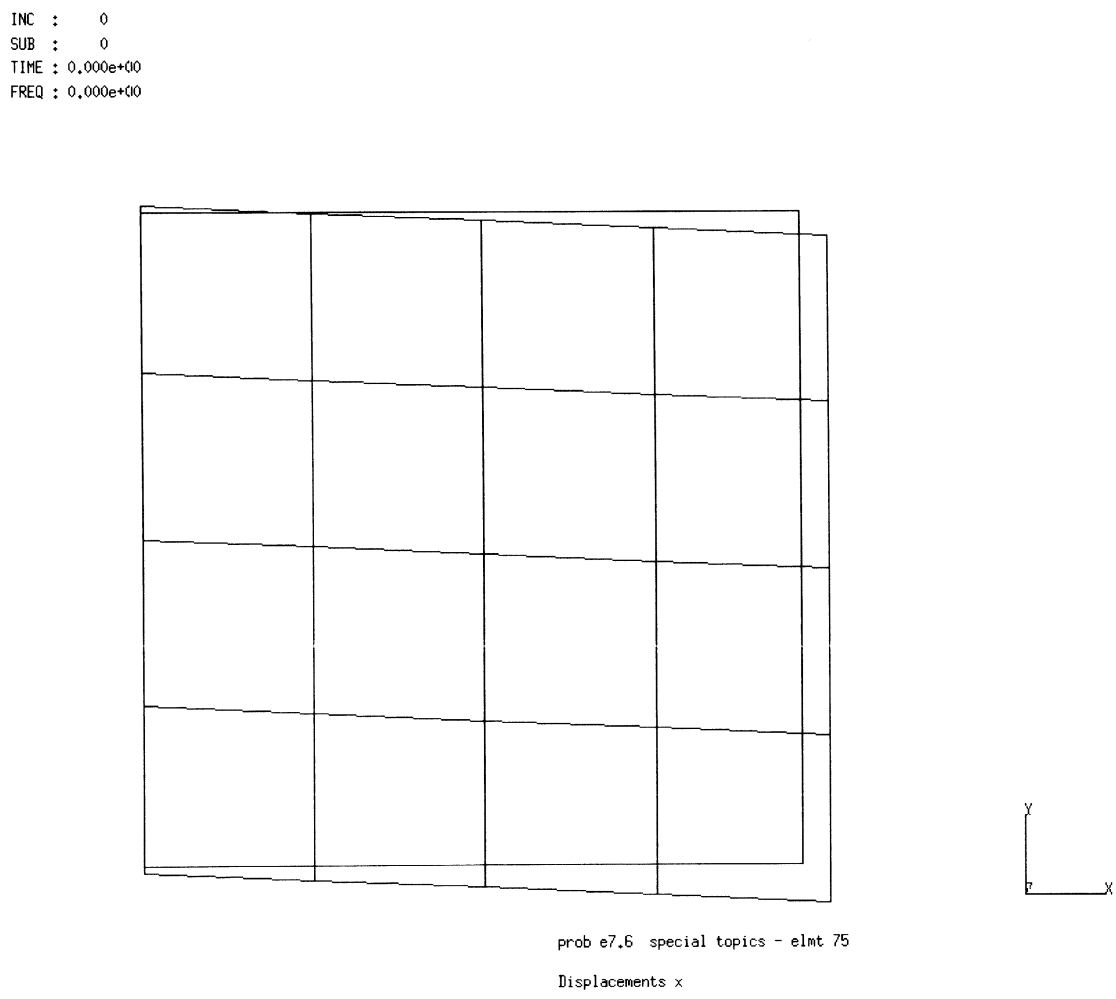

Figure E 7.6-3 Deformed Mesh Plot

E 7.16 Hydrodynamic Journal Bearing Of Finite Width

In this example, a journal bearing of finite width is analyzed. The load-carrying capacity as well as stiffness and damping properties are determined for a stationary bearing system. In addition, the procedure to be followed when analyzing the dynamic behavior of a nondeformable bearing system due to a change in the applied load vector is demonstrated.

Element

Element type 39, which is an arbitrary 4-node isoparametric quadrilateral element with bilinear pressure interpolation, is used to model the lubricant.

Model

The details of the journal bearing problem are given in Figure E 7.16-1. In bearing analyses, the lubricant is modeled by means of planar finite elements. This is possible because it is assumed that the pressure does not vary over the lubricant thickness. Due to symmetry conditions, only half the bearing width needs to be modeled. The incremental mesh generators CONN GENER and NODE FILL are used to generate the element mesh.

Boundary Conditions

It is assumed that atmospheric pressure is acting on the end faces of the bearing system. The BC FILL option is used to generate these boundary conditions.

Tying

Tying was applied to the nodal pressures at both sides of the mesh to simulate the continuous pressure distribution in the circumferential direction.

Thickness Field

The variation of the lubricant thickness over the mesh due to the eccentric position of the rotor is specified in user subroutine UTHICK. This subroutine will determine the nodal thickness values using the following expression:

$$h(\theta) = (20 - 10 \cos \theta)\ 10^{-6}\ m$$

Velocity Field

The relative velocity of the lubricant at the rotor surface, with respect to the stationary surface, is specified in the VELOCITY block. The angular velocity is 1250 rad/sec.

Material Properties

All elements will have lubricant properties as follows: viscosity of .015 N-sec/m^2 and density of 800 kg/m^3.

Load-Carrying Capacity

The pressure distribution for the given bearing system will be calculated in increment 0. Because no external mass flux is prescribed, FLUXES need to be specified. The resulting pressure distribution will be integrated to calculate the actual bearing force components. User subroutine UBEAR is included to specify at each node the physical orientation of the lubricant film. The following expressions are used:

$X = r \sin \theta$ $\quad\quad$ $n_X = -\cos \theta$
$Y = r \cos \theta$ $\quad\quad$ $n_Y = -\sin \theta$
$Z = -y$ $\quad\quad$ $n_Z = 0$

In addition, the resulting bearing moment components with respect to the origin of the global coordinate x, y, z system are calculated. Figure E 7.16-2 shows a path plot of the calculated pressure distribution along the circumference.

The resulting bearing force yields:

$W_X = -1046$ N
$W_Y = -1814$ N
$W_Z = 0$

The resulting bearing moment yields:

$M_X = -6.846$ Nm
$M_Y = 3.938$ Nm
$M_Z = 0$

Because half of the structure was modeled, the components M_X and M_Y are not zero.

Damping and Stiffness Properties

The calculation of bearing characteristics (i.e., damping and stiffness properties) will be performed in subincrements based on a specified change in lubricant film thickness or thickness rate. This is achieved by activating the DAMPING COMPONENTS and the STIFFNS COMPONENTS options. The variation of the film thickness is again specified in user subroutine UTHICK. In total, four subincrements are specified. A displacement of the rotor center of 1.0×10^{-7}m in each global direction is given for both damping and stiffness properties.

The calculated properties are as follows:

Specified Thickness Rate	Damping Components	
$\dot{h} = -1 \times 10^{-7} * \cos\theta$ m/s	$B_{XX} = -54.3 \times 10^{-3}$ N-sec/m	$B_{YX} = -22.4 \times 10^{-3}$ N-sec/m
$\dot{h} = -1 \times 10^{-7} * \sin\theta$ m/s	$B_{XY} = -16.8 \times 10^{-3}$ N-sec/m	$B_{YY} = -28.4 \times 10^{-3}$ N-sec/m

Stiffness

Specified Thickness Rate	Stiffness Components	
$\Delta h = -1 \times 10^{-7} * \cos\theta$ m/s	$K_{XX} = -62.6$ N/m	$K_{YX} = -84.1$ N/m
$\Delta h = -1 \times 10^{-7} * \sin\theta$ m/s	$K_{XY} = 119.8$ N/m	$K_{YY} = 31.4$ N/m

Load-Carrying Capacity at New Rotor Position

Assume that the actual loading of the bearing system increases to the force F = (1408, 1390, 0). Since the resultant load-carrying capacity is not in equilibrium with this force, the rotor will move to a new position. Based on the calculated damping and stiffness properties, a new rotor position, which implies an incremental thickness change in a particular time period, may be estimated. This is done by investigating the mechanical equilibrium of the total system.

The force equilibrium conditions for a nondeformable bearing requires that:

$$F + W + \Delta W = 0$$

From this equation, the required correction for the load-carrying capacity can be calculated. This yields:

$$\Delta W = (-1362, 424, 0)$$

Any incremental change in position of the rotor center will cause a change in the load-carrying capacity according to the following relation:

$$[B]\,\Delta\dot{u} + [K]\,\Delta u = \Delta W$$

where u is the incremental movement of the rotor center.

After substituting the previously calculated stiffness and damping properties, the above equation may be solved, which yields:

$$\Delta u = (-.450, -1.832, 0)\ 10^{-6}\ \text{m}$$

where a time increment of 10^{-3} seconds is assumed.

From the difference in magnitude of the damping and stiffness properties, it can be concluded that the initial response is dominated by the damping effects.

The above procedure is applied in increment 1. The incremental thickness change is defined in user subroutine UTHICK, based on the previous calculated bearing properties at the original rotor position. This change in film thickness is automatically added to the previous thickness field if the calculation of damping and/or stiffness properties is not activated.

According to the calculated pressure distribution for increment 2, this results in a bearing force of:

W_X = -1296 N
W_Y = -1513 N
W_Z = 0.0 N

Summary of Options Used

Listed below are the options used in example e7x16.dat:

Parameter Options

BEARING
ELEMENT
END
SIZING
TITLE

Model Definition Options

BC FILL
CONN GENER
CONNECTIVITY
CONTROL
COORDINATE
END OPTION
FIXED PRESSURE
ISOTROPIC
NODE FILL
THICKNESS
TYING
VELOCITY

Load Incrementation Options

CONTINUE
DAMPING COMPONENTS
STIFFNS COMPONENTS
THICKNS CHANGE

Listed below are the user subroutines found in u7x16.f:

UTHICK
UBEAR

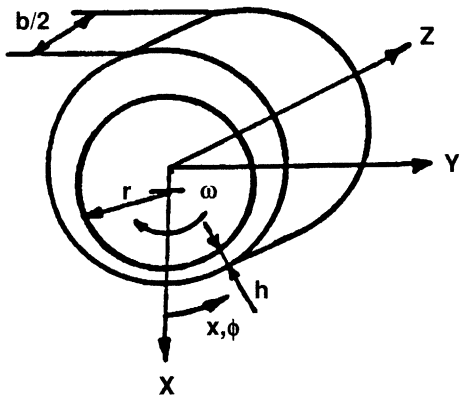

r = 20 mm

b = 10 mm

η = 0.015 N-sec/m^2

h = (20 – 10cosθ) 10^{-6} m

ω = 1250 rad/sec

MARC

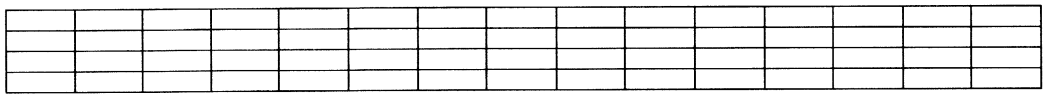

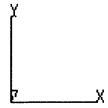

Figure E 7.16-1 Journal Bearing of Finite Width

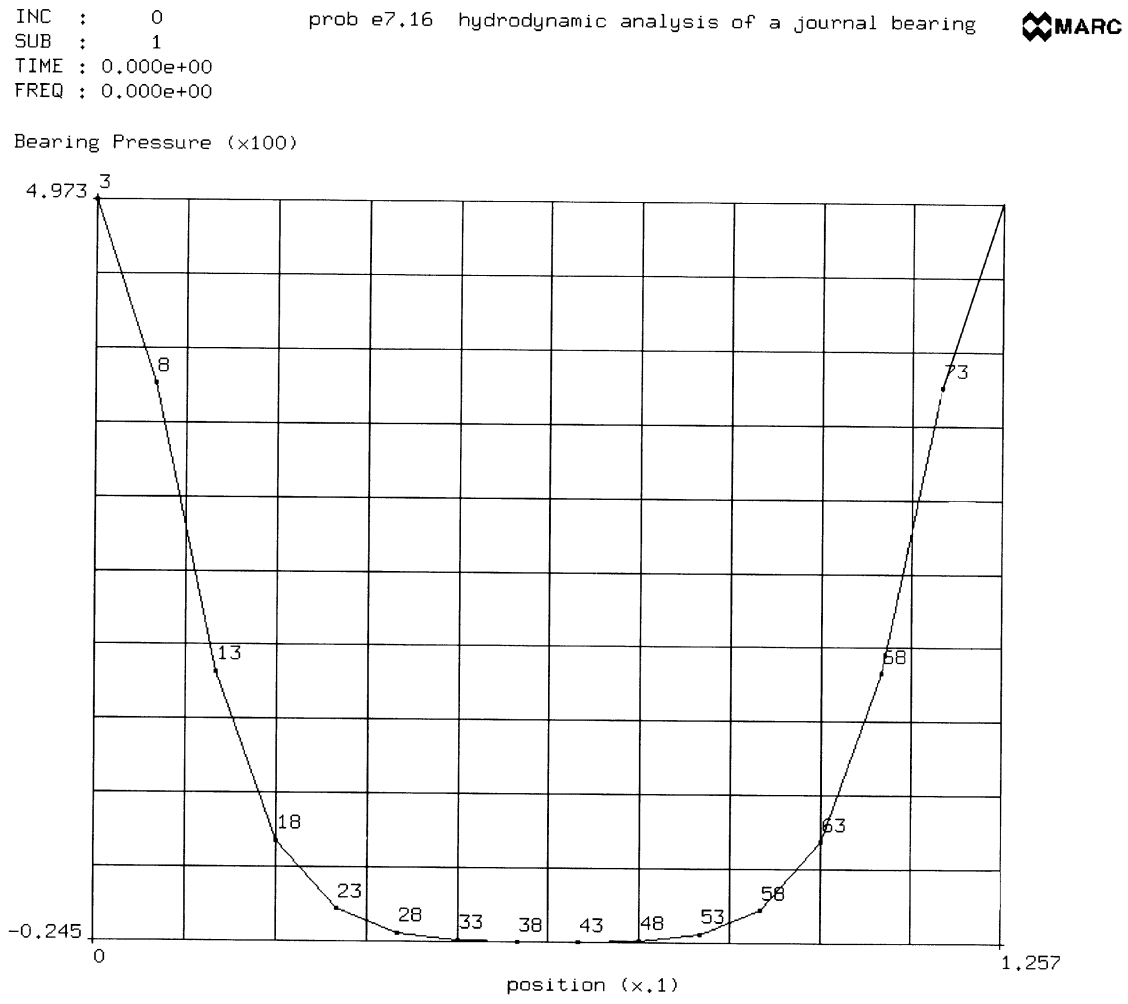

Figure E 7.16-2 Path Plot of Pressure Distribution

E 7.19 Stretching Of A Rubber Sheet With A Hole

This example demonstrates the use of the Mooney-Rivlin and Foam material model for a thin rubber sheet analysis with a hole.

Model

A square sheet of 6.5 cm x 6.5 cm with a hole of radius 0.25 cm is to be analyzed. One quarter of the model is represented due to symmetry. The mesh shown in Figure E 7.19-1 has 80 elements and 277 nodes. Element 26, the conventional displacement formulation 8-node quadrilateral, is used. When using the Mooney-Rivlin in compressible material mold, you normally use Herrmann elements. Because this is a plane-stress analysis, the use of Herrmann elements is not necessary. When using the Foam model, conventional elements should always be used. The thickness of the sheet is 0.079 which is entered through the GEOMETRY option.

Material Properties

The material is modeled using the general third-order deformation model with:

C_{10} = 20.300 N/cm^2
C_{01} = 5.810 N/cm^2
C_{11} = 0.000 N/cm^2
C_{20} = -0.720 N/cm^2
C_{30} = 0.046 N/cm^2

for all elements. This data is entered through the MOONEY option.

The material of problem e7.19b is modeled using the three-term rubber-foam model:

Term	μ (N/cm)	α	β
1	1.48269	7.56498	-10.4156
2	-1.48269	-0.504321	-10.4155
3	π0.0041819	12.1478	-5.67921

for all elements. This data is entered through the OGDEN option.

Boundary Conditions

The nodes along x = 0 (edge 1) are fixed in the x-direction. The nodes along y = 3.25 (edge 2) and along y = 0 (edge 4) are fixed in the y-direction. The nodes which are originally along x = 3.25 (edge 3) are all tied to node 277. This will allow you to keep this edge straight and easily calculate the total pulling force. The displacement of node 277 is first set to 0 in the x-direction and then changed through the DISP CHANGE option. The incremental displacement will be 0.325 cm/increment. A total of 10 increments are executed. Hence, the dimension in the x-direction doubles.

Results

For the Incompressible Model:

The deformed mesh is shown in Figure E 7.19-2. The load-deflection curve for node 277 is shown in Figure E 7.19-3. There is substantial thinning of the sheet.

For the Foam Model:

The deformed mesh is shown in Figure E 7.19-4. The load deflection curve for node 277 is shown in Figure E 7.19-4. Note that the deformation is significantly different near the hole.

Summary of Options Used

Listed below are the options used in the example e7x19.dat:

Parameter Options

ELEMENT
END
SIZING
TITLE

Model Definition Options

CONNECTIVITY
CONTROL
COORDINATES
END OPTION
DEFINE
FIXED DISP
GEOMETRY
MOONEY
POST
PRINT CHOICE
TYING

Load Incrementation Options

AUTO LOAD
CONTINUE
DIST CHANGE

Listed below are the options used in the example e7x19b.dat:

Parameter Options

ELEMENTS
END
LARGE DISP
SIZING
TITLE

Model Definition Options

CONNECTIVITY
COORDINATE
DEFINE
END OPTION
FIXED DISP
FOAM
GEOMETRY
POST
PRINT CHOICE
TYING

Load Incrementation Options

AUTO LOAD
CONTINUE
DIST CHANGE

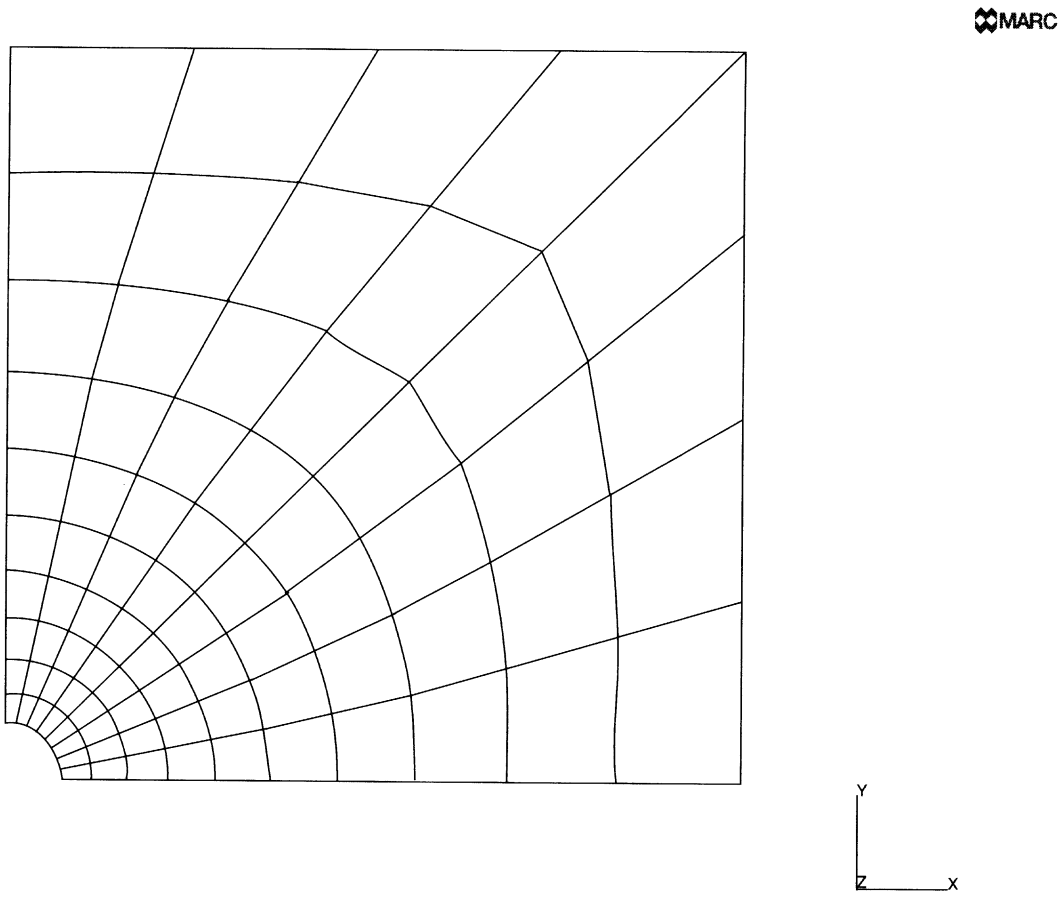

Figure E 7.19-1 Finite Element Mesh

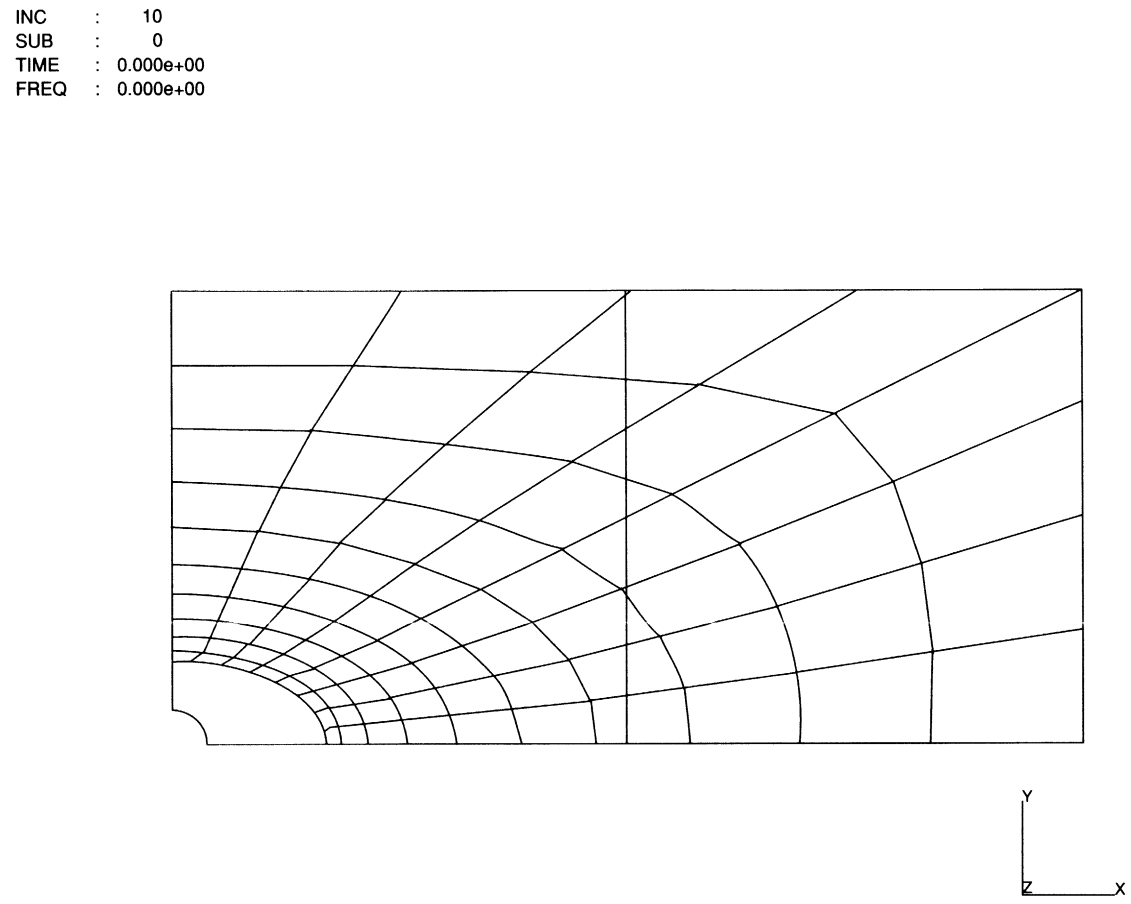

Figure E 7.19-2 Incompressible Model Deformed Mesh

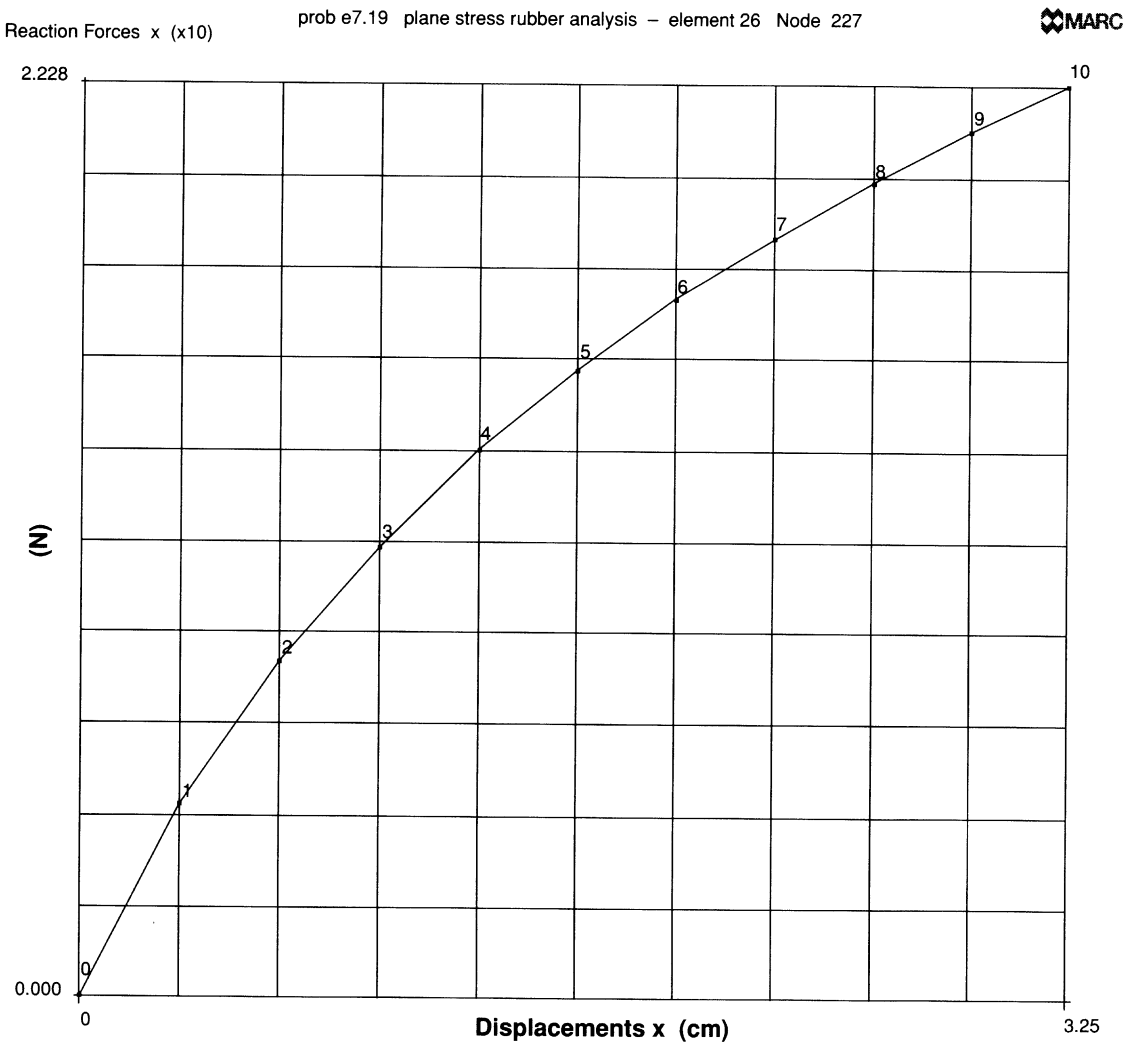

Figure E 7.19-3 Incompressible Model Load Deflection Curve at Node 277

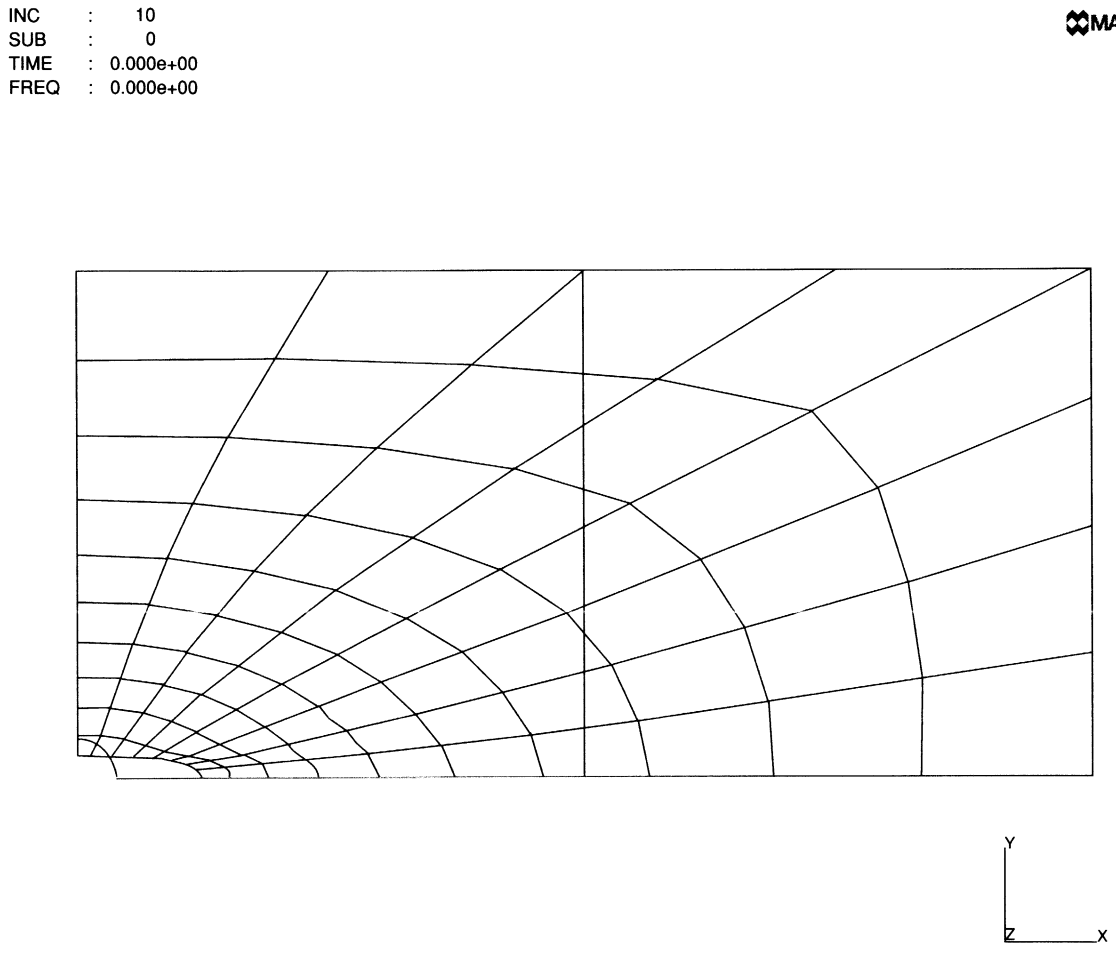

Figure E 7.19-4 Foam Model Deformed Mesh

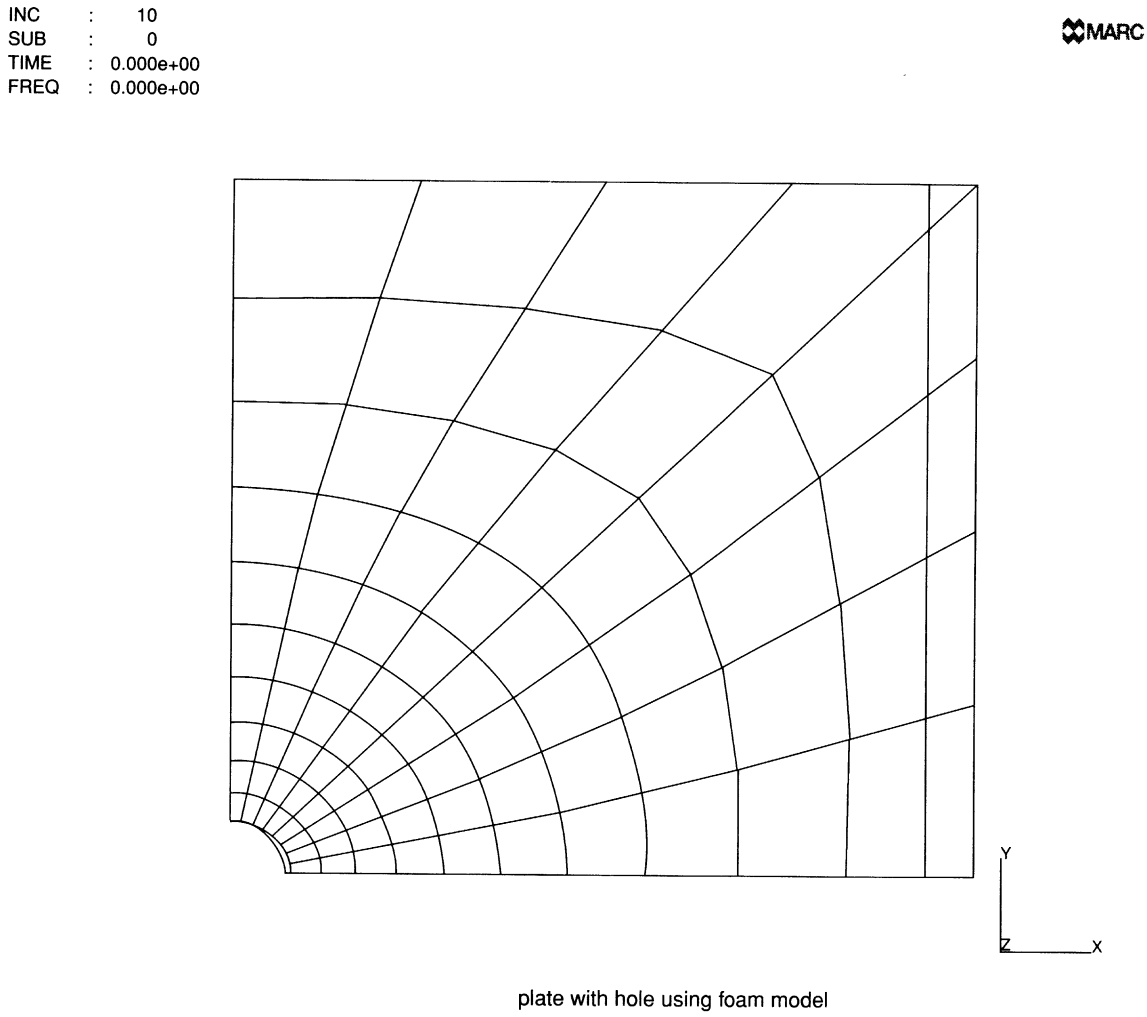

Figure E 7.19-5 Foam Model Load Deflection Curve at Node 277

E 7.20 Compression Of An O-Ring Using Ogden Model

This example demonstrates the use of the Ogden rubber model for the high compression of an O-ring. The ring is compressed into a rigid channel. The second analysis is of the same problem, but the follower force stiffness is included. The third analysis uses a simpler mesh to begin with and then demonstrates the adaptive meshing capability.

Element

Library element 82, a five-node axisymmetric element using the Herrmann formulation, is used for this analysis. In the first two analyses, there are 544 elements and 1149 nodes as shown in Figure E 7.20-1. Three rigid bodies are used to simulate the channel. The ring has a mean radius of 12 cm and the loading radius is 1.5 cm. In the third analysis, the crude mesh shown in Figure E 7.20-2 is used. This mesh begins with 29 elements and 69 nodes.

The rigid surface at the outside radius is first moved inwards a distance of 0.5 cm in a period of 50 seconds. The surface is then frozen and an external pressure of 18.8 N/cm^2 is applied onto the left face during 47 increments. The FOLLOW FOR option is used to insure that the load is applied on the deformed geometry. In the second analysis, the follower force stiffness is included. This should improve the convergence behavior.

Material Properties

The O-ring can be described using the Ogden material model using a three term series. The stress-strain curve for this model is shown in Figure E 7.20-3. The data was fit such that:

Term	μ (N/cm^2)	α
1	6.30	1.3
2	0.12	5.0
3	-0.10	-2.0

and the bulk modulus was 1.0E9 N/cm^2.

Contact/Boundary Conditions

All of the kinematic constraints are provided using rigid contact surfaces. Coulomb friction with a coefficient of friction of 0.1 is specified.

Controls

The full Newton-Raphson iterative method is used with a convergence tolerance of 10% on residuals requested. Because of the large compressive stresses that are generated, the solution of nonpositive definite systems is forced. Additionally, a flag is set that tells the program to only use the deviatoric stresses in the initial stress stiffness matrix. While this may slow convergence, it tends to improve stability. The PRINT,5 option is used to obtain more information regarding the contact behavior. The NO PRINT option is used to suppress the printout.

Adaptive Meshing

In the third analysis, the adaptive meshing technique is demonstrated. The mean strain energy criteria is used with a factor of 0.9. The maximum number of subdivisions allowed is two. As the O-ring initially is round, this additional information is provided using the SURFACE option. A circle at origin (1.5, 12.0 cm) and a radius of 1.5 cm is defined. The ATTACH NODE option is used to associate the original nodes with this geometry.

Results

The deformed mesh at increments 10, 30, and 50 are shown in Figure E 7.20-4 through Figure E 7.20-6. One observes that at increment 50, the ring almost completely fills the corner regions. The mean second Piola-Kirchhoff stresses are shown in Figure E 7.20-7. One should note that in all these plots, the free surface to which the pressure is applied remains almost perfectly circular. Finally, the contact forces are shown in Figure E 7.20-8.

The progression of meshes using the adaptive meshing is shown in Figure E 7.20-9 through Figure E 7.20-12. At the end of the analysis, the total number of elements is 104 and the number of nodes is 148.

Summary of Options Used

Listed below are the options used in example e7x20.dat and e7x20b.dat:

Parameter Options

ELEMENT
END
FOLLOW FOR
LARGE DISP
PRINT
SIZING
TITLE

Model Definition Options

CONNECTIVITY
CONTACT
CONTROL
COORDINATES
DEFINE
DIST LOADS
END OPTION
OGDEN
OPTIMIZE
POST

Load Incrementation Options

AUTO LOAD
CONTINUE
DIST LOADS
MOTION CHANGE
TIME STEP

Listed below are the options used in example e7x20c.dat:

Parameter Options

ADAPTIVE
ELEMENT
END
FOLLOW FOR
LARGE DISP
PRINT
SETNAME
SIZING
TITLE

Model Definition Options

ADAPTIVE
ATTACH NODE
CONNECTIVITY
CONTACT
CONTROL
COORDINATES
DEFINE
DIST LOADS
END OPTION
OGDEN
OPTIMIZE
POST

Load Incrementation Options

AUTO LOAD
CONTINUE
DIST LOADS
MOTION CHANGE
TIME STEP

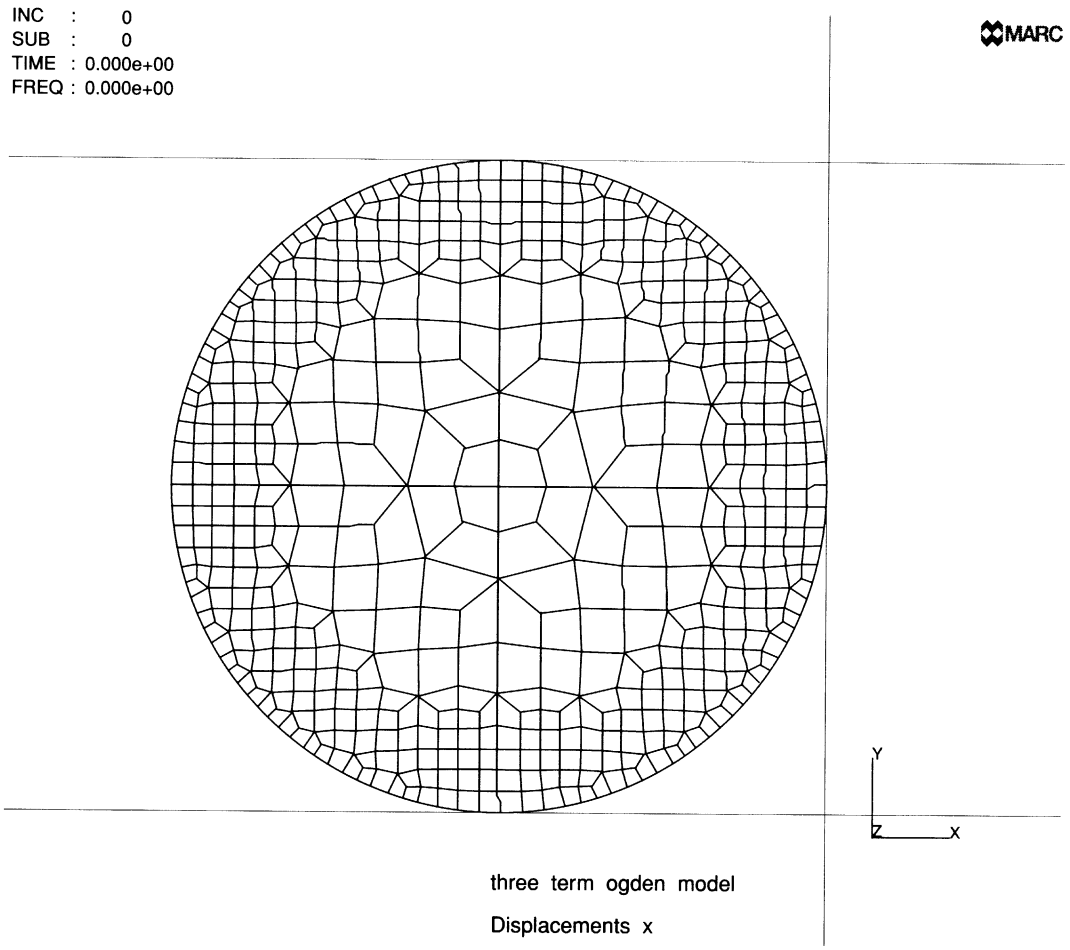

Figure E 7.20-1 O-ring Mesh

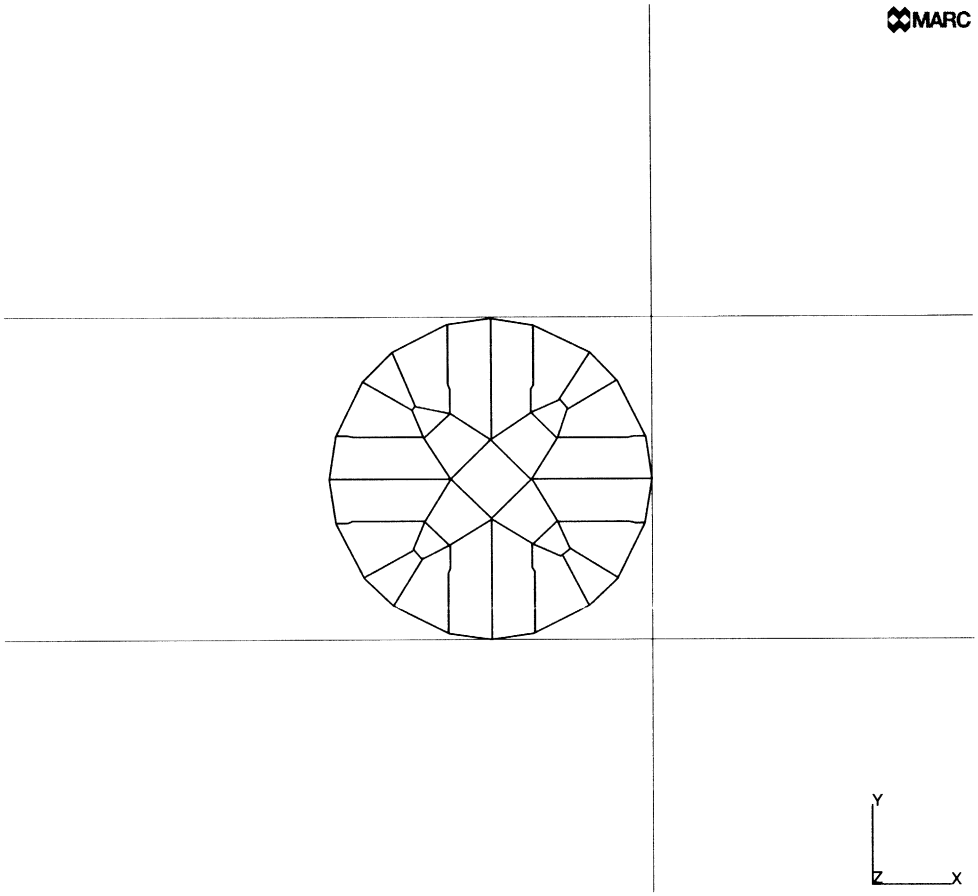

Figure E 7.20-2 Crude O-ring Mesh

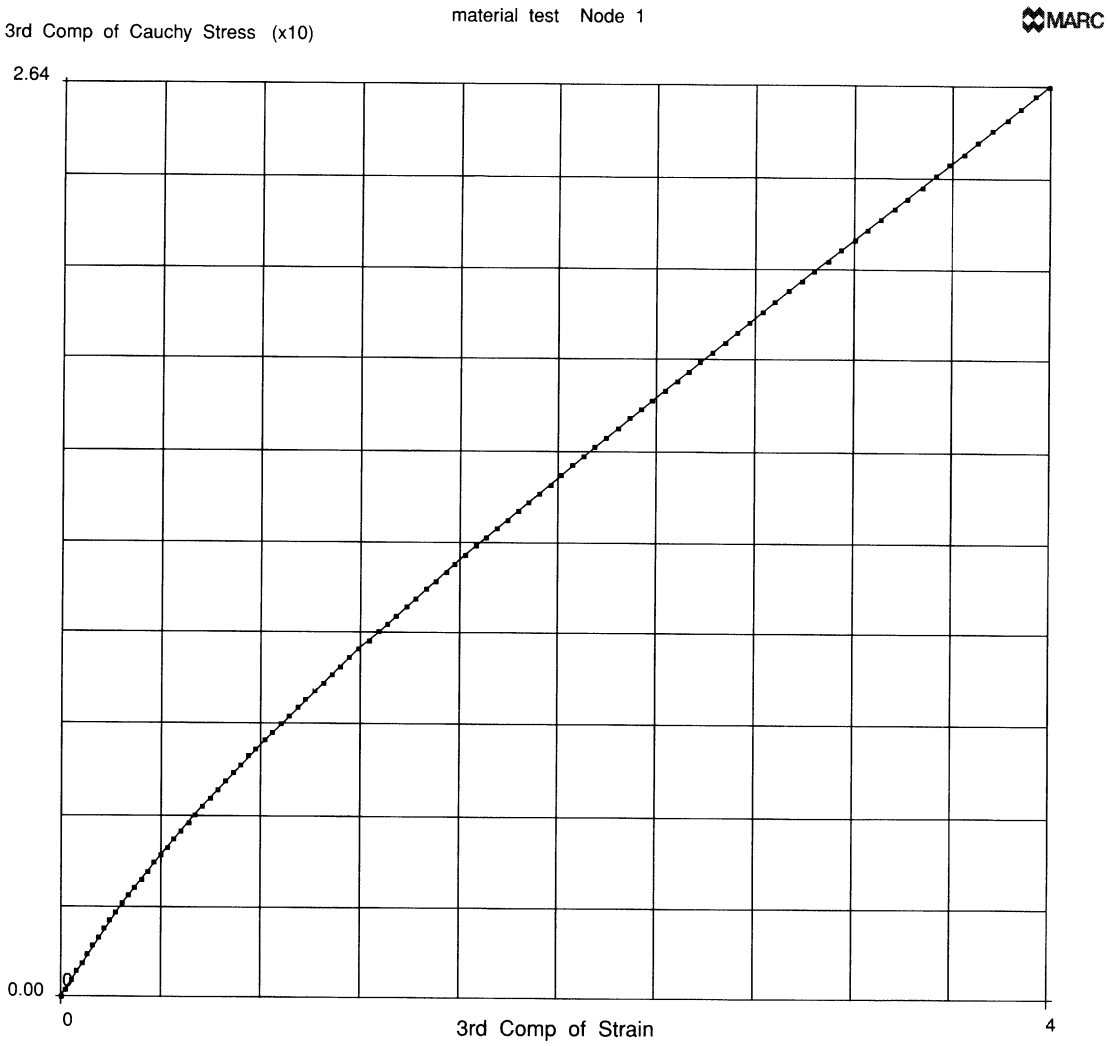

Figure E 7.20-3 Stress-Strain Curve

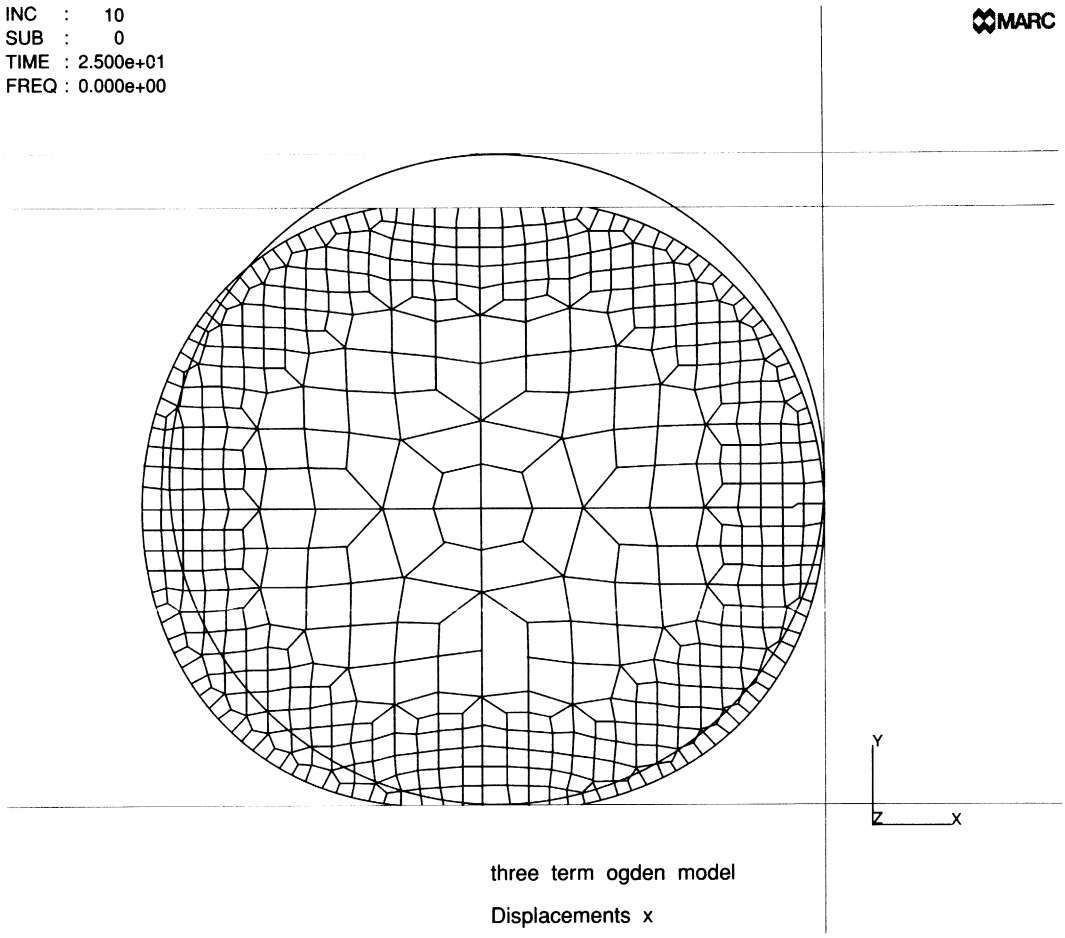

Figure E 7.20-4 Deformed Mesh, Increment 10

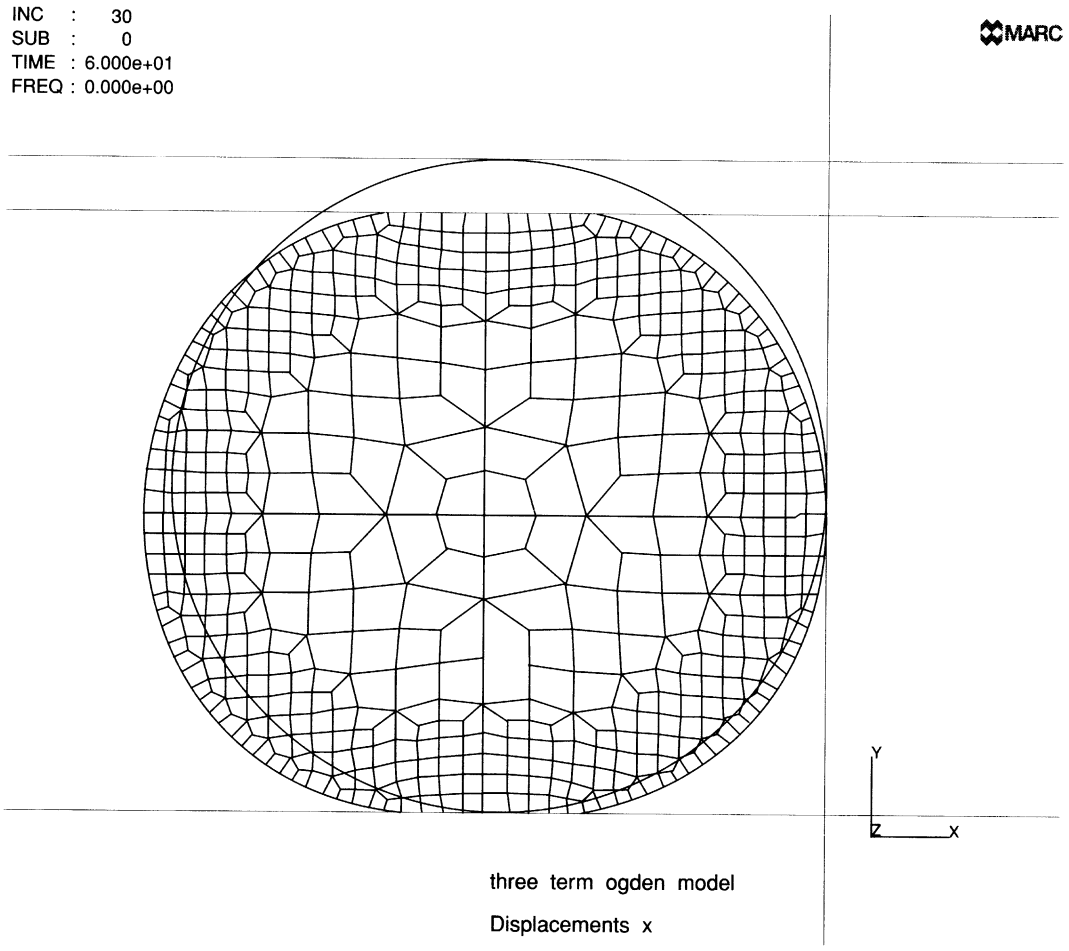

Figure E 7.20-5 Deformed Mesh, Increment 30

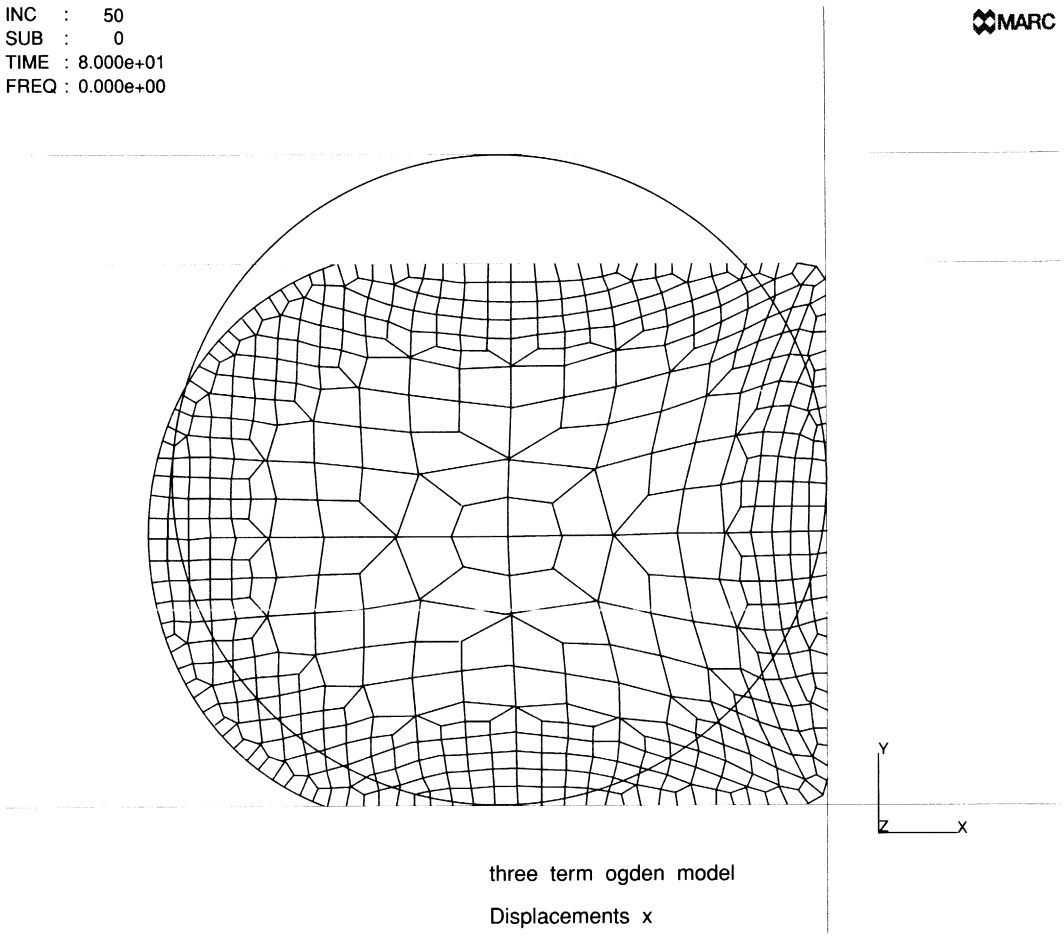

Figure E 7.20-6 Deformed Mesh, Increment 50

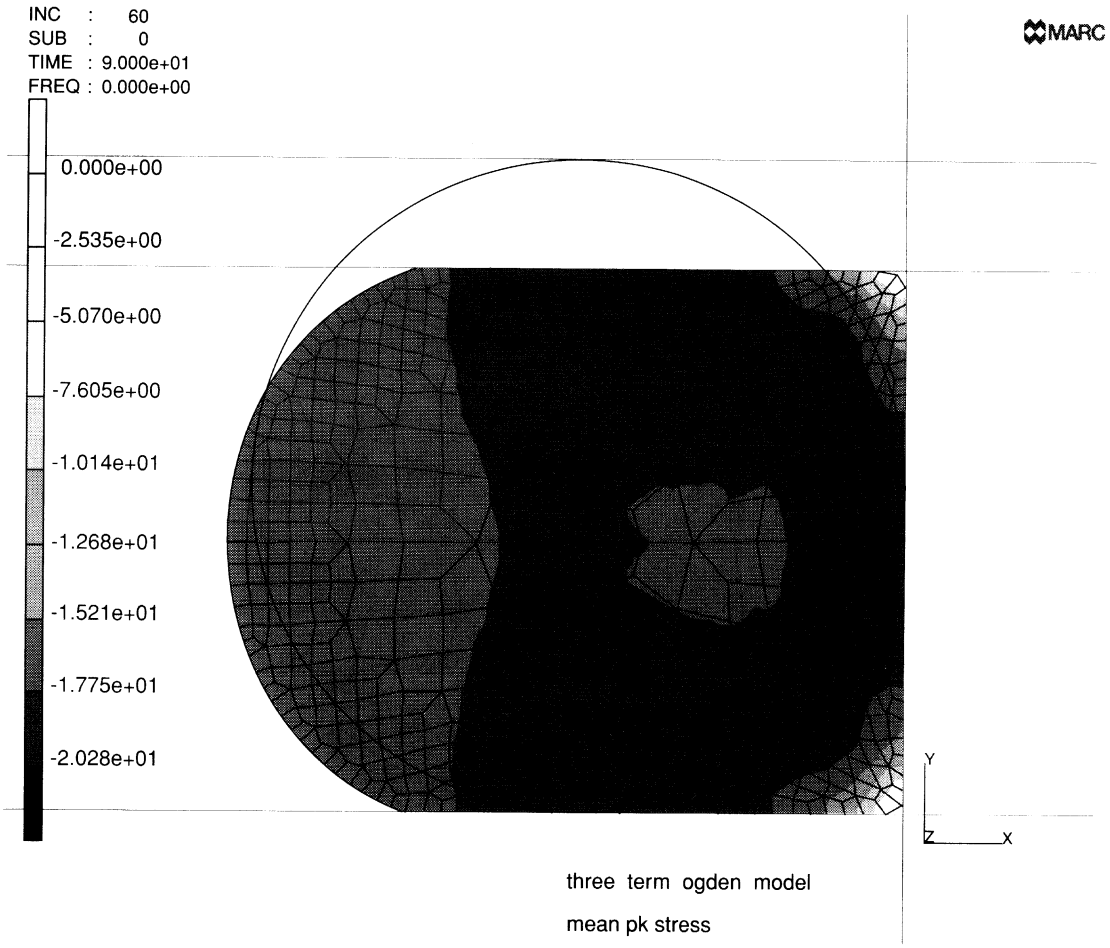

Figure E 7.20-7 Mean Stress Distribution

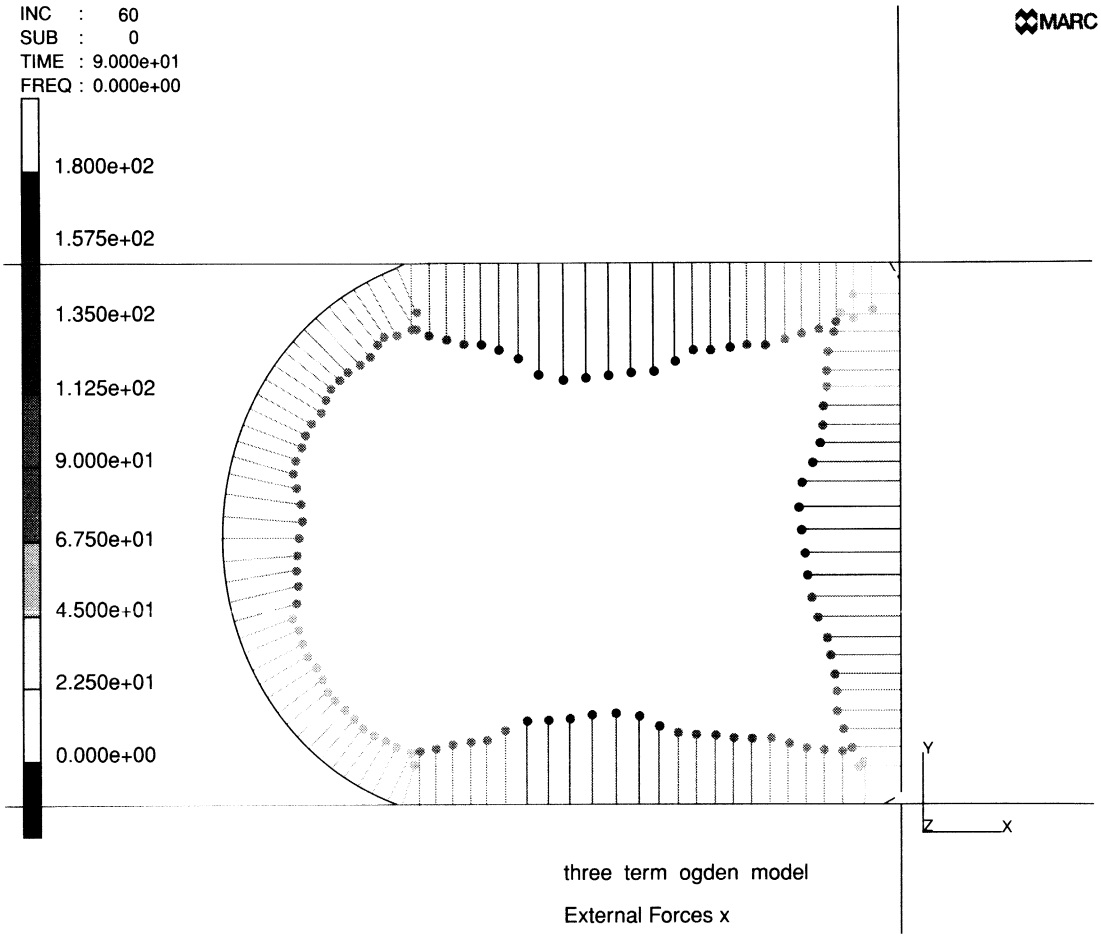

Figure E 7.20-8 Contact Forces

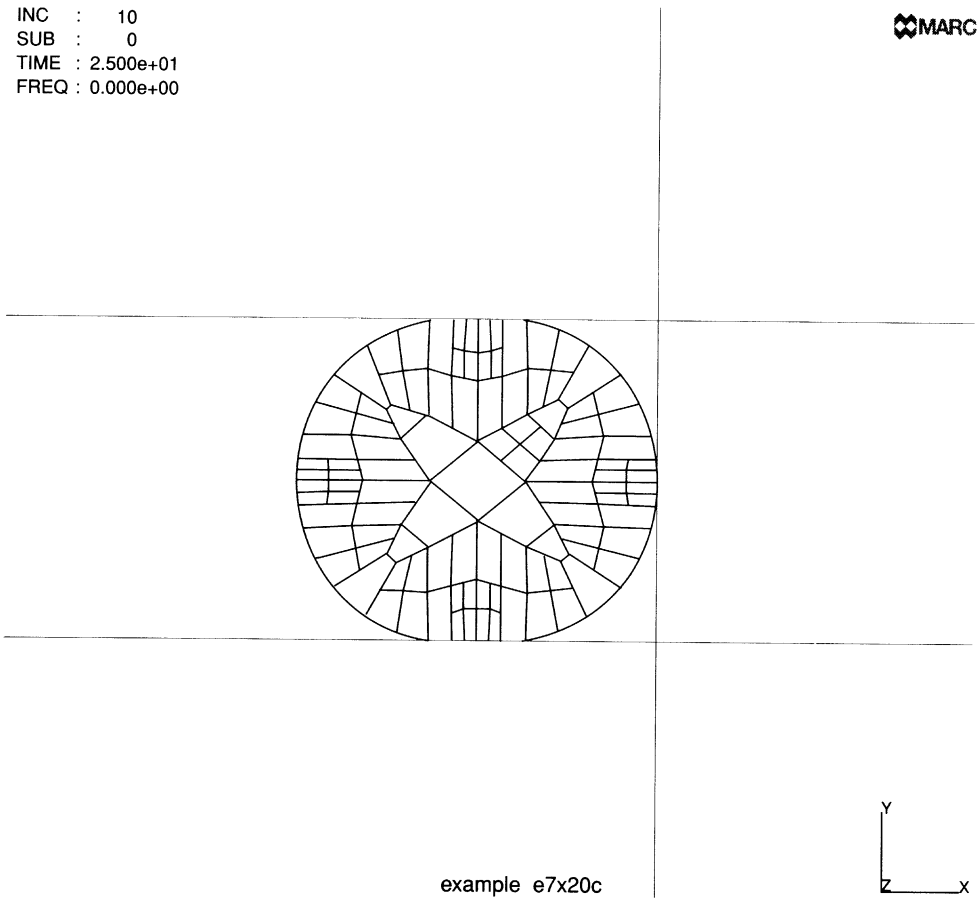

Figure E 7.20-9 Adaptive Mesh at Increment 10

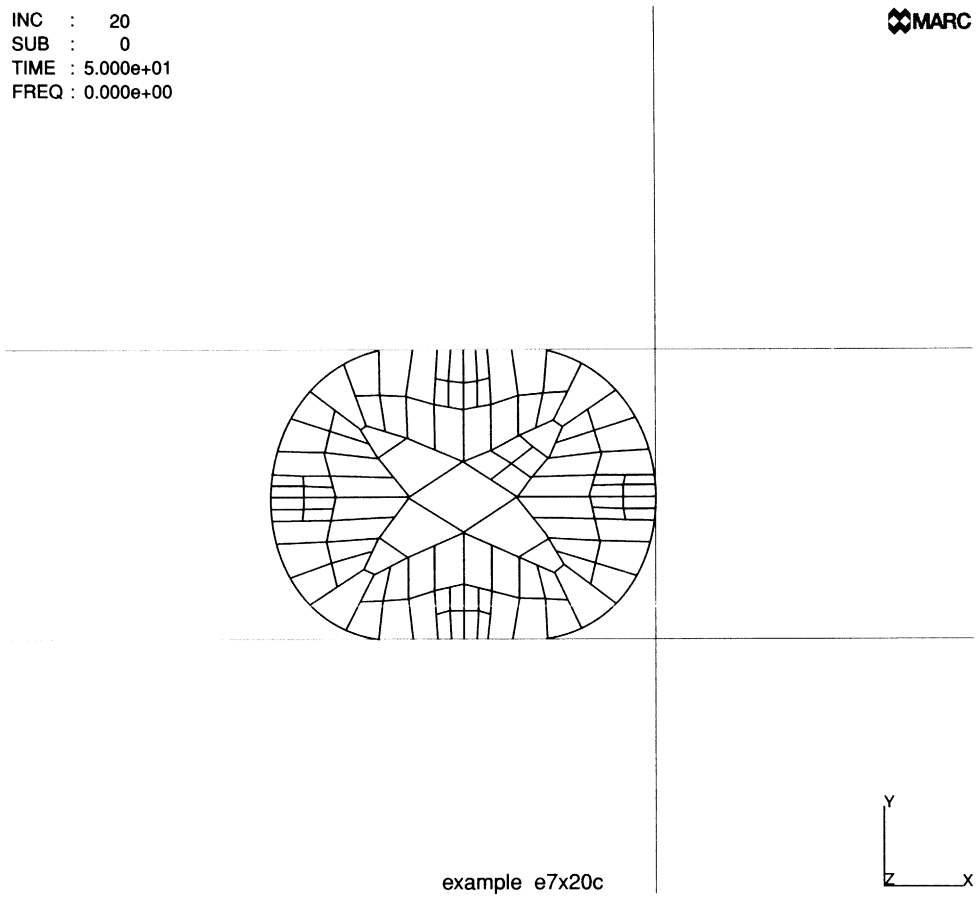

Figure E 7.20-10 Adaptive Mesh at Increment 20

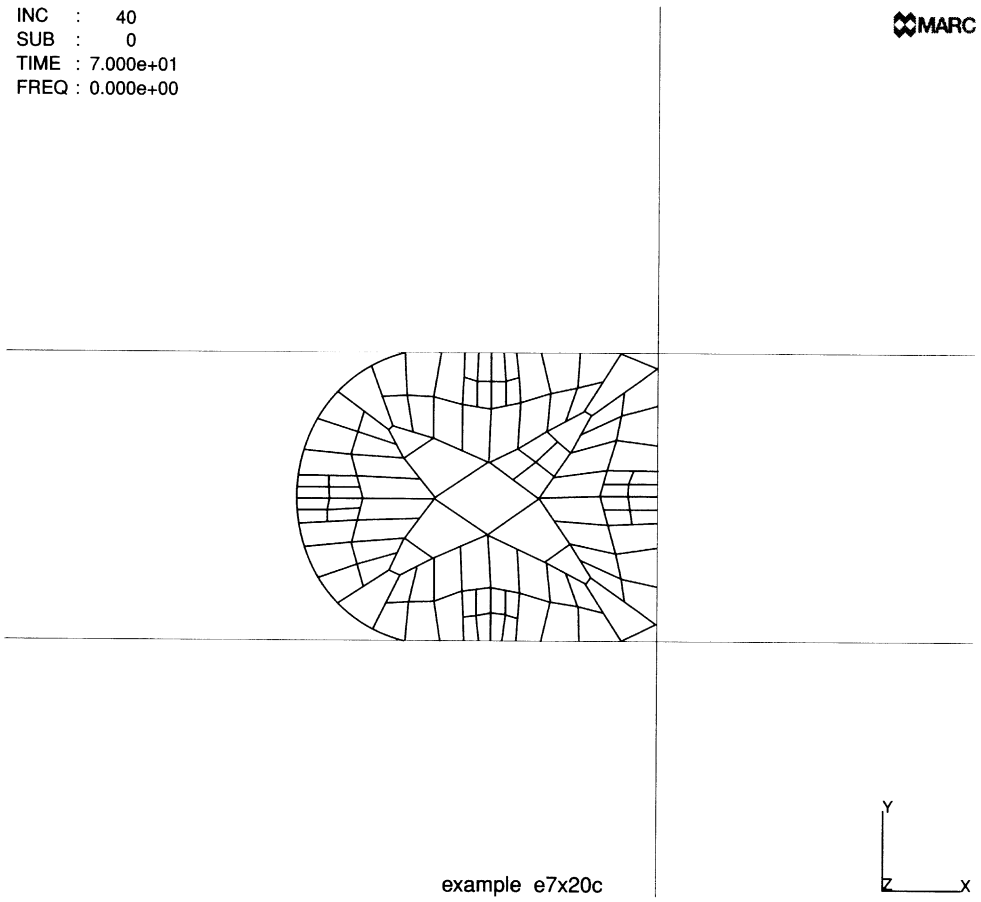

Figure E 7.20-11 Adaptive Mesh at Increment 40

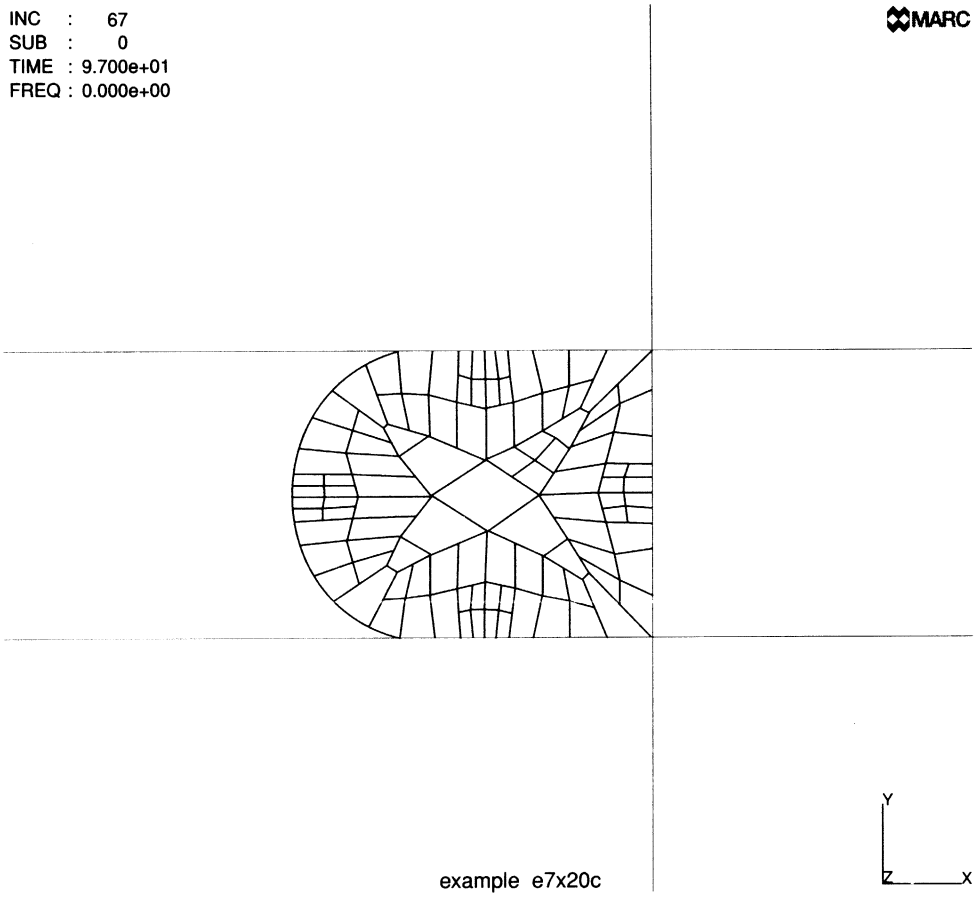

Figure E 7.20-12 Adaptive Mesh at Increment 67

E 7.22 Loading Of A Rubber Plate

This example illustrates the analysis of a rubber plate under cyclic loading. The analysis uses three different material models. The first analysis uses simply a three-term Ogden series; the second model incorporates damage; the third and most complex model incorporates both damage and viscoelasticity.

Element

Element type 75, a 4-node shell element, is used for this analysis. A 60 cm x 60 cm simply-supported plate is to be modeled. Because of symmetry, only one-quarter of the plate is represented using 25 elements as shown in Figure E 7.22-1. The SHELL SECT option is used to prescribe three layers. This is adequate because it is a linear analysis. The thickness of 3 cm is specified in the GEOMETRY option.

Loading

The first and second models are rate insensitive. Two increments are taken to apply a distributed load of 0.004 on the complete plate followed by two increments to remove the load. In the third analysis, the initial load is also applied in two increments instantaneously; that is, the time step is zero. Hence, creep (viscoelasticity) will not occur. This is followed by a period of one second in which relaxation occurs in which no additional load is applied. Then, two increments follow during which the load is removed again and instantaneously followed by a final relaxation period of five seconds.

Material Properties

The rubber material is defined as a three-term Ogden series with a finite compressibility. The bulk modulus = 6000 N/cm^2 and the coefficients are:

Term	μ (N/cm^2)	a
1	6.300	1.3
2	0.012	5.0
3	-0.100	-2.0

The stress-strain law is shown in Figure E 7.22-2.

The rubber damage model is used in the second and third analyses. Only deviatoric damage will be considered with the damage rate being 0.050 and the maximum damage factor = 0.90. This is specified through the DAMAGE option.

The third model includes viscoelastic deviatoric behavior. Two terms are included in the Prony series to express the strain energy relaxation function:

Series	Multiplier	Relaxation Time (Seconds)
1	0.6	1.0
2	0.1	10.0

Notice that the total time of the analysis falls within the relaxation times specified.

Boundary Conditions

Displacements are prescribed such that nodes 1 to 6 and 1 to 31 by 6 have no normal displacement or rotations about the edge, and nodes 31 to 36 and 6 to 36 by 6 are symmetric boundary conditions. The in-plane rotation is constrained at all nodes.

Controls

The full Newton-Raphson method is used in this analysis. In those increments where the total applied load is nonzero, a five percent tolerance on residuals is required. When the applied load is zero, we would be attempting to measure residual/noise so the convergence is changed to displacement control. This is very important to insure efficient convergence to a meaningful accuracy.

Results

Figure E 7.22-3 shows the displacement of the center node (36) as a function of the increment number for the first model. You can observe that the material goes back to the original configuration when the load has been removed. Displacement is of the order 10^{-6}. In Figure E 7.22-4, one observes the displacement history when damage is included. Note that the maximum displacement is larger and the slope of the loading and unloading curve is substantially different. Upon unloading, there is a permanent deformation of the order 2.5×10^{-2}. Finally, Figure E 7.22-5 shows the displacement history when both damage and viscoelasticity occur. You observe that there are four different regions: loading, creep, unloading and creep. Figure E 7.22-6 is the same information but now plotted as a function of time.

Summary of Options Used

Listed below are the options used in example e7x22a:

Parameter Options

ELEMENT
END
LARGE DISP
SHELL SECT
SIZING
TITLE

Model Definition Options

CONNECTIVITY
CONTROL
COORDINATES
DIST LOADS
END OPTION
FIXED DISP
GEOMETRY
OGDEN
OPTIMIZE
POST

Load Incrementation Options

AUTO LOAD
CONTINUE
DIST LOADS

Listed below are the options used in example e7x22b:

Parameter Options

ELEMENT
END
LARGE DISP
SHELL SECT
SIZING
TITLE

Model Definition Options

CONNECTIVITY
CONTROL
COORDINATES
DAMAGE
DIST LOADS
END OPTION
FIXED DISP
GEOMETRY
OGDEN
OPTIMIZE
POST

Load Incrementation Options

AUTO LOAD
CONTINUE
DIST LOADS

Listed below are the options used in example e7x22c:

Parameter Options

ELEMENT
END
LARGE DISP
SHELL SECT
SIZING
TITLE

Model Definition Options

CONNECTIVITY
CONTROL
COORDINATES
DAMAGE
DIST LOADS
END OPTION
FIXED DISP
GEOMETRY
OGDEN
OPTIMIZE
POST
VISCELOGDEN

Load Incrementation Options

AUTO LOAD
CONTINUE
DIST LOADS

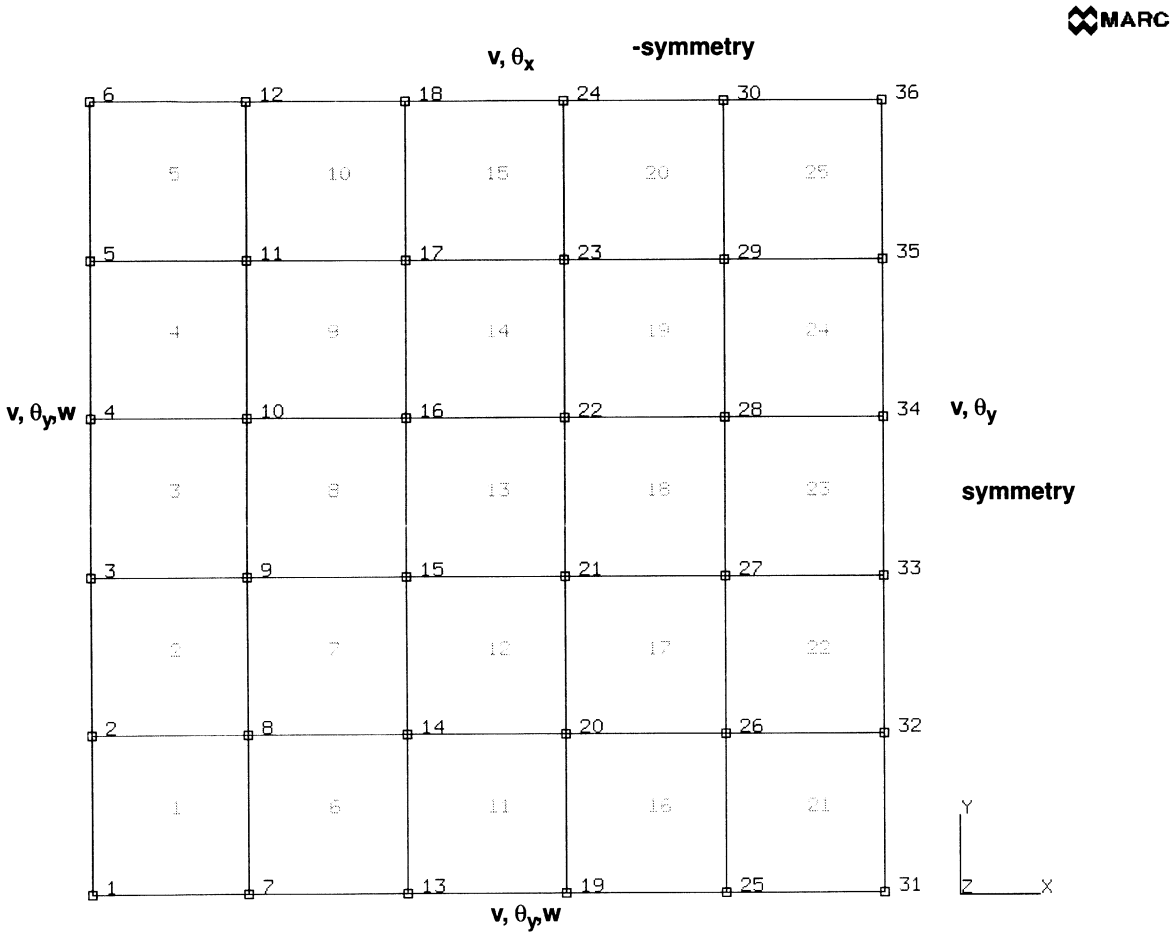

Figure E 7.22-1 Finite Element Mesh

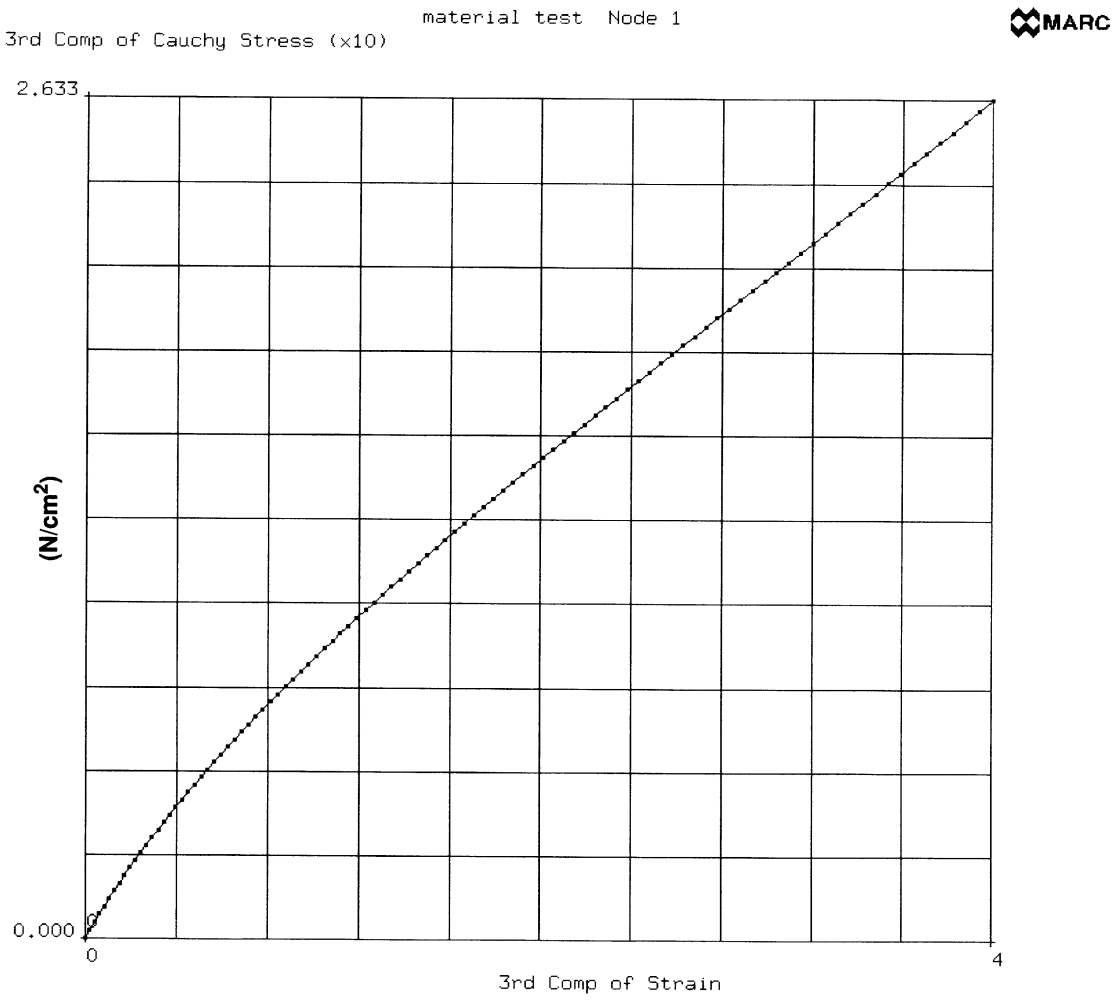

Figure E 7.22-2 Stress-Strain Curve

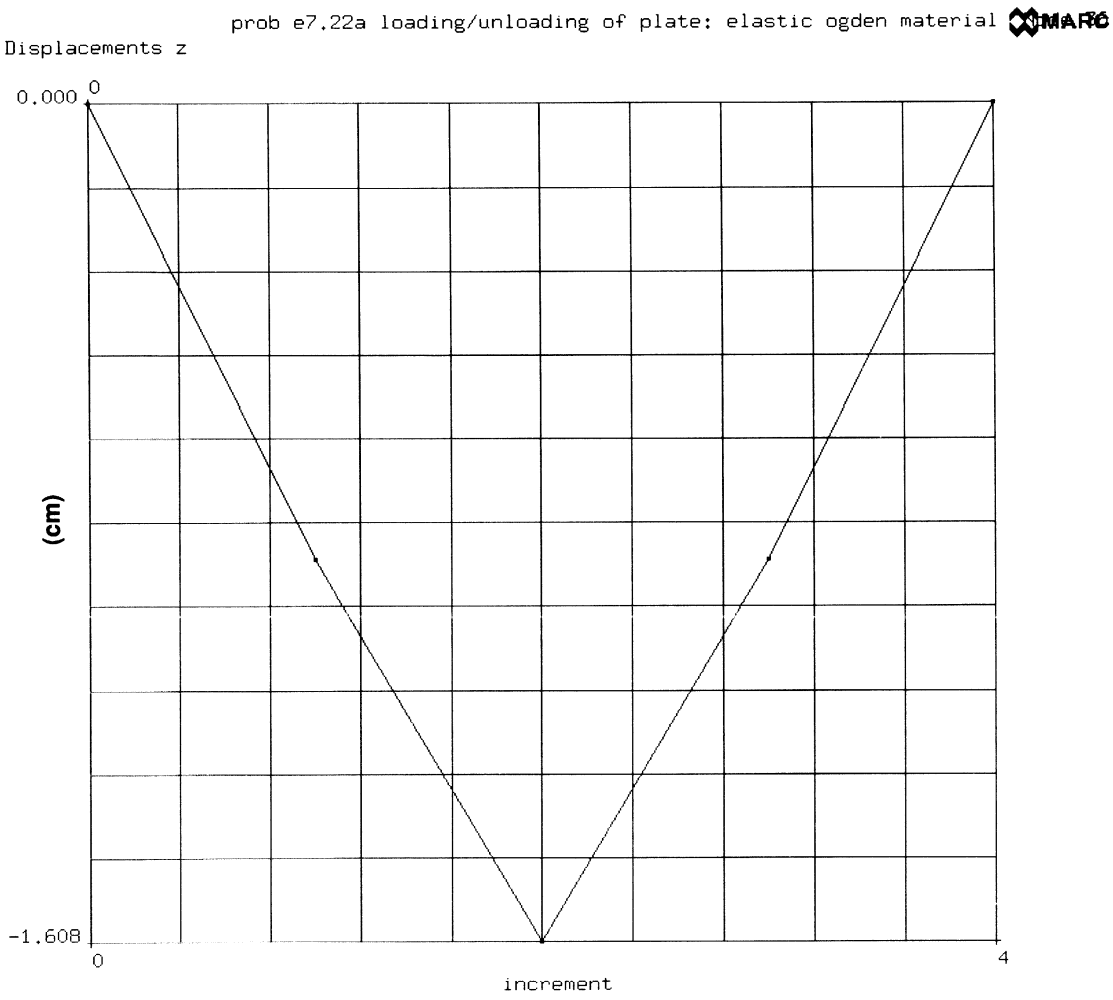

Figure E 7.22-3 Displacement History of Center Node – Elastic Effects Only

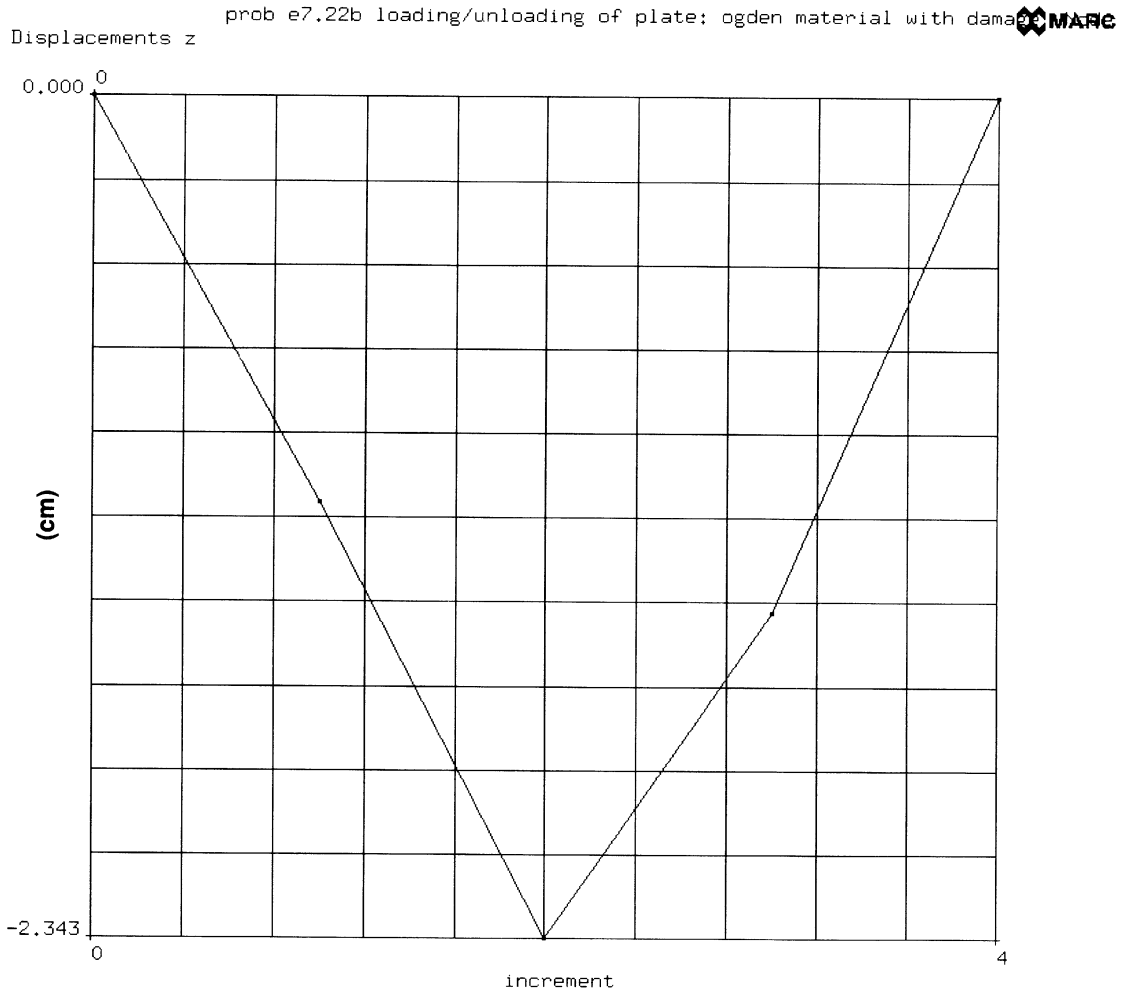

Figure E 7.22-4 Displacement History of Center Node – Including Damage Effects

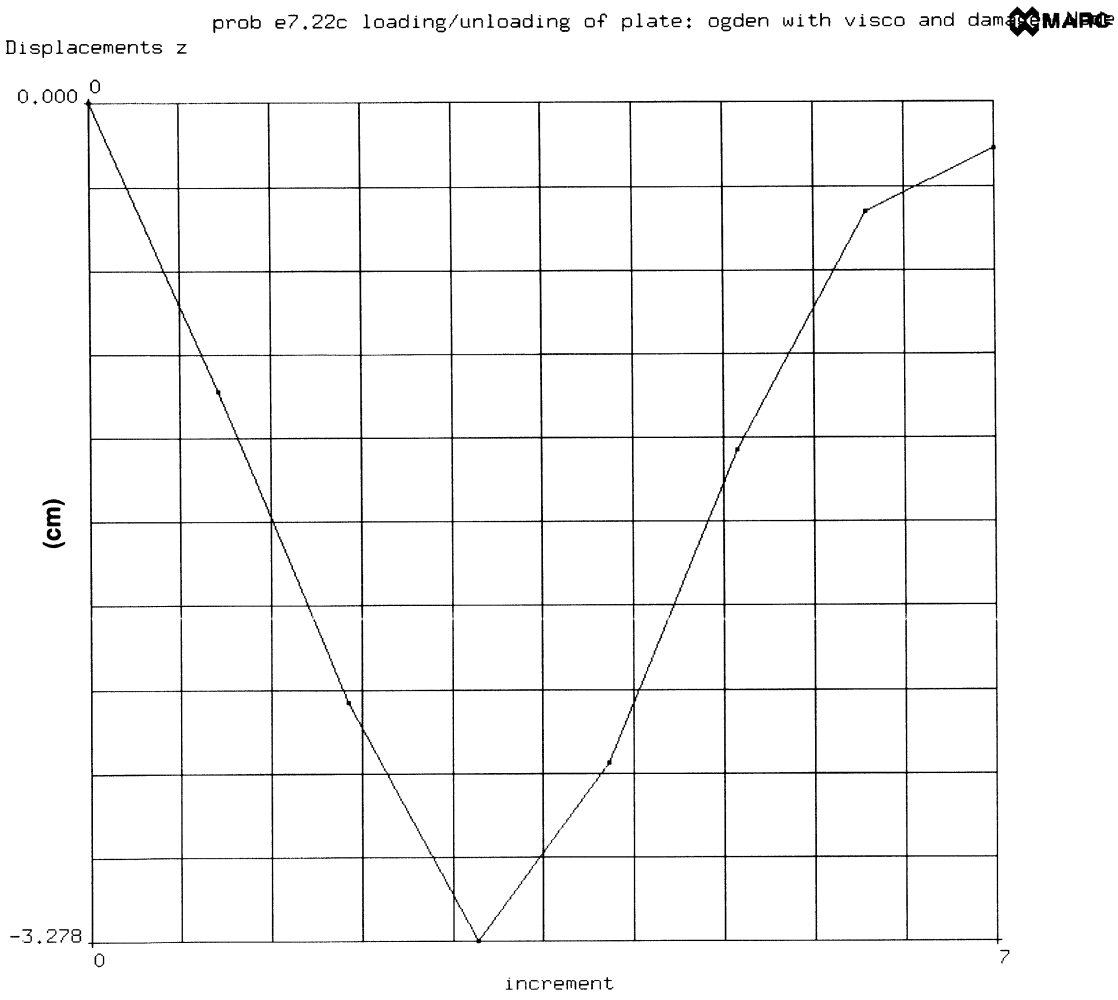

Figure E 7.22-5 Displacement History of Center Node – Including Damage and Viscoelastic Effects

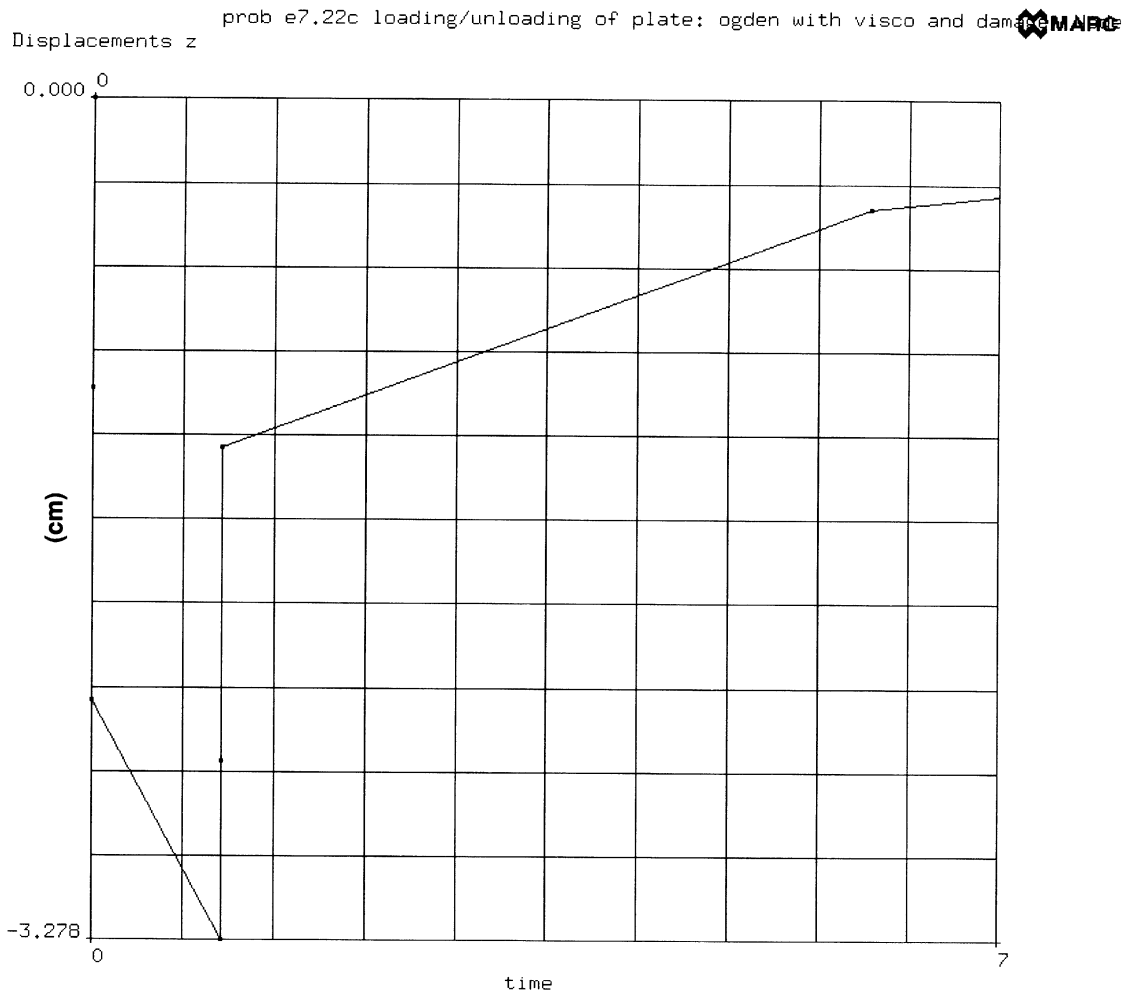

Figure E 7.22-6 Displacement History as a Function of Time – Including Damage and Viscoelastic Effects

Volume E
Demonstration Problems

Chapter 8
Advanced Topics

E 8.12 Forging Of The Head Of A Bolt

This example demonstrates the contact capability of the program, using rigid surfaces for a simple forging analysis. An originally cylindrical block is sitting in a surface with the shape of a cavity, and is deformed by another rigid surface which has the shape of the bolt head and moves at constant speed (Figure E 8.12-2). The block is considered an elastic-plastic deformable material.

This analysis is done using three different approaches. In the first method (e8x12.dat), a fixed time step approach is used and the rezoning capability is used to improve the mesh when distortion occurs. In the second approach (e8x12b.dat), a variable time step approach is used by requesting the AUTO TIME option. In the third approach (e8x12c.dat), a fixed time step method is again used, but here the adaptive meshing capability is utilized. The restart capability is demonstrated based upon the first analysis (e8x12r.dat), which is typically used in rezoning analyses.

Parameters

The UPDATE, FINITE, and LARGE DISP options are included to trigger a finite deformation analysis. Element 10, a 4-node bilinear axisymmetric element is used. The PRINT,5 card requests printed information on change in contact status of boundary nodes. In the first analysis, the SIZING option reserves space for 120 elements, 150 nodes, and 60 boundary conditions. The amounts are larger than the starting model which contains 70 elements and 90 nodes. This is done so that there is freedom to increase the size of the model later using the REZONING option. The REZONING parameter is included to indicate that this may be required.

In the second analysis, the same SIZING option is used even though rezoning is not performed. This will result in an over allocation of memory, but is insignificant for this small problem.

In the third problem, the number of elements and nodes is not specified on the SIZING option, but an upper bound is defined on the ADAPTIVE option. Here, the analysis will initially start with 70 elements and 90 nodes and re-allocate memory as the adaptive meshing process occurs. Two levels of refinement will be allowed; so if all elements refine, the total would be 1120 which is less than the number specified on the ADAPTIVE parameter option. Note that the SIZING option specifies an upper bound on the number of boundary conditions and distributed loads.

Mesh Definition

CONNECTIVITIES and COORDINATES were brought from a pre-processor. The mesh depicted in Figure E 8.12-2 is quite regular over the rectangular block. Due to symmetry, only half of the cylinder needs to be modelled.

No gap elements are used in this problem, as the contact with the rigid surfaces are governed by the CONTACT option.

Geometry

A '1' is placed in the second field to indicate that the constant dilatation formulation is used.

Boundary Conditions

Symmetry displacement boundary conditions are applied to all nodes on the axis.

Material Properties

The bolt is treated as an elastic plastic material with a Young's modulus of 17,225., Poisson's ratio of 0.35, mass density of 1., and initial yield stress of 34.45. The material work-hardens from the initial yield stress up to 150 at a strain of 400% according to the piece-wise linear curve entered in WORK HARD DATA.

Control Options

A formatted post tape is requested every twenty increments, as well a RESTART tape. PRINT CHOICE is used to minimize the amount of output. In the third analysis, the print out is suppressed using the NO PRINT option. Convergence control is done by relative residuals, with a tolerance of 10%.

Contact

This option defines three bodies with no friction between them. The code is expected to determine by itself a contact tolerance. (See Figure E 8.12-1.)

The first body is deformable and is made out of all the elements in the model.

The second body is the top rigid surface, defined by three sets of geometrical entities. It has a reference point along the axis, and is given a translational velocity of 1 parallel to the axis of symmetry. The first geometrical entity is a straight line, the second is a concave arc of a circle, and the third is another straight line. The last line was added so that the top node on the axis would not encounter the end of the rigid surface definition.

The third body is the bottom rigid surface, defined by one set of geometrical entities. It does not need a reference point and is not given any motion. The geometrical entities are three straight lines, defined by four points.

Note how the sequence of entering the geometrical data of the second and third bodies corresponds to following the profiles of such bodies in a counterclockwise direction.

Based upon information obtained in the first two analyses, a redesign of the third body was performed such that a circular fillet was placed between what was the second and third entities. This may be seen in Figure E 8.12-3. The third body now consists of three entities:

the first entity is a line segment with three points,

the second entity is a circle using method 2 (starting point, end point, center, and radius), and

the third entity is a straight line.

Load Control

The first part of the analysis was performed with a fixed TIME STEP of 0.1 in a sequence of 100 increments.

As an alternative in the second input file, the AUTO TIME option was used to control the time step procedure. The initial time step was 0.1 second and a maximum of 150 steps were allowed to reach a total time of 10 seconds. Only 51 increments were necessary using this procedure.

In the third analysis, only 60 increments using a fixed TIME STEP of 0.2 were used.

Rezoning

The next increment performs a rezoning operation. A new mesh was created with a preprocessor, which covers the profile of the previously deformed mesh (Figure E 8.12-4). This mesh is defined by means of CONNECTIVITY CHANGE and COORDINATE CHANGE. Both the number of elements and the number of nodes was increased. The ISOTROPIC CHANGE option was also used to extend material properties to the new elements. Similarly, the CONTACT option was repeated to account for the new element definition of the deformable body; the contact tolerance was decreased because much thinner elements were created.

One increment of deformation, with a TIME STEP of 0.05, was executed then. At this point, it is necessary to include the DISPLACEMENT CHANGE to account for the new node numbers that are located along the axis of symmetry. An extra node at the convex corner of surface 3 was fixed. This was done to allow a very coarse mesh to represent a sharp corner without cutting it.

The rest of the deformation proceeded. Twenty increments with five steps of 0.04 were completed first, followed by seventy increments of time step 0.02. The reason for decreasing the time step is that as the deformation proceeds, the height of the bolt head becomes smaller and a constant movement of the second surface would produce larger and larger strains per increment.

Adaptive

In the third problem, the adaptive meshing technique is demonstrated. Such that the first 50 elements are enriched based upon the contact criteria. That is, if nodes associated with these elements come into contact, the element will be refined. A limit of two levels of refinement is prescribed.

Results

Figure E 8.12-5 through Figure E 8.12-7, show the contour plots of the equivalent plastic strain, the equivalent von Mises stress, and the average stress in the deformed configuration before rezoning. The block completely fills the bottom surface, and is folding into the top surface. The need to rezone stems from the fact that soon thereafter there will be too few nodes in the free surface that has to fit in the narrow gap between the two rigid bodies. The rezoning method allows us to represent the material flash.

Virtually all the deformation takes place in the part of the block above the bottom surface.

Figure E 8.12-8 through Figure E 8.12-10 show the same contour plots in the final deformed configuration. At this stage, the full shape of the head of the bolt has been acquired by the original block and flash formed in the gap between surfaces. The strains are very concentrated in the part which folded on the bottom surface. The von Mises stress shows that the bottom cavity was elastic at the end of deformation.

The progression of the deformed adaptive mesh is shown in Figure E 8.12-11 through Figure E 8.12-13, for increments 20, 40, and 60, respectively. You can observe that, based upon the adaptive criteria, additional elements are formed as the workpiece comes into contact with the dies. At the end of the analysis, there are 187 elements and 250 nodes. Based upon this analysis, perhaps you would perform the analysis also with an adaptive criteria based upon strain energies or plastic strains.

The printed results of an analysis with the contact option include general information about rigid surfaces, such as the updated position of the reference point, the velocity of the surface, the loads on the surface, as well as the moment with respect to the reference point.

Summary of Options Used

Listed below are the options used in example e8x12.dat:

Parameter Options

END
FINITE
LARGE DISP
PRINT
REZONE
SIZING
TITLE
UPDATE

Model Definition Options

CONNECTIVITY
CONTACT
CONTROL
COORDINATE
END OPTION
FIXED DISP
GEOMETRY
ISOTROPIC
POST
PRINT CHOICE
RESTART
WORK HARD

Load Incrementation Options

AUTO LOAD
DISPLACEMENT CHANGE
COMMENT
CONTINUE
TIME STEP

Rezone Options

CONNECTIVITY CHANGE
CONTACT
CONTINUE
COORDINATE CHANGE
END REZONE
ISOTROPIC CHANGE
REZONE

Listed below are the options used in example e8x12b.dat:

Parameter Options

END
FINITE
LARGE DISP
PRINT
REZONE
SIZING
TITLE
UPDATE

Model Definition Options

CONNECTIVITY
CONTACT
CONTROL
COORDINATE
END OPTION
FIXED DISP
GEOMETRY
ISOTROPIC
POST
PRINT CHOICE
RESTART
WORK HARD

Load Incrementation Options

AUTO TIME
CONTINUE

Listed below are the options used in example e8x12c.dat:

Parameter Options

ADAPTIVE
END
FINITE
LARGE DISP
PRINT
SIZING
TITLE
UPDATE

Model Definition Options

ADAPTIVE
CONNECTIVITY
CONTACT
CONTROL
COORDINATES
END OPTION
FIXED DISP
GEOMETRY
ISOTROPIC
NO PRINT
POST
WORK HARD

Load Incrementation Options

AUTO LOAD
CONTINUE
TIME STEP

Listed below are the options used in example e8x12r.dat:

Parameter Options

END
FINITE
LARGE DISP
PRINT
REZONE
SIZING
TITLE
UPDATE

Model Definition Options

CONNECTIVITY
CONTACT
CONTROL
COORDINATE
END OPTION
FIXED DISP
GEOMETRY
ISOTROPIC
POST
PRINT CHOICE
REAUTO
RESTART
WORK HARD

Load Incrementation Options

AUTO LOAD
COMMENT
CONTINUE
DISP CHANGE
TIME STEP

Rezone Options

CONNECTIVITY CHANGE
CONTACT
CONTINUE
COORDINATE CHANGE
END REZONE
ISOTROPIC CHANGE
REZONE

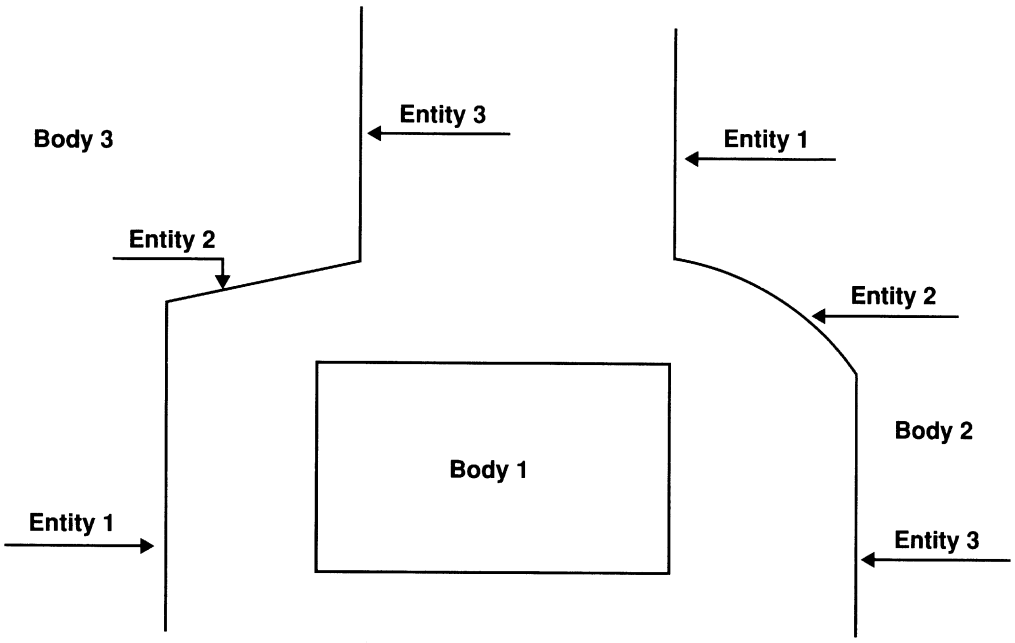

Figure E 8.12-1 Model

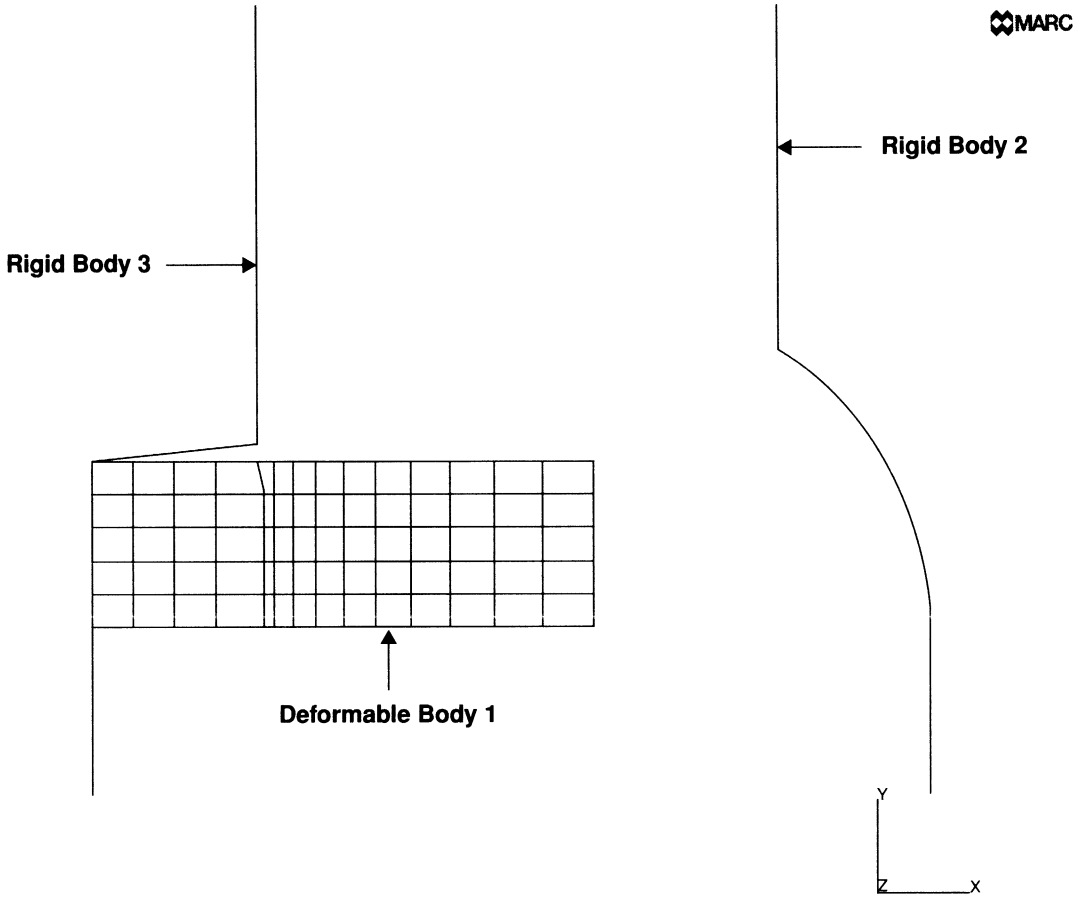

Figure E 8.12-2 Initial Mesh

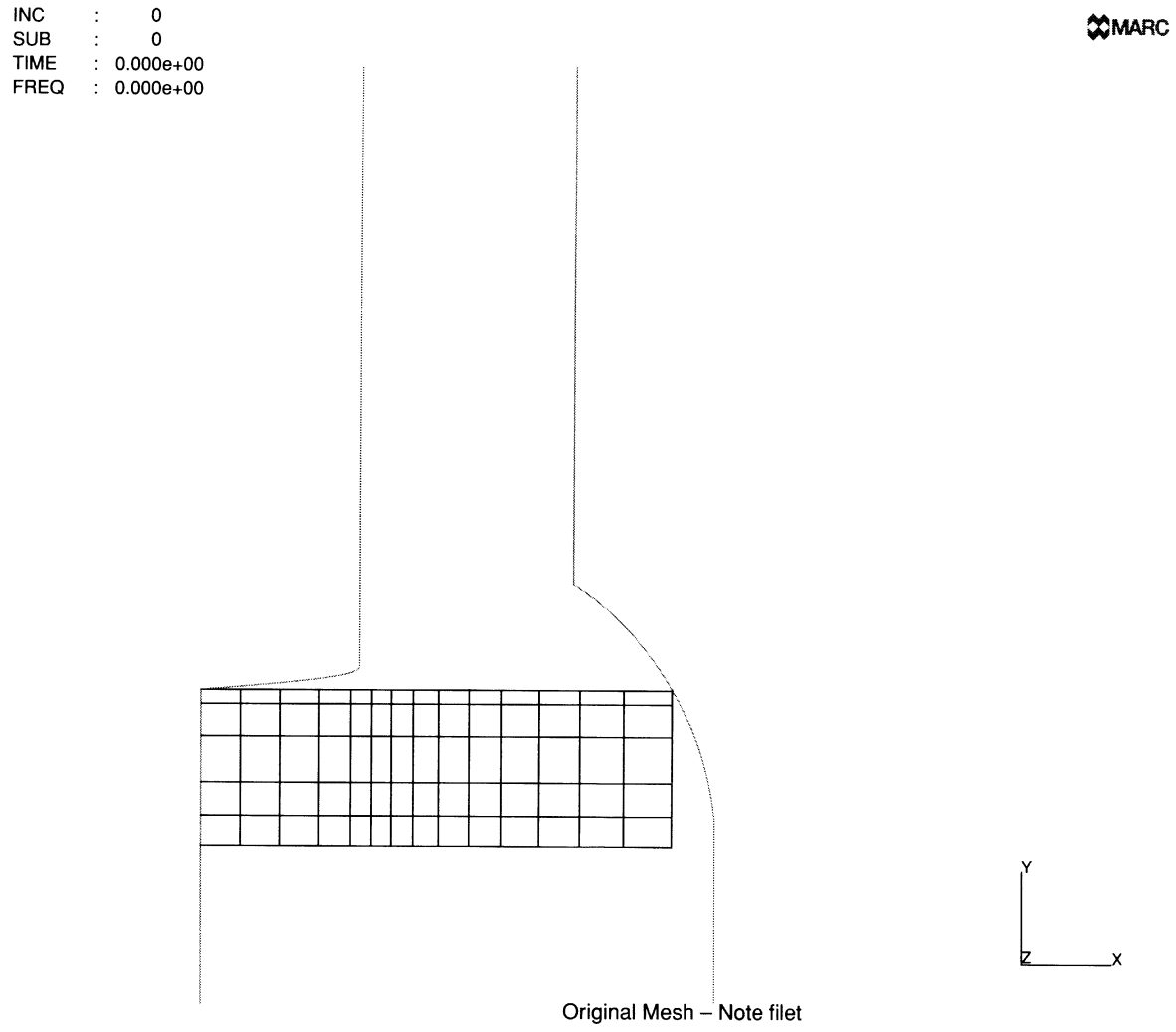

Figure E 8.12-3 Initial Mesh with Modified Rigid Body 3 for Adaptive Analysis

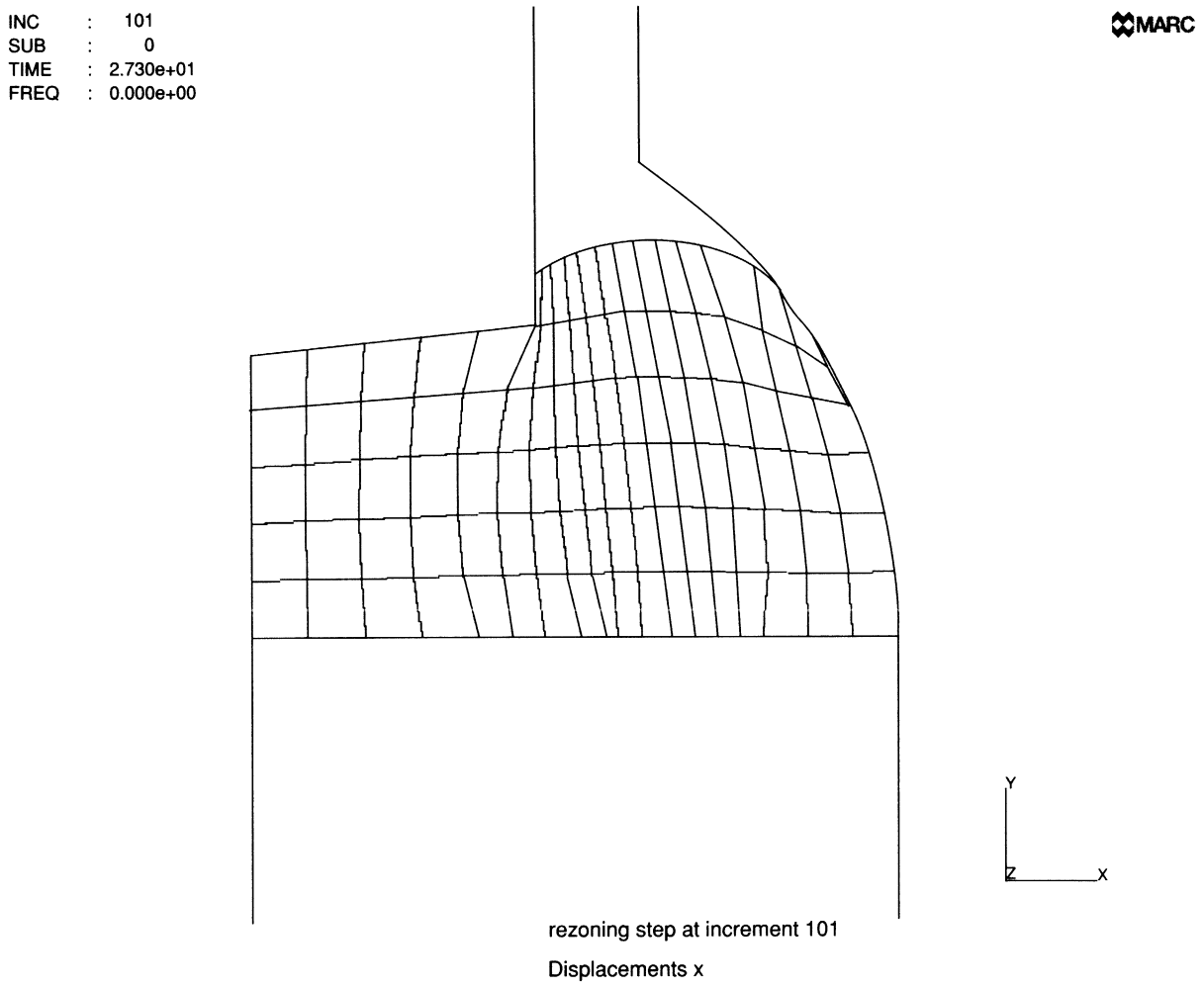

Figure E 8.12-4 Rezoning Mesh

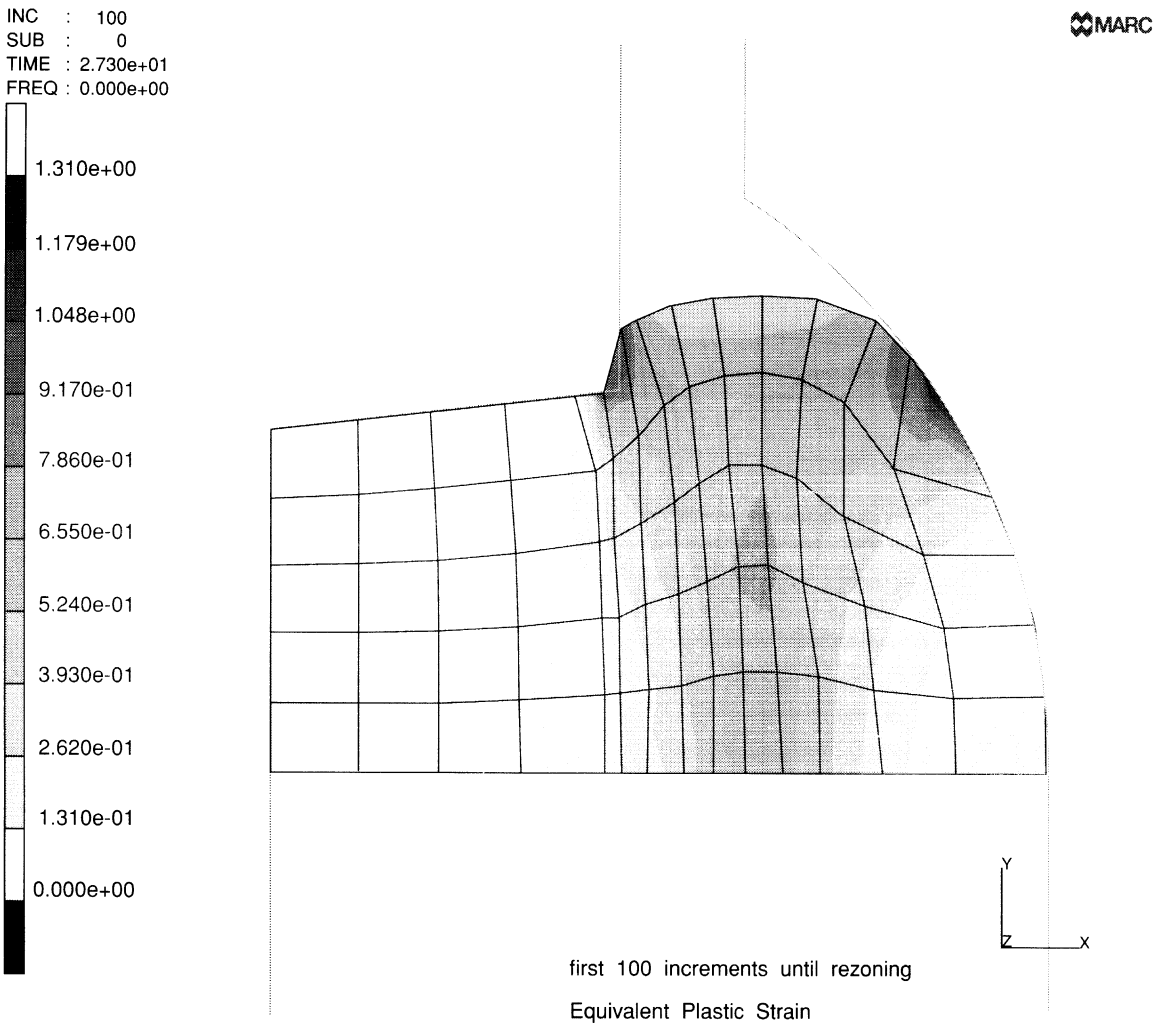

Figure E 8.12-5 Equivalent Plastic Strain until Rezoning

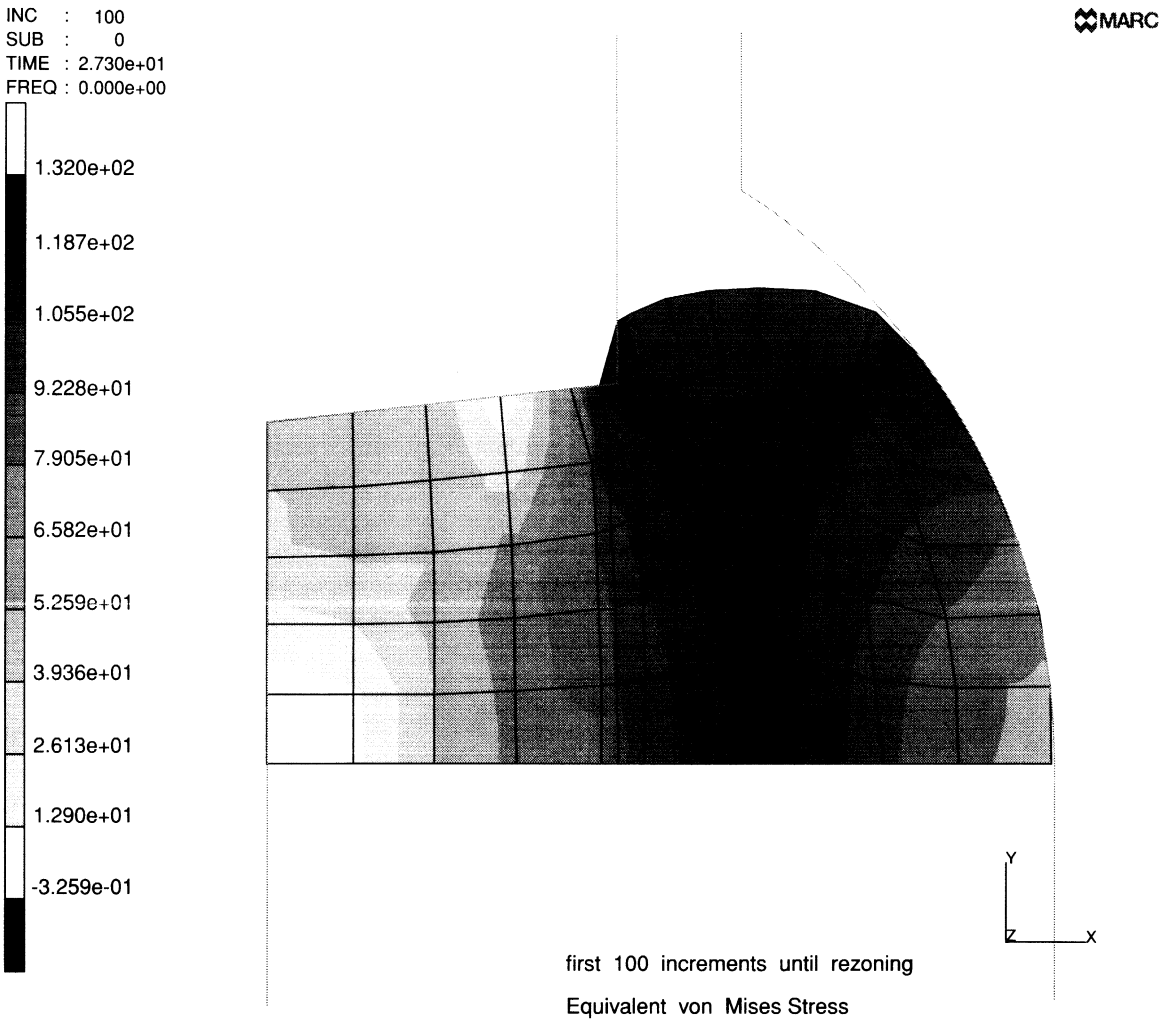

Figure E 8.12-6 Equivalent Mises Tensile Stress Until Rezoning

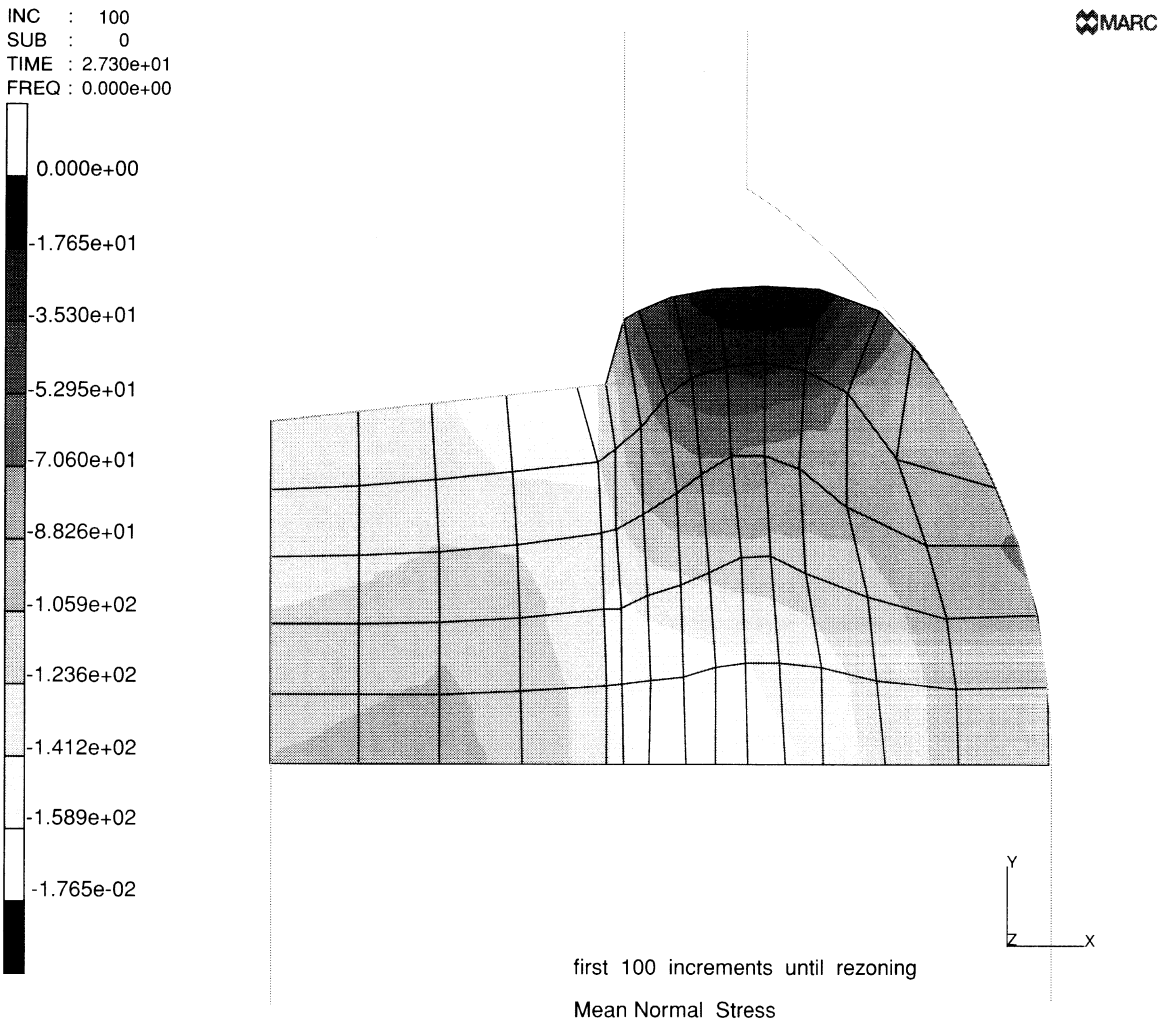

Figure E 8.12-7 Mean Normal Stress Until Rezoning

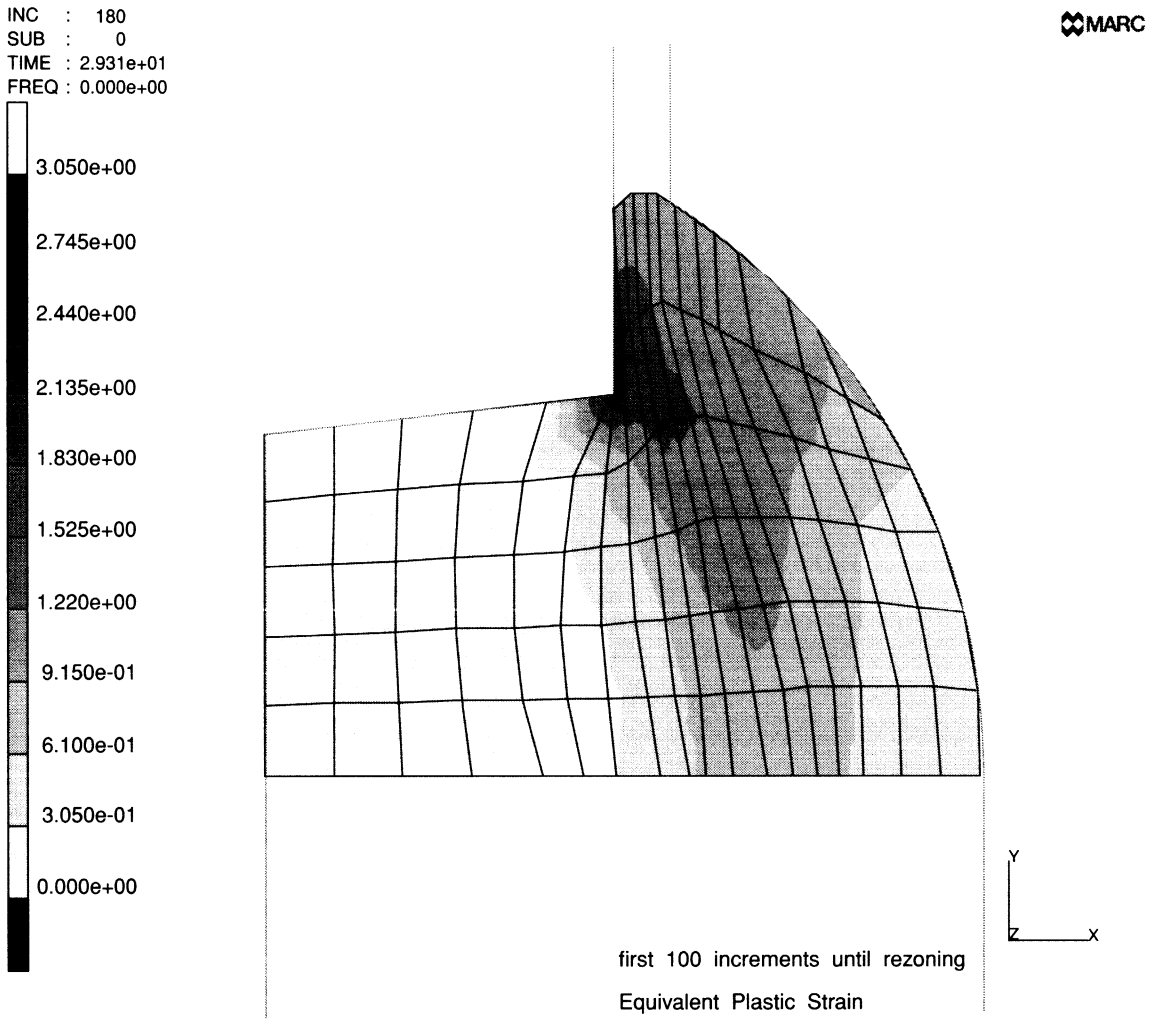

Figure E 8.12-8 Final Equivalent Plastic Strain

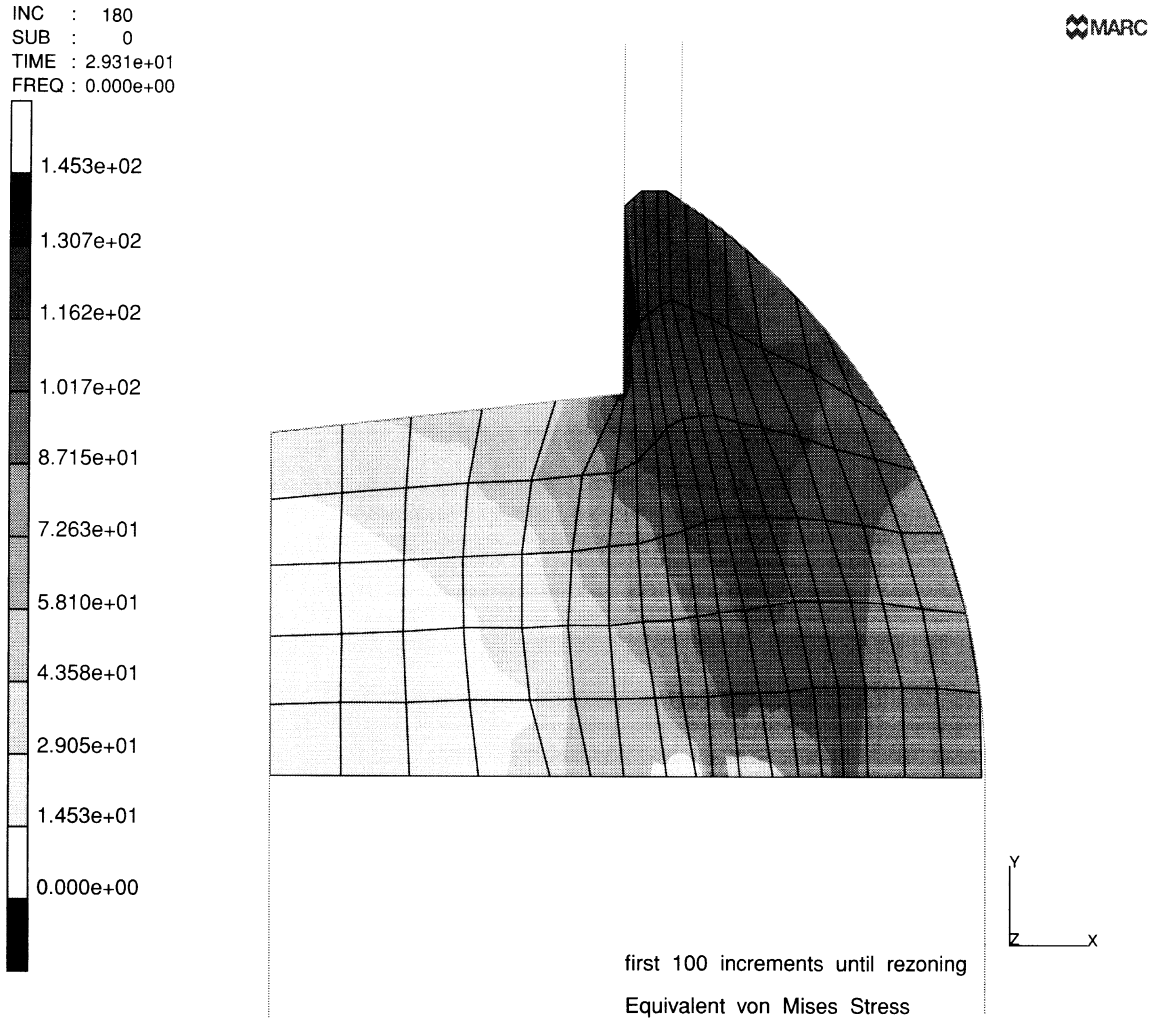

Figure E 8.12-9 Final Equivalent von Mises Tensile Stress

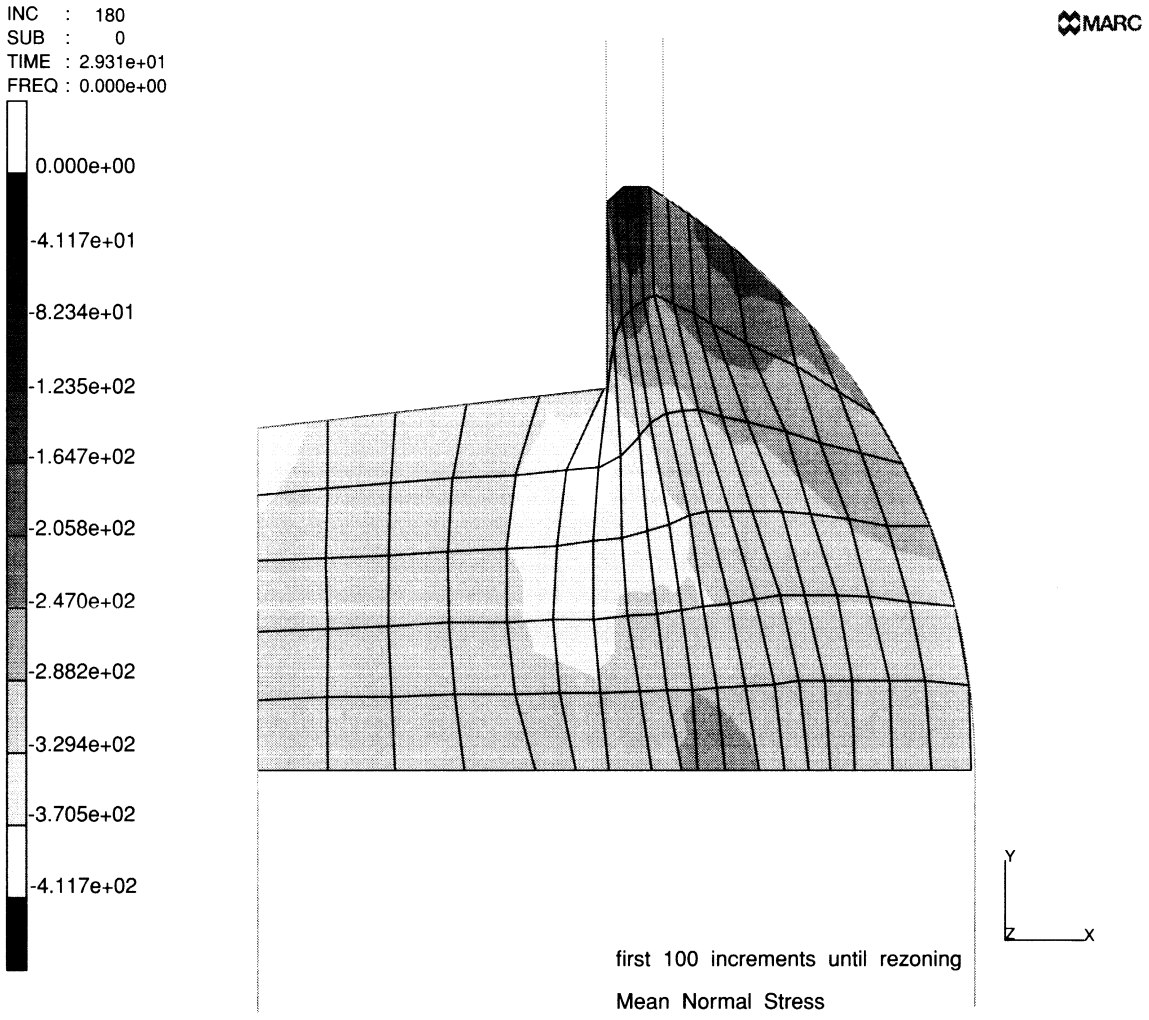

Figure E 8.12-10 Final Mean Normal Stress

Figure E 8.12-11 Adapted Mesh at Increment 20

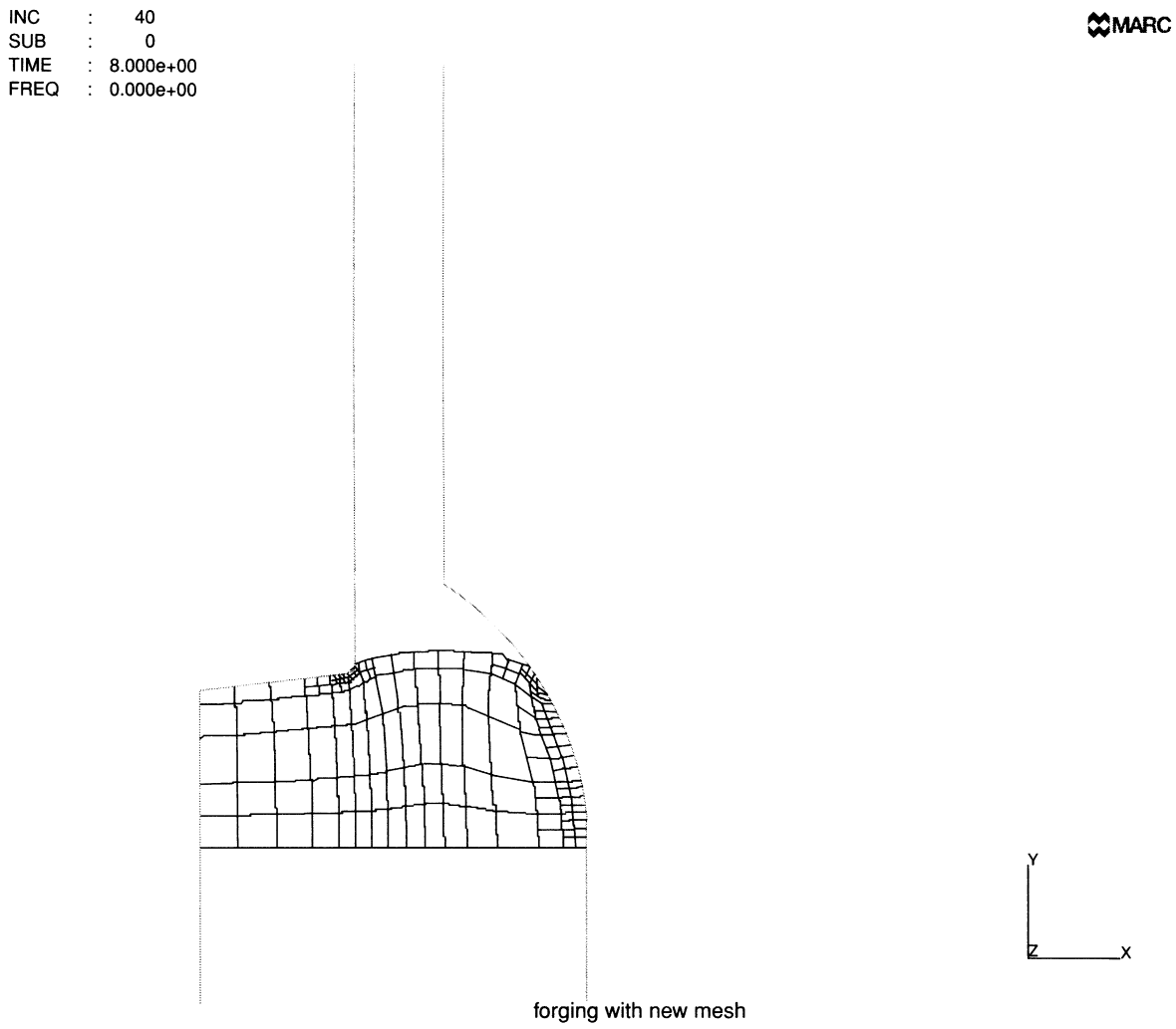

Figure E 8.12-12 Adapted Mesh at Increment 40

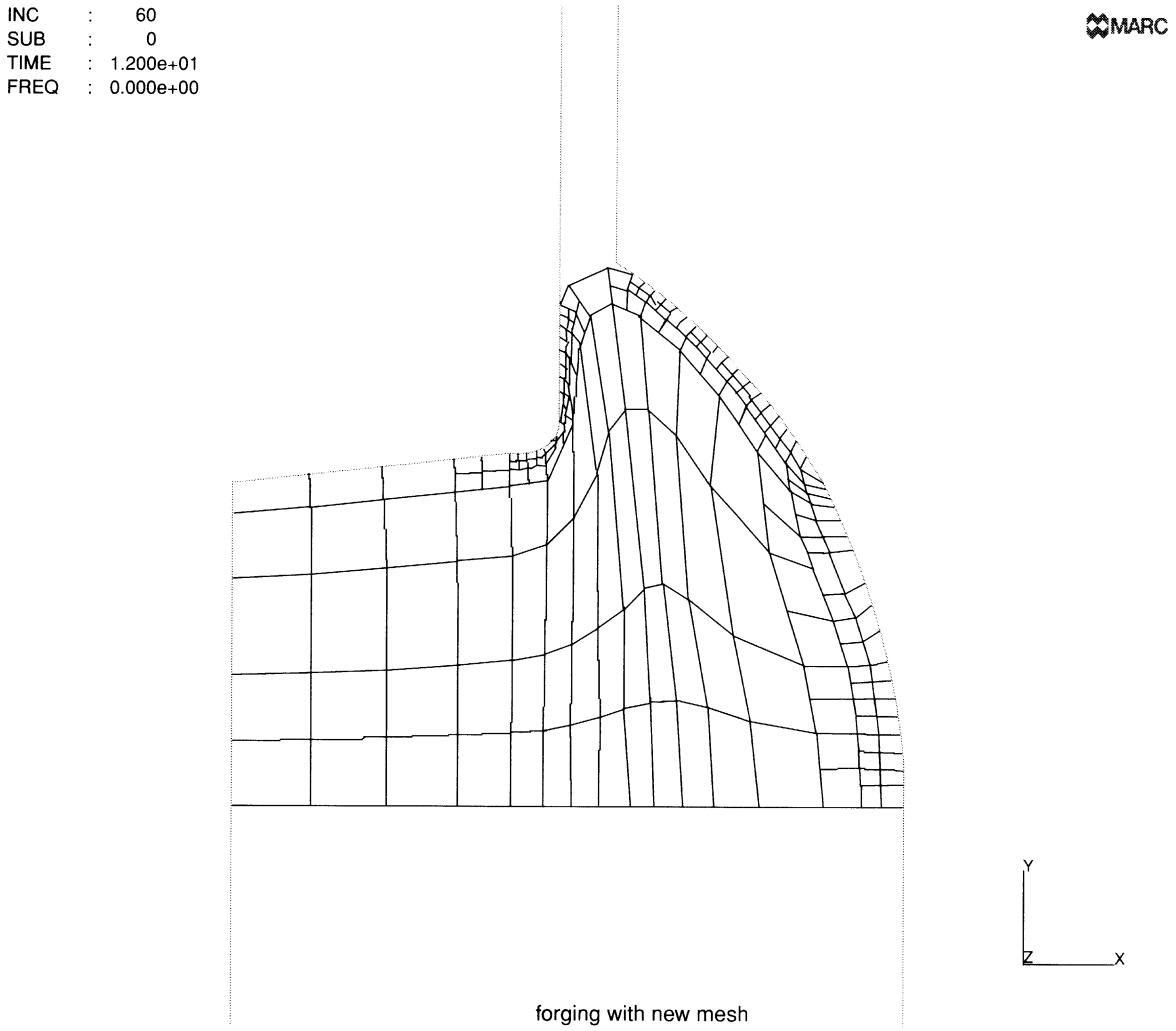

Figure E 8.12-13 Adapted Mesh at Increment 60

E 8.14 3-D Contact With Various Rigid Surface Definitions

This problem demonstrates the program's ability to perform contact analysis between a deformable body and a rigid die described through various surface definitions. It also demonstrates the program's ability to perform contact analysis between a flexible body and a rigid die described through the NURBS definition.

Parameters

The UPDATE, FINITE and LARGE DISP options are included in the parameter section to indicate that this is a finite deformation analysis. The PRINT,5 option requests additional information in the output regarding nodes acquiring or losing contact.

Geometry

A "1" is placed in the second data field to indicate that the constant dilatation formulation is used. This is particularly useful for analysis of approximately incompressible materials and for structures in the fully plastic range.

Boundary Conditions

To prevent rigid body motions, several nodes are restrained from displacing in the global x-, y-, z-directions. These constraints are given through the FIXED DISP option.

POST/PRINT Control

It is requested that the E_{xx} strain (post code 1) be written onto a formatted post file. The NO PRINT option limits the amount of printed output to a minimum.

Control

A maximum of 200 increments is allowed, with no more than 20 recycles per increment. Displacement control is used, with a relative error of 10%. However, keep in mind that control parameters under the CONTACT option set will generally govern the convergence of the problem.

Material Properties

The material for all elements is treated as an elastic-perfectly plastic material, with Young's modulus of 1.75E+07 psi, Poisson's ratio of .3, and an initial yield stress of 35,000 psi.

Contact

This option declares that there are two bodies in contact with no friction between them. The distance tolerance is specified as 0.005 inches. The reaction and velocity tolerances will be computed by the program. A die velocity of -0.3 in/sec in the global z-direction constitutes the driving motion for this problem.

Load Control

This problem is loaded by the application of number of increments specified in the AUTO LOAD option of the prescribed die velocities in the CONTACT option. The load increment will be applied once.

Die Surface Definitions

The only difference between problems e8x14a, b, c, d, and e is the type of surface defined for the rigid die. In data set 14a, it is a 3-D ruled surface with straight line generators. In 14b, it is again a ruled surface with circular arc generators. In 14c, it is a surface of revolution. In 14d, it is a 4-node patch. Finally, in 14e, a 3-D polysurface defines the rigid die.

In e8x14f, the second body is described by NURBS. The "1" in the fifth field (surface definition) indicates the analytical form of NURBS is used to implement contact conditions. If "0" is entered in the field, the surface is still divided into 4-node patches and uses the piecewise linear approach to do the analysis.

The NURBS is defined by 9 x 5 control points with four cubic degrees along the u- and v-directions. The surface is divided into 20 x 5 patches for visualization.

Results

Figure E 8.14-2 shows the deformed body at the end of increment one with the deformation at the same scale as the coordinates.

Summary of Options Used

Listed below are the options used in example e8x14a.dat:

Parameter Options

ELEMENT
END
FINITE
LARGE DISP
PRINT
SIZING
TITLE
UPDATE

Model Definition Options

CONNECTIVITY
CONTACT
CONTROL
COORDINATE
END OPTION
FIXED DISP
GEOMETRY
ISOTROPIC
NO PRINT
POST

Load Incrementation Options

AUTO LOAD
CONTINUE
TIME STEP

Listed below are the options used in example e8x14b.dat:

Parameter Options

ELEMENT
END
FINITE
LARGE DISP
PRINT
SIZING
TITLE
UPDATE

Model Definition Options

CONNECTIVITY
CONTACT
CONTROL
COORDINATE
END OPTION
FIXED DISP
GEOMETRY
ISOTROPIC
NO PRINT
POST

Load Incrementation Options

AUTO LOAD
CONTINUE
TIME STEP

Listed below are the options used in example e8x14c.dat:

Parameter Options

ELEMENT
END
FINITE
LARGE DISP
PRINT
SIZING
TITLE
UPDATE

Model Definition Options

CONNECTIVITY
CONTACT
CONTROL
COORDINATE
END OPTION
FIXED DISP
GEOMETRY
ISOTROPIC
NO PRINT
POST

Load Incrementation Options

AUTO LOAD
CONTINUE
TIME STEP

Listed below are the options used in example e8x14d.dat:

Parameter Options

ELEMENT
END
FINITE
LARGE DISP
PRINT
SIZING
TITLE
UPDATE

Model Definition Options

CONNECTIVITY
CONTACT
CONTROL
COORDINATE
END OPTION
FIXED DISP
GEOMETRY
ISOTROPIC
NO PRINT
POST

Load Incrementation Options

AUTO LOAD
CONTINUE
TIME STEP

Listed below are the options used in example e8x14e.dat:

Parameter Options

ELEMENT
END
FINITE
LARGE DISP
PRINT
SIZING
TITLE
UPDATE

Model Definition Options

CONNECTIVITY
CONTACT
CONTROL
COORDINATE
END OPTION
FIXED DISP
GEOMETRY
ISOTROPIC
NO PRINT
POST

Load Incrementation Options

AUTO LOAD
CONTINUE
TIME STEP

Listed below are the options used in example e8x14f.dat:

Parameter Options

ELEMENTS
END
FINITE
LARGE DISP
PRINT
SIZING
TITLE
UPDATE

Model Definition Options

CONNECTIVITY
CONTACT
CONTROL
COORDINATE
END OPTION
FIXED DISP
GEOMETRY
ISOTROPIC
NO PRINT
POST

Load Incrementation Options

AUTO LOAD
CONTINUE
TIME STEP

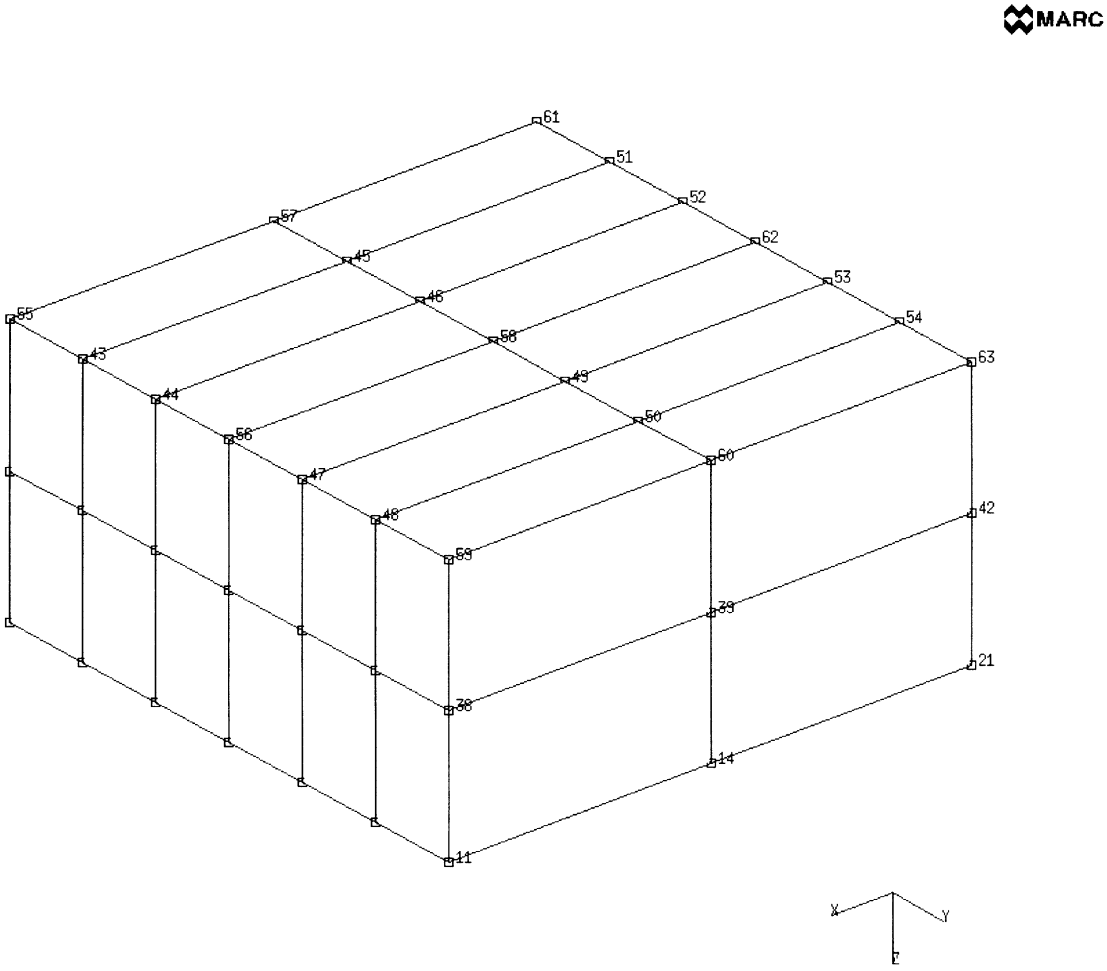

Figure E 8.14-1 Undeformed Block

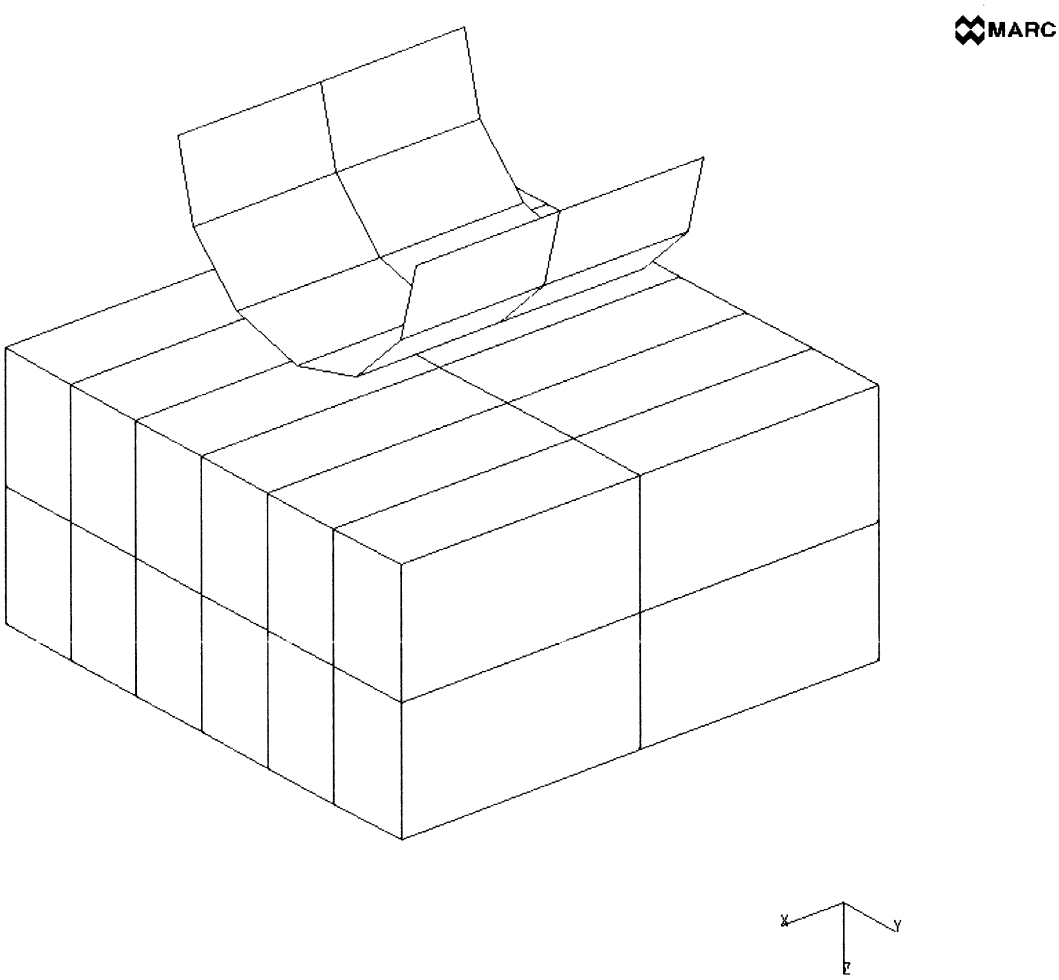

Figure E 8.14-2 Block and Indentor

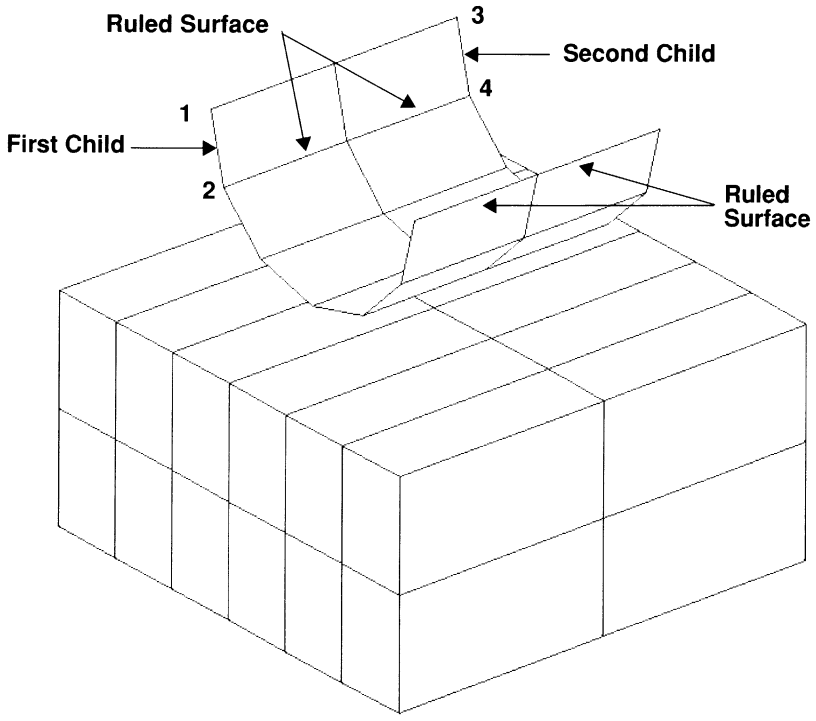

(a) Straight Line Generator

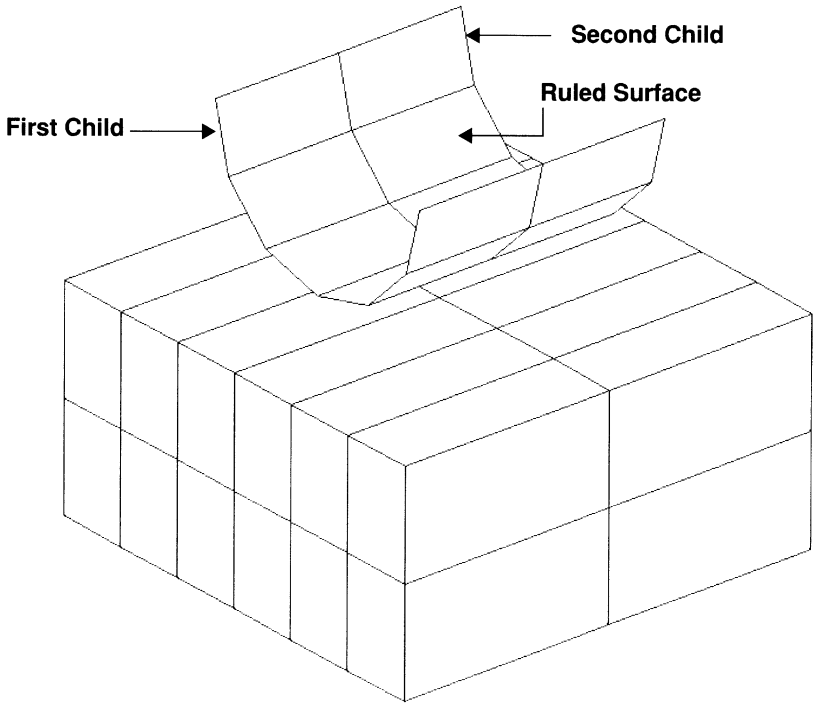

(b) Circular Arc Generator

Figure E 8.14-3 Ruled Surface

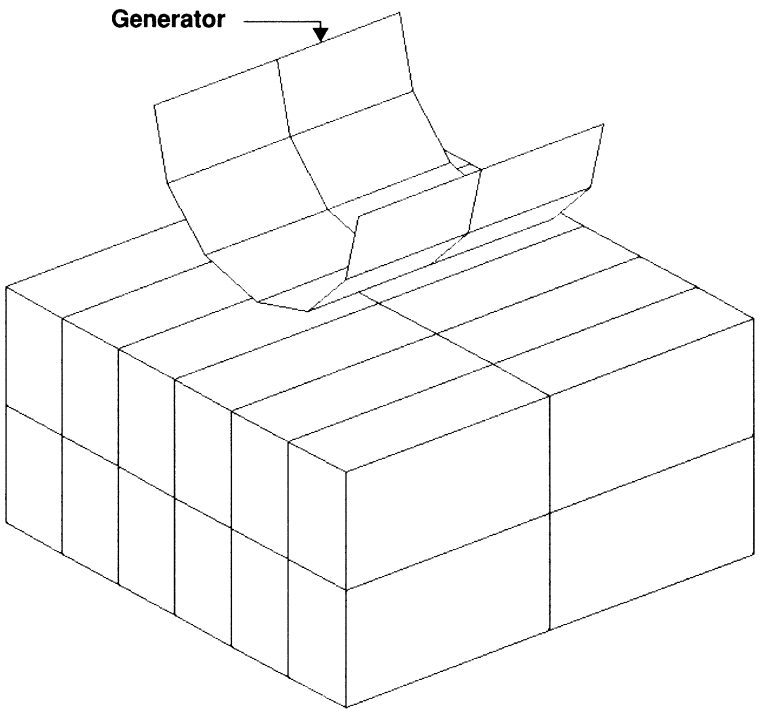

(c) Surface of Revolution

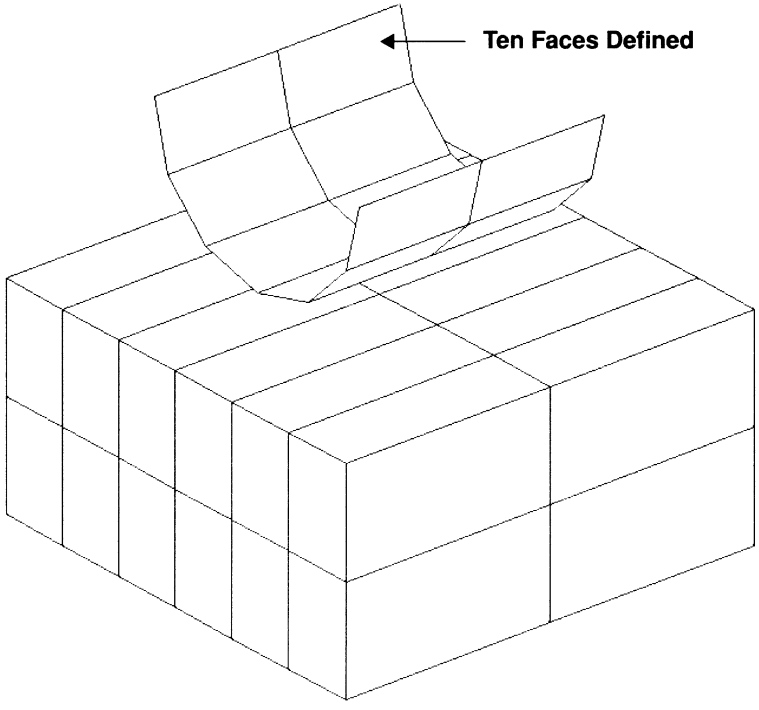

(d) Four Node Patches

Figure E 8.14-3 Ruled Surface (Continued)

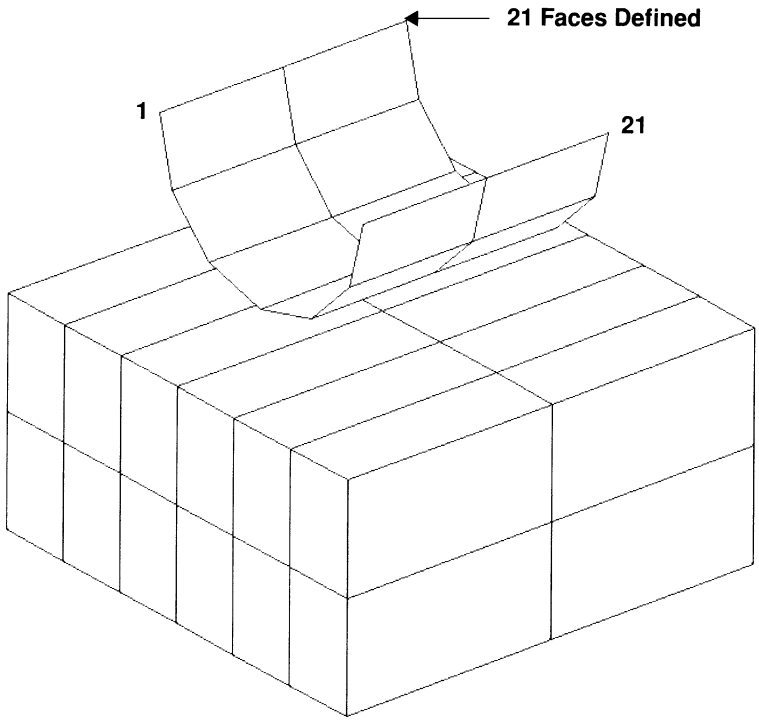

(d) Poly Surface

Figure E 8.14-3 Ruled Surface (Continued)

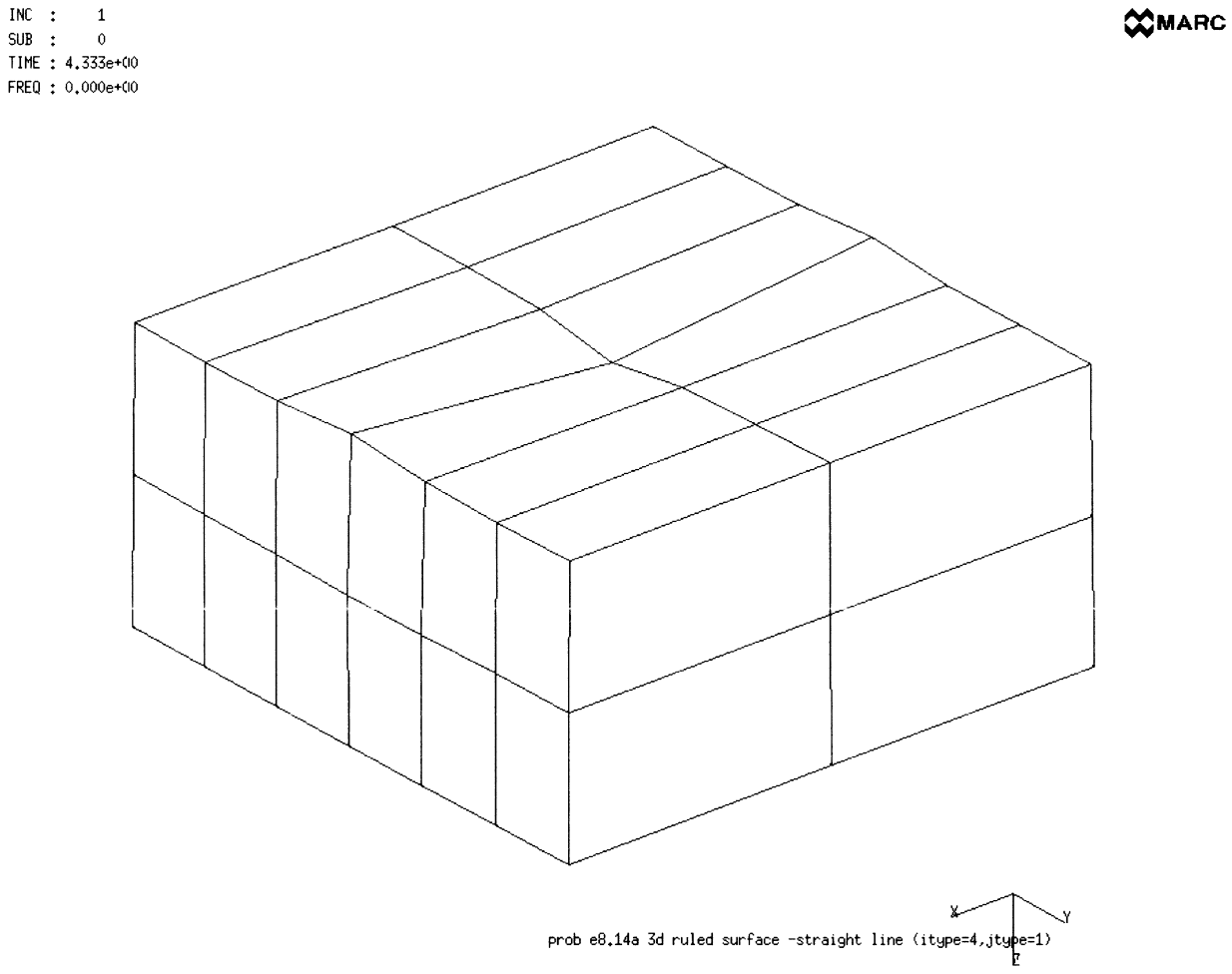

Figure E 8.14-4 Deformed Block

E 8.15 Double-Sided Contact

This problem demonstrates the program's ability to perform multibody contact, incorporating automated double-sided contact with friction between the contact surfaces for linear and parabolic elements. It is not necessary to assign either body as a master or slave.

Parameters

The UPDATE, FINITE and LARGE DISP options are included in the parameter section to indicate that this is a finite deformation analysis. The PRINT,5 option requests additional information in the output regarding nodes acquiring or losing contact.

Elements

Element types 11 and 27 are plane strain quadrilaterals with 4 and 8 nodes respectively.

Mesh Definition

Mentat was used to determine the CONNECTIVITY and COORDINATES of the mesh. The mesh is shown (with the units in inches) in Figure E 8.15-1. In a contact analysis, double-sided contact is automatically checked during this deformation.

Geometry

A "1" is placed in the second data field to indicate that the constant dilatation formulation is used. This is particularly useful for analysis of approximately incompressible materials and for structures in the fully plastic range. The "1.0" placed in the first data field indicates the thickness of 1 inch.

Boundary Conditions

The nodes on the top surface (y = 3) are moved uniformly downward. The left (x = 0) and bottom (y = 0) side are constrained.

Material Properties

The material for all elements is treated as an elastic-plastic material, with Young's modulus of 31.75E+06 psi, Poisson's ratio of 0.268, a mass density of 7.4E-04 lbf-sec^2/in^4, a coefficient of thermal expansion of 5.13E-06 in/(in-deg F), corresponding reference temperature of 70°F, and an initial yield stress of 80,730 psi. The material work-hardens from the initial yield stress to a final yield stress of 162,747 psi at a strain of 1.0 in the WORK HARD DATA block.

Contact

This option declares that there are two bodies in contact with adhesive friction between them. The relative ship velocity is defined as 0.01 in/sec. The contact tolerance distance is 0.01 inches. The coefficient of friction associated with each body is 0.7. The reaction tolerance will be computed by the program.

The CONTACT TABLE is used to indicate that body 1 will potentially come in contact with body 2. Because the contact table is used, no contact between body 1 and itself or body 2 and itself will be checked. Also the CONTACT NODE option is used to only check contact for the corner nodes for the parabolic element, type 27.

Load Control

This problem is loaded by the repeated application of the load increment created by the prescribed boundary conditions in the AUTO LOAD option. The load increment will be applied 20 times. The TIME STEP option allows the user to enter the time variable for static analysis. All contact analyses are time driven and require the definition of a time step. A formatted post tape containing the equivalent plastic strain, the first two stress components, von Mises equivalent stress, and the mean normal stress. The NO PRINT option limits the amount of printed output to a minimum. Displacement control is used, with a relative error of 20%. The RESTART LAST option is used to save the last increment of data if a later restart is required.

Results

Figure E 8.15-1 shows the original mesh with the elements labeled of double-sided contact problem for both element types. Figure E 8.15-2 and Figure E 8.15-3, respectively, show the nodal labels for element types 11 and 27. Figure E 8.15-4, Figure E 8.15-5, and Figure E 8.15-6 show the deformed body at the end of 10, 20 and 30 increments with the deformation at the same scale as the coordinates. Figure E 8.15-8, Figure E 8.15-9, and Figure E 8.15-10 show the deformed body at the end of 10, 20 and 30 increments for element type 27. Due to the high level of friction, significant transverse deformation is shown along the contact surfaces. Figure E 8.15-7 and Figure E 8.15-11 show the equivalent plastic strain at the end of increment 30. The peak values of equivalent plastic strain are 137% and 151% for element types 11 and 27, respectively. The additional degrees of freedom in the model using element type 27 makes the structure more flexible. The larger plastic strain found for the higher degrees of freedom model is on the high side of convergence tolerance.

A user-written subroutine, IMPD, is used in conjunction with the UDUMP model definition option to sum the nodal loads across the y = 3 (top) surface and print the nodal load and displacement for each increment into the output file. This information is plotted and shown in Figure E 8.15-12 for both element types. The overall force-displacement behavior of the two element types is in good agreement with all differences occurring in the early portion of the contact.

Summary of Options Used

Listed below are the options used in example e8x15.dat:

Parameter Options

ELEMENT
END
FINITE
LARGE DISP
PRINT
SIZING
TITLE
UPDATE

Model Definition Options

CONNECTIVITY
CONTACT
CONTACT TABLE
CONTROL
COORDINATE
DEFINE
END OPTION
FIXED DISP
GEOMETRY
ISOTROPIC
NO PRINT
POST
RESTART LAST
WORK HARD

Load Incrementation Options

AUTO LOAD
CONTINUE
TIME STEP

Listed below are the options used in example e8x15b.dat:

Parameter Options

ELEMENT
END
FINITE
LARGE DISP
PRINT
SETNAME
SIZING
TITLE
UPDATE

Model Definition Options

CONNECTIVITY
CONTACT
CONTACT NODE
CONTACT TABLE
CONTROL
COORDINATE
DEFINE
END OPTION
FIXED DISP
GEOMETRY
ISOTROPIC
NO PRINT
OPTIMIZE
POST
RESTART LAST
WORK HARD

Load Incrementation Options

AUTO LOAD
CONTINUE
TIME STEP

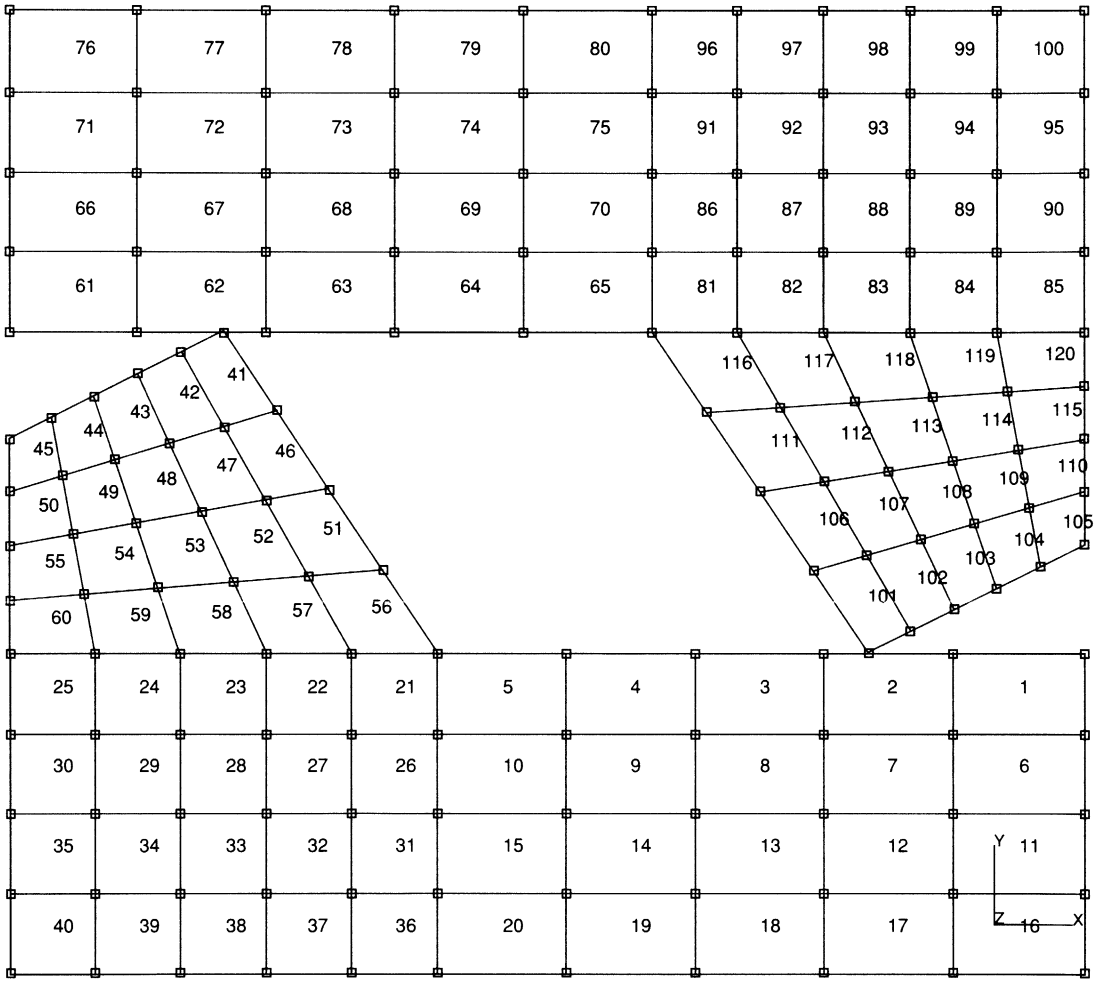

Figure E 8.15-1 Mesh

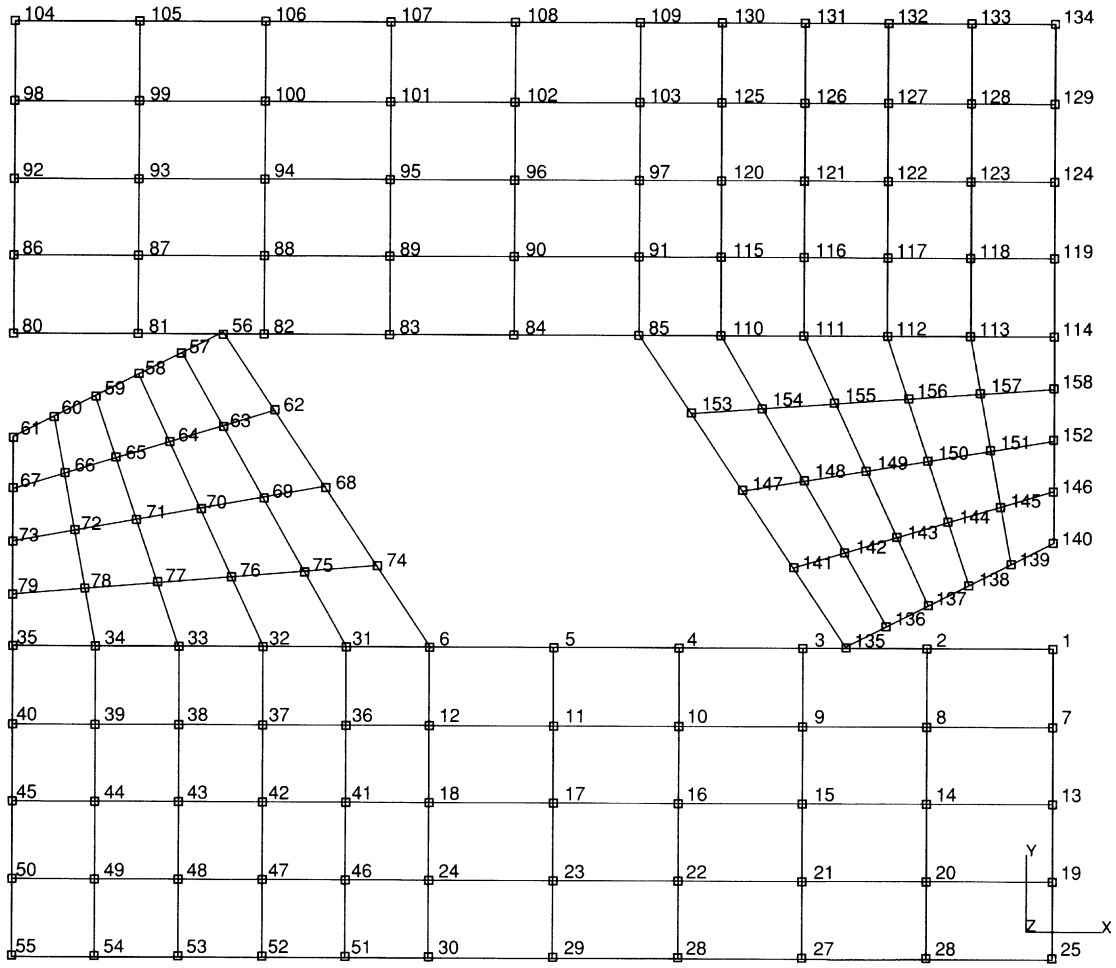

Figure E 8.15-2 Nodal Configuration, Element Type 11

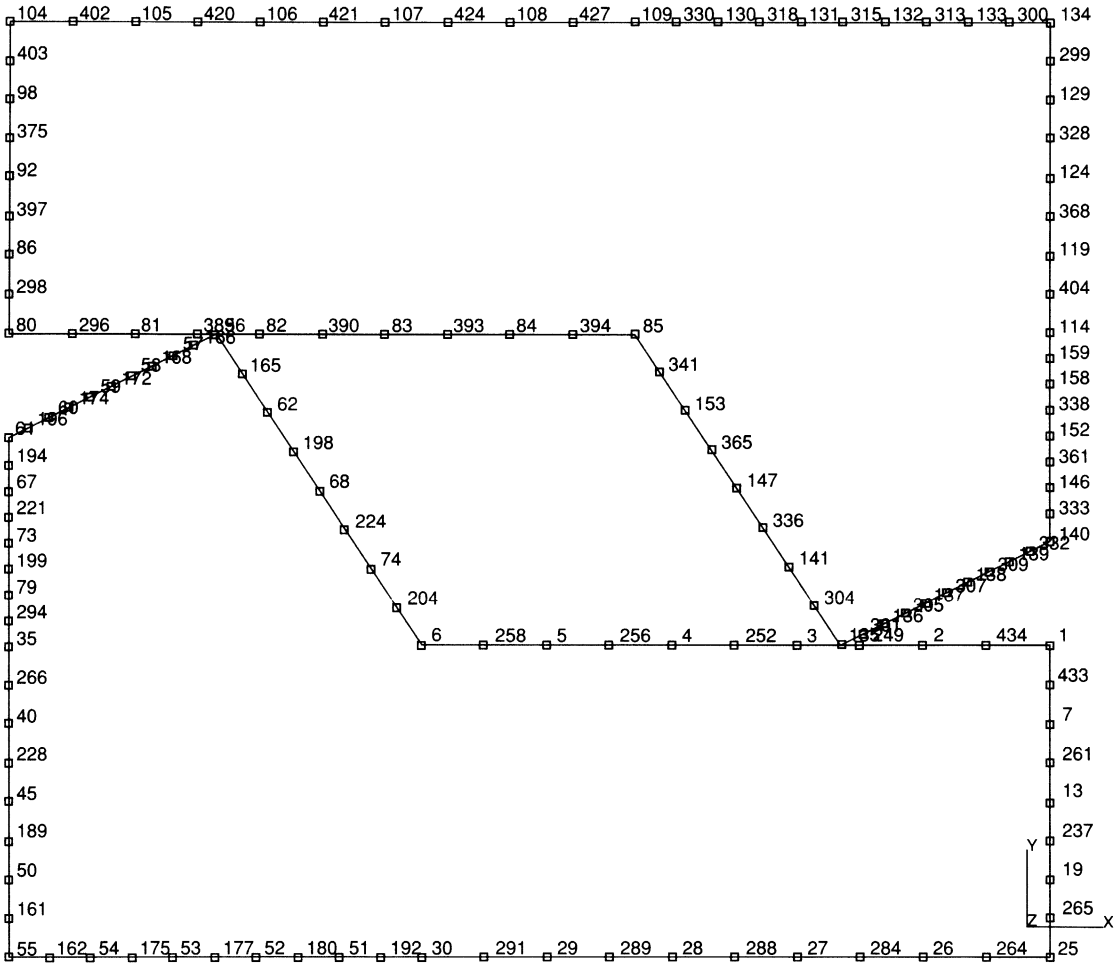

Figure E 8.15-3 Nodal Configuration, Element Type 27

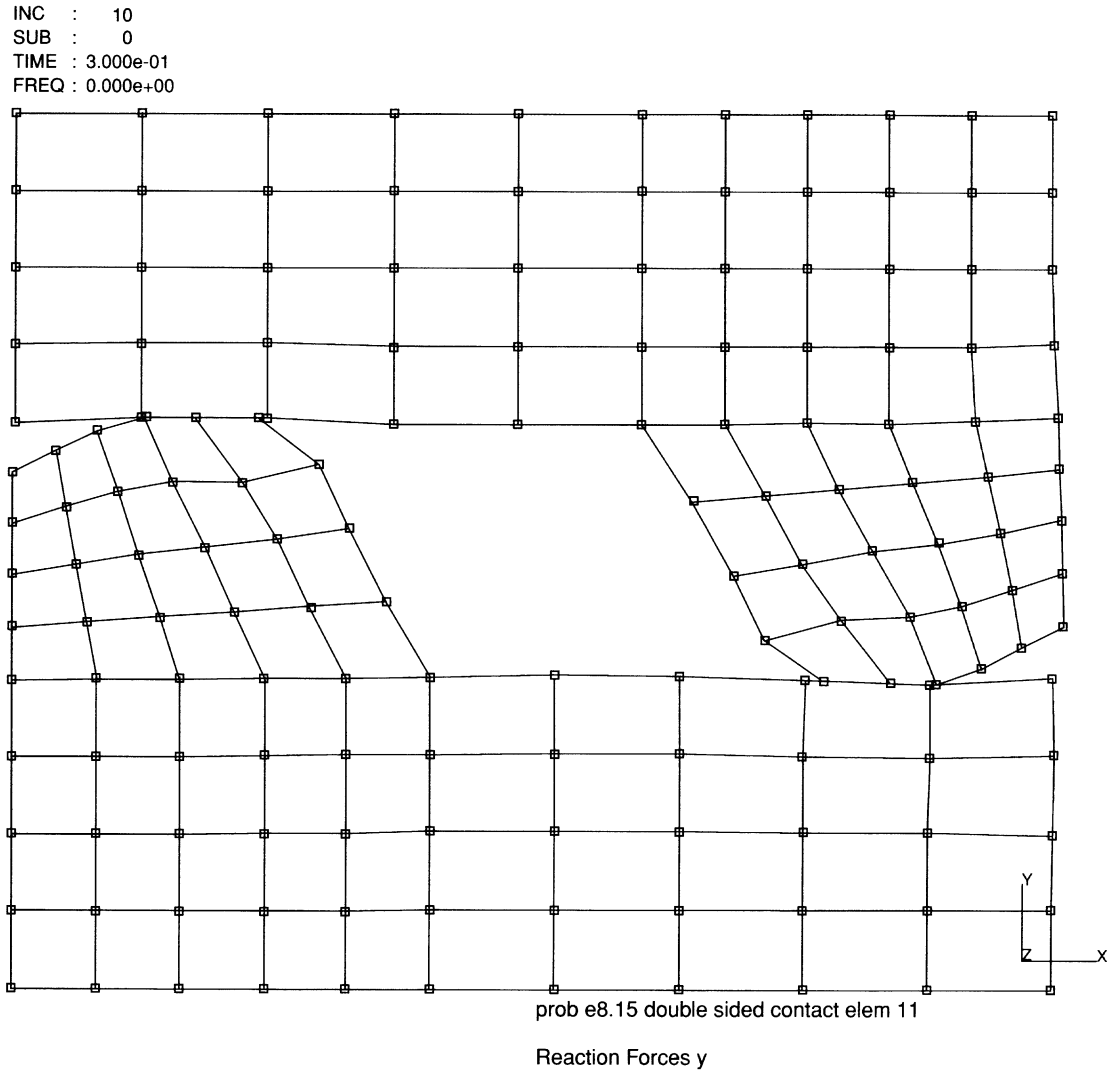

Figure E 8.15-4 Nodal Displacements at Increment 10, Element Type 11

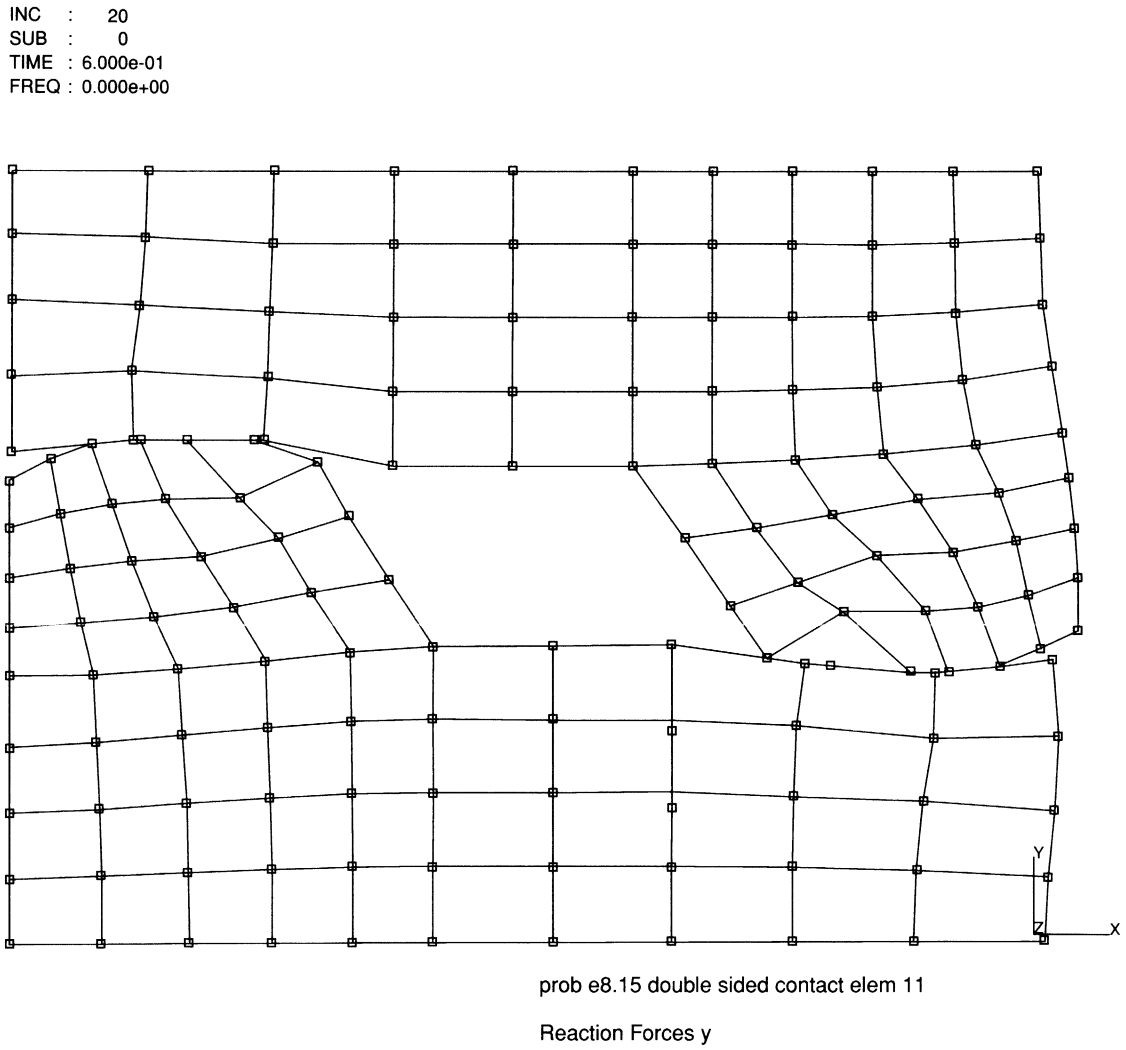

Figure E 8.15-5 Nodal Displacements at Increment 20, Element Type 11

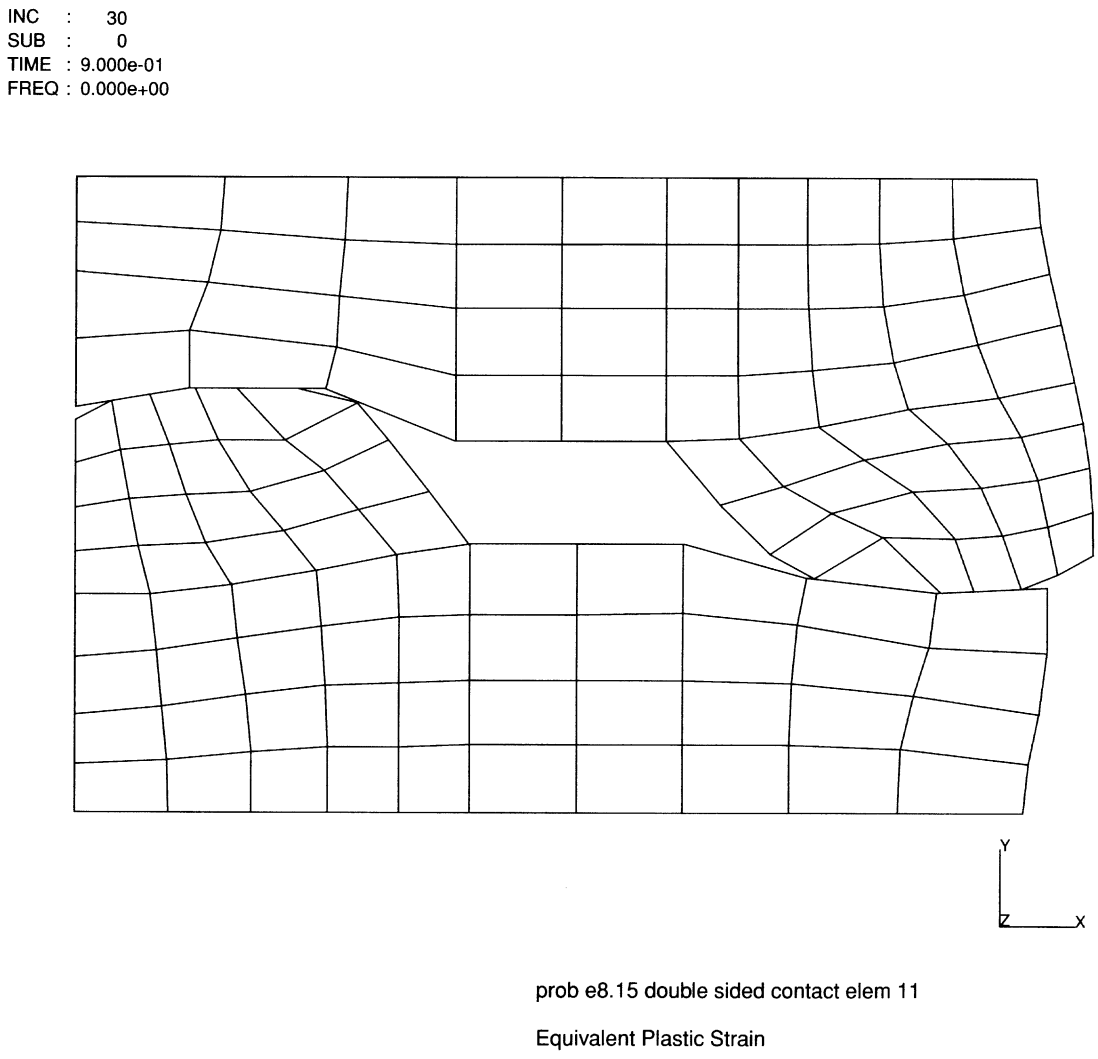

Figure E 8.15-6 Nodal Displacements at Increment 30, Element Type 11

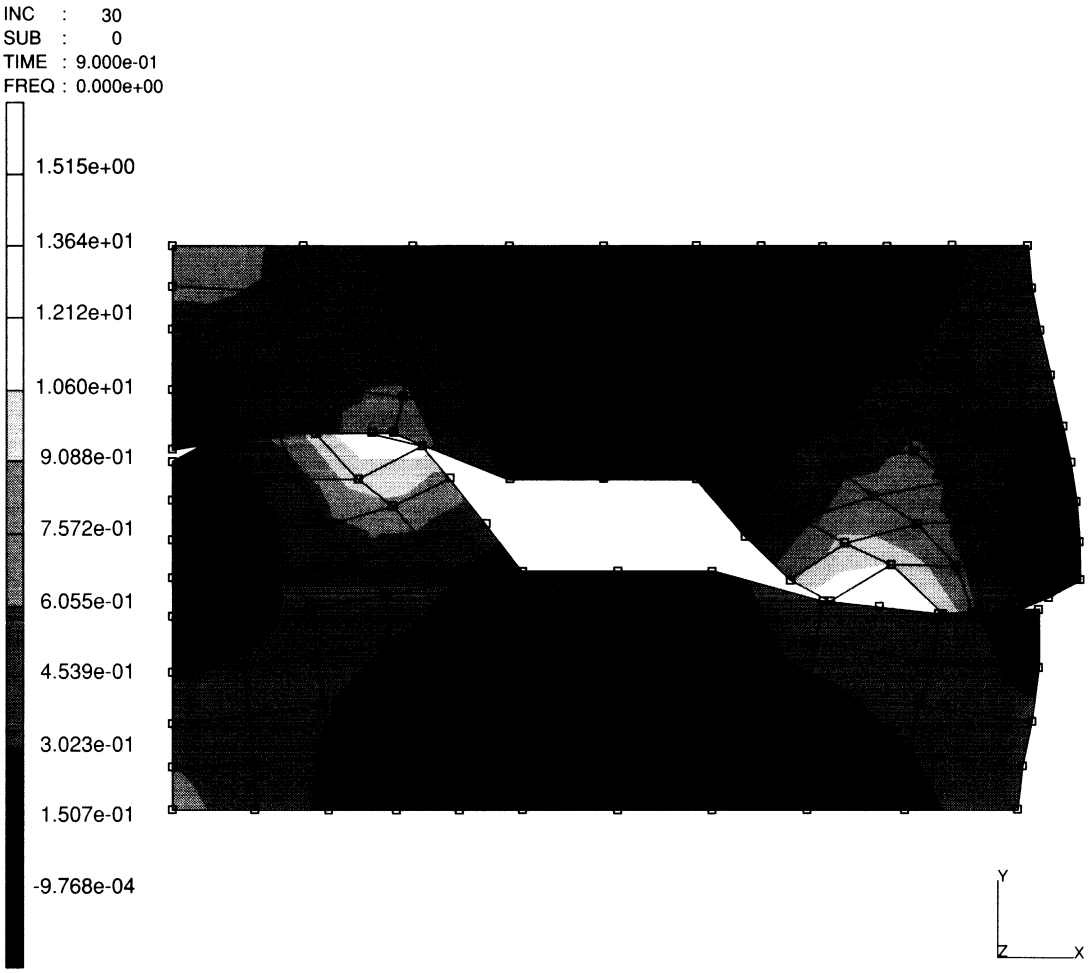

Figure E 8.15-7 Equivalent Plastic Strain at Increment 30, Element Type 11

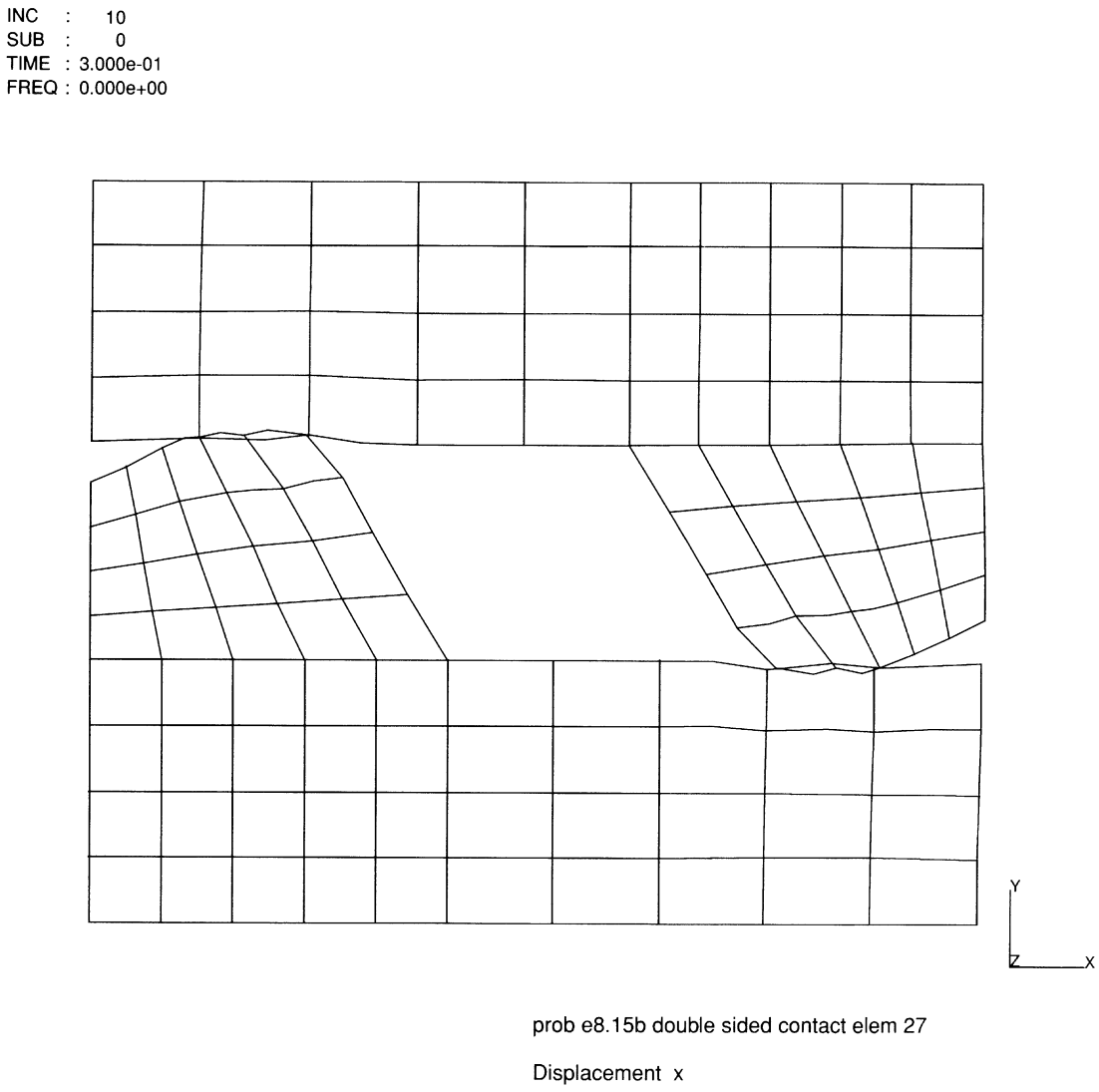

Figure E 8.15-8 Nodal Displacements at Increment 10, Element Type 27

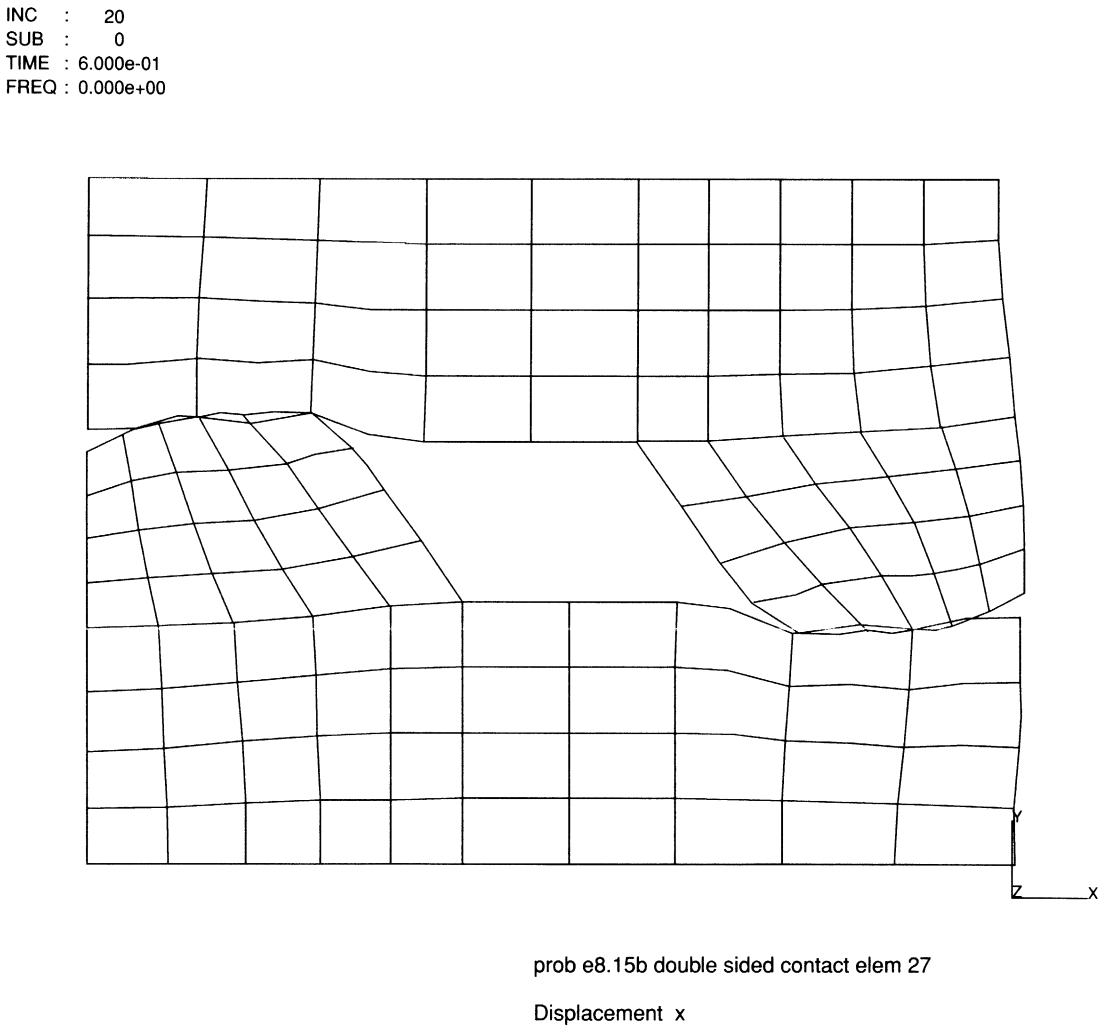

Figure E 8.15-9 Nodal Displacements at Increment 20, Element Type 27

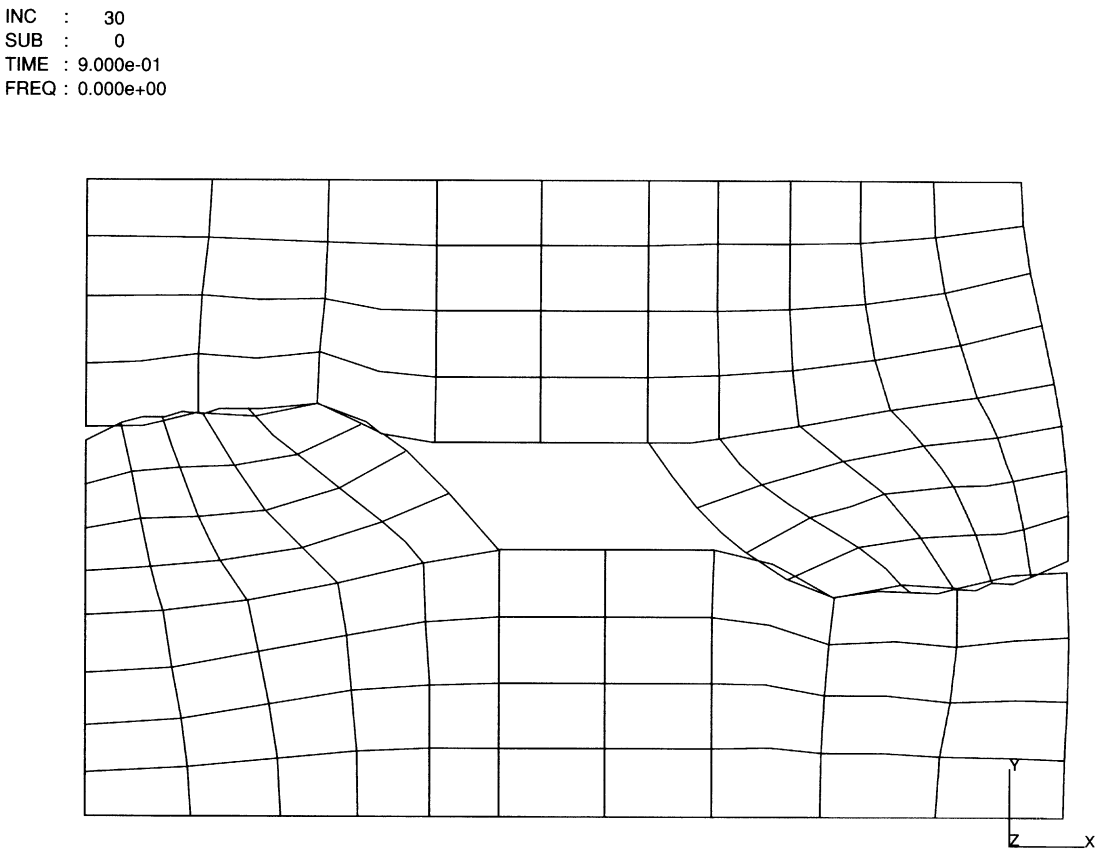

Figure E 8.15-10 Nodal Displacements at Increment 30, Element Type 27

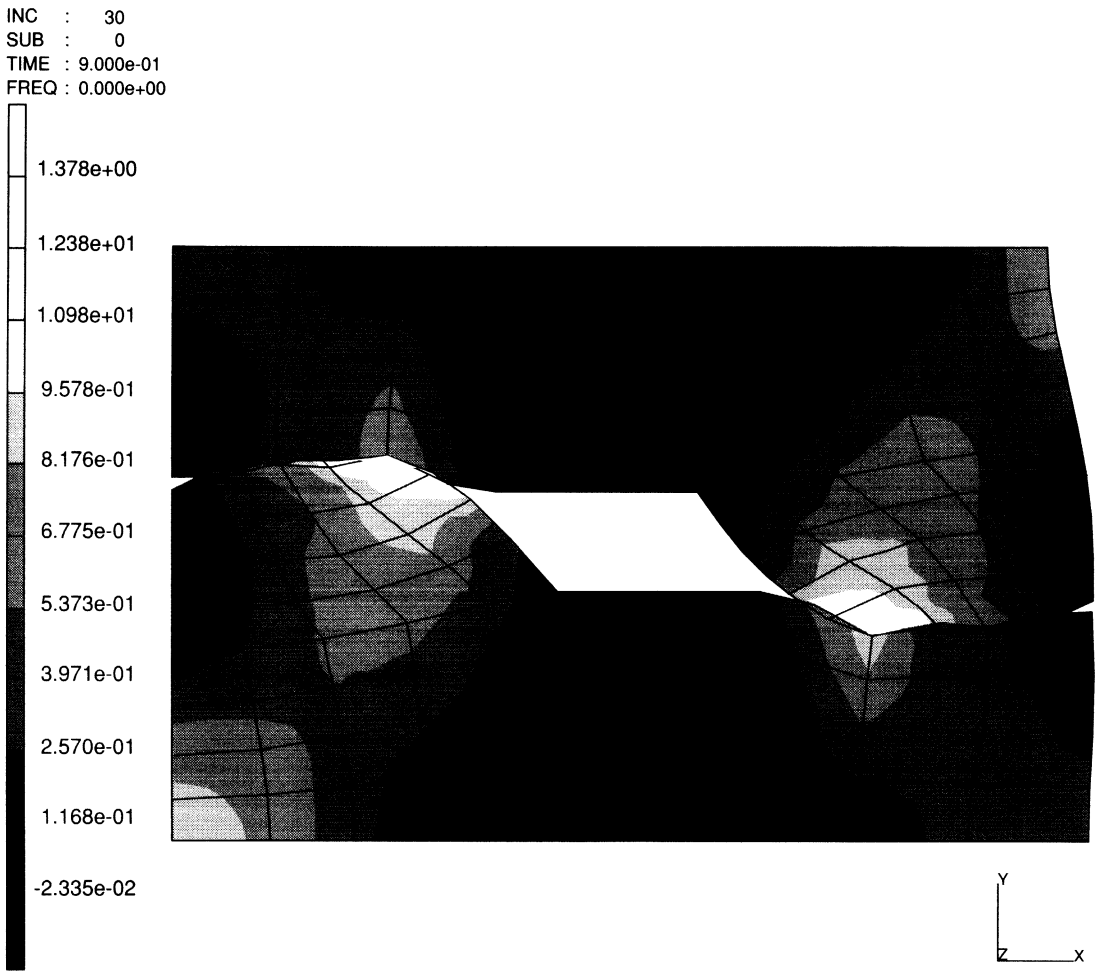

Figure E 8.15-11 Equivalent Plastic Strain at Increment 30, Element Type 27

Disp (x-1e+0)	Load (x-1e+5)		Disp (x-1e+0)	Load (x-1e+5)	
	Type 11	Type 27		Type 11	Type 27
0.00000E+00	0.00000E+00	0.00000E+00	4.50000E-01	5.73937E+00	5.76850E+00
3.00000E-02	1.49358E+00	9.65015E-01	4.80000E-01	5.82146E+00	5.92706E+00
6.00000E-02	1.36351E+00	1.34468E+00	5.10000E-01	5.88858E+00	6.02711E+00
9.00000E-02	1.40418E+00	1.61070E+00	5.40000E-01	5.95362E+00	6.11778E+00
1.20000E-01	3.59213E+00	2.52490E+00	5.70000E-01	6.01384E+00	6.20322E+00
1.50000E-01	3.26189E+00	3.02085E+00	6.00000E-01	6.28412E+00	6.28309E+00
1.80000E-01	3.31538E+00	3.35550E+00	6.30000E-01	6.35279E+00	6.35828E+00
2.10000E-01	3.52452E+00	3.70196E+00	6.60000E-01	6.39055E+00	6.42653E+00
2.40000E-01	4.55123E+00	4.33235E+00	6.90000E-01	6.43786E+00	6.52579E+00
2.70000E-01	4.74629E+00	4.63125E+00	7.20000E-01	6.56095E+00	6.55766E+00
3.00000E-01	4.89159E+00	4.88421E+00	7.50000E-01	6.72437E+00	6.52325E+00
3.30000E-01	5.03333E+00	5.07415E+00	7.80000E-01	6.77405E+00	6.70139E+00
3.60000E-01	5.16167E+00	5.23750E+00	8.10000E-01	6.70833E+00	6.79742E+00
3.90000E-01	5.39677E+00	5.41752E+00	8.40000E-01	6.89754E+00	7.02602E+00
4.20000E-01	5.51851E+00	5.60917E+00	8.70000E-01	6.97591E+00	7.14885E+00
			9.00000E-01	7.01286E+00	7.24298E+00

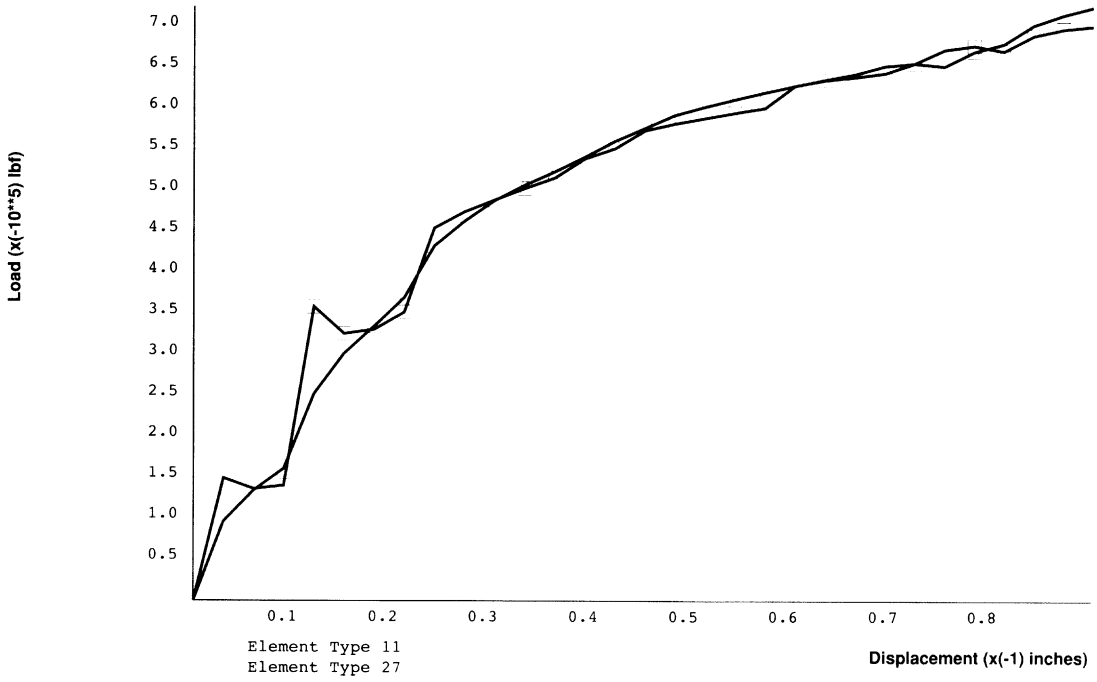

Figure E 8.15-12 Load History for Both Element Types

E 8.16 Demonstration Of Springback

A metal part is formed and the springback is examined.

Model

The original part is shown in Figure E 8.16-1 and is composed of 197 elements type 11 plane strain quadrilaterals. A rigid cylinder is used to deform the part.

Parameters

The LARGE DISP, FINITE and UPDATE options are included because it is anticipated that large plastic strains will occur. The PRINT, 5 option results in additional output regarding contact.

Geometry

The "1" in the second field invokes the constant dilatation option. This gives improved behavior for nearly incompressible behavior that occurs during plastic deformation. The "1" in the third field invokes the assumed strain formulation for element type 11. This gives improved behavior in bending which will be the dominant mechanism in this problem.

Boundary Conditions

The left side is constrained in the first degree of freedom. A spring is used to constrain the motion in the y-degree of freedom, so there will not be any rigid body modes.

Material Properties

The part is made of aluminum with a Young's modulus of 10.6E+6 psi^2. The material strain hardens such that at 5.8% strain the flow stress will be 50,355 psi. It is important that the first stress in the WORK HARD DATA be the same as given through the ISOTROPIC option.

Contact

Two contact bodies are defined. The first is the deformable body, consisting of 147 elements. The second body is the rigid pin, defined as four circular arcs. Each arc is subdivided into ten segments. The circular pin has a velocity of 0.2 in/sec.

Control

The full Newton-Raphson procedure is used in this analysis. Displacement control is requested with a tolerance of 2%. The Cuthill-McKee method is used to minimize the bandwidth. The POST tape frequency is specified through the POST and POST INCREM options. The post tape will be written at increments 0 (default), 18, and 19.

The AUTO LOAD and TIME STEP options are used to request 18 increments each with a time step of 0.1 second. At this point, the pin is removed from the model.

This is done in one step by using the RELEASE and MOTION CHANGE options. The RELEASE option is used to ensure that all of the nodes separate from body 2, the rigid pin. The MOTION CHANGE option is used to move the pin away from the body, so that it will not make any further contact.

Results

The deformed shape at increment 18 is shown in Figure E 8.16-2. The stresses at this point are shown in Figure E 8.16-3. After release of the pin, there is a slight amount of springback. Recall that the elastic strain is, at the most, 5.4 E4/10.6E6 = 0.5% which will limit the amount of springback.

Summary of Options Used

Listed below are the options used in example e8x16.dat:

Parameter Options

ELEMENT
END
FINITE
LARGE DISP
PRINT
SIZING
TITLE
UPDATE

Model Definition Options

CONNECTIVITY
CONTACT
CONTROL
COORDINATES
END OPTION
FIXED DISP
GEOMETRY
ISOTROPIC
OPTIMIZE
POST
PRINT CHOICE
WORK HARD

Load Incrementation Options

AUTO LOAD
CONTINUE
POST INCREMENT
RELEASE
TIME STEP

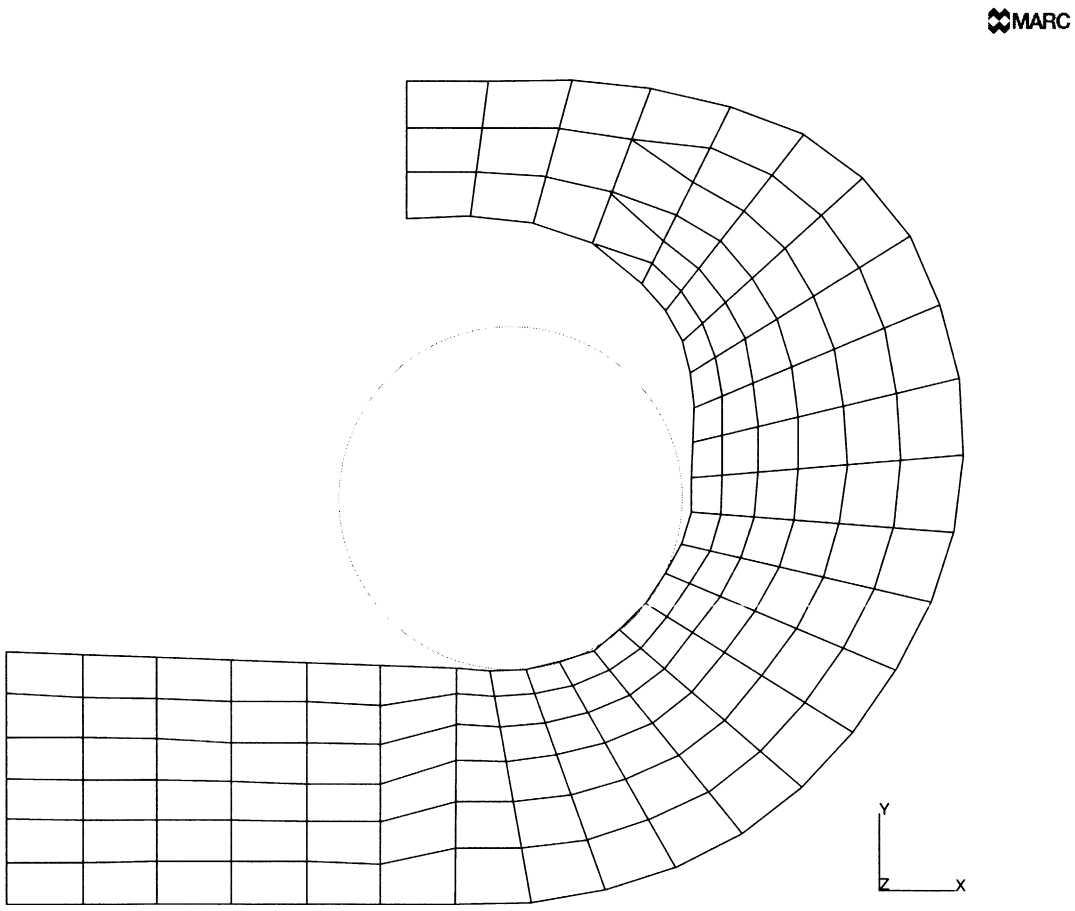

Figure E 8.16-1 Original Configuration

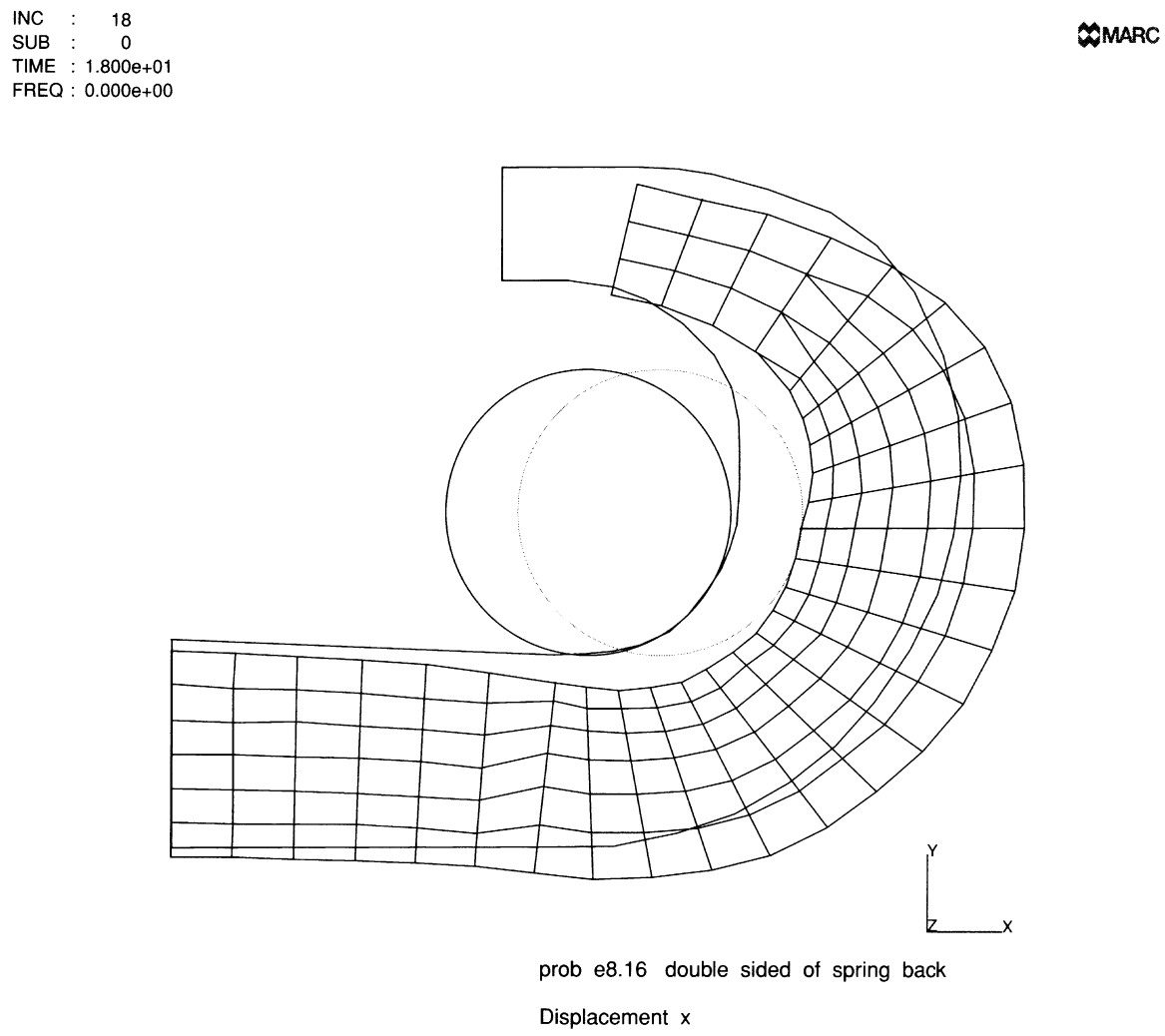

Figure E 8.16-2 Deformed Mesh

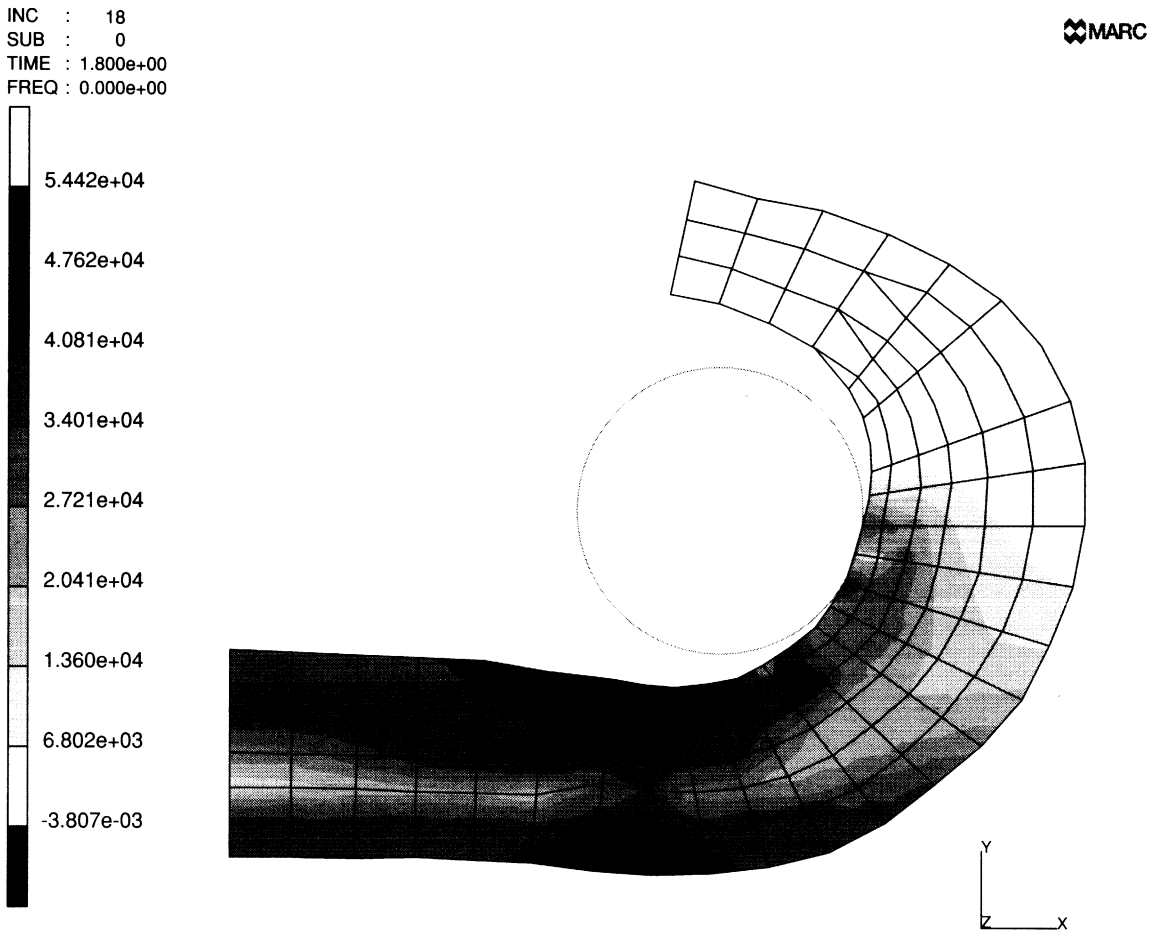

Figure E 8.16-3 Equivalent Stress

E 8.18 3-D Forming Of A Circular Blank Using Shell Elements And Coulomb Friction

This problem demonstrates the program's ability to perform stretch forming by a spherical punch using the CONTACT option and shell elements. The second example demonstrates the same problem using the analytical form (quadratic equation) of the spherical punch.

Parameters

The UPDATE, FINITE and LARGE DISP options are included in the parameter section to indicate this is a finite deformation analysis. The PRINT,8 option requests the output of incremental displacements in the local system. Element type 75, the four-node thick-shell element, is used in this analysis. Seven layers are used through the thickness of the shell.

Geometry

A shell thickness of 1 cm is specified through the GEOMETRY option in the first field (EGEOM1).

Boundary Conditions

The first boundary condition is used to model the binding in the stretch forming process. The second and third boundary conditions are used to represent the symmetry conditions.

POST

The following variables are written to a formatted post tape:

7 } Equivalent plastic strain
20 } Element thickness
17 } Equivalent von Mises stress

Furthermore, the above three variables are also requested for all shell elements at layer number 4, which is the midsurface.

Control

A full Newton-Raphson iterative procedure is requested, along with the mean normal method approach to solve plasticity equations. Displacement control is used, with a relative error of 5%. Twenty-six load steps are prescribed, with a maximum of twenty recycles (iterations) per load step.

Material Properties

The material for all elements is treated as an elastic-plastic material, with Young's modulus of 690,040 lbf/cm^2, Poisson's ratio of 0.3, and an initial yield stress of 80.6 lbf/cm^2. The yield stress is given in the form of a power law and is defined through the WKSLP user subroutine.

Contact

This option declares that there are three bodies in contact with Coulomb friction between them. A coefficient of friction of 0.3 is associated with each rigid die. The first body represents the workpiece. The second body is the lower die, defined as three surfaces of revolution. The first and third surfaces of revolution use a straight line as the generator, the second uses a circle as the generator. In example e8x18, the third body (the punch) is defined as two surface of revolution. These surfaces are extended from -0.5 to 101.21 degrees. In example e8x18b, the third body (the punch) is represented by a sphere. Its initial center is at 0, 0, 51.3 and the radius is 50. In problem e8x18, the rigid surfaces are discretized into 4-node patches. This results in a piecewise-linear representation of the surface. In e8x18b, the analytical form is used. This results in a smooth representation of the surface. The relative slip velocity is specified as 0.01 cm/sec. The contact tolerance distance is 0.05 cm.

Load Control

This problem is displacement controlled with a velocity of 1 cm/sec applied in the negative z-direction with the AUTO LOAD option. The load increment will be applied 40 times. The MOTION CHANGE option is illustrated to control the velocity of the rigid surfaces.

Results

Figure E 8.18-2 shows the deformed body at the end of 40 increments with the deformation at the same scale as the coordinates. Due to the high level of friction, significant transverse deformation is shown along the contact surfaces.

Figure E 8.18-3 shows the equivalent plastic strain contours on the deformed structure at increment 40, with the largest strain level at 60%.

Figure E 8.18-4 shows the equivalent von Mises stress contours on the deformed structure at increment 40 with peak values at 527.4 lbf/cm^2.

Figure E 8.18-5 shows the deformed body at the end of 40 increments. The computational performance and results are improved by using the analytical form.

Summary of Options Used

Listed below are the options used in example e8x18.dat:

Parameter Options

ELEMENT
END
FINITE
LARGE DISP
PRINT
SHELL SECT
SIZING
TITLE
UPDATE

Model Definition Options

CONNECTIVITY
CONTACT
CONTROL
COORDINATE
END OPTION
FIXED DISP
GEOMETRY
ISOTROPIC
POST
PRINT CHOICE
WORK HARD

Load Incrementation Options

AUTO LOAD
CONTINUE
MOTION CHANGE
TIME STEP

Listed below are the options used in example e8x18b.dat:

Parameter Options

ELEMENTS
END
FINITE
LARGE DISP
PRINT
SHELL SECT
SIZING
TITLE
UPDATE

Model Definition Options

CONNECTIVITY
CONTACT
CONTROL
COORDINATE
END OPTION
FIXED DISP

GEOMETRY
ISOTROPIC
POST
PRINT CHOICE
WORK HARD

Load Incrementation Options

AUTO LOAD
CONTINUE
MOTION CHANGE
TIME STEP

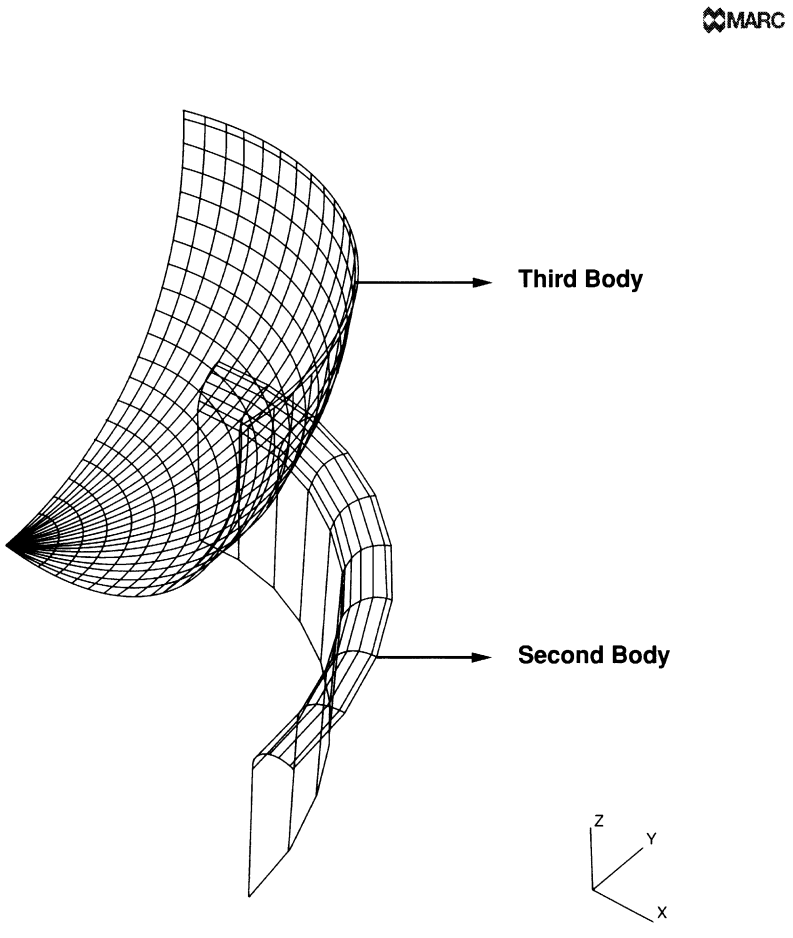

Figure E 8.18-1 Circular Blank Holder and Punch

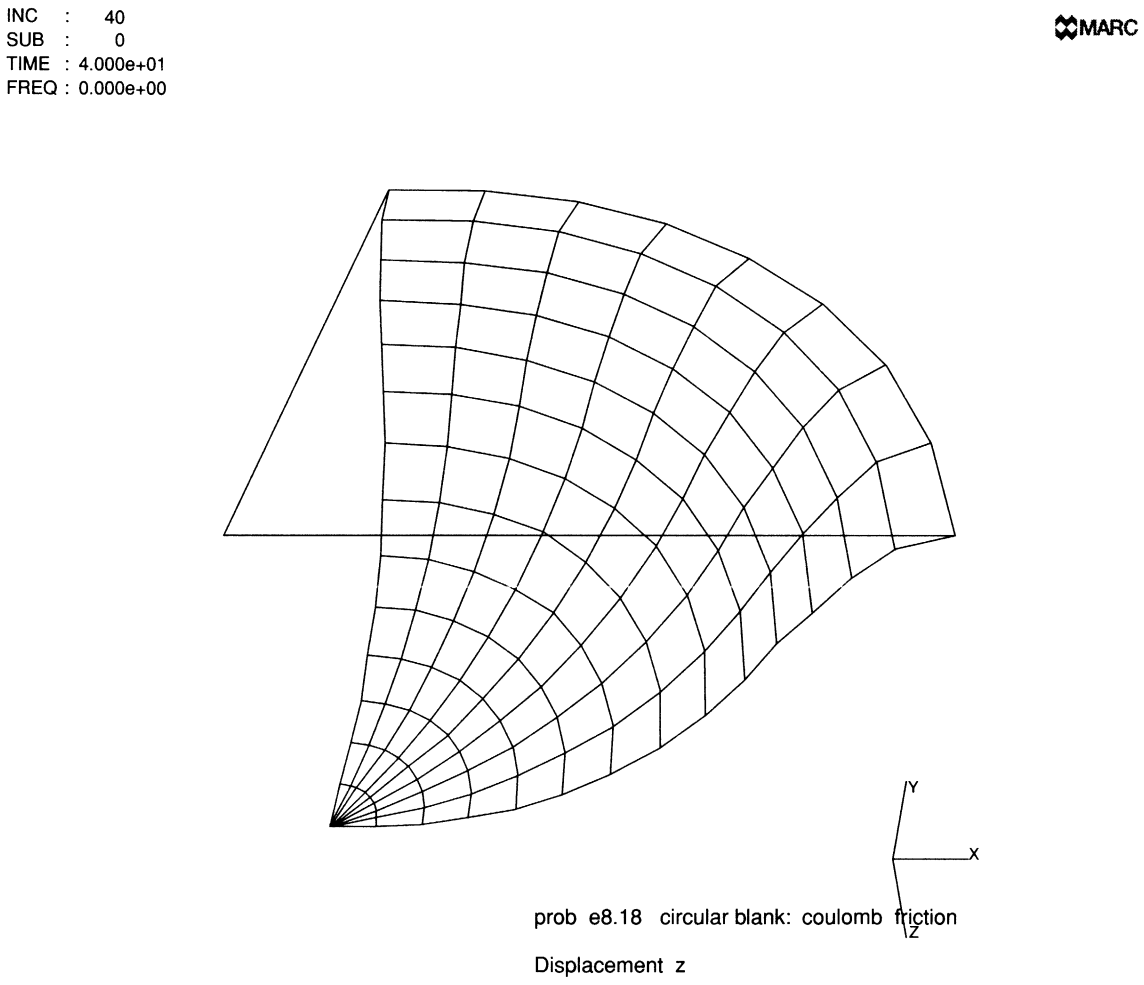

Figure E 8.18-2 Deformed Sheet at Increment 40

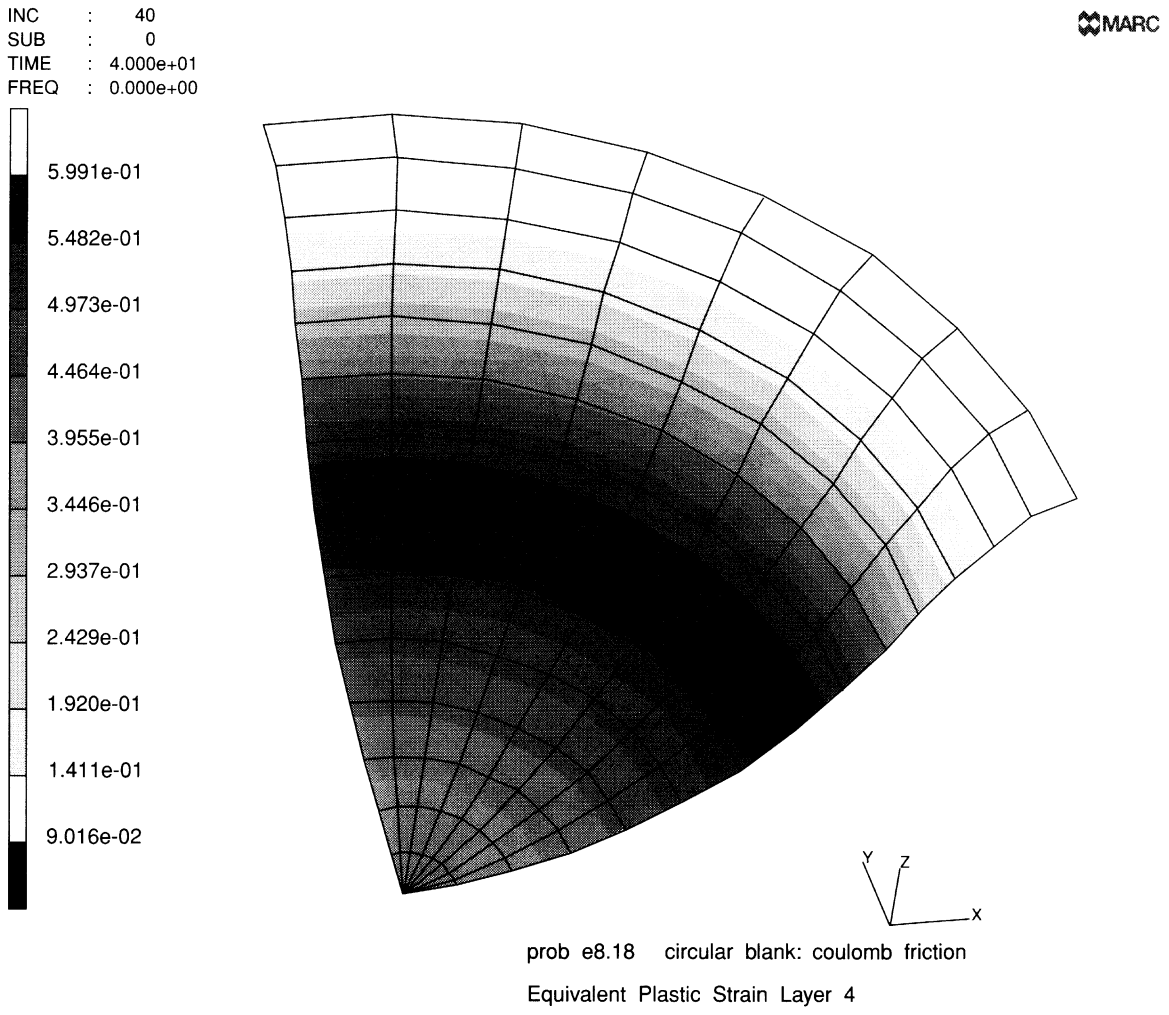

Figure E 8.18-3 Plastic Strain at Increment 40

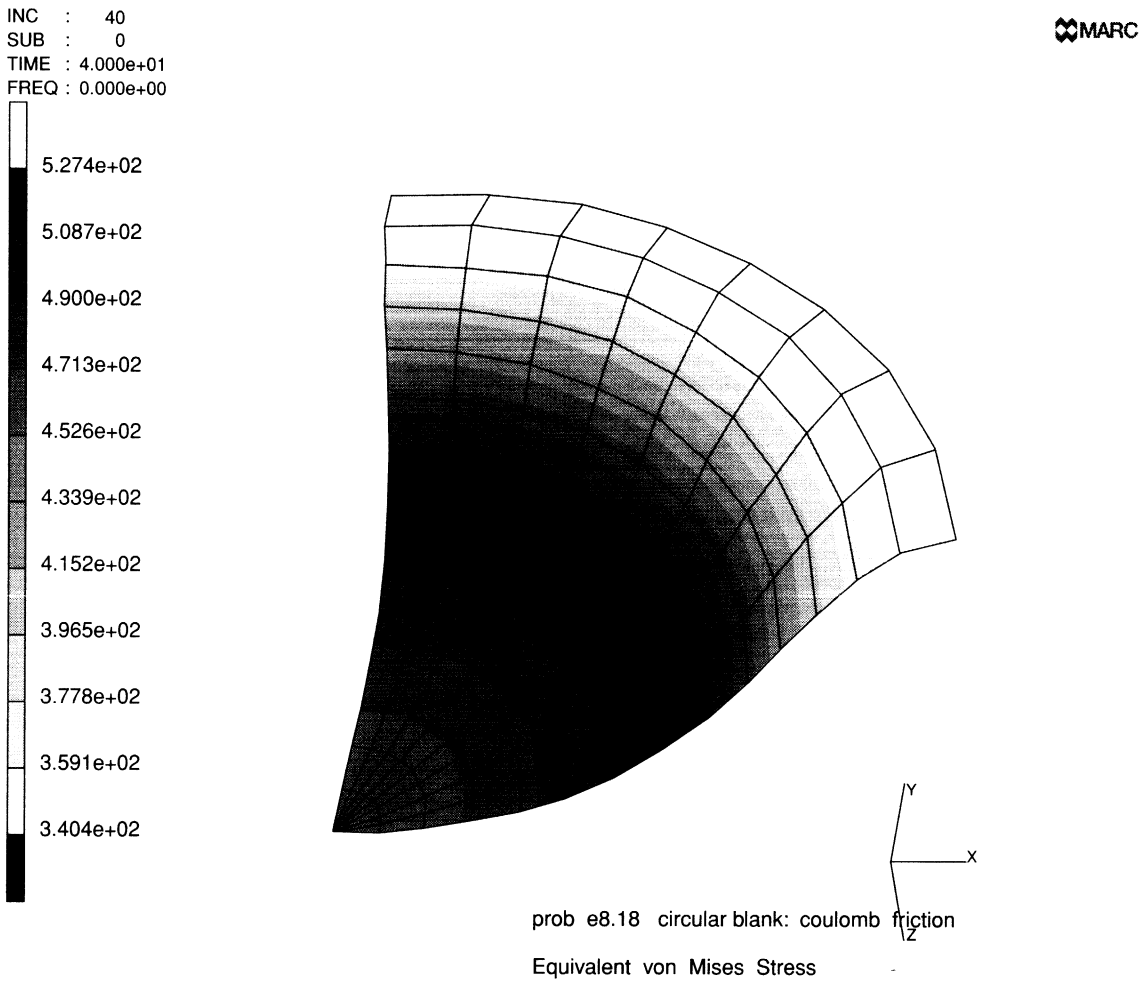

Figure E 8.18-4 Equivalent Stress at Increment 40

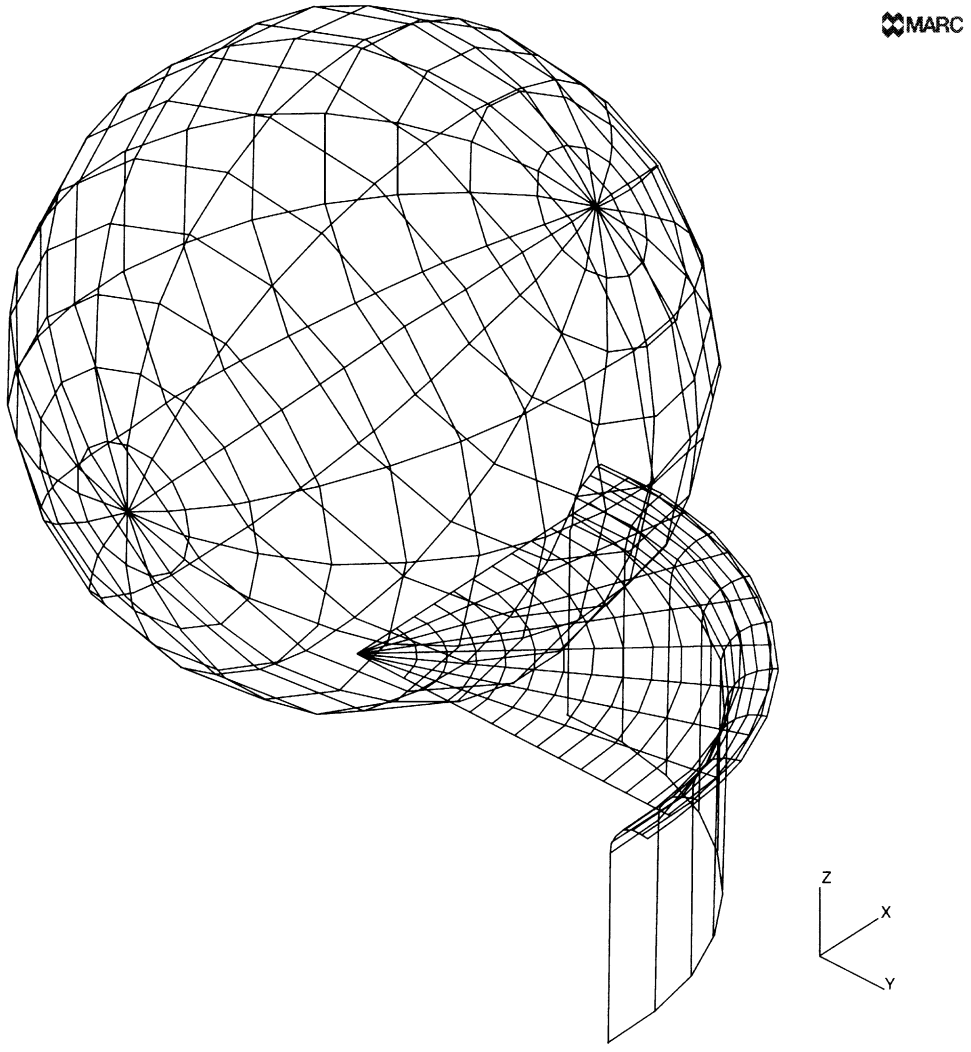

Figure E 8.18-5 Analytical Form of Rigid Contact Surfaces

MARC Corporate Headquarters
260 Sheridan Avenue, Suite 309
Palo Alto, CA 94306, USA
Tel: (415) 329-6800
Fax: (415) 323-5892
Email: support@marc.com

MARC Analysis Research Corporation
Bredewater 26
2715 CA Zoetermeer
The Netherlands
Tel: 31-(0)79-510411
Fax: 31-(0)79-517560
Email: support@marc.nl

Nippon MARC Co.,Ltd.
P.O.Box 5056
Shinjuku Daiichi Seimei Bldg.
2-7-1 Nishi-Shinjuku
Shinjuku-ku, Tokyo 163, Japan
Tel: 81-(0)3-3345-0181
Fax: 81-(0)3-3345-1529
Email: system@marc.co.jp

MARC Software Deutschland GmbH
Ismaningerstrasse 9
85609 Aschheim
Germany
Tel: 49-(0)89-9045033
Fax: 49-(0)89-9030676
Email: support@marc.de

Nippon MARC Co.,Ltd.
Dai 2 Kimi Bldg.
2-11 Toyotsu-cho
Suita-city,Osaka 564, Japan
Tel: 81-(0)6-385-1101
Fax: 81-(0)6-385-4343

MARC Software Deutschland GmbH
Alte Dohrener Str. 66
D-30173 Hannover, Germany
Tel: 49-(0)511-800211
Fax: 49-(0)511-801042

MARC UK Ltd.
35, Shenley Pavilions, Chalkdell Drive
Shenley Wood
Milton Keynes, MK5 6LB, UK
Tel: 44-1908-506505
Fax: 44-1908-506522

Espri-MARC S.r.l.
Viale Brigata Bisagno 2/10
16129 Genova
Italy
Tel: 39-(0)10-585949
Fax: 39-(0)10-585949

Document Title: **Volume E, Demonstration Problems, K6 Changes**
Part Number: RF-3020-06
Revision Date: July, 1995